

F.P. Bos



There are two things everybody knows about glass: it is transparent ... and it breaks! And it is these two qualities (transparency and fragility) that provide it its unique position in the building industry. Transparency is the prime architectural driving force, and fragility a key property making engineers hesitant to apply it quite to the extent architects would like, i.e. as a load bearing material. In spite of several decades of development, there is still no comprehensive method to assess the safety of a structural glass element, that agrees with its specific failure behaviour. Therefore, this dissertation proposes the *Integrated Approach to Structural Glass Safety*, based on four clearly defined element safety properties, *damage sensitivity*, *relative resistance*, *redundancy*, and *fracture mode*. The *Element Safety Diagram* (ESD) is introduced to provide an easy-to-read graphical representation of these properties. The safety performance of a large number of glass beam designs has been compared through experimental testing based on the proposed approach. The effects of a wide range of safety enhancing design measures on each element safety property is extensively discussed. Elastic strain energy release is identified as a, hitherto underexposed, parameter with major influence on redundancy – the most important safety property. Finally, the Integrated Approach is applied to re-evaluate the safety of two full-scale case-study projects which started this study.

Towards an Integrated Approach
Safety Concepts in Structural Glass Engineering

Safety Concepts in Structural Glass Engineering

Towards an Integrated Approach

ISBN 978-90-8570-428-7



9 789085 704287 >



F.P. Bos

Stellingen behorend bij het proefschrift:

Safety Concepts in Structural Glass Engineering – Towards an Integrated Approach

F.P. Bos

1. De veiligheid van een glazen element in een bouwkundige constructie kan worden beschreven door middel van de – fysisch slechts indirect afhankelijke – eigenschappen: schadegevoeligheid, relatieve weerstand, redundantie en breukpatroon (hoofdstuk 6, paragraaf 4).
2. Er dient een testprogramma te worden opgezet om vooral de eigenschappen schadegevoeligheid en redundantie van glazen elementen vast te leggen. Daartoe moeten de maatgevende types impact worden vastgelegd, hun grootte om de model schadeniveaus I, II, en III te bereiken, alsmede de reststerkte die bij elk van die niveaus overblijft.
3. In een enkellaags, ongeharde glasplaat – staande belast in drie- of vierpuntsbuiging – kan het totale scheuoppervlak eenvoudig lineair worden gerelateerd aan de totale elastische rekenergie in de glasplaat op het moment van bezwijken, door middel van een constante en enkele geometrische parameters.
4. Het vrijkomen van elastische rekenergie uit externe belastingen bij het initieel falen van glazen constructie-elementen uit ongehard of thermisch versterkt glas beïnvloedt de capaciteit van het post-faal draagmechanisme in die zin, dat meer vrijkomende energie leidt tot een lagere post-faal sterkte. De invloed van de hoeveelheid energie die vrijkomt, neemt echter af naarmate de stijfheid van het post-faal draagmechanisme groter is.
5. Het ‘spontane’ verkrumelen van een plaat thermisch gehard glas wordt niet – zoals algemeen aangenomen – simpelweg veroorzaakt door een verlies aan intern krachterevenwicht. Er is een additioneel bezwijkmechanisme dat dit specifieke breukpatroon veroorzaakt.
6. Verder onderzoek naar de (statistische beschrijving van de) sterkte van natronkalk vlakglas is zinloos zolang er niet meer kennis is over het fysisch-chemische proces dat ten grondslag ligt aan scheurgroei in dat materiaal.
7. Beter dan onderzoeksplannen, vormen prestaties uit het verleden een indicatie voor de te verwachten kwaliteit van onderzoek in de toekomst.
8. Voor ernstig slechthorende en dove kinderen moet een tweetalige opvoeding en educatie (in gebarentaal en een gesproken taal) het uitgangspunt zijn, waarvan alleen afgeweken moet worden indien dit een te grote belasting voor het kind is.
9. Na 35 jaar is ‘Onder professoren’ (*W.F. Hermans*) onverminderd actueel.
10. De menselijke domheid is oneindig (*Einstein*); de menselijke inventiviteit gelukkig ook.

Deze stellingen worden oponeerbaar en verdedigbaar geacht en zijn als zodanig goedgekeurd door de promotor, prof. dr. ir. J.G. Rots

Propositions to the dissertation:

Safety Concepts in Structural Glass Engineering – Towards an Integrated Approach

F.P. Bos

1. The safety of a glass element in a building construction can be described by the – physically only indirectly related – properties: damage sensitivity, relative resistance, redundancy, and fracture mode (Chapter 6, Section 4).
2. An extensive test program should be initiated to determine specifically the properties damage sensitivity and redundancy of glass elements. Therefore, the governing impact types need to be established, as well as their magnitude to obtain model damage levels I, II, and III, and the residual resistance that remains at each of those levels.
3. In single layer, annealed glass sheets – loaded in a standing position in three- or four point bending – the total fracture surface area can be related linearly to the total elastic strain energy in the sheet at the moment of failure, through a constant and some simple geometrical parameters.
4. The release of elastic strain energy from external loads at initial failure of a structural glass element from annealed or heat strengthened glass, influences the capacity of the post-failure load transfer mechanism in such a way that a larger quantity of energy release will cause a lower post-failure strength. However, the importance of the amount of energy release decreases with increasing stiffness of the post-failure load transfer mechanism.
5. ‘Spontaneous’ disintegration of a sheet of thermally tempered glass is not – as commonly assumed – caused simply by a loss of equilibrium of internal forces. Rather, there is an additional failure mechanism that causes this specific fracture pattern.
6. Further research into the (statistical description of the) strength of soda-lime silicate flat glass, is senseless as long as there is not a more fundamental understanding of the physico-chemical processes that control crack growth in that material.
7. Better than research proposals, does past performance provide an indication for the quality to be expected from future research.
8. For severely hearing impaired and deaf children, a bilingual (in sign language and a spoken tongue) upbringing and education should be the premise, of which should be diverted only when this places too high a demand on the child.
9. After 35 years, ‘Onder professoren’ (*W.F. Hermans*), is still as relevant as ever.
10. Human stupidity is infinite (*Einstein*); fortunately, so is human resourcefulness.

These propositions are considered opposable and defensible and as such have been approved by the supervisor, prof. dr. ir. J.G. Rots.

**Safety Concepts in
Structural Glass Engineering**
*Towards an Integrated
Approach*

Proefschrift

ter verkrijging van de graad van doctor
aan de Technische Universiteit Delft,
op gezag van de Rector Magnificus prof. dr. ir. J.T. Fokkema,
voorzitter van het College van Promoties,
in het openbaar te verdedigen op donderdag 17 december 2009 om 10:00 uur
door

Freek Paul BOS

bouwkundig ingenieur
geboren te Amsterdam

Dit proefschrift is goedgekeurd door de promotor en copromotor:

Prof. dr. ir. J.G. Rots
Dr. ir. F.A. Veer

Samenstelling promotiecommissie:

Rector Magnificus	voorzitter
Prof. dr. ir. J.G. Rots	Technische Universiteit Delft, promotor
Dr. ir. F.A. Veer	Technische Universiteit Delft, copromotor
Prof. ir. R. Nijssse	Technische Universiteit Delft
Prof. dr.-ing. U. Knaack	Technische Universiteit Delft
Prof. ir. F. van Herwijnen	Technische Universiteit Eindhoven
Prof. dr.-ing. J. Schneider	Technische Universität Darmstadt
T. Macfarlane BSc CEng MIStructE	Dewhurst Macfarlane & Partners, Londen

ISBN 987-90-8570-428-7

Printed by Wöhrmann Print Service, Zutphen, the Netherlands

Copyright © 2009 Freek Bos

No part of this publication may be reproduced in any form, by print, copy, or in any other way, without prior written permission from the author.

Voor

Lonneke,
Caspar en Emilia

Acknowledgements

Many institutes, companies, and persons have been helpful in different stages of my research. I would like to thank everyone of them, some of whom I would like to mention in particular.

All float glass used during the research was supplied for free by the van Noordenne Groep. In doing so, they have enabled experimental testing on a scale that would otherwise have been impossible to perform. This has led to (proof of) decisive insights. I therefore sincerely thank the van Noordenne Groep for its commitment to the Zappi Glass & Transparency research. Delo GmbH and DuPont have also supported the research by providing their products. Their contribution is gratefully acknowledged as well.

Through the intensive team work during the All Transparent Pavilion (ATP) project, I was able to quickly gain hands-on experience with glass – a crucial step in the growth of my understanding of the material and its structural use. I thank the ATP team members.

Kees Baardolf has been of unequalled value in the manufacturing of test specimens, auxiliary gear and *oliebollen*. Prof. Alan Brookes was a crucial support in getting together speakers for the 2004 symposium There / Not there. My first paper on a new safety approach for structural glass was critically reviewed by prof. Ton Vrouwenvelder. I express my sincere gratitude to all of them.

The Chair of Mechanics of the TU Delft Faculty of Architecture, of which I was a part during my research, is not only a friendly and sympathetic environment to work in, but also a place where the unusual and the far-fetched is met with sincere interest and enthusiasm. Thus, it is a great place to conduct science. My promotor and co-promotor, prof. Jan Rots and dr. Fred Veer, allowed me to pursue activities besides the research, like the organization of the Challenging Glass conferences, which I consider to be incredibly important for my personal development as well as a lot of fun. Furthermore, Fred has been an extremely helpful and supportive mentor who deserves a particularly warm ‘thank you’. A special mention is also due for Christian Louter who, as my close colleague in the glass research, was my primary sounding board, conference travelling companion, and coffee pal. But even more importantly, he took over my responsibilities as a matter-of-course, when I could not be present as often as I would have liked to. I owe him a debt of gratitude.

Jan Tom and Annemiek Bos, Geert and Jelly Bosch, my parents and parents-in-law: I need not explain what you have done for me and my family. You truly are the ever-burning lighthouse marking the safe harbour. Caspar and Emilia, my son and daughter: you are miracles! Lonneke, my love: words are futile. Thank you.

Freek Bos
Zwolle, November 2009

Extended Summary

1. Safety Concepts in Structural Glass Engineering (Chapters 1 – 5)

1.1. Introduction (Chapter 1)

There are two things everybody knows about glass: it is transparent ... and it breaks!

It is these two qualities (transparency and fragility) that provide glass its unique position in the building industry. Transparency is the prime architectural driving force, and fragility a key property making engineers hesitant to apply it quite to the extent architects would like, i.e. as a load bearing material. As part of the Zappi Glass & Transparency research program, this doctorate research aims at increasing the confidence in the structural use of glass.

The research objectives of this thesis were:

- **To suitably define quantifiable criteria to determine the structural risk for various glass applications in building construction,**

and:

- **To determine the design parameters relevant to minimize structural risk for glass applications in building construction.**

With regard to the first objective, theoretical and codified safety approaches in structural engineering, as well as theory on glass failure mechanisms were studied. Safety approaches in structural glass engineering practice have been inventoried through a survey and interviews. A new, integrated approach based on the introduction of four element safety properties was presented. Based on experimental testing, the safety of a range of glass beam designs was evaluated and compared according to this approach.

For the second objective, the effect of existing and innovative safety enhancing techniques on each element safety property was assessed. Elastic strain energy was identified as a, hitherto neglected, important parameter that partially determines the post-failure resistance through the crack pattern in glass and shock loading on tensile components.

Glass has been used in buildings for many centuries. Aesthetically, its first surge came with the Gothic age. Structures were minimized, stained glass windows maximized. The 19th century conservatories as well as the glass clad iconic buildings of the Modern Movement marked subsequent milestones in the development of the use of glass in buildings.

Structurally (i.e. not only carrying external loads, but also transferring actions within a structure, other than self weight), glass was not used until a few decades ago. Two lines of development of structural glass can be identified. Linear structural elements loaded in bending and/or compression (e.g. façade fins, columns, beams) have been developed since the late 1970's, when glass fins were applied in the Sainsbury Art Centre and Willis Faber Dumas office building. Other key-projects include a glass bridge in Rotterdam (1994) and a cantilevering canopy structure in Tokio, Japan (1997). The other line started with the iconic hanging façades of the Serres of La Villette (1986), where in-plane bearing glass sheets were applied.

The development of glass structures was held back, though, by the unsafe failure behaviour of the material. Due to the fact that glass fracture is governed by stress concentrations around surface defects, the strength of an individual piece of glass is difficult to predict with a satisfying degree of certainty. Furthermore, glass gives no warning signal before breaking and tends to break completely once a crack has started.

In practice, two techniques are commonly applied to overcome these problems: creating an internal prestress by heat treatment and laminating sheets of glass, usually with polyvinylbutiral (PVB) foils to obtain residual strength after glass breakage. Application of these techniques, however, does not make glass match the safety of the most common structural materials: steel and reinforced concrete.

The cause of the structural problems of glass lies in its molecular composition and microstructure. Most generally, a glass is defined as an amorphous solid. This definition is independent of any kind of matter. The material commonly referred to as 'glass' and the subject of this study, is more accurately known as soda lime silicate glass. This material consists for approximately 70 % of SiO_2 , organized in tetrahedras, but without any repetitive character on a higher level of scale. It lacks a crystal structure, interlocking molecule side strands or cross links. Therefore, several fracture delaying mechanisms, such as plasticity and visco-elasticity, are impossible. Glass is thus highly susceptible to surface defects, which act as stress concentrators. As a result, statistically reliable failure prediction of an individual piece of glass is extremely difficult, even though it globally behaves linear elastically up to failure.

The Zappi Glass & Transparency research program was initiated in the mid-1990's to develop transparent structural elements with safe failure behaviour.¹ Initially, glass-polycarbonate laminated beams and plates were devised. Several other concepts were tested as well. Currently, the concept of steel reinforced elements is in an advanced stage of development.

By the end of 2003, at the start of the present study, the Zappi research was at a crossroads. There were several options with respect to the direction subsequent research should take, but their relative importance and relevance was unclear. The All Transparent Pavilion project, which beheld designing and building an all glass pavilion with Zappi concept elements, provided opportunity not only to investigate numerous

¹ Veer, F.A., *The Limitations of Current Transparent Sheet Material in Buildings*, internal memo (unpublished), TU Delft, the Netherlands, 1996.

problems related to combining existing concepts into one structure, but, even more importantly, to determine the research focus for the following years.

1.2. Case Studies (Chapter 2)

1.2.1. All Transparent Pavilion

In the All Transparent Pavilion (ATP) project,² a glass structure was designed and constructed, making use of several innovative concepts that had been developed in previous Zappi-research. Probably the most radical innovation was that only annealed glass was used. Although it is less strong than heat treated glass and more susceptible to stress corrosion and thermal breakage, it had been shown in a range of experimentally tested design concepts that annealed glass is very suitable to create elements with significant residual strength, i.e. that retain resistance after glass breakage. Thereby, the need to absolutely avoid glass fracture was obviated. Instead it could be accepted as a possibility: if, against expectation, failure would happen, it would not have catastrophic results. This was deemed a more fundamentally correct approach, as the possibility of glass breakage can never be avoided completely.³

Besides a range of technical issues mostly related to the joining of glass elements, the ATP project laid bare a fundamental issue to be addressed. A whole array of safety measures had been incorporated in the design. They all aimed particularly at providing post-failure strength in case of failure of one or more elements, and included:

- Resin laminated columns with significant post-failure resistance ($r_{\text{res,III}} = 200 - 343 \%$),⁴
- Steel reinforced glass cantilever main beams with $r_{\text{res,III,mid-span}} \approx 140 \%$ and $r_{\text{res,III,cantilever}} \approx 80 \%$,
- Aluminium reinforced, PVB laminated, ‘double’ purlins with $r_{\text{res,III}} \approx 50 \%$,
- PVB laminated roof plates spanning two fields,
- PVB laminated façade panels with a shifted grid respective to the roof plate grid,
- Steel clamp back-up provision in the main beam-purlin joints.

However, although the elements performed in a manner that was intuitively perceived to be safe, there were no *a priori* requirements to which their behaviour could be checked or optimized. Nor were the principles of designing safe elements really understood.

1.2.2. Transparent Façade Struts

The much smaller Transparent Façade Struts (TFS) project⁵ provided the opportunity to address some of the technical problems which had also been encountered with the columns of the ATP project, particularly producing elements longer than the standard

² Freek, F.P., Veer, F.A., Hobbelman, G.J., Romein, T., Nijssse, R., Belis, J., Louter, P.C., Nieuwenhuijzen, E.J. van, *Designing and planning the world's biggest experimental glass structure*, Proceedings of the 9th Glass Processing Days, Tampere, Finland, June 2005.

³ See extensive discussion in Chapters 3 and 4.

⁴ $r_{\text{res,III}}$ is the residual strength after initial failure, defined as the maximum post-failure resistance as a percentage of the initial failure resistance. Initial failure is equal to model damage level III, see Chapter 6, Section 3.3.2.

⁵ Bos, F.P., *Hybrid Glass-Acrylic Façade Struts*, Proceedings of the 10th Glass Performance Days, Tampere, Finland, June 2007.

1.5 m trade length of glass tubes and developing joints to connect to the tube ends (the cylindrical shape provides specific difficulties).

Three 1:1 scale TFS prototypes were tested in tension, compression/buckling, and three-point bending. The specimens showed post-failure strength in all experiments. However, the quantity varied significantly per experiment type, ranging from 9.7 to 119 % of the initial failure strength. Especially the difference between the post-failure resistance in bending and in buckling was remarkable. In the bending test, the glass tube still contributed to the overall element bending stiffness as it suffered only a limited amount of fracture. In the compression/buckling test the tube fractured much more densely upon failure, thus making any contribution to the overall bending stiffness impossible. This difference in glass fracture, and consequently element failure behaviour, was attributed to the difference in elastic strain energy release.

As with the ATP project, the assessment of the TFS prototype tests brought to light there was no performance criterion to which the failure behaviour could be checked. Thus, there was no means to compare the results of the three tests either to the calculable loads or to one another. It was, therefore, concluded that a safety assessment method was needed to be developed in order to allow the Zappi research to progress.

1.3. Theoretical and Codified Safety Approaches in Structural Engineering (Chapter 3)

Generally, not the safety, but the risk (which could be defined as its inverse) of a structure is determined. Simplified, risk is defined as the product of the probability of an event (e.g. structural collapse) and its consequence. In order to assess whether a structure meets risk requirements, the consequence of a collapse is usually considered (im- or explicitly) as a given. The probability of failure is calculated. Failure is generally defined as an action S exceeding the resistance R .

Though being valuable as a comparative tool, this probabilistic approach has several shortcomings. First, the data to make a full probabilistic approach are usually incomplete. Thus, approximations and simplifications are used. Second, in reality failure is hardly ever caused by those actions considered in the formal probability analysis. Rather, all kinds of errors, defects, or unexpected events (often a combination) cause failure. Overloading of the structure by causes considered in the probability analysis is rare.

Furthermore, in most structural elements there is an important margin between failure and collapse. In steel this is most strikingly illustrated by the difference in yield strength applied in structural calculations, and the ultimate strength that determines whether an element tears and thus collapses. This introduces a hidden extra safety reserve.

Finally, structure codes focus on individual elements. However, the collapse of a single component bears little relation to the collapse probability of the complete structure. Their relation is depends on the type of structural system. The failure probability of a pure serial system is in the order of the sum of the individual element collapse probabilities, while that of a pure parallel system is in the order of the product of the individual element collapse probabilities.

The limitations of a purely probabilistic approach have been recognized for several decades. It has resulted in the introduction of notions such as robustness, redundancy, and collapse resistance into the field of safety in structural engineering. However, these concepts and the way in which they can be quantified are still heavily debated today. Structural engineering codes such as the Dutch NEN 6700⁶ (basis of design) usually only provide very general guidelines (e.g. ‘collapse of a single component should not lead to excessive damage’). The Eurocode, in NEN-EN 1991-1-7,⁷ is more extensive by describing strategies to be applied to the design of building structures in order to limit the extent of localized failure of whatever cause.

However, compared to the quantitative probability requirements, demands with regard to the consequence of a local failure are still relatively limited. Furthermore, they aim at complete structures rather than individual elements. Due to the particular failure behaviour of glass, specific requirements on element level are needed first.

1.4. Glass Failure (Chapter 4)

1.4.1. Fracture Strength

Based on the molecular bonds, soda lime silicate glass should be extremely strong, capable of withstanding stresses of some 32 000 MPa. In practice, the strength of a piece of flat glass is approximately three orders of magnitude smaller. A representative (5%-fractile) strength of 45 MPa is usually maintained. The difference is attributed to the presence of surface flaws, which act as stress concentrators. As glass has no possibility to even out stress concentrations, they induce fracture when exceeding the material strength. Fracture mechanics is required to analyse this kind of failure. In comparison to the classical material strength approach, it compares applied stresses not only to the material strength but also to surface defect size and geometry. The strain energy release approach and the stress intensity approach both provide – for linear elastic materials equivalent – failure criteria based on the flaw depth a as the essential variable.

Thus, to predict failure of a glass sheet, the properties of its surface flaws need to be determined. For two reasons, this has caused difficulty:

- There is a certain distribution of non-identical cracks over the glass surface. Two types of cracks are generally recognized: more or less regularly distributed, small Griffith flaws, and larger accidental flaws that may arise during the glass sheet life time. But it has also been suggested the surface of a glass sheet should be divided into 3 – 5 areas (face, edge, fillet, angles), each with its own type(s) of flaws. Even within one type, flaws are not identical, but rather (only) similar (i.e. statistically distributed).
- Cracks in glass are not static. Their geometry changes with temperature, humidity, time, and presence of tensile stresses (stress corrosion). Despite the development of complex mathematical models, no explanations have yet been

⁶ Nederlands Normalisatie Instituut, *NEN 6700: Technische grondslagen voor bouwconstructies – TGB 1990 – Algemene basiseisen*, Delft, 2005.

⁷ Nederlands Normalisatie Instituut, *NEN-EN 1991-1-7 Eurocode 1: Belastingen op constructies – Deel 1-7: Algemene belastingen – Buitengewone belastingen: stootbelastingen en ontploffingen*, Delft, the Netherlands, 2006.

found that describe these phenomena completely satisfactorily in a physical-chemical sense.

Not surprisingly, the scatter in strength tests in ambient conditions is considerable. Values of 5 – 40 % can be found in literature. The correct statistical description of the distribution (Weibull, Normal, Log-Normal, or other) is also still subject of debate.

1.4.2. Dimensioning Methods for the Application in Building

For the application of glass as a load bearing material in buildings, a range of methods has been developed which relate an allowable load or stress level to a target failure probability through relatively simple equations. Besides simple deterministic models, two families have been developed. The *European methods* follow the system of the current generation of codes in which parameters are expressed with partial factors. The *North American methods*, founded on the Glass Failure Prediction Model, are directly derived from Weibull statistical theory of failure for brittle materials. Haldimann⁸ has concluded, after extensive analysis, that neither of the existing methods is free of shortcomings.

1.4.3. Glass Failure Causes

The complete inability of glass to redistribute peak stresses or stop crack growth, has made the material susceptible to a much broader range of failure causes, than that explicitly considered in glass engineering codes. Failure causes may include surface damage (degradation by chemicals such as alkalis, or mechanical surface damage, e.g. scratches), accidental impact (hard or soft body), purposeful impact (vandalism, break-in, terrorism), thermal stress (both under normal conditions and fire), Nickel Sulfide or other inclusions, and human error (design, calculation, manufacturing and post-processing, handling and transport, and construction). The relative importance of each of the mentioned possible failure causes is difficult to estimate as little has been published on the subject, even though glass failure is common. Interviews with several glass engineering specialists⁹ indicated the primary failure cause is human error during the design/build process.

1.4.4. Limitations of a Probabilistic Approach for Structural Glass Engineering

In addition to the general limitations of the probabilistic approach to assess safety in structural engineering, it can now be concluded it has additional weaknesses for glass in construction.

The reliability of the formal probability analysis is less as there is still significant debate on the proper method to calculate glass resistance.

Additionally, more than common structural materials, glass is susceptible to a wide variety of unconsidered failure causes (i.e. failure causes not included in the probability analysis).

Collapse of glass elements is also more likely to cause injury because of the shards.

⁸ Haldimann, M., *Fracture Strength of Structural Glass Elements – Analytical and numerical modeling, testing and design*. Thèse No 3671, Ecole Polytechnique Fédérale de Lausanne (EPFL), Switzerland, 2006.

⁹ Appendix C.

Finally, the hidden safety margin between failure and collapse, present in common structural materials, hardly exists in glass. The nature of crack growth through glass is such that a glass sheet will almost certainly collapse at failure.

1.4.5. Extension of the Probabilistic Approach in Structural Glass Engineering Codes

Thus, additional safety measures are required beyond the basic probability requirement. Many glass engineering codes are still in the early stages of development. The extent of non-probabilistic safety requirements that can be found varies considerably in specificity. Several German codes and guidelines, e.g. the Guideline for the approval of glass structures of the State of Hessen,¹⁰ currently have the highest available degree of detail, specifying not only strength requirements and compulsory impact tests (drop/pendulum) but also required residual strength after impact. Importantly, layers that have not been broken by the impact should be fractured, e.g. by a hammer, before the residual strength test is performed, thus incorporating the eventuality of breakage of all glass layers, whether or not by the specified impact test.

Nevertheless, codes and guidelines generally lack an overall *integrated safety approach*. It should be noted that such an approach is not only absent in codes, but also in scientific treatises. As a consequence, there is a need for improvement of existing safety requirements:

- Different types of safety requirements should be related.
- Safety requirements should be suitable for all structural elements.
- Safety requirements should be described in terms of structural performance and depend on structural role.
- Safety requirements should be detailed and quantitative.

Even though an integrated safety approach is lacking, structural glass safety is well known as a general problem, under increasing attention in codes and guidelines. Building practice is, off course, also well aware of the difficulties.

1.5. Structural Glass Safety in Practice (Chapter 5)

An analysis of realized projects showed a range of techniques is being applied to obtain sufficient safety, such as prestressing and laminating. Several design solutions, like the application of protective covers or provision of alternative load paths, may also be applied. Some recent innovations include high strength laminates and steel or carbon fibre reinforcement. However, despite the effort put into the investigation of safety enhancing design concepts, it remains generally unclear what (quantitative) performance is aimed at. It is therefore impossible to decide which measures and techniques should be applied to which extent, and to assess whether a certain design actually meets the required safety.

A survey was held among structural glass engineers in order to discover which general premises with regard to safety are being held, how they translate into practice, and to explicate to what extent opinions on these issues differ. The need to provide some form

¹⁰ Hessisches Ministerium für Wirtschaft, Verkehr und Landesentwicklung, *Anwendung nicht geregelter Bauarten nach § 20 der Hessischen Bauordnung (HBO) im Bereich der Glaskonstruktionen, Anforderungen an Bauarten im Zustimmungsverfahren und Freistellung vom Erfordernis der Zustimmung im Einzelfall nach § 20 Abs. 1 HBO*, Erlass vom 26. Juni 2001, Wiesbaden, Germany, 2001.

of residual strength is universally recognized in the field. However, there seems to be no quantitative elaboration of this concept. There is no generally accepted view on the extent of glass breakage to be taken into account, and what loads should be considered in such cases. For glass floors, a considerable majority considers three layers to be the minimum. Glass beams should also have a minimum of three layers according to the majority of respondents. However, this majority was much smaller (55 %). For glass fins, the votes for a minimum of one or multiple layers were practically tied, although the latter option got the preference of most respondents. Heat strengthened or annealed glass are appreciated for their cracking patterns enabling residual strength. Thermally tempered glass is preferably only used when its high resistance is required (e.g. with bore holes). PVB was¹¹ often preferred over ionoplast interlayers because of the large body of available practical and scientific knowledge.

Six of the survey respondents were interviewed more extensively on the issue of structural glass safety. Discussed subjects included the position of safety considerations in the design process, failure experiences, project dependency / independency of safety measures, and (differences in) safety approaches.

The interviews have shown that, by and large, the safety approaches are in line with each other. Generally, breakage of all glass sheets in a structural element should be considered possible. Should breakage occur, residual strength has to be provided to prevent injury or disproportionate collapse. However, there are significant differences in the extent to which these safety approaches are made explicit. A trend towards further quantification of residual strength requirements seems to develop, in which *a priori* a certain performance is demanded for each stage of failure (formulated in terms of increasing numbers of broken glass sheets). Complex analyses to calculate the failure probability with a high degree of certainty are not commonly executed. There does not seem to be a high demand to further increase failure probability calculation by adopting more complex models in codes. Ignorance and negligence in manufacturing, transport, and construction are identified as the most common cause of premature failure. Codes that place a major responsibility at the engineer by formulating safety requirements in general terms, are appreciated.

The analysis of existing projects, the survey, and the interviews have shown that there is no unifying safety concept taking all relevant aspects of safety into account. Hence, there is no generally accepted and complete quantitative set of performance requirements to which design solutions can be tested and compared. As a result, the effect of safety related design measures on the safety of the glass element is often only very globally known.

2. Towards an Integrated Approach of Structural Glass Safety (Chapters 6 – 10)

2.1. The Integrated Approach to Structural Glass Safety (Chapter 6)

These conclusions call for the development of a new systematic safety concept for structural glass engineering. Therefore, the *Integrated Approach to Structural Structural Glass Safety* is presented, as a method to assess structural glass safety objectively, taking into account *all relevant factors simultaneously*. The approach is, for the time being,

¹¹ At least at the time of the survey: 2007.

limited by two important constraints: it deals with the *design* (rather than to incorporate also manufacturing and construction aspects) of *elements* (rather than complete structures). The Integrated Approach identifies four element safety properties to which requirements can be set and performance can be tested. The element safety properties are: *damage sensitivity*, *relative resistance*, *redundancy*, and *fracture mode*. These properties have been chosen to address the shortcomings of a purely probabilistic approach as formulated above. Importantly, they are not physically or mathematically related, but nevertheless all together constitute the safety of a glass element.

A number of underlying concepts was introduced and defined in order to develop the element safety properties:

- **Load Transfer Mechanism; primary, secondary (LTM).**

The mechanism as a mechanics model, with which the element transfers loads acting on it, to its supports. An element may (latently) possess the possibility of more than one LTM. The primary LTM has the highest stiffness and will initially be addressed when the element is loaded. However, a secondary LTM may be activated after the primary LTM has, for whatever reason, lost its capacity (Figure S.1). The concept of LTMs is extremely important to discern damage from failure.

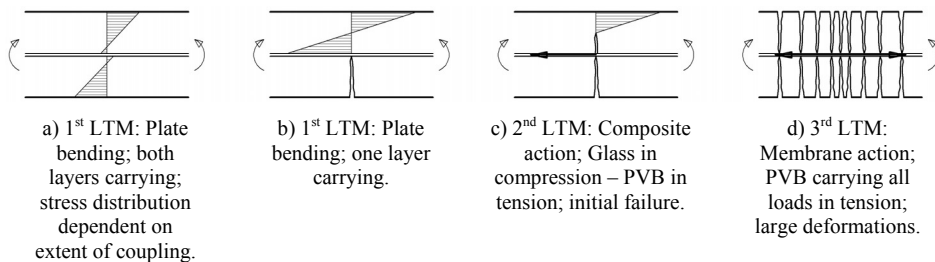


Fig. S.1 Load transfer mechanisms in a laminated glass sheet, loaded in plate bending and developing into membrane action.

- **Failure; initial, final, collapse.**

Initial failure occurs when the element is no longer capable of transferring loads according to its primary LTM. Final failure occurs when the element is no longer capable of transferring loads through any LTM. This usually coincides with collapse.

- **Damage; physical (D_ϕ), structural (D_s), model levels of ... (D_n , with $n = I, II, III$).**

Structural damage is the loss of load transferring capacity of the 1st LTM. Physical damage is the physical phenomenon (e.g. fracture) that has caused the structural damage. Model levels of damage are qualitatively described cases of (increasing) physical damage to a glass element (for each level residual resistance requirements may be formulated).

- **Impact Im.**

The effort required to create damage (chemical, mechanical, etc).

- **Residual resistance $R_{res,n}$ (with $n = I, II, III$)**
The maximum resistance at a model damage level.
- **Post-failure resistance.**
The maximum resistance after initial failure; equal to the $R_{res,III}$.

With the help of these concepts, the element safety properties can be further developed.

- **Damage sensitivity Σ .**
Addresses the vulnerability of a glass element to (probabilistically) unconsidered failure causes. As there are many possible failure causes, this is a multi-modal concept that can not be completely quantified. However, it may be possible to identify governing impact types and to define damage sensitivity in terms of the minimum impact of the governing type.
- **Relative resistance r .**
Addresses the formal failure probability. The relative resistance is the ratio between the calculable actions on and resistance of an element (i.e. the inverse of the unity check).
- **Redundancy m .**
Addresses the margin between damage and failure, and failure and collapse. Redundancy is the development of residual resistance over increasing levels of damage from 0 to III (i.e. from the undamaged state over increasing damage to initial failure).
- **Fracture Mode.**
Addresses the injury potential in case of failure. Three different typical fracture patterns a glass element is likely to break into are discerned, similar to the categorization already existent in glass engineering codes: A, B, C.

The Element Safety Diagram (ESD) was introduced to combine the four element safety properties into one clear picture (Figure S.2). A central place is given to the redundancy curve, considered to be the most important safety property, at least from a structural point of view. The time dependency of resistance can be incorporated by adding a third axis, but the use of time tags results in easier readable diagrams.

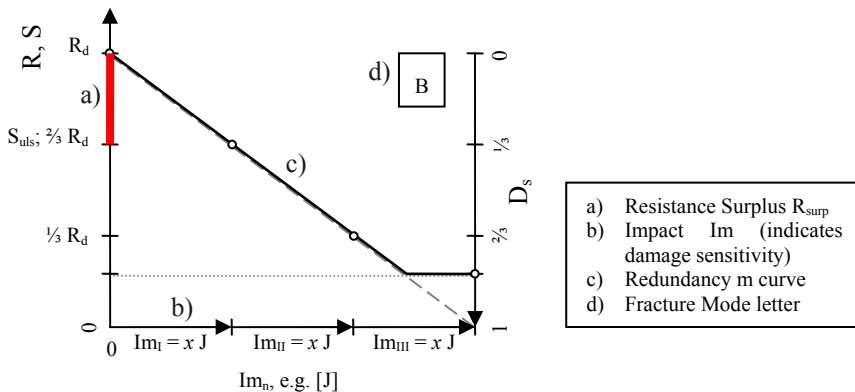


Fig. S.2 Example of an indicative ESD for a three-layer, SG laminated glass beam from annealed glass.

The identification of element safety properties can be used to determine safety requirements for an element for each property. The required resistance can be taken from existing glass and action codes. Damage sensitivity requirements may follow from several codified impact tests. However, further research is required to identify reasonable impact types for different element types, determine which impact types are governing, and what magnitude they may have.

Redundancy requirements are given as residual resistance for a certain period of time at a certain damage level. The survey and interviews have shown the residual resistance requirements are quantified rather arbitrarily e.g. as (a percentage of) the unfactored load. As the unfactored loads are applicable to serviceability limit states rather than ultimate limit states, this is a fundamentally incorrect approach. Rather, it is suggested to use the time correction factor ψ_t and the safety class (and thus the action partial safety factor γ) as instruments to define the required residual resistance levels at damage or failure. Their magnitudes can be decreased for increasing levels of damage and/or decreasing importance of the considered element. The time period for which certain resistances are required should be determined by relevant durations, such as time-to-evacuate, and time-to-support. Their magnitudes may differ per element type and application which makes them project dependent.

If any quantity of post-failure resistance is required, the fracture mode will automatically be B.

Element safety requirements should be diversified per application, depending on the vulnerability of an element and the severity of an eventual collapse. Providing such requirements on scientific grounds requires much more research and could therefore not be incorporated in this study. Nevertheless, a range of example requirements was formulated as well as an example evaluation and redesign of a glass element in a structure.¹²

The development of the Integrated Approach has raised many issues in need of further research, including:

- To determine founded requirements for each element safety property: development of application classes; failure causes in reality; actions and action histories, and correlation between damage and actions.
- For the design of safe glass elements: the relation between physical and structural damage; the relation between design parameters and damage sensitivity; comparative research on different designs for common elements to determine their Element Safety Diagrams; the influence of connection design on failure behaviour.
- For the evaluation of the Integrated Approach as a method, and its development: practicality; expansion of the approach to complete structures; expansion of the approach to include manufacturing and construction processes.
- Other relevant subjects: injury potential of various types of glass elements and shards.

¹² Appendix D.

2.2. Experimental Exploration of the Integrated Approach (Chapter 7)

The Element Safety Diagrams (ESDs) of 14 different glass beam designs were constructed in an attempt to practically evaluate the theoretical Integrated Approach and the ESD as a method to assess structural glass element safety. The beam designs differed by the most common design parameters: double- or triple-layer; annealed, heat strengthened, or thermally tempered; PVB or SentryGlas (SG) laminated. Additionally, two stainless steel reinforced glass beams were tested (bonded with UV-curing adhesive and laminated with SG).

To obtain data for the ESDs, a specific test method was developed.¹³ To construct the redundancy curves, the residual resistance at each model level of damage (0, I, II, III) was determined. For level 0, a direct four-point bending test was applied. For the damage levels I – III, a governing impact type had to be established. A concentrated hard-body impact on the edge of each glass sheet was chosen. A spring-loaded device (Figure S.3) was custom made to apply this kind of impact. Specimens were tested in four-point bending after having been damaged to level I or II in combination with a static load, or to level III without a static load. Figure S.4 shows one of the constructed ESDs.

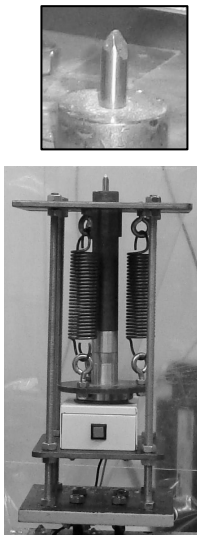


Fig. S.3 Impact device used create model damage levels in glass beams.

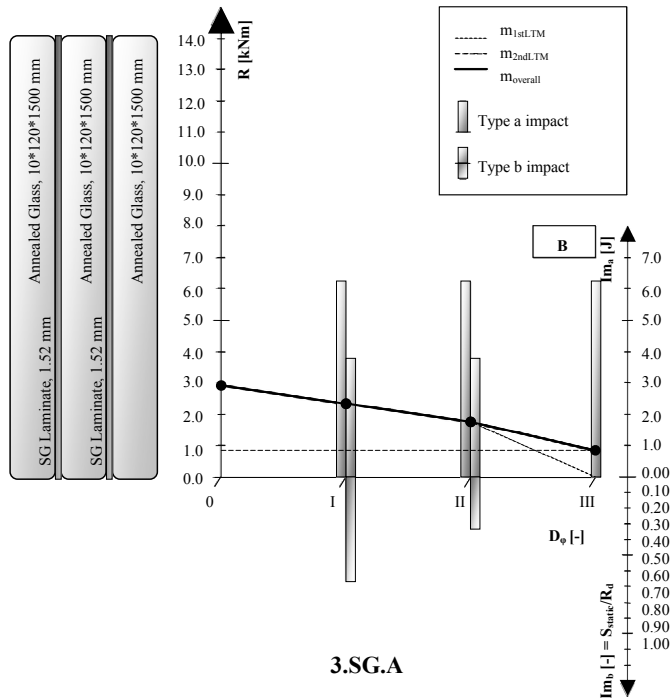


Fig S.4 Element Safety Diagram for triple layer, SG laminated, annealed glass beams.

¹³ Appendix E.

The experiment provided valuable insight into glass beam failure behaviour, showing that:

- The presence of a static load during impact greatly enhances the physical damage caused by that impact.
- In laminated glass beams, the post-failure strength depends on the fracture pattern density, the laminate stiffness and the laminate tensile strength. The former two determine to which extent compressive forces can be build up in the (broken) glass and thereby the type of LTM activated after initial failure.
- As the elastic strain energy released at failure determines the fracture pattern density, it also influences the 2nd LTM. Thus, different test methods which yield varying levels of energy at failure, result in different LTMs and thus differences in post-failure strength.

From the results, ESDs could be constructed, although they have to be interpreted as preliminary as residual resistance values had to be interpolated or deduced from very few experimental data. Besides individual ESDs, the relative redundancy curves were compared in combined diagrams.

The triple layer designs perform much better than the double layer ones. They are harder to damage to failure. The inner layer is well protected by the outer ones. The redundancy of triple layer beams is also much better.

As expected, the safety of the SG laminated beams is significantly higher than of the PVB laminated designs – even though their damage sensitivities are equal. Their safety stems particularly from their post-failure strength, which exceeds that of PVB laminated beams even more than to be expected from the difference in laminate layer thickness and strength; its stiffness allows for a different LTM.

Annealed and heat strengthened glass perform similarly with regard to damage sensitivity from physical impact. However, annealed glass provides higher post-failure strength, both relatively and absolutely. Annealed, PVB laminated beams even have a higher relative post-failure strength r_{III} than heat strengthened, SG laminated ones. On the other hand, heat strengthened glass is more resistant to some other impacts like thermal stress. Thermally tempered glass behaves poorly compared to annealed and heat strengthened glass. Its damage sensitivity from the applied impact is approximately three times as high and it results in less post-failure resistance.

From a safety point of view, the reinforced beams out perform the other designs by far. They pair very low damage sensitivity with very high redundancy. With the resistance of the 2nd LTM consistently above that of the 1st LTM, the amount of damage has practically no influence on the total load carrying capacity. Importantly, this justifies effectively using the *complete* glass section in engineering calculations (without sacrificial layers). SG laminated reinforced beams perform somewhat better than GB368 bonded ones, as they allow for a slightly different 2nd LTM.¹⁴

¹⁴ Appendix I.

The ESD provides a clear overview of the safety properties of a (structural) glass element. Combined with the possibilities to provide it with structural safety prerequisites, swift conclusions with regard to the suitability of a design can be drawn.

Although a number of values can be obtained from deduction and previously published research, the ESDs require a significant amount of experimental data yet unavailable. However, such research would be required anyway if we were to fully understand failure behaviour of glass elements. The introduction of the ESD tool allows the gradual build up of databases of relevant glass element behaviour data that can be presented in a uniform method.

2.3. Designing for Glass Element Safety (Chapter 8)

Although the Integrated Approach does not provide a single definite answer to the question ‘what is structural glass safety?’, it does offer a reasonably objective, clear, quantitative, and opposable method to assess and compare the safety of glass elements. Subsequently, the fundamental design principles and techniques to obtain and optimize the safety performance were investigated per element safety property, on three levels of scale: material, element, and structure.

2.3.1. Relative resistance

Despite the fact that glass failure is not generally caused by the considered actions exceeding the considered resistance, it is obvious that a stronger element (higher relative resistance) is safer than a weaker one. The accuracy of the formal probability analysis therefore does influence the safety of an element. The two common safety enhancing techniques, prestressing and laminating both complicate this problem.

Recent experimental studies have questioned assumptions with regard to prestressing, namely that the prestress can be described by a single value (while in fact it seems to vary at various locations on a glass sheet) and the fact that the resistance of a prestressed element may be described as the sum of an inherent strength and the level of prestress. The complex time and temperature behaviour of laminates makes an accurate failure probability analysis of such elements even more difficult than for single sheet glass.

Improving edge quality has not been found to improve engineering strength as it does not remove the most severe flaws, and thus does not eliminate the low failure strength specimens from a batch.

2.3.2. Damage Sensitivity

Physical damage generally causes, usually by stress concentrations, a reduction in resistance compared to the nominal resistance, i.e. structural damage. It is a diverse phenomenon with many different causes.

Some options to decrease damage sensitivity on material level include the alteration of the chemical composition or microstructure, application of thermal or chemical prestress, the application of coatings, or the use of altogether different transparent materials (polymers). Of these, only the application of prestress is a well-known technique. Its effect on damage sensitivity, however, is ambiguous as it may decrease sensitivity to some impact types (e.g. thermal stress), but increase sensitivity to others (e.g. hard body impact). Alterations in chemical sense require much more research and are not likely to be introduced on commercial scale because of the rigidity of the float

glass manufacturing process. Furthermore, it is questionable whether fundamental differences in safety behaviour could be obtained. Coatings are being applied for purposes other than safety. Their effect may be beneficial, but a local damage to the coating may nullify its effectiveness. Polymers generally suffer from too low Young's moduli and environmental dependencies (temperature and time) rendering them unsuitable for most of the glass applications in construction.

On element level, damage sensitivity may be decreased by laminating. This has been proven to be highly effective, especially when three or more layers are applied. Design measures such as applying receding inner layers or protective covering can also reduce damage sensitivity.

There is a very wide range of possible impacts, of which the relative importance is largely unknown (what impact occurs how often and on which parameters does it depend?). Very little is quantitatively known about the effectiveness of damage decreasing measures. This makes it virtually impossible to develop a general strategy to minimize damage sensitivity. Much more research in this area is required.

2.3.3. Redundancy

Since there can always be unexpected damage causes, optimizing redundancy is the principle approach to provide maximum safety for glass in construction. Two fundamentally different stages were recognized: partial damage ($0 < D_\phi < 1$) and full damage or failure ($D_\phi = 1$). Optimizing redundancy requires different strategies for these two stages.

For the stage of partial damage, the (only) point of interest is the resistance ratios of the undamaged versus the damaged parts at the model (partial) damage levels. By altering these ratios in the direction of more resistance for the undamaged parts, the redundancy may increase.

To obtain post-failure behaviour, a 2nd LTM has to be introduced. There are many ways to incorporate 2nd LTMs into an element. Three starting points govern their design:

- The stiffness of the 2nd LTM is, by definition, lower than that of the 1st LTM.
- Failed glass layers are considered to be broken; broken glass can not carry any tensile loads. Therefore, a complementary component will have to be present to carry the post-failure tensile loads.
- Failed, broken glass layers can still transfer compressive loads.

From these starting points it follows that any glass element with post-failure resistance will have to be a composite. Post-failure resistance may be obtained with several design concepts and manufacturing techniques:

- Laminating.
The post-failure resistance of laminated elements, is highly dependent on load conditions, support conditions, aspect ratio, relative glass sheet thicknesses, glass type, and laminate type. Laminated plates with additional steel mesh or perforated sheet metal achieve very high post-failure resistances.

- Application of additional polymer sheets.
A combination of glass and polymer sheets, either or not laminated together, has seldom been applied. Nevertheless, several studies as well as practical experience has shown favourable post-failure behaviour.
- Reinforcement (beams).
A hitherto rarely in practice applied, but highly effective method of obtaining post-failure strength, is reinforcing beams with a strand of another, stronger and more stiff material. Concepts with two materials, steel and carbon-fibre reinforced polymers (CFRP) have been developed at several institutes and engineering offices
- Hybrid Composite elements.
Several concepts have also been developed that can be described as hybrid between glass and other materials. Contrary to the reinforced concepts (where in the pre-failure state, the glass is primarily responsible for load transfer), the glass and other material work together both before and after failure. Glass-wood, glass-steel, and glass-reinforced concrete hybrids (mostly beams) have been developed.

The one design measure available at structure level to provide redundancy for an element (not necessarily for the complete structure) is to provide alternative load paths. This approach is widely used. It is shown this method can be highly efficient and effective.¹⁵

2.3.4. Comments

With the development of safety enhancing concepts, high post-failure resistance $r_{\text{res,III}}$ is generally aimed at, while minimizing damage sensitivity does not seem of primary concern. However, although many options are available to obtain/increase glass element safety, it is difficult to see how the presented concepts could progress without clear *a priori* performance criteria – which are generally lacking in publications concerning both tried and true techniques and innovative concepts. The integrated approach, provides the opportunity to work towards specific goals.

Usually, predictive models to determine the post-failure resistance of glass elements are not presented. Extensive FE-modeling is used to analyze experimental results, but generally (semi-) static in character. FE-models usually do not take dynamic (energy related) crack growth into account, and therefore only roughly predict post-failure resistance. Further research is required.

2.4. Elastic Strain Energy (Chapter 9)

Several observations in different experiments both within this and other research prompted the hypothesis to be put forward that elastic strain energy release is an important parameter for the determination of post-failure resistance by its influence on the crack pattern density and shock load on tensile components.

When a load is exerted on a linear elastic body, this body will deform proportionally to the load. The amount of work W [$J = 10^3 \text{ Nmm}$] performed by the load is the load-displacement function integrated over the displacement. It is stored in the body as an

¹⁵ Appendix D.

equal amount of elastic strain energy U_ε . The amount of strain energy at a certain point in a body is known as the strain energy density χ [Nmm^{-2}], and the result of integrating the stress at that point over the strain. The total elastic strain energy in the body can thus also be obtained from integrating the strain energy density over the body volume.

Crack growth requires energy to form new surfaces. The surface energy U_γ is provided by the release of strain energy around the growing crack. However, upon glass failure, only a small portion of the elastic strain energy is consumed by crack formation. The rest is dissipated by other forms of energy, most notably kinetic energy.

Experiments¹⁶ on a large series of single sheet, standing, annealed glass beams have shown there is a linear relation between total crack length, the elastic strain energy released at failure, and some geometry parameters, Eq. (1) (Figure S.5). The elastic strain energy cracking constant was found to be $C_{U_{\varepsilon,f}} = 27.1 \text{ m}^2/\text{J}$. Importantly, a similar dependency between total crack length and failure stress (as opposed to total strain energy or strain energy density), was not found.

$$U_{\varepsilon,f} = \frac{A_{fr}}{C_{U_{\varepsilon,f}} h \alpha_{config}} = \frac{A_{fr}}{27.1 \frac{\text{m}^2}{\text{J}} \cdot h \alpha_{config}} \quad (1)$$

With:

- $U_{\varepsilon,f}$ Elastic Strain Energy content at failure [J] = [Nm]
- A_{fr} Crack surface area [mm^2]
- $C_{U_{\varepsilon,f}}$ Elastic Strain Energy Cracking Constant [m^2/J]
- h Beam Height [mm]
- α_{config} Load Configuration Factor [m^{-1}]

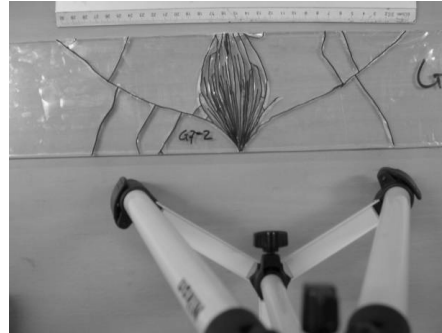


Fig. S.5 Investigation of total fracture surface area in an annealed glass beam tested in 3-point bending.

The results of two experiments were used to assess the actual hypothesis. The differences in failure behaviour between glass beams with varying levels of predamage, also used for the construction of the ESDs in Chapter 7,¹⁷ were analyzed with regard to elastic strain energy release. The failure behaviour of reinforced glass beams with varying strain energy content¹⁸ (by varying the section dimensions so that $W_1 = W_2$, but $I_1 > I_2$) was also compared.

It was concluded that the *external* elastic strain energy release at the moment of initial failure of a glass element, influences the maximum post-failure resistance, in a way that

¹⁶ Appendix G.

¹⁷ Appendix E.

¹⁸ Appendix H.

a release of more energy generally results in less post-failure resistance, either by premature failure of the tensile component as a cause of the shock load or through the extent of crack growth/branching. However, the importance of the extent of crack growth reduces with increasing tensile stiffness of the 2nd LTM. The fracture pattern density may become irrelevant with high tensile stiffness elements, such as steel reinforced glass beams.

It should be noted that because of the geometry dependency of strain energy content, negative scaling effects can be expected when increasing the size of (innovative) elements. Thus, test results on smaller size specimens can not be extrapolated to larger sizes without further consideration.

In order to avoid excessive energy release to induce premature failure or sub standard post-failure resistance, two strategies are basically available. The elastic strain energy content in structural elements at failure can be minimized by:

- Increasing the effective elastic modulus ($E_{\text{eff}} \uparrow$)
- Decreasing the stress ($\sigma \downarrow$), by:
 - Reducing the material failure stress ($\sigma_{\text{max}} \downarrow$),
 - Reducing the external moment ($M \downarrow$),
 - Reducing the external load ($F \downarrow$)
 - Increasing the section surface area or the moment of resistance ($A \uparrow$; $W \uparrow$)

Alternatively or additionally, the effects of energy release can be counteracted through:

- An increase of the fracture toughness of the complementary component – either its material toughness or its geometry (e.g. laminate thickness).
- An increase in stiffness of the 2nd LTM.

2.5. Case Studies Revisited (Chapter 10)

Finally, the All Transparent Pavilion and Transparent Façade Strut designs were re-evaluated using the Integrated Approach and ESD. Where necessary the designs were improved.

For the ATP, an application (waiting room at a bus station) was first defined in order to be able to set safety requirements. Subsequently, for each element the relevant time periods, time correction factors and safety classes for each model damage level were determined. The actions for $D = 0$ were calculated. The governing load cases were established. From the result, the required residual resistances at each model damage level were determined. The resistance and redundancy of each element was then checked.

Indicative governing impacts and damage sensitivity requirements were also formulated, but could not be evaluated as the elements had not been tested to those types of impact. In general, it was not always possible to fully assess the element behaviour as they had not been tested suitably (as the safety requirements had not been clear at the time).

Although the column had shown considerable post-failure strength, it was doubted whether this could be maintained under horizontally orientated impact. Furthermore, the

failure stress was very low. In the main beam, the mid-span section met all requirements. The cantilevers, however, which had suffered premature failure in testing through adhesive failure, had to be reconsidered. In the original design, the maximum tensile stresses in the purlins could appear in the top, for which the reinforcement was not designed. Furthermore, the use of aluminium as reinforcement was not very efficient. Redesigns were proposed for each of these elements.

A similar analysis of the TFS design yielded that it did meet safety requirements. As there were no major technical problems during the prototype manufacturing, the design was left unaltered.

A subtle aspect when formulating the safety requirements is that they should be detached completely from the already developed (preliminary) design. It may be tempting, for instance, with the TFS to estimate the consequence of their collapse as practically zero because the façade panels they support will not collapse when one strut does. In fact, the large façade panels ‘span’ more struts and thus provide an alternative load path for the TFS – and should therefore be assessed as such (whether it provides sufficient redundancy). It should *not* be used as an argument to reduce the safety requirements on the one hand. The consequence class of an element should be determined by the area it supports, not by whether or not alternative load paths are available.

If this trap is sufficiently recognized, the Integrated Approach and ESD provide valuable insight in the failure behaviour required for structural glass elements in certain applications and consequence classes. The designs can be adjusted accordingly.

2.6. Conclusion and Outlook (Chapter 11)

A solely probabilistic approach, in which the material resistance is compared to a limited number of actions, is principally insufficient to determine the safety of glass structures and structural glass elements. In spite of this being generally recognized by glass engineering specialists, this issue is only addressed to a limited extent both in codes and guidelines, as well as in scientific treatises. A comprehensive approach, in which all relevant factors are observed simultaneously, is lacking. Safety requirements are not described in terms of continuous structural performance properties, but merely as single value pass/fail criteria.

The proposed *Integrated Approach to Structural Glass Safety* introduces four element safety properties, with which element behaviour can be characterized and safety can be assessed. The element safety properties can be combined into an *Element Safety Diagram* (ESD).

The Integrated Approach makes it possible to build a body of knowledge on glass element safety by project-independent testing, as well as to compare reasonably objectively between designs and material selections. Furthermore, it allows adjustment of requirements in an easy and insightful way, so that they can be subjected to discussion.

Experimental testing to create ESDs for a range of glass beam designs has shown the presence of a static load during impact greatly enhances the physical damage caused by that impact. Furthermore, in laminated glass beams, the post-failure strength depends on

the fracture pattern density, the laminate stiffness and the laminate tensile strength. The elastic strain energy released at failure, which, among others, depends on the failure cause, determines the post-failure load transfer mechanism (LTM). *Therefore, requirements with regard to residual resistance should be formulated with consideration of the failure cause.*

From a safety point of view, reinforced annealed glass beams perform very well. They pair very low damage sensitivity with very high redundancy. The amount of damage has practically no influence on the total load transfer capacity. Importantly, this justifies effectively using the *complete glass section* in engineering calculations (instead of applying sacrificial sheets).

From an evaluation of common as well as innovative safety enhancing options and their effects on the element safety properties, it may be concluded that increasing redundancy by introducing/improving post-failure LTMs is the most effective strategy.

Elastic strain energy release is an important parameter for the determination of post-failure resistance by its influence on the crack pattern density and shock load on tensile components. Negative scaling effects may be expected when increasing the size of (innovative) elements.

As recent large structural glass projects have shown, it is likely architects and their clients will desire ever more, greater, and more complex glass structures. The Integrated Approach provides a step towards the development of a comprehensive safety method for glass in construction. The next step should be the pilot-application and evaluation by engineers and building authorities in actual structural glass projects.

Further extensive research into failure causes in reality, actions and action histories, and correlation between damage and actions, should facilitate the development of final application classes and safety requirements for structural glass elements.

There will be an increasing demand for project independent data on glass element failure behaviour to allow for a more conscious selection of element designs. Together with universities and/or other research institutes, the glass industry is recommended to instigate an extensive program of glass element testing aimed at failure behaviour, rather than failure stress, to supply these data.

The increasingly daring structural applications of glass will continue to drive the development of structural glass elements with high post-failure resistances, e.g. the reinforced concepts. It is likely such elements will become common place in the coming years. Optimization with regard to structural performance and aesthetical appearance (transparency) may be expected.

In the end, everybody will know about glass: it is transparent ... but it doesn't just break!

Table of Contents

ACKNOWLEDGEMENTS	v
EXTENDED SUMMARY	vii
1. Safety Concepts in Structural Glass Engineering (Chapters 1 – 5).....	vii
1.1. Introduction (Chapter 1).....	vii
1.2. Case Studies (Chapter 2).....	ix
1.2.1. All Transparent Pavilion	ix
1.2.2. Transparent Façade Struts	ix
1.3. Theoretical and Codified Safety Approaches in Structural Engineering (Chapter 3).....	x
1.4. Glass Failure (Chapter 4).....	xi
1.4.1. Fracture Strength.....	xi
1.4.2. Dimensioning Methods for the Application in Building.....	xii
1.4.3. Glass Failure Causes.....	xii
1.4.4. Limitations of a Probabilistic Approach for Structural Glass Engineering.....	xii
1.4.5. Extension of the Probabilistic Approach in Structural Glass Engineering Codes	xiii
1.5. Structural Glass Safety in Practice (Chapter 5).....	xiii
2. Towards an Integrated Approach of Structural Glass Safety (Chapters 6 – 10).....	xiv
2.1. The Integrated Approach to Structural Glass Safety (Chapter 6).....	xiv
2.2. Experimental Exploration of the Integrated Approach (Chapter 7)	xviii
2.3. Designing for Glass Element Safety (Chapter 8).....	xx
2.3.1. Relative resistance	xx
2.3.2. Damage Sensitivity	xx
2.3.3. Redundancy.....	xxi
2.3.4. Comments	xxii
2.4. Elastic Strain Energy (Chapter 9)	xxii
2.5. Case Studies Revisited (Chapter 10).....	xxiv
2.6. Conclusion and Outlook (Chapter 11)	xxv
TABLE OF CONTENTS	xxvii
LIST OF SYMBOLS	xxxix
1. Symbols	xxxix
2. Generally Used Subscripts	xli
3. Abbreviations.....	xli
1 INTRODUCTION	1
1. Two Things	1
2. Research Questions and Objectives, Method and Thesis Outline.....	1
3. Brief History of the Use of Glass in Buildings	4
4. Structural Use of Glass in Buildings.....	11
5. Glass Material Properties	17

5.1. Definition	17
5.2. Silicate glasses; Structure and Composition	19
5.3. Failure Behaviour.....	21
5.4. Overview of Soda-Lime Silicate Glass and Borosilicate Glass Properties	21
6. The Zappi Glass & Transparency research project	21
2 CASE STUDIES.....	25
1. All Transparent Pavilion	25
1.1. Introduction.....	25
1.2. Architectural and Structural Design.....	26
1.3. Safety Approach.....	27
1.3.1. Scale Level of Elements.....	27
1.3.2. Structure level	29
1.4. Individual Members	30
1.4.1. Columns	30
1.4.2. Main Beams	31
1.4.3. Purlins	32
1.5. Realisation	33
1.6. Evaluation and Conclusions of the ATP project	33
2. Transparent Façade Struts	35
2.1. Introduction.....	35
2.2. TFS Design, Safety and Stability Concept.....	35
2.3. Prototype testing	37
2.3.1. Compression Test.....	37
2.3.2. Tensile Test.....	38
2.3.3. Impact and three point bending test	39
2.4. Discussion	41
3. General Discussion and Evaluation of Case-Studies	43
3 THEORETICAL AND CODIFIED SAFETY APPROACHES IN STRUCTURAL ENGINEERING	45
1. Safety and Danger.....	45
2. Risk	46
3. Risk analysis; Cause and Consequence.....	46
4. Probability analysis.....	50
4.1. Variables and Distributions.....	50
4.2. The Reliability Problem of Structural Members: $G(\xi) = R(\xi) - S(\xi)$	52
4.3. Probabilistic Approach in Dutch and European Engineering Codes for the Basis of Design on Structures	53
5. Systems	53
6. General Limitations of the Probabilistic Approach.....	55
7. Extension of the Probabilistic Approach.....	58
7.1. Recognition of Unknown Actions and Measures against Progressive Collapse	58
7.2. Structural Robustness and Other Properties.....	60
7.3. Extension of the Probabilistic Approach in Dutch and European Codes	62
8. Acceptability of Risk	63

4 GLASS FAILURE	65
1. Fracture Strength.....	65
1.1. Fracture Mechanism.....	65
1.1.1. The Strain Energy Release Rate-Criterion to Glass Failure	67
1.1.2. The Stress Intensity-Criterion for Glass Fracture.....	69
1.2. The Problem of Glass Surface Flaws	70
1.2.1. Non-Identical Character of Glass Surface Flaws	70
1.2.2. Non-Static Character of Glass Surface Flaws	71
1.3. Life Time Prediction Models of Glass Surface Flaws	74
1.4. Glass Fracture Strength Scatter.....	74
2. Dimensioning Methods for the Application of Glass in Buildings	75
3. Glass Failure Causes	80
4. Limitations of a Probabilistic Approach for Structural Glass Engineering.....	84
5. Extension of the Probabilistic Approach in Structural Glass Engineering Codes	88
5.1. Discussion of Several Codes and Guidelines	88
5.1.1. NEN 2608, Parts 1 and 2.....	88
5.1.2. NEN 3569	88
5.1.3. Dutch Guideline for Approval of Glass Structures: Constructief Glas, toetsingshulpmiddel voor Bouwtoezichten.....	88
5.1.4. Draft NEN-EN 13474-1	89
5.1.5. Draft DIN 18008, Parts 1 and 2	89
5.1.6. German Technical Guidelines on linear supported glazing (TRLV), point fixed glazing (TRPV), and glazing acting as a barrier (TRAV).....	90
5.1.7. Requirements on Glass Constructions for exemption of Individual Approval and Guidelines for Individual Approval, State of Hessen, Germany	91
5.1.8. German Guideline for Approval of Accessible Glass: DIBt 04.17 Anforderungen an begehbbare Verglasungen; Empfehlungen für das Zustimmungsverfahren	92
5.2. Comments on Impact and Failure Behaviour Related Requirements.....	92
5 STRUCTURAL GLASS SAFETY IN PRACTICE	95
1. Projects.....	95
1.1. Prestressing	97
1.1.1. Thermal	97
1.1.2. Chemical	98
1.2. Laminating	98
1.3. Design Solutions	99
1.4. Innovative and Experimental Safety Enhancing Techniques.....	100
1.5. Remaining Questions.....	106
2. Short Survey on Material and Design Specifications for Structural Glass Components	108
2.1. Questions	108
2.2. Results & Analysis.....	108
2.2.1. Responses.....	108
2.2.2. Question 1: Could you briefly describe your premises with regard to safety, when you're working on a project involving structural glass?	108
2.2.3. Question 2: Consider a GLASS BEAM (span approx. 5 m).....	109
2.2.4. Question 3: Consider a GLASS FAÇADE FIN	110

2.2.5. Question 4: Consider a GLASS FLOOR PANEL.....	110
2.2.6. Question 5: Is there any other comment you would like to add?	111
2.2.7. Conclusions from Survey	111
3. Interviews.....	112
3.1. Finding a useable value for the strength of glass	113
3.2. Thermally prestressed glass: a failed idea of safety?	113
3.3. Failure cases.....	114
3.4. Structural Design and Safety.....	115
3.5. Load, Time and Temperature Requirements.....	117
3.6. Codes and Guidelines	119
3.7. Conclusions from Interviews	120
4. General Conclusions	121
6 AN INTEGRATED APPROACH TO STRUCTURAL GLASS SAFETY.....	123
1. Introduction.....	123
2. Towards an Integrated Safety Approach of Structural Glass	125
2.1. Goal and Prerequisites	125
2.2. Scope.....	125
2.3. Structure.....	127
3. Underlying Concepts for Element Safety Properties	129
3.1. Load Transfer Mechanisms; Primary and Secondary	129
3.2. Initial Failure, Final Failure, and Collapse.....	131
3.3. Damage D	132
3.3.1. Physical Damage D_{ϕ} and Structural Damage D_s	133
3.3.2. Model Levels of Physical Damage $D_{\phi,I}$, $D_{\phi,II}$, $D_{\phi,III}$	135
3.4. Residual Resistance R_{res} and Relative Residual Resistance r_{res}	137
3.5. Impact I_m	138
4. Element Safety Properties.....	138
4.1. Damage Sensitivity Σ and relative damage sensitivity ζ	138
4.2. Relative Resistance r	140
4.3. Overall Redundancy m	141
4.4. Fracture Mode.....	143
4.5. The Glass Element Safety Diagram (ESD).....	143
4.5.1. Incorporating the Time-component.....	145
4.5.2. Incorporating the Temperature-component.....	146
4.6. Alternative Presentations of the Safety Diagram	147
4.6.1. Using a Dimensionless Horizontal Axis	147
4.6.2. Using a Relative Representation of Measures.....	147
4.7. Comments	149
5. Formulating Safety Requirements With the Element Safety Diagram.....	149
5.1. Damage Sensitivity	150
5.2. Resistance	151
5.3. Redundancy.....	152
5.3.1. Time axis demarcations	153
5.3.2. Resistance Axis Demarcations.....	154
5.3.3. Redundancy through Alternative Load Paths.....	159
5.4. Fracture Mode at Failure.....	159
6. Element Categories	159
7. Required Further Research for Finalizing the Integrated Approach	161

7 THE INTEGRATED APPROACH APPLIED TO THE SAFETY ASSESSMENT OF GLASS BEAMS	163
1. Constructing Element Safety Diagrams (ESDs) from Experimental Data	163
2. Absolute ESDs for 14 Glass Beam Designs.....	166
2.1. Impact and Damage Sensitivity	183
2.2. Resistances, Post-failure Strength, and Redundancy Curves	184
2.2.1. Resistances	184
2.2.2. Post-Failure Strength.....	184
2.2.3. Redundancy Curves	186
2.3. Fracture Mode.....	186
3. Relative Overall Redundancy Curves	187
4. Safety Comparison.....	191
5. Evaluation of the ESD as a Tool.....	192
8 DESIGNING FOR GLASS ELEMENT SAFETY.....	195
1. Element Safety Properties and Scale Levels of Approach	195
2. Relative Resistance	196
2.1. Prestressing; Influence on the formal probability analysis.....	197
2.2. Laminating.....	199
2.3. Improving Product Quality	200
3. Damage Sensitivity	201
3.1. Decreasing Damage Sensitivity on Material Level.....	201
3.1.1. Altering the Chemical Composition or Microstructure.....	201
3.1.2. Prestressing	203
3.1.3. Coatings	205
3.1.4. Transparent Polymers	206
3.2. Decreasing Damage Sensitivity on Element Level.....	207
3.2.1. Laminating	207
3.2.2. Design measures	208
3.3. Decreasing Damage Sensitivity on Structure Level.....	208
3.3.1. Compound members	209
3.3.2. Alternative Load Paths.....	210
3.3.3. Specific Design Measures.....	210
3.4. Conclusions with Regard to Minimizing Damage Sensitivity	210
4. Redundancy and Post-Failure Strength.....	210
4.1. Optimizing Redundancy in the Stage of Partial Damage.....	211
4.1.1. Laminating.....	212
4.2. Optimizing Redundancy in the Stage of Full Damage (Generating Post-Failure Resistance); Material Level	212
4.3. Element Level.....	213
4.3.1. Principles of Designing Secondary Load Transfer Mechanisms.....	213
4.3.2. Laminating	216
4.3.3. Additional Transparent Polymer Sheets.....	222
4.3.4. Reinforced Glass Beams	224
4.3.5. Hybrid Elements	229
4.4. Structure Level; Alternative Load Paths	233
5. Comments	234

9 ELASTIC STRAIN ENERGY AND ELEMENT FAILURE BEHAVIOUR..	237
1. Introduction.....	237
2. Elastic Strain Energy and Crack Growth	241
3. Experimental Determination of an Energy Release-Crack Growth Relation.....	243
3.1. Experimental Method.....	244
3.2. Investigated Relations	244
3.3. Results and Discussion.....	244
3.3.1. Energy Dissipation by Crack Growth	245
3.4. Conclusions.....	245
4. Effect of Energy Release on the Failure Behaviour of Glass Beams	246
4.1. Elastic Strain Energy Release and Failure Behaviour of Glass Beams with Different Levels of Damage	246
4.1.1. Double and Triple Layer PVB Laminated Annealed Glass Beams.....	248
4.1.2. Double and Triple Layer PVB Laminated Heat Strengthened Glass Beams	250
4.1.3. Double and Triple Layer PVB Laminated Thermally Tempered Glass Beams	252
4.1.4. Double and Triple Layer SG Laminated Annealed Glass Beams	253
4.1.5. Triple Layer GB368 Bonded, Steel Reinforced, Annealed Glass Beams	253
5. Failure Behaviour of Reinforced Glass Beams with Varying Energy Content ..	253
5.1. Experimental Method.....	254
5.2. Results.....	254
5.3. Discussion	255
6. Conclusions.....	257
7. Relevance.....	258
7.1. Elastic Strain Energy Release and The Effective 2nd LTM.....	259
7.2. Consequences of the Elastic Strain Energy Release Parameter	261
8. Elastic Strain Energy and Structural Design	262
8.1. Minimizing Elastic Strain Energy Content in Structural Elements.....	262
8.2. Reducing the Effects of Strain Energy Release on a Structural Element	265
8.3. Application of Effect-Reducing Measure: SG-Laminated Reinforced Glass Beams	265
10 CASE STUDIES REVISITED	269
1. Introduction.....	269
2. All Transparent Pavilion Revisited	270
2.1. Specification of Use, Load Cases, and Ultimate Limit State Actions	270
2.2. Columns	272
2.2.1. Element Safety Diagram	272
2.2.2. Safety Evaluation of Original Design	276
2.2.3. Redesign.....	278
2.3. Main Beams	279
2.3.1. Element Safety Diagram	279
2.3.2. Safety Evaluation of Original Design	281
2.3.3. Redesign.....	283
2.4. Purlins	285
2.4.1. Element Safety Diagram	285
2.4.2. Safety Evaluation of Original Design	285
2.4.3. Redesign.....	285
3. Transparent Façade Struts Revisited.....	289

3.1. Specification of Use, Load Cases, and Ultimate Limit State Actions, and ESD.....	289
3.2. Safety Evaluation of the Original Design	292
4. Evaluation of ATP en TFS Revisited.....	293
11 CONCLUSIONS AND OUTLOOK.....	295
1. Conclusion	295
2. Outlook	297
12 BIBLIOGRAPHY.....	299
1. Books, Theses, Chapters	299
2. Articles, Papers	301
3. Codes, Guidelines	308
4. Other Documents	310
5. Websites.....	310
6. Illustration Credits	311
13 VEILIGHEIDSCONCEPTEN BIJ HET CONSTRUCTIEF GEBRUIK VAN GLAS - NAAR EEN GEÏNTEGREERDE AANPAK.....	313
Nederlandse samenvatting	313
APPENDIX A CASE STUDIES	317
1. All Transparent Pavilion	317
1.1. Team	317
1.2. Design Stress and Safety Factors	317
1.2.1. Plate bending in roof and façade panels.....	318
1.2.2. Mid-field stress concentrations	318
1.2.3. Bending stresses in glass sheet edges in beams and purlins.....	319
1.2.4. Compression stresses in borosilicate glass columns	319
1.3. Individual Members	320
1.3.1. Columns	320
1.3.2. Main Beams	321
1.3.3. Purlins	323
1.3.4. Roof and Façade Panels	324
1.4. Joints	325
1.4.1. Column to Main Beam.....	325
1.4.2. Main Beam to Purlin	327
1.4.3. Roof to Façade Panel	328
1.5. Realisation	328
1.6. Redesign.....	334
1.6.1. Columns	335
1.6.2. Main beams.....	339
1.6.3. Purlins	343
1.6.4. Roof Plates and Façade Panels.....	343
2. Transparent Façade Struts	347
2.1. Existing façade structure	347
2.2. Transparent Façade Struts Design.....	348
2.2.1. Material Selection	348
2.2.2. Section dimensions and strut head design.....	351

2.3. Conclusions.....	353
-----------------------	-----

APPENDIX B SHORT SURVEY ON MATERIAL AND DESIGN

SPECIFICATIONS IN STRUCTURAL GLASS COMPONENTS	355
1. Introduction.....	355
2. Method.....	356
2.1. Survey questions	356
2.2. Distribution	356
3. Results.....	357
3.1. Respondents	357
3.2. Responses.....	358
3.2.1. Responses to question 1: Could you briefly describe your premises with regard to safety, when you're working on a project involving structural glass?....	358
3.2.2. Responses to question 2: Consider a GLASS BEAM (span approx. 5 m)...	360
3.2.3. To question 3: Consider a GLASS FAÇADE FIN:	364
3.2.4. To question 4: Consider a GLASS FLOOR PANEL	367
3.2.5. To question 5: Is there any other comment you would like to add?.....	371
3.3. Analysis	372
3.3.1. Analysis of Question 1: Could you briefly describe your premises with regard to safety, when you're working on a project involving structural glass?....	372
3.4. Analysis of question 2: Consider a GLASS BEAM (span approx. 5 m).....	372
3.4.1. 2a: How many layers of glass would you prescribe?	372
3.4.2. 2b: What type, if any, of prestressing would you prescribe?	372
3.5. 2c: What kind of laminate material would you prescribe?.....	373
3.5.1. 2d: Would you prescribe any other special measures?.....	373
3.6. Analysis of question 3: Consider a GLASS FAÇADE FIN:.....	374
3.6.1. 3a: How many layers of glass would you prescribe?	374
3.6.2. 3b: What type, if any, of prestressing would you prescribe?	374
3.6.3. 3c: What kind of laminate material would you prescribe?	374
3.6.4. 3d: Would you prescribe any other special measures?.....	374
3.7. Analysis of question 4: Consider a GLASS FLOOR PANEL	374
3.7.1. 4a: How many layers of glass would you prescribe?	374
3.7.2. 4b: What type, if any, of prestressing would you prescribe?	374
3.7.3. 4c: What kind of laminate material would you prescribe?.....	375
3.7.4. 4d: Would you prescribe any other special measures?.....	375
3.8. Analysis of question 5: Is there any other comment you would like to add?..	375
3.9. General.....	375
4. Conclusions.....	377
5. Acknowledgements.....	378

APPENDIX C INTERVIEWS ON STRUCTURAL GLASS AND SAFETY.....379

1. Explanatory Notes to the Interview.....	379
2. Report of the Interview with Rob Nijse.....	382
2.1. Introduction by Interviewer	382
2.2. Background and Experience of the Interviewee.....	382
2.3. Experiences with Structural Glass and General Safety Issues	382
2.3.1. Experiences with failure cases	383
2.3.2. General premises and project specific parameters	384
2.3.3. Residual strength, load and time requirements	384

2.4. Codes and Guidelines	385
2.5. Future Developments	386
2.6. Conclusion	386
3. Report of the Interview with Graham Dodd.....	386
3.1. Introduction by Interviewer	386
3.2. Background and Experience of the Interviewee.....	386
3.3. Experiences with Structural Glass and General Safety Issues	386
3.3.1. General Approach to Safety in Structural Glass Projects	387
3.3.2. Consistency.....	388
3.4. Codes and Guidelines	388
3.5. Future Developments	389
3.6. Other Subjects.....	389
3.7. Conclusion	390
4. Report of the Interview with Tim Macfarlane	390
4.1. Introduction by Interviewer	390
4.2. Background and Experience of the Interviewee.....	390
4.3. Experiences with Structural Glass and General Safety Issues	390
4.3.1. Glass strength.....	391
4.3.2. Thermally tempered glass	392
4.3.3. Design procedure and consistency	392
4.4. Codes and Guidelines	393
4.5. Future Developments	393
4.6. Conclusion	393
5. Report of the Interview with Holger Techen	393
5.1. Introduction by Interviewer	393
5.2. Background and Experience of the Interviewee.....	393
5.3. Experiences with Structural Glass and General Safety Issues	394
5.3.1. General premises.....	394
5.3.2. Time requirements	395
5.3.3. Load requirements	395
5.3.4. Annealed, Heat Strengthened and Thermally Tempered glass.....	395
5.4. Codes and Guidelines	396
5.5. Past and Future Developments.....	396
5.6. Further Subjects	397
5.7. Conclusion	397
6. Report of the Interview with Jens Schneider	397
6.1. Introduction by Interviewer	397
6.2. Background and Experience of the Interviewee.....	397
6.3. Experiences with Structural Glass and General Safety Issues	398
6.3.1. General premises.....	398
6.3.2. Time requirements	398
6.3.3. Temperature requirements	398
6.3.4. DIN 18008 and testing requirements	399
6.3.5. Construction.....	399
6.3.6. Annealed, Heat Strengthened and Thermally Tempered glass.....	399
6.3.7. Residual Strength and Safety Factors.....	400
6.3.8. Structural vs other safety issues	400
7. Report of the Interview with Frank Wellershof	401
7.1. Introduction by Interviewer	401

7.2. Background and Experience of the Interviewee.....	401
7.3. The Allied Irish Bank (AIB), PLC, Bankcentre, Dublin.....	401
7.3.1. Short project description.....	401
7.3.2. The structural analysis report.....	401
7.4. Discussion of the ‘Consequence-based Safety Requirements for Structural Glass Members’, GPD2007 paper by the author.....	403
7.4.1. Time requirement.....	403
7.4.2. Residual strength.....	404
7.5. Conclusion.....	405
APPENDIX D SUGGESTED SAFETY REQUIREMENTS AND EXAMPLE APPLICATION	407
1. Some Suggested Performance Criteria.....	407
1.1. Glass Façade Fin.....	408
1.2. Glass Floor Plate.....	410
1.3. Glass Beam.....	414
2. Example Application of the Integrated Approach and ESD: a Glass Beam	417
2.1. Initial Design.....	417
2.2. Safety Requirements.....	418
2.3. Evaluation of the Initial Design.....	419
2.4. Redesign 1: Three-layer SG Laminate Beam.....	422
2.5. Redesign 2: Alternative Load Path.....	425
APPENDIX E FAILURE BEHAVIOUR OF GLASS BEAMS	429
1. Introduction.....	429
2. Experimental Method.....	430
2.1. Specimens.....	430
2.2. Test Methods.....	433
2.2.1. Direct.....	433
2.2.2. Pre-damaged.....	433
2.2.3. Static and Impact Load.....	435
2.3. Impactor.....	436
3. Results.....	438
3.1. Direct Four-Point Bending Tests.....	438
3.2. Predamaged.....	443
3.3. Static + Impact.....	452
4. Analysis.....	461
4.1. Overview of Resistances per Specimen Type.....	461
4.2. Impact and Damage Sensitivity.....	464
4.3. Load Transfer Mechanisms.....	466
4.3.1. Level I and II Mechanisms.....	466
4.3.2. Level III Mechanisms.....	466
5. Conclusions.....	469
APPENDIX F ELASTIC STRAIN ENERGY	473
1. General Equation.....	473
2. Beam in Three-Point Bending.....	473
2.1. Method 1: From Individual Stress and Strain Components.....	474
2.2. Method 2: From M, κ - and V, η -curves.....	479

2.3. Method 3: From Load Displacement	480
3. Beam in Four-Point Bending	481
3.1. Section I	482
3.2. Section II.....	483
3.3. Total.....	485
3.4. Load Displacement	485
4. Strain Energy Induced by Heat Treatment.....	485
 APPENDIX G EXPERIMENTAL DETERMINATION OF THE RELATION BETWEEN ELASTIC STRAIN ENERGY RELEASE AND CRACK GROWTH IN STANDING, SINGLE SHEET GLASS BEAMS.....	
489	489
1. Introduction.....	489
2. Investigated Relations	490
3. Experimental Method.....	494
4. Results.....	495
5. Discussion	492
5.1. Hypothetical Relations.....	502
5.2. Results for Individual Groups	502
5.3. Influence of added geometry and loading configuration parameters	502
5.4. Specimen Thickness t	503
5.5. Specimen Height h	504
5.6. Specimen Loading Configuration Factor α_{config}	505
5.7. Results for All Specimens.....	506
5.8. Ignored specimens G3-5, G7-3, G7-6	507
5.9. Energy Dissipation by Crack Growth	508
6. Conclusions.....	508
 APPENDIX H COMPARISON BETWEEN FAILURE BEHAVIOUR OF REINFORCED GLASS BEAMS WITH VARYING ELASTIC STRAIN ENERGY CONTENT.....	
511	511
1. Introduction.....	511
2. Experimental Method.....	511
3. Results.....	513
4. Discussion	522
4.1. Theoretical and Experimental Energy Release	525
4.2. Crack Growth.....	527
4.3. Final Failure	528
5. Conclusions.....	528
 APPENDIX I COMPARISON BETWEEN FAILURE BEHAVIOUR OF SG AND GB368 LAMINATED REINFORCED GLASS BEAMS	
537	537
1. Introduction.....	531
2. Experimental Method.....	531
3. Results.....	533
4. Discussion	543
4.1. Failure Behaviour of GB368 Bonded Reinforced Glass Beams	543
4.2. Failure Behaviour of SG Bonded Reinforced Glass Beams.....	544
4.3. Causes for the Differences in Failure Behaviour	547
4.4. Crack Growth Behaviour and Elastic Strain Energy Release	547

5. Conclusions.....548

List of Symbols and Abbreviations

1. Symbols

A	Area	[m ²], [mm ²]
A_{fr}	Fracture surface area	[mm ²]
a	General distance parameter	[m], [mm]
b	General distance parameter	[m], [mm]
D	Damage (Chapter 6, Section 3.3)	
D_s	Structural damage (Chapter 6, Section 3.3.1)	[kN], [N]
D_φ	Physical damage (Chapter 6, Section 3.3.2)	
D_n	Model level of damage, with $n = 0, I, II, III$ (Chapter 6, Section 3.3.3)	
E	Young's modulus of elasticity	[GPa], [MPa]
E_{shear}	Shear modulus	[GPa], [MPa]
F_X(ξ)	Cumulative distribution function of event X as a function of ξ.	
f_X(ξ)	Probability density function of event X as a function of ξ.	
G_C	Critical strain energy release rate, dU_c/dU_a .	
G(ξ)	Probability density function of $S(ξ) ≥ R(ξ)$ (= failure)	[year ⁻¹]
h	Height	[mm]
I	Moment of inertia	[mm ⁴]
Im	Impact	[J], or other
K_{Ic}	Mode I critical stress intensity factor	
k_b	Fracture mode factor	
k_e	Edge quality factor	
k_{mod}	Load duration correction factor	
L, l	Length	[m], [mm]
l_{fr}	Fracture length	[mm]
M	Bending moment	[kNm]
m	Redundancy (Chapter 6, Section 4.3)	
P_X	Probability of event X	
P	Action, Load, as pressure	[kN/m ²]
R	Resistance, Strength	[kN], [N]
R(ξ)	Probability density function of S as a function of ξ	
R_{res,n}	Residual resistance at model damage level n ($= 0, I, II, III$; Chapter 6, Section 3.4)	

x1 |

R_{surp}	Surplus resistance, (Chapter 6, Section 4.2)	[kN], [N]
r	Relative resistance, (Chapter 6, Section 4.2)	
r_{res}	Relative residual resistance, (Chapter 6, Section 3.4)	
S	Action, Load	[kN], [N]
S(ξ)	Probability density function of S as a function of ξ	
S	Action, Load, linearly distributed	[kN/m], [N/mm]
T	Time	[s]
T	Thickness	[mm]
U	Energy	[J = Nm],
U_K	Kinetic energy	[mJ = Nmm]
U_ε	Elastic strain energy	
U_{ε,f}	Elastic strain energy at failure	
U_v	Surface energy	
V	Shear Load	[kN], [N]
v	Speed	[m/s]
W	Moment of resistance	[mm ³]
W_o	Work	[J = Nm]
w	Displacement	[mm]
w₀	Atom equilibrium spacing	[nm]
Y	Stress intensity shape factor	
z	Internal moment arm	[mm]
α_{config}	Loading Configuration Factor (Appendix G, Section 2)	[m ⁻¹]
γ	Safety factor	
ε	Strain	
ε_y	Yield strain (steel, polymers)	
ε_{ult}	Ultimate strain (polymers)	
η	Shear angle	[rad]
Θ	Temperature	[° C]
Θ_g	Glass (transition) temperature	[° C]
κ	Curvature	[rad ⁻¹]
μ	Median value	
ν	Poisson's ratio	
Σ	Damage sensitivity (Chapter 6, Section 4.1.)	
ς	Relative damage sensitivity (Chapter 6, Section 4.1.)	
σ	Stress	[MPa = N/mm ²]
σ_y	Yield stress (steel, polymers)	[MPa = N/mm ²]

σ_{ul}	Ultimate failure stress (polymers)	[MPa = N/mm ²]
σ_f	Fracture stress (glass)	[MPa = N/mm ²]
υ	Fracture surface energy	[J/m ²]
χ	Strain energy density	[J/m ³], [N/mm ²]
ψ	Momentary factor	
ψ_T	Time correction factor	

2. Generally Used Subscripts

d	Calculable, i.e. including safety factors
f	Failure
fr	Fracture
inc	Incidental
ini	Initial
max	Maximum
perm	Permanent
post	Post initial failure
rep	Representative
res	Residual
surp	Surplus
var	Variable
y	Yield

3. Abbreviations

CDF	Cumulative Distribution Function
CFRP	Carbon Fibre Reinforced Polymer
ESD	Element Safety Diagram (Chapter 6, Section 4.5)
LTM	Load Transfer Mechanism (Chapter 6, Section 3.1)
PC	Polycarbonate
PDF	Probability Density Function
PMMA	Polymethylmethacrylate (popularly known as ‘ acrylic ’)
PVB	Polyvinylbutiral
sc	Safety class
SG	SentryGlas
sls	Serviceability limit state
s.w.	Self weight
uls	Ultimate limit state

1 Introduction

This chapter presents the main research questions and objectives of this thesis, as well as an outline per chapter. It goes on to introduce the field of building engineering to which it belongs: that of structural glass. A brief history of the use of glass in buildings concludes with the observation that glass is ever more used in a structural role. The key difficulties of such applications are identified and linked with some characteristic glass material properties. The most important results of the Zappi research project, of which this thesis is a part, are reviewed.

1. Two Things

There are two things everybody knows about glass: it is transparent... and it breaks!

Transparency provides glass with its unique position among building materials. It allows it to both open up and close. It brings light in, but keeps climate out. As a material, it is there and not there at the same time. But glass is hardly ever invisible. It can vary from a subtle presence to an untouchable and impenetrable appearance caused by complete reflection.

In recent decades, architects and structural engineers have sought new and daring applications for glass, further stressing its architectural impact by applying it to the part of the building where we least expect it: the load bearing structure.

Why don't we expect glass in the load bearing structure? Perhaps because of what we also all know: it breaks! Its fragility renders glass the prima donna of all building materials. Complete failure occurs without the slightest warning.

When one studies the properties of glass and the use of glass in building, one soon discovers much needs to be said to nuance both these two common perceptions of glass characteristics. A glass structure is certainly not always the optimum in terms of transparency – high strength, tension loaded steel structures may perform much better in this respect. And it need not be very fragile either.

Nevertheless, it is these two qualities that rightfully draw the attention of those active in the building industry. Transparency is the prime architectural driving force, and fragility a key property making engineers hesitant to apply it quite to the extent architects would like. We are still a long way from using glass as confidently as concrete or steel. How to incorporate safety is the inevitable question when designing a glass structure.

2. Research Questions and Objectives, Method and Thesis Outline

This thesis is part of the Zappi Glass & Transparency research program, running at the TU Delft Faculty of Architecture since 1996. Its main research goal is to develop safe

structural glass elements.¹ However, despite the development of a range of innovative glass element design concepts, within this research group as well as (more recently) at other universities, and the steadily increasing number of realized projects, a proper, preferably quantifiable criterion (or set of criteria) for structural safety of a glass element has never been developed. To go from the contemporary mostly intuitive approach to a rational one, the crucial question both in structural glass engineering in general as in the Zappi research project, is:

What is structural glass safety?

Only when this matter has been resolved satisfactorily, a systematic approach is possible of the obvious follow-up question:

How can it (structural glass safety) be obtained?

It is these two questions that are addressed in this thesis. The subsequent sections of this chapter will provide an introduction into the use of glass in buildings, structural glass, glass material properties and the Zappi research project. In Chapter 2, two case study projects are discussed that specifically gave rise to treating the issues of structural glass safety in this work. They have been reformulated into more specific research objectives so that a matching research approach could be determined.

General research question: **What is structural glass safety?** →

Reformulated research objective: **To suitably define preferably quantifiable criteria to determine the structural risk for various glass applications in building construction.**

In Chapters 3 – 5, existing safety concepts are investigated.

Chapter 3 presents a literature study on safety engineering and safety requirements in general structural engineering codes. The limitations of the most widely used safety concept in structural engineering, the probabilistic approach, are discussed.

Chapter 4 goes on to focus particularly on glass. The theoretical background to glass failure (fracture mechanics, materials science), dimensioning methods, failure causes, and safety requirements in codes and guidelines (additional to probabilistic strength calculation), is critically reviewed. It is concluded that, because of its specific material properties, the limitations that apply to the probabilistic approach in general, apply all the more to structural glass engineering. Additional safety requirements in codes² lack coherence, are not described in terms of structural performance, are insufficiently detailed, and often very general and/or non-quantitative.

In Chapter 5, the attention shifts from theory to practice. Safety measures in realized projects are analyzed. The results of a survey among structural glass engineers

¹ Initially, Zappi was described as ‘a material strong as steel and transparent as glass’. However, later it was acknowledged it is not so much the strength the safety that is the key issue in structural glass engineering.

² Beyond the probabilistically based strength calculations.

regarding design and material specifications are presented. Subsequent interviews with six glass engineers lead to the conclusion that there is no unifying structural glass safety concept and a quantitative elaboration thereof. This is likely to be an important cause of the ongoing debate. It makes it practically impossible to objectively discuss the different views and develop a commonly accepted set of performance requirements.

Therefore, from the analyses presented in the previous chapters, a new approach, the *Integrated Approach to the Safety of Structural Glass*, is developed in Chapter 6. It is based on the introduction of four, rather than one (resistance), element safety properties: *damage sensitivity*, *relative resistance*, *redundancy*, and *fracture mode*. These can be graphically combined into one *Element Safety Diagram* (ESD). A range of underlying concepts is introduced as well.

The Element Safety Diagrams for 14 different glass beam designs are constructed from experimental test data in Chapter 7. The results are then used to discuss and compare the safety of each design, for which it is concluded the Integrated Approach together with the Element Safety Diagram, is a workable method.

Chapters 6 and 7 thus comprise the result of the first research objective. The second research question, reformulated into an objective as below, is treated in Chapters 8 – 10.

General research question: **How to obtain structural glass safety?** →

Reformulated research goal: **To determine the design parameters relevant to minimize structural risk for glass applications in building construction.**

For each element safety property, the effect of common and innovative safety enhancing techniques is extensively discussed in Chapter 8. It is argued the realisation of post-failure resistance through the introduction of secondary load transfer mechanisms is the most fundamental strategy to obtain safety. The principles for incorporating secondary load transfer mechanisms are presented.

One hitherto neglected parameter which partially determines the post-failure capacity, and thus the most important element safety property, is elastic strain energy. Based on experimental research, it is shown in Chapter 9 that energy release can be related to total crack length in a glass beam with the use of some geometrical parameters. Subsequently, drawing upon other elaborate tests, it is proven elastic strain energy release influences both the post-failure compressive capacity through the crack pattern density and the post-failure tensile capacity through shock loading on the tensile component. However, the relevance of elastic strain energy release on post-failure strength decreases with increasing post-failure tensile stiffness of an element.

The second research objective is concluded with a review in Chapter 10 of the case studies presented in Chapter 2. The Integrated Approach is applied to the element design and conclude on their safety. Redesigns are proposed were necessary. Thus, this chapter also serves as a test case for the developed approach in terms of validity and suitability.

Finally, Chapter 11 presents the general conclusions with regard to the research questions and objectives and provides an outlook regarding future developments.

3. Brief History of the Use of Glass in Buildings³

The material we commonly refer to as ‘glass’ was probably discovered, or perhaps we should say invented, over 9000 years ago, judging from glass beads found in the tombs of ancient Egyptian pharaohs⁴. How the discovery of glass came about is not entirely sure. It has been suggested that sea salt (soda, NaCl), bones or shells (lime, CaO) and sand (silicate, SiO₂) underneath fires lit on the beaches of the Mediterranean provided the right mix of ingredients and heat to create drops of soda-lime silicate glass. Nowadays, we know this material for a whole range of applications, but most obviously from containers (bottles) and windows.

Originally glass was used for jewelry; later it was pressed or molded into vessels.⁵ It only made its entrance into buildings after the invention of the glass blowing process, approximately around 100 B.C., when the Romans started to use it in bath houses. Sheets up to about 1 m² could be produced and were coloured greenish blue. At that time, glass was still used sparingly in buildings. Roman architecture did not generally feature glazed windows, partially because the warm climate did not directly call for that.

The subsequent centuries saw a gradual development of glass mixes and manufacturing techniques as well as a geographical spread around Europe. Especially in western and northern Europe, glass was increasingly used for windows. By the end of the first Millennium, there were two techniques in use to create flat glass. The eldest, originating from Syria, the ancient centre of the glass industry, was *spinning*. This involved rapid spinning of the blow pipe in order for the glass bubble to turn into a disc of 600 – 700 mm diameter. The cylinder process on the other hand was based on using several tools to blow a glass cylinder, longitudinally cutting it open and flatten it.

The development of Gothic architecture saw the first surge of glass use in buildings. Contrary to the Roman period which preceded it, Gothic churches featured very slender, minimized structures. Building heights and spans were optimized. The space that became available between the structural elements was filled with stained glass windows of ever increasing size, partially driven by competition between rivaling cities and congregations. These compiled windows of small glass pieces caught in lead framing, could measure several tens of metres in height, including secondary steel and stone supporting structure. The cathedrals of Chartres and Aachen feature famous examples of Gothic stained glass windows (Figures 1.1a and b).

³ The history of the use of glass in buildings has been described to greater or lesser extent in numerous publications. See among others: Nijse, R., Glass in Structures, Birkhäuser, Basel, Switzerland, 2003; or Knaack, Konstruktiver Glasbau 1, Rudolf Müller Verlag, Cologne, Germany, 1998.; or Schittich, C., Glass Construction Manual, 2nd Edition, Birkhäuser, Basel, Switzerland, 2007. An especially elaborate overview is given in Wigginton, M., Glass in Architecture, Phaidon, London, UK, 1996. The brief history presented in this paragraph is based on that publication, unless noted otherwise.

⁴ Shelby, J.E., Introduction to Glass Science and Technology, 2nd Edition, The Royal Society of Chemistry, Cambridge, United Kingdom, 2005, p. 1.

⁵ Doremus, R.H., Glass Science, 2nd Edition, John Wiley & Sons Inc., New York, USA, 1994, p. 2.



Fig. 1.1a and b Stained glass windows in the cathedrals of Chartres (a, left) and Aachen (b, right).

Glass became more and more common during the Renaissance and by end of the seventeenth century it was available for private use for all social classes. Besides improving the spinning and cylinder processes, flat glass was also produced by casting and subsequent grinding and polishing. Sheets up to almost 2 x 3 m² became available in the late 1800's.

A radical breakthrough occurred with the development of conservatories. Using glass protection to grow plants out of season dates back as far as 2000 years (to the Romans), but complete conservatories depending on the greenhouse effect were developed from the mid sixteenth century onwards, both to grow out of season and to conserve exotic plants from the colonies of European countries. Conservatory construction reached an aesthetical peak in the nineteenth century, as orangeries⁶ had become fashionable with wealthy private patrons who were the clients before botanical gardens were socially funded. Many astonishing examples can still be found, especially in the UK (Figures 1.2a, b, c). Not only did they instigate a new kind of architectural expression, they also brought structural innovations: to get as much light in as possible, the number of structural frame members was minimized and stability was obtained by in-plane action in the glass sheets.

The emergence of these structures was facilitated by the development of cast iron. The technique of iron frames and glass cladding was also applied to new building types which followed from the industrial revolution, such as railway stations and factory halls.

⁶ Orangeries are conservatories meant specifically for orange trees.

The most well-known example of this new architectural type is probably the Crystal Palace (Figure 1.3), designed by Joseph Paxton and built in Hyde Park, London. The initially accepted brick and iron design for this exhibition hall by Brunel was cancelled. The commission was granted to Paxton instead since his scheme was not only much cheaper, but also showed much more potential that it would actually be built in time for the London World Exhibition of 1851. Chrystal Palace consisted entirely of off-the-shelf designs and products, which allowed the over 70 000 m² building featuring almost 84 000 m² of glass to be built in nine months. After the Exhibition, Crystal Palace was demounted and rebuilt at an even larger scale in Sydenham. Unfortunately, fire destroyed the new Palace in 1936.



Fig. 1.2a, b, c Some highlights of 19th century conservatory construction in the UK: Palm House, Bickton, Devon, 1820 – 1840 (a, left); Temperate House, Royal Botanical Gardens, Kew, London, 1860 (b, top right); Palm House, Royal Botanical Gardens, Kew, London, 1845 - 1848 (c, bottom right).

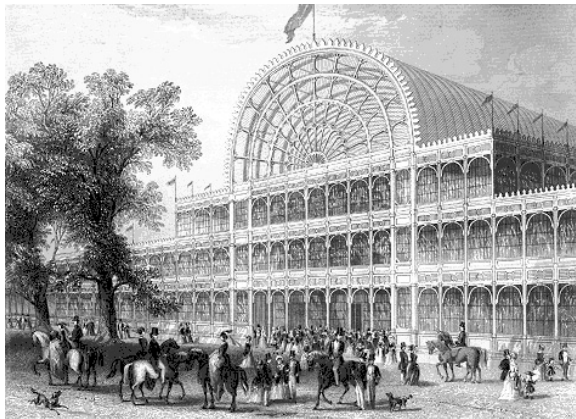


Fig. 1.3 Crystal Palace, London, 1851.

During the nineteenth century there was much debate on the architectural qualities of the new glass and iron building types. Generally, the new language of form and materials was rejected by the architecture establishment which, being in a neo-classical phase, focussed on the compositional rules of the Renaissance. Nevertheless, the possibilities of glazed cast iron frames gradually conquered the built environment, appearing in shops, offices and housing from the second half of the nineteenth century onwards.



Fig. 1.4 Mies van der Rohe's design for a completely glazed skyscraper, 1922, Friedrichstrasse, Berlin, Germany.

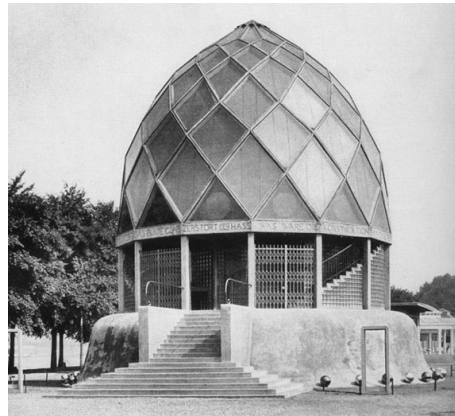


Fig. 1.5a Werkbund Pavilion, architectural design by Walter Gropius and Adolf Meyer, 1914, Cologne, Germany.



Fig. 1.5b Van Nelle factory, architectural design by Brinkman en van der Vlugt, 1927-1929, Rotterdam, the Netherlands.



Fig. 1.5c Sanatorium Zonnestraal, architectural design by Jan Duiker, Bernard Bijvoet, and Jan Gerko Wiebenga, 1928, Hilversum, the Netherlands.

It was not until the early twentieth century though, with the rise of the Modern Movement, that technological breakthroughs in the production of iron, reinforced concrete and glass became the leading means in architectural theory. The development of trains, cars and airplanes quickly changed the people's perspective of time and distance and brought a spirit of progression and a fascination with machines. In architecture, it led to a machine induced aesthetic. In his influential book

Glasmarchitektur⁷, Paul Scheerbart thrusts glass into the most important material in architecture because of its ability to open up the hitherto enclosed spaces in which people spend most of their time. He claimed only thus society could hope to raise its culture to a higher level. Through its transparency, glass was symbolically strongly related to openness. Especially dissolving the closed corner by applying glass, was a powerful new architectural instrument creating new character for built spaces. Many designs appeared with complete glass claddings, such as the famous glass clad skyscraper design by Mies van der Rohe (1922, never built, Figure 1.4), exploring the aesthetical possibilities of glass. Examples which *have* been constructed include the Werkbund Pavilion, the van Nelle factory, and the Sanatorium Zonnestraal⁸ (Figures 1.5a, b, c).

Even today, symbolism often plays an important role in the application of glass. The glass dome over the new Reichstag (Figure 1.6) in Berlin not only serves to bring light into the parliament meeting room, but also serves as a sign of transparency and democracy after decades of communism. Glass façades cover the Bibliotheque National (Figure 1.7) in Paris to symbolize the accessibility of knowledge – even though from a perspective of book preservation, this is far from logical.



Fig. 1.6 Reichstag renovation and extension, architectural design by Norman Foster & partners, 1999, Berlin, Germany. Interior view of the glass covered dome, on the left part of the Reichstag building, on the right a view over Berlin city. The mirror clad pillar in the centre reflects daylight into the main meeting room of the German parliament.

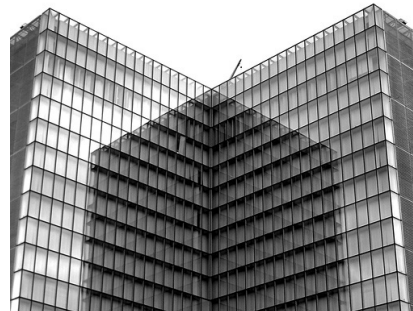


Fig. 1.7 Bibliotheque National, architectural design by Jean Nouvel, 1996, Paris, France (detail of façade).

The development of iron-glass façades starting in the mid-1800's, increased the pressure on glass manufacturers to produce higher quality glass (less distortions, constant thickness) at a lower price. By the start of the twentieth century, this resulted in the first mechanical, mass production methods for flat glass, such as the Fourcault (1914 Belgium, Figure 1.8), Pittsburgh (1921 USA) and Colburn/Libbey-Owens (1915 USA, 1923 Belgium, Figure 1.9) processes. These all featured pulling a continuous ribbon of viscous flat glass from a molten glass bath. The latter produced the best results as it did

⁷ Scheerbart, P., *Glasmarchitektur*, Germany, 1914.

⁸ Off course, the use of glass was not just symbolical, but also brought real improvements in the indoor environment. Nevertheless, symbolism was an important driving force to get the use of glass to the level it obtained.

not pull the ribbon vertically all the way, but rather bent it by 90° to become horizontal about 75 cm above the glass bath. This allowed more constant thickness and better annealing, thus avoiding uncontrolled thermal residual stress.

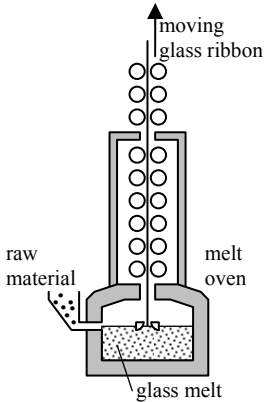


Fig. 1.8 Fourcault process (simplified).

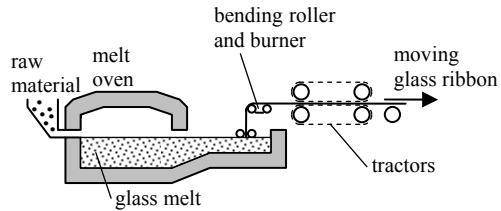


Fig. 1.9 Colburn/Libbey-Owens process (simplified).

However, all these processes were swiftly swiped off the market with the introduction of the float glass process by Pilkington in 1959 (Figure 1.10) – still the primary flat glass production process today. Rather than pulling glass out of a bath of molten glass vertically, it is poured on another bath of molten tin on which it floats perfectly, without mixing. From the tin bath, the glass ribbon goes into an annealing lehr and is finally cut to size. The standard maximum trade sizes has been 6.00 x 3.21 m² for decades, but possibilities of obtaining greater lengths are increasing. Compared to the earlier processes, the float process gives high quality flat glass with a constant thickness at a very low price.

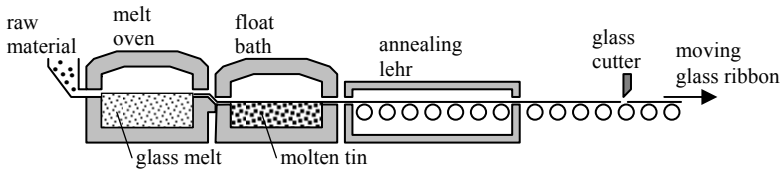


Fig. 1.10 Float glass process (simplified).

Coloured and tinted glass became en vogue after WO II, especially to clad large office buildings and high rise towers with curtain wall façades. It was used to reduce glare and solar heat gain, but often also because of its glamorous appearance. At first, the glass itself was coloured by adding various metaloxides to the glass mix. The Seagram Building⁹ (Figure 1.11) in New York is a famous example of the use of mass tinted glass. Mies van der Rohe chose the glass colour to harmonize with the colour of the framing and spandrels.

⁹ Design by L. Mies van der Rohe, 1954-1958, New York, USA.

When float glass put cast glass out of business, however, mass tinted glass largely disappeared as it was no longer commercially possible to custom produce tinted glass. Instead, metaloxide coatings were devised. These had a much higher reflectivity and were often referred to as ‘mirror glass’. Countless buildings have been clad with these bronze, green and blue glasses in the 1960’s, 70’s, and 80’s.

The disadvantage of these early coatings was that they blocked light primarily in the range of visible wavelengths, while at the same time not being hugely effective in blocking heat radiation. Thus the spaces behind them became gloomy. Furthermore, their appearance, which was initially conceived as glamorous, changed to an image of impersonality and unpleasantness (perhaps also because it became associated with the poor indoor climates in general, e.g. ‘sick buildings’).

Fortunately, technological developments hugely improved the appearance and performance of coatings. More coating techniques and coating materials became available, coating layers got much thinner, and it became possible to superpose coatings on one another to create custom light and heat transmittance behaviour. The last two decades saw the development of colourless coatings that can transmit large amounts of visible light while simultaneously blocking most heat gain.



Fig. 1.11 Seagram Building, architectural design by Mies van der Rohe, 1954-1958, New York, USA.



Fig. 1.12a and b Two examples of the use of curved and bended glass: Curved glass wall in the Casa de Música, architectural design by OMA, glass design by ABT, 2005, Porto, Portugal (a, top); Double curved glass cladding of the Lentille St. Lazare subway entrance, architectural design by A.R.T.E. Jean-Marie Charpentier & Associés, glass design by RFR, 2003, Paris, France (b, bottom).

Significant development has also been made in the field of insulated glazing by the appearance of triple glazing and gas filled cavities. Current developments include vacuum insulated panels capable of reaching even higher insulation values. The thermal performance of glazing profiles has also been improved hugely by the introduction of thermal bridge interrupters. Together, these developments nowadays allow the design of practically completely transparent buildings which can still maintain contemporary indoor environment standards.

Besides completely glazed, transparent façades and structural uses, the application of curved and bended glass, either through hot or cold deformation, is one of the most important developments in the use of glass in buildings today (Figures 1.12a and b). A range of production techniques already exists.¹⁰ The increasing popularity of non-orthogonal architecture forms a powerful driving force.

4. Structural Use of Glass in Buildings

With the exception of the greenhouses, glass was not used in load bearing building structures until some sixty years ago. It transferred external actions (most notably wind) to the substructure, but did not carry any parts of the building except itself. This changed in the 1950's. Basically, two lines in the development of the structural use of glass can be discerned:

- The development of linear structural glass members loaded in bending and/or compression.
- The development of in-plane bearing glass sheets in façades, first loaded in tension later also compression.



Fig. 1.13 Exposition pavilion by Glasbau Hahn firm, 1950's.

¹⁰ An overview of production methods and some example applications can be found in Bos, F.P., *Maak een buiging, het warm en koud vervormen van glas*, DAX, nr. 10, October 2006.

The first line of development starts with the construction of adhesively bonded all glass (temporary) pavilion structures by the German Glasbau Hahn firm in the 1950's (Figure 1.13). These remarkable structures particularly served to convey the ability of the company to manufacture high quality, fully transparent showcases for museums, etc. The possibilities of structural glass inspired Norman Foster to apply glass fins in two permanent projects. Both in the Willis Faber Dumas office building (1975, Figure 1.14) and the Sainsbury Centre for Visual Arts (1978, Figure 1.15), these fins act as (cantilevering) beams carrying actions through bending and providing lateral stiffness to the glass façade. In the façade itself, mullions are replaced by silicone sealed joints, thus minimising the lining around the edges of the glass sheets and optimising surface smoothness.



Fig. 1.14 Willis Corroon (originally Willis Faber Dumas) office building, architectural design by Norman Foster & Partners, glass design by Anthony Hunt Associates, 1975, Ipswich, UK.



Fig. 1.15a and b Sainsbury Centre for Visual Arts. Outside view of the glass façade, and inside close-up with glass fins. Architectural design by Norman Foster & Partners, glass design by Anthony Hunt Associates, 1978, Norwich, UK.

The Louvre extension¹¹ of 1991 features an early application of glass roof beams, engineered by RFR. Much of the pioneer work was done from the second half of the eighties onwards by Rob Nijse¹² and Tim Macfarlane¹³. From 1989, Tim Macfarlane developed a series of over 30 glass staircases with architect Eva Jiricna (Figure 1.16). He also pioneered on joining glass columns and beams by splice joints in two projects featuring half-portals: the Keats Grove private house extension in Hampstead, London (1992, Figure 1.17) and the Broadfield House Glass Museum extension¹⁴ in Kent (1994). In 1997 he took structural glass to a new level by designing the Yurakucho glass canopy (Figure 1.18), cantilevering some 9 m over the entrance to a subway station. A more complex beam-column structure followed with the glass reading room of the Arab Urban Development Institute (1998, Figure 1.19).

¹¹ Architectural design by I.M. Pei, structural glass design by RFR, 1991, Paris, France.

¹² For ABT in Velp, the Netherlands.

¹³ Dewhurst Macfarlane & partners, London, UK.

¹⁴ Architectural design by Design Antenna, 1994, Dudley West, Midlands, UK.



Fig. 1.16 Joseph store staircase, architectural design by Eva Jiricna, glass design by Tim Macfarlane, 1989, London, UK.



Fig. 1.17 Extension to a private house in Keats Grove, architectural design by Rick Mathers, glass design by Tim Macfarlane, 1992, London, UK.



Fig. 1.18 Yurakucho canopy, architectural design by Rafael Viñoly, glass design by Tim Macfarlane, 1997, Tokio, Japan.



Fig. 1.19 Reading room of the Arab Urban Development Institute, architectural design by Nabil Fanous Architects, glass design by Tim Macfarlane, 1998, Riyadh, Saudi Arabia.

Nijsse used flat glass columns as early as 1986 in a temporary exhibition structure, the Sonsbeek Pavilion (Figure 1.20). Half-portals consisting of a beam and a column connected by a splice joint were the load carrying elements in a small private conservatory (2002, Figure 1.21a, b). Several covered glass bridges (Figures 1.22 and 1.23) featuring glass beams carrying the bridge floor and load bearing walls for the roof, have also been engineered by Nijsse. The first one was to connect office spaces in two adjacent buildings for architects firm Kraaijvanger Urbis in 1994.

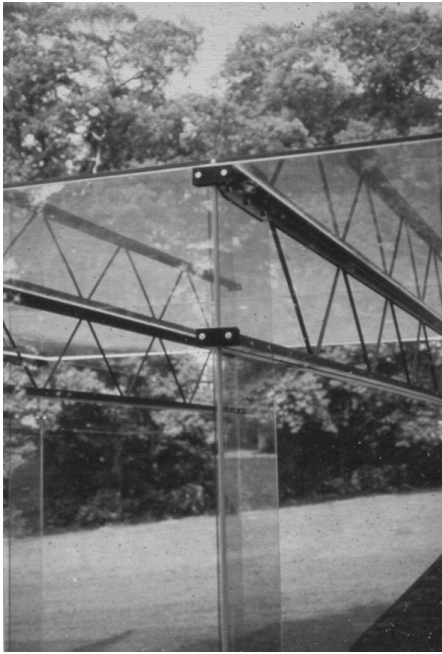


Fig. 1.20 Sonsbeek Pavilion (detail of the joint between the glass column and the steel truss), architectural design by Benthem & Crouwel, glass design by Rob Nijssse and Michel Maarschalkerwaard (ABT), 1986, Arnhem, the Netherlands.



Fig. 1.21 a, b Private conservatory, architectural design by B&D Architecten, glass design by Rob Nijssse (ABT), 2002, Leiden, the Netherlands.



Fig. 1.22 Glass bridge, architectural design by Dirk-Jan Postel (Kraaijvanger Urbis), glass design by Rob Nijssse (ABT), 1994, Rotterdam, the Netherlands.



Fig. 1.23 brug arnhem: Glass bridge with stairs, architectural design by Wiegierck Architecten, glass design by Rob Nijssse (ABT), 1996, Arnhem the Netherlands.

The other line of development starts with the iconic cable-stayed hanging facades of the Serres of the National Museum of Science, Technology and Industry in the Parc de la Villette in Paris¹⁵ (Figure 1.24). Peter Rice, as the structural engineer, co-founded RFR based on this project. Instead of connecting each glass panel directly to the substructure

¹⁵ This project has been described extensively in: Rice, P. Dutton, H., *Structural Glass*, E&FN Spon, London, UK, 1995.

to transfer vertical forces, the glass panels are hung from each other and connected to the substructure only once every four panels. Thus the upper panels carry the dead load of the lower ones. Only the horizontal (wind) loads on the glass panels are carried directly to a cable-stayed substructure. The panels were connected by four point-fixings, one in each corner. Because the behaviour of structurally used glass was only known to a limited extent and the stress distributions around the holes were hard to determine precisely¹⁶, the steel joint pieces were elaborately designed making sure they would not induce any bending moment in the glass. One joint piece got four legs connecting four panels in their corners to one point of the substructure. This later became the prototypical ‘spider-joint’. The advantage was that if a top panel would break, the panels directly underneath would be carried by the neighbouring panels instead of falling down with the top one. The principle of the hanging façade with glass carrying dead load in plane and a substructure carrying wind loads has been copied countless times over the last two decades. An early application in the Netherlands was the hanging facades of the AGA-music room in the Berlage Exchange, Figure 1.25.



Fig. 1.24 Serres of the National Museum of Science, Technology and Industry in the Parc de la Villette, architectural design by Adrien Fainsilber, structural glass design by RFR, 1986, Paris, France.



Fig. 1.25 Hanging glass façade of the AGA Music Room in the Berlage Exchange. Architectural design by Pieter Zaanen and Mick Eekhout, structural design and construction by Octatube, 1990, Amsterdam, the Netherlands.

In the last 10 to 15 years, there has been a slow, but steady increase of structural glass projects by a variety of engineers and architects, both in the bending and in-plane loaded applications. There is a definite tendency to stretch the possibilities of structural glass ever further. Float glass is now available in lengths up to 12 m from some plants. Large hanging façades, such as the 24 m atrium façade of 50 Avenue Montaigne, Paris (1993), have been realized. At 16 m, Glasgow now boasts the world’s longest glass beams in the atrium roof of the Wolfson Building (2002, Figure 1.26). New York hosts

¹⁶ This was before FE-analysis became common practice.

the impressive $10 \times 10 \times 10 \text{ m}^3$ glass cube entrance to an underground Apple store on 5th Avenue (2006, Figure 1.27).



Fig. 1.26 Atrium roof of the Wolfson Building, architectural design by Reich and Hall, glass design by Arup, 2002, Glasgow, UK.



Fig. 1.27 Glass cube over the entrance to the Apple Store on 5th Avenue, architectural design by Bohlin Cywinski Jackson, glass design by Eckersley O'Callaghan, 2006, New York, USA.

Glass is, in itself, a material which is unsafe to use in structural applications. This hampers the development of glass structures. Although ‘structural glass’ is actually a broad term used for any glass application from four sided supported glass floor panels to complex column-beam glass structures, the safety problems are generally the same:

- The strength of an individual piece of glass is difficult to predict with a satisfying degree of certainty. Equal individual sheets from the same batch may still show strength values varying as much as a factor 2 or more.
- Glass gives no warning signal before breaking and tends to break completely once a crack has started.

Furthermore, glass not only yields structural safety problems, the shards are also a direct risk for personal injury as they are so sharp they can cause dangerous cuts much more easily than bits of other materials.¹⁷

Two standard solutions, taken from the car industry, are commonly applied to avoid personal injury and excessive structural damage: tempering and laminating. During thermal tempering, glass is heated to approximately $150 \text{ }^\circ\text{C}$ above the glass transition temperature¹⁸, causing it to become viscous. Subsequently, it is then quenched by blowing cool air onto the surface. This causes the outer layer to solidify without shrinking. The inner layer cools more slowly and (tries to) shrink normally, putting the outer layer in compression while ending up in tension itself. The resulting residual stress follows a parabolic shape over the glass thickness. The amount of prestress

¹⁷ These safety problems of glass will be elaborated in Chapter 3, along with a diversification of the term ‘structural glass’.

¹⁸ The glass transition temperature Θ_g for soda-lime silicate glass is around $545 \text{ }^\circ\text{C}$. This concept is further explained in Section 5 of this chapter.

obtainable is thus dependent on the sheet thickness. Thin glass ($\leq 4\text{mm}$) is very hard to temper.

This technique is used to increase the practical strength of the glass piece (the outer compression has to be overcome before breakage) and decrease the sensitivity to several common failure causes such as thermal breakage and peak stresses. Furthermore, for a long time the common perception has been that the small fragments into which thermally tempered glass breaks, are relatively harmless. More recently however, awareness is growing that glass treated this way does not necessarily disintegrate immediately, but may do so only after contact with another object on which it may be falling, thus still causing considerable injury.

The other solution is laminating two or more glass sheets together with polymer resin or sheet materials. By far the most common laminating material is polyvinylbutiral foil (PVB). Under elevated temperature and pressure, this foil is bonded to glass sheets in autoclaves. The material has little strength and stiffness of its own. It is mainly used to avoid glass shards from coming off and usually relies on the load carrying capacity of some unbroken glass sheets for residual strength.

Over the last decade, several innovations have been developed that can provide more residual strength to structural glass. They include the introduction of stiff and strong foils as well as reinforcement techniques and will be discussed in Chapter 8.

5. Glass Material Properties

5.1. Definition

The cause of the structural problems of glass lies in its material properties. To understand the properties of glass, it is imperative to know about their molecular composition and microstructure.

What is glass? The material we commonly refer to as ‘glass’ is actually a specific type of glass, more accurately described as soda-lime silicate glass. The term ‘glass’, when used in materials science, is a description of the state of the microstructure of a material, rather than of its composition. Doremus¹⁹ defines a glass as follows:

Glass is an amorphous solid.

Thus, with the term ‘glass’ a solid state material is described, i.e. a material which does not flow when subjected to moderate forces. Doremus quantifies a solid as a material with a viscosity of more than approximately 10^{15} P^{20} . The popular belief that window glass is actually an extremely high viscous fluid is therefore false; the molecules in a glass can not flow.

‘Amorphous’ means there is no long range regularity in the arrangement of molecular constituents. Contrary to most solids, a glass does not have a crystalline structure in which molecular groups are ordered in a repetitive way. If a solid is created by cooling

¹⁹ Doremus, R.H., *Glass science, 2nd Edition*, John Wiley & Sons Inc., New York, USA, 1994, p. 1.

²⁰ Poise; $10^{15} \text{ P} = 0.1 \cdot 10^{18} \text{ mPa}\cdot\text{s}$.

from a liquid state, the creation of a crystalline network is dependent on the cooling rate. Materials forming crystalline solids do so because they can form crystals very quickly, faster than they usually cool down and freeze (i.e. stop moving). Vice versa, materials forming glasses do so because their crystal forming process is too slow to create a crystalline structure before they freeze. Thus it is possible to create crystalline solids by extremely slow cooling of materials normally producing glasses, just as it is also possible to create glass versions by rapid cooling of materials that normally make crystalline solids. This has been applied in the production of metallic glasses which are used for a variety of applications such as (high-end) sportswear, toughened consumer electronics and coatings on industrial machinery, because of their high wear and tear resistance, tensile strength²¹, and shaping possibilities (like other glasses they have a glass transition range before becoming fluid).

The lack of a crystal structure results in a relatively high volume and enthalpy²² at a certain temperature, compared to crystalline solids. These properties can be plotted versus temperature in a graph (Figure 1.28)²³.

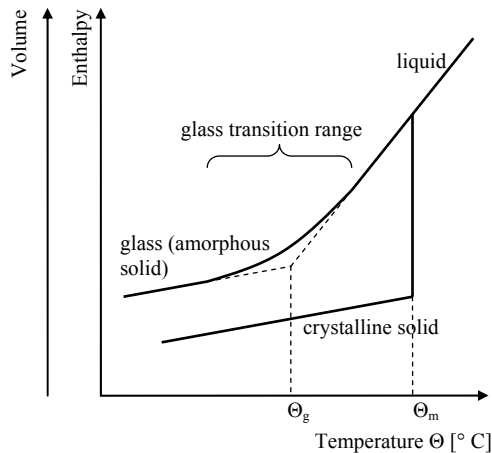


Fig. 1.28 Volume and enthalpy versus temperature for glass and crystalline materials.

In this graph, another difference between glasses and crystalline solids also becomes clear. Where crystalline solids exhibit a clear melting point at which the volume instantly decreases due to crystallization, glasses show a transition range in which the manoeuvrability of molecules relative to each other gradually decreases over a range of decreasing temperature, until the glass solidifies. This range is called the *glass transition range*. This zone between solid state and full fluidity is used in several

²¹ Their failure behaviour, however, is brittle. Also note that these glasses are not transparent.

²² 'In thermodynamics and molecular chemistry, the **enthalpy** or **heat content** (denoted as H , h , or rarely as χ) is a quotient or description of thermodynamic potential of a system, which can be used to calculate the "useful" work obtainable from a closed thermodynamic system under constant pressure and entropy.' www.wikipedia.org, dd 09-06-2008.

²³ According to Shelby, the choice of ordinate is somewhat arbitrary, as volume and enthalpy behave similarly. Shelby, J.E., *Ibid*, p. 3.

important glass treatment processes such as thermal tempering, hot-shaping (bending) and welding.

Because it is convenient to be able to use a single value to define the transition behaviour of a glass, the *glass temperature* Θ_g has been introduced. This is the temperature at which the linear volume-temperature curves from beneath and above the transition range would intersect. Although this gives some indication of the temperature at which glass transition occurs, it provides no definite data on the size of the glass transition range.

With the additional properties *strain point* and *softening point*, respectively indicating the lower and upper end of the glass transition range, a more complete picture of the glass transition range is obtained. However, as the glass transition range also depends on the cooling rate, none of these properties are true glass-specific material properties.

Because all glasses exhibit glass transition behaviour, Shelby²⁴ expands Doremus' definition:

A glass is an amorphous solid completely lacking in long range, periodic atomic structure, and exhibiting a region of glass transformation behaviour.

Some other definitions have been proposed, such as:

Glass is a frozen, super cooled melt.²⁵

or:

Glass is an inorganic product of fusion which has been cooled to a rigid condition without crystallisation.²⁶

Although these definitions are more specific and describe most common glasses well, they are not completely correct as they ignore some less common manufacturing methods such as sintering, as well as the fact that glasses, theoretically, can be produced from any material.

5.2. Silicate glasses; Structure and Composition

With considerable margin, soda-lime silicate glass is the eldest glass mankind produces. It belongs to the family of silicate glasses. These glasses consist for over 70% of siliciumdioxide (SiO_2), which forms tetrahedra building blocks with a silicium atom in the middle and four oxide atoms at the corners (Figure 1.29). Each of the corner oxide

²⁴ Shelby, J.E., *Ibid*, p. 3. His definition seems considerably longer than that of Doremus, but that is caused by the somewhat superfluous explanation of 'amorphous' as '...completely lacking in long range, periodic atomic structure...'

²⁵ Original German definition: 'Glas ist eine eingefrorene unterkühlte Schmelze'. Frischat, Günther-Heinz, *Glas – Struktur und Eigenschaften*. In: Lohmeyer, S., *Werkstoff Glas I: Sachgerechte Auswahl, optimaler Einsatz, Gestaltung und Pflege*, 2. Aufl., Ehningen bei Böblingen: expert Verlag, 1987. Translation into English by the author.

²⁶ American Society for Testing of Materials, *ASTM Standards for Glass*, as quoted in: Doremus, R.H., *Ibid*.

atoms can connect to other silicium atoms, to simultaneously become part of two tetrahedras. Silicate glasses are thus built from regular groups in the extremely short range. Irregularity is introduced by varying Si-O-Si bond angles as well as rotations between neighbouring tetrahedras (Figure 1.30).

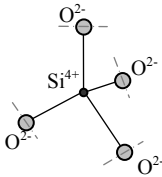


Fig. 1.29 The building blocks for silicate glasses: tetrahedras of four oxide atoms and one silicium atom. The O^{2-} connect to other Si^{4+} .

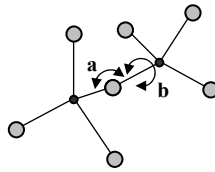


Fig. 1.30 The irregularity of the structure in silicate glasses stems from **a**) varying Si-O-Si bond angles and **b**) rotations between neighbouring tetrahedras.

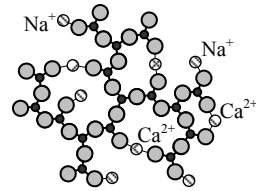


Fig. 1.31 Soda and lime disrupt the silicate network which therefore becomes less dense (schematic 2d representation).

Although by definition glasses do not possess a regular long range molecule structure, two pieces of glass will behave similarly. Therefore, their structures must be similar in some fashion. Shelby²⁷ remarks that although several structural models have been proposed, such as the microcrystal model, the crystallite model and models based on random network theory, none of these succeeds in explaining all experimental data. They should therefore be used with caution and awareness of their limitations.

Vitreous silicate glass (also called fused silica or quartz) consists almost solely out of siliciumdioxide. Thus there is relatively much possibility for oxide atoms to connect to silicium atoms, leading to a high density network. This in turn results in a high glass transition temperature and a highly viscous melt. The glass transition temperature can be significantly reduced by introducing salts and oxide additives, such as soda (natriumchloride, NaCl) and lime (calciumoxide, CaO) in soda-lime silicate glass. The soda and calcium atoms also connect to the oxide atoms, thus less oxide atoms are available to form a network with silicium atoms (Figure 1.31).

With additives, some important characteristics of silicate glasses can be influenced significantly. The composition of some glasses is shown in Fig. 1.32. Vitreous silica (quartz) is difficult and expensive to produce because of its high working temperatures ($\Theta_g = 1082\text{ }^\circ\text{C}$). It is valued for its extremely low thermal expansion coefficient and high chemical resistance and used in high end applications such as laboratory ware and light guides. Borosilicate glass has similar advantages over soda-lime silicate glass, although not to the same extent. Its thermal expansion is three times as low as that of soda-lime silicate glass, but still six times as high as that of quartz. In price, it is also between these two extremes. It finds a wide range of applications from (laboratory) containers to lamps to kitchen utensils. Lead glasses can be used for radiation shielding. Soda-lime silicate glass is by far the most common. All flat glass you see in buildings and cars is soda-lime silicate glass, as is the glass used in bottles, vases and other containers and the glass in most ordinary lamps.

²⁷ Shelby, J.E., *Ibid*, pp. 72-74.

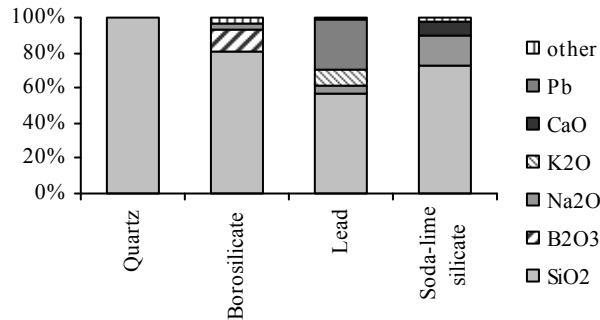


Fig. 1.32 Composition of some silicate glasses.²⁸

Borosilicate glass is the only other glass which, besides soda-lime silicate glass, appears in this research. It has been applied in the Transparent Façade Struts case study (Chapter 2.2) for glass tubes because, contrary to soda-lime silicate glass, its low thermal expansion coefficient allows it to be welded and hot-shaped.²⁹ But all other glass used and discussed in this research is soda-lime silicate glass. For easy reading, soda-lime silicate glass is simply referred to as ‘glass’, unless noted otherwise.

5.3. Failure Behaviour

Despite its linear elastic stress-strain behaviour, glass failure is a complex phenomenon, to which Chapter 4 is entirely devoted.

5.4. Overview of Soda-Lime Silicate Glass and Borosilicate Glass Properties

The material properties of soda-lime silicate glass and borosilicate glass vary somewhat depending on the source you consult. This is due to the complexity of the material behaviour (Chapter 4). Tables 1.1a and b list some relevant properties as found in various sources.

6. The Zappi Glass & Transparency research project

The notion of ‘Zappi’ was introduced at the faculty of Architecture of the Delft University of Technology in 1992 as the name of a new, conceptual transparent sheet material that could be used for structural purposes.³⁰

²⁸ Stacked column charts based on Wigginton, M., *Ibid*, p. 242. The subsequently listed uses of these types of glasses are taken from the same source. The composition of soda-lime silicate glass is codified in NEN-EN 572-1 (SiO₂ 69 – 74 %; CaO 5 – 14 %; Na₂O 10 – 16 %; MgO 0 – 6 %; Al₂O₃ 0 – 6 %; Others 0 – 5 %). Borosilicate glass composition is codified in NEN-EN 1748-1-1 (SiO₂ 70 – 87 %; B₂O₃ 7 – 15 %; Na₂O 0 – 8 %; K₂O 0 – 8 %; Al₂O₃ 0 – 8 %; Others 0 – 8 %).

²⁹ It therefore also features in supporting research into glass welding presented in *AdDoc III: Welding and Hot-Shaping Borosilicate Glass Tubes; Possibilities, Strength and Reliability*, additional document to this PhD, www.glass.bk.tudelft.nl.

³⁰ An extensive overview of the results of the Zappi Glass & Transparency research project in the period before the start of this thesis, was written by the author, but never formally published. This report, *AdDoc I: Zappi, 1996 – February 2004*, can be found on the website of the research group, www.bk.tudelft.nl/glass, as an additional document to this thesis.

Table 1.1a Selection of soda-lime silicate glass material properties according to various sources.

Property	Symbol	Soda-lime silicate glass			Dimension
		Source 1*	Source 2**	Source 3***	
Density	ρ	2500 – 2535	2500	2490 - 2500	kg/m ³
Young's Modulus	E	68 – 72	70	50 - 74	GPa
Poisson's Ratio	ν	0.22 – 0.24	0.2	n/a	-
Tensile Strength	σ_t	31 – 35	n/a	n/a	MPa
Compressive Strength	σ_c	360 – 420	n/a	n/a	MPa
Bending Strength	σ_b	31 – 35	45	42 - 50	MPa
Fracture Toughness	K_{Ic}	0.55 – 0.7	n/a	n/a	MPa·√m
Glass Temperature	Θ_g	441.9 – 591.9	n/a	720 – 735	°C
Thermal Exp. Coef.	α	8.5 – 9.5	9	7.9 – 8.5	10 ⁻⁶ ·°C

* Granta Design Limited, CES Edupack 2007, version 4.7.0.

** Nederlands Normalisatie Instituut, NEN-EN 572-1:2004 Glas voor gebouwen - Basisproducten van natronkalkglas - Deel 1: Definities en algemene fysische en mechanische eigenschappen, Delft, the Netherlands, 2004.

*** www.matbase.com

Table 1.1b Selection of borosilicate glass material properties according to various sources.

Property	Symbol	Borosilicate glass			Dimension
		Source 1*	Source 2**	Source 3***	
Density	ρ	2200 – 2300	2200 – 2500	2230	kg/m ³
Young's Modulus	E	70 – 76	60 – 70	63	GPa
Poisson's Ratio	ν	0.19 – 0.21	0.2	0.2	-
Tensile Strength	σ_t	22 – 32	n/a	n/a	MPa
Compressive Strength	σ_c	264 – 384	n/a	n/a	MPa
Bending Strength	σ_b	20 – 29.09	45	n/a	MPa
Fracture Toughness	K_{Ic}	0.5 – 0.7	n/a	0.77	MPa·√m
Glass Temperature	Θ_g	449.9 – 601.9	n/a	530	°C
Thermal Exp. Coef.	α	3.2 – 4	3.1 – 6.0	3.25	10 ⁻⁶ ·°C

* Granta Design Limited, CES Edupack 2007, version 4.7.0, Database Architecture & Structural Sections.

** Nederlands Normalisatie Instituut, NEN-EN 1748-1-1 Glas voor gebouwen – Bijzondere basisproducten - Borosilicaatglas - Deel 1-1: Definitie en algemene fysische en mechanische eigenschappen, Delft, the Netherlands, 2004.

*** www.matweb.com (Schott Borofloat).

Actual preliminary research started in 1995 and resulted in an internal memo by Veer in May 1996.³¹ This memo aimed both at a more clearly defined research problem by investigating the limitations of current transparent sheet materials for building structures, and at the theoretical exploration of a number of principally different conceptual solutions. Considering the available time and financial frame, as well as the theoretically possible material properties, the concept of a composite laminate consisting of layers of chemically toughened glass segments and continuous polycarbonate foils was chosen as a starting point for the Zappi Glass & Transparency research project. This concept is based on combining the positive qualities of existing materials, in this case joining the bending stiffness of glass with the ductility of polymers. More accurately, the addition of polycarbonate provides the laminate with:

- A micro scale crack bridge which will allow the glass around a single crack to keep transferring forces. Thus local failure within the glass will not lead to global failure of the structural component.
- A macro scale crack bridge, i.e.: a constituent to carry tensile forces (at large strains) after multiple cracks have appeared in the glass.
- A constituent to dissipate fracture energy by deformation thereby stopping or retarding crack growth.
- A constituent to redistribute peak stresses thus increasing shock damage resistance.

This concept was first tested on beams in 1997 (Figure 1.33a and b), followed by plates in 1998. Especially for plates, the glass-polycarbonate laminate worked very well. Investigations into Zappi plates were therefore limited. Glass-polycarbonate laminate beams posed more problems, and were thus subjected to more extensive research. After several years of development, the 50% drop between peak- and residual strength of the Zappi beams remained a crucial problem, which prompted the introduction of a minimal amount of stainless steel to the design of the section. This second generation design gave very promising results and is currently in the final stages of development.³²

In 1998, the development of transparent structural columns was also started. Because columns mainly carry compressive loads instead of bending forces, the design was completely different. It consisted of an outer and an inner tubular glass column with a cavity filled with a cast resin. The glass carries the loads, the resin only holds the glass together after the growth of cracks has started, thereby ensuring that the glass will keep transferring the compressive forces that are exerted on it. In compression testing, stresses of over 450 MPa were reached, before specimens failed by buckling. However, it proved very difficult to obtain a bubble free cast resin. In 2004, van Nieuwenhuijzen³³ developed a production method with which such defects could be avoided.

As is clear from the development of columns, beams and plates, Zappi is not so much a defined material, but the notion of a variable complex composite, the design of which is governed by its desired application as a structural component and anticipated force flow. In other words, a Zappi beam, loaded with bending moment and shear forces, will be

³¹ Veer, F.A., *The Limitations of Current Transparent Sheet Material in Buildings*, internal memo (unpublished), TU Delft, the Netherlands, 1996.

³² Ph.D. research by P.C. Louter, completion expected in 2010.

³³ Nieuwenhuijzen, E.J. van, Bos, F.P., Veer, F.A., *The Laminated Glass Column*, Proceedings of the 9th Glass Performance Days, Tampere, Finland, June 2005.

completely different from a Zappi column, which is loaded by compression and prone to buckling. This characteristic of variability meant that the various studies within the Zappi project were directly linked to specific structural components. Starting with the beams, the project spread like a tree to form a family of Zappi structural components. The beam and plate were followed by a column, various joints and specific building units like a door, a staircase, a dome, a folded plate shell, a 3D-lattice and an integrated façade system.

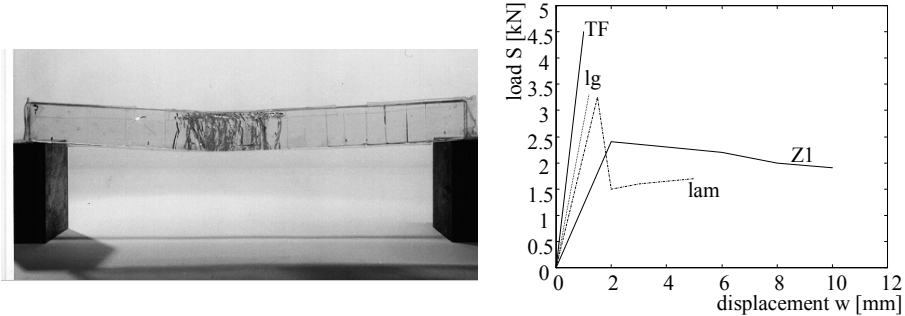


Fig. 1.33a, b From the first generation of Zappi beams (1997): a 40 cm long glass-PC laminate after a four-point bending test (a, left) and its load-displacement graph (b, right, Z1 curve).

To support the development of the various composites, research was also conducted into the (structural) properties of the separate materials that are used in Zappi, i.e. glass, polymers and adhesives. Besides investigating structural aspects, several subjects of building physics, like acoustics and thermal conductivity, were also treated. However, these subjects fall outside the scope of this dissertation.

Up until now, the Zappi project has had a predominantly qualitative character. Research concentrated on the testing of principals (does this work or does it not?), mainly by experimental testing of prototypes. This gave very valuable insight into the possibilities of Zappi composites. It also produced numerical data about the loads Zappi elements could carry. However, for the time being, it led only to tentative material properties. During the Zappi project, increasing use of computational modelling has been made. With a complex finite element model including an algorithm for smeared cracking, produced with the FEM programme DIANA, it was possible to describe the behaviour of a first generation Zappi beam with sufficient accuracy. However, there is by no means a readily available method to model various Zappi composites which will reliably predict the structural response.

By the end of 2003, the Zappi research was at a cross-roads. There were several options with respect to the direction subsequent research should take, but their relative importance and relevance was unclear. The All Transparent Pavilion project, which beheld designing and building an all glass pavilion with Zappi concept members, provided opportunity not only to investigate numerous problems related to combining existing concepts into one structure, but even more importantly to determine the research focus for the following years.

2 Case Studies

Two case study projects are being presented: the All Transparent Pavilion (ATP) and the Transparent Façade Struts (TFS). Design considerations, experimental research and construction are presented briefly. It is explained how these projects gave rise to the research questions already introduced in the Chapter 1 (Section 2): ‘what is safe failure behaviour?’ and ‘how can that be obtained?’, and thus formed the direct occasion for this thesis.

1. All Transparent Pavilion

1.1. Introduction

By the beginning of 2004, the Zappi research program had progressed to a stage in which several design concepts for individual structural glass components with safe failure behaviour had been presented. Their conceptual validity had been proven in varying level of detail. The primary concepts were:

- Stainless Steel Reinforced Glass Beams,
- Resin Laminated Tubular Glass Columns,
- The Use of Transparent Polymers for Mechanical Joints,
- The Use of Adhesives for Chemical Joints.¹

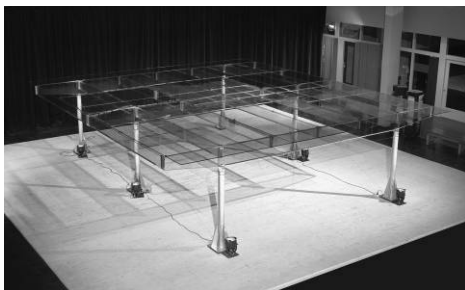


Fig. 2.1 Roof Structure of the All Transparent Pavilion.



Fig. 2.2 Transparent Façade Strut in an extension of the TU Delft Architecture Faculty (impression).

Zappi seemed ready for a next step in the research, from single components to integrated structures. With the All Transparent Pavilion (ATP) project, which ran from March until December 2004, the Zappi Glass & Transparency Research Group aimed at realizing for the first time a structure of considerable size.

The ATP project investigated the possibilities to integrate the developed concepts into one structure, but, more importantly, it served to provide direction to the subsequent

¹ Refer to *AdDoc I: Zappi, 1996 – February 2004*, additional document to this thesis, www.bk.tudelft.nl/glass, for an extensive overview of these and other concepts developed in the Zappi research, as well as literature references.

research by revealing the fundamental bottlenecks in designing such structures. Section 1 of Appendix A provides additional information on the ATP project.

1.2. Architectural and Structural Design

The pavilion design consists of a relatively simple box of four 9 m long, 3.6 m high walls in a square. The roof panels cantilever 30 cm on each side. Three π -shaped portals make up the vertical load carrying structure (Figures 2.3a – d). Each portal (Figure 2.4) is made up out of two glass columns of 1.5 m high on a steel footing and one main beam, which has a mid-span of 4.8 m and cantilevers 1.2 m to both sides. The portals stand at 3.6 m centre distance and are connected to each other by a two sets of seven purlins. Except for the columns, which are made of borosilicate glass, only ordinary annealed float glass was used.

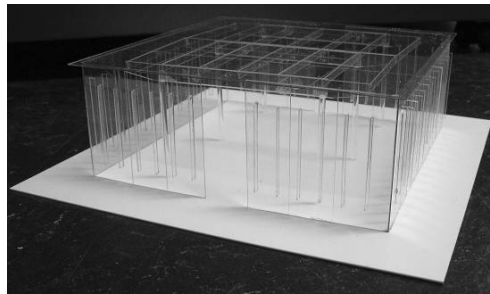


Fig. 2.3a Model of the All Transparent Pavilion design.

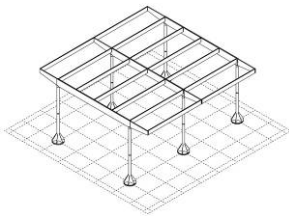


Fig. 2.3b Main load bearing structure: three π -shaped portals connected by purlins.

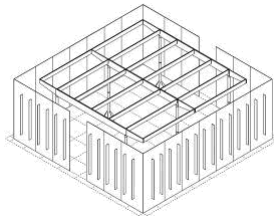


Fig. 2.3c Façade panels with glued on fins.

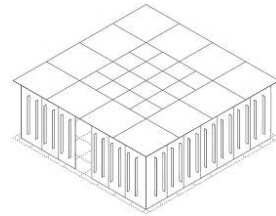


Fig. 2.3d The roof panel layout.

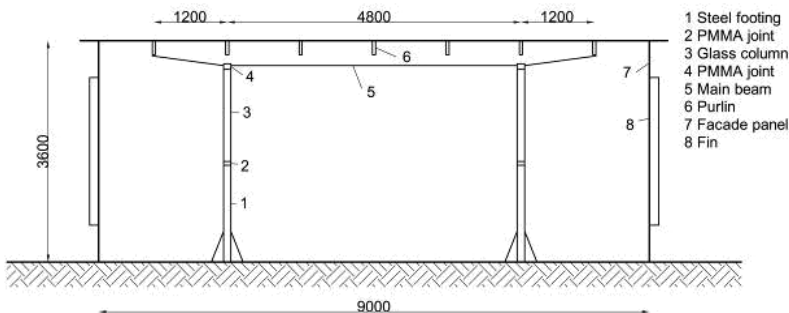


Fig. 2.4 Elevation of a π -portal.

The overall stability of the pavilion is provided by the façade walls. This separation of the portals in structural function was underlined by making them appear to be standing free. The walls are composed of 1.5 and 1.2 m wide and 3.6 m high panes. A very minimal joint connects them to the roof panels and thereby to the rest of the structure. Glued on fins limit bending under wind loading. This allows the façade panes to be only 2 x 8 mm thick. The fins are positioned where they are most effective, i.e. in the mid area of the panel. By not touching the ground or the roof, a lot of problematic joints were avoided.

Twelve large sheets of 2.4 x 2.4 m at the edges and sixteen smaller panes of 1.2 x 1.2 m in the centre, all 2 x 6 mm thick, make up the roof. The smaller plates were chosen for practical mounting purposes.

By connecting the purlins rigidly to the main beams, the latter are prevented from tilting. The column-main beam joint was specifically designed not to perform this function as it might introduce bending in the top of the column.

1.3. Safety Approach

The safety approach that was adopted for the ATP was based on two strategies. On the scale level of elements, a margin between initial failure and collapse is aimed at. For the level of the complete structure, the principle that a local damage (element failure) should not result excessive (global) failure is maintained.

1.3.1. Scale Level of Elements

There are several techniques that are commonly adopted to obtain safety in structural glass elements:

- Thermal prestressing (strengthening or tempering). The failure stress is increased while the sensitivity to certain common failure causes such as thermal breakage is decreased.²
- Laminating, commonly with PVB foil.
- Dimensioning with high safety factors.
- Applying sacrificial sheets.

Basically, these techniques are based on the same concept – although this is hardly ever explicitly formulated in publications. This concept assumes that safety is guaranteed by the fact that there is always at least a part of glass that is never broken and that this part is dimensioned so that it will be able to carry the applied loads on its own. To put it in terms of a load-displacement graph (Figure 2.5): this concept hypothesizes that the maximum load of the component is never reached.^{3,4}

² A thermally prestressed glass sheet may become more sensitive to some other failure causes like Nickel Sulfide inclusions and (edge) scratching.

³ The resistance of PVB itself is small and usually neglected. Extensive discussion on the failure behaviour of laminated glass beams in Chapter 7, based on experimental research presented in Appendix E, as well as literature review of tested laminated glass plates (Chapter 8, Section 4.3.2) show this should be nuanced somewhat. In cooperation with broken glass, PVB can provide a small amount of residual resistance, depending on glass type, geometry, loading configuration, etc.

⁴ The development of newer, stiffer interlayer foils like DuPont's SentryGlas (SG) may alter this significantly. Residual strength of SG laminated components seems possible, even when all the glass sheets of a laminate have been broken, especially when the foil is loaded in in-plane stress. If such a laminate is used in a beam

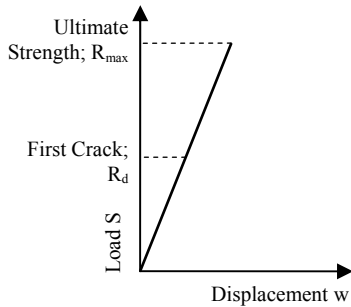


Fig. 2.5 Failure behaviour as it commonly designed in glass structural components. It is assumed that F_{\max} will never be reached.

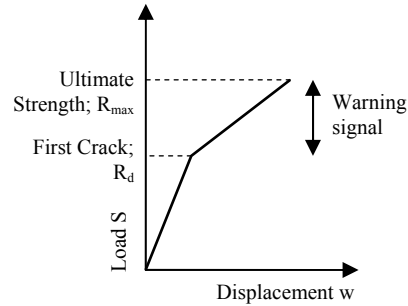


Fig. 2.6 Failure behaviour of transparent Zappi components. By combining materials into composites, a yielding behaviour can be obtained.

The Zappi research project adopts a different safety philosophy. By developing composites of glass and other materials such as plastics, adhesives, resins and stainless steel, a failure behaviour similar to yielding is aimed at (Figure 2.6). It is actually the safety principle applied in all other common structural materials, like steel and reinforced concrete: at some point a maximum load is reached, and then there remains a safety margin in which the material starts to seriously deform, thereby giving off a warning signal.

In general, a yielding-like failure behaviour is reached by making the failure process gradual instead of sudden. Of course, the glass itself does not yield, but similar behaviour can be obtained by allowing it to slowly crumble under an increasing load.⁵

A consequence of the adoption of this strategy was that thermally tempered glass could not be applied. When it breaks, it shatters into very small pieces (often referred to as ‘dice’; Figure 2.7). It was assumed that with such a fracture pattern, no integrity can remain after breakage.⁶ Instead, ordinary annealed glass was to be used as its fracture pattern (Figure 2.8) still allows to transfer (compressive) forces – especially through overlapping sheets.

(with the glass standing on its side), structurally it should come close to the concept of a glass-PC laminate, presented by Veer et al. in 1997: Veer, F.A.; Liebergen, M.A.C. van; Vries, S. de, *Designing and engineering transparent building components with high residual strength*, Proceedings 5th Glass Processing Days, Tampere, Finland, June 1997.

⁵ Previous results of the Zappi research program indicated, though not proved conclusively, that, for two reasons, crumbling can only occur if the energy release during failure is limited. The correlation between elastic strain energy release and post-failure behaviour is extensively discussed (and proven) in Chapter 9.

⁶ There are, however, now some indications the stiffness of the tensile component after failure mainly determines the influence of the fracture pattern density on post-failure resistance. This was shown by experiments presented in Appendix E. As the reinforced beams have relatively very stiff tensile components (i.e. small steel sections), their post-failure behaviour may not depend as much on the glass heat treatment as previously expected.

This implied that pin joints in drilled holes could not be used, as this would lead to unacceptable stress concentration.⁷ Therefore, the design only contained surface- and line-shaped connections.

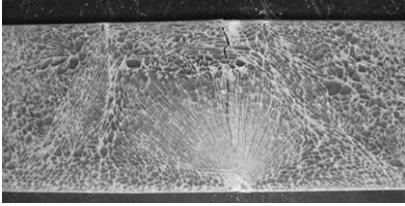


Fig. 2.7 Cracking pattern in tempered glass.

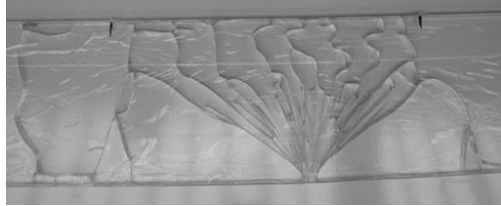


Fig. 2.8 Cracking pattern in annealed glass.

1.3.2. Structure level

Four strategies on structure level were identified in order to ensure a local failure does not result in excessive damage to the structure:

- Providing alternative load paths, for example by having components span more than one field or the interconnection of multiple components.
- Loading structures in compression rather than tension (stacking components instead of hanging them; i.e. using gravity to keep components in place).
- Designing hyperstatic structures (like three dimensional lattices), thus ensuring that the failure of a single component or a limited amount of components does not lead to global instability and complete structural failure.
- Providing back-up in joints.

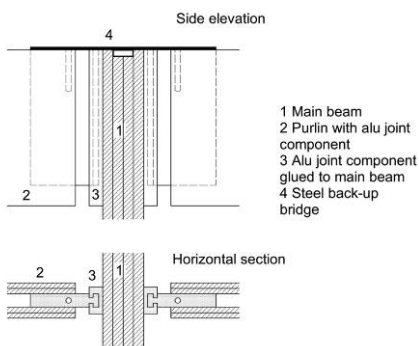


Fig. 2.9 Main beam to purlin-joint.



Fig. 2.10 A steel bridge over the main beam serves as a back-up for the adhesive bond between the aluminium joint component and the glass.

⁷ That was common perception at the time of the ATP project. An unpublished FE-parameter study indicated pin-joints may be feasible if combined with friction or for in-plane bending applications, e.g. beams (some results were used in Chapter 10, Section 2.3.2). See also, for instance, Callewaert, D., Belis, J., Impe, R. van, Lagae, G., Beule, M. de, *Glued and preloaded bolted connections for laminated float glass*, Proceedings of the 10th Glass Performance Days, Tampere, Finland, June 2007.

Most of these strategies have been applied in the ATP design. The grid of the façade is shifted 60 cm to that of the roof (Figure 2.3d). The roof panels therefore always rest on more than one façade panel, thus ensuring that the failure of one façade panel will not cause a roof panel to come falling down. The large roof panels themselves always span two fields, so even in case of complete failure of one purlin, the roof panel will remain in place. Furthermore, the joints between the main beams and the purlins are provided with a back-up (Figures 2.9 and 2.10)⁸. Finally, the main beams are stacked on the columns.

1.4. Individual Members

1.4.1. Columns⁹

The design of the columns had to meet strict requirements for transparency, strength and safety. During previous Zappi research, a concept had been developed of tubular glass columns consisting of two glass tubes laminated together with a clear resin.¹⁰ It assumes the resin to slow down crack growth and keep the fragments of broken glass together, thereby allowing them to keep transferring compressive loads. This concept had been tested and shown to work on small scale specimens and was consequently also adopted for the ATP columns. A custom manufacturing process was developed by van Nieuwenhuijzen¹¹ to ensure defect free curing in full size elements. In experimental compression tests (Figure 2.11), post-failure strengths of over 300 % were found (Table 2.1).

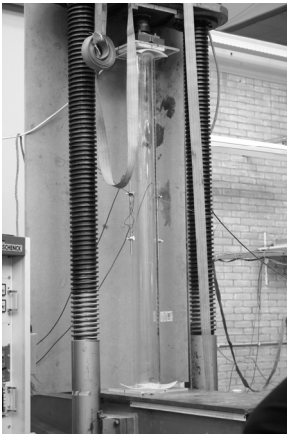


Fig. 2.11 ATP Column prototype during compression test.

Table 2.1 Results of compression tests on several ATP column prototypes.

Prototype	$R_{\max,ini}$ [kN]	$R_{\max,post}$ [kN]	$r_{res,III}^*$
1.2m column	73	146	200 %
1.5m column 1	61	196	321 %
1.5m column 2	40	137	343 %

* relative residual strength at initial failure (= model damage level III, see Chapter 6, Section 3.4) = $R_{\max,post} / R_{\max,ini}$ · 100%.

⁸ The connection primarily depends on the adhesive bond between the aluminium component and the glass to transfer moment and thereby ensure the rigidity of the main beam-purlin grid. However, if this layer would fail, a steel strip which goes over the main beam will keep the purlin hanging in place. It will not provide the same contribution to the stability, but as there are seven purlins connected to the main beam, this should not be an immediate problem.

⁹ An extensive discussion on the column design, manufacturing and testing can be found in: Nieuwenhuijzen, E. van, Bos, F.P., Veer, F.A., *The laminated glass column for the All Transparent Pavilion*, Proceedings 9th Glass Processing Days, Tampere, Finland, June 2005. This section is based on that paper.

¹⁰ F.A.Veer, J.R. Pastunink, *Developing a transparent tubular laminated column*, Proceedings 5th Glass Processing Days, Tampere Finland, 1999.

¹¹ During her graduation project under supervision of dr. Veer and the author.

1.4.2. Main Beams¹²

The ATP features three main beams. Their design was based on the reinforced glass beam concept which had been developed from 2001 onwards within the Zappi research.¹³ Such beams consist of annealed glass layers, glued together with UV-curing acrylate adhesives and provided with a stainless steel section or profile in the tensile zone. Up until the ATP project, only single span beams had been tested. To obtain lengths beyond the standard glass sheet length (6.00 m), the glass layers can be segmented in longitudinal direction. Upon failure, the steel profile starts to act as a crack-bridge, both slowing further crack growth and taking tensile loads. The top glass section remains unbroken and carries compressive loads¹⁴, resulting in a closed system comparable to reinforced concrete.

The full-section glass main beams for the ATP were 7.2 m long, with a mid-span of 4.8 m and two additional tapered cantilever ends of 1.2 m each (Figure 2.12). The cantilevers allow a more favourable bending moment distribution and thereby reduce the height and weight. One full scale prototype has been subjected to three 3-point bending tests to validate its structural behaviour, two on either cantilevering side, and one on the mid section.

Figures 2.13a, b and c show the load-displacement curves of the respective tests, and list the recorded post-failure strengths as a percentage of the initial failure strength. Although in principle they showed failure behaviour similar to previous tests on reinforced glass beams, there is a significant difference between the first two tests on the cantilevers and the final test on the mid-span. Where the latter reaches a residual strength of approximately 150 % of the initial crack strength, the former ones only reach about 66 - 75 %¹⁵. In terms of safety, this difference is fundamental as the latter would not fail upon overloading the initial crack strength, whereas the former two would. They would only survive if (part of) the load would be removed.

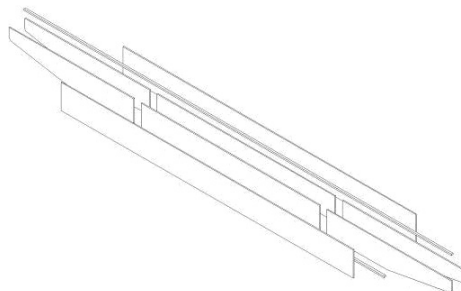


Fig. 2.12 ATP main beam layout.

¹² An extensive discussion on the main beam design, manufacturing and testing can be found in: Christian Louter, Jan Belis, Freek Bos, Fred Veer, Gerrie Hobbelman, *Reinforced Glass Cantilever Beams*, Proceedings 9th Glass Processing Days, Tampere, Finland, June 2005.

¹³ *AdDoc I: Zappi, 1996 – February 2004*, additional document to this PhD, www.glass.bk.tudelft.nl.

¹⁴ Sometimes the top part of the beam was also (partly) cracked; the cracked glass then also carries compressive loads.

¹⁵ The residual strength as percentage of the initial crack strength varies because the initial crack strength varies. The residual strength absolute however, is remarkably constant at 18.4 kN on each side.

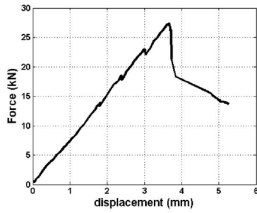


Fig. 2.13a Load-displacement curve of first cantilever test. Relative post-failure resistance $r_{res,III} = 66\%$

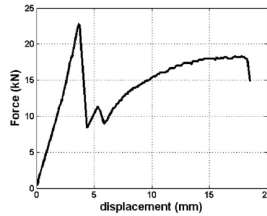


Fig. 2.13b Load-displacement curve of second cantilever test. Relative post-failure resistance $r_{res,III} = 75\%$

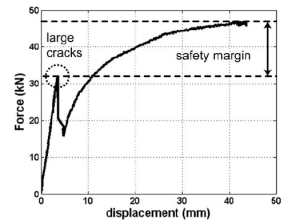


Fig. 2.13c Load-displacement curve of central section test. Relative post-failure resistance $r_{res,III} = 150\%$

According to the design, the main beam would be rigidly connected to the roof purlins through aluminium intermediate components, that would be glued to each element (i.e. the main beam and the purlins; Figures 2.9 and 2.14a, b). A steel bridge served as back-up to prevent the purlins coming down in case of adhesive layer failure. The aluminium pieces slide into each other in a kind of swallow tail design.



Fig. 2.14a, b Aluminium components glued to the main beam (a, left) and to the purlins (b, right).

1.4.3. Purlins¹⁶

Fourteen purlins carry the roof panels of the ATP, spanning 3.6 m. In section, they consist of two two-layer PVB-laminated glass sheets joined by an aluminium profile at the bottom (Figure 2.15). The profile serves both as a spacer and as reinforcement, similar to that in the stainless steel glass beams.

After the pavilion was demounted, all 14 purlins have been tested in a lateral torsional buckling installation developed at Ghent University. The purlins have been subjected to three different loading cases to study the effect of asymmetrical loading on failure behaviour. The load-displacement curves are given in Figures 2.16a, b, and c.

¹⁶ An extensive discussion on the purlin design, manufacturing and testing can be found in: J. Belis, R. van Impe, P.C. Louter, F.A. Veer, F.P. Bos, *Design and Testing of Glass Purlins for a 100 m² Transparent Pavilion*, Proceedings 9th Glass Processing Days, Tampere, Finland, June 2005.

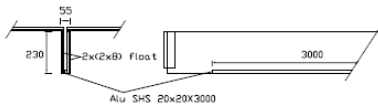


Fig. 2.15 ATP purlin design.

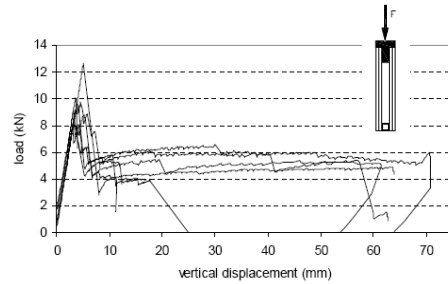


Fig. 2.16a Load-displacement curves of centrally loaded specimens (load case 1).

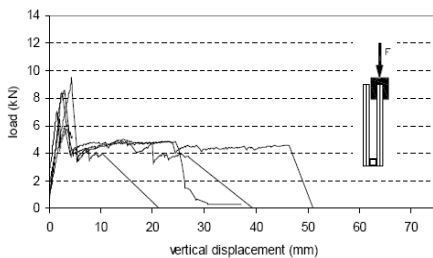


Fig. 2.16b Load-displacement curves of specimens loaded asymmetrically on one laminate (load case 2).

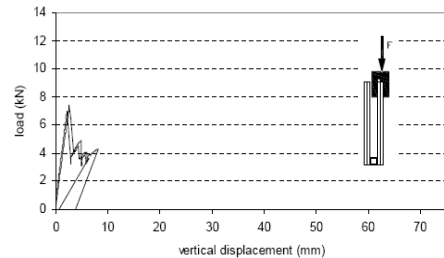


Fig. 2.16c Load-displacement curves of specimens loaded asymmetrically on one sheet (load case 3).

As could be expected, the average initial strength of the centrally loaded purlins is the highest. The difference however, is not very big. The residual strength is also quite close, about 4 kN for load case 3, 4-5 kN for load case 2 and 4-6 kN for load case 1. With residual strengths varying from 33 – 66 % of the initial crack strength, the purlins behave somewhat similarly to the main beam cantilever ends. It is significant to note none of the purlins obtained residual strength anywhere near the initial crack strength.

1.5. Realisation

The ATP was only partly constructed (Figure 2.17). The problems that surfaced were of technical and practical nature, and are extensively discussed in Appendix A, Section 1.

1.6. Evaluation and Conclusions of the ATP project

The structural use of annealed glass requires a high degree of scrutiny for the joint design. The use of adhesive joints seems a logical consequence of working with annealed glass, but care should be taken to avoid inappropriate loading of the bonds. The joint design should allow stress-free mounting. The damage threshold value of an adhesive is therefore a much more important characteristic than its ultimate strength.

Probably the most striking design feature was the successful application of continuous 7.2 m long beams. The concept of these components not only allows for failure behaviour similar to that of reinforced concrete, but also frees the designer of glass sheet size availability and laminating facilities. Because the reinforcement profile is situated at the glass sheet edge, the transparency was hardly compromised.

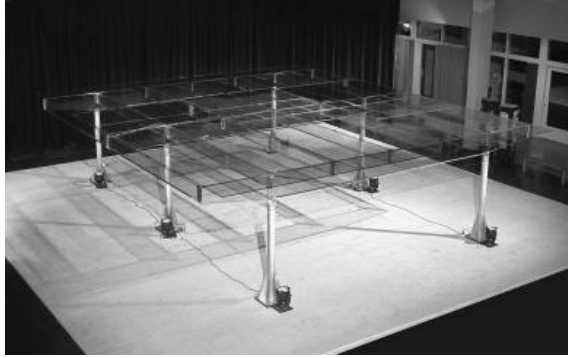


Fig. 2.17 Realized result: the ATP roof structure.

Another important innovation was the development of completely transparent laminated glass columns. A manufacturing process had been developed that solved the perpetual problem of this concept, i.e. the defect free curing of the resin.

Although the joints were lagging behind in development, no technically insurmountable problems had been encountered. Most obstacles during the design and building process were of practical nature, like the availability of several materials and site, and time limitations.

With the ATP project, a safety concept was presented that was new for structural glass components. It aimed at gradual crumbling failure behaviour. It was shown that it was possible to design structural components according to this concept. Transparent building structures can be designed completely out of ordinary annealed and borosilicate glass. The low design stresses do not necessarily result in extreme dimensions, because the inherent safety in the components make it unnecessary to add extra mass. The use of non-tempered glass allows failure behaviour that gives a warning signal before collapse. This was a significant improvement over existing structural glass components, that may stand up to impact damage, but do not warn against overloading.

On the other hand, while the ATP shows an alternative safety strategy (introduction of a safety margin by gradual failure behaviour vs. overdimensioning) can be realized for several different individual elements that can be combined into a complete structure, it also puts forward the question of how to assess and compare safety measures. In the ATP, a range of design measures to increase and ensure safety was applied. Summarized, they are:

- Resin laminated columns with significant post-failure resistance ($r_{\text{res,III}} = 200 - 343 \%$),
- Steel reinforced glass cantilever main beams with $r_{\text{res,III,mid-span}} \approx 150 \%$ and $r_{\text{res,III,cantilever}} \approx 70 \%$),
- Aluminium reinforced, PVB laminated, ‘double’ purlins with $r_{\text{res,III}} \approx 50 \%$,
- PVB laminated roof plates spanning two fields,
- PVB laminated façade panels with a shifted grid respective to the roof plate grid,

- Steel clamp back-up provision in the main beam-purlin joints.

But, as can be seen from the relative post-failure resistances, there are significant differences in their performance. Thus, it is the question what is to be regarded as sufficient. Additionally, it should be considered whether the performance of a single element influences the requirements for another, and/or the complete structure. Can the lack of performance of one element, say a purlin, be compensated by that of another, e.g. a main beam? Finally, reducing a safety assessment to a comparison of post-failure resistances, may not at all be valid. There is only intuitive support for the emphasis on this parameter, but perhaps there are other parameters, of greater or lesser importance, that should also be considered.

consider

Thus, the ATP project raised fundamental questions which can not be answered easily and swiftly.

2. Transparent Façade Struts

2.1. Introduction

Tubular structural glass elements, like columns and struts, possess an inherent aesthetical beauty. But although there is an increasing demand by architects, few realized examples exist. There are several difficulties associated with their development, of which structural safety is perhaps the most important one. Other problems are of a technical nature and associated with the use of glass tubes.¹⁷

Some of these problems had already been encountered during the ATP project. The Transparent Façade Struts (TFS) project, conducted in 2006, provided an opportunity to do more in-depth partial research in these areas and to find a satisfying integrated solution.¹⁸ The objective was to design and test a maximally transparent alternative for a number of existing steel façade struts (Fig. 2.18), with safe failure behaviour both in tension and compression. A design was proposed for hybrid glass-acrylic façade struts.

2.2. TFS Design, Safety and Stability Concept

In a structural glass element loaded in tension (or bending), an auxiliary component is necessary to carry tensile forces in case of glass breakage. The concept of resin laminated glass tubes, previously developed at the TU Delft, was not suitable in this situation because the cured resin is neither strong nor stiff enough to carry significant tensile loads. Alternatively, the TFS design relies on a transparent *polymer* tube rather than a glass one, as its primary load carrying component. Most polymers show plastic and thus safe failure behavior. Furthermore, they are more resistant to impact and do not

¹⁷ The design and manufacturing issues of the TFS project that are not directly related to the main research questions, are presented in Appendix A, Section 2.

¹⁸ These studies have been published in a range of conference papers, to which is referred where relevant. They have also been collected in three documents additional to this thesis, and published on the website of the Zappi Glass & Transparency research group, www.bk.tudelft.nl/glass. The additional documents are:

- *AdDoc II: Transparent Polymers for Joint Applications in Glass Structures.*
- *AdDoc III: Welding and Hot-Shaping Borosilicate Glass Tubes; Possibilities, Strength and Reliability.*
- *AdDoc IV: Glass-to-Acrylic and Acrylic-to-Acrylic Cylindrical Adhesive Bonds.*

The complete TFS project was published as: Bos, F.P., *Hybrid Glass-Acrylic Façade Struts*, Proceedings of the 10th Glass Performance Days, Tampere, Finland, June 2007.

produce dangerous shards upon breakage. This concept also allowed the application of fully transparent polymer strut heads with which they can be connected to the external structure.



Fig. 2.18 The Faculty of Architecture has been extended with a smoking room; essentially a glass box added to the existing glass façade (picture taken from inside the Faculty building). The two steel struts which are to be replaced are visible in the centre of the picture.

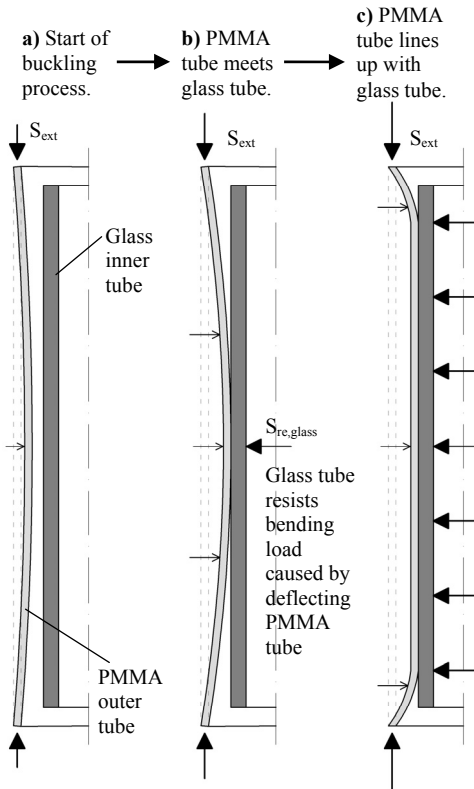


Fig. 2.19a, b, c The TFS stability concept demonstrated.

With a maximum Young's modulus of approximately 3.3 GPa, transparent polymers are very flexible compared to other building materials. A strut consisting only of a polymer tube would therefore have to have had a very large diameter. As this was deemed unacceptable from an architectural point of view, the strut was supplied with a glass tube inside. This prevented the polymer outer tube from buckling. By making sure that the glass tube was a bit shorter than the polymer one, direct normal action on the glass tube is avoided. Instead it was only loaded in bending when the polymer tube starts to buckle and meets the glass tube. This concept is demonstrated in Figures 2.19a, b, and c. It was proven also in a 1:2 scale test (not shown) before the 1:1 prototypes were manufactured. By placing the glass tube inside, there was no risk of shards injuring people in case of glass breakage and the high fracture toughness of the polymer tube provides impact resistance for the strut.

2.3. Prototype testing

2.3.1. Compression Test

Three prototypes were produced. The first specimen was aligned horizontally and subjected to a force-controlled compression/buckling test. This set-up resembled the actual situation best (incorporating self weight in the behaviour) and made it easy to predict the buckling direction. The load was applied through a hand-controlled hydraulic jack (displacement controlled). The load-displacement graph is presented in Figure 2.10. The displacement is axial (thus the shortening along the x-axis of the element).

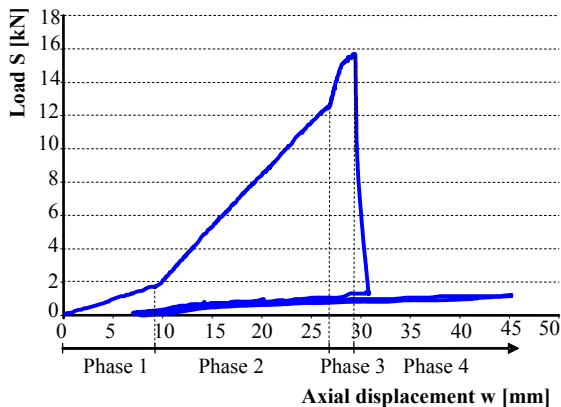


Fig. 2.20 Force-displacement graph of the compression/buckling test on a TFS prototype.

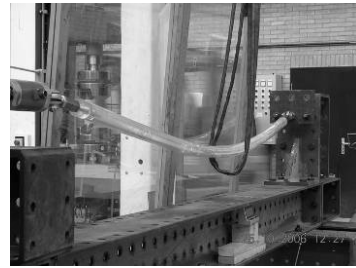


Fig. 2.21 TFS prototype during compression/buckling test (phase 4).

Four phases can be distinguished in the loading and failure process:

- Phase 1 (pre-failure): The acrylic tube shortens elastically and bends (buckles) sideways freely, making use of the 1 mm wide cavity between the glass and the acrylic tube.
- Phase 2 (pre-failure): Then, it touches the glass tube which starts to contribute to the bending resistance of the strut. This is expressed by a seriously increased steepness of the graph.
- Phase 3 (pre-failure): Meanwhile the acrylic tube was also shortening elastically, until at some point the sliding joint on one side of the strut meets the end of the glass tube. Now, the glass tube not only carries bending loads, but also transfers the axial compressive loads. The stiffness increases again. Finally, the glass tube breaks at 15.5 kN.
- Phase 4 (post-failure): After failure, the load was removed. The specimen was then loaded again. The glass tube had been shattered to such an extent that it could not provide a significant contribution to the bending stiffness anymore and buckling of the failed member occurred at approximately 1.5 kN, which is close to the theoretical Euler buckling load of 1.2 kN of just the acrylic tube. Figure 2.21 shows the first prototype during phase 4.

2.3.2. Tensile Test

The tensile test on the second specimen was conducted in the same experimental set-up. The load-displacement diagram is given in Figure 2.22. Again, a number of phases could be identified:

- Phase 1 (pre-failure): The graph follows a more or less linear path until, at 10.9 kN, failure occurs by breakage of the acrylic tube on one side of the specimen. The break occurs just between the cylindrical adhesive joint and the end of the glass tube (Figure 2.23).
- Phase 2 (post-failure): This trajectory of increasing axial displacement at zero force is caused by the sliding of the acrylic joint piece at one side, until the widening hits the thickened glass tube end.
- Phase 3 (post-failure / collapse): A linear load-displacement curve is registered until the specimen collapses at 12.9 kN, as a result of breakage of the glass tube about halfway the glass-acrylic adhesive joint on the other side. Contrary to expectation, the acrylic tube broke again, approximately at the same point as the glass tube.

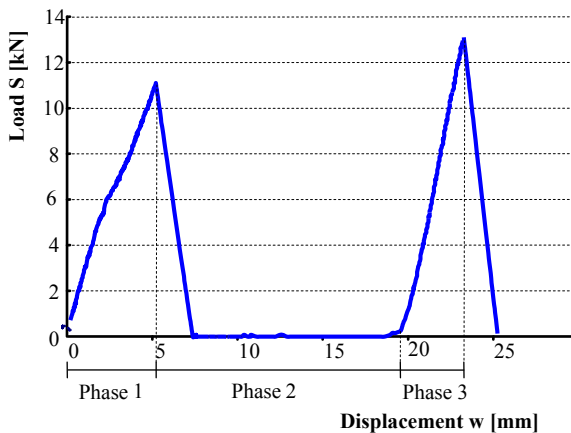


Fig. 2.22 Force-displacement graph of the tension test on a TFS prototype.

Two observations immediately draw attention when analyzing these results. First, the initial failure occurred by breakage of the acrylic tube at only 10.9 kN. Failure was expected at approximately this load, but through breakage of one of the cylindrical adhesive bonds, rather than by breakage of the tube. The failure load coincides with a nominal tensile failure stress of only 15.6 N/mm^2 in the tube, while the tensile strength of PMMA is usually listed to be approximately 70 N/mm^2 . Secondly, the tensile stiffness ($\Delta F/\varepsilon = EA$) of the specimen during phase 3 is only about twice that as during phase 1. This is remarkable because the actions are supposed to be transferred solely through the acrylic before failure, and only through the glass after failure. Therefore, EA_{phase1} should be equal to $E_{\text{acrylic}}A_{\text{acrylic}} = 3300 \cdot 703.7 = 2.3 \times 10^6 \text{ N}$, while EA_{phase3} should be $E_{\text{bo-glass}}A_{\text{bo-glass}} = 64000 \cdot 1159.2 = 74.2 \times 10^6 \text{ N}$, thus $EA_{\text{phase1}}:EA_{\text{phase3}}$ was expected to be 1:31.9 N.

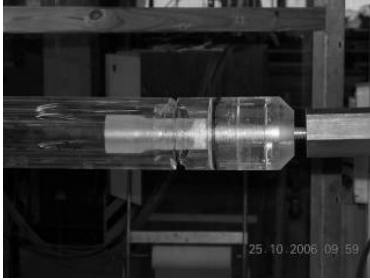


Fig. 2.23 Failure of the tension tested TFS prototype occurred by breakage of the outer acrylic tube at the A-side, between the cylindrical adhesive bond with the strut head and the end of the glass tube.

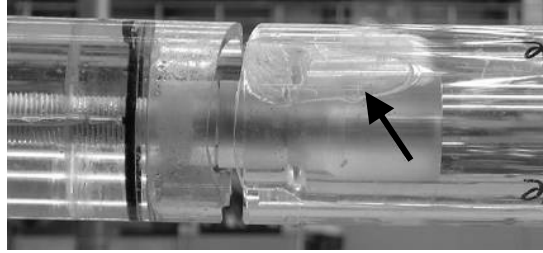


Fig. 2.24 The arrow indicates a large spot of accidentally cured adhesive between the acrylic and glass tubes. This probably caused stress concentrations in the acrylic tube leading to premature breakage.

Both observations can be explained by the presence of a large spot of adhesive between the glass and acrylic tubes, right at the end of the glass tube (Figure 2.24). This patch has cured in that location by accident, and could not be removed before testing. The consequence of this erroneous adhesive bond was that when the specimen was loaded in tension, the forces were transferred through the glass tube, rather than through the acrylic one. The glass tube had a much higher stiffness and thus drew forces to it. This explains the small stiffness difference in the first and third phase of the experiment. Because this adhesive patch is local, it causes a peak stress in the acrylic tube between the glass tube end and the A-side head (because here, the forces can not go through the glass). The premature acrylic tube failure which occurred here can thus also be explained by the presence of the adhesive patch. The fact that this erroneous adhesive bond was indeed transferring forces is underlined by the fact cracks were observed in it.

The breakage of the glass tube at 12.9 kN coincided with a relatively low nominal tensile stress of 11.1 N/mm² in the glass, but breakage was probably caused by some form of stress concentration at the point where the forces have to be transferred from the glass into the acrylic.

2.3.3. *Impact and three point bending test*

Additionally, a series of tests was conducted on a third prototype to investigate its behaviour under lateral action. This time, a Zwick universal test rig with a 10 kN load cell was used. The experiment was carried out as a 3-point bending test. A load was repeatedly applied by a piece of steel angle profile at a speed of 2000 mm/min (machine maximum). The load maximum was set to increasing values. At the fourth attempt, the inner glass tube broke at a failure load of 1093.0 N. All glass shards remained inside the acrylic tube, thus there was no risk of personal injury.

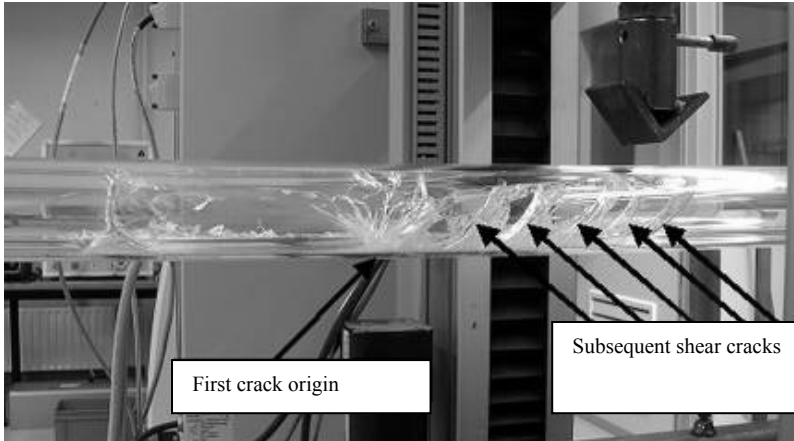


Fig. 2.25a Fracture pattern in the TFS prototype after failure in the impact/bending experiment. Cracking pattern development during post-failure in impact/bending test (b, bottom).

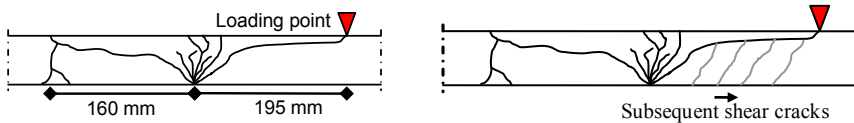


Fig. 2.25b, c Schematic fracture pattern, directly after failure (left) and development of shear cracks (right).

The primary cracking occurred 195 mm from the loading point on the A-side. The crack branched into a fan. One branch reached the loading point, while another turned back to the underside approximately 160 mm from the crack origin. After the load was removed, the specimen recovered deformation almost completely. The cracking pattern is shown in Figure 2.25a, b, and c.

Although the failure load seems quite low (just under 110 kg), it coincided with a peak stress in the glass under the loading point of 72.2 N/mm^2 . Hence, failure was not premature. Although the speed of a random falling object will probably be higher, the exerted load will most probably be much lower as the object will bounce away (because of the small smooth curved surface). The impacts hardly inflicted any damage. The acrylic tube only suffered minor scratches and the glass was not affected. The failure was not caused by the effect of the impact, but rather by an expectable bending stress.

Subsequently, the prototype was further tested in 3-point bending at a speed of 5 mm/min. First, the force-displacement graph is linear (Figure 2.26). From approximately 370 N, new cracks appear, mostly in the existing cracked area. The curve slowly turns towards the horizontal, indicating decreasing member stiffness caused by the ongoing cracking of the glass tube. The new cracks (Figure 2.25b) seem to be caused by shear and to work towards the creation of a hinge directly underneath the loading point. The prototype could not be loaded to collapse because of the flexibility of the acrylic outer tube. The maximum lateral displacement of 180 mm was reached at a load of 538.6 N. The final collapse load is expected to be governed completely by the acrylic tube strength. For literature values of 70 N/mm^2 , this would mean a maximum load of 958.4 N.

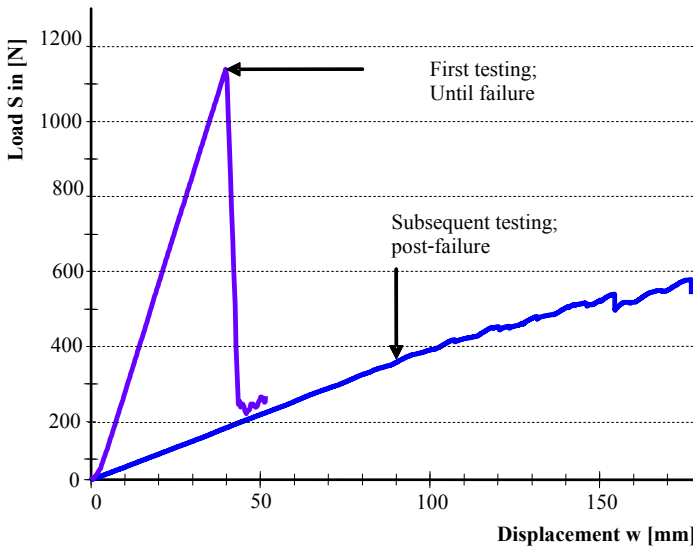


Fig. 2.26 Force-displacement graph of the impact/bending test on a TFS prototype.

2.4. Discussion

Considerable levels of post-failure resistance were obtained in all loading cases (Table 2.2). However, the levels of post-failure strength and the ratio between pre- and post-failure strength varied widely per loading case, from 9.7 % in compression to 118 % in tension. Similarly to the evaluation of the ATP, this raises the obvious question of how these results compare to one another, and how the safety of this element should be assessed. Particularly the post-failure resistance in compression, which is below the ultimate limit state action, deserves consideration.

Another interesting point is made by the difference in post-failure stiffness in the bending and compression/buckling cases. In the former, it is approximately $1/6^{\text{th}}$ of the pre-failure stiffness, while in the latter it is only $1/16^{\text{th}}$, which means the bending stiffness is almost solely provided by the acrylic tube. In the bending test, the broken glass still contributes significantly to the overall bending stiffness. This difference seems to be caused by the crack pattern density in the glass tube.

Table 2.2 Summary of results of different tests on TFS prototypes.

Test	Initial failure load $R_{\max,ini}$	Maximum post-failure load $R_{\max,post}$	Relative post-failure resistance $r_{\text{res,III}}$	Ultimate limit state action S_d
Tension	10.9 kN	12.9 kN	118 %	3.6 kN
Compression	15.5 kN	1.5 kN	9.7 %	3.9 kN
3-Point Bending	1093 N	537* (958)** N	49* (92)** %	-

* Measured value, maximum displacement experimental set-up reached.

** Expected maximum value.

In the compression test, the glass tube fractured in multiple places at once upon failure. Thus any significant contribution to the member's stiffness was lost immediately. In this situation, the behaviour differs from the bending experiment. There, the glass cracking upon failure was limited, and the glass tube continued to contribute to the element's stiffness after failure, only to gradually crack further and decrease stiffness contribution.

But in both cases, failure is caused by bending-induced tensile stresses. It is, therefore, not immediately clear what causes the difference in fracture behaviour and, thus, post-failure stiffness. This may indicate a fundamental parameter in the determination of post-failure behaviour.¹⁹



Fig. 2.27a, b, c Some impressions of the TFS in the Architecture building extension.

¹⁹ See Chapter 9.

3. General Discussion and Evaluation of Case-Studies

Within the ATP and TFS projects, many design innovations have been explored and various design concepts for safety have been tested. There is still much opportunity for the development of transparent structures.

Two principle and recurring problems were encountered in both projects:

- safety: *how to design a safe structure?*
- joints: *how to connect the parts together (safely)?*

Both problems required extensive research on many partial aspects of the structures. During the ATP project, especially the joint related problems were not solved satisfactorily within the short time frame available for that project. In the TFS project, several of these were brought closer to a solution, but much research still remains for the structural application of transparent polymers, adhesives and glass welding. Designing joints in annealed float glass without the use of load bearing holes in the glass also remained a challenge yet to be addressed.

However, the safety problem proved to be the more fundamental of the two. A mass of intuitive conceptual solutions has been applied, both on component and structure level, to obtain safe failure behaviour, i.e. a type of failure which is not sudden and immediate but rather allows for a margin between initial failure and collapse, either in terms of load, deformation, and/or time.

However, the extent of this margin obtained in each element, varied significantly. The mid-span of the ATP main beams showed 150 % residual strength; but the cantilevers only provided 66 - 75 %. The residual strength of the purlins hovered between 33 and 66 %, and appeared to be load case dependent; the columns on the other hand had a residual strength of 300 %, but this also depended highly on the way the joints transferred the loads into the glass.

The failure behaviour of the façade struts was highly dependent on the load type. The residual strength in tension was almost 120 %, but initial failure was actually premature due to a manufacturing error, thus the residual strength as a percentage of the initial strength may be different in error free prototypes. In compression, on the other hand, the residual strength was only 10 % and buckling governed – a phenomenon depending on the residual bending stiffness. In direct 3-point bending however, the residual strength could not be measured. It was at least 50 %, but more likely close to 100 % with very high deformation capacity.

Thus, the principle validity of the presented design concepts has been proven: it is possible to obtain margin between failure and collapse by applying them. But in order for these concepts to be developed further, selection criteria are desperately needed.

If the primary goal of the Zappi Glass & Transparency research is

To create transparent structural components and structures with safe failure behaviour,

the question is:

‘What is safe failure behaviour?’

An unambiguous answer to this question will be difficult to give, but a useful, detailed handhold to assess and compare design solutions is imperative and possible.

Only once this question has been tackled, the subsequent question can be addressed:

‘How can we achieve safe failure behaviour (in transparent structural components and structures)?’

Uncovering the fundamental parameters to achieve this is required to optimize the concepts which have had an intuitive character up until now. But a systematic approach is needed. Only thus can the differences in performance between the investigated concepts be explained, and the performance of the individual concepts be optimized.

The objectives and methods derived from these research questions, were already presented in Chapter 1, Section 2 (based on the analyses presented here). Chapter 3 will start systematic treatment of these issues with an analysis of existing safety approached in general structural engineering.

In Chapter 10, the ATP en TFS designs will be re-analyzed with regard to safety, based on the safety approach that will be developed in the preceding Chapters. A redesign of the ATP will be proposed in Appendix A (Section 1.6). Besides the safety issues, this redesign also addresses the practical and technical problems of the initial design.

3 Theoretical and Codified Safety Approaches in Structural Engineering

This Chapter gives an introduction into structural safety engineering, of which probabilistic analysis forms the basis. Concepts such as risk, probability, consequence, and systems are introduced, as well as robustness and residual strength. The relation between theoretical probability analysis and real failure causes is discussed and the limitations of the probabilistic approach are explained. Extensions to this approach are being discussed.

1. Safety and Danger

According to the Oxford Advanced Learner's Dictionary, safety is being safe, i.e. not being dangerous or not being in danger.¹ The importance of being safe for a human being is so obvious, it is hard to objectively describe. It is arguably the first condition for survival, even before water, food, and shelter. It is the *raison d'être* for much of our legislation, as well as for our extensive system of insurances.

Danger to people may entail a threat to one's life, health, financial situation, or (indirect) to one's emotional welfare (e.g. by threat to loved ones). It may originate from a wide range of sources, such as diseases, accidents, natural phenomena and disasters (fire, floods, storms, earthquakes, volcanic eruptions, etc.), environmental hazards (UV-light, (bio-) chemical substances, etc.), and – certainly not unimportant – other human beings (error, dangerous activity, war, crime, neglect, etc.).

One source of peril, is human engineering. Countless pieces of engineering have been produced by mankind, some very small, others extremely big, often to increase his standard of living. However, these enterprises have also frequently augmented the dangers to which he is exposed. Planes crash, cars collide, buildings collapse.

The structural safety of buildings is an important field in engineering related safety issues. It is concerned with controlling the threat building structures pose to humans, so that they remain within acceptable limits. This thesis particularly addresses the safety related to the structural use of glass.

Throughout this study, 'glass in construction' refers to any glass element that is part of the building: windows, balustrades, roofs, floors, etc. The term 'structural glass' is used for glass applied in a way that it not only carries external (i.e. from out of the structure) actions and self weight but also internal (i.e. from other parts of the structure) loads to a substructure or another structural member. Hence, structural glass is a small sub set of glass in construction.

¹ Cowie, A.P. (Ed.), *Oxford Advanced Learner's Dictionary of Current English*, 4th Edition, Oxford University Press, Oxford, UK, 1989.

When addressing the second general question ‘how structural glass safety can be obtained?’, it should first be noted that safety, by definition, is not an absolute concept. The concept of safety is only meaningful to the extent it means not being in danger, which, by the way, therefore also is not an absolute concept either. Thus both safety and danger are *measures*, one being the inverse of the other. Especially in engineering, a threat, however remote, to the engineering feat is always imaginable, underlining the relativity of safety. Since we are usually primarily concerned with the amount of danger, rather than the amount of safety (it is, for instance, more insightful to know how many lives may be in danger than to know how many lives are safe – even though these measures are directly dependent on each other), the notion of ‘risk’ has been introduced as a quantity of danger. It will be explored further in the next sections.

2. Risk

To be able to adjust engineering designs to accepted safety levels, ‘risk’ has been introduced as a quantifiable concept for the level of danger (or the inverse of the level of safety). Although several quantified definitions of risk exist, risk as the product of probability of a cause event times the consequence of that event (Eq. 3.1) is most commonly used² and fairly insightful.

$$\text{risk} = \text{probability} \cdot \text{consequence} \quad (3.1)$$

This definition appears to be quite simple and indeed it clearly brings out the two important constituents of risk: the probability that an event will occur and the consequences of that event. If the consequence of an event is small, a high probability of that event is likely to be accepted; if, on the other hand, the effect is large, a low probability will be required. Thus, it also seems clear there are two principal ways to minimize risk: diminish consequence or reduce probability (or both).

However, several problems arise when one tries to get tangible results from this equation. First, there is a problem of units. Probability is principally dimensionless, but since risk is usually related to a certain relevant time period (probability density, see below), the probability constituent gets the character of a frequency unit, such as yr^{-1} . Thus, the unit of risk is often a unit of consequence over a unit of time. However, the multisided character of consequence makes it difficult to agree on a unit for this constituent. The consequence of a structural failure may be financial, but could also be described in terms of injuries or loss of life. To overcome this problem, all consequences are often translated into their equivalent in one single unit. Off course, this is a source of ongoing debate: what is the financial value of a life?

3. Risk analysis; Cause and Consequence

More fundamentally though, an event and its consequence never form an isolated system. Rather, the consequence is an event in itself which has further consequences.

² See for instance: Schneider, J., Introduction to Safety and Reliability of Structures, Structural Engineering Document 5, IABSE, Zurich, Switzerland, 1997, p. 11; or: Vrouwenvelder, A.C.W.M., Vrijling, J.K., Probabilistisch Ontwerpen (b3), TU Delft, The Netherlands, p. 8-1. The latter also list three other definitions: *risk = probability*; *risk = consequence*; *risk = probability·consequence*ⁿ. These, however, are not commonly used.

Likewise, the cause event is the consequence of previous causes. Thus, the cause and consequence events are part of a cause-and-effect chain (Figure 3.1), tracing of which would lead to infinite regression on either side.

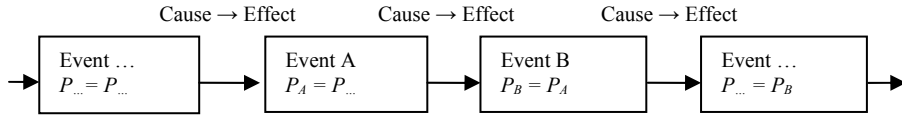


Fig. 3.1 Cause-and-effect chain. The subsequent events X and X+1 are fully correlated: $P_{X+1|X} = 1$, thus $P_{X+1} = P_X$. Both the initial event and the final effect can not be found, tracing the chain leads to infinite regression on either side.

To make matters even more complex, there is generally not a unique relation between a cause and a consequence. Rather, a specific consequence may depend on the occurrence of multiple events which together cause the consequence. On the other hand, one cause may have multiple possible consequences. Thus, the cause and consequence events are actually part of a cause-and-effect mesh (Figure 3.2) rather than a simple chain.

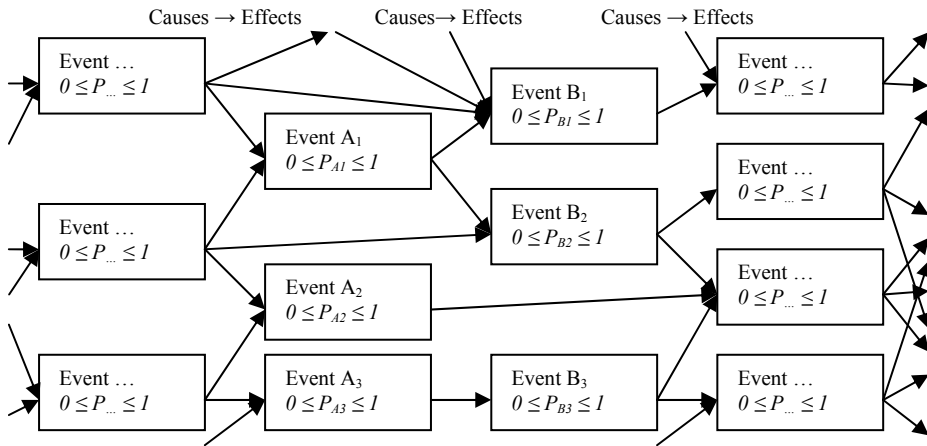


Fig. 3.2 Cause-and-effect mesh. The subsequent events are not fully correlated. An event may rely on multiple causes and may have multiple effects. Thus, the probability of an event X is $0 \leq P_X \leq 1$.

The infinite character of this mesh makes the problem of minimizing risk mathematically unsolvable, unless discrete boundaries in the mesh of events are chosen. It is a *choice* to consider the relation between a certain possible start cause event, possible intermediate events, and a certain possible end consequence event and to neglect previous causes and subsequent consequences.

Event trees (implicitly) provide such boundaries. They are crucial instruments in risk analysis of engineering works and give qualitative insight into the relation between causes and effects, which serves as the basis for further quantitative elaboration. Basically, there are two types. Cause event trees (Figure 3.3) are based on forward logic and consider the possible consequences of one cause event up to a certain stage, while fault trees (Figure 3.4) seek to trace the causes that lead up to a certain governing

consequence event, down to a certain stage. Usually, the considered effect in a fault tree is the most serious consequence that could occur; if various consequences are considered, individual fault trees have to be constructed for each one. Likewise, a new cause event tree needs to be set up for each cause event. Both tree types are in fact a cut-out of the cause-and-effect mesh (Figures 3.3, 3.4), and either ignore or assume the events outside of the tree.

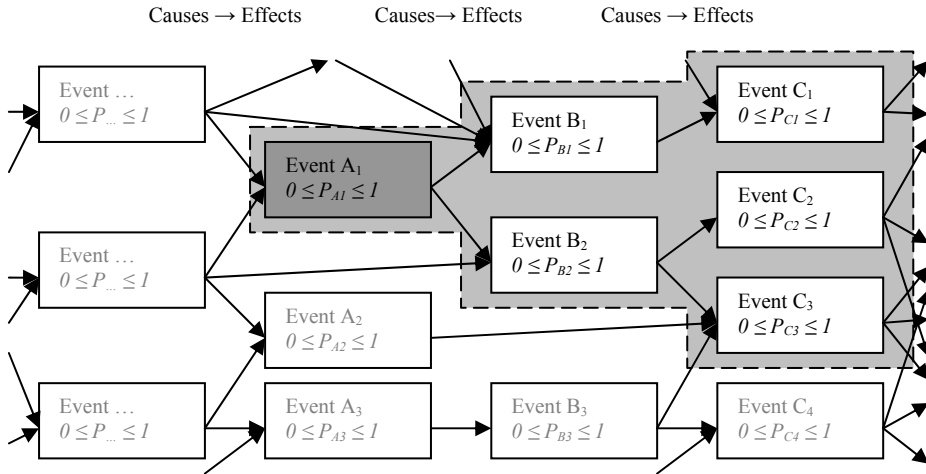


Fig. 3.3 Cause Event Tree. To avoid infinite regression in determining cause and effect, only a certain part of the cause-and-effect mesh can be considered. A cause event tree starts at one cause event and considers the possible consequences of that event, possibly considering intermediate events.

For a meaningful risk analysis, it is of primary importance to recognize all relevant hazards or hazard scenarios (combination of events which together can form a hazard), i.e. determine the appropriate logic trees. Several creative techniques and cognitive aids, can be applied to trace as many relevant hazards as possible; brainstorming in interdisciplinary teams is often appropriate³.

Both cause event trees and fault trees are useful tools in the subsequent stages of risk analysis:⁴

- Describe the engineering work as a system.
- Make an inventory of all possible undesirable start events and investigate what the reactions (consequences) of the system could be. A cause event tree is a useful tool for this stage.
- Investigate how the most unwanted reaction(s) can occur. Effectively this means combining the most undesirable branches of the cause event trees to one error tree. The single, grave consequence event in this tree is called the *top event*.

³ Schneider, J., *Introduction to Safety and Reliability of Structures*, Structural Engineering Documents 5, IABSE, Zurich, Switzerland, 1997, pp. 19-20.

⁴ Vrouwenvelder, A.C.W.M., Vrijling, J.K., *Ibid*, p. 7-1. See this reference for an elaborate explanation of the risk analysis procedure.

- Calculate the probability of the top event by determining the probabilities of the start (cause) events and using the conventions of probability analysis to determine the top event probability.

Subsequently, the risk can be evaluated and it can be decided whether counter measures are required, which may consist of a range of actions. Schneider recognises five categories⁵:

- Eliminate the hazard by taking action at its source.
- By-pass the hazard by changing intentions or concepts.
- Control the hazard by checks, warning systems, etc.
- Overcome the hazard by providing sufficient reserves.
- Consciously accept the hazard as a risk which can not be avoided at reasonable cost.

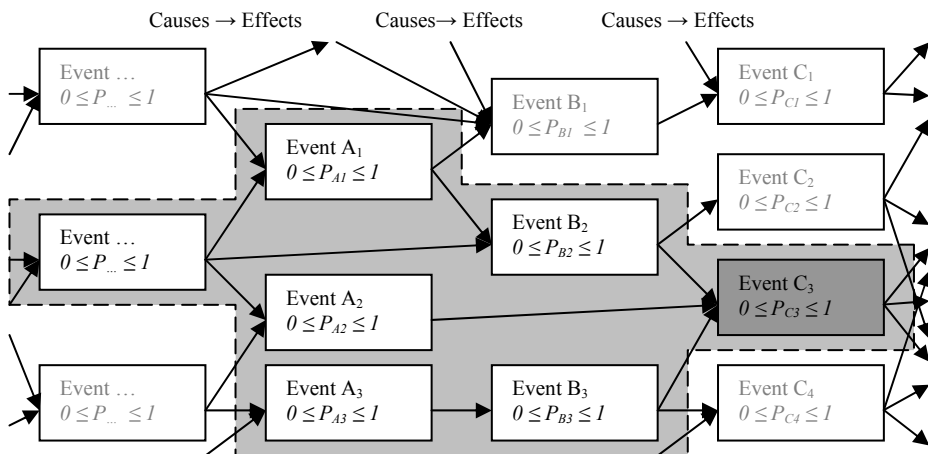


Fig. 3.4 Fault Tree. To avoid infinite regression in determining cause and effect, only a certain part of the cause-and-effect mesh can be considered. A fault tree starts from a certain consequence event and traces to find possible causes.

In structural analysis, however, such a full risk analysis is usually not conducted unless failure of the structure could harvest extremely grave consequences (e.g. nuclear power plants, dams, dikes, or high-rise buildings). A full risk analysis is very time consuming and usually considered excessive for ordinary building structures. Rather, the risk analysis is limited to considering one critical top event, i.e. failure by mechanical overload, for each individual structural member through exceeding its resistance (strength) for a governing load case. The member resistance is a function of material properties and geometry, while the governing load case is determined by permanent, variable and accidental loads.

⁵ Schneider, J., Ibid, p. 22.

With the consequence event given (structural failure of an individual member), the risk problem is thus reduced to a probability problem: the probability of failure has to be determined from the member resistance and load case probabilities (Figure 3.5).

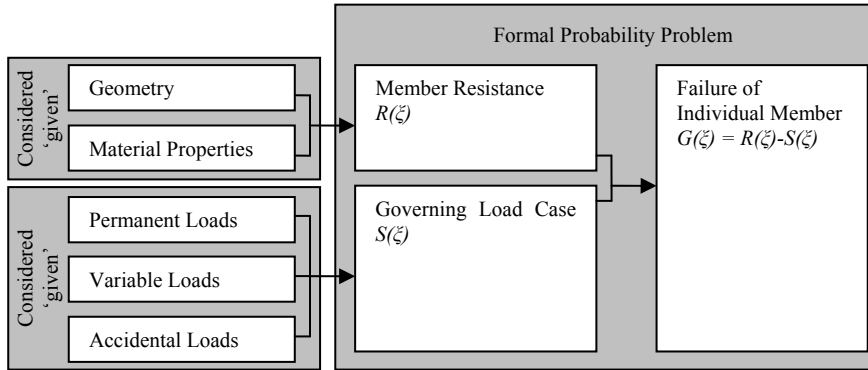


Fig. 3.5 For most structures, the risk analysis is limited to considering the probability $G(\xi)$ of the top event ‘member failure’, for each individual member, as a function of member resistance $R(\xi)$ depending on material properties and geometry, and the governing load case $S(\xi)$, depending on permanent, variable and accidental loads.

4. Probability analysis

4.1. Variables and Distributions

By definition, probability analysis is based on the mathematical theory of sets: the probability of an event is considered a partial set of all possible events. Thus, it follows its mathematical rules⁶, which can be visually represented with Venn Diagrams. As an example Figure 3.6 represents the probability of a failure event as a partial set of the set of all events.

Stochastic variables are used to calculate the probability of an event. The continuous stochastic variable X is a variable which can be described with the continuous probability function $F_X(\xi)$, also known as the cumulative distribution function (CDF; Figure 3.7a). The CDF is defined as the probability that the variable X at a certain value ξ does not exceed ξ ⁷ (Eq. 3.2). It has a monotonously non-decreasing character from $F_X = 0$ for $\xi = -\infty$ to $F_X = 1$ for $\xi = +\infty$. Probability functions have no unit.

The derivative of the probability function (Eq. 3.3) is called the probability density function (PDF), which gives the probability that the stochastic variable takes a certain value within the infinitesimally small interval $\xi + d\xi \approx \xi$. The unit of the probability density function is $[\xi]^{-1}$. Experimental results are often presented in histograms which can then be fitted into probability density functions (Figure 3.7b).

⁶ Based on three central axioms, Vrouwenvelder and Vrijling provide 11 mathematical theorems, which provide the fundament for all further probability calculations. Vrouwenvelder, A.C.W.M., Vrijling, J.K., Ibid., pp. 2-1 – 2-5. The axioms are: $P(A) \geq 0$; $P(\Omega) = 1$; $P(A \cup B) = P(A) + P(B)$ if $A \cap B = \phi$. With: A, B arbitrary events; Ω certain event; ϕ impossible event.

⁷ Vrouwenvelder, A.C.W.M., Vrijling, J.K., Ibid, p. 2-12.

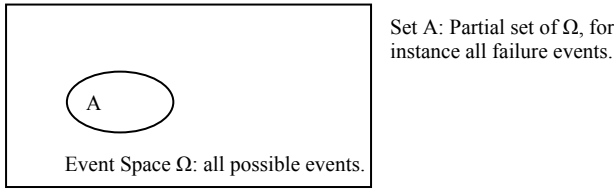
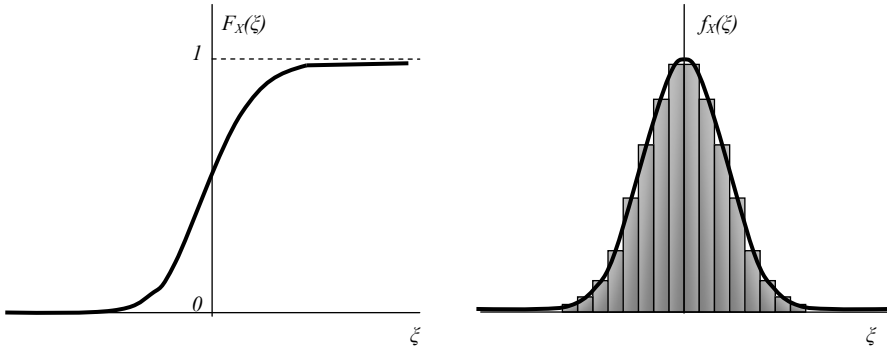


Fig. 3.6 Probability analysis is based on the mathematical theory of sets; the failure events form a partial set of all possible events.



$$F_X(\xi) = P(X \leq \xi) \quad (3.2)$$

$$f_X(\xi) = \frac{dF_X(\xi)}{d\xi} \quad (3.3)$$

Fig. 3.7a, b Example of a (normal) Cumulative Distribution Function (CDF) and a (normal) Probability Density Function (PDF), with their respective equations Eqs (3.3) and (3.4).

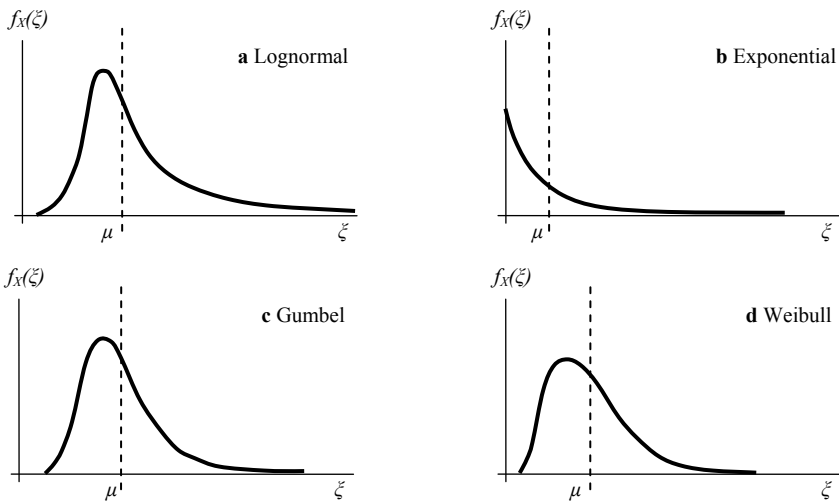


Fig. 3.8a - d General shape of Log-normal, Exponential, Gumbel, and Weibull distributed probability density functions.⁸

⁸ After: Schneider, J., Introduction to Safety and Reliability of Structures, Structural Engineering Document 5, IABSE, Zurich, Switzerland, 1997, p. 117. More distribution functions can also be found in this reference.

There are a considerable number of standard probability density functions, appropriate through their shape for the description of various kinds of stochastic variables. The Normal, Log-normal, Exponential, Gumbel and Weibull distributions are fairly common; their general shape is shown in Figure 3.8a – d. The latter is often used to describe the statistical distribution of the bending tensile strength of glass sheets. The strength of steel or the magnitudes of mechanical loads are usually considered to have a Normal or Log-Normal distribution.

4.2. The Reliability Problem of Structural Members: $G(\xi) = R(\xi) - S(\xi)$

The reliability G of a structure is generally considered to be a continuous stochastic variable, depending on the resistance $R(\xi)$ of the structure and load $S(\xi)$ exerted on the structure through Eq. 3.4.

$$G(\xi) = R(\xi) - S(\xi) \quad (3.4)$$

The boundary of failure is defined by the limite state condition $G(\xi) = 0$. Failure occurs when the exerted load $S(\xi)$ exceeds the structure resistance $R(\xi)$, thus when $G(\xi) < 0$. The probability of failure is then determined by all cases for which $R(\xi) < S(\xi)$, as Eq. 3.5.

$$P_f = P_{G(\xi) \leq 0} = P_{R(\xi) \leq S(\xi)} \quad (3.5)$$

Since $R(\xi)$ and $S(\xi)$ are also stochastic variables, as opposed to single value parameters, the solution of $G(\xi) = R(\xi) - S(\xi)$ is not obvious. Literature presents several methods to solve this problem, such as the classical solution with the convolution integral, the Monte Carlo method, the Basler/Cornell method, and the Joint probability density method. An extensive treatment falls outside the scope of this research. The interested reader is referred to probability method handbooks.⁹

In reliability analysis, three¹⁰ levels of statistical accuracy are recognized. In increasing order of mathematical complexity, they are¹¹:

- Level I: Instead of using probability density functions, the variables (R and S) are introduced by a single characteristic value. Often a 5% fractile value is used, multiplied by a partial safety factor to account for the statistical scatter. Low partial safety factors indicate small scatter of the variable, while high factors point to the opposite.
- Level II: The exact reliability is approximated by using two parameters, e.g. the mean and the standard deviation, to describe the variables. Correlation between variables has to be avoided.

⁹ E.g. Schneider, J., Ibid, pp.73-83; or: Kottegoda, N.T., Rosso, R., Applied Statistics for Civil and Environmental Engineers, 2nd edition, Blackwell Publishing, Oxford, United Kingdom, 2008.

¹⁰ Sometimes, a fourth level, Level 0, is added, which is considered to be the level of deterministic calculation, i.e. the variables are assumed to have one single value and no statistical distribution. Calculations on this level only give absolute reliability results, i.e. the reliability is 0 or 1, and have long been removed from structural engineering codes as an acceptable calculation method.

¹¹ Vrouwenvelder, A.C.W.M., Vrijling, J.K., Ibid, p. 3-1.

- Level III: The probability density functions for all relevant variables are determined and used to calculate the exact failure probability.

Level I is commonly used in structural analysis, but gives no actual failure probability. The higher levels produce more accurate results but are much more elaborate and therefore usually not economical. More importantly though, they require data which are often not available. However, Level I codes and guidelines are calibrated by Level II and III computations as much as possible, to obtain consistent reliability requirements.

4.3. Probabilistic Approach in Dutch and European Engineering Codes for the Basis of Design on Structures

The basic requirements towards building structures in the Netherlands are defined in the NEN 6700.¹² In this code, the maximum failure probability is limited primarily by requiring a structure to meet a minimum reliability index β , which is a measure for the probability that an ultimate limit state or a serviceability limit state is exceeded during the reference life time of the structure (clauses 5.3.1 and 5.3.2). The required value of β is dependent on the safety class into which the structure can be categorized. The safety class is determined by the consequences of collapse of the structure in question.¹³ The higher the safety class, the higher the required value for β . The semi-probabilistic Level I method is the minimum level of probabilistic analysis allowed by the NEN 6700.

To check whether a structure meets the reliability requirements, extensive rules are laid down in NEN 6702,¹⁴ which defines the actions on structures, and several material codes, such as NEN 6720 (reinforced concrete) and NEN 6770 (steel), giving rules of how to check a designed structure against those actions. The basic method of checking is the unity check, such as Eq. 3.6. If structures are designed according to these codes, they are assumed to meet the reliability requirements formulated in NEN 6700.

$$\frac{\sigma_d}{f_d} \leq 1 \quad (3.6)$$

At the moment, the Dutch codes coexist with codes that have been developed in European context by the CEN, which follow the same general format. Basic requirements towards building structures are formulated in NEN-EN 1990¹⁵. This code sets requirements to the reliability of structures similar to those in the NEN 6700. Actions are formulated in NEN-EN 1991; NEN-EN 1992 – NEN-EN 1999 are the material codes.

5. Systems

In structural engineering, the reliability analysis is usually limited to an analysis of each component individually. However, these components together form a structural system.

¹² Nederlands Normalisatie Instituut, NEN 6700 Technische grondslagen voor bouwconstructies – TGB 1990 – Algemene basiseisen, Delft, 2005.

¹³ According to note 2 of Table 1 in the NEN 6700, which provides an overview of required values for β .

¹⁴ Nederlands Normalisatie Instituut, NEN 6702 Technische grondslagen voor bouwconstructies – TGB 1990 – Belastingen en vervormingen, Delft, 2007.

¹⁵ Nederlands Normalisatie Instituut, NEN-EN 1990 Eurocode – Grondslag van het constructief ontwerp, Delft, 2006. The Dutch versions of the European EN codes have the prefix NEN-EN.

The consequence of failure of one component for the structure as a whole depends on the way the system is organized. Two fundamental system types can be distinguished:

- Serial systems (e.g. a truss beam, Figure 3.9a), and
- Parallel systems (e.g. a floor on multiple clamped columns, Figure 3.9b).

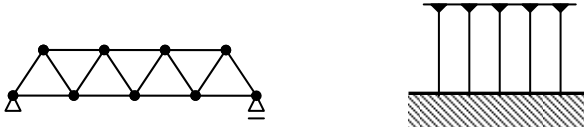


Fig. 3.9a, b Examples of a serial and a parallel system: a) a truss beam (left) and b) a floor on multiple clamped columns.

In a serial system, failure of one component will induce failure of the complete system. Failure of a component in a parallel system on the other hand, will cause other components to take over its function: there is an alternative path, e.g. for the transfer of loads. Serial systems are associated with statically determined structures; parallel systems with statically undetermined structures. Although pure examples occur regularly, a lot of building structures are a mix of parallel and serial systems, with some crucial serial elements and some other parallel elements for which alternative load paths are present.

The significance of appreciating the presence of structural systems is that their failure probability may deviate considerably from the failure probability of individual components. For a serial system, the failure probability lies between the boundaries of the maximum failure probability of one component and the sum of the failure probabilities of all components (Eq. 3.7), depending on the extent of correlation between the failure probabilities of the individual components. Thus, the failure probability of the system may be much higher than that of an individual component.

$$\max P_{f_i} \leq P_f \leq \sum_{i=1}^n P_{f_i} \quad (3.7)$$

Whereas the failure probability of an individual member is the minimum failure probability in a serial system, it is the maximum failure probability in a parallel system. It occurs when failure of all components is fully correlated: failure of one component implies failure of the others. If the failure probabilities of components are completely independent, the minimum system failure probability is obtained through the product of the failure probabilities of the components (Eq. 3.8).

$$\prod_{i=1}^n P_{f_i} \leq P_f \leq \max P_{f_i} \quad (3.8)$$

It should be noted that the failure probabilities of the individual components in building structures are rarely completely independent.¹⁶ When the correlation is high, the failure probability of the system approaches that of a critical individual member, and thus that of a serial system. The extent of correlation is often also load type dependent.

6. General Limitations of the Probabilistic Approach

Although the probabilistic approach is a powerful tool in assessing and minimizing the risk of structures, it has several limitations.

(1) Firstly, for a full probabilistic analysis, it would be required that all relevant data concerning structural properties (e.g. material composition, material quality, geometry) and actions on that structure (self weight, static, semi-static, dynamic, shock/impact) are known, so that they can be described in accurate statistical functions. Usually, this is impossible. In practice, this is solved by using approximations and estimations based experience from the past and research. For common structural materials with a constant quality over large periods of time and well known behaviour combined with common static or semi-static actions, these approximations will work quite well. In structural engineering codes, the focus is on those kinds of actions, combined with a check of more infrequent actions like impacts of which the force can still be relatively well be assessed. But as a consequence, probabilities of failure are notional, i.e. they can be used for mutual comparison, but do not represent absolute values.¹⁷

(2) Secondly, many authors present observations to the effect that structural failures are hardly ever caused by the considered resistance being exceeded by the considered action(s). Instead, failure can be caused by a number of different deficiencies and errors, many of which are not even inside the domain of the structural engineer. Popovic and Nugent¹⁸ note that technical errors may be a lack of consideration for tolerances, design errors in structural details, unanticipated loading or insufficient stability during construction and a lack of communication between designer and builder. However, the British Standing Committee on Structural Safety has concluded that the prevailing political, financial, scientific, professional and industrial conditions may have an overriding effect.¹⁹ Menzies²⁰ remarks that especially financial pressure can cause errors to be made and warning signals to be ignored. Also, organisational failures may cause information not to arrive at the right person. All these influences can be grouped under human error, which, Schneider²¹ notes, is what essentially governs actual failure probabilities and is the reason why, again, failure probabilities should be regarded as

¹⁶ Failure of a component usually results in a load redistribution which influences the failure probability of the other elements.

¹⁷ Schneider, J., Ibid, p. 13.

¹⁸ Popovic, P.L., W.J. Nugent, *Common causes of structural collapses*, In: IABSE (Ed.), Proceedings of the International conference on Safety, Risk and Reliability – Trends in Engineering, Malta, 2001.

¹⁹ Standing Committee on Structural Safety, *Structural Safety 1996-99: Review and recommendations*, SETO, London, UK, 1999.

²⁰ Menzies, J., *Hazards and controlling the risks to structures*, In: IABSE (Ed.), Proceedings of the International Conference on Safety, Risk and Reliability – Trends in Engineering, Malta, 2001.

²¹ Schneider, J., Ibid, p. 13.

notional. Importantly, Matousek²² concludes that 13% of all errors could *not* possibly have been detected in advance.

Thus, for any structure, there is a *residual risk* which is the result of²³:

- Failure causes that could not have been known (objectively unknown risk),
- Failure causes that could have been known, but were unknown to the project parties (subjectively unknown risk),
- Unsuitable or wrongly applied counter measures,
- Consciously accepted (but not necessarily communicated) risk.

Together, these causes will be henceforth be referred to as '*unconsidered causes*', in the sense that they have not been incorporated in the formal probability analysis (even though they may have been recognized during the design process). Generally, the probability of unconsidered failure causes is deemed sufficiently small when small failure probabilities for considered loads are required. Failures usually only occur when multiple errors occur simultaneously, the probability of which thus lies in the order of the product of the probability of the individual errors.

(3) An important extra hidden safety measure stems from the margin between *failure* and *collapse*. Failure is usually defined as ceasing to perform an intended function.²⁴ However, failure does not necessarily mean collapse, which is the falling down or caving in of a structure through breakage and/or loss of stability. Rather, collapse is an excessive case of failure (Figure 3.10). This is a distinction that is usually not explicitly made (e.g. not in the codes). In common structural materials like steel and reinforced concrete, failure and collapse do not coincide upon overloading. Thus, $P_f \neq P_c$ (with P_c = the probability of collapse). This is most easily illustrated by a structural steel beam. In stress checks, the yield strength of steel is used. Thus, a steel element is considered to have failed (i.e. have reached its ultimate limit state) when it yields, although local yielding may occasionally be accepted as a settling mechanism. However, collapse will not occur until the ultimate (tensile) stress is reached. Depending on the steel quality and the (detail) design, the ultimate strength of steel may range from 100 to 150 % of the yield strength. Even if the nominal yield strength is exceeded (failure), the consequences will most likely remain limited because of this reserve. Similar observations, though not as obvious, hold for reinforced concrete because it also heavily relies on the plastic behaviour of steel.

(4) Finally, to be able to determine structural element dimensions based on their failure probability, the consequence constituent has to be considered as a given²⁵. In order to obtain constant risk levels, the magnitude of the reliability requirement (usually formulated as meeting a minimal reliability index β) depends on the expected number of

²² Matousek, M., Schneider, J., *Untersuchungen zur Struktur des Sicherheitsproblems bei Bauwerken*, Institut für Baustatik und Konstruktion an der ETH Zürich, Bericht no. 59, Switzerland, 1976, as quoted in: Schneider, J., *Ibid*, p. 15.

²³ Schneider, J., *Ibid*, p. 15.

²⁴ A more specific definition is presented in Chapter 6, Section 3.2., in relation to a newly formulated integrated safety approach to structural glass elements.

²⁵ Otherwise, the risk function would have two unknowns, and thus become unsolvable.

casualties in case of *collapse* of the structure. In structural engineering codes, the expected number of casualties is determined by a categorization of building types.

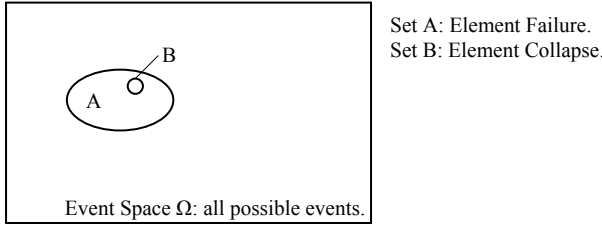


Fig. 3.10 The probability of *collapse* of a element does not coincide with its *failure* probability. Rather, collapse is an excessive case of failure, with significantly smaller probability in common structural materials.

The probability analysis, however, usually does not focus on the probability of collapse of the structure, but rather on the failure probability of an individual element. The relation between probability and consequence is thus indirect, as at least two intermediate stages between member failure and structural collapse can be recognized (Figure 3.11).

1. Failure of a member does not necessarily mean collapse of that member (see above); $P_{f,member} \neq P_{c,member}$.
2. Collapse of a member obviously does not necessarily mean collapse of the structure; $P_{c,member} \neq P_{c,structure}$. As explained in Section 2.4, the relation between these collapse probabilities is highly dependent on the structural system and may vary from the order of the product to the order of the sum of individual failure probabilities.

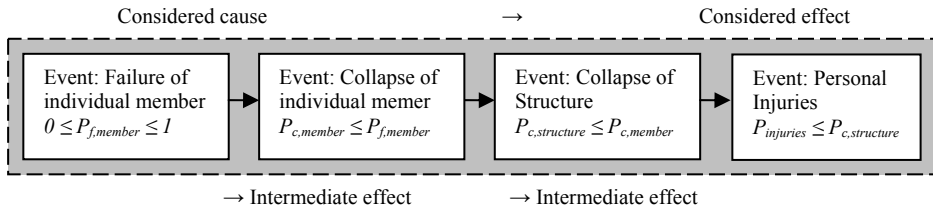


Fig. 3.11 The relation between the considered cause (of which the probability is calculated) and considered consequence in structural safety engineering is indirect. At least two intermediate events can be identified which are certainly not fully correlated with the failure event.

It should also be noted that the number of casualties is in itself a stochastic variable, as, for instance, the number of people within the structure is not constant.

The result of all these considerations is that the reliability requirements towards individual elements (maximum allowable $P_{f,element}$) in different structures may be consistent, but the effective probability of injuries and thus the risk level of various structures is not.

7. Extension of the Probabilistic Approach

7.1. Recognition of Unknown Actions and Measures against Progressive Collapse

Early morning May 16th 1968, just two months after the completion, disaster struck a 23-story housing block known as Ronan Point, in Newham, East London. A relatively small gas explosion in a corner apartment on the 18th floor blew out a load bearing wall, and all walls above it came crashing down, destroying the corner apartments of the building over the entire height. Four people were killed; seventeen injured.²⁶

The Ronan Point incident clearly illustrates why a probabilistic check of the resistance of structural members against codified static, semi-static and incidental loads is insufficient to ensure an appropriate safety level for the complete building structure. On the one hand, there was a failure cause (gas explosion) outside the scope of considered possible actions.²⁷ On the other hand, failure of the member (a load bearing wall) not only meant collapse of the element but even collapse of a significant part of the building. Indeed, the collapse raised awareness in the UK for the problem of progressive collapse and measures to avoid it were incorporated into the British Standards in the early 1970's.

Basically, two strategies can be followed to try to avoid calamities as the one at Ronan Point. Following the lay-out of Figure 3.12, there can be a cause-oriented approach which aims at (more actively) tracing hazards and hazard scenarios, e.g. by requiring a (full) risk analysis rather than (just) dimensioning according to codes. Consequently, the identified scenarios can be treated in one of the ways mentioned earlier: eliminate, bypass, control, overcome, accept.

Another strategy is a consequence-directed approach, i.e. create an extra safety margin between the failure probability of an element and the collapse probability of the structure, i.e. avoid progressive collapse after failure and collapse of the element. As there usually already is a margin between failure and collapse of the element extra measures in that step are generally not considered.

Following some general sensible structural design rules can significantly decrease the probability of progressive collapse. These can include²⁸:

- Providing sufficient reserve capacity in individual members and redundancy in the structure (i.e. alternative load paths),
- Providing sufficient ductility, which allows alternative load paths to be activated before collapse of an individual member, thus achieving higher total load carrying capacity.
- Minimizing the number of serial elements in the system.

A full probabilistic analysis of the structural system would be required to quantify the effects of such measures, but this is usually omitted.

²⁶ www.wikipedia.org, dd 27.07.2008.

²⁷ This is an assumption by the author. However, if a gas explosion of this kind *has* been considered in the design, the possible consequences have obviously been overlooked (the only other option, that it has been accepted as an unavoidable risk seems highly unlikely), which could be classified as a human error (which is in itself an unconsidered failure cause).

²⁸ Vrouwenvelder, A.C.W.M., Vrijling, J.K., Ibid, p. 4-22.

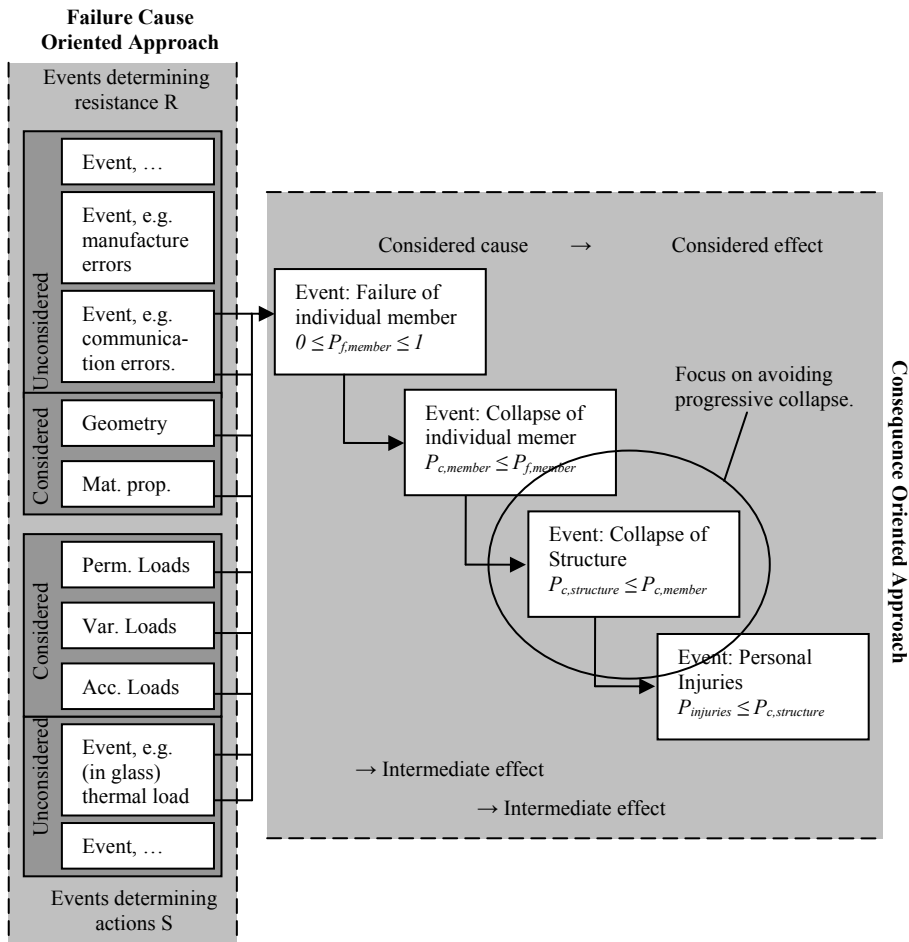


Fig. 3.12 Extension of the probabilistic safety approach for structural members with failure cause oriented measures aiming at avoiding failure through unknown causes by extensive risk inventarization and consequence oriented measure aiming at creating a margin between member collapse and structure collapse, i.e. avoiding progressive collapse.

Both the cause- and the consequence-oriented approach are valuable in reducing the risk of structures. However, considering the fact that it is impossible to avoid all failures completely because not all failure causes can reasonably be foreseen and human nature implies people will keep making errors, especially a consistent consequence-oriented approach to avoid progressive collapse is of vital importance. This approach assumes that the possibility of failure and collapse of an element, although unfortunate, has to be accepted. The structural consequences, however, should remain in proportion to the original failure cause, e.g. a local gas explosion should not result in collapse of a significant part of the building structure.

An additional advantage of this approach is the fact that the damage will provide a clear warning signal of the deteriorated state of the structure. This should lead to extra

counter measures to avoid further damage and collapse. The effect of failure cause related measures will be less visible. Unfortunately, *before* failure a structure of compromised quality is usually not visibly discernable²⁹ from a structure in pristine condition.

7.2. Structural Robustness and Other Properties

Extending the common probabilistic element based safety approach with system related measures to avoid progressive collapse, is a field which still is under development. Starossek³⁰ notes ‘there is neither a uniform theory of progressive collapse nor any agreement on terms and nomenclature.’ He attempted in several publications³¹ to come to an agreed set of definitions of terms such as robustness, collapse resistance, continuity, damage tolerance, ductility, integrity, redundancy, and vulnerability.

For this research, *robustness* and *redundancy* are the most important concepts. Several similar definitions can be found for robustness in literature. Starossek³² defines robustness as ‘insensitivity of a structure to local failure’, and considers robustness ‘a property of the structure alone and independent of the possible causes and probabilities of the initial local failure.’ A similar description can be found with Biondini et al.³³ who describe robustness as ‘the ability of the system to suffer an amount of damage not disproportionate with respect to the causes of the damage itself.’ In these publications, robustness is considered a *property of the structure alone* – regardless of action or defect. Maes et al.³⁴ give another view. They present definitions of robustness from several fields of engineering and generally conclude that robustness indicates a tendency of a system to remain stable under perturbations. Contrary to the previously mentioned authors, they require robustness to be defined for ‘specified performance objectives for specified perturbations.’ Thus, they hold the term robustness is idle without a cause consideration. Actually, their definition is close to what Starossek defines as *collapse resistance*: ‘Insensitivity of a structure to accidental circumstances, which comprise unforeseeable or low-probability events.’

This discussion touches upon a fundamental difficulty in the definition of a descriptor for the resistance of a structure against unconsidered failure causes. In order to assess and compare the reaction of a structure to unforeseeable events, it seems very useful to introduce robustness independently of failure causes – just as strength for instance, is a property independent of the cause of the load. Furthermore, an important *raison d’être* for robustness requirements is to deal with unknown failure causes. Thus, it seems a definition of robustness for specified perturbations misses the point.

However, in reality the failure behaviour of a structure *directly depends* to greater or lesser extent on its failure cause. This rightful conclusion by Maes et al. is supported by

²⁹ Observation made in Chapter 5 by one of the interviewees, Graham Dodd, see there.

³⁰ Starossek, U., Haberland, M., *Measures of Structural Robustness – Requirements & Applications*, Proceedings of the Structures 2008 Congress: Crossing Borders, of the ASCE, Vancouver, April, 2008.

³¹ Besides the paper mentioned in the previous footnote, also: Starossek, U., *Progressive Collapse of Structures: Nomenclature and Procedures*, Structural Engineering International, No. 2, 2006, pp. 113 – 117.

³² Starossek, U., Haberland, M., *Ibid.*

³³ Biondini, F., Frangopol, D.M., Restelli, S., *On Structural Robustness, Redundancy and Static Indeterminacy*, Proceedings of the Structures 2008 Congress: Crossing Borders, of the ASCE, Vancouver, April, 2008.

³⁴ Maes, M.A., Fritszons, K.E., Glowienka, S., *Structural Robustness in the Light of Risk and Consequence Analysis*, Structural Engineering International, No. 2, 2006, pp. 101 – 107.

experimental testing on glass beams with various failure inducing methods, presented in Appendix E. A robustness descriptor will *always*, implicitly or explicitly, have to include an assumption about the failure cause.³⁵

The further claim that robustness should be defined for specified performance objectives, also seems very sensible. Maes et al. introduce three robustness parameters, each related to a specific performance objective as presented in Table 3.1.

Table 3.1 Structure robustness parameters according to Maes et al.³⁶

Performance Objective	Robustness Parameter	Short Description
Maintaining Sufficient System Structural Resistance	$R_1 = \min_i \frac{RSR_i}{RSR_0}$ (3.9a)	R_1 is the smallest value of the reserve strength ratio (RSR) of the system with member i impaired over the RSR of the system with no impaired members.
Maintaining Sufficient System Reliability	$R_2 = \min_i \frac{P_{s0}}{P_{si}}$ (3.9b)	R_2 is the smallest value of the system failure probability of the undamaged state over the failure probability of the system with member i impaired.
Containing Severe System Consequences	$R_3 = \frac{1}{H}$ (3.9c)	R_3 is a more complex term including the severity of the consequences of a failure, for which H , the ‘tail heaviness of the log-exceedence curve’ is a measure. This descriptor can be useful if the system ‘can not easily be expressed as an assembly of members or components.’ For a system in which the consequences are approximately linear to the hazard intensity, $R_3 \approx 1$. In a robust structure, the consequences increase less than the hazard intensity, thus $R_3 < 1$. For a non-robust structure, the consequences quickly exceed the hazard intensity and $R_3 > 1$. The complexity of R_3 lies in the fact that all consequences have to be quantified along with a statistical distribution.

Starossek³⁷ provides an overview of several methods that have been developed from 1995 until 2008. He concludes that ‘most of the approaches lead to performance-based measures defined by the change in structural behaviour due to an assumed initial local failure and quantified by probabilistic or deterministic comparative values.’ According to him ‘some measures require the determination of collapse scenarios, which is numerically challenging’. He furthermore notes that ‘no approach has shown itself to be clearly superior.’

Contrary to robustness, the term *redundancy* is not used as an overall structure performance indicator. Possibly as a result it seems less disputed. According to Starossek³⁸ it ‘refers to the multiple availability of load-carrying components or

³⁵ In the Integrated Approach to Structural Glass Safety, presented in Chapter 6, this is incorporated by requiring specification of a ‘governing impact’, after which residual resistance levels have to be determined.

³⁶ Maes, M.A., Fritzsos, K.E., Glowienka, S., Ibid.

³⁷ Starossek, U., Haberland, M., Ibid.

³⁸ Starossek, U., Haberland, M., Ibid.

multiple load paths which can bear additional loads in the event of a failure.’ Biondini et al.³⁹ define redundancy as ‘the ability of the system to redistribute among its members the load which can no longer be sustained by some other damaged members.’ Thus, redundancy can be a means to achieve robustness.⁴⁰

7.3. Extension of the Probabilistic Approach in Dutch and European Codes

The NEN 6700, in clause 5.3.3, states that collapse of a single component should not lead to excessive damage. It specifies that damage should remain localized after collapse of a part of the structure and that essential parts of the main load bearing structure should have an extremely small probability of collapse by taking preventive measures and paying specific attention to the quality of the design and construction process. Thus, this clause goes beyond the general probabilistic approach to structural members to include both a cause- and a consequence-oriented approach.

The material codes also contain consequence-oriented measures, but they are usually not clearly recognizable as such. They turn up as design or detailing rules that aim at allowing the supposed plastic behaviour of a material to actually develop and, by doing so, avoiding brittle failure. Besides the general requirements formulated in clause 5.3.3 in NEN 6700, the background to these rules is unclear and the desired behaviour not explicitly formulated. It is therefore questionable if they are consistent, especially when considering different materials.

With regard to the consequences of element failure, the NEN-EN 1990 is more extensive. In 4(P) under clause 2.1, it is stated that a structure should not be disproportionately damaged by explosion, impact or human error. Identifying human error as a cause of damage is important because it is virtually impossible to describe by probabilistic means. Not only is there not enough data available, it is also unlikely that the effects of human error would fit a known statistical distribution – even though there may be some consistency in the mistakes we make. Sub clause 5(P) names several strategies that can be deployed to limit or avoid potential damage. Avoiding as far as possible structural systems that can collapse without *warning*⁴¹ is one of them.

Although being more specific than the Dutch codes, the requirements in the NEN-EN 1990 are still quite generally formulated. However, part 7 of Eurocode 1 (NEN-EN 1991-1-7⁴²), deals with the structural resistance both to identified accidental actions, like vehicle impact and explosions, and unspecified failure causes in more detail. Especially the acceptance in the code that ‘unspecified failure causes’ may occur, is important, because it calls for consequence-oriented safety measures. And indeed, clause 3.3 of NEN-EN 1991-1-7 describes strategies to be applied to the design of building structures in order to limit the extent of localised failure of whatever cause: key structural elements should be designed to withstand a (large) accidental action, and the structure should be designed in a way that failure of a local member will not endanger

³⁹ Biondini, F., Frangopol, D.M., Restelli, S., Ibid.

⁴⁰ Chapter 6, Section 4.3 provides another, more specific definition of redundancy, specifically developed for the integrated safety approach (which is presented in Chapter 6).

⁴¹ Quite remarkably, the value in terms of safety of warning signals of damaged structures is rarely treated in publications on the subject (not in any of the papers studied by the author).

⁴² Nederlands Normalisatie Instituut, NEN-EN 1991-1-7 Eurocode 1: Belastingen op constructies – Deel 1-7: Algemene belastingen – Buitengewone belastingen: stootbelastingen en ontploffingen, Delft, 2006.

the stability of the structure or a significant part of it. Design and detailing rules should provide an acceptable robustness for the structure.

The informative annex A of NEN-EN 1991-1-7 gives a guideline to design for consequences of localised failure in buildings from an unspecified cause. It categorizes building types into consequence classes (CC) CC1, CC2a, CC2b and CC3, depending on the severity in case of collapse; 1 is low consequence, 3 is high consequence). The extent of the measures that should be taken to avoid disproportionate collapse are dependent on consequence class and range from no further measures (CC1), to a complete systematic risk assessment (CC3). Of course, it can be debated what amount of damage can be accepted, and when damage will be 'disproportionate'. NEN-EN 1991-1-7 proposes a limit of 15% of the floor area or 100 m², whichever is smaller, of localised damage caused by failure of a structural column on each of the two adjacent storeys. It furthermore provides guidelines for horizontal and vertical structural tyings to ensure the robustness of the structure.

The quantitative requirements with regard to the consequence of a local failure are still relatively limited compared to all requirements regarding the probability of a failure. Nonetheless, contrary to the Dutch codes, the European codes provide more explicit general requirements on how structural system related requirements should be met. However, the requirements are still predominantly formulated in terms of design rules, rather than quantifiable structure characteristics, for which the methods are still under development.

8. Acceptability of Risk

The fact that safety can not be absolute implies there is always a level of (residual) risk to which man is exposed. Part of the responsibility of the (structural) engineer is to reduce the risk of structures to a level that is acceptable to its owners, users, and society in general. Estimating what level of risk is acceptable, however, is a very complex multidisciplinary undertaking, involving psychological, sociological, political, economical, and other factors.

First, there is an authority issue: who determines how much risk is acceptable? As it is, in the end, a subjective and personal choice of how much risk one is willing to run, there may be significant differences in risk allowance between individuals or groups within a society. In (Western) democracies, this is formally solved by minimum requirements laid down in codes, enforced by approved law. However, these codes are formulated by a relatively small group of specialists, who usually are not a part of the democratic system.⁴³ The client of a project can require more extensive safety measures. The user, however, usually can not (unless he is also the client); his interests are supposedly protected by society.

Next, it is actually very hard to grasp the meaning of the risk function constituents probability and consequence, especially in cases of very small probabilities and very high consequences. A probability of 10⁻⁴ year⁻¹ will most likely be perceived as 0. It is

⁴³ I.e. they not elected by vote. The author does not wish to imply this would be desirable or even possible. It is just to indicate the relativity of the risk establishing authority.

also questionable if the meaning of, for instance, a serious flooding can be fully understood on forehand.

Risk evaluation by laymen usually depends on the consequence rather than the probability. Thus, large consequences with low frequencies are deemed less acceptable than small consequences with higher frequencies, as illustrated by the level of media attention to large consequence events. Actually, psychometric field research⁴⁴ has shown individuals will base a risk evaluation primarily on the possible consequence, rather than the probability.⁴⁵

An important factor in the acceptance of risk is the (perception) of avoidability. The easier it is to avoid a certain consequence, the less risk is acceptable. Thus, people are also willing to run much higher risks if they do so voluntarily than they would if they were forced to run a risk. Linked to this is the fact that higher risks are accepted when an individual has direct influence on the events, for instance in driving.

People spend a lot of time in or near buildings, usually not completely voluntary, and they have no influence on the quality of the structure. Furthermore, buildings are not perceived as overly complicated (like e.g. airplanes) or difficult to understand; we have several thousands of years experience with them. Therefore, only very low levels of risk are accepted for building structures. This is reflected by high reliability factors (Sections 2.5 and 2.6) in structural engineering codes, even though we have seen they do not directly relate to consequences; a fact that is gaining increasing attention in the field of structural safety engineering (Section 4).

Several methods exist to estimate the risk acceptance levels of individuals and society.⁴⁶ An elaborative study of that, however, falls outside the scope of this research. Rather, as the acceptable level of risk for glass structures, the remainder of this research understands a level of risk that is comparable to the risk level that should be achieved for other structures composed of more common structural materials such as steel and reinforced concrete.

⁴⁴ Vlek, C.A.J., Stallen, P.J.M., *Beoordeling van riskante activiteiten: een psychometrische analyse*, De Ingenieur, 29 November 1979; as quoted in Vrouwenvelder & Vrijling, *Ibid.* p.8-3.

⁴⁵ This is, perhaps, a reason for the popularity of gambling and lotteries.

⁴⁶ Vrouwenvelder and Vrijling provide an overview in: Vrouwenvelder & Vrijling, *Ibid.* Chapter 8.

4 Glass Failure

Contrary to what the simple linear nominal stress-strain curve of a glass piece loaded to failure suggests, its failure behaviour is quite complex. It depends on surface flaws, of which various types may be present. These flaws are not static, but rather change characteristics over time, depending on temperature, moisture, and present tensile stress levels. In this Chapter, first some theoretical models of glass fracture are introduced. Subsequently, the dimensioning methods used in glass engineering are briefly presented, followed by an overview of typical glass failure causes. As an extension of the general limitations presented in Chapter 3, specific shortcomings of a probabilistic approach to structural glass elements are discussed. The additional safety requirements in several codes and guidelines are presented. Finally, their general validity and suitability is analysed.

1. Fracture Strength

1.1. Fracture Mechanism

Despite its linear elastic stress-strain behaviour, glass failure is a complex phenomenon. The fracture process is still a subject of debate within the glass science community.¹ According to Orowan², the theoretical failure stress σ_m of a material is determined by the energy required to create two new surfaces (on both sides of an appearing crack) as in Eq. (4.1).

$$\sigma_m = \sqrt{\frac{E v_s}{w_o}} \quad (4.1)$$

E	Young's Modulus	= 70 000 MPa
v_s	Fracture Surface Energy	≈ 2 - 4 J/m ²
w_o	Atom Equilibrium Spacing	≈ 0.2 nm

However, with the values mentioned above, this results in a theoretical failure stress of 32 000 N/mm², whereas the characteristic bending tensile strength of float glass obtained from practical experience and experimental testing (see Chapter 1, Section 5.4) is only 45 N/mm². This extreme difference was attributed by Griffith³ to randomly distributed microscopic flaws in the glass surface, which henceforward became known as Griffith flaws, acting as stress concentrators. Earlier, based on experiments with notched steel specimens, Inglis⁴ had derived Eq. (4.2)⁵ as an approximation of the stress

¹ See, for instance, the 3rd International Workshop on Flow and Fracture in Advanced Glasses (FFAG), Pennsylvania State University, USA, October 2005.

² Quoted in many publications, for instance: Shelby, J.E., Introduction to Glass Science and Technology, 2nd Edition, The Royal Society of Chemistry, Cambridge, United Kingdom, 2005, p. 191.

³ Griffith, A.A., *The Phenomenon of Rupture and Flow in Solids*, Philosophical Transactions of the Royal Society of London, Vol. A221, 1921, pp. 163-198.

⁴ Inglis, C.E., *Stresses in a plate due to the presence of cracks and sharp corners*, Transactions of the Institution of Naval Architects, 55 (219), 1913, as quoted in: Haldimann, M., Luible, A., Overend, M., Structural Use of Glass, Structural Engineering Documents 10, IABSE, Zurich, Switzerland, 2008.

concentration around the tip of a crack. The ratio of the crack depth over the crack tip radius a/ρ determines the stress concentration σ_{tip}/σ_E .

$$\sigma_{tip} = 2\sigma_E \sqrt{\frac{a}{\rho}} \quad (4.2)$$

a Crack depth (for surface cracks, or half the crack depth for volume cracks)

ρ Crack tip radius

Because glass can not redistribute peak stresses originating from the flaws, through local plastic flow or any other mechanism, glass failure is in fact governed by their presence and behaviour.

The significance of flaw-induced stress concentrations initiated the development of Fracture Mechanics. Rather than traditional structural analysis, which uses two variables to determine failure (i.e. applied stress and yield or tensile strength), in Fracture Mechanics three parameters are used (Figure 4.1): applied stress, flaw size (or geometry), and fracture toughness. Fracture toughness replaces yield or tensile strength as the material property. The importance of an additional flaw descriptor (a/ρ) can be readily seen from Eq. (4.2).

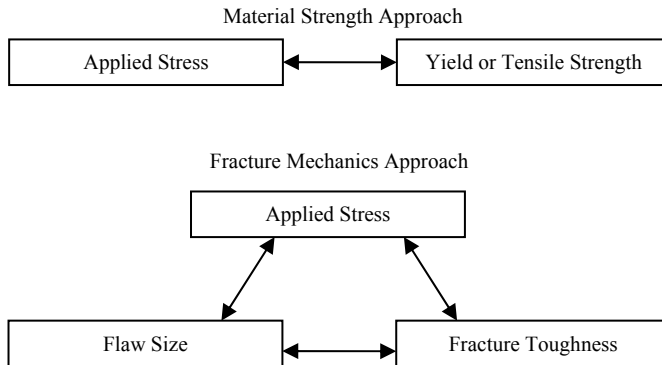


Fig. 4.1 Traditional strength of materials approach (top) and fracture mechanics approach (bottom) to design.⁶

The material's fracture toughness can be expressed in two alternative criterions, *strain energy release* and *stress intensity*, which are equivalent for linear elastic materials. They are based on two different approaches to fracture analysis.

⁵ It is, actually, questionable if this formula derived from steel specimens with macroscopic notches is valid for the microscopic flaws in glass. Nevertheless, it gives a good impression of the effect of cracks on stress distributions.

⁶ After Figure 1.7 in: Anderson, T.L., *Fracture Mechanics, Fundamentals and Applications*, 3rd Edition, CRC Press, Taylor & Francis, Boca Raton, USA, 2005.

1.1.1. The Strain Energy Release Rate-Criterion to Glass Failure

The *energy approach* was first suggested by Griffith⁷ and later on developed by Irwin⁸. According to this approach, to create a crack of a certain size, a total amount of fracture energy is needed equal to the sum of all the energies required to separate all the individual molecule bonds through the crack surface area. The fracture energy required per unit of crack area is the material property *fracture surface energy* ν_s [J/m²]. In a plastic material, further energy is required for plastic flow (i.e. dislocation slip). This is ν_p [J/m²], and its magnitude is strain rate dependent. Thus the total energy required to create new surface area is $\nu = \nu_s + \nu_p$. In glass however, $\nu_p = 0$, and is therefore further ignored. Since a crack generates two surfaces, the required fracture energy is the fracture surface energy times *twice* the product of the crack length and material thickness. For volume cracks and surface cracks, this yields Eq. (4.3a) and Eq. (4.3b), respectively (Figure 4.2).

The total amount of potential energy in a system, consisting of the inner elastic strain energy and the outer applied force displacement is dependent on crack size⁹. Thus, the creation of fracture surface is related with energy consumption. To obtain a criterion for crack growth, Griffith formulated this system in terms of an energy balance as Eq. (4.4)¹⁰, known as the *Griffith energy balance*.

$$U_{pot,system} = U_0 - U_a - U_v \quad (4.4)$$

$U_{pot,system}$ The total potential energy of the system

U_0 The elastic strain energy of the uncracked plate.

U_a The decrease in the elastic strain energy caused by introducing the crack in the plate.

U_v The increase in the elastic-surface energy caused by the formation of the crack surfaces.

When more energy is available than required for the creation of new surfaces, the system becomes unstable (crack growth accelerates rapidly until the terminal velocity, governed by the speed of elastic waves, is reached; 1 500 – 2 500 m/s for soda lime silicate glass¹¹). To account for this situation, Mott¹² expanded Eq. (4.4) by a constituent for kinetic energy U_K into Eq. (4.5). This term, however, is irrelevant for a failure criterion, as it only comes into play after the system has lost its stability.

$$U_{pot,system} = U_0 - U_a - U_v - U_K \quad (4.5)$$

⁷ Griffith, A.A., Ibid.

⁸ Irwin, G.R., *Onset of Fast Crack Propagation in High Strength Steel and Aluminium Alloys*, Sagamore Research Conference Proceedings, Vol. 2, 1956, pp. 289 – 305. As quoted in: Anderson, T.L., Ibid.

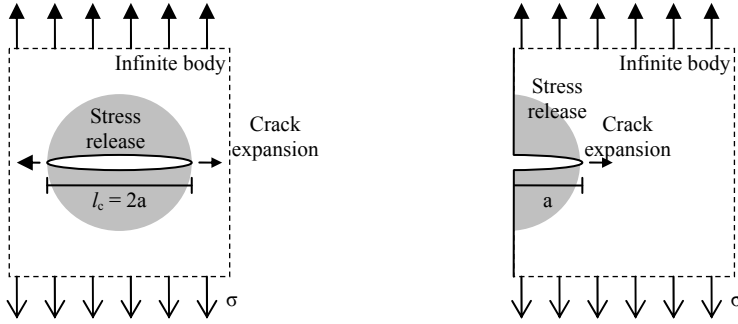
⁹ A larger crack means more surface energy, thus less potential energy in system and vice versa.

¹⁰ Jireh J. Yue, Energy Concepts for Fracture.

http://www.sv.vt.edu/classes/MSE2094_NoteBook/97ClassProj/anal/yue/energy.html.

¹¹ Haldimann, M., Luible, A., Overend, M., *Structural Use of Glass*, Structural Engineering Documents 10, IABSE, Zurich, Switzerland, 2008, p. 71.

¹² Mott, N.F., *Brittle Fracture in Mild Steel Plates*, Engineering 165 (16), 1948. As quoted in: Haldimann, M., Luible, A., Overend, M, Ibid.



Crack area :

$$A_{vol-crack} = l_c t = 2at$$

Crack surface energy :

$$U_v = 2l_c t \nu_s = 4at \nu_s \quad (4.3a)$$

Strain energy release around crack:

$$U_a = \frac{1}{2}(\sigma^2 / E)\pi a^2 t \quad (4.7a)$$

$$\pi a^2 t$$

$$\frac{1}{2}(\sigma^2 / E) = \frac{1}{2}\epsilon^2 E = \chi$$

Volume released of strain energy

Elastic Strain Energy Density, i.e. the Elastic Strain Energy stored per unit volume; [Nmm/mm³] = [N/mm²].

$$G_c = \frac{\pi \sigma_f^2}{E_s} a_c = 2\nu_s \quad (4.8)$$

Crack area :

$$A_{surf-crack} = at$$

Crack surface energy :

$$U_v = 2at \nu_s \quad (4.3b)$$

Strain energy release around crack:

$$U_a = \frac{1}{4}(\sigma^2 / E)\pi a^2 t \quad (4.7b)$$

(since $A_{vol-crack} = 2A_{surf-crack}$, the critical strain energy release rate $dU_a/dA = G_c$ of volume and surface cracks is equal)

Fig. 4.2 Volume crack, surface crack and required fracture energy.

If there are no cracks ($U_a=0$; $U_v=0$), the potential energy in the system is equal to the elastic strain energy as calculated by mechanics¹³ $U_{pot,system} = U_0$. Now, a crack can be introduced. The energy required for this (U_v) is provided by the elastic strain energy release of the area around the crack (U_a). Therefore $U_a = U_v$.

For a crack to keep growing it is required the elastic strain energy release provided by the area around the crack, is equal to or greater than the increase in surface energy per unit surface area of crack that is created (Eq. 4.6).

$$\frac{dU_a}{dA} \geq \frac{dU_v}{dA} \quad (4.6)$$

In this equation, $dU_a/dA = G$ is the *strain energy release rate*, i.e. the amount of strain energy that is released during crack growth per unit area of increase of crack length.¹⁴

¹³ See also Chapter 9.

¹⁴ It should be noted that the term ‘rate’ does not mean ‘speed’ in this case; it is not related to time. Rather it refers to the amount of energy released per crack area.

The increase in surface energy per unit area of increase of crack length is represented by dU_v/dA .

The energy required to create fracture surface area is provided by the elastic strain energy release of the area around the crack. Thus, the question whether a crack can grow depends on the amount of strain energy that can be released by the area around the crack. According to Cottrell¹⁵, the area being relieved of elastic strain energy around a crack is approximately circular with a radius equal to the crack length a (or half length a with a volume crack). The elastic strain energy in this area can be calculated with Eqs. (4.7a) and (4.7b).

From Eqs. (4.3), (4.6), and (4.7), it can be deduced that the critical strain energy release rate G_c which is the boundary condition for failure¹⁶, is a material property dependent on the Young's Modulus E or surface energy ν of the material and a combination of fracture stress σ_f and critical crack length a_c , as in Eq (4.8). Thus, G_c is the first fracture toughness criterion.

1.1.2. The Stress Intensity-Criterion for Glass Fracture

Where the energy method is related to stresses indirectly, through the dependence of the stored strain energy on the exerted stress, the stress intensity approach is based on stress considerations directly. The stresses σ_{xx} , σ_{yy} , and τ_{xy} at a Mode I-loaded crack tip are proportional to a single constant called the stress intensity factor K_I , which is determined by the nominal stress σ and the crack (half-)length a , Eq. (4.9)¹⁷. For cracks deviating from the ideal shape, a shape factor Y has to be added, which ranges from $Y = 0.637$ to 0.713 for half-penny shaped cracks in a semi-infinite specimen often assumed in glass.¹⁸ Failure occurs when K_I exceeds the critical stress intensity K_{Ic} , which is related to the strain energy release rate through Eqs. (4.10a) and (4.10b) for plane stress and plain strain conditions, respectively.

$$K_I = Y\sigma\sqrt{\pi a} \quad (4.9)$$

$$G_c = \frac{K_{Ic}^2}{E}; G_c = \frac{K_{Ic}^2(1-\nu^2)}{E} \quad (4.10a); (4.10b)$$

Haldimann et al.¹⁹ present an overview of experimentally determined critical stress intensity factors for soda-lime silicate glass and indicate a value of $K_{Ic} = 0.75 \text{ MPa}\sqrt{\text{m}}$ is sensible for all practical purposes. With $E = 70\,000 \text{ MPa}$, the critical strain energy release rate then becomes $G_c = 8.0 \text{ J/m}^2$ and the fracture surface energy $\nu_s = 4.0 \text{ J/m}^2$.

¹⁵ A.H. Cottrell, *The Mechanical Properties of Matter*, Robert E. Krieger Publishing Company, Huntington NY, USA, 1981, p. 345.

¹⁶ For $G = G_c$, crack growth is stable. When, $G > G_c$ crack growth becomes unstable and accelerates.

¹⁷ Refer to Fracture Mechanics literature for the derivation of the stress intensity factor, e.g. Anderson, T.L., *Ibid.*

¹⁸ Haldimann, M., Luible, A., Overend, M., *Ibid.*, p. 56.

¹⁹ Haldimann, M., Luible, A., Overend, M., *Ibid.*, p. 57.

1.2. The Problem of Glass Surface Flaws

For linear elastic materials, both the strain energy release and the stress intensity approach are equivalent. They both introduce the flaw depth a as an essential variable in the determination of a failure criterion. Thus, to predict failure of a glass sheet, the properties of its surface flaws need to be determined. For two reasons, this has caused considerable difficulty in predicting the strength of individual glass sheets:

- There is a certain distribution of non-identical cracks over the glass surface. Various types of cracks can be recognized, but even within one type, they are not identical, but rather (only) similar (i.e. statistically distributed).
- Cracks in glass are not static. Their behaviour and geometry change with temperature, humidity, time, and presence of tensile stresses.

Both these issues, the non-identical and non-static character of flaws, still cause considerable debate concerning their nature. Consequently, there is still substantial argument as to how they should be processed to arrive at a satisfying fracture criterion.

1.2.1. Non-Identical Character of Glass Surface Flaws

Although it is generally accepted glass failure is (almost always) the result of surface flaw-induced stress concentrations, experimental data²⁰ indicate there are different types of flaws leading to different failure strengths. Veer²¹ suggests to discriminate between 3 to 5 areas on the surface of a glass sheet, Figure 4.3, each with their typical flaw type(s). This view is supported by the repeatedly found²² difference in glass strength between specimens loaded in their flat surface versus specimens loaded on their edge (i.e. sheets tested in bending while lying flat versus sheets tested while standing up). The strength of standing sheets may be only 0.7 times that of sheets laying flat.²³ This is usually attributed to the presence of a critical type of flaw in the glass sheet edge, different from the ones in the face surface. Considering the different manufacturing and processing treatments to which these different areas are exposed, such a distinction between areas and their flaw types seems convincing.

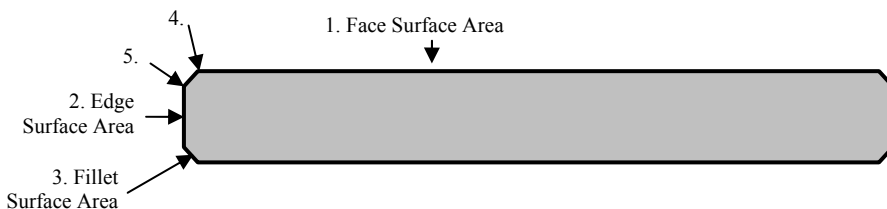


Fig. 4.3 Suggested surface areas around a glass sheet, each with its own type(s) of flaws.

²⁰ Veer, F.A., Louter, P.C., Bos, F.P., Romein, T., Ginkel, H. van, Riemsdag, A.C., *The Strength of Architectural Glass*, Proceedings of the Challenging Glass Conference, IOS Press, Delft, the Netherlands, May 2008.

²¹ Dr. F.A. Veer, in private communication.

²² See for instance: Hess, R., *Glasträger*, vdf Hochschulverlag AG an der ETH Zürich, Switzerland, 2000; or: Veer, F.A., Bos, F.P., Zuidema, J., Romein, T., *Strength and Fracture Behaviour of Annealed and Tempered Float Glass*, Proceedings of the 11th International Conference on Fracture (ICF), Turin, Italy, 2005.

²³ See also discussion on calculable stress in beams of the All Transparent Pavilion: Section 2.3.3 of Chapter 2.

Nevertheless, glass failure models are usually limited to considering the face surface area only (eliminating effects from other areas by ring-on-ring tests). Then, generally, two types of flaws are distinguished. *Griffith flaws* are distributed over the face surfaces of glass sheets and originate during solidification in the manufacturing process.²⁴ They are assumed to be randomly distributed over the face surface in a way that can statistically be described with a two-parameter Weibull distribution. The shape parameter m_0 and the scale parameter θ_0 ²⁵ mathematically describe the so-called *random surface flaw population* (RSFP).

Besides the relatively small, homogeneously spread Griffith flaws, a glass piece may also suffer *accidental flaws*. The first of these flaws usually already appear in the glass sheet edge when the glass ribbon is cut at the end of the float glass production line. However, accidental flaws can originate from numerous other sources during the glass sheet life time, such as debris, accidental scratching, impact, etc. Accidental flaws are larger than Griffith flaws²⁶ and their distribution over the glass edge and surface can not be described by statistical functions. Therefore, when assuming an accidental flaw to be governing failure, *single surface flaw* (SSF) models are used, applying a specific design flaw which is assumed to be caused by some specific incident.

1.2.2. Non-Static Character of Glass Surface Flaws

Time-dependency of glass strength was already reported in 1899 by Grenet.²⁷ It decreases from about 70 MPa for very short duration loads to approximately 10 MPa for permanent loads. This phenomenon, known as *static fatigue* or *stress corrosion*, has later been attributed to alterations of the surface flaws in glass, which in turn influence the stress field around the crack tips. Eq. (4.11) is generally quoted to represent the ratio between time-to-failure of two identical glass pieces subjected to two different magnitudes of (tensile) stress. A crack growth constant of $N_t = 16$ was found by Evans,²⁸ and used in many methods to determine glass strength.

$$\frac{t_1}{t_2} = \left(\frac{\sigma_1}{\sigma_2} \right)^{N_t} \quad (4.11)$$

According to the mostly accepted²⁹ explanation, a stress-enhanced reaction between water (vapor) and the silicium-oxide network, represented by Eq. (4.12), Figure 4.4, alters the geometry of flaws present in the glass surface.³⁰

²⁴ A reason for their existence was not encountered in literature studied by the author.

²⁵ These parameters refer to the properties of the Weibull curve; not to the shape or scale of the flaws themselves. Belis presents methods to calculate these parameters: Belis, J., *Kipsterkte van monolithische en gelamineerde glazen liggers*, Ph.D. Thesis, Ghent University, Belgium, 2005, pp. 3-9 – 3-11.

²⁶ Or they would not be relevant.

²⁷ Grenet, L., *Mechanical Strength of Glass*, Enc. Industr. Nat. Paris, 5 (4): 838 – 848, 1899. As quoted in: Haldimann, M., Luible, A., Overend, M., Ibid, p. 50.

²⁸ Evans, A.G., *A Method for Evaluating the Time-Dependent Failure Characteristics of Brittle Materials – and its Application to Polycrystalline Alumina*, Journal of Materials Science, no. 7, 1972, pp. 1137 – 1146.

²⁹ See: Doremus, R.H., Ibid, p.182, and: Shelby, Ibid, p. 196.

³⁰ Thus if there is sub-critical crack growth, it is caused by chemical reactions enhanced by stress, rather than mechanical load directly.

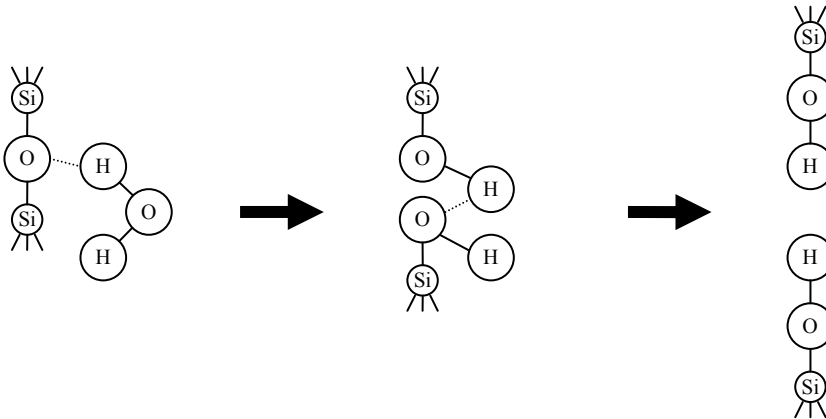


Fig. 4.4 Generally assumed reaction at the crack tip in soda-lime silicate glass. However, this model has been challenged as not fitting some of the details of glass fatigue.

Although according to Shelby³¹, this model does not fit some of the details of glass fatigue (other models have been proposed), it does explain the gross fatigue behaviour. Naturally, the reaction speed depends on several environmental conditions, such as³² humidity, temperature, corrosive media and pH value, glass chemical composition, load, and loading rate.

Thus, the strength-time relation Eq. (4.11) is also environment dependent. When the ambient conditions change, other ratios would result. Therefore, to obtain reliable surface flaw data from experimental, testing should ideally occur at inert conditions rather than ambient conditions. As this is usually difficult to achieve, Haldimann³³ proposes an alternative method to obtain near-inert conditions which gives reliable test results.³⁴

The reaction of Eq. (4.12) both sharpens and lengthens the crack tip. Each of these effects increases the peak stress around the crack tip, but Doremus remarks that according to theoretical relations between failure time and stress developed by Hillig and Charles³⁵, the rate of crack tip sharpening is more than ten times greater than the crack growth speed caused by this reaction. The crack growth is not as much a direct effect of mechanical loading, but rather the consequence of the chemical reaction.

The conclusion that the reaction mainly sharpens the crack tip, rather than expand its length, is not completely compatible with the usual representation of the glass strength

³¹ Shelby, *Ibid*, p.197.

³² Haldimann, M., Luible, A., Overend, M., *Ibid*, p. 53. This source does not separately mention 'load'.

³³ Haldimann, M., Fracture Strength of Structural Glass Elements – Analytical and numerical modeling, testing and design, Thèse No 3671, Ecole polytechnique fédérale de Lausanne (EPFL), Switzerland, 2006.

³⁴ The experiments presented in other parts of *this* research, however, do not aim at obtaining those parameters with such precision and have therefore not been executed in ambient conditions.

³⁵ Quoted in Doremus, *Ibid*, p. 180, as Hillig, W.B., Charles, R.J., in *High Strength Materials*, V.F. Jackey, Ed., Wiley, New York, 1965, p. 682.

applied stress intensity-dependency through v, K diagrams³⁶ such as Figure 4.5. In such diagrams, the crack growth velocity is presented as a speed v (unit of distance over time) which increases for increasing values of K between the threshold K_{th} ³⁷ to K_{Ic} (when the crack accelerates to terminal velocity). Perhaps v should be read more as a general crack altering parameter over time than as a real geometrical descriptor of a crack growing distance over time.

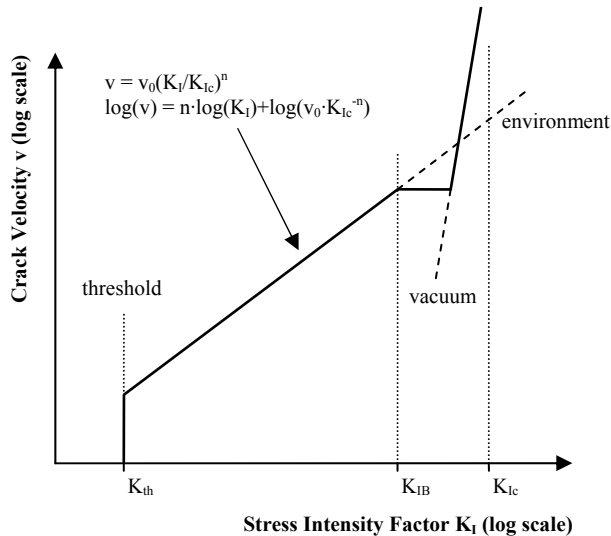


Fig. 4.5 Crack growth velocity versus stress intensity.³⁸

Another remarkable characteristic of glass is that the fracture strength of specimens with induced flaws *increases* if no stress is applied over a period of time. This phenomenon is referred to as *crack healing*. This was originally attributed to blunting of the crack tip, but recent investigations have supported the hypothesis that a change in chemical composition at the crack tip by alkali leaching out of the glass causes this effect.³⁹

³⁶ Indirect, such diagrams also link glass strength to time, as the crack speed determines the time for a crack to reach a critical length a_c .

³⁷ $K_{th} = 0.2 - 0.3 \text{ MPa}\sqrt{\text{m}}$, thus about $\frac{1}{3}$ of the K_{Ic} . Haldimann, M., *Ibid*.

³⁸ Taken from: Haldimann, M., *Fracture Strength of Structural Glass Elements – Analytical and numerical modeling, testing and design*, Thèse No 3671, Ecole polytechnique fédérale de Lausanne (EPFL), Switzerland, 2006.

³⁹ Haldimann, M., Luible, A., Overend, M., *Ibid*, p. 52. In support of the blunting-theory they quote:

- Bando, Y., Ito, S., Tomozawa, M., *Direct observation of crack tip geometry of SiO₂ glass by high-resolution electron microscopy*, Journal of the American Ceramic Society, 67 (3):C36-C37, 1984.
- Charles, R.J., Hillig, W.B., *The kinetics of glass failure by stress corrosion*, Symposium on Mechanical Strength of Glass and Ways of Improving it, Charleroi, Belgium, 1962.

The alkali hypothesis finds support in:

- Gehrke, E., Ullner, C., Hähner, M., *Fatigue limit and crack arrest in alkali-containing silicate glasses*, Journal of Materials Science, 26:5445-5455, 1991.
- Guin, J.-P., Wiederhorn, S., *Crack growth threshold in soda-lime silicate glass: role of hold-time*, Journal of Non-Crystalline Solids, 316 (1):1-11, 2003.
- Nghiem, B., *Fracture du verre et hétérogénéités à l'échelle sub-micronique*, Ph.D. Thesis Nr 98 PA06 6260, Université Paris-VI, 1998.

1.3. Life Time Prediction Models of Glass Surface Flaws

The non-identical, non-static character of glass surface flaws, makes an accurate prediction of glass strength very difficult. Actually, it makes it impossible to speak of glass strength. Rather, the glass piece life time can be predicted with two types of failure models: Single Surface Flaw models determine the time-to-failure from one governing design crack while Random Surface Flaw Population models calculate the failure probability over a period of time from a statistically distributed population of flaws. Generally, the first type of model is more suitable for aged glass in which you may assume some kind of accidental damage. The second kind is more appropriate for pristine glass direct from the float line, with only Griffith flaws in its surface, or perhaps artificially (evenly) weathered glass.

Taking all environmental and load history effects as well as flaw properties into account requires complex models. Haldimann⁴⁰ provides an extensive analysis of proposed models, and also proposes an SSF and an RSFP model himself, which he claims considers all relevant parameters. He furthermore provides suggestions for simplification so that these models can be used in structural design. Remarkably, though taking many influences into account, these models ignore the crack growth stress intensity threshold K_{th} ⁴¹ for reasons which are not entirely clear.⁴²

1.4. Glass Fracture Strength Scatter

With the fracture strength dependencies as presented above, it is not surprising that experimental test results in ambient conditions will result in considerable scatter. Actually, relative standard deviations of 5 to 40 % can be found. Several authors⁴³ have questioned the Weibull distribution for glass fracture strength based on such tests and suggested Log-Normal or even Normal distributions might fit the results just as well. However, Haldimann et al.⁴⁴ comment this ignores the theoretical background of glass failure, and attributed the deviations from a Weibull distribution to non-inert testing conditions, the influences of which are not always taken into account in the evaluation of test results. Veer et al.⁴⁵ have suggested – au contraire – that, as other statistical distributions fit experimental results better than the Weibull distribution, the underlying fracture mechanics failure mechanism for glass has to be questioned. More recently, Veer & Rodichev claimed, on the basis of experimental tests on AR glass rods⁴⁶ in various environmental conditions which resulted in bi-linear Weibull curves also found in earlier research by Veer, there must be several (competing) physical mechanisms governing glass fracture. This would mean fracture models based on two-parameter Weibull statistics are fundamentally flawed.

⁴⁰ Haldimann, M., Ibid. Refer to this document or Haldimann, M., Luible, A., Overend, M., Ibid, for an extensive explanation of these models.

⁴¹ Haldimann, M., Luible, A., Overend, M., Ibid, pp. 59, 62.

⁴² See Section 5 of this chapter for further comments on this assumption.

⁴³ See for instance: Veer, F.A., *The Strength of Glass; a Non-Transparent Value*, HERON, Vol. 52, Is. 1/2, 2007, pp. 87-104; or: Calderone, I., Jacob, L., *The Fallacy of the Weibull Distribution for Window Glass Design*, Proceedings of the 7th Glass Processing Days, Tampere, Finland, June 2001.

⁴⁴ Haldimann, M., Luible, A., Overend, M., Ibid, pp. 105-106.

⁴⁵ Veer, F.A., Louter, P.C., Bos, F.P., Romein, T., Ginkel, H. van, Riemsdag, A.C., *The Strength of Architectural Glass*, Proceedings of the Challenging Glass Conference, IOS Press, Delft, the Netherlands, May 2008.

⁴⁶ Thereby, alternatively to ring-on-ring testing, eliminating the problem of different types of surface areas being loaded at the same time.

Clearly, the actual processes governing glass fracture are yet evasive. Further studies in the field of material science are required before it would be possible to arrive at a single convincing fracture prediction or life time prediction model. Such research, however, falls outside the scope of this study.

2. Dimensioning Methods for the Application of Glass in Buildings

For the application of glass as a load bearing material in buildings, a range of methods has been developed which relate an allowable load or stress level to a target failure probability through relatively simple equations. They differ from the previously discussed (Life Time Prediction) models in the sense that they are not general (i.e. limited to certain conditions) and based on experimental test results rather than full consideration of the glass failure behaviour in a physico-chemical sense⁴⁷.

In literature, these methods are often referred to as ‘design methods’. However, the author prefers the term ‘dimensioning methods’ as they primarily aim at determining the right geometrical dimensions to ensure the allowable load or stress will not be exceeded, rather than defining the complete design.

Extensive overviews of dimensioning methods are provided by Haldimann⁴⁸, Haldimann et al.⁴⁹, and Belis.⁵⁰ Table 4.1 summarizes the checking equations and parameters for the most important methods.⁵¹

Easy-to-use deterministic models simply use a verification format as Eq. (4.13)⁵². These models should only be used in the preliminary design stages as only one global safety factor is used to include the effect of many parameters. Dimensions based on such rules should be checked with more sophisticated methods before finalizing the design.

The more elaborate dimensioning methods which try to take several or all glass failure variables in account, can be grouped into two families, according to Haldimann et al. The *European methods* follow the system of the current generation of codes in which parameters are expressed with partial factors. Several methods were under development simultaneously from the late 1990’s into the first years of the third millennium. The Damage Equivalent Load and Resistance Method (DELRL) was presented by Sedlacek et al.⁵³ in 1999. Its checking formula is presented by Eq. (4.14) (See Table 4.1 below). Other methods with similar formats include the (withdrawn) draft NEN-EN 13474

⁴⁷ They are *methods* to conveniently determine dimensions, not *models* that seek to accurately describe the glass fracture behaviour.

⁴⁸ Haldimann, M., Ibid.

⁴⁹ Haldimann, M., Luible, A., Overend, M., Ibid.

⁵⁰ Belis, J., Ibid.

⁵¹ Refer the mentioned publications for a more detailed account of the glass dimensioning methods. Here, they will be only briefly touched upon.

⁵² Haldimann, M., Luible, A., Overend, M., Ibid, p.86. The TRLV and TRAV (see Section 5 of this Chapter) are mentioned as guidelines that use this method.

⁵³ Sedlacek, G., Blank, K., Laufs, W., GÜsGen, J., Glas im Konstruktiven Ingenieurbau, Ernst & Sohn Verlag, Berlin, Germany, 1999.

method, Eqs. (4.15)⁵⁴, the NEN 2608 method, Eqs. (4.16), the draft DIN 18008 method, Eqs. (4.17) and the methods proposed by Shen⁵⁵, Eqs (4.18), and Siebert⁵⁶, Eqs. (4.19).

Another family is formed by the *North American methods*, which are founded on the Glass Failure Prediction Model (GFPM, Eqs. (4.20)) presented by Beason and Beason & Morgan,⁵⁷ directly derived from Weibull statistical theory of failure for brittle materials. Experiments therefore aim at obtaining the required Weibull parameters. Both the American ASTM 1300 E and the Canadian CAN/CGSB 12.20 are based on the GFPM. Contrary to the European methods, these codes require a check of actions versus resistances rather than occurring versus allowable stresses, using a very simple format as Eq. (4.21) or (4.22). In the ASTM 1300 E, the failure parameters are incorporated in the Non-Factored Load, for which extensive charts are provided. The Canadian code determines the glass resistance from the product of four variables and tabulated reference resistance of the glass.

The Porter-Houlsby method⁵⁸ is the odd-one-out. Instead of checking stresses or actions and resistances, it proposes to check the stress intensity factor caused by a design flaw against the critical stress intensity of glass (multiplied by a reduction factor, Eq. 4.23a). Although this method theoretically is more appropriate for a brittle material like glass than methods based on nominal stress fields, Belis notes the accuracy of such a method is highly dependent on the correct assumption of the design flaw. This will, in turn, depend on a correct prediction of the stress history, which is extremely difficult, if not impossible, for glass applied in buildings.

The European and North-American methods have been analysed extensively by Haldimann. He has found significant shortcomings, such as⁵⁹

- with regard to time dependency of glass strength: Crack velocity parameters have been determined from optical measurement of large through-thickness cracks in ambient conditions. It is questionable whether these parameters are as valid for microscopic crack development. Also, the influence of a variance of ambient conditions is unclear.
- with regard to laboratory testing to obtain strength data: The methods depend on surface flaw data obtained from testing in ambient conditions. Thus the factors inevitably include effects of sub-critical crack growth. Besides the fact that it may be undesirable to include two different effects in one parameter, it is

⁵⁴ Nederlands Normalisatie Instituut, *NEN-EN 13474-1 Ontw.: Glass in building - Design of glass panes - Part 1: General basis of design*, Delft, the Netherlands, 1999.

⁵⁵ Shen, X., *Entwicklung eines Bemessungs- und Sicherheitskonzeptes für den Glasbau*, Ph.D. thesis, Technische Hochschule Darmstadt, Germany, 1997.

⁵⁶ Siebert, G., *Beitrag zum Einsatz von Glas als tragendes Bauteil im konstruktiven Ingenieurbau*, Ph.D. thesis, Technische Universität München, Germany, 1999.

⁵⁷ Quoted in Haldimann, M., Luible, A., Overend, M., Ibid, as:

- Beason, W.L., *A failure prediction model for window glass*, NTIS Accession no. PB81-148421, Texas Tech University, Institute for Disaster Research, USA, 1980.
- Beason, W.L., Morgan, J.R., *Glass Failure Prediction Model*, Journal of Structural Engineering, 110(2): 197-212, 1984.

⁵⁸ Porter, M.I., Housby, G.T., Development of crack size and limit state design methods for edge-abraded glass members, *The Structural Engineer*, Volume 79, No. 8.17 (April 2001), pp. 29-35, as quoted in: Belis, J., Ibid.

⁵⁹ For a derivation of these shortcomings, refer to Haldimann, M., Ibid.

difficult to estimate the crack growth that occurs during an experiment. This may yield unsafe values for the surface flaw parameters.

- with regard to load duration effect: All dimensioning methods use a single variable to account for load duration. However, the load duration effect depends on many other factors such as action history and element geometry.
- with regard to residual stress: Some methods include the effect of thermal prestress in the inherent glass resistance. However, since sub-critical crack growth does not occur in compressed parts, they should be separated. Furthermore, their partial factors refer to different uncertainties and can therefore not be combined in one factor.
- with regard to size effect: the effect of the factor which takes the size effect into account (probability of critical flaws in a certain tensile stressed area) in North American codes is significant, while its influence in European codes is almost negligible. Size dependency has been experimentally proven in pristine glass, but not for weathered glass.
- with regard to bi-axial stress fields:
 - o European methods: Assume cracks to be orientated perpendicular to the major principal stress. This is conservative for design, but not for derivation of glass strength from test results.
 - o North American methods: The single biaxial stress correction is calculated for each point on the surface and assumed to be valid for all load intensities, although it is based on the load intensity dependent principal stress ratio.

Haldimann therefore concludes the current dimensioning methods suffer from notable shortcomings and proposes to develop design methods based on the SSF and RSFP Life Time Prediction models.

Table 4.1 Summary of structural glass dimensioning methods.⁶⁰

Method and checking equations	Parameter description
Deterministic allowable stress method $\sigma_E \leq \sigma_{adm} \quad (4.13)$	σ_E Maximum in-plane principal stress. σ_{adm} Allowable in-plane principal stress, determined from experiments multiplied by one global safety factor.
Damage Equivalent Load and Resistance Method (DELRL) $\sigma_{max,d} \leq \frac{\sigma_{bB,A_{test},k}}{\alpha_\sigma(q, \sigma_V) \cdot \alpha(A_{red}) \cdot \alpha(t) \cdot \alpha(S_v) \cdot \gamma_{M,E}} + \frac{\sigma_{V,k}}{\gamma_{M,V}} \quad (4.14)$	$\sigma_{max,d}$ design value of maximum in-plane principal stress in the element $\sigma_{bB,A_{test},k}$ characteristic inherent bending fracture strength in R400 coaxial double ring test $\sigma_{V,k}$ characteristic of the residual surface stress $\alpha_\sigma(q, \sigma_V)$ coeff. for stress distribution $\alpha(A_{red})$ coeff. for tensile loaded surface area $\alpha(t)$ coeff. for load duration $\alpha(S_v)$ coeff. for load combination and environmental conditions $\gamma_{M,E}$ partial factor for inherent strength $\gamma_{M,V}$ partial factor for residual stress
NEN-EN 13474-1 Draft $\sigma_{eff,d} \leq f_{g,d} \quad (4.15a)$ $\sigma_{eff,d} = \left[\frac{1}{A} \int_A (\sigma_1(x, y))^\beta dx dy \right]^{1/\beta} \quad (4.15b)$ $f_{g,d} = \left(k_{mod} \frac{f_{g,k}}{\gamma_M k_A} + \frac{f_{b,k} - f_{g,k}}{\gamma_V} \right) \cdot \gamma_n \quad (4.15c)$	$\sigma_{eff,d}$ effective stress for design $f_{g,d}$ allowable effective stress A element total surface area $\sigma_1(x, y)$ major principal stress at point x,y β Weibull distribution shape parameter k_{mod} coeff. for load duration, load combination, and environmental conditions k_A coeff. for element surface area $f_{g,k}$ characteristic value of inherent strength $f_{b,k}$ characteristic value of fracture strength (inherent strength + residual stress) γ_M partial factor for inherent strength γ_V partial factor for residual stress γ_n national partial factor
NEN 2608-2 ⁶¹ $\sigma_{mt;u;d} \leq f_{mt;u;d} \quad (4.16a)$ $f_{mt;u;d} = \frac{f_{g;k} k_b k_e k_{mod}}{\gamma_m} + \frac{f_{b;k} - f_{g;k}}{\gamma_v} \quad (4.16b)$	$\sigma_{mt;u;d}$ calculable value of the bending tensile stress $f_{mt;u;d}$ calculable value of the allowable bending tensile stress; $f_{g;k}$ characteristic bending tensile strength of annealed glass; $f_{b;k}$ characteristic bending tensile strength of prestressed glass. k_b coeff. for fracture behaviour; k_e coeff. for edge treatment; k_{mod} modification factor for loading period. γ_m partial factor for inherent strength; γ_v partial factor for residual stress; The last term of Eq.

⁶⁰ Unless noted otherwise, notations are taken from Haldimann, M., Luible, A., Overend, M., Ibid, pp. 86-101.

⁶¹ Nederlands Normalisatie Instituut, NEN 2608-2: *Vlaskglas voor gebouwen - Deel 2: Niet-verticaal geplaatst glas - Weerstand tegen eigen gewicht, wind- en sneeuwbelasting en isochore druk - Eisen en bepalingmethode*, Delft, the Netherlands, 2007.

4.16b equals 0 for annealed glass.

Table 4.1 (Continued) Summary of structural glass dimensioning methods.

Method and checking equations	Parameter description
DIN 18008-1 ⁶² $E_d \leq R_d$ (4.17a) $R_d = \frac{k_{\text{mod}} f_k}{\gamma_M}$ (4.17b)	E_d calculable value of the actions R_d calculable value of the resistance f_k characteristic bending tensile strength k_{mod} modification factor for loading period γ_m partial factor for inherent strength, is omitted for prestressed glass.
Shen $\sigma_{\text{max},d} \leq \sigma_k \frac{\eta_F \eta_D}{\gamma_R}$ (4.18)	$\sigma_{\text{max},d}$ design maximum principal stress σ_k characteristic inherent bending fracture strength in R400 coaxial double ring test η_F coeff. for surface area stress distribution η_D coeff. for load duration γ_R partial factor for resistance
Siebert $\sigma_{\text{ges},d,\text{max}} \cdot f_A \cdot f_\sigma \cdot f_{IS} \leq \frac{\theta}{f_P}$ (4.19a) $\sigma_{\text{ges},d,\text{max}} = \sigma_{d,\text{max}} + \sigma_E$ (4.19b) $f_P = \left[\ln \left(\frac{1}{1 - G_a} \right) \right]^{-1/\beta}$ (4.19c)	$\sigma_{\text{ges},d,\text{max}}$ maximum principal surface stress $\sigma_{d,\text{max}}$ maximum principal stress due to actions σ_E maximum residual surface stress f_A coeff. for surface area f_σ coeff. for stress distribution f_{IS} coeff. for load duration and relative magnitudes of different loads f_P factor for target failure probability θ Weibull distribution scale parameter G_a target failure probability β Weibull distribution shape parameter
Glass Failure Prediction Model (GFPM) $P_f = 1 - e^{-B}$ (4.20a) $B = \tilde{k} \int_A \left[\tilde{c}(x, y) \sigma_{\text{eq},\text{max}}(q, x, y) \right]^{\tilde{m}} dA$ (4.20b)	P_f failure probability B risk of failure as a function of all relevant aspects \tilde{k} surface flaw parameter \tilde{m} surface flaw parameter $\tilde{c}(x, y)$ biaxial stress correction factor $\sigma_{\text{eq},\text{max}}(q, x, y)$ maximum equivalent principal stress as a function of the lateral load q and the position x, y . A Surface area
ASTM 1300 E $q \leq LR = NFL \cdot GTF$ (4.21)	q uniform lateral load LR load resistance NFL non-factored load GTF glass type factor

Table 4.1 (Continued) Summary of structural glass dimensioning methods.

⁶² Deutsches Institut für Normung, *DIN 18008-1 Entwurf: Glas im Bauwesen – Bemessungs- und Konstruktionsregeln – Teil 1: Begriffe und allgemeine Grundlagen*, Berlin, Germany, 2006.

Method and checking equations	Parameter description
CAN/CGSB 12.20	E_d combination of all actions
$E_d \leq R_d$ (4.22a)	R_d resistance of the pane
$E_d = \alpha_D D + \gamma \cdot \psi \cdot (\alpha_L L + \alpha_Q Q + \alpha_T T)$ (4.22)	α_D partial factor
$R = c_1 \cdot c_2 \cdot c_3 \cdot c_4 \cdot R_{ref}$ (4.22c)	α_L partial factor
	α_Q partial factor
	α_T partial factor
	D dead loads
	γ importance factor
	ψ load combination factor
	L live loads (snow, rain, use, var. hydrostatic pressure)
	Q live loads (wind, stack effect, earthquake, climatic and altitude load for IGU's)
	T effects for temperature differences
	c_1 glass type factor
	c_2 heat treatment factor
	c_3 load duration coefficient
	c_4 load sharing coefficient
	R_{ref} reference factored resistance of glass
Porter – Houlsby ⁶³	K_I design stress intensity factor
$K_I^* \leq \phi K_{Ic}$ (4.23a)	K_{Ic} critical stress intensity factor
$K_I^* = Y \cdot \sigma^* \sqrt{\pi a^*}$ (4.23b)	Φ reduction factor for strength
	Y flaw shape parameter
	σ^* design stress
	a^* design flaw depth

3. Glass Failure Causes

The range of models and methods introduced in the preceding sections, have been developed to determine the resistance of glass elements and their failure probability from permanent, variable and (a limited number of) accidental actions, represented as static or semi-static loads. However, the complete inability of glass to redistribute peak stresses (by (local) plastic deformation) or stop crack growth (through energy dissipation or crack-stopping discontinuities), has made the material susceptible to a much broader range of failure causes.

In fact, glass failure is quite common and several specialized publications⁶⁴ have appeared concerning glass failure causes and their qualitative identification. The crack pattern plays a key role in such forensic investigations. Only rarely quantitative analyses

⁶³ Belis, J., Ibid, p. 3 – 23.

⁶⁴ For instance: Loughran, P., *Falling Glass*, Birkhäuser, Basel, Switzerland, 2003; *Glass Breakage, Technical Note No. 13*, Centre for Window & Cladding Technology (CWCT), Bath, UK, 2000; Wagner, E., *Glasschades – Oppervlaktebeschadigingen, glasbreuk in theorie en praktijk*, Kenniscentrum Glas, Gouda, the Netherlands, 2006. Original (German) title: *Glasschäden – Oberflächenbeschädigungen, Glasbrüche in Theorie und Praxis*, Verlag Karl Hofman, Schorndorf, Germany, 2002.

are included. Overend et al.⁶⁵ presented an equation, here represented as Eq. (4.24)⁶⁶, from a review of fracture mechanics publications on glass failure with which the glass failure stress can be determined from measuring the distance from the failure origin to the first crack branching.

$$\sigma_f - \sigma_{ar} = \frac{\alpha}{\sqrt{r}} \quad (4.24)$$

σ_f Failure Stress [MPa]

σ_{ar} Apperent Residual Compressive Surface Stress [MPa]⁶⁷ (a value of 11 MPa for annealed glass is proposed)

α Branching Constant [MPa \sqrt{m}]: α_m , α_h , or α_b (a macroscopic branch constant α_b of 2.1 MPa \sqrt{m} is proposed)

r Radius [m] : r_m , r_h , or r_b

Glass failure may result from any of the causes discussed below.

- **Surface Damage**

During its life time, the surface of a glass sheet may be exposed to many influences which deteriorate the surface quality to greater or lesser extent. This may result in loss of visual quality, but also loss of strength as damage may develop critical crack lengths immediately or over time (through stable crack growth). Generally, surface damage can have mechanical or chemical causes.

- o *Degradation by chemicals*

Glass will react with substances of similar chemical composition. This can result in corroded or hazy / cloudy surfaces. Some sources of degrading chemicals are⁶⁸ strongly alkaline façade cleaners, fluor-hydrogenacid and façade cleaners containing fluor-hydrogenacid, cement and concrete, mineral paints and mineral plaster, lye, and conservation and impregnation solutions.

- o Scratches (mechanical surface damage)

Any material with a Mohs hardness equal to or greater than that of glass, can cause scratches on the surface. There is a whole range of possible causes. Wagner⁶⁹ describes more than a dozen in detail.

- **Accidental impact**

As most building parts, glass elements may encounter collision with people or objects. This may cause unexpected stress distributions and stress concentrations, which the glass may not be able to accommodate. Testing of glass or glazed assemblies is often required by codes to ensure their resistance to such loads.

⁶⁵ Overend, M., Gaetano, S. de, Haldimann, M., *Diagnostic Interpretation of Glass Failure*, Structural Engineering International, no. 2, 2007, pp. 151-158.

⁶⁶ This will be further discussed in Chapter 9.

⁶⁷ The physical meaning and explanation of this constituent is still unknown. It was suggested to fit experimental results.

⁶⁸ List from Wagner, E., *Ibid.*, p. 20.

⁶⁹ Wagner, E., *Ibid.*, pp. 27-46.

- o *Soft body impact*
People falling or bumping on/into glass elements. Especially applicable for glass balustrades, full height glazing without further fall-through protection, or glass floors.
- o *Hard body impact*
Objects, often with a hard nature such as bolts, stones, roof tiles, etc., falling on/into glass elements, accidentally or as air borne debris in storms.⁷⁰ Roofs and floors are more prone to falling objects; glass in façades is more susceptible to air borne debris.
- **Purposeful impact / damage**
Often, glass is the subject of purposeful damage.
 - o *Vandalism*
Particularly tempered glass seems to have a irresistible attraction on vandals, as can occasionally be experienced at bus stops.
 - o *Break-in*
The glass parts (especially windows) are often considered the weak part in the enclosure of a building. They can be attacked with a range of (handheld) tools and weapons such as hammer, axes, glass cutters, centre punches, thrown objects, etc.⁷¹
 - o *Terrorism*
Bombs, bullets, etc. Terrorist attacks over the last decade, such as those in New York, Madrid and London, have raised the attention for the performance of glazing under such assaults.
- **Thermal Stress**
Thermal stress breakage is caused by a combination of low thermal conductivity and a high thermal expansion coefficient. This causes irregular thermal expansion and high stresses.
 - o *Normal*
Thermal breakage of annealed glass may occur when part of the glass sheet is in the shade (for instance, through a glazing rebate), and an adjacent part is exposed to a high intensity of (direct) sun light. The sun lit part will want to expand causing thermal stresses in the shaded part. Especially when the shaded part is already damaged or stressed through another cause, this may induce early failure. Since the outer surface of thermally prestressed glass is in compression, that type is less susceptible to thermal breakage at normal conditions.
 - o *Fire*
During a fire, one side of the glass will usually experience a severe temperature increase, while the other side is still cool. This will cause glass breakage. Fire resistant glass makes use of thermally prestressed borosilicate glass with a thermal expansion coefficient of only one third of that of soda-lime silicate glass. Other types of fire resistant glazing are laminated with foam-forming resins, which expand and sacrifice the glass itself.

⁷⁰ Air borne debris is probably of less concern in Europe. However, it requires serious consideration in large parts of North America as well as other parts of the world.

⁷¹ NEN-ISO 16936, parts 1 through 4 define test criteria to classify glazing behaviour against such attacks.

- **Inclusions, e.g. Nickel Sulfide (NiS)**

Inclusions results from impurities in the glass forming batch. When they are present in the tensile zone in thermally tempered glass, they may induce glass breakage. This is probably the only ordinary failure cause which originates from inside the glass, rather than from the surface.

Failure from Nickel Sulfide inclusions is the most well documented type of inclusion induced failure. Nickel Sulfide particles change from their β -phase into their smaller α -phase during tempering. However, when exposed to heat (i.e. direct sun light), they return to their β -phase, causing large stresses and often breakage. The transition from α - to β -phase may take a long time and failure may occur at any time after manufacturing (incidents peak after 4-5 years, but may occur up to 20 years later⁷²).

Many spontaneous failures of tempered glass are attributed to Nickel Sulfide. The presence of a butterfly-shaped fracture origin is often considered sufficient proof. Generally, glass remains are not further investigated to actually find the Nickel Sulfide inclusion. It is thus not entirely certain whether Nickel Sulfide inclusions or another, yet unknown, failure cause, are responsible for all cases in which spontaneous tempered glass failure has been attributed to the former.

- **Human error**

In the process of designing, manufacturing and construction, many things can go wrong due to error, ignorance, or negligence.

- o *Design*

Incorrect detailing design, glass type selection, or selection of intermediate materials in joints, etc.

- o *Calculation*

Incorrect modeling, incorrect use of checking formulae, incorrect or insufficient check of peak stresses, etc.

- o *Manufacturing, post-processing*

Incorrect thermal treatment (insufficient prestressing), crude drilling of holes, misaligning multiple layers, dimensional inaccuracies, lack of or rough edge treatment (polishing), etc.

- o *Handling and Transport*

Bumping, colliding, dropping, etc. of glass; exposure to degrading substances e.g. at a building site, exposure to environmental conditions, etc.

- o *Construction*

Incorrect placement, incorrect use of tools or use of inappropriate tools, incorrect last-minute solutions,⁷³ deviating from the original design, etc.

The relative importance of each of the mentioned possible failure causes is difficult to estimate as little has been published on the subject, even though glass failure is common.⁷⁴ Ledbetter et al.⁷⁵ indicate the most important failure causes are impact,

⁷² Ledbetter, S.R., Walker, A.R., Keiller, A.P., *Structural Use of Glass*, Journal of Architectural Engineering (ASCE), Vol. 12, no.3, September 1, 2006, pp. 137 – 149.

⁷³ Some improvising is always part of building.

⁷⁴ The author did not find any comprehensive studies on the relative importance of glass failure causes or their occurrence frequency.

⁷⁵ Ledbetter, S.R., Walker, A.R., Keiller, A.P., Ibid.

thermal stress, inclusions, and malicious damage through small projectiles, scratching, deliberate impact, failure of the compressive layer in heat treated glass, or blast.⁷⁶ Contrary though, interviews by the author with several glass engineering specialists⁷⁷ have revealed the primary failure cause is human error during the design/build process. Most failures seem to originate from design errors, badly manufactured or post-treated glass, or errors and carelessness during handling, transport, or construction. Unfortunately, it is practically impossible to completely avoid such errors. To make matters worse, they are usually undetectable until failure actually occurs.

It will, in any case, be clear the sensitivity of glass elements to certain failure causes will be highly dependent on application, measure of accessibility, glass type, project partners, etc. But proper treatment of glass and quality control is of paramount importance.

4. Limitations of a Probabilistic Approach for Structural Glass Engineering

In Chapter 3, Section 6, it was shown a probabilistic approach for failure on element level alone, is not enough to provide sufficiently safe building structures. This observation holds for any structural material. However, the relevance of the probabilistic approach to the safety of *glass* structures is even more limited. Five principal reasons can be traced when considering the cause-consequence diagram of glass structure failure as in Figure 4.6 – an elaboration of Figure 3.14 in Chapter 3:

① Unconsidered Influences on the Resistance $R(\xi)$ and the Actions $S(\xi)$

As has been argued in the previous section, glass is susceptible to a high number of events which adversely influence either the resistance of the glass element or the actions on it. Except for the codified actions, none of these are explicitly considered in the probability analysis.

② Uncertainties in the Formal Probability Problem $G(\xi) = R(\xi) - S(\xi)$

It may be assumed the uncertainties concerning the codified actions S on a glass structure are similar to those on other structures. However, probably more than other materials, there is still considerable debate on how to accurately predict the resistance R of a structural glass element.⁷⁸

According to Haldimann⁷⁹, all existing engineering dimensioning methods suffer from a greater or lesser extent of shortcomings and thus do not accurately predict R . He has proposed two models to determine the failure probability over a life time, based on a Single (design) Surface Flaw (SSF) or on a Random Surface Flaw Population (RSFP). However, several remarks should also be made concerning the validity and suitability of those models.

First, they are based on face surface flaws, while failure in reality often originates from the glass sheet edge. Other types of flaw are likely to be present there.⁸⁰

⁷⁶ Other publications usually do not present any indication on the issue.

⁷⁷ Appendix C presents extensive reports of these interviews. In Chapter 5, the views of the interviewees are presented by subject.

⁷⁸ See Sections 1 and 2 of this Chapter.

⁷⁹ Haldimann, M., Ibid.

⁸⁰ See discussion in Section 1.2.1 of this Chapter.

Furthermore, the models rely on an accurate statistical and geometrical description of the SSF and RSFP. Especially the properties of the SSF, which should be considered in an analysis as design flaws, are still evasive.

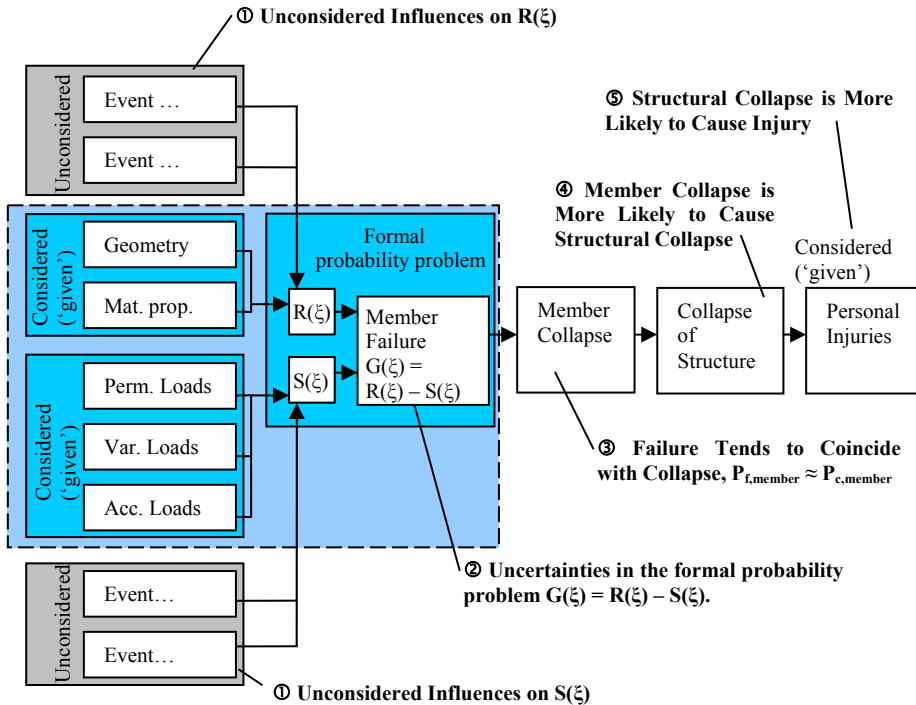


Fig. 4.6 Cause-consequence diagram for structural glass failure, with five principal reasons why a probabilistic approach has significant limitations.

It is, additionally, questionable if a separation between an SSF based and an RSFP based probability analysis for different glass elements is appropriate. Veer⁸¹ has suggested from experimental research at least two types of flaw compete as governing failure causes in glass beams. These should be included in one analysis to obtain an accurate failure probability.

Also, the stable crack growth stress intensity threshold K_{th} (under which no crack growth occurs) is ignored. The reasons to do this are not completely clear, as Haldimann himself presents four studies in which such a threshold has been reported.⁸² Off course, taking this threshold into account would complicate the

⁸¹ Veer, F.A., *The Strength of Glass; a Non-Transparent Value*, HERON, Vol. 52, Is. 1/2, 2007, pp. 87-104.

⁸² Haldimann, M., Ibid. On page 80 Haldimann quotes:

- Wiederhorn, S. M., Bolz, L. H., *Stress corrosion and static fatigue of glass*, Journal of the American Ceramic Society, 53(10):543-548, 1970.
- Simmons, C. J., Freiman, S. W., *Effect of corrosion processes on subcritical crack growth in glass*, Journal of the American Ceramic Society, 64, 1981.
- Gehrke, E., Ullner, C., Hähner, M., *Effect of corrosive media on crack growth of model glasses and commercial silicate glasses*, Glastechnische Berichte, 63(9):255-265, 1990.

models even further, but with their complexity already considerable, it seems arbitrary to exclude this specific effect. Ignoring K_{th} is a safe assumption as there is no risk of overestimating the crack growth threshold and thus the long term glass strength. However, the presence of such a threshold is not disputed in itself. Disregarding it eliminates the permanent contribution of the inherent glass strength to the overall strength of an element. Effectively, annealed glass is thus excluded for permanently loaded structural applications as cracks would always develop a critical length sooner or later. As has been shown already in Chapter 2, annealed glass is extremely useful in creating safe structural glass elements. An expansion of the Life Time prediction models is, therefore, desirable.

Finally, the models proposed by Haldimann are considerably more complex than those used in the engineering methods. Even if they would be adopted by engineering practice, it will take considerable time for engineers to familiarize themselves with them.

Thus, no generally accepted and applicable dimensioning method is yet available. The complexity of the material behaviour in relation to stress and environmental conditions over time make it unlikely this will change in the near future.

③ In Single Sheet Glass, Failure Tends to Coincide with Collapse

As indicated in Chapter 3, Section 6 under (3), the failure of a structural element from common structural materials does not necessarily mean its collapse ($P_{f,member} \neq P_{c,member}$, Figure 4.7a). There can, for instance, be a considerable safety margin that stems from the difference between yield and ultimate tensile strength in steel elements. In glass however, failure will almost certainly also lead to collapse ($P_{f,member} \approx P_{c,member}$, Figure 4.7b), as very little energy or driving force is required to drive an unstable crack through a piece of glass completely. Thus, this hidden safety margin disappears without notice.

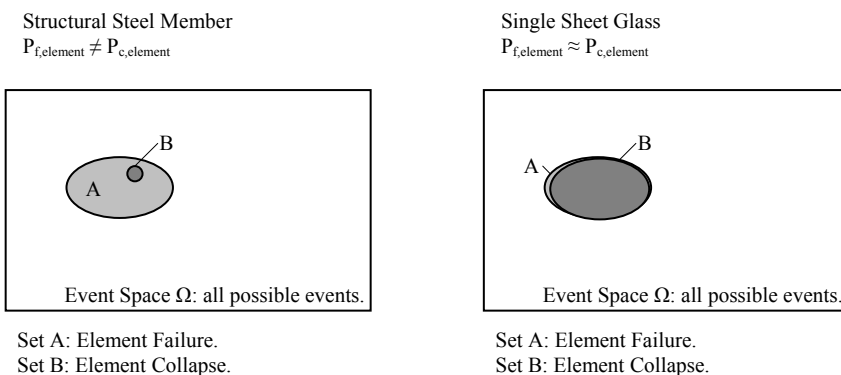


Fig. 4.7a and b Indicative comparison between failure and collapse probabilities of a steel structural element (a, left) and a single glass sheet (b, right). Whereas $P_{f,element} \neq P_{c,element}$ for the steel member, $P_{f,element} \approx P_{c,element}$ for the glass sheet.

The only case in which failure will not coincide with collapse is the combination of a very short impact (causing failure) without a static load (to drive the cracks further). Note that even self weight can provide enough load to drive cracks. Especially in prestressed glass, it is apparent that failure means collapse, as cracks running through the compressive layer into the tensile zone will unleash the stored strain energy causing extensive cracking.

④ **Element Collapse is More Likely to Cause Structural Collapse**

Generally, brittle structures lack deformation capacity which can help load redistribution before members or parts of the structure collapse.

⑤ **Structural Collapse is More Likely to Cause Injury**

When glass breaks, unlike other structural materials, it does so in very sharp shards. Therefore, the risk of people getting seriously injured because of a collapse of a glass structure is higher than from collapse of another structure.

Thus, it may be concluded that for every stage between failure cause and considered final consequence, glass poses extra safety hazards compared to more common structural materials. A single probabilistic approach for the failure probability of a structural element is therefore especially insufficient for structural glass engineering. Extra measures are required at each stage to provide a safety level more comparable to that obtained with other structural materials. Fortunately, measures at one stage often automatically also have an effect on other stages.

In glass engineering practice, the insufficiency of a probabilistic failure analysis of members is generally recognized and additional measures are applied to ensure adequate safety. However, the implications of these shortcomings are hardly ever systematically analysed. Structural glass engineering codes, discussed in the next section, provide insufficient guidance on the subject. As a consequence, additional safety measures are applied to highly varying extent. An investigation of the approach of the safety problem of glass by engineers in practice is presented in Chapter 5.

5. Extension of the Probabilistic Approach in Structural Glass Engineering Codes

There is a wide range of codes related to glass in building engineering. Codes usually apply to relatively common uses. Only a small part of structural glass qualifies as such. Technical guidelines and approval guidelines from building authorities and/or standardization institutes form a set of less formal documents with additional requirements and regulations for the use of structural glass. Some of these are also discussed below.

5.1. Discussion of Several Codes and Guidelines

5.1.1. NEN 2608, Parts 1 and 2⁸³

At the moment of writing, the first two parts of the NEN 2608 have come into force. Part 1 deals with wind loading on vertical glazing; while part 2 is concerned with wind loading, snow and self weight on non-vertically installed glass. Parts 3 and 4, about specific loads on non-vertical glazing accessible for maintenance and glass separations for floors respectively, are still in preparation. The scope of NEN 2608-2 excludes glass in primary load carrying applications (like beams and columns) and even in floors. Nevertheless, it usually serves as a starting point to evaluate glass structures because of a lack of alternatives.

Besides the stress checks already introduced in Section 2, this code provides rules to calculate the maximum bending tensile stress and the bending tensile strength of the glazing. Surprisingly though, it does not specify *any* requirements with regard to failure behaviour, testing for specific load conditions, or residual strength.⁸⁴

5.1.2. NEN 3569⁸⁵

The Dutch standard NEN 3569 specifically aims at providing personal safety against fall through and injury from glass shards. It does so by requiring that glass in certain applications in a building needs to conform to a certain fracture pattern and coherence after breakage. It does *not* describe any requirements with regard to structural performance or dimensioning. Thus, it acts complementary to NEN 2608.

NEN 3569 categorizes glass types based on fracture pattern and minimum drop height of a predefined body at which a failure type occurs. The code recognizes three types of failure pattern (type) and three drop heights (class), definitions of which have been taken from NEN-EN 12600, which describes an experimental method to assess the failure type and class of a piece of glass. The required glass type depends on 6 building types and 7 kinds of construction. Additionally, the NEN 3569 demands glass with a B-type (e.g. laminated safety glass) failure pattern does not come out of its framing after breakage.

5.1.3. Dutch Guideline for Approval of Glass Structures: *Constructief Glas, toetsingshulpmiddel voor Bouwtoezichten*⁸⁶

To harmonize approval in the Netherlands, the Dutch building authorities use an unpublished auxiliary guideline to assess glass constructions. It treats vertical glazing acting as a fall through barrier, and horizontal glazing (i.e. floors, roofs, and porches). It requires all these constructions to resist actions as defined in the Dutch code for actions

⁸³ Nederlands Normalisatie Instituut, *NEN 2608-1: Glass in building - Resistance against windload - Requirements and determination method*, Delft, the Netherlands, 1997; and: *NEN 2608-2: Vlakglas voor gebouwen - Deel 2: Niet-verticaal geplaatst glas - Weerstand tegen eigen gewicht, wind- en sneeuwbelasting en isochore druk - Eisen en bepalingmethode*, Delft, the Netherlands, 2007.

⁸⁴ A new preliminary version of the NEN 2608 is planned for publication around September 2009. It will combine and replace the earlier parts 1 and 2. Contrary to the versions discussed here, the new NEN 2608 will include further requirements with regard to residual resistance and fracture mode. As such it will also replace much of NEN 3569.

⁸⁵ Nederlands Normalisatie Instituut, *NEN 3569: Safety glazing in buildings*, Delft, the Netherlands, 2001.

⁸⁶ Centraal Overleg Bouwconstructies (COBc), *Constructief glas, toetsingshulpmiddel voor Bouwtoezichten*, 1999. In Dutch; not publicly published.

on structures, NEN 6702. Furthermore, it states that an alternative load path should always be present if single layer thermally tempered glass is used, as spontaneous breakage through Nickel Sulfide inclusions or contact with sharp objects can never be ruled out. Also, a construction protocol has to be present, which should include at least the construction order, acceptable tolerances, acceptable levels of damage to the glass before, during, and after construction, the method of attachment, and rejection criteria. In the light of the observation that most failures originate from errors in the design or build phase, this seems very sensible.

Besides permanent and variable loads, vertical barriers should be able to withstand an impact load simulating collision with a human being coming in with a kinetic energy of approximately 500 J. This can either be proven by applying a static load to the calculation model or testing with a sandbag pendulum test. The sandbag weighs 50 kg and the drop height is 1.0 m. The test is successful if either the glass does not break or, if it does, it still prevents the sandbag from going through.

Glass floors need to be able to withstand an impact load as simulated by a cylinder drop test. The steel cylinder should have a wooden disk underneath of 100 mm diameter and 25 mm thickness with which it hits the floor. The total weight is 75 kg and the drop height 0.5 m. Roofs and porches also need to withstand an impact load. Like the vertical glazing, this can be proven by applying a static load to the calculation model or executing a 50 kg sandbag drop test from a height of 0.7 m. In all horizontal glass applications, the top layer should be considered to be sacrificial and has to be ignored in strength calculations. In this case, the glazing is considered to have passed the test if it does not break, or, if it does, it can still hold the sandbag up to 15 minutes and no particles larger than 100 mm² fall off.

5.1.4. Draft NEN-EN 13474-1⁸⁷

On European level, a provisional code for structural glass, the EN 13474, has been circulating for 8 years, but was withdrawn early 2007. This code had a wider scope than the NEN 2608-2. In principle, it was applicable to all glazing required to resist actions according to NEN-EN 1991-2 that are acting normal to the surface. This effectively ruled out beams and columns. Like the NEN 2608-2, the NEN-EN 13474 focused on checking the design stress against the bending tensile strength of the glass. However, in clause 5.1 it stated that breakage of the glazing should not result in further damage if the glazing is part of the 'supporting structure'. How this general remark was to be interpreted was not elaborated further.

5.1.5. Draft DIN 18008, Parts 1 and 2⁸⁸

The German structural glass code DIN 18008 appears to be the first to treat the failure behaviour aspect more extensively. Provisional versions of part 1 (concepts and general basis of design) and part 2 (linear supported glazing) have been published in March 2006. At the moment of writing no further parts had been published.

⁸⁷ Nederlands Normalisatie Instituut, *NEN-EN 13474-1 Ontw.: Glass in building - Design of glass panes - Part 1: General basis of design*, Delft, the Netherlands, 1999.

⁸⁸ Deutsches Institut für Normung, *DIN 18008-1 Entwurf: Glas im Bauwesen – Bemessungs- und Konstruktionsregeln – Teil 1: Begriffe und allgemeine Grundlagen*, Berlin, Germany, 2006; and *DIN 18008-2 Entwurf: Glas im Bauwesen – Bemessungs- und Konstruktionsregeln – Teil 1: Linienförmig gelagerten Verglasungen*, Berlin, Germany, 2006.

Part 1 requires glazed structures not only to be able to carry actions during their reference life time with a certain level of probability, but also demands sufficient residual strength (*Resttragfähigkeit*) for certain structures or installation situations (clause 4.1.2). It defines residual strength as the capacity of a glazed construction to remain sufficiently stable in case of glass breakage (clause 3.1.5). Rightfully, it is stated that this can not be realized by applying a safety factor (clause 4.1.3) as this would influence the probability of failure, not the behaviour should one occur. Residual strength should ensure sufficient safety for persons in case of breakage of a single glass element, and refers both to the glass element itself and the construction of which the glass element is a part (clause 4.2.1).

Importantly, the DIN 18008-1 considers the residual strength requirements to be *one part* of the overall safety concept (clause 9.1). The requirements for residual strength are considered fulfilled for specific constructions when the regulations in the code are followed. Alternatively, for constructions not explicitly covered in the codes, they can be proven by calculation for partially damaged glass elements with sufficient glass layers in tact, or by experiment (clauses 9.1 and 9.2).

Part 2 formulates some very brief design requirements which have to be interpreted as related to safety and residual strength. For horizontal glazing, clauses 6.1 and 6.2 demand only wired glass or laminated float, or heat-strengthened glass is used, unless extra construction measures can ensure no dangerous shards will reach traffic areas in case of glass breakage. Vertical glazing which breaks into large pieces should be supported along all sides (clause 7.1).

The various clauses in the DIN 18008-1 concerning safety and residual strength seem to indicate a more systematic and integral approach than the provisional NEN-EN 13474. Clauses 4.2.1 and 9.2 imply that various levels of damage can be identified: partial breakage (one or more layers) and complete breakage. However, for now it remains unclear how the residual strength requirements are quantified and when partial and complete breakage should be reckoned with.⁸⁹

5.1.6. German Technical Guidelines on linear supported glazing (TRLV), point fixed glazing (TRPV), and glazing acting as a barrier (TRAV)⁹⁰

The TRLV, TRPV and TRAV cover relatively common glass applications with simple dimensioning rules and additional, mostly qualitative design rules (e.g. with regard to glass type choice and detailing). The DIN 18008 will have a broader range of application and will, in time, supersede these guidelines.

Like the DIN 18008-2, the TRLV requires overhead glazing to consist of wired or laminated glass (annealed or heat-strengthened, clause 3.2.1). Accessible horizontal glazing (stair treads, floor panels) should consist of at least three layers of laminated glass; the top layer is ignored in stress calculations (clauses 3.4.3 and 3.4.4). Not only should they be linearly supported along all edges, they should also not be exposed to an

⁸⁹ However, such elaborations may be under development at the moment of writing.

⁹⁰ *Technische Regeln für Verwendung von linienförmig gelagerten Verglasungen (TRLV), Entwurfsfassung September 2005, Technische Regeln für die Bemessung und Ausführung punktförmig gelagerten Verglasungen (TRPV), Entwurfsfassung August 2005, and Technische Regeln für die Verwendung von Absturzsichernden Verglasungen (TRAV), Fassung Januar 2003, Deutsches Institut für Bautechnik (DIBt), Berlin, Germany.*

increased risk of impact or collision (clause 3.4.1). Thus, an extra consideration is added to prevent failure from actions that are otherwise not considered in the structural calculations.

For point fixed overhead glazing, the TRPV requires laminated heat strengthened glass of two sheets of equal thickness (clause 6.1).

The guideline for vertical barriers TRAV recognizes three categories of fall through prone glazing (clause 1.2):

- A- All-sided linearly supported glazing according to the TRLV,
- B- One-sided linearly, clamped glass balustrades, and
- C- In-fill panels, further subdivided into C1, C2 and C3.

For all categories except C1 and C2, laminated glass is always required (for insulated glass either the in- or the outside panel; clause 3.1). The edges should be protected from damage (clause 3.2).

Additional to the resistance to static actions regulated in clause 5, clause 6 requires the resistance under impact to be sufficiently proven. It provides three methods: by experiment (clause 6.2), by using a construction of which the resistance has previously been sufficiently proven (clause 6.3), or by using stress tables (clause 6.4).

The experimental method requires a double-tire pendulum impact test according to DIN-EN 12600⁹¹, where the drop height is 900, 700, or 450 mm depending on the glazing category (A, B, or C, respectively). The complete glazing construction should be tested, rather than just the glass. If the construction is damaged by the test, a subsequent pendulum test with a drop height of 100 mm should be executed. The test is considered successful when the glazing remains in place after testing, no shards fell down, and no holes with a width of 76 mm or more appeared.

5.1.7. Requirements on Glass Constructions for exemption of Individual Approval and Guidelines for Individual Approval, State of Hessen, Germany⁹²

This decree provides requirements for glass structures, which, when fulfilled, exempts the construction of a more elaborate individual approval. In its appendices it furthermore provides guidelines for individual approvals of six construction types: generally accessible glazing, incidentally accessible glazing,⁹³ non-accessible overhead glazing, fall through proof double skin facades, single sheet thermally tempered glass in facades, and glazing constructions with filigree load carrying structures.

For accessible glazing, the impact safety and residual strength has to be proven experimentally (Appendix 2, clause 4). A drop test with a prescribed steel cylinder and a bolt (M8) head of 40 kg from a height of 800 mm should proof the impact safety. Consequently, the residual strength has to be proven by adding half the working load to

⁹¹ German version of the EN 12600.

⁹² Hessisches Ministerium für Wirtschaft, Verkehr und Landesentwicklung, *Anwendung nicht geregelter Bauarten nach § 20 der Hessischen Bauordnung (HBO) im Bereich der Glaskonstruktionen, Anforderungen an Bauarten im Zustimmungsverfahren und Freistellung vom Erfordernis der Zustimmung im Einzelfall nach § 20 Abs. 1 HBO*, Erlass vom 26. Juni 2001, Wiesbaden, Germany, 2001.

⁹³ In German, distinction is made between *begehrbar* and *betretbar*. The former indicates general accessibility (floors), while the latter describes incidental accessibility only for cleaning, maintenance and replacement (usually roofs).

the damaged construction including the impact body. Any glass sheets that had not yet broken, should be broken by a hammer or centre punch, preferably in a way that cracks are statically unfavourable. Sufficient residual strength is proven when the damaged construction can carry the loads for more than 24 hours⁹⁴.

The impact safety of incidentally accessible glazing (Appendix 3) has to be proven by two drop tests, which both differ from the one described above. A 50 kg sack of glass spheres has to be dropped from minimally 1.20 m. The glazing has to be predamaged to account for the fact that damages may always be present, and loaded with an additional evenly spread static load. A consequent test involves a combination of a drop test with a 4.1 kg steel sphere from 1 m height and a 1 kN static load at an unfavourable location on the glazing. The residual strength is tested directly after the first drop test by removing the sack with glass spheres and replacing it with a 1 kN load. After 30 minutes, the 1 kN load can be removed. The construction passes the test if it does not collapse within 24 hours.

Non-accessible glazing (Appendix 4) is tested for impact safety with the 4.1 kg steel sphere drop test. A 24 hour residual strength has to be demonstrated with a half of the evenly distributed working load.

5.1.8. German Guideline for Approval of Accessible Glass: DIBt 04.17 Anforderungen an begehbare Verglasungen; Empfehlungen für das Zustimmungsverfahren⁹⁵

This guideline treats accessible glass floors. It produces drop-tests and residual resistance requirements similar to those in the glass construction guideline from Hessen.

5.2. Comments on Impact and Failure Behaviour Related Requirements

Safety requirements which extend beyond the probabilistic analysis of glass elements thus appear in various codes and guidelines. However, when comparing these with the limitations of a probabilistic approach to structural glass described in Section 4, it has to be concluded they do not sufficiently cover those – although some better than others.

Generally, codes and guidelines lack an overall integrated safety approach. A systematic explicit analysis of the failure process from possible failure causes to the consequences of failure and all intermediate stages is not provided. The safety requirements therefore suffer from a shortage of coherence and an ad-hoc character. It is unclear at what part of the failure process they aim. They appear at various places and have a wide range of characters, varying from very general ('breakage of the glazing should not result in further damage if the glazing is part of the supporting structure', NEN-EN 13474 – aiming primarily at providing a safety margin between failure and collapse) to qualitatively prescriptive ('Overhead glazing should consist of wired or laminated glass', DIN 18008-2 and TRLV – to prevent injury. Or: 'The free edge ... should be protected from unintended impact', TRAV – to avoid damage) to extensive testing procedures to prove impact resistance and residual strength (to assess resistance to impact loads and to prevent injury).

⁹⁴ Or only 30 minutes if there is no accessible area underneath. However, that is quite unlikely for glass floors.

⁹⁵ Deutsches Institut für Bautechnik, *DIBt 04.17 Anforderungen an begehbare Verglasungen; Empfehlungen für das Zustimmungsverfahren*, Fassung März 2000, Berlin, Germany, 2000.

Partially because of this lack of an integrated approach, the impact resistance and residual strength requirements are not particularly suitable for important structural elements like columns and beams. Experimental tests like drop or pendulum tests primarily aim at demonstrating resistance to specific impacts and at avoiding injury, either from fall through, shards, or glass dropping onto somebody. Requirements are therefore mostly formulated in terms of resistance to incoming hard or soft body objects – not, or just barely, in terms of structural performance e.g. as percentage of the original load carrying capacity. Neither are distinctions made based on the role of the element in the structure, although this would be highly important to assess the safety of the structure as a whole. Actually, most requirements aim at elements which only carry external loads to a sub structure but not at elements performing a significant role in a structure, i.e. elements that carry (internal) loads from one element to another.

Furthermore, a glazing construction is usually considered to have passed a pendulum or drop test if the glass breaks and retains the object for a certain period but also if the glass does not break (e.g. according to the Dutch COBc auxiliary guideline for the approval of glass constructions, or the German TRAV). Although the latter case seems more favourable, in those cases, *no information* is obtained on the post-breakage behaviour. As other failure causes may always occur (Section 3), e.g. by faulty construction, explicit residual strength requirements should not be omitted, even if a certain impact test does not induce immediate failure.⁹⁶

The requirements for glass floors and overhead glazing in the decree on structural glass of the State of Hessen form a notable exception to some of these observations. By demanding tests for both impact resistance and a subsequent residual strength – the severity of which depends on the application (generally accessible/incidentally accessible/overhead), these requirements have a more integrated character. If not all glass layers were broken by the impact, they should be broken during the residual strength test, thus taking into account that some unknown failure cause may always cause all glass layers to break. However, this decree is still limited in scope, aiming only at elements carrying external loads.

Additionally, the relevancy of the described testing methods for other structural elements like beams and columns is questionable. Perhaps it would make sense to subject a beam to a drop test, but it is doubtful if such a test is severe enough to assess the beam's structural safety. The same could be said of a standard pendulum test on a column. But codes and guidelines do not even apply to such elements, thus it is unclear what demands they should meet.

Another important shortcoming is the fact that the relation between safety measures which address different stages of the failure process, is not treated. For instance: the TRAV requires edge protection of glazing in specific cases. But if I would insist on omitting edge protection, could that be compensated e.g. by more strict residual strength requirements (or vice versa)?

⁹⁶ Also note that the testing which does not cause breakage may have caused invisible damage that leads to premature failure in the future.

Fundamental omissions thus exist within the set of structural glass safety requirements, resulting from the lack of an integrated safety approach. It should be noted that such an approach is not only absent in codes, but also in scientific treatises. But even in the practical execution and assessment of codified experiments, at least in the Netherlands, there appear to be many ambiguities that mainly stem from an incomplete or insufficiently detailed description of the experiments.⁹⁷

Summarized, safety requirements in codes and guidelines suffer from the following shortcomings:

- Lack of an overall integrated safety approach.
- It is often unclear what part of the failure process safety requirements address.
- Safety requirements for different parts of the failure process are unrelated.
- Safety requirements are not suitable for all structural elements.
- Safety requirements are not described in terms of structural performance and independent of structural role.
- Safety requirements are insufficiently described in detail.
- Safety requirements are often very general and/or non-quantitative.

Even though an integrated safety approach is lacking, structural glass safety is well known as a general problem, under increasing attention in codes and guidelines. Building practice is, of course, also well aware of the difficulties. The subsequent chapter will explore which safety approaches and strategies are applied by engineers working in glass construction on a daily basis.

⁹⁷ CUR Bouw en Infra, Kenniscentrum Glas, Construeren met glas, stand der techniek, CUR rapport 2007-1, Gouda, the Netherlands, 2007.

5 Structural Glass Safety in Practice

The previous Chapters 3 and 4 have shown existing published and formalized safety requirements to structural glass are inadequate to actually provide sufficient safety. In this Chapter, the way safety is treated in glass engineering practice is investigated. First, a number of realized projects is introduced which have made use of more or less common safety enhancing techniques. Subsequently, some innovative and experimental concepts which are in various stages of development, are introduced. Analysis of both projects and concepts reveals they are not based on a fundamental safety analysis and generally lack *a priori* defined performance criteria to which failure behaviour can be assessed. A subsequently presented survey among structural glass engineering specialists shows that although providing residual strength is commonly held as a premise in the design of glass structures, there is no quantitative elaboration of this concept. To obtain more insight in engineer's approaches to safety related issues, six glass specialists have been interviewed on subjects such as failure experiences, residual strength and time requirements, thermal tempering, and design approach. A development towards explicitly formulated residual strength requirements was found. Nonetheless, from the projects, survey, and interviews it can be concluded that – similar to the result from the analysis of codes – a comprehensive approach to structural glass is still lacking.

1. Projects

In the previous Chapters 3 and 4 it was shown the existing published and formalized safety approaches to structural glass are insufficient to function as an overall safety concept for all structural glass applications. Codes do not provide a suitable philosophy which allows application beyond their usually limited scope. But, even within their field of application, they possess important shortcomings (Chapter 4, Section 5.2). Although there are significant developments of existing safety approaches beyond the probabilistic problem, these still hardly constitute an integrated approach to all stages of the failure process.

However, a quick scan of some structural glass projects shows that the specific safety issues of glass that stem from its brittle failure behaviour, are certainly reckoned with by practicing engineers and controlling bodies: a range of measures additional to the probabilistic analysis (i.e. stress calculation and dimensioning), was taken in various projects.

Several examples of glass beams, portrayed in Figures 5.1 – 5.3, illustrate this. Instead of using monolithic glass of a thickness as determined from simple stress analyses, composite sections of varying complexity are applied with a total section significantly larger than required from the stress calculation.



Fig. 5.1 Broadfield House Glass Museum extension, Dudley West. Span 5.7 m, 3 layers (3x10 mm), resin laminated, thermally tempered. 1994. Structural glass engineer: Dewhurst Macfarlane, London, UK.



Fig. 5.2 Laboratoires des Grand Louvre, Paris. Span 4.6 m, 4 layers (4x15 mm), PVB laminated, annealed. 1991. Structural glass engineer: RFR, Paris, France.



Fig. 5.3 Roof of the renovated ING Office, Budapest. Span 4.5 m, 3 layers (8-12-8 mm), PVB laminated, annealed & thermally tempered. 1994. Structural glass engineer: ABT, Velp, the Netherlands.

Thermal prestressing and laminating are the two techniques most often encountered to obtain safe failure behaviour. Safety-awareness can also yield various design interventions such as protective covering, compound members, and alternative load paths. Some more innovative and experimental techniques are also being developed, often aiming at obtaining significant residual strength even in when all glass layers have been broken. These techniques are briefly introduced in the subsequent sections (1.2 – 1.5). Their effect on safety is discussed in Chapter 8.¹

1.1. Prestressing

1.1.1. Thermal

The principle of thermal prestressing has been introduced in Chapter 1, Section 4. Depending on the level of prestress, two types can be distinguished: heat strengthened glass and thermally tempered glass². Figures 5.4a and b show the resulting typical stress distributions through the thickness of a glass sheet. For both types, the prestressing process is similar. The level of prestress depends on the speed of the quenching, which is lower for heat strengthened glass. In the American codes³, heat treated glass qualifies as thermally tempered when it has a surface compression of at least 69 MPa or an edge compression of at least 67 MPa. Heat strengthened glass should have a surface compression of 24 – 52 MPa. These values should be verified by polariscopic or light reflection methods.

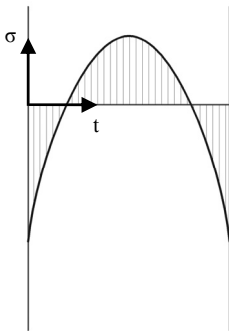


Fig. 5.4a Typical stress distribution through the glass sheet thickness from thermal tempering.

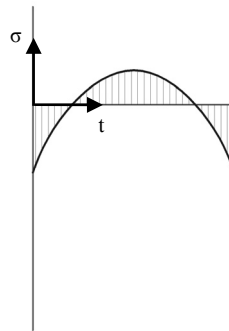


Fig. 5.4b Typical stress distribution through the glass sheet thickness from heat strengthening.

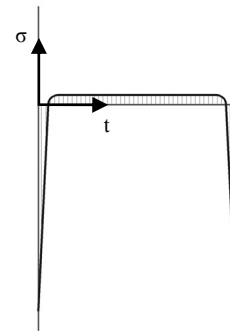


Fig. 5.4c Typical stress distribution through the glass sheet thickness from chemical prestressing.

The European codes⁴, on the other hand, qualify heat treated glass by their fracture pattern from hard pin point impact near the edge, rather than by direct surface

¹ After the introduction of the Integrated Approach to Structural Glass Safety in Chapters 6 and 7.

² Heat strengthened glass is occasionally also referred to as half-tempered glass; thermally tempered glass is also known as (fully) toughened glass.

³ American Society for Testing of Materials, *ASTM C 1048-04, Standard Specification for Heat-Treated Flat Glass—Kind HS, Kind FT Coated and Uncoated Glass*, USA, 2004.

⁴ Nederlands Normalisatie Instituut, *NEN-EN 1863-1, Glass in building - Heat strengthened soda lime silicate glass - Part 1: Definition and description*, Delft, the Netherlands, 2000, and: Nederlands Normalisatie Instituut, *NEN-EN 12150-1, Glass in building - Thermally toughened soda lime silicate safety glass - Part 1: Definition and description*, Delft, the Netherlands, 2000.

compression measurement. The fracture pattern is related to the stored strain energy: thermally tempered glass breaks into the characteristic ‘dice’ (i.e. small, more or less dice-shaped particles), while heat strengthened glass breaks into a pattern similar to annealed glass, albeit more dense (i.e. smaller fragments).⁵ This indirect checking method is less precise but much easier to execute than the American one, while still providing the information that is often the critical distinction between the two, i.e. the fracture pattern. Remarkably, however, the European codes require the fracture pattern test to be executed on specimens of specific size: 1100 x 360 mm². Apparently, when heat treated glass sheets of this size meet the required fracture specifications, than the process is deemed sufficiently accurate to obtain equal results with other sizes.

1.1.2. Chemical

Besides thermally, soda lime silicate glass can also be chemically prestressed. Chemically prestressed glass is obtained by submerging a sheet in a K⁺-solution. The potassium ions exchange place with the surface sodium (Na⁺) in the glass. Since K⁺-ions are larger than Na⁺-ions, a thin outer layer of the glass sheet (variable; usually several tens of μms) thick, is put into compression. Consequently, the inside of the glass is forced into slight tension. This process yields a stress profile through the thickness completely different from that of thermally treated glass, see Figure 5.4c. Contrary to thermally treated glass, this process induces only small amounts of elastic strain energy into the glass.⁶ As a result, the fracture pattern is equal to that of annealed glass.

The level of compressive surface stress can be controlled by treatment parameters such as temperature, solution percentage, and submersion time. Prestresses of 100 MPa or more can easily be obtained. According to the NEN-EN 12337-1⁷, the characteristic bending tensile stress of chemically strengthened float glass is 150 MPa (including inherent strength) – and thus very strong.

1.2. Laminating

Glass laminates are manufactured by joining sheets of glass together with thin, transparent adhesives or adhesive foils (see also Chapter 1, Section 4). If so desired, glass sheets with different heat treatments can be combined to obtain certain combinations of resistance and failure properties. Usually, however, only one type of glass is applied in a laminate.

The resistance and failure behaviour of laminated glass is strongly influenced by the type of laminate. Roughly, three kinds can be distinguished: castable adhesive resins, soft adhesive foils, and stiff adhesive foils. They are all visco-elastic polymers and their material behaviour is thus complex, depending on load duration, temperature, moisture, and other environmental influences.

⁵ Interestingly, recent research has shown a strong dependency of the fracture pattern on the impact location (e.g. near the edge or in the middle of the face surface). Jacob, L., Davies, P.S., Munz, N., *Fracture Characteristics of Heat Treated Glass – Safety Classification Characteristics*, Proceedings of the Glass Performance Days, Tampere, Finland, June 2009.

⁶ The total amount of elastic strain energy is proportional to the area under the graph of Figure 5.4a – c. See Chapter 9.

⁷ Nederlands Normalisatie Instituut, NEN-EN 12337-1, Glass in building - Chemically strengthened soda lime silicate glass - Part 1: Definition and description, Delft, the Netherlands, 2000.

Contrary to foils, resins can fill relatively large cavities, which may specifically occur between sheets of tempered glass. However, foils are often preferred whenever possible, because of their ease of application and better mechanical properties (tear resistance).

Soft foils are most often employed for laminated glass. As a rule, Polyvinyl Butiral (PVB) is used, but some other foils exist, such as Ethylene Vinyl Acetate (EVA), which is often used for laminated glass with photovoltaic cells. PVB is stored on rolls, typically 0.38 mm thick, and applied in two or four layers.

Ionomer foils have a much higher modulus of elasticity⁸ and were introduced in the building industry relatively recently,⁹ originally to obtain better impact performance from airborne debris in hurricane prone areas. SentryGlas (SG), developed by DuPont de Nemours, is the best known commercially available brand. The standard thickness used to be 1.52 mm, but recently other thicknesses have been introduced. SG is manufactured in sheets of 1220 x 1520 mm².

1.3. Design Solutions

Besides altering the glass panel by heat treatment and/or laminating, various design solutions are being applied to increase the safety of glass structures and structural glass elements, such as:

- Receding inner layers,
The outer protruding layers protect the edge of the inner layer, making failure from incidental impact highly unlikely (Figures 5.5a and b).
- Protective covering of the glass element edge,
To avoid impact damage.¹⁰



Fig. 5.5a, b Structural glass column, town hall of Saint-Germain-en-Laye, France, 1994. Overview (left) and detail (right), with the receding inner layer visible. In this design, only the inner layer is load carrying.
Architect: Brunet et Saunier, Structural Engineer: OTH/Alto – M. Malinowski.

⁸ $E_{PVB} = 0.018$ MPa, whereas $E_{SG} = 0.3$ MPa. Belis, J., Kipsterkte van monolithische en gelamineerde glazen liggers, Dissertation, Laboratory for Research on Structural Models, Ghent University, Ghent, Belgium, 2005.

⁹ The SentryGlas (SG) ionomer interlayer of DuPont de Nemours has been commercially available since 1998. It was initially known as SentryGlas Plus (SGP).

¹⁰ This has not been done in the previously mentioned projects, but has been repeatedly suggested by structural glass engineers. See Section 2 of this Chapter.

- Compound Elements,
Dividing a structural element into multiple parts to limit possible damage one segment (Figures 5.6 and 5.7).
- Alternative load paths.
Designing the structure so that loads can be redistributed when a structural members loses its load carrying capacity (Figure 5.8a and b).



Fig. 5.6 Subway Entrance Canopy, Tokio, Japan. Total span 10.8 m, 4 segments (3 of which double), two 19 mm thermally tempered glass layers, with an acrylic layer in between, 1996. Structural glass engineer: Dewhurst Macfarlane, London, UK.



Fig. 5.7 Atrium roof of the Chamber of Commerce, Munich, Germany. Total span 14 m, 5 segments (2 double, 3 triple), double and triple layers, PVB laminated, thermally tempered and heat strengthened, 2002. Structural glass engineer: Ludwig und Weiler, Germany.



Fig. 5.8a Allied Irish Bank (AIB), Dublin, Ireland. Span: 8 m. 2 Sections of 3x12 mm heat strengthened glass. PVB laminated. 2007. Façade design: Arup, London, UK. Structural glass engineer: Gartner Steel and Glass,¹¹ Würzburg, Germany.

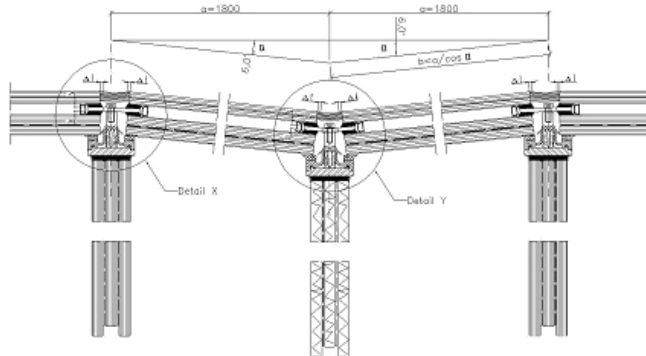


Fig. 5.8b Alternative load path designed in the glass roof structure of the AIB in Dublin, Ireland. If the beam would lose its load carrying capacity completely by breakage of all layers, a catenary mechanism in the roof plates is activated, perpendicular to the main span, to prevent collapse. Note that also a receding inner layer has been applied.

1.4. Innovative and Experimental Safety Enhancing Techniques

Various research institutes, engineering offices, and other companies have been involved in the development of new glass design concepts to increase safety. Their effect on element safety is extensively discussed in Chapter 8, along with the more traditional methods. These concepts are in various stages of maturity – some have been

¹¹ Part of the Permasteelisa Group.

applied in a number of projects, some in a single one, and others have yet to leave the laboratory. They include:

- High-stiffness and/or high-strength interlayers,
 - Additional polymer sheet materials (e.g. PC, PMMA),
*Glass treads have been simply provided with a non-laminated PMMA sheet beneath them in several projects by Dewhurst Macfarlane.*¹²
*Glass-PC laminates were originally introduced as bullet-proof glazing, but already in 1997, Veer et al.*¹³ *showed they can also posses considerable post-failure strength in both plates and beams (Figure 5.10). More recent work by Weller et al.*¹⁴ *confirmed this.*
 - Ionomer laminating foils (e.g. SG),
*The safety effect of ionomer laminating foils is comparable to the application of glass-adhesive-polymer sheet laminates (Fig. 5.11).*¹⁵
 - Steel-wire mesh or perforated steel sheet,
*Feirabend and Sobek*¹⁶ *presented the possibility of laminating steel-wire mesh or perforated steel sheet between two layers of PVB or SG to obtain even better post-failure resistance (Figure 5.12).*

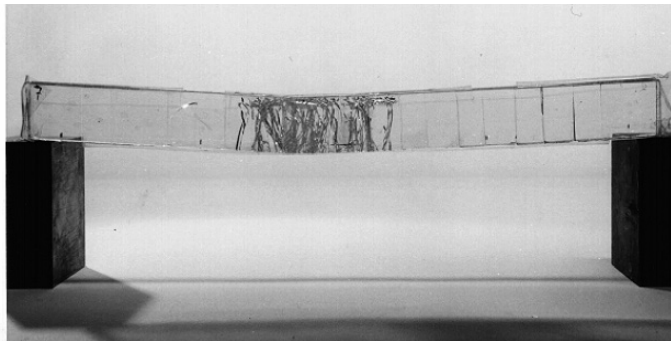


Fig. 5.9 Original Zappi Concept: a 400 mm glass-PC laminate beam, after failure.

¹² Figure 8.13, Chapter 8, Section 4.3.3.

¹³ For (standing) beams: Veer, F.A., Liebergen, M.A.C. van, Vries, de S.M., *Designing and engineering transparant building components with high residual strength*, Proceedings 5th glass processing days, Tampere, Finland, 1997, and later publications. For plates: Veer, F.A., Vries, S.M. de, *Transparant laminated composites for novel architectural structures*, Proceedings 9th European Conference on Composite Materials, Brighton, UK, 2000. See also *AdDoc I: Zappi, 1996 – February 2004*, additional document to this PhD, www.glass.bk.tudelft.nl.

¹⁴ Weller, B., Weimar, T., *Glass-Polycarbonate-Sandwich-Elements as Overhead Glazing*, Proceedings of the 10th Glass Performance Days, Tampere, Finland, 2007.

¹⁵ See e.g. Belis, J., Depauw, J., Callewaert, D., Delincé, D., Impe, R.van, *Failure Mechanisms and Residual Capacity of Annealed glass/SGP Laminated Beams at Room Temperature*, Engineering Failure Analysis, 2008; or: *Verbund sicherheitsglas mit SentryGlas Plus erstmals in Europa eingesetzt*, Glas; Architektur und Technik, issue 4/2002, pp 51-53.

¹⁶ Feirabend, S., Sobek, W., *Reinforced Laminated Glass*, Proceedings of the Challenging Glass Conference, Delft, the Netherlands, May 2008. Fig. 5.11 is taken from this publication.



Fig. 5.10 Post-failure behaviour of an SG laminated glass plate.

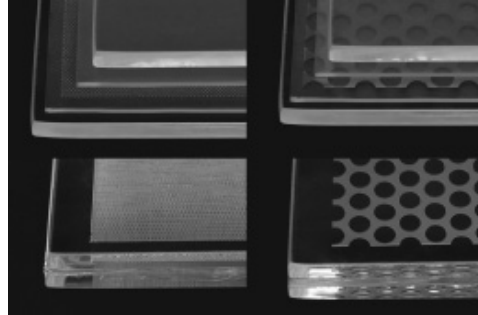


Fig. 5.11 Perforated steel sheet laminated in a glass plate, between PVB layers.

- Linear Reinforced elements,

- Steel reinforced,

The possibility of reinforcing a glass beam with a steel profile was introduced by Veer et al.¹⁷ – then still in combination with a glass-PC laminate. In later designs, the PC was considered obsolete and omitted (Figure 5.12).¹⁸ More recently, Nielsen & Olesen¹⁹ presented studies on the same concept (Figure 5.13).

Separately from the developments at the universities, this concept was applied for a project in Badenweiler, Germany by Schlaich Bergermann und Partner (Figures 5.14a and b).²⁰

- Carbon-fibre reinforced polymer (CFRP) reinforced,

Another reinforcement concept evolved around the same time in Italy, where CFRP reinforced glass beams were applied in a tri-hinged frame to restore the roof of a 13th century building, presented by Palumbo (Figures 5.15a and b).²¹ Recently, further research on this concept was presented.²²

¹⁷ Veer, F.A., H. Rijgersberg, D. Ruytenbeek, P.C. Louter, J. Zuidema, *Composite glass beams, the third chapter*, Proceedings of the Glass Processing Days, Tampere, Finland, 2003.

¹⁸ E.g. Bos, F.P., F.A. Veer, G.J. Hobbelman, P.C. Louter, *Stainless steel reinforced and post-tensioned glass beams*, Proceedings of the 12th International Conference of Experimental Mechanics (ICEM12), Bari, Italy, 2004; Louter, P.C., J. Belis, F.P. Bos, F.A. Veer, G.J. Hobbelman, *Reinforced glass cantilever beams*, Proceedings of the 9th International Conference on Architectural and Automotive Glass (GPD), Tampere, Finland, 2005; Louter, P.C., *Adhesively bonded reinforced glass beams*, HERON Volume 52 (2007) issue 1/2 special issue: Structural glass, <http://heron.tudelft.nl>.

¹⁹ Nielsen, J.-H., Olesen, J.F., *Mechanically Reinforced Glass Beams*, Proceedings of the 3rd International Conference on Structural Engineering, Mechanics, and Computation, Cape Town, South Africa, 2007.

²⁰ Schober, H., Gerber, H., Schneider, J., *Ein Glashaus für die Therme in Badenweiler*, Stahlbau 73, Heft 11, 2004, pp. 886-892. Figures 5.14a and b were taken from this publication.

²¹ Palumbo, M., *A new roof for the XIIIth Century “Loggia de Vicari” (Arquà Petrarca –PD, Italy) based on structural glass trusses: a case study*, Proceedings of the 9th international conference on Architectural and Automotive Glass (GPD), Tampere, Finland, 2005. Fig. 5.15b is based on this publication.

²² Antonelli, A., Cagnacci, E., Giordano, S., Orlando, M., Spinelli, P., *Experimental and Theoretical Analysis of C-FRP Reinforced Glass Beams*, Proceedings of the 3rd International Symposium on the Application of Architectural Glass (ISAAG), Munich, October, 2008. And: Cagnacci, E., Orlando, M., Pecora, M.L., Spinelli, P., *Application of C-FRP Strengthened Glass Beams in Façade Design*, Proceedings of the 3rd International Symposium on the Application of Architectural Glass (ISAAG), Munich, October, 2008.

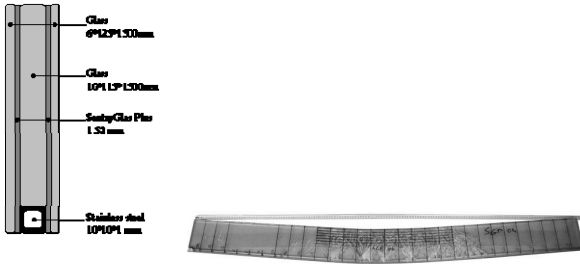


Fig. 5.12 One of many stainless steel reinforced glass beams developed by the Zappi Glass&Transparency Research Group, TU Delft: $l \times h \times t = 1500 \times 125 \times (3 \times 10)$ mm, SG-laminated, stainless steel reinforcement profile (10 x 10 x 1).

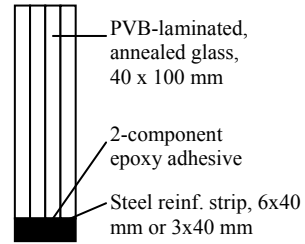


Fig. 5.13 Steel reinforced glass beam concept by Nielsen & Olesen.



Fig. 5.14a Glass roof at the Spa Thermen in Badenweiler. Span: 6.2m. 3x10 mm thermally toughened glass. PVB laminated. Steel reinforced and post-tensioned. 2004. Structural glass engineer: Schlaich Bergemann, Stuttgart, Germany.

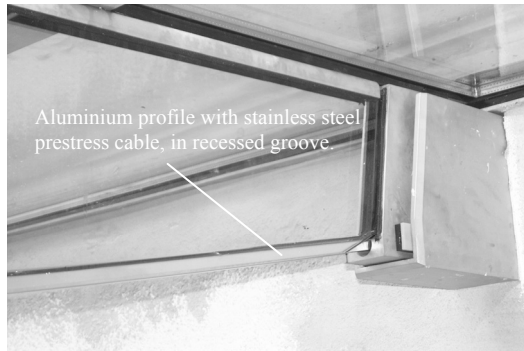


Fig. 5.14b Glass beam (detail) at the Spa Thermen in Badenweiler.



Fig. 5.15a Loggia dei Vicari, Arquà Petrarca (PA), Italy. Span: 11 m. 2 Sections. 4 layers, annealed glass. PVB laminated. Carbon fibre reinforcement strip. ~ 2004. Structural glass engineer: Vetrostrutturale, Brescia, Italy.

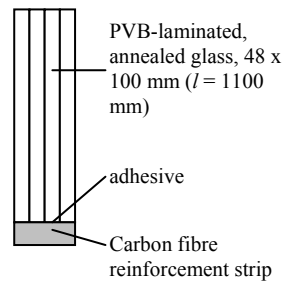


Fig. 5.15b Section of the CFRP reinforced glass beams applied at the Loggia dei Vicari, Arquà Petrarca.

- Hybrid elements,²³
 - Glass-Wood,
Extensive work on Glass-Wood hybrid beams has been presented by Hamm²⁴ and Kreher,²⁵ specifically so they could be applied in the construction of a hotel in Switzerland (Figure 5.16a and b). Lately, research by Cruz & Pequeno²⁶ targeted the same concept. Additionally, they introduced glass-wood composite panels (Fig. 5.17).²⁷
 - Glass-Steel,
Composite beams with steel flanges and a glass web have been presented by Wellershof & Sedlacek²⁸ (Figure 5.18). Froli & Lani²⁹ developed a beam concept consisting of post-tensioning rods in a lattice truss layout with glass filling the interstitial spaces (Figure 5.19).
 - Glass-Reinforced Concrete.
A beam with a glass web and flanges consisting of a high-performance concrete section with up to 4 reinforcement strands was published by Freytag (Figure 5.20).³⁰

²³ The distinction between ‘reinforced’ and ‘hybrid’ elements is somewhat arbitrary. It was made as in some concepts the influence of the additional components on both the pre-failure resistance and the aesthetical character is minimal (reinforced elements), while in others the presence of other materials highly influences both the pre-failure performance and the aesthetical character of the element (hybrid elements).

²⁴ Hamm, J., *Tragverhalten von Holz und Holzwerkstoffen im statischen Verbund mit Glas*, PhD Thesis Nr. 2065, IBOIS/EPFL, Lausanne, Switzerland, 2000.

²⁵ Kreher, K., *Tragverhalten und Bemessung von Holz-Glas Verbundträgern unter Berücksichtigung der Eigenspannungen im Glas*, PhD Thesis Nr. 2999, IBOIS/EPFL, Lausanne, Switzerland, 2004. And: Kreher, K., Natterer, J., Natterer, J., *Timber-Glass-Composite Girders for a Hotel in Switzerland*, Structural Engineering International, 2/2004, pp. 149-151.

²⁶ Cruz, P., Pequeno, J., *Timber-Glass Composite Beams: Mechanical Behaviour & Architectural Solutions*, Proceedings of the Challenging Glass Conference, Delft, the Netherlands, 2008.

²⁷ Cruz, P., Pequeno, J., *Timber-Glass Composite Structural Panels: Experimental Studies & Architectural Applications*, Proceedings of the Challenging Glass Conference, Delft, the Netherlands, 2008. Fig. 5.18 is taken from this publication.

²⁸ Wellershof, F., Sedlacek, G., *Structural Use of Glass in Hybrid Elements: Steel-Glass Beams, Glass-GFRP Plates*, Proceedings of the Glass Processing Days, Tampere, Finland, 2003. Fig. 5.18 is taken from this publication.

²⁹ Froli, M., Lani, L., *Towards Ductile Glass Beams*, Proceedings of the IASS Symposium, Venice, Italy, 2007. Fig. 5.19 is taken from this publication.

³⁰ Freytag, B., *Glass-Concrete Composite Technology*, Structural Engineering International, 2/2004, pp. 111-117.



Fig. 5.16a Hotel Palafitte, Monruz (NE), Switzerland, 2002. Structural glass engineer: IBOIS Institute, EPFL, Lausanne, Switzerland.

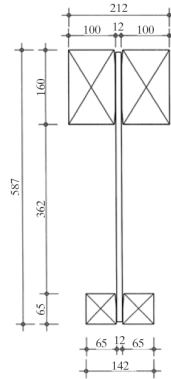


Fig. 5.16b Section of the glass-wood beams applied at the Hotel Palafitte.³¹ A thermally tempered 12 mm single sheet of glass was used.

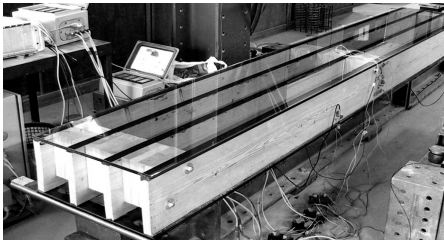


Fig. 5.17 Glass-wood panels (Cruz et al.).

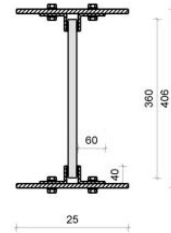


Fig. 5.18 Glass-steel beams (section), by Wellershof & Sedlacek.

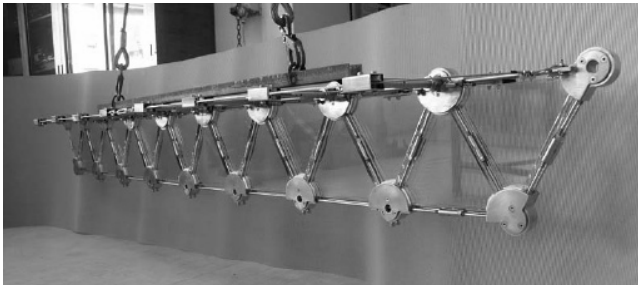


Fig. 5.19 Glass-filled post-tensioned steel lattice truss, presented by Froli & Lani.

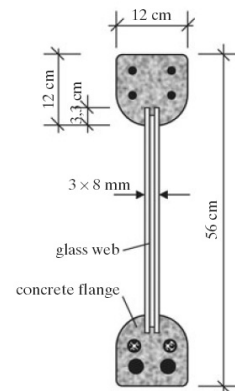


Fig. 5.20 Glass-Reinforced Concrete beam (section), proposed by Freytag.

³¹ Taken from: Kreher, K., Natterer, J., Natterer, J., Timber-Glass-Composite Girders for a Hotel in Switzerland, Structural Engineering International, 2/2004, pp. 149 – 151.

1.5. Remaining Questions

A wide variety of strategies is available to obtain safety in structural glass, and more are being developed. They are applied to varying extent; experimental concepts are in different stages of maturity. The effect of these techniques on the safety of glass elements will be discussed in Chapter 8.

For now, it is highly important to note that, despite the effort put into the investigation of safety enhancing design concepts, it remains generally unclear what (quantitative) performance is aimed at. Neither in studies concerning the developed techniques of (PVB-) laminating and thermal prestressing, nor in those regarding more experimental concepts,³² can a comprehensive analysis be found with regard to specific (preferably) quantifiable safety goals that need to be obtained. Only general notions are provided, such as: ‘structures must warn before collapsing...’^{33,34} – usually translated as providing a margin between initial and final failure in terms of resistance, deformation, or both.³⁵ Often initial resistance (when cracking starts) and the maximum resistance before collapse is listed (usually determined from 4-point bending tests),³⁶ tacitly assuming their ratio is a measure for safety. Additionally, in practice sometimes protective measures are taken to decrease the possibility of failure from unconsidered causes. This, however, does not appear consistently in either projects or concept developments, and thus seems to be applied rather randomly.

The lack of any significantly developed (set of) a priori goal(s), to which the performance of an element may be compared, results in some fundamental flaws in the development of safe glass elements:

- It is rather single-sided.³⁷ When considering the failure process as sketched in Figure 4.6³⁸, it will be clear that providing a margin between the initial cracking resistance and the maximum resistance aims at reducing the probability of collapse, given a failure. However, the same Figure indicates there may be more aspects to consider, most notably the probability of unconsidered circumstances causing failure, but also the accuracy of the formal probability problem as well as the injury potential of the element.

³² Including, admittedly, those of the Zappi research group.

³³ Nijse, R., *Glass in Structures*, Birkhäuser, Basel, Switzerland, 2003, p. 12.

³⁴ Also: Hamm, J., *Tragverhalten von Holz und Holzwerkstoffen im Statischen Verbund mit Glas*, PhD Thesis Nr. 2065, IBOIS/EPFL, Lausanne, Switzerland, 1999, p. 125. Even though extensive research was done at the EPFL on glass-timber composite elements, those studies did not present a priori requirements for post-failure resistances.

³⁵ See e.g. Cruz, P., Pequeno, J., *Timber-Glass Composite Beams: Mechanical Behaviour & Architectural Solutions*, Proceedings of the Challenging Glass Conference, Delft, the Netherlands, 2008; or: Bos, F.P., Veer, G.J. Hobbelman, P.C. Louter, *Stainless steel reinforced and post-tensioned glass beams*, Proceedings of the 12th International Conference on Experimental Mechanics (ICEM12), Bari, Italy, 2004.

³⁶ See e.g. practically all publications mentioned in the footnotes to Section 1.4.

³⁷ It will be concluded in Chapter 8, Sections 3.4 and 5, that this is indeed the most fundamental aspect of providing safety. The attention for post-failure resistance is therefore in itself not mistaken, but also not complete as a safety approach.

³⁸ Chapter 4, Section 4.

- It yields illogical results. Various authors³⁹ have noted that direct overloading of a PVB laminated element causes collapse and results in no residual strength. Thus, from the above assumption of requiring a margin between initial and post-failure strength, it would have to be concluded laminated glass is as unsafe as single sheet glass is, while it obviously is not as the probability of an inner layer cracking is much smaller.
- The testing method (direct overloading in e.g. bending tests) is considered valid to assess the safety performance, while considering the previous point, this should be doubted. A method should be adopted that at least allows distinction between performance of laminated and single sheet glass.⁴⁰
- Finally, it does not provide a quantified goal. No study specifies a post-failure resistance target. Thus, it can not be concluded whether a desired level of safety is actually obtained.

These deficiencies make it difficult to see how the presented concepts could progress. Furthermore, it is impossible to decide consistently on a range of design measures, such as:

- the number of layers to use,
- the respective thickness of the layers,
- the number of failed layers to be reckoned with,
- the required strength after failure,
- the required time that strength has to be maintained,
- the amount of prestress,
- the kind of interlayer,
- the application of other strategies such as alternative load paths,
- etc.

From reviewing realized projects as well as innovative concepts, it may be deduced that practising engineers and researchers have their opinions on these matters, probably with a varying level of focus and possibly with different priorities. It is not clear if project specific parameters are the main source of different solutions or if they stem from fundamentally different views. Therefore, these issues have been investigated by means of a survey among glass engineers, followed by a series of interviews with some recognized experts in the field.

³⁹ For (standing) beams: Hess, R., *Glasträger*, vdf Hochschulverlag AG an der ETH Zürich, Switzerland, 2000; for plates: Feirabend, Sobek, *Reinforced Laminated Glass*, Proceedings of the Challenging Glass Conference, Delft, the Netherlands, May 2008. Additionally, it should be noted the author has obtained slightly different results for directly tested, PVB laminated annealed glass standing beams. Very small post-failure resistances were found for double and triple layer beams (in the order of 1 – 3 %, see App. H). For heat strengthened and thermally tempered glass beams though, the conclusions with regard to post-failure resistance would be identical: when obtained from direct overloading it is less than the elements self-weight and thus leads to collapse.

⁴⁰ It is shown in Appendix E that the post-failure behaviour of PVB laminated glass beams heavily depends on the failure cause. Direct overloading results in significantly less residual capacity than overloading after significant pre-applied damage.

2. Short Survey on Material and Design Specifications for Structural Glass Components

The goal of this survey was threefold:

- To find out what general premises are held with regard to safety of structural glass projects.
- To investigate how these premises translate into practice, i.e. what material and design specifications result from them.
- To explicate to what extent opinions of structural glass specialists differ on these issues.

The survey yielded 21 responses. A full report and the questionnaire can be found in Appendix B.

2.1. Questions

The opening question of this five-question query, inquired about the general premises of the respondent with regard to safety in glass structures. In the consecutive questions 2 through 4, the respondent was asked to consider three specific structural elements: a beam, a façade fin and a floor panel. The sub questions *a* through *d* deal with the material- and design specifications for these elements, particularly with regard to the number of layers in a laminate, the required level of thermal prestressing, the laminate type, and other measures. Thus, these questions tried to shed light on the way general premises are translated into practice solutions. Finally, question five gave room for further comments by the respondent.

2.2. Results & Analysis

2.2.1. Responses

Not all questions were answered by each respondent. Table 5.1 lists the number of responses per question.

Table 5.1 Number of responses per question.

Question	1	2a	2b	2c	2d	3a	3b	3c	3d	4a	4b	4c	4d
# of responses	18	19	19	19	18	13	11	12	12	18	18	17	18

2.2.2. Question 1: Could you briefly describe your premises with regard to safety, when you're working on a project involving structural glass?

Realizing residual strength is by far the most important point of attention when using glass for structures. In 17 out of 18 answers with regard to the premises for a structural glass project, this is mentioned in one way or another. However, there seem to be significant differences in the level of detail this principle is carried through in the design. While a few consider multiple stages of damage of a member, most others simply indicate 'residual strength needs to be realized'. The type or area of application is mentioned by some to be of influence on the level of residual strength required.

In most cases, the level of required residual strength is not quantified further. Only one respondent states he uses a safety factor of 1.1 in case of failure, while another said to

use three layers in a beam, and count only two in the calculations. Yet another indicated to work with lower safety factors when considering glass breakage, depending on the location and application.

Thus, although the necessity for residual strength is commonly felt, there seems to be no clear idea what ‘residual strength’ actually is in quantifiable terms and on which factors it may depend. Therefore, there can also be no common agreement on how much residual strength is needed in which application.

2.2.3. Question 2: Consider a *GLASS BEAM* (span approx. 5 m)

- 2a: How many layers of glass would you prescribe?
A small majority (57.9 %) has developed in favour of a three layer minimum for glass beams of 5 m span (Figure 5.21).
- 2b: What type, if any, of prestressing would you prescribe?
The responses to this question gave a more diffuse picture (Figure 5.22). Most respondents (36.8 %) would prescribe heat strengthened glass, but an almost equally large group (31.6 %, a difference of 1 respondent) indicated that any type of prestress is, in principal, possible.
- 2c: What kind of laminate material would you prescribe?
Again, a significant group considered any laminate material possible (21.1 %), but the majority indicated that it would have to be either PVB or Ionomer (52.6 %), see Figure 5.23.
- 2d: Would you prescribe any other special measures?
This question yielded a host of varying answers. No clear picture emerged with regard to other/special measures that might be required.

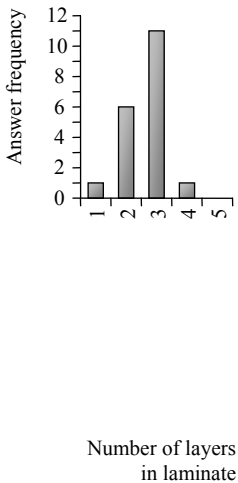


Fig. 5.21 Overview of responses to question 2a.

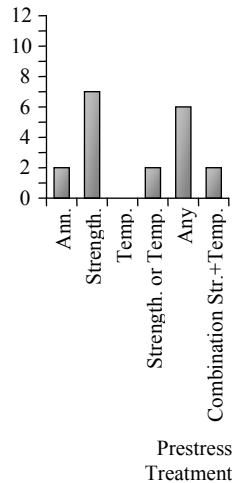


Fig. 5.22 Overview of responses to question 2b.

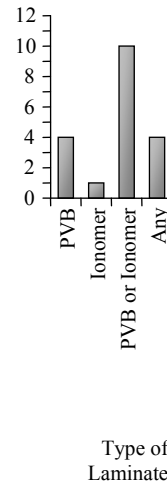


Fig. 5.23 Overview of responses to question 2c.

2.2.4. Question 3: Consider a GLASS FAÇADE FIN

- 3a: How many layers of glass would you prescribe?
Almost half of the respondents (46.2 %; Figure 5.24) found a one-layer solution suitable in cases where there is no risk of people bouncing into the fins. However, one of those noted he would prefer a two layer solution, although he did not find that the absolute minimum. A slight majority of 53.8 % specified a multi-layer (2-3) solution in any case.
- 3b: What type, if any, of prestressing would you prescribe?
A large majority (Figure 5.25) considers any type of prestressing possible, depending on parameters such as the presence of point fixings, required strength, maximum weight and price.
- 3c: What kind of laminate material would you prescribe?
Contrary to the similar question with regard to 5 m beams, there is a considerable consensus on the use of laminate in fins (Figure 5.26).
- 3d: Would you prescribe any other special measures?
Some general heeds were given regarding detailing, but there is no generally felt need for further measures.

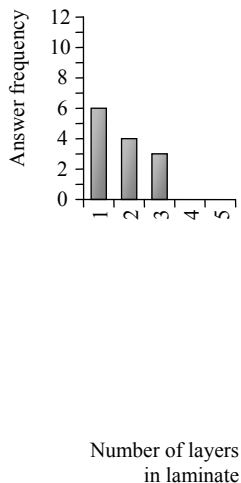


Fig. 5.24 Overview of responses to question 3a.

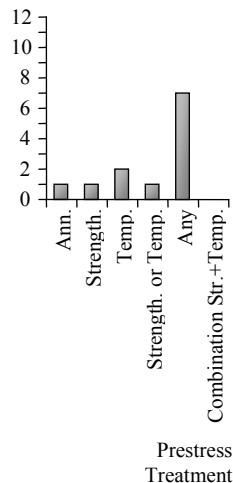


Fig. 5.25 Overview of responses to question 3b.

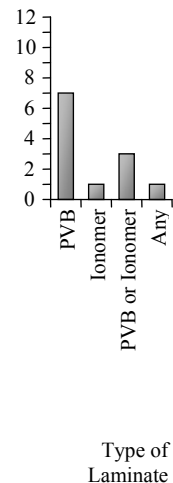


Fig. 5.26 Overview of responses to question 3c.

2.2.5. Question 4: Consider a GLASS FLOOR PANEL

This question yielded the most agreement in the answers. Especially question 4a gave a clear picture.

- 4a: How many layers of glass would you prescribe?
Fourteen respondents (77.8 %) opted for at least three layers, while four (22.2 %) choose two layers (Figure 5.27).
- 4b: What type, if any, of prestressing would you prescribe?

As with questions 2b and 3b, the largest group (33.3 %) felt any prestress treatment could be possible (Figure 5.28).

- 4c: What kind of laminate material would you prescribe?
Again, a high preference for PVB was found (Figure 5.29).
- 4d: Would you prescribe any other special measures?
Some general remarks concerning detailing were given. However, four respondents explicitly required residual strength tests.

2.2.6. Question 5: Is there any other comment you would like to add?

Most answers to question 5 contained the notion that there should *not* be a definite design and/or material prescription for certain applications, but rather that clear criteria are necessary to which designs can be checked.⁴¹

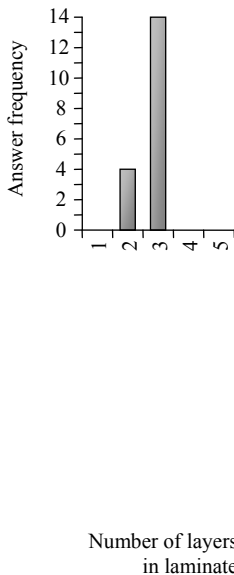


Fig. 5.27 Overview of responses to question 4a.

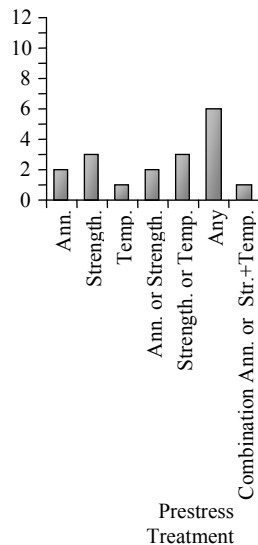


Fig. 5.28 Overview of responses to question 4b.

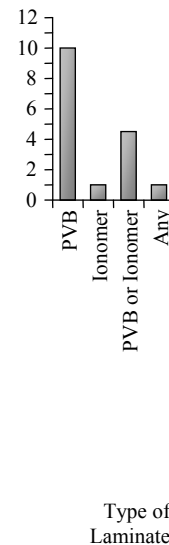


Fig. 5.29 Overview of responses to question 4c.

2.2.7. Conclusions from Survey

This survey sought to find out a) what premises are held with regard to safety of structural glass projects, b) how they work out in practice, and c) how big opinion differences are on these issues.

⁴¹ It was not the intention of this survey to arrive at definite member designs by inventorizing what the majority of the field thinks of certain design issues. In the framework of this survey, the word choice in the questions ('prescribe') was perhaps misleading. Maybe a more neutral word like 'use' would have been more suitable.

The need to provide some form of residual strength is universally recognized by professionals in the field. However, views on how residual strength should be obtained in practical designs vary. There seems to be no quantitative elaboration of this concept. No other generally carried premise with regard to the safety of structural glass was encountered.

In practice, residual strength is provided by multi-layer designs in beams and floors. For both these types of members, a majority finds three layers to be the minimum (regardless of project specifics), but for floors this majority is more significant than for beams (over 75 % vs approximately 55 %). However, there is no generally accepted view on what extent of glass breakage should be taken into account (1, 2, or all layers broken) and what loads should be considered in those cases. The level of detail in which such scenarios are considered also seem to vary widely, although this impression may depend on the amount of time and effort put in the survey by the individual respondents.

More than three layers are not necessary from a safety point of view, neither for beams nor for floors.

Fins are judged differently. Almost half of the respondents find one layer to be the minimum, although some prefer two layers. The other half requires a multi-layer solution. That group can again be approximately equally split between respondents requiring 2 and those requiring 3 layers. Residual strength for this type of members is thus not as important.

Residual strength is also provided by using annealed or heat strengthened glass, which have favourable cracking patterns. Thermally tempered glass is appreciated for point fixings and other peak stress applications, but its breakage pattern is a major disadvantage for the safety. Possibly as a result, the level of prestress required in structural glass members is highly dependent on the specific project details, much more so than the other investigated parameters. Relevant project specifics may include presence of point fixings / type of support, risk of bumping into, actions on the element, required maximum weight, etc.

The large body of knowledge on PVB, both in terms of scientifically acquired data and practical experience, is greatly appreciated and is one of the reasons why it is often preferred over ionomer interlayers.

3. Interviews⁴²

The survey on material and design specifications of structural glass elements has given some insight into safety premises held in structural glass practice and the extent of the variation of differences in opinion in the field. However, the inevitable brevity of the questions and the answers as well as the lack of direct interaction with the respondents has left several issues in need of further elaboration. Therefore, six highly respected professionals in the field of structural glass engineering, all of whom also filled out the survey previously described, have been interviewed. Refer to Appendix C for the

⁴² This was a study of opinions *held in practice*. In the discussion of various safety related subject, the views of the interviewees have been presented as objectively as possible. They do not necessarily coincide with those of the author. Neither have all the assertions of the interviewees been factually checked.

interview agenda with explanatory notes as well as full reports of each interview. The interviewees were Rob Nijse, Graham Dodd, Tim Macfarlane, Jens Schneider, Holger Techen, and Frank Wellershof.⁴³

The interviews served to gain more in-depth insight into the same subjects as the survey, specifically issues such as:

- The position safety considerations take in the structural glass design process.
- Failure experiences and (perceived) common failure causes.
- Project dependency / independency of safety measures.
- Differences in safety approaches.

3.1. Finding a useable value for the strength of glass

A problem both Nijse and Macfarlane encountered in the 1980's, was the fact that very little was known about the strength of glass. **RN**: "The small amount of data available suggested a tensile strength of about 40 N/mm². I used to divide that number by an (arbitrary) material partial factor of 5, which lead to a design strength of 8 N/mm²." Macfarlane ended up with a similar figure, albeit through a different way. **TM**: "After a long search, I ended up using 7 N/mm² for the long-term strength. This was based on a mean value of approximately 70 N/mm², which I found in *Mark's Handbook*, an engineering handbook from 1941, and divided by 10, an intuitive *factor of ignorance*." Remarkably, these figures are very close to the long term strength of annealed glass according to, for instance, the NEN 2608-2:2007: 7,25 N/mm².

3.2. Thermally prestressed glass: a failed idea of safety?

Since the beginning of the 1990's, there have been extensive discussions on which type of glass (annealed or thermally toughened, later also heat strengthened) would be most safe to use in glass structures. Nijse as well as Dodd and Macfarlane claim the traditional trust in the safety of thermally tempered glass is out-dated. Although tempered glass has significantly higher strength than annealed glass, it can, off course, also break. Because of the breakage pattern in countless small humps, there will be no residual strength left, especially in unlaminated applications. Furthermore, the internal stress state makes thermally tempered glass actually more prone to failure from local hard impact or scratching, because, while this would only chip of small bits of annealed glass, it could disintegrate a toughened panel completely.⁴⁴

When considering personal safety, it should be noted that tempered glass does not always immediately break into small humps completely (Figure 5.30). Techen did experiments for a green house project with puppets covered with leather, situated beneath a heavily tempered (150 MPa) 4 mm thick glass pane which was subsequently broken. The test showed the glass falls down in large pieces⁴⁵ which only break into

⁴³ When quoted in the following, their names are abbreviated with the first letters of their given name and surname, e.g. **RN** = Rob Nijse.

⁴⁴ As was confirmed by experimental research presented in Appendix E.

⁴⁵ Similar observations have been noted by Isselmans, C., *Schadagevallen met Glas*, in: Stichting Postacademisch Onderwijs in Civiele Techniek en Bouwtechniek, Bouwkundige en constructieve toepassingen met glas, professional post-academic course, Delft, the Netherlands, 2007.

small ones upon hitting an object (i.e. the puppets). The leather skin was punctured numerous times. Although perhaps not as lethal as large shards from annealed glass, the toughened glass humps are not innocent.

Contrary to common practice, Macfarlane actually used annealed glass regularly in structural applications. In many of his staircases, the treads consist of a single sheet of 19 mm thick annealed glass with a 15 mm acrylic layer underneath. The glass and acrylic sheets are not laminated together. The argument is that because of the glass type (annealed) and thickness, failure is likely to result in a single (transverse) crack breaking the glass in two parts, leaving the acrylic to carry the loads (although with much more deflection). Over the years, only one tread has actually broken in all those staircases, and it happened exactly in the predicted fashion.

On the subject of suitability for structural applications, however, Schneider disagrees with Macfarlane and feels annealed glass should not be used in structural applications. Heat strengthened and thermally tempered glass can both be options as long as they are heat-soaked to exclude nickel-sulfide induced failures. **JS:** “I’m not convinced that, because of the cracking pattern, heat strengthened glass in a reinforced beam is much better than thermally tempered glass. Experiments executed on beams for the Spa Thermen extension resulted in considerable residual strength even in case all three layers were broken.”



Fig. 5.30 Thermally toughened glass does not always break into small humps immediately upon failure.

Heat strengthened glass is favoured by Techen for overhead applications because of its combination of impact resistance and cracking pattern (resulting in residual strength). These characteristics are also valued by Nijssse, who applied it frequently, especially in balustrades.

3.3. Failure cases

Nijssse emphasizes that negligent work (manufacturing, transport and mounting) is the most common cause of premature failure. In one of his projects, a series of glass beams

all broke shortly after installment. The inside edges of bolt holes had not been polished, contrary to specification. Unfortunately, the client got so disturbed by this experience, he demanded the glass beams to be replaced by steel ones. Improvements in the material composition, manufacturing, handling, and construction would therefore be much desired in the future.⁴⁶

Thus, it is extremely important not only to deliver a safe design, but also to remain particularly vigilant during the construction. This plea is wholeheartedly supported by Macfarlane and Dodd, but the latter adds: “It is impossible to ban such errors completely. Besides accidental mistakes, there can always be crucial errors caused by time or financial pressure, or plain ignorance.” **JS:** “Even if you maintain very low stresses in the glass, you will not be protected from construction errors.”

3.4. Structural Design and Safety

The general approach to a structural glass project varies somewhat between the interviewees. Determining the sizes of the individual components in relation to the architecture and the available glass sizes is usually the first step.

Nijssen indicated that he then continues by calculating the structure, using the strengths and safety factors as given by the Dutch code NEN 2608-2. Consequently, the glass elements should be laminated, meanwhile considering the possible breakage of one or two layers, depending on the risk of vandalism. **RN:** “One time, vandals tried to bring down the glass bridge in Rotterdam at the office of Kraaijvanger Urbis. The outer sheets of the roof panel and one (load carrying) wall panel got broken by thrown pavement tiles (Fig. 5.31). These, however, formed a protective cover for the inner sheets which survived unscathed and kept doing their job. Disillusioned, the vandals took off.”

Glass structures are divided into three types by Schneider: façades, overhead glazing, and ‘special stuff’ (columns, beams, etc). Besides the category, there are basically three important issues to think of when getting started on a structural glass project. The first is sizes, which is an important parameter in the structural system and connections. Second is thickness (stress check) and third are safety issues. A safe structure needs to provide redundancy: local failure of one component should not lead to collapse of the structure. In laminated glass, it depends on the application whether or not you should consider situations with more than one layer broken. In four side supported overhead glazing, it is highly unlikely both layers will break simultaneously, thus this need not be considered. In cases where the glass edge is unprotected though, such as glass staircases, at least three layers should be used. A situation with two sheets broken should be reckoned with. Three layers broken seems a very severe condition. A paradox then arises: if you would use a 2 layer laminate, you only have to consider two layers broken, but when you use a 3 layer laminate, you have to reckon with three layers broken. Techen also feels that whether or not you consider breakage of the complete section should be dependent on the presence of (edge) protection. A well protected sheet has very little chance of breaking.

⁴⁶ Dodd and Macfarlane also experienced severe manufacturing and construction errors, narrated in Sections 3 and 4 of Appendix C, respectively.



Fig. 5.31 Glass bridge in Rotterdam after treatment by vandals: the inner layers of the roof and wall panels proved to be sufficiently protected not to break and to keep carrying loads.

Macfarlane follows an approach similar to that of Nijssen. **TM:** “First I just do the numbers. Then, I try to think of what could go wrong, and adjust the design so that those situations will not cause excessive damage or injury. The design should not only limit the consequences of glass failure, but also facilitate easy replacement – a failure should not bankrupt your client. The general problem in providing safety is that there are always ‘unknown unknowns’ (i.e. unpredictable situations you can not even imagine). Thus, a universal equation for safety is impossible. Because of the unknown unknowns, the basic attitude should be ‘assume that any piece of glass may break.’” Macfarlane does not specify specific a priori safety requirements beforehand, as this would lead to general statements that may not be relevant to a particular design problem. He admits this approach does not bring quantitative consistency in the safety of his structural glass projects, other than that resulting from maintaining a consistent attitude. But, according to Macfarlane, this is not necessarily a problem because in daily life you are constantly subjected to varying levels of risk. Furthermore, safety thinking develops as you go along and also therefore not consistent. However, an acute awareness of general engineering principles and a responsible attitude are indispensable.

Stimulated by the steadily increasing number of realized structural glass projects, more and more engineers enter the field of structural glass. This poses an increasing risk of faulty copies. Especially structural measures applied to provide safety may not

necessarily be obvious. Dodd sees hazards for the future. **GD**: “The development of glass structures is at a turning point. It has passed the initial pioneering stage in which the pioneers had to be extremely careful and thorough because nobody yet knew how to do it, but has not yet arrived at the point where all difficulties of glass are generally understood and laid down in guidelines or codes. There is an increasing risk that engineers, stimulated by a steadily increasing number of examples, will start copying without truly understanding the point of the original structure.” Dodd therefore recommends a working method in which safety is explicitly put forward. When designing a structural glass member, he considers all stages of failure (1, 2, ..., n layers broken, with n = the total number of layers). He quantitatively formulates residual strength requirements for each stage and also specifies the time period for which the member has to maintain that strength. As Macfarlane, he bases these requirements on a scenario approach (“what can go wrong?”). This approach implies that breakage of the complete glass section should also always be considered, although the performance criteria for that case can be lenient. **GD**: “I usually do not trust designs completely that rely on one layer being unbroken. Unfortunately, you can not always avoid that in practice.” In a number of projects, such as the Wolfson Building atrium roof, Dodd solved this by connecting the roof plates to create an alternative load path, perpendicular to the beam axis.

Contrary to Nijse, Macfarlane and Dodd, the design of a glass structure for Wellershof starts with conceptually determining how safety will be arranged. The member dimensions follow after that. Just as Dodd, he sets quantitative requirements to the residual strength in each phase of failure. **FW**: “The discussions (with structural engineers, authorities, etc.) arise when the required residual strength levels have to be determined. The problem of the scenario approach is that it is very difficult to objectively decide which ones are reasonable and which are not. As a consequence, the required scenarios can vary widely from project to project, even if the projects themselves are similar.” Techen therefore argues that the more far-fetched scenarios should be discussed with the client – he should decide for which occasions he wants his structure built. To avoid arbitrariness as well as having to do the same discussion over and over again, Wellershof feels explicit requirements towards residual strength levels should be incorporated in codes or guidelines.

Adjusting the safety factor for structural glass elements with safe failure behaviour (i.e. using a factor lower than one for elements with unsafe behaviour), is a complicated issue according to Schneider. First of all, it would require a definition of what is ‘safe’. Second, to calculate the value of such a factor, you would need to know either:

- the probability of irregular actions (e.g. a pistol shot, thunder storm debris, etc.), the statistics of which are not available,
- or the load resistance of the broken glass for regular loads (e.g. snow, wind, etc.) and for a given temperature scenario which acts at the same time. This is difficult because broken glass is seldom behaves consistently in a series of tests.

3.5. Load, Time and Temperature Requirements

The basic requirement Macfarlane sets is that upon breakage of any piece of glass, the structure should not collapse. Furthermore, the part must be replaceable without

bankrupting the client. This seems trivial, but it is sometimes so difficult to replace certain elements, that they are either just left there or enormous expenses are made. The specific residual strength requirements depend on the particular project.

Contrary, Nijssse has a relatively specific basic rule for the amount of residual strength required: if one layer breaks (or two in case of vandalism prone elements), the remaining layer(s) should be able to carry the load at an arbitrary point in time multiplied by a safety factor of 1.1. If that load equals 0 (e.g. wind load), Nijssse does a reasonable estimate based on experience instead, usually about 25 % of the serviceability limit state load.

Techen notes there is much discussion on this subject. Like Nijssse, Techen feels only relatively small loads need to be considered in failure situations. Glass breakage is likely to be noticed quickly and it is improbable high loads will occur during that time. However, the amount of residual strength should also be dependent on the level of maintenance, on which the speed with which elements are replaced, is highly dependent.

For time requirements (i.e. the time a failed structure should be able to maintain a certain level of residual strength), Techen points to an enactment of the Hessisches Ministerium für Wirtschaft, Verkehr und Landesentwicklung⁴⁷, which specifies that overhead glazing under certain loads must remain in place after breakage for:

- 30 minutes, if the area underneath the glass not accessible or
- 24 hrs, if the area underneath is accessible.

According to Schneider, these requirements seem acceptable. **JS**: “It is a duration that can still be reasonably tested, without disproportionately delaying the building process. Furthermore, the critical phase is usually between 0 – 2 hrs after failure. If a structure holds a load for 24 hrs, it is likely it will also hold for 2 months. Nevertheless, despite being reasonable, the 24 hr requirement is also quite arbitrary.”

German building authorities will often require residual strength to be maintained for 24 or 72 hrs, Wellershof accounts, depending on the building usually being open or closed during weekends. He himself distinguishes three important stages:

1. The time needed for the damage to be discovered. This is usually a day or several days.
2. The time needed to erect a supporting structure. This can usually also be done relatively quickly.
3. The time needed to replace the component. Complex structural glass components may take several months to manufacture. This would require the supporting structure to be present for a long period of time. Since glass structures are usually applied in high-profile buildings, this is commonly not desired by the client and the damaged structure itself often has to be able to provide residual strength for a longer period of time.

⁴⁷ Hessisches Ministerium für Wirtschaft, Verkehr und Landesentwicklung, *Anwendung nicht geregelter Bauarten §20 der Hessischen Bauordnung (HBO) im Bereich der Glaskonstruktionen*, VII 2-2 – 64 b 16/01 – 8/2003, 17. Januar 2003.

Thus, similarly to Macfarlane's notion, Wellershof indicates the time requirement is often not purely governed by the safety aspect, but also by important commercial and/or psychological motivations.

Specific temperature requirements for proof testing structural glass elements, are not set by Schneider. The main reason is that governing actions (such as excessive snow or wind loads) will hardly ever coincide with high temperatures.⁴⁸ Nevertheless, elevated temperature tests are frequently required by German building authorities. **JS:** "This may lead to ridiculous scenarios, such as a maximum snow load on a glass roof at 50 °C ambient temperature."

3.6. Codes and Guidelines

The development of glass engineering codes is desirable and they should basically do two things, Macfarlane notes: provide a common set of numbers (most notably strength) to design by and describe general principles and minimal requirements for safety.

In this respect, Nijse is reasonably satisfied with the Dutch code NEN 2608-2:2007. It contains an easy-to-use strength formula which takes all important parameters into account. Specific requirements with regard to residual strength are not formulated in the code,⁴⁹ this remains up to the individual engineer. This is not very remarkable as discussion on how to define and quantify residual strength are new to the field of structural engineering in general, also in relation to common structural materials such as steel and reinforced concrete.

Dodd claims that obtaining a consistent approach to structural glass safety by different engineers in different projects would be a distinct advantage of developing common rules. However, because there are such big differences in projects, it is unlikely that such rules could be prescriptive codes. Rather, they should be guidelines on what is reasonable and at what point residual risk is acceptable. Another advantage of the development of codes or guidelines may be that it will ease the commercial pressure by contractors on engineers to approve of minimal designs.

According to Schneider, the new DIN 18008 will bring more unity into testing requirements and abolish ridiculous scenarios.

Dodd and Techen agree that it is essential in structural glass not to 'think' in codes and blindly follow the rules within them. Instead, scenario thinking should be encouraged, the latter says. Dodd notes that the CDM regulations⁵⁰, which have been developed in the UK and require a risk assessment by the engineer, aim at preventing blind code-following and creating an active involvement instead.

⁴⁸ For wind loads in Germany, this has been proven by extensive statistical research in: Wellershoff, F., *Nutzung der Verglasung zur Aussteifung von Gebäudehüllen*, Ph.D. thesis, RWTH Aachen / Shaker Verlag, Germany, 2006.

⁴⁹ The forthcoming edition of the NEN 2608, however, will include such requirements. It is due around September 2009.

⁵⁰ The Health and Safety Executive (HSE), *The Construction (Design and Management) Regulations 2007*, Statutory Instrument 2007 No. 320, UK, 2007.

Techen furthermore thinks a serious drawback of codes is that they are adjusted to low-quality companies (even they should be able to meet the code requirements). Effectively, this makes it very difficult for high-quality companies realize profit from their quality, and thus slows down innovation. He therefore praises the Swiss codes which place much responsibility at the engineer. Nijssse recognizes the risk that codes may suffocate innovations, but feels this should not be an excuse not to develop them. Rather, it should be an incentive for the profession to formulate the codes in a clever way, so that they provide useful rules without blocking innovation.

3.7. Conclusions from Interviews

The interviews have shown that, by and large, the safety approaches of the interviewees are in line with each other. Generally, breakage of all glass sheets in a structural element should be considered possible (although there may be some exceptions). Should breakage occur, residual strength has to be provided to prevent injury or disproportionate collapse.

However, there are significant differences in the extent to which these safety approaches are made explicit. A trend towards further quantification of residual strength requirements seems to develop, in which *a priori* a certain performance is demanded for each stage of failure (formulated in terms of increasing numbers of broken glass sheets).

The residual strength requirements should be formulated in terms of resistance for a certain period of time. The magnitude of the resistance is subject of continuous debate. It may depend on the accessibility and maintenance level of the glass structure as well as on the failure stage. The tendency seems to be to consider relatively small actions (in the order of the load at an arbitrary point in time multiplied by a small safety factor).

The duration for which the residual strength has to be maintained should be in the order of days (one to several). This should allow for sufficient time for the failure to be noticed and consequent action to be taken (evacuating, erecting extra support, closing off). In non-supervised applications, this time requirement should be considerably longer (in the order of expected inspection frequency).

However, it should be noted that the residual strength and duration requirements may not be governed by safety considerations only. Failure of a structural glass element should not cause excessive financial damage or image loss to the owner of a glass structure. It can take considerable time to manufacture complex structural glass elements (weeks to months) and long-term scaffolding may be unacceptable in such applications. Thus, residual strength over a considerable time period may be required from the element itself. As the probability of higher loads increases over time, the magnitude of the residual strength than also has to be higher.

Additional temperature requirements deviating from normal room temperature, e.g. demanding that a certain degree of residual strength has to be proven over a temperature range of, say, -20 to +60 °C, is felt to make experimental proof testing unnecessarily complicated.

Complex analyses to calculate the failure probability with a high degree of certainty are not commonly executed. There does not seem to be a high demand to further increase

failure probability calculation by adopting more complex models in codes. Remarkably, the strength values adopted by Nijssen and Macfarlane in the early years (1980's) of the development of structural glass were very close to those that result from dimensioning methods provided by contemporary codes.

Ignorance and negligence in manufacturing, transport, and construction are identified as the most common cause of premature failure. Thus, attention to safety should not only be in the design, but also in the execution phase of a glass structure, although it should be realized that such failures can never be completely avoided – another reason why investing in more accurate failure probability analysis beyond a certain point becomes futile.

Codes that place a mayor responsibility at the engineer by formulating safety requirements in general terms, such as the Swiss codes and the British CDM regulations, are appreciated. They do not hinder innovations through detailed design prescriptions and avoid mindless 'code following'. On the other hand, there is a definite need for clarity on safety requirements to avoid repetitive discussions, which is not provided by today's codes. Code development should aim at clear performance requirements without hampering innovations.

Scenario thinking (actively pursuing the question 'what could go wrong?') is an important tool to develop safe designs. However, Wellershoff noted this does not solve the issue of the magnitude of residual strength and leads to inconsistencies, even within a single project.

As also put forward by the survey results, annealed and heat strengthened glass are favoured over thermally tempered glass for their cracking patterns which provides better opportunities for residual strength. However, the applicability of annealed glass in structures, while deemed possible by some, is disputed by others. Furthermore, Schneider questioned the influence of the cracking pattern on the failure behaviour for reinforced glass beams.⁵¹

4. General Conclusions

In Section 1, a range of measures applied to provide safety in glass structures was presented. These measures usually aim at reducing damage sensitivity and/or providing residual strength. The need to provide residual strength in case of glass breakage is universally felt in the field of structural glass engineering. However, judging from the variety of design solutions, it was expected that there is disagreement or confusion about how this general need is to be translated into practice. This was confirmed by the survey and the interviews, which, along with the analyses made in the previous chapters, have shown there is no unifying safety concept taking all relevant aspects of safety into account, on which the application of the safety measures can be founded.

Consequently, there is no generally accepted and complete quantitative set of performance requirements to which design solutions can be tested and compared.

⁵¹ The discussion on the influence of elastic strain energy release on post-failure resistance in Chapter 9, sheds some light on this issue.

Existing safety requirements in codes and guidelines (extensively discussed in Chapter 4) do not provide generally applicable and sufficiently clear requirements.

As a result, the effect of safety related design measures on the safety of the glass element is often only very generally known. This goes even for the influence of the most well known measures, heat treatment and (PVB-) laminating.

The lack of a unifying structural glass safety concept and a quantitative elaboration thereof, is likely to be an important cause of the ongoing debate on how safety should be achieved (how many layers should be used in a laminate, type of heat treatment, actions to consider, etc.). Furthermore, this makes it practically impossible to objectively discuss the different views and develop a commonly accepted set of performance requirements. Therefore, such a concept will be proposed in Chapter 6.

6 An Integrated Approach to Structural Glass Safety

In the previous chapters, it was shown that existing methods to assess the safety of glass structures are insufficient. Although it is generally recognized that a (codified) probability analysis does not consider all relevant structural safety aspects, for structures in general and for structural glass in particular, there is no explicit elaboration of the cause-and-effect chain that leads from failure causes to personal injury or economic loss. In an attempt to achieve some clarity in the debate and to obtain objective criteria to compare structural glass designs with regard to safety, the *Integrated Approach to Structural Glass Safety* is proposed. Four properties of the glass structure and its elements are defined: *damage sensitivity*, *relative resistance*, *redundancy*, and *fracture mode*. Several underlying concepts, such as load transfer mechanisms, initial and final failure, and damage, are also introduced. Performance requirements can be formulated to which each element safety property can be checked. The *Element Safety Diagram (ESD)* is introduced, a graphical tool to combine all element safety properties into one overview. Together, the defined safety properties and performance criteria form a new approach to structural glass safety. This chapter closes with an inventory of required additional research to finalize the Integrated Approach.

1. Introduction

In the previous Chapters 3, 4, and 5, existing approaches to structural glass safety have been presented. It was shown that a sole failure probability analysis based on element strength is not sufficient to guarantee an actual failure probability and adequate safety. For structures in general, the shortcomings can be summarized as follows (Chapter 2, Section 2.5):

- Only a part of the relevant variables reasonably accurate statistical distributions are known.
- Structural failure is hardly ever caused by a considered resistance being exceeded by the considered action(s). Many other events, that have not been included in the probabilistic analysis, may cause failure. Some of these could not even have been reasonably foreseen.
- The probability of collapse of an element is often significantly smaller than the probability of failure. As this is not considered in the probability analysis, this introduces a hidden safety margin.
- There is no direct relation between the event that governs probability requirements (personal injuries by structural collapse) and the probability analysis itself (limited to an individual structural element).

These observations hold for structures in general. For glass structures, the relevance of a probability analysis to safety is even more limited:¹

¹ Also see Figure 4.6 in Chapter 4, Section 4.

- Glass is very sensitive to a high number of failure causes, besides the ordinarily considered actions on a structure.
- There is still much discussion on the processes governing glass failure. Thus, the accurate description of the statistical distribution of glass strength is a subject of scientific debate. The validity of the results of the formal probability analysis is therefore less certain than with more common structural materials.
- Macro-cracks do not tend to stop once they have started as there is no crack stopping mechanism present. Therefore, the probability of collapse of a glass element is practically equal to the probability of failure. Glass does not have the hidden safety margin present in other materials.
- Brittle structures lack deformation capacity that can help redistribution of loads.²
- Broken glass is more likely to cause injury than other materials because of its sharp shards.

As the limitations of probabilistic analyses for the safety of glass structures are generally recognized, additional safety requirements have been formulated to varying extent in codes and guidelines. They relate to the impact resistance, residual strength, and fracture behaviour³ of glass elements – but still suffer from significant shortcomings.⁴

Most importantly, they do not appear to be related to each other, or to an analysis of the failure process from possible failure causes to the consequences of failure. It is often unclear at what part of the failure process specific requirements aim. An overall integrated safety approach is lacking. Furthermore, safety requirements may:

- not be suitable for all structural elements,
- not be described in terms of structural performance and may be independent of structural role,
- be insufficiently described in detail,
- be very general and/or non-quantitative.

In structural glass engineering practice, a range of safety enhancing techniques and design solutions has been developed. Remarkably, there is very little a-specific⁵ data available of the actual effect of the most well known measures (like thermal treatment and laminating) on failure behaviour.

The premise that residual strength should be provided in some form for all structural glass elements is generally held. However, there is no accepted quantitative criterion for this concept, and neither is there a clear picture on what the required amount of residual strength should depend. As a result, the solutions applied in practice vary considerably.

The lack of an integrated safety approach that qualitatively incorporates all relevant aspects of the failure process, makes it impossible to objectively compare structural

² As will be argued in Section 2.2 of this Chapter, the safety approach presented here is limited to the level of individual structural elements. This issue will, therefore, not be pursued further.

³ Related to the possibility of injury from shards.

⁴ Chapter 4, Section 5.2.

⁵ Project independent.

glass designs with regard to safety and select an optimal solution. Furthermore, it can lead to inconsistent requirements from building authorities and extensive, but confused, discussion. The development of such an approach should therefore be pursued. Besides solving the before mentioned problems, it would open the way for broad a-specific testing and comparison of glass element designs and compositions, so that the effect of design decisions on safety can be estimated better without the need for experimental testing for each project.

The remainder of this Chapter aims at the theoretical development of such an approach, its key concepts and parameters as well as qualitative performance criteria.

2. Towards an Integrated Safety Approach of Structural Glass

Before starting an extensive elaboration of a new safety approach, the main goal(s), prerequisites, scope and underlying structure need to be explicated.

2.1. Goal and Prerequisites

The primary goal of the introduction of a new safety approach in structural glass engineering is to obtain a method to assess structural glass safety objectively, taking into account *all relevant factors simultaneously*, thus arriving at an integrated approach. Concepts should be quantified whenever possible. The method should be clear. Requirements should be adjustable so that, for instance, authorities can apply their specific demands – but in a way that all modifications are easily identifiable, so that they can be debated and criticized. The shortcomings of existing sets of requirements described previously, most specifically the lack of coherence, should be overcome.

Since it seeks to incorporate all relevant safety aspects in the safety assessment of glass structures, the new approach will henceforth be referred to as the *Integrated Approach* (to structural glass safety).

2.2. Scope

Perhaps even more important than explaining the structure of the proposed approach, is setting its scope. Development of the Integrated Approach revealed further research is required in quite a number of areas. It could therefore not be completed here. The final section of this chapter is devoted to an inventory of required further research. Nevertheless, this chapter does present the required key concepts, element properties, and considerations as how to formulate performance criteria. This should suffice to further develop and finalize the integrated approach in subsequent research.

Up until now, the term ‘structural glass’ was used, assuming it is clear what it means. However, upon closer scrutiny, this may not be so obvious. The author would propose to define a structural glass element as an element that, besides external loads and self weight, transfers internal actions from one part of the structure to another, or to a foundation. This definition, however, excludes e.g. glass floor plates and balustrades, for which the safety issues are just as important. For these and all other applications of glass (including façade cladding and windows), it is suggested to speak of ‘glass in construction’. The safety approach presented here, though primarily developed for structural glass, *is just as well suitable for any application of glass in construction* (it only requires adjustment of the requirements per application).

Two important constraints apply to the presented approach. In the first place, the approach is limited to the *design* of glass in construction, rather than to include also the execution phase (manufacturing and construction). Notwithstanding the fact that manufacturing and construction errors are the primary reason for glass failure⁶, the basis for a safe structure lies in its design. The performance criteria of the design need to be defined before one can start to worry about how to make sure a structure is built to optimally resemble the design. Such quality management of industrial processes is a professional field in itself. Also for that reason, it has not been incorporated here.

Rather, the performance criteria assume an average execution quality including possible errors as unpredictable failure causes. A structural glass element has to be insensitive to such errors to an extent depending on its application. Nevertheless, the performance of any design will ultimately depend on the execution quality. Even when designed to be insensitive to errors, faulty execution can always render an element prone to failure. It is therefore recommendable to review quality control in structural glass manufacturing and construction, in relation to the presented design approach.

The second major constraint applied here is its limitation to structural *elements*. It does not include requirements for structures. Previously,⁷ it has been shown that safety assessment of structural systems instead of individual elements, is a subject still very much in need of crystallization for structural engineering in general. The definition of relevant structure properties and related performance criteria is debated by many experts in the field. A valuable contribution would be a study in itself and could therefore not be included in this work. Furthermore, it should be expected that, when element performance requirements are met, the structure performance requirements need not be different for glass structures than for steel, reinforced concrete, or any other structure, because structure safety performance properties are mostly related to the configuration of elements, independently of their material.⁸

Even when it remains limited to the *design* of structural glass *elements*, an integrated safety approach requires the introduction of an extensive set of concepts, properties, and requirements. These will all be introduced below in qualitative terms. However, again the extent of this research did not allow all to also be defined in quantitative terms. Especially relating various performance criteria in a mathematically and physically meaningful way, will have to remain subject of further research given the state of existing structural glass safety approaches.

⁶ Chapter 5, Section 3.

⁷ Chapter 3, Section 7.

⁸ At least in those publications discussed in Chapter 3 (including the Eurocode).

2.3. Structure

Consider Figures 6.1a and b. Ideally, any validity assessment consists of checking a single, unambiguous object property to a single, quantitative pass/fail criterion (Figure 6.1a). In reality, in many assessments a set of object properties which are not (fully) related to each other, has to be compared to (a set of) often qualitative or only partially quantitative pass/fail criteria.⁹ Nevertheless, defining the relevant object properties is the first step in an attempt to develop a maximally objective assessment – at least, it will provide opportunity to identify subjective choices of preference for one object over another.

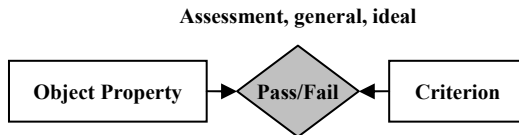


Fig. 6.1a Ideal assessment: comparing one unambiguous object property to one objective criterion.

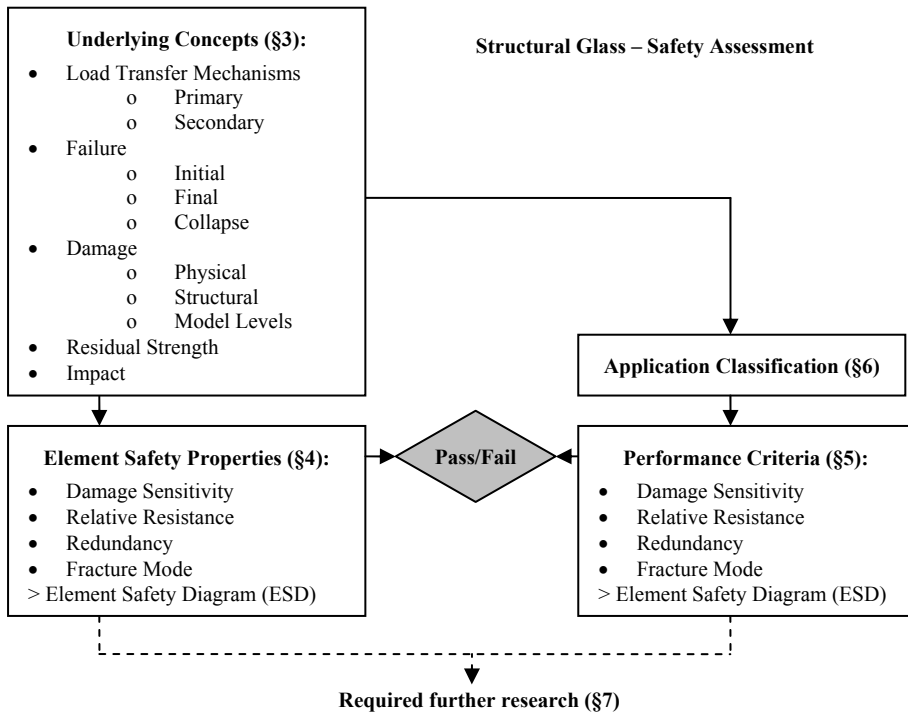


Fig. 6.1b Structural Glass Safety Assessment: object properties, performance criteria, and underlying concepts.

⁹ Consider for instance a car. Airbags, seatbelts, traction control, and brake assist, are some of the instruments contributing to its safety. Yet they are not directly physically related, and can therefore not (or not all) be combined into one quantitative safety property. A similar observation holds for glass elements: they have several properties contributing to their safety, which can not be directly combined into one quantity.

The Integrated Approach makes use of four element safety properties, listed in the element safety property box in Figure 6.1b. Each of these properties relates to specific areas in the cause-and-effect chain from failure cause to injury, as depicted in Figure 6.2. They are:

- Damage Sensitivity
Gives an indication of the vulnerability of the element to failure causes that have not been considered in the formal probability problem, e.g. hard-body impact or thermal stress.
- Relative Resistance
Relates to the formal failure probability from considered causes.
- Redundancy
Quantifies the reserves between damage and failure, and failure and collapse.
- Fracture Mode
Relates to the injury potential of the element.

These concepts will be further elaborated in Section 4.¹⁰ In Section 4.5, the *Element Safety Diagram (ESD)* is introduced, a graphical tool to combine all element safety properties into one overview.

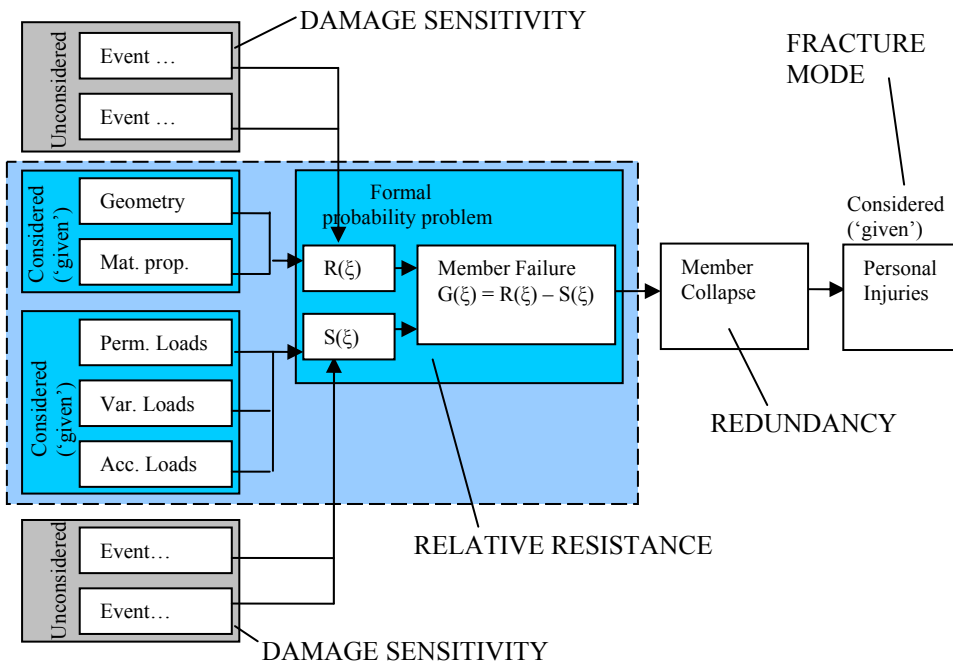


Fig. 6.2 Cause-consequence diagram for structural glass failure, with the four element safety properties introduced in the Integrated Approach. The diagram is based on Figure 4.6 (Chapter 4, Section 4), but the box ‘collapse of structure’ was omitted since this approach is – for now – limited to the scale level of elements.

¹⁰ Including reasoning for their selection.

To define the element safety properties, a number of supporting concepts has to be introduced, some of which are new to the field of structural glass engineering. These are therefore discussed first in Section 3.

The other side of the development of a safety approach is the definition of minimum performance criteria for each of the defined element safety properties. Section 5 discusses the way safety requirements can be formulated for each element safety property, by using the Element Safety Diagram. As there is a wide range of glass in construction applications, it is sensible to produce multiple sets of performance criteria for categories of elements so that reasonable requirements can be formulated for each application. This is discussed principally in Section 6. Appendix D contains suggested quantitative performance criteria for several element categories, as well as a worked out example of the use of the Integrated Approach to assess the safety of a structural glass design.

In Section 7 finally, an inventory is made of required further research to develop the integrated approach to maturity.

3. Underlying Concepts for Element Safety Properties

In this Section, a number of underlying concepts is introduced and defined. Their use will become clear in Sections 4 – 6, in which the Integrated Approach is elaborated.¹¹

3.1. Load Transfer Mechanisms; Primary and Secondary

In mechanics terms, there are several ways in which a structural element can carry loads to its supports. Such a *load transfer mechanism* (LTM) is determined by the stress distribution through the element; different load transfer mechanisms yield principally different stress distributions. Thus, the method to calculate the stress distribution varies with each load transfer mechanism. The applicable stress calculation method is therefore the criterion to distinguish between various load transfer mechanisms. Perhaps the most common load transfer mechanisms are linear elastic bending, compression, and tension.

A structural element may be able to carry loads through more than one mechanism. Consider, for example, a rectangular, solid steel beam loaded in bending (Figure 6.3). Hooke's Law applies and the stresses and section moment capacity can simply be calculated with Eqs. (6.1) and (6.2). Linear elastic bending can be considered the first load transfer mechanism of this beam. Now, when the beam is loaded to the point that $\sigma_{\max} = \sigma_y$, steel starts to deform plastically. The linear relation between stress and strain is lost. The maximum stress is simply the yield stress and the maximum moment capacity is reached when the complete section is in yielding and given by Eq. (6.3). The second load transfer mechanism thus has a moment capacity 1.5 times as high as the first one.

¹¹ A number of these concepts have been previously introduced in Bos, F.P., *Towards a Combined Probabilistic/Consequence-based safety approach of structural glass members*, HERON, Vol. 52, Is. 1/2, 2007. However, the definitions presented here all deviate to greater or lesser extent from those applied in that publication.

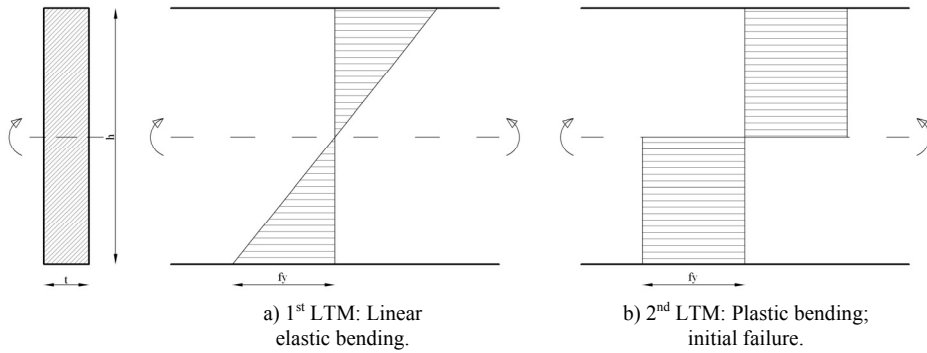


Fig. 6.3 Load transfer mechanisms in a solid section steel beam, loaded in bending.

$$\sigma_{\max} = \frac{M}{W} \quad (6.1)$$

$$M_{\max,el} = \sigma_y W = \sigma_y \cdot \frac{1}{6} th^2 \quad (6.2)$$

$$M_{\max,pl} = \sigma_y \cdot \frac{1}{4} th^2 \quad (6.3)$$

A second example is shown in Figure 6.4a – d¹². The laminated glass plate will act in plate bending as long as the glass is unbroken. The stress distribution will depend on the degree of coupling. When the bottom sheet breaks, actions are still carried by plate bending in the top layer (Figure 6.4b). However, when the top sheet also starts breaking, the load transfer mechanism changes into composite bending: the laminating foil takes the tensile stresses while the glass top layer keeps carrying compressive loads. The moment capacity was initially determined by the bending tensile strength of the glass, but is now governed by the tensile (yield) strength of the foil, the glass compressive strength and the internal lever arm. When the glass in the compressive zone crumbles and loses compressive stiffness, the load transfer mechanism changes again. The laminating foil carries all the loads in membrane action.

¹² This example is based on a classification presented by Kott & Vogel: Kott, A., Vogel, T., *Structural Behaviour of Broken Laminated Safety Glass*, in: Crisinel, M., Eekhout, M., Haldimann, M., Visser, R. (Eds.), *EU Cost C13 Final Report, Glass & Interactive Building Envelopes*, Research in Architectural Engineering Series, Volume 1, IOS Press, Amsterdam, the Netherlands, 2007, pp. 123 – 132. However, the LTMs identified here do not follow their classification. Kott & Vogel refer to the undamaged state (Figure 6.4a) as stage I. The element enters stage II when the bottom layer is broken and no longer carries tensile actions. However, in principle the load carrying mechanism is still the same: plate bending, only now with only one sheet active. The contribution of the PVB is still negligible. By the author, this state is referred to as ‘damaged’ (see also Section 3.3). The 2nd LTM only becomes active when the top sheet also partially cracks and a composite action between glass (in compression) and PVB (in tension), is activated. Kott & Vogel identify this state as stage III. The final state, when the top layer is crumbled to an extent it can no longer carry compressive forces, is also referred to as stage III by Kott & Vogel. But this ignores the fact that yet another mechanism is activated: membrane action. The forces are transferred by tension in the PVB under large deformations. The author identifies this stage as the 3rd LTM.

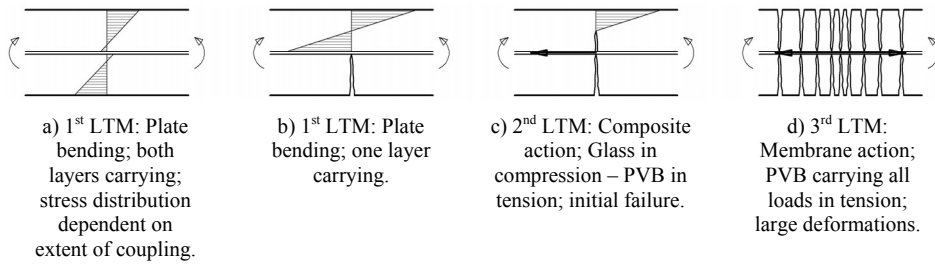


Fig. 6.4 Load transfer mechanisms in a laminated glass sheet, loaded in plate bending and developing into membrane action.

From the moment an element is loaded, there is principally one load transfer mechanism active, even though the element may latently possess the capability to activate others. The mechanism to be activated first will be the one with the greatest stiffness and henceforth referred to as the *primary* load transfer mechanism. A subsequent mechanism can be activated when the primary one loses stiffness, e.g. through overloading (steel beam) or damaging (glass plate). The mechanisms that are then activated are named *secondary* load transfer mechanisms.¹³

The concepts of primary and secondary load transfer mechanism are crucial, among others, for the quantification of redundancy in Section 4.3 of this Chapter.

3.2. Initial Failure, Final Failure, and Collapse

Generally, failure is defined as ‘ceasing to perform an intended function.’¹⁴ However, as has been pointed out in Chapter 3, elements from common structural materials usually do not collapse immediately upon failure. They have secondary LTMs with resistances higher than or equal to that of the primary LTM. These secondary LTMs thus provide an important, often not explicitly considered, safety margin. To incorporate requirements into the Integrated Safety Approach to obtain a similar margin in structural glass, it is necessary to discriminate between *initial failure* and *final failure* of an element.

The concept of *initial failure* is introduced to mark the transition between the primary and secondary load transfer mechanism. Initial failure occurs when the load transfer mechanism that was initially active, is superseded by a subsequent one (Figures 6.3b and 6.4c).

Final failure, on the other hand, denotes that a structural element has lost all of its load carrying capacity. It identifies the state that none of the primary or secondary LTMs can be activated anymore. For an element with only one load transfer mechanism (e.g. a single sheet of glass), initial and final failure will coincide.

¹³ The glass plate in the example has one primary load carrying mechanism (plate bending) and two secondary load carrying mechanisms (composite bending and membrane action).

¹⁴ Chapter 3, Section 6.

Final failure and collapse will often occur simultaneously, but they are not synonyms. Collapse is ‘falling down or caving in of a structure through breakage and/or loss of stability.’¹⁵ Unless somehow supported, an element will collapse upon final failure.

Derived from the concept of initial failure, are the terms pre- and post-initial failure state,¹⁶ indicating a state before or after initial failure, respectively.

3.3. Damage *D*

Even before initial failure, the resistance of the primary load transfer mechanism may decrease from its original, nominal value. The element is then damaged.

Damage can arise, for instance, as a small crack or dent in the glass (Figure 6.5). In more serious cases, one or more layers of a laminate can be broken completely. As long as one layer remains unbroken, the primary load transfer mechanism will often still be active, although with less capacity. Consider a three-layer thermally tempered, PVB laminated glass beam, as in Figures 6.6a – d¹⁷. In Figure 6.6a, the beam is undamaged, the primary load transfer mechanism has its original value. Figure 6.6b shows one layer broken. Nevertheless, mechanically the beam still works according to the primary LTM, although its capacity has decreased to $\pm \frac{2}{3}$ of the original value. In figure 6.6c, a second layer is broken; the primary LTM is still active at $\pm \frac{1}{3}$ of its original value. The element thus still has not failed, rather, it is (badly) damaged. Only when the third and final layer breaks (Figure 6.6d), the primary LTM loses its capacity completely and the beam suffers initial failure. A secondary LTM is activated: composite action with the PVB foil in tension and cracked glass in compression. Depending on the dimensions of the beam, the capacity of this secondary mechanism may only be about 0.2 %¹⁸ of its primary one.

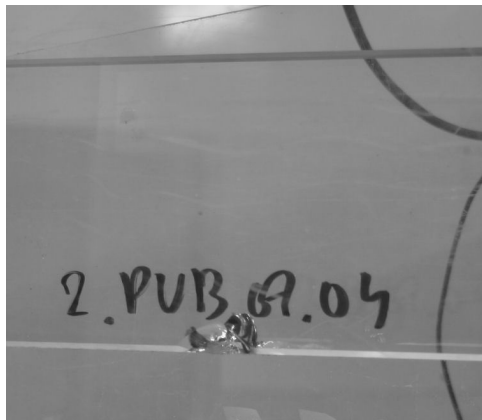


Fig. 6.5 Small damage (dent) in glass beam.

¹⁵ Chapter 3, Section 6.

¹⁶ Or ‘stage’. Though being similar terms, there is a subtle difference in their meaning: ‘state’ refers to the state of an element itself, while ‘stage’ is used to identify stages in an experimental procedure, e.g. in a load-displacement curve.

¹⁷ The pictures are taken from the experimental research presented in Chapter 7 and Appendix E. More elaborate analyses on the failure behaviour of such beams can be found there.

¹⁸ See experimental results in Chapter 7 and Appendix E.

The definition of failure described in the previous section, deviates from what is commonly understood by it, even though no generally accepted definition yet exists. The elements presented in Figure 6.6b and c, would probably be described by most to be failed. However, this not only raises the question of how much cracking is required to call an element failed, but more importantly combines fundamentally different stages in the failure process, determined by the active load transfer mechanism, into one concept. The introduction of damage allows the distinction between active load transfer mechanisms to be made and thus to describe more accurately in what state an element is. According to the definitions presented here, the element of Figure 6.6b and c is *damaged*, but did not yet *fail*.

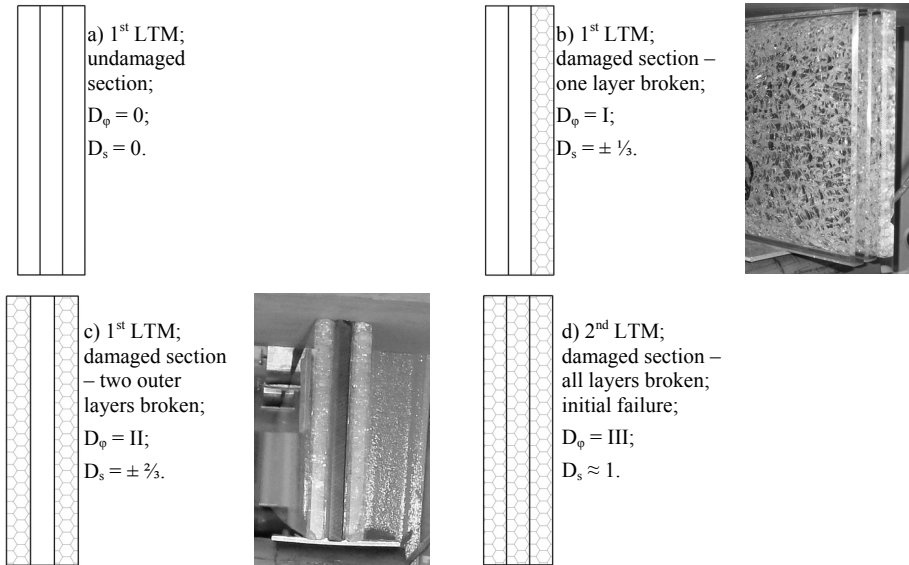


Fig. 6.6 Increasing damage in a 3 layer thermally tempered, PVB laminated glass beam (D_ϕ = physical damage; D_s = structural damage).

3.3.1. Physical Damage D_ϕ and Structural Damage D_s

In engineering applications, damage is often defined in terms of the amount of loss of resistance, Eq. (6.4)¹⁹. This definition, however, needs a small but important alteration in order to be sensibly applicable in the assessment of structural glass failure behaviour.²⁰ When Eq. (6.4) is applied to a reinforced concrete beam, cracking in the

¹⁹ Budden, P.J., J.K. Sharples, A.R. Dowling, *The R6 procedure: recent developments and comparison with alternative approaches*, International Journal of Pressure Vessels and Piping 77, 2000, pp. 895-903.

²⁰ The insufficiency of the general damage definition has been previously discussed by the author (Bos, F.P., *Towards a Combined Probabilistic/Consequence-based Safety Approach of Structural Glass Members*, HERON, Vol. 52, Is. 1/2, 2007, and Bos, F.P., Veer, F.A., *Consequence-based Safety Requirements for Structural Glass Members*, Proceedings of the 10th Glass Performance Days, Tampere, Finland, June 2007). It was proposed to solve this by the introduction of the concept of 'glass damage' (D_{glass}), which was defined by the loss of load carrying capacity of the glass in the element rather than the element completely. It was further simplified by defining that loss in terms of the ratio of cracked glass over total glass area in a (governing) section. This approach, however, *should be abandoned* as it is less universal than the damage definition proposed here. Furthermore, it is highly questionable if the remaining resistance of the section can be linearly related to the extent of crack growth (e.g. because of stress concentrations). But most importantly,

tensile zone would not be considered as damage, as the initial maximum resistance is unchanged. In a similar glass element,²¹ this would be unacceptable. For a safety assessment of glass elements, it is especially relevant to be able to evaluate intermediate stages between undamaged and initial failure. Therefore, the definition of structural damage as maintained here, is related to the (loss of) resistance of the *primary* load transfer mechanism, Eq. (6.5).

$$D = 1 - \frac{R}{R_{ini}} \quad (6.4)$$

D Damage
R Actual resistance
R_{ini} Initial resistance

$$D_s = 1 - \frac{R_{1stLTM}}{R_{ini,1stLTM}} \quad (6.5)$$

D_s Structural damage
R_{1st LTM} Actual resistance of the primary load transfer mechanism
R_{ini,1st LTM} Initial resistance of the primary load transfer mechanism

As with the common damage definition, D_s can range from 0 to 1. The state of D = 1 is referred to as ‘full damage’. From the previous Section it can be deduced that full damage coincides with initial failure (the capacity of the primary load transfer mechanism is reduced to 0). When 0 < D < 1, an element has suffered ‘partial damage’. Henceforth, an element will be referred to as ‘damaged’ when it has sustained partial damage and failed when it has suffered full damage.

The damage definitions Eq. (6.4) and (6.5) describe damage as a structural effect rather than, as one would perhaps expect, a physical²² phenomenon (e.g. an amount of cracking, corrosion, microstructure alteration, etc.). The advantage of such a presentation is that damage is defined in terms relevant for the evaluation, i.e. the loss of resistance, independent of its cause. However, when using the concept of damage for the safety evaluation of structural glass elements, this is inappropriate. Rather, it is vital to explicitly distinguish between the physical *phenomenon* and its *effect* (i.e. a resistance reduction). This allows to consider the relation between the extent of the physical phenomenon and the resulting effect on the resistance as a property that can be used in the description of the failure behaviour of an element and thus its safety.²³ This property is of crucial importance as it determines the sensitivity of the structural performance of the primary load transfer mechanism to physical effects regardless of their origin or probability. Even the more while most glass element designs lack a secondary load transfer mechanism of significant capacity. The phenomenon and the

the extent of cracking does not coincide completely with the transition between load carrying mechanisms which, in fact, govern the element failure behaviour. The definitions of failure, damage, and residual strength cover the actual failure behaviour much better.

²¹ Several reinforced concepts are being developed, see Chapters 1 and 8.

²² Or chemical. Both terms are grouped here as ‘physical’ for brief.

²³ See also Sections 3.4 on residual strength and 4.3 on redundancy.

effect are therefore considered as separate concepts, the former being henceforth referred to as *physical damage* D_ϕ while the latter is named *structural damage* D_s . Their relation is the *redundancy of the primary load transfer mechanism* m_{1stLTM} , an important element safety property (Section 4.3).

3.3.2. Model Levels of Physical Damage $D_{\phi,I}$, $D_{\phi,II}$, $D_{\phi,III}$

Structural damage D_s is caused by physical phenomena (e.g. cracks) called physical damage D_ϕ . For a glass element, they can be plotted against one another, as in Figure 6.7. The curve indicates the 1st LTM redundancy of the element. A curve towards the top-left corner is less redundant, one towards the bottom-right is more redundant. However, when trying to determine such a curve, one runs into the problem of quantifying D_ϕ . The effect of a phenomenon such as cracking on the resistance is highly dependent on the various factors such as the location, direction, and shape of the crack. Therefore, a certain amount of physical damage does not always result in the same amount of structural damage, as demonstrated in Figure 6.8a and b: although the amount of crack area is approximately equal in both damaged beams, the structural damage in a) is less than in b). A quantification in terms of relative crack length or area is therefore futile. Rather, it is suggested to introduce a finite number of qualitatively described amounts of physical damage, numbered in Roman: the *model levels* of physical damage.

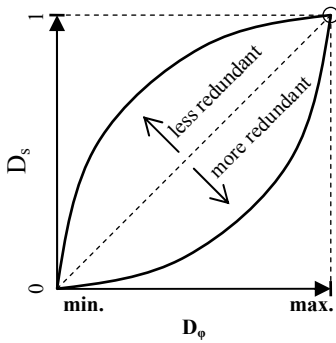


Fig. 6.7 Element 1st LTM redundancy curve: structural damage D_s vs physical damage D_ϕ .

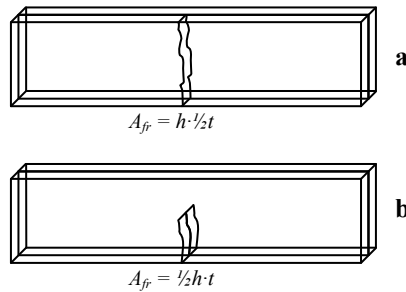


Fig. 6.8a and b Equal amounts of physical damage (crack surface area) in two beams with significantly different residual load transfer capacity (and thus different structural damage).

Consider Figure 6.9. The demarcations between the model levels of damage need to coincide with actual important differences in the probability of those levels occurring. Defining the top level (III) is easiest: it is the level at which the damage is so extensive that initial failure has occurred ($D_s = 1$, the primary load transfer mechanism has ceased to be active). For $0 < D_s < 1$, a number of model levels have to be introduced that are relevant for glass elements. Thus, they may vary for different elements, but, generally, it seems the introduction of two intermediate demarcations should cover many applications. Level I relates to one outer layer, level II to all outer layers (usually two). A demarcation per glass layer makes sense, as the laminates between them will usually work as a crack growth barrier. The distinction between one outer layer, all outer layers and all layers, relates to the vulnerability: one outer layer is more likely to be damaged

than two simultaneously and even more than all layers. A distinction between inner layers (e.g. introducing four model levels of physical damage for a four-layer laminate beam) introduces a level of detail irrelevant for a safety evaluation of such an element. Failure of inner layers probably only comes from vandalism, construction errors or very severe impacts that may be just as likely (or even more likely) to break all layers rather than leave one inner layer unscathed.

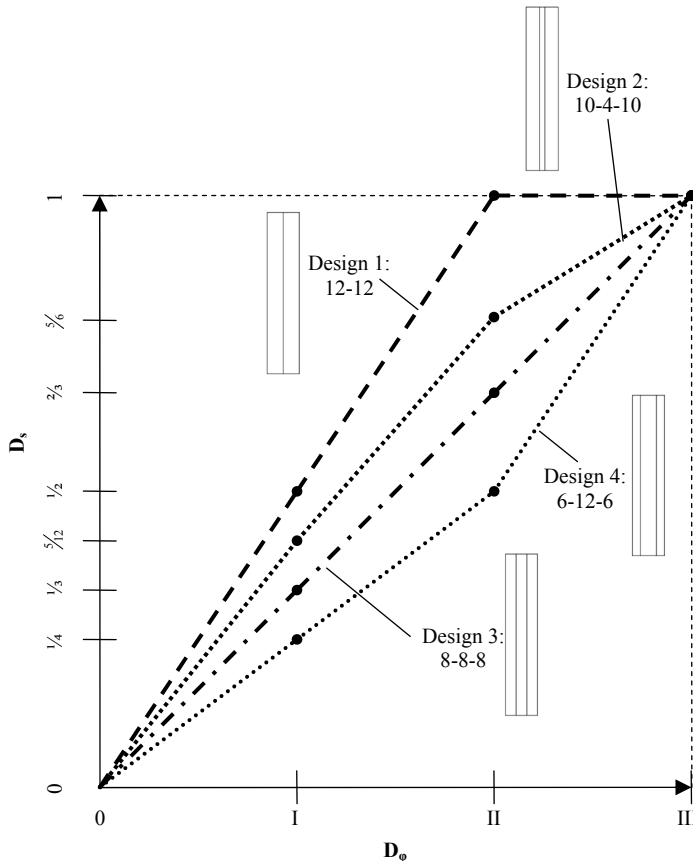


Fig. 6.9 1st LTM redundancy curves for four different beam section designs of equal total thickness.

The most obvious way to define the three model levels that have been introduced here, is to describe them in terms of glass layers, cracked to an extent that they have lost their load carrying capacity, so that they are ignored in the calculation of the residual load carrying capacity (basically, as if they disappear). For instance, level I could be ‘one outer layer broken’, level II ‘all (2) outer layers broken’, and level III ‘all layers broken’. This method is usually applied in structural engineering practice.²⁴ For four beam

²⁴ As can be concluded from several answers given in the survey presented in Chapter 5 Section 2 and (full report) in Appendix B, as well as from the interviews presented in Chapter 5 Section 3 and (full report) Appendix C.

designs with equal total section width and height, this could lead to the redundancy curves as presented in Figure 6.9.

Although this method of describing the model damage levels provides a basic means to define a 1st LTM redundancy curve, it has two drawbacks. Because the model damage is effectively described in terms of structural damage (i.e. total loss of load carrying capacity of one or more layers), it does not allow for consideration of a residual compression capacity in the broken layer or residual tensile capacity in areas away from the crack, both of which may be dependent on the actual (density of) the fracture pattern, the laminate material, or other factors. This may result in resistances higher than can be attributed solely to the unbroken layers. Furthermore, it may be difficult to actually obtain the levels of cracking required for a layer to fulfil these definitions in an experimental setting. Therefore, it is proposed to alter the model level damage description to the effect that they assume loss of the tensile capacity of the layer(s) concerned, so that the general²⁵ model levels of damage are:

- I: Physical damage to the extent that *one outer glass layer* does not transfer principal tensile stresses related to the governing load case anymore in at least one section of the element.
- II: Physical damage to the extent that *all outer glass layer* does not transfer principal tensile stresses related to the governing load case anymore in at least one section of the element.
- III: Physical damage to the extent that *all glass layer* does not transfer principal tensile stresses related to the governing load case anymore in at least one section of the element.

3.4. Residual Resistance R_{res} and Relative Residual Resistance r_{res}

The (overall) residual resistance R_{res} is the resistance of an element that remains after damage.²⁶ Thus, it is the highest value of the primary or secondary load transfer mechanism at a certain level of damage, as Eq. (6.6). By definition, $R_{res,III}$ (the residual resistance at damage level III) indicates the capacity of the 2nd LTM, as the 1st LTM is no longer active at that stage.

Although in practice the highest value for residual resistance determines the resistance of the element, it may be useful to also introduce the concept of residual resistance of the primary load transfer mechanism $R_{res,1stLTM}$, Eq. (6.7), for theoretical considerations especially on elements with high capacity secondary LTMs. This measure indicates the residual strength of the primary LTM only, and ignores the possible presence of a 2nd LTM.

$$R_{res,n} = \max(R_{D\phi,n} \vee R_{2ndLTM=D\phi III}), \text{ with } n = \text{I, II, III.} \quad (6.6)$$

$$R_{res,n,1stLTM} = R_{D\phi,n,1stLTM}, \text{ with } n = \text{I, II, III.} \quad (6.7)$$

²⁵ Some other descriptions are presented for specific elements in Appendix D.

²⁶ It may be used synonymously with ‘residual strength’.

To generally evaluate redundancy, residual resistance can be related to the capacity of the 1st LTM to obtain the relative residual strength r_{res} as in Eq. (6.8).

$$r_{res,n} = \frac{\max(R_{D\phi,n} \vee R_{2ndLTM=D\phi III})}{R_{1stLTM}}, \text{ with } n = \text{I, II, III.} \quad (6.8)^{27}$$

3.5. Impact Im

Damage originates from some cause. The impact Im is the qualified and possibly quantified damage cause, or, in other words, the effort to produce damage. As there can be many different damage causes for glass, impact may have a variety of characters: thermal, soft body, hard body, static, dynamic, environmental, etc, or a combination of these. The resistance of a glass element to a range of impacts is an important parameter determining the safety of that element. If a governing impact is identified (e.g. a soft body pendulum impact test), the impact Im_n is the impact that results in physical damage level n .

4. Element Safety Properties

With the help of the concepts introduced in the previous Section, four safety properties can be defined for structural glass elements.²⁸ *damage sensitivity*, *relative resistance*, *redundancy*, and *fracture mode*. These properties relate to different areas in the cause-and-effect chain from failure cause to injury as depicted in Figure 6.1. They are explained in Sections 4.1 through 4.4 and combined into one graphical overview in Section 4.5. Together, they define the safety of an element, by covering *all* relevant aspects that influence the ability of a glass element to, ultimately, injure:

- **Damage sensitivity:** determines the failure likelihood from actions unconsidered in the failure probability analyses.
- **Relative resistance:** determines the notional failure probability through the considered actions S exceeding the element resistance R .
- **Redundancy:** determines the probability of collapse after sustaining partial damage and/or failure.
- **Fracture Mode:** determines the probability of injury from shards.

4.1. Damage Sensitivity Σ and relative damage sensitivity ς

Although the probabilistic approach of comparing the element resistance R to the actions S provides the basis for structural engineering, actual failures are hardly ever caused by the considered actions simply exceeding the nominal resistance. Rather, there are numerous other possible damage causes. Depending on the design and material selection, an element may be more or less sensitive to such unconsidered actions.²⁹ A 3x8 mm three layer laminate glass beam will be less susceptible to failure from

²⁷ Off course, relative residual strength can also be presented as a percentage. The results of Eq. (6.8) should then be multiplied by 100%.

²⁸ It has argued in Section 2 of this Chapter why this method is restricted to elements, rather than complete structures.

²⁹ ‘Unconsidered’ refers to the fact that they are not taken into account in the probability analysis. It does not necessarily mean the designer is not aware of them (although the designer may indeed not be conscious of some of the unconsidered causes).

vandalism – it is very difficult to damage the inner layer of a laminate by impact (thrown stones) on the outer layers – than a 2x12 mm two layer laminate, even though the (relative) resistance is practically equal.

The safety property *damage sensitivity* Σ describes how susceptible a glass element is to damage and failure from unconsidered causes. Since these have a wide variety of natures³⁰, some of which are even, by definition, unknown, the damage sensitivity of an element can only partially be assessed qualitatively and even less quantitatively, by identifying the impacts *Im* that may affect the element. Common impacts could be:

- Thermal stress,
- Soft body impact,
- Hard body impact,
- Powerful and repetitive hard body impact (vandalism),
- Vehicle collision,
- Scratches or chipping,
- Local peak stressing by errors in detailing or in the execution of details during construction,
- Etc.

Further variations in these impacts is often possible through parameters of e.g. impact body, speed, etc.

The relative likelihood and thus importance of each of these impacts may vary significantly per project. Also, there may be project specific impacts, such as bullet fire or explosions. Consequently, many design or material specification measures can be taken to decrease damage sensitivity. Alternatively, it may be possible to take measures to decrease the magnitude of the governing impact.

Generally, little nothing is known about the physico-mechanics of damage evolution in glass by impact. For practical reasons there are standardized impact tests, such as pendulum and drop tests,³¹ which evaluate an element or construction only in terms of pass/fail, but do not require recording of the extent of crack growth and a post-impact strength test to determine the damage caused by the impact. If any further testing is required (which often is not the case), it is a static load test over a prescribed time period. Again, the result is given only as ‘pass’ or ‘fail’. Thus, although this may give an indication as to the suitability of a certain constructions, it does not provide much information on the actual limits and failure behaviour of the construction – which would be required to compare the safety of different design solutions.

Although it is not possible to fully quantify damage sensitivity, it can at least partially be quantified by identifying a governing impact type and determining (e.g. by experimental testing³²) the magnitude thereof required to create the model levels of

³⁰ Chapter 4, Section 3.

³¹ See codes and guidelines discussed in Chapter 4, Section 5.1.

³² It should be noted that there are developments towards FE-modelling of (soft-body pendulum) impact tests, see: Lamers, E., Derkink, M., *Towards Design Rules for Structures with Glass Panels During Impact*, Proceedings of the Challenging Glass Conference, Delft, The Netherlands, May 2008. Provided corroborated by experimental research, this could provide an opportunity to establish the damage sensitivity of a large

damage I, II, and III³³. The damage sensitivity Σ for each level is then provided by Eq. 6.9. The impact can be presented in a measure suitable for the chosen governing impact type, for instance a temperature difference (°C) for thermal impact, or a drop height (mm), impulse (Ns), or energy (J) for a drop impact.

$$\Sigma_n = \frac{D_{\varphi,n}}{\text{Im}_n}, \text{ with } n = \text{I, II, III} \quad (6.9)^{34}$$

The *relative damage sensitivity* can be defined as the ratio between the damage sensitivity and the maximum allowable damage sensitivity. This parameter allows for a more general evaluation of the element safety than absolute damage sensitivity.

In general, the damage sensitivity of an element does not depend on its application. However, the importance of damage sensitivity as well as the magnitude of governing impact can be much greater in one project than in another.

4.2. Relative Resistance r

The resistance R^{35} of an element is the nominal calculable strength of its primary load transfer mechanism under (semi-) static loads and the value commonly checked against codified actions. For an evaluation of element safety, it is not so much the absolute resistance of the element that is of importance, but rather the *relative resistance* r : the magnitude of the resistance related to the ultimate limit state load³⁶ - in fact, the relative resistance is the inverse of the outcome of the unity check as prescribed by many codes, Eq. (6.10).

$$r = \frac{R_d}{S_{uls}} \quad (6.10)$$

Compare, for instance, two beam designs A and B as in Figure 6.10: both double PVB laminated, annealed glass beams. Assume a short term tensile strength of $\sigma_f = 25$ MPa, and a short term ultimate limit state load of $q_{uls} = 4$ kN/m. For both designs, $u.c._{A/B} \leq 1.0$ - thus both pass. But just as the actual outcome of the u.c. for A and B is different ($u.c._A = 0.50$; $u.c._B = 0.75$), so is the relative resistance for A and B: they result in $r_A = 1.33$ and $r_B = 2.00$. This indicates that, although both designs are strong enough, design B is

variety of element designs to this type of impact. The development of such modelling for other impact types should be encouraged.

³³ The impact type is not necessarily the same for each model level impact. E.g. the governing impact type for a floor panel may be a hard body drop test. When the panel is composed of annealed or heat strengthened glass sheets, drop tests will probably only cause crushing, chipping, and possibly some small cracks in the top layer, or cracking of the whole panel. Thus, it may be impossible to obtain crack extent level II (all outer layers broken), with this type of test; levels I (one outer layer broken - the bottom one would be logical in this case) and III, on the contrary can be achieved with this impact type. For level II, another impact type could be identified, e.g. centre punch on the edge, or a crack line produced by a glass cutter.

³⁴ Note that the safety is higher when the (relative) damage sensitivity is lower.

³⁵ As in ordinary structural calculations, the 'R' presented here is a single value parameter, contrary to the probabilistic function $R(\xi)$ discussed in Chapter 3 (the probabilistic scatter is incorporated through safety factors).

³⁶ Obviously, when one element is twice as strong as another, but the actions on it are three times larger, it is more likely to break.

likely to be more safe. This may be quite obvious, but it should not be overlooked in a safety assessment.

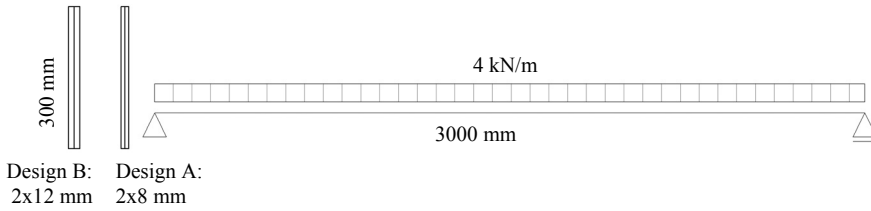


Fig. 6.10 Two example glass beams to illustrate the concept of relative resistance.

The greater r is, the less likely the element is to fail. To obtain a prescribed failure probability, $r = 1.0$. When, instead $r > 1.0$, this means the formal failure probability is smaller than required. Hence, the element is more safe. The exact magnitude of the failure probability reduction depends on the momentary factor ψ , but even for a relatively slight increase in r , the failure probability reduces by orders of magnitude.³⁷

However, this also means the formal failure probability quickly becomes irrelevant, even when resistances are several decimals above 1.0. Rather, actual failure will be determined by damage sensitivity (to actions not considered in the formal probability analysis) – although these are often not independent properties.

Additionally, the concepts of resistance surplus R_{surp} and relative resistance surplus r_{surp} are introduced because they can be incorporated more easily into the graphical presentation of safety properties, the Element Safety Diagram (Section 4.5). They relate to the relative resistance reserve through Eqs. (6.11a and b).

$$R_{surp} = R_d - S_{uls} \tag{6.11a}$$

$$r_{surp} = \frac{R_{surp}}{S_{uls}} = \frac{R_d - S_{uls}}{S_{uls}} = \frac{R_d}{S_{uls}} - 1 = r - 1 \tag{6.11b}$$

4.3. Overall Redundancy m

In Chapter 3, Section 7.2, two definitions of ‘redundancy’ were quoted, both in relation to the behaviour of structures. According to Starossek³⁸, redundancy ‘refers to the multiple availability of load-carrying components or multiple load paths which can bear additional loads in the event of a failure.’ Biondini et al.³⁹ define redundancy as ‘the ability of the system to redistribute among its members the load which can no longer be sustained by some other damaged members.’

³⁷ Consider e.g. Eq (6.12) (Section 5.3.1. of this Chapter), taken from NEN 6702, which relates the failure probability density to the momentary factor. The effect of r is comparable to that of ψ_t . Actually, when $\psi = 1$, as e.g. for self weight, and $r > 1.0$, then the failure probability becomes 0, or: once during infinity)

³⁸ Starossek, U., Haberland, M., *Measures of Structural Robustness – Requirements & Applications*, Proceedings of the Structures 2008 Congress: Crossing Borders, of the ASCE, Vancouver, April, 2008.

³⁹ Biondini, F., Frangopol, D.M., Restelli, S., *On Structural Robustness, Redundancy and Static Indeterminacy*, Proceedings of the Structures 2008 Congress: Crossing Borders, of the ASCE, Vancouver, April, 2008.

In the context of the integrated safety approach presented here, it is proposed to describe the *overall redundancy*⁴⁰ m as the development of residual strength over increasing model damage levels from 0 to III. It differs from m_{1stLTM} by the fact that m is the highest value of $R_{res,1stLTM}$ and $R_{res,2ndLTM}$ at any value of $D_{\phi,n}$, whereas m_{1stLTM} only considers $R_{res,1stLTM}$. Additionally, the redundancy of the 2nd LTM m_{2ndLTM} can also be defined, namely as the development of $R_{res,2ndLTM}$ over $D_{\phi,n}$. However, in the system being developed here, $R_{res,2ndLTM}$ is constant over $D_{\phi,n}$, thus m_{2ndLTM} is equal to $R_{res,III}$ (i.e. a horizontal line in the D_s, D_{ϕ} -graph).

Figure 6.11 presents the expected indicative m , m_{1stLTM} , and m_{2ndLTM} curves for a three layer, SG laminated annealed glass beam.⁴¹ In comparison to Figures 6.7 and 6.9, the axis organization in Figure 6.11 was altered to obtain a decreasing curve over increasing values of $D_{\phi,n}$ by turning the direction of the D_s axis upside down. This allows to add an alternative vertical axis for resistance in the same graph so that damage and residual strength can simultaneously be read off. Furthermore, the relative resistance axis can expand beyond 1, allowing for elements with secondary load transfer mechanisms with greater capacity than their primary ones. Finally, it results in curves that can be interpreted more intuitively: a higher curve indicates more safe behaviour rather than less safe behaviour.

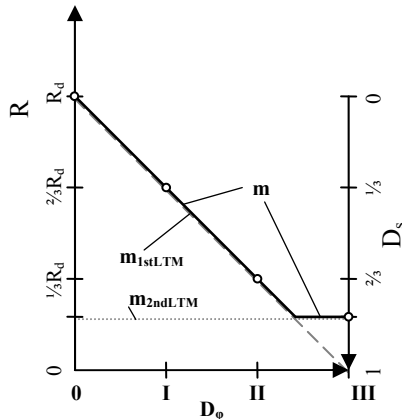


Fig. 6.11 Expected indicative redundancy curves M , M_{1stLTM} , and M_{2ndLTM} for a three-layer, SG laminated, annealed glass beam.

The behaviour of (partially) broken glass elements may often be both time and temperature dependent. Section 4.5 presents a method to incorporate these aspects along with the other element safety properties into one diagram.

⁴⁰ Or just ‘redundancy’, for short.

⁴¹ Experimental results of four-point bending tests on such beams as well as many other designs, are presented in Appendix E. Actually, from the tests it could be concluded the actual residual strength of a damaged specimen can diverge from a simple proportionate section reduction. The actual, experimentally determined redundancy curves are extensively discussed in Chapter 7.

4.4. Fracture Mode

Finally, the fracture mode of the glass element directly influences the possibility of getting injured when coming into contact with a broken/breaking element, either by collision or by it falling on someone. Glass engineering codes such as the NEN-EN 12600⁴² distinguish three kind of fracture modes:

- A – numerous cracks appear forming separate fragments with sharp edges, some of which are large; typical of annealed glass.
- B – numerous cracks appear, but the fragments hold together and do not separate; typical of laminated glass.
- C – disintegration occurs, leading to a large number of small particles that are relatively harmless; typical of thermally tempered glass.⁴³

NEN-EN 12600 further accompanies the fracture mode letter with two figures indicating the drop height with a prescribed drop test device, required to actually obtain the fracture mode. However, in the system presented here, such results should be part of the damage sensitivity characterization of an element (with the drop test being the governing impact type). Furthermore, within type B, there can still be important differences between various (broken) laminates in terms of residual strength and residual stiffness. These properties, though, can be incorporated through the redundancy requirements. For application in the integrated approach, it is proposed just to use a letter (A, B, or C) based on the fracture mode that occurs at failure from the prescribed failure impact type.⁴⁴

4.5. The Glass Element Safety Diagram (ESD)

Having identified the four properties that determine the safety of a glass element, it is now possible to construct an *element safety diagram* (ESD) for the glass element, which combines (relative) resistance, damage sensitivity, redundancy, and fracture mode in one clear picture.

Figures 6.12a and b present two examples, developed from Figure 6.11. They are on scale with one another and indicate the expected ESDs of a three-layer, SG laminated glass beam from annealed glass and thermally tempered glass, respectively. The element safety is basically presented by (see also markings in the Figures):

⁴² Dutch Institute for Standardization, *NEN EN 12600: Glass in building - Pendulum test - Impact test method and classification for flat glass*, Delft, the Netherlands, 2003.

⁴³ This assumption has been challenged before, see Chapter 5, Section 3.2. Despite objections to the assumed safety of tempered glass, it is imaginable its shards are at least less dangerous than those of annealed and strengthened glass. Extensive comparative research with regard to the injury potential of each glass type is unknown to the author. This could be extremely valuable to the discussion regarding the sensibility of tempering glass. However, the distinction in fracture mode is actually only relevant for glass in construction applications; for structural glass, fracture mode B will always be applicable as it would not be possible to obtain residual resistance with type A or C.

⁴⁴ It should be noted that in some cases, the test method for determining the fracture mode does matter for its characterization. In experiments presented in Appendix E, it was found that heat strengthened, PVB-laminated glass beams may fail by breaking into two when subjected to direct four point bending, thus behaving as fracture pattern A. When, however, specimens had been predamaged, they behaved like you would expect from laminated glass: as type B.

- a) The resistance reserve: a fat line on the vertical resistance axis, indicating the margin between the ultimate limit state action and the calculable resistance of the element, at $D_\varphi = 0$ (contrary to the other properties, the resistance reserve is application dependent),
- b) The horizontal impact axis, which replaces the D_φ axis to quantify the effort required to obtain each model damage level,
- c) The redundancy curve,
- d) The fracture mode letter.

a) Resistance Surplus R_{surp}
 b) Impact Im (indicates damage sensitivity)
 c) Redundancy m curve
 d) Fracture Mode letter

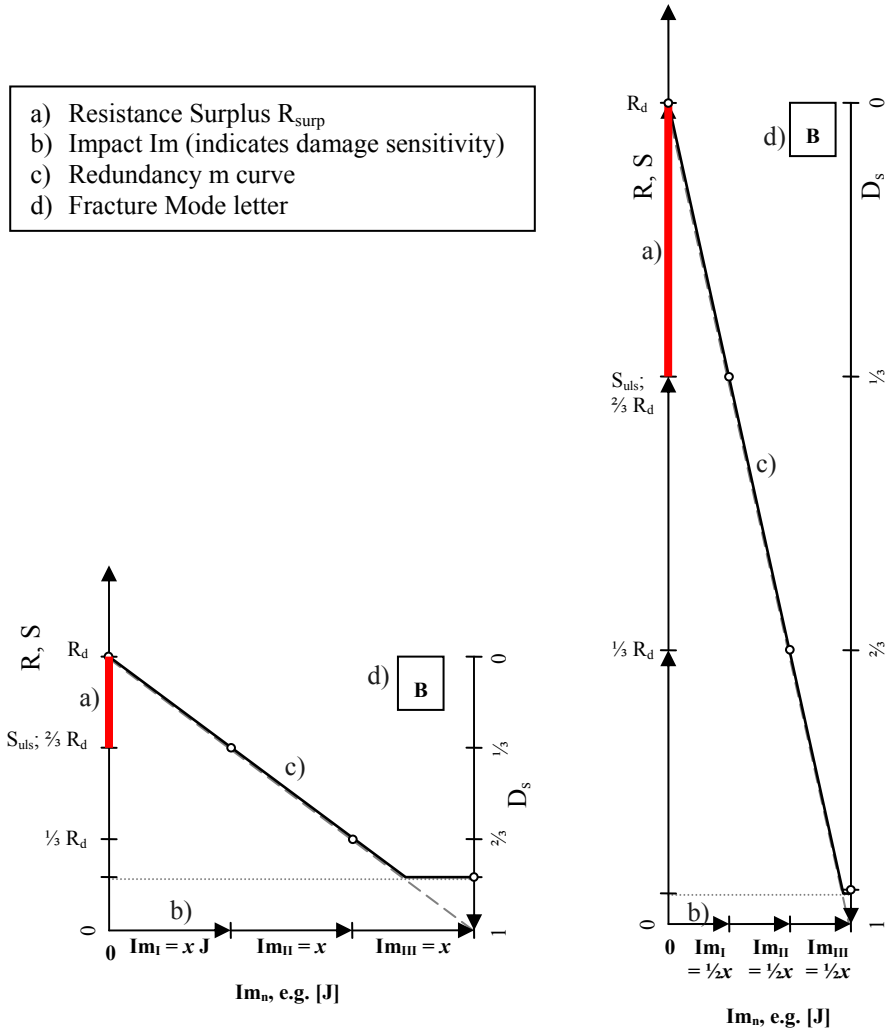


Fig. 6.12a, b Expected indicative ESD for a three-layer, SG laminated glass beam from annealed glass (a, left) and thermally tempered glass (b, right). The position of S_{uls} is application dependent and was here assumed at $\frac{2}{3}R_d$ for both beams as an example. Obviously, the resistance of the thermally tempered beam is expected to also be significantly higher (it requires less impact energy to break a layer), resulting in smaller sections on the horizontal impact axis. Because of the dense fracture pattern (which generates less stiffness in compression), $R_{res,III}$ is also expected to be lower.

The left vertical axis indicates the element resistance in undamaged state as well as the decreasing resistance under increasing levels of physical damage. The right vertical axis shows the increasing level of structural damage.

The horizontal distance between the model crack levels is determined by the (quantitative) impact required to create the model crack levels. The horizontal axis is constructed as a stacked summation of the impact required to go from 0 to I, I to II, and II to III. Thus, the length of each segment as well as the total length indicates the element damage sensitivity, which is also in the steepness of the primary load transfer mechanism curve.

It should be noted that the shape of the curve between the model crack levels will be hard to determine in reality. Most likely, it will not be straight, but, rather, have a hyperbolic character as in Figure 6.13. However, the exact determination of the continuous relation between crack level and strength is not relevant for safety assessment – the model crack levels form the governing boundary cases. Therefore, the curve is presented with straight lines between the model damage levels.

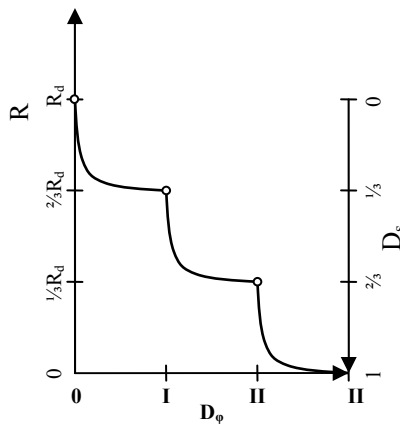


Fig. 6.13 Expected real relation between physical and structural damage. Probably the 1st LTM redundancy curve would have to follow a hyperbolic shape between model damage levels, rather than a linear one.

4.5.1. Incorporating the Time-component

It is well known that the failure behaviour of both glass and commonly used additional polymeric materials such as PVB, is highly time dependent. The precise nature of the time dependency of glass and the way to incorporate that into strength calculations, is still debated⁴⁵. However, it has long been clear that the resistance, either in the pristine state or after damage, can not be presented as one value. To fully assess the element resistance and failure behaviour, a time axis should therefore be added to the ESD, turning it into a 3D figure. A log-scale would be most practical as the duration of relevant actions is of highly increasing nature (wind gust: seconds – snow load: months – permanent load: decades).

⁴⁵ Chapter 4, Section 1.2.2.

An example of an ESD expanded with a time-axis is given in Figure 6.14a (expansion of Figure 6.12a). Again, it will be difficult, if not impossible to determine the complete relation between resistance, physical damage, and time. However, it is only really relevant at the model damage levels.⁴⁶ Curves can be drawn from these points (as in Figure 6.14a), however it is often only relevant to indicate the minimum time a resistance can be maintained for a limited number of resistance levels. The time axis can therefore be omitted and replaced by a number of time-tags in the 2D diagram. Figure 6.14b shows how the 3D diagram with the time axis is thus reduced again to a 2D one – arguably a more clear representation of the vital data.

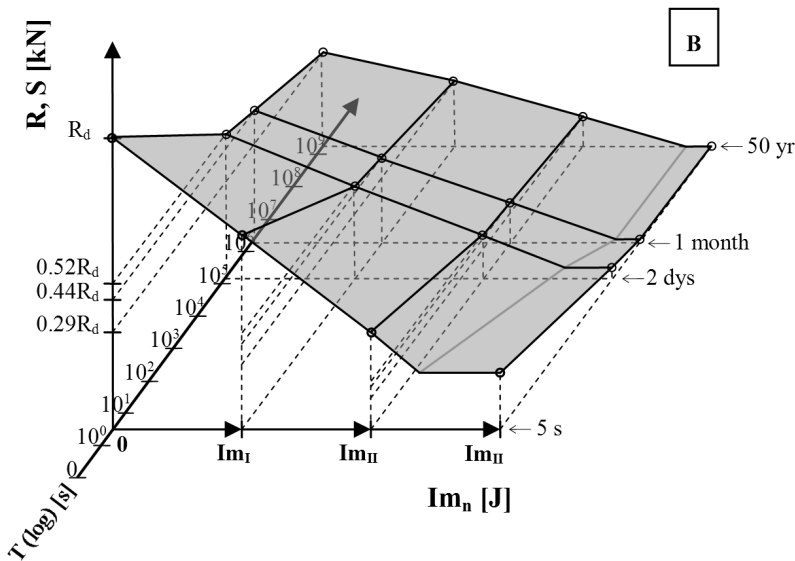


Fig. 6.14a Expansion of the ESD with a time-axis. The resistance, time, impact relation becomes a surface. The time periods relevant according the NEN 2608-2⁴⁷ are indicated on the left: 5 s, 2 days, 1 month, 50 years. The demarcations 0.52, 0.44, and 0.29 on the resistance axis are the values of the time factor k_{mod} for those durations. The impact axis is positioned at 5 s as this is the duration for which $k_{\text{mod}} = 1$ and the initial value of R_d is calculated. As in Figure 6.12, the behaviour in between the model damage levels has been simplified by linearization.

4.5.2. Incorporating the Temperature-component

Additional to the time-dependency, the behaviour of most additional polymeric materials is also temperature dependent. A full incorporation is difficult as it requires the addition of another, 4th, axis (and thus dimension). It is therefore proposed to incorporate this parameter in the form of an (indicative) range for which the curves are valid. This range should coincide with the temperature range assumed for the required resistance and redundancy.

⁴⁶ As long as at least one layer of glass is still unbroken and functions as the primary load transfer mechanism, with lack of more detailed data, it should be assumed the resistance-time relation for that sheet is equal to that of a single, undamaged glass sheet.

⁴⁷ Nederlands Normalisatie Instituut, *NEN 2608-2: Vlakglas voor gebouwen - Deel 2: Niet-verticaal geplaatst glas - Weerstand tegen eigen gewicht, wind- en sneeuwbelasting en isochore druk - Eisen en bepalingmethode*, Delft, the Netherlands, 2007.

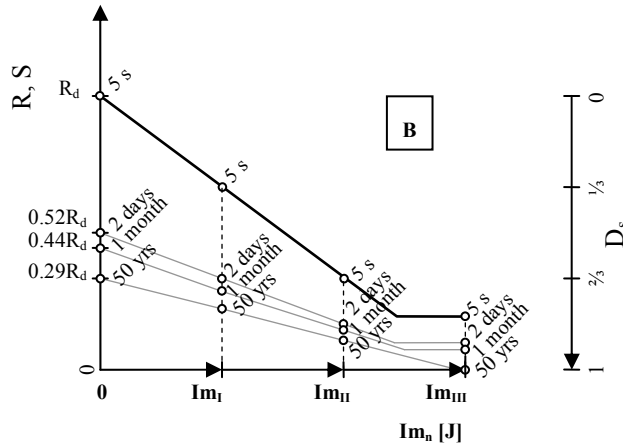


Fig. 6.14b Replacement of the significant time-related demarcations with time tags instead of an extra axis.

4.6. Alternative Presentations of the Safety Diagram

4.6.1. Using a Dimensionless Horizontal Axis

The way the safety diagram is presented above requires a quantitative explication of the model level impact for each model crack level. Since there is little research data available with regard to the relation between impact (of whatever kind) and crack growth, this may not be commonly possible. Alternatively, the horizontal axis can again represent D_ϕ and be divided in equal, dimensionless sections between crack level 0 (no damage) and failure, as in Fig. 6.15. The sections then no longer represent any quantitative measure, but only serve to graphically differentiate between stages of cracking. If, for one or more stages, the required impact is known, it can be added e.g. as a vertical bar at the relevant crack level. It also becomes possible to present a multitude of such bars, if the required impact quantity of different kinds of impact is known that result in the model crack level. These bars then represent the damage sensitivity, for as far as known.

4.6.2. Using a Relative Representation of Measures

In order to obtain a clear understanding of the safety of an element, it may be suitable to present the safety diagram in relative terms, rather than absolute ones (Figure 6.16). This is especially suitable to interpret and compare the safety of different elements in different applications. The resistance can be divided by the ultimate limit state action to obtain relative resistance. As the relative residual resistance is related to R_d and thus has another scale than relative resistance, this requires an additional vertical axis for the latter.

On the horizontal axis, the impact levels could also be made relative by dividing the quantities by the required minimum level impact for each model crack level (Figure 6.16) Alternatively, the dimensionless horizontal axis can be used, either with or without relative vertical bars for impact.

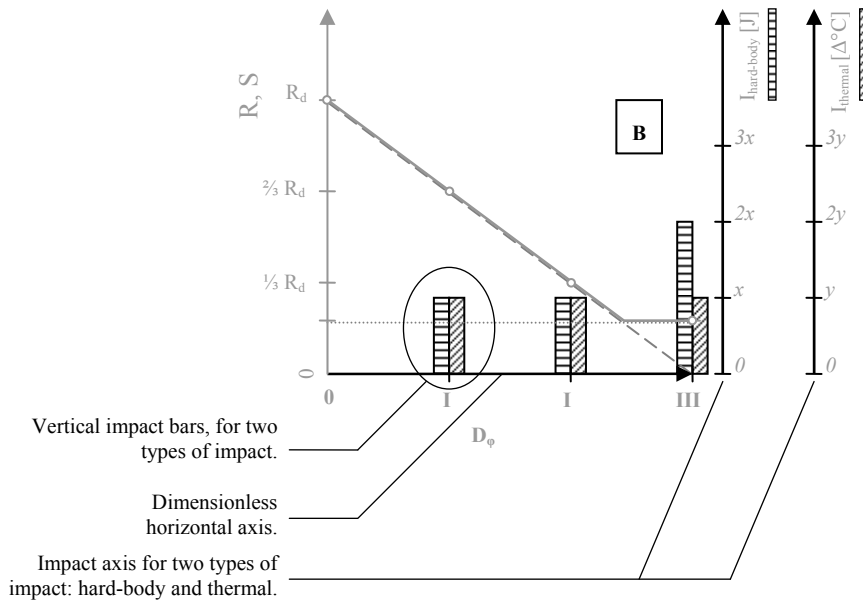


Fig. 6.15 ESD for a triple layer, SG laminated, annealed glass beam, with a dimensionless horizontal axis, representing D_ϕ . For clarity, the (right) structural damage axis has been omitted. The required impact is represented by vertical bars. This also allows identification of multiple types of multiple impact types, e.g. a hard body impact and a temperature difference. In this example, the inner layer is thicker than the others, requiring a higher hard body impact to obtain breakage.

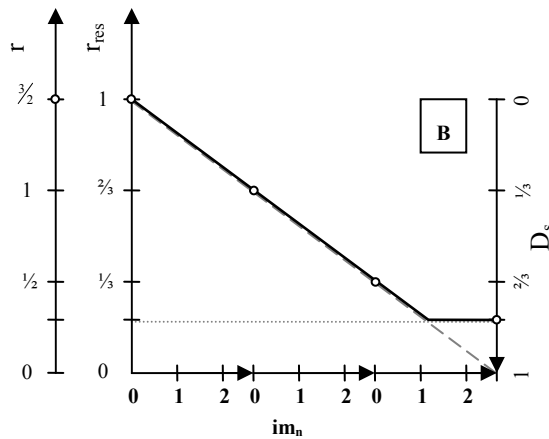


Fig. 6.16 ESD with relative presentations on the axes. An extra vertical axis has to be added because the scaling of relative resistance and relative residual strength is unequal. The former is related to the ultimate limit state load S_{uls} , while the latter is derived from the calculable resistance R_d .

4.7. Comments

Although damage sensitivity, relative resistance, redundancy, and fracture mode are all properties that influence the safety of an element that can be quantified to a considerable extent individually, it is difficult to join them in one quantitative relation or model. It is questionable whether that is even theoretically possible in a meaningful way. In the case of the safety of glass elements, it would require a probabilistic model combining the influences of all properties on the probability of injury. Such a model would be extremely complicated. More importantly though, there are fundamental objections to such an approach, as extensively argued earlier.⁴⁸

Consider assessing a car: relevant properties could be reliability, size, fuel economy, and top speed. But how much reliability can one sacrifice for a certain increase in top speed? As these properties are not (or hardly) physically related, the choice is rather subjective, even though minimum requirements may be formulated for each property. Nevertheless, it can be extremely useful to list the individual properties in a fixed format to make the differences insightful. Tables and diagrams aiming at that can be found in practically any car magazine. The goal of the ESD is the same: to get a comprehensive overview of all relevant safety properties of a glass element.

The most important safety property in the ESD is redundancy. While both resistance and damage sensitivity provide information on the likelihood of damage and failure, redundancy informs on the element performance once that has happened. As there may always be unexpected damage and failure causes, redundancy is of key significance and has therefore been given a central position in the ESD. Nevertheless, considering redundancy only, and disregarding resistance and damage sensitivity could lead to overly conservative designs.

The integrated safety approach as developed here may lose relevancy when extremes are being sought in the design. For instance, in case of a three layer laminate with very thin outer layers and a thick inner one, the relative importance of model damage level III should weigh heavier than in a design with evenly distributed thicknesses, although a qualitative impact axis could already indicate the abnormality of such a design (as it would require much less impact to obtain model damage levels I and II, than it would to obtain III).

Robustness⁴⁹ has not been applied in the integrated approach, mainly because it is still a heavily debated concept in the field of safety engineering of structures. It seems robustness would somehow combine several or all introduced safety properties into one figure. However, as argued above, it is questionable whether this is meaningfully possible. At least, it would require much additional research.

5. Formulating Safety Requirements With the Element Safety Diagram

Requirements with regard to the four safety properties already appear to varying extent in glass engineering codes. However, they do not appear to bear much relation to each other. The introduction of the glass element safety diagram allows the integrated definition of safety requirements.

⁴⁸ Chapter 3, Section 6, and Chapter 4, Section 4.

⁴⁹ Chapter 3, Section 7.2.

5.1. Damage Sensitivity

In the current state of structural glass engineering, impact-based performance requirements for structural glass elements, such as pendulum and drop tests, are not related to model damage levels that have to be obtained. They simply require a construction to pass such a test without collapse. Occasionally it is stated that layers not broken after the impact test, should be broken (e.g. by hammer or centre punch) before a residual strength test is executed.

This method, however, provides very little information on the actual damage sensitivity of the element. Ideally, a quantifiable governing impact type is defined and provided with a required minimum to obtain each model crack level. In the cases that this is possible, the required minimum impacts can be outlined on the horizontal axis and stacked for each model damage level.

Consider, for instance, a laminate glass beam. It could be argued the governing impact is a hard, concentrated impact (e.g. a thrown or falling object) on the edge. Chapter 7 and Appendix E present extensive research into the failure of glass beams damaged with a device to simulate such impact (Figure 6.17). The minimum impact for each level could be defined as a minimum energy in the impacting device, required to create the model level crack growth.

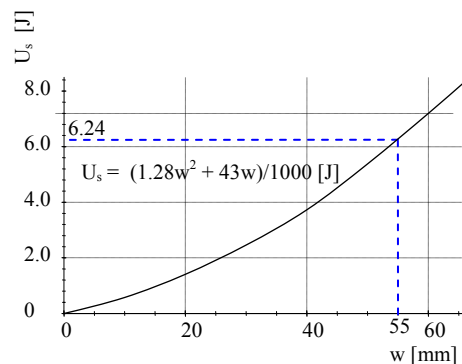
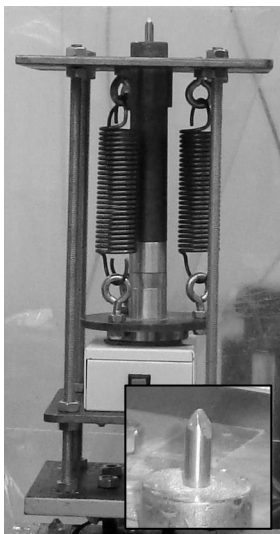


Fig. 6.17 Impact device used in the experiments described in Appendix E to create model damage levels in glass beams. It consists of a spring loaded flat impact head from hardened steel. The intensity of the impact can be controlled by setting the spring extension. The graph indicates the relation between the spring extension and stored spring energy.

However, with many impact types available, this kind of presentation may not be possible, or only to a limited extent (e.g. only for level III). The dimensionless horizontal D_ϕ should then be used, along with additional qualitative and/or quantitative remarks concerning damage sensitivity. When presenting test results, it should at least

be indicated how the model damage levels were obtained (e.g. by impact, glass cutter, additional static load, etc.).

A problem may arise when assessing the redundancy of an element with a quantified impact method, because the residual strength depends on the intensity of the impact with which model damage level III is obtained. Experimental research presented in Appendix E shows that the failure behaviour of heat strengthened, two-layer PVB-laminated glass beams is significantly different in direct overloading then when either one or both layers had been predamaged. In the former case, the laminate foil tears upon failure and the beam breaks in two. In the latter case, a (weak) secondary load transfer mechanism (composite action between PVB in tension and glass in compression) is activated which generates some residual strength $R_{res,III}$.⁵⁰ Testing the same geometry with either annealed or thermally tempered glass does not result in PVB-tearing upon direct overloading, and thus in some residual strength $R_{res,III}$. This means the selection of the impact type (in this case direct overloading or overloading after predamage) significantly influences the redundancy assessment of the element, and may therefore also result in different conclusions when various designs are compared. Accordingly, the choice of impact (impact requirement) is of crucial importance in the assessment of the safety of an element.

5.2. Resistance

The required resistances for the undamaged state can be outlined on the left resistance-time face of the diagram. Alternatively, they can be indicated on the resistance axis with time tags (Figures 6.18a and b, respectively). The resistances should be determined from existing action-defining codes such as the NEN-EN 1991 (Eurocode 1);⁵¹ the relevant time demarcations from glass engineering codes such as the NEN 2608-2.⁵²

The actual element resistances (calculable value) can also be outlined on the face of the diagram or indicated on the resistance axis with time tags. Off course, the element resistance should consistently exceed the required resistance.⁵³

⁵⁰ Kott and Vogel found similar results when testing laminated glass plates: in direct loading they yielded no residual strength of significance, while they did after having previously been damaged. Kott & Vogel: Kott, A., Vogel, T., *Structural Behaviour of Broken Laminated Safety Glass*, in: Crisinel, M., Eekhout, M., Haldimann, M., Visser, R. (Eds.), *EU Cost C13 Final Report, Glass & Interactive Building Envelopes*, Research in Architectural Engineering Series, Volume 1, IOS Press, Amsterdam, the Netherlands, 2007, pp. 123 – 132.

⁵¹ Nederlands Normalisatie Instituut, *NEN-EN 1991 Eurocode 1: Actions on Structures, (various parts)*, Delft, the Netherlands.

⁵² Nederlands Normalisatie Instituut, *NEN 2608-2: Vlakglas voor gebouwen - Deel 2: Niet-verticaal geplaatst glas - Weerstand tegen eigen gewicht, wind- en sneeuwbelasting en isochore druk - Eisen en bepalingmethode*, Delft, the Netherlands, 2007.

⁵³ It should be noted that even the determination of the calculable resistance of a pristine glass element over time still requires more research. It has been argued extensively in Chapter 4, Section 1.2.2., questions remain concerning sub-critical crack growth as well as with regard to the relation between thermal treatment and strength.

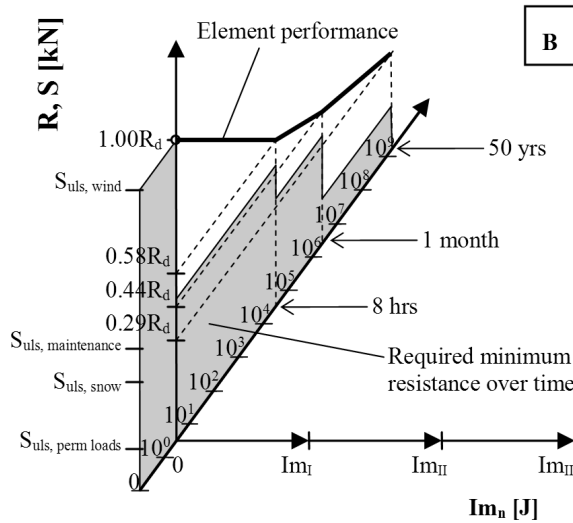


Fig. 6.18a Required minimum resistance for several time periods, presented two-dimensionally on the R,t-face of the ESD. The element performance is outlined in bold. The element performance curve should consistently exceed the gray area. In this example, the wind load case (5 s) is governing ($R_d = S_{uls,wind}$).

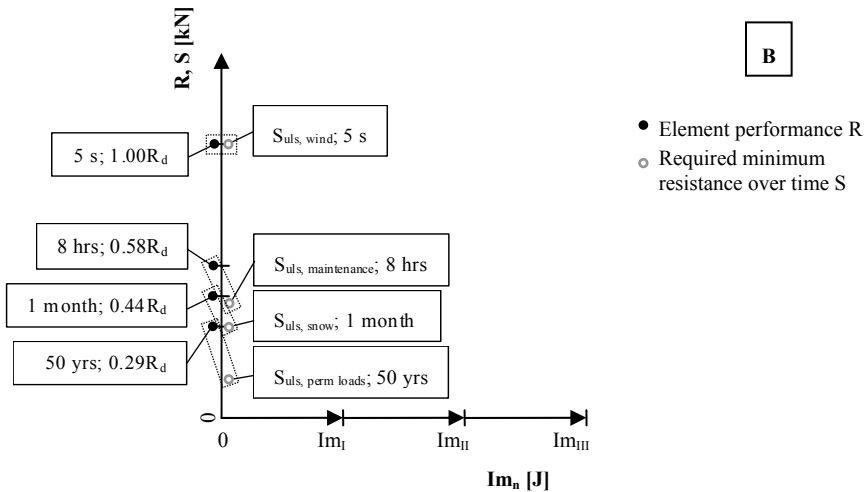


Fig. 6.18b Required minimum resistance for several time periods, presented by dots on the vertical resistance axis, along with time tags. The element performance for each time period is presented by black dots, which should always exceed the corresponding hollow gray dot for the same time period.

5.3. Redundancy

The redundancy requirements consist of a series of minimum residual resistance levels required at *each* model damage level for a required minimum period of time.

The relevant damage axis demarcations (level 0, I, II, and III) have been previously argued. The next sections discuss the relevant demarcations on the time and resistance axes.

5.3.1. Time axis demarcations

Based on the interviews presented in Chapter 5, Section 3, it can be argued that, relative to the reference life time, four time periods may be relevant:

- (a) time-to-discovery
 - (b) time-to-evacuate
 - (c) time-to-support
 - (d) time-to-replace
- ↔ (e) reference life time

Table 6.1 gives an indication of their magnitude and some remarks per time period. The time-to-evacuate was not explicitly mentioned, but seems a logical addition. The reference life time is relevant because in some cases it may not be acceptable to make structural safety dependent on the fact whether or not required measures are actually taken. This may be the case for low damage levels, low inspection frequencies or even at high damage levels for major structural elements (although it is questionable whether this would apply to any glass structure that has been built up until now).

Table 6.1 Relevant time periods for the determination of residual strength requirements.

	Time period description	Order of magnitude	Remarks
(a)	Time-to-discovery	1 – 3 days	Time until the damage or failure is likely to be discovered. This depends on the inspection frequency ⁵⁴ (the approximate frequency that the element in question is observed by somebody likely to take measures in case of damage, e.g. a janitor or security personnel. In most building applications, the inspection frequency will be in the order of 1 – 3 days. However, outside applications may be much less frequently be inspected.
(b)	Time-to-evacuate	Seconds to hours	The time to flee from under a damaged element may only be seconds. When an element plays a vital role in a structure, more time may be required. This time frame may include evacuating people that have lost consciousness for whatever reason as well as closing off of an area immediately endangered by the damaged element, e.g. under a canopy.
(c)	Time-to-support	1 – 7 days	The time required to support the damaged element and thereby provide an alternative load path strong enough for the actions the element was designed for. This time frame may include removing variable loads such as snow or (interior) furniture.
(d)	Time-to-replace	1 – 6 months	This time frame is not directly important for safety. However, for prestige as well as avoiding costly temporary supports it may be important to require an element to be able to provide residual strength for this time period.

The time components can be combined to arrive at time periods for which the element is required to maintain a certain resistance at a certain level of damage. For instance: residual strength has to be maintained for level I for a period equal to (a)+(c), level II for a period of (a)+(b), and level III for a period of (b). It is proposed the component combinations should be based on an application classification. The actual quantification

⁵⁴ It should be noted that the general public may not report damage if the element in question does not seem to be about to collapse. Holger Techen and Jens Schneider have made remarks with regard to this issue when being interviewed by the author. See Appendix C, Sections 5.3.2. and 6.3.2., respectively.

of the time components could be based on such a classification as well, but may also be subject to project specific specification.

It should be noted that the time component influences redundancy requirements in two ways. First, off course, it defines the duration for which a certain level of residual strength has to be guaranteed. But, consequently, the duration itself influences the maximum action that can be expected during that time. If the time period for which residual strength has to be maintained gets longer, than the most severe action that can be expected during that period also increases because of the stochastic character of variable actions such as wind and snow loads.

In the NEN 6702⁵⁵, the time-dependent character of the variable loads is accounted for with the reference period correction factor ψ_T which depends on the momentary factor ψ (e.g. $\psi_{\text{wind}} = 0$) and the reference life time through Eq. (6.12).

$$\psi_T = 1 + \left(\frac{1 - \psi}{9} \right) \cdot \ln \left(\frac{T}{T_{50}} \right) \quad (6.12)$$

However, for two reasons this factor can not be applied to the determination of residual strength requirements without further ado. First, if residual strength requirements were to be based on the usual action calculations and a reference period correction factor for the relevant time period as introduced above, it would mean the damage is considered as a given uncorrelated to the action history (i.e. the average statistical action history would start at the time of the damage), while in fact it may be more likely that the probability of damage increases with increasing actions. Damage and action history may be correlated to a certain extent.

Furthermore, it is questionable whether the value of ψ_T is valid for small values of T .⁵⁶ The NEN 6702 requires the use of a minimum value of $T = 1$ yr, even for structures with a shorter life time. However, one year is still well beyond any of the relevant time periods relating to glass damage and failure (as introduced above). Both these issues should be subject of further research.

5.3.2. Resistance Axis Demarcations

Codes for the determination of actions recognize a number of relevant loading combinations (LC). NEN 6702 distinguishes five loading combinations, some of which apply to ultimate limit (ul) states (Eqs. (6.13a, b, c)), while others regard serviceability limit (sl) states. In terms of calculus, the main difference lies in the value of the load safety factor γ , which for sl-states is always equal to 1.0, while for ul-states it may range from 1.0 to 1.5, depending on the load type, building safety classification, and loading combination.⁵⁷

Fundamental combinations:

⁵⁵ Dutch code for the determination of actions on structures. Momentarily co-exists with the Eurocode 1, by which it will eventually be superseded. Nederlands Normalisatie Instituut, *NEN 6702, Technical principles for building structures - TGB 1990 - Loadings and deformations*, Delft, the Netherlands, 2007.

⁵⁶ Actually, $\psi_T \leq 0$, for $T \leq 0.006$ yr (≈ 54 hrs).

⁵⁷ Hence, serviceability limit state actions are also known as 'unfactored loads'.

$$S_{f;u;d} = \gamma_{f;g;u} S_{perm,rep} + \gamma_{f;q;u} \psi_T S_{var,1;rep} + \sum_{i \geq 2}^n \gamma_{f;q;u} \psi_i S_{var,i;rep} \quad (6.13a)$$

$$S_{f;u;d} = \gamma_{f;g;u} S_{perm,rep} \quad (6.13b)$$

Exceptional combinations:

$$S_{a;u;d} = \gamma_{f;g;u} S_{perm,rep} + \gamma_{f;a;u} S_{inc,rep} + \sum_{i \geq 1}^n \gamma_{f;q;u} \psi_i S_{var,i;rep} \quad (6.13c)$$

Serviceability limit states are to be used in calculations related to the practical performance of the structure. Thus, they are generally used to calculate whether acceptable maximum values of displacement and deformation are exceeded, which may cause damage to surrounding construction, render parts of the structure less useable (e.g. through uneven floors), or cause anxiety or loss of aesthetic quality by becoming otherwise noticeable (e.g. visible). Statistically, they have a probability density of $p_{sls} = 1/t$ [yr⁻¹] with t = reference life time in years.

Ultimate limit states, on the other hand, are to be used in calculations relating to structural failure. By multiplying the actions with the load safety factor γ , the probability of exceeding during the reference life time is significantly decreased to the order of $P_{uls} = 10^{-3} - 10^{-4}$. Since the ul-state values of loading combinations relate to failure, these are the values to be used when determining redundancy requirements for structural glass. Applying serviceability limit state actions as requirements, as is often done, is – at least theoretically – mistaken, because the analysis made in these calculations is one of safety and not of serviceability. The argument that an actual damage (I, II, or III = failure) is in itself unlikely and the residual strength requirements should therefore be lenient seems intuitively correct, but should not be solved by applying sl- rather than ul-state loading combinations.

It could also be suggested to consider a damage as an exceptional action and that residual strength requirements thus have to be determined from Eq. (6.13c). The damage itself would have no quantity ($S_{inc,rep} = 0$) and the remaining residual strength should be equal to the permanent load ($\gamma_{f;g;u} S_{perm,rep}$) plus the momentary variable load

($\sum_{i \geq 1}^n \gamma_{f;q;u} \psi_i S_{var,i;rep}$). However, this approach is also mistaken, as Eq. (6.13c) applies to

the required resistance at the time of the special action, not after it. Rather, the damaged state should be considered a given, for which requirements have to be determined.

There are two ways to arrive at residual strength requirements below the initial ul-state resistance requirement for the undamaged state:

- a) Considering a small reference life time for the damaged structure, and thus applying a small value for the life time correction factor ψ_T .

- b) Allowing for a greater probability of collapse in case of damage or failure, and thus a smaller value of the reliability index β .

Ad a. Ideally, further research would have to provide reliable values for ψ_T for small values of T and given a certain damage. However, as these data may not be available any time soon, it is suggested to (subjectively) select a limited number of values for ψ_T to be used in the formulation of redundancy requirements. Figures 6.19a and b show the development of ψ_T as determined from Eq. (6.12) for $\psi = 1.0$ and $\psi = 0.0$, keeping in mind the curves may not correspond with reality for $T < 1$ yr. For $0 < \psi < 1$, the value of ψ_T is between these boundaries. The proposed selectable values for ψ_T for $\psi = 0.0$ (e.g. wind), $\psi = 0.5$ (e.g. furniture), and $\psi = 1.0$ (e.g. self weight) are presented in Table 6.2. The values approximately correspond with $T = 0.25$ yr, $T = 0.5$ yr, and $T = 1.0$ yr. However, as the above hesitations apply (extent correlation and validity over small time frames) these values are, to an extent, *arbitrarily* chosen and do not necessarily coincide with the time periods/combinations that are deemed relevant as discussed in the previous Section.

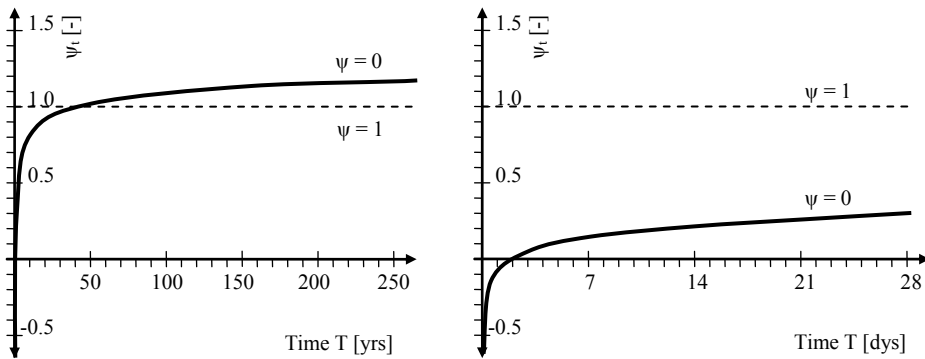


Figure 6.19a, b Development of ψ_T over T for $\psi = 0.0$ and $\psi = 1.0$ (straight line); for a long time scale (0 – 250 years, left) and a shorter one (0 – 4 weeks, right)

Table 6.2 Selectable values for ψ_t to determine redundancy requirements.

	$\psi = 0.0$	$\psi = 0.5$	$\psi = 1.0$	Corresponding T
ψ_T	0.3	0.6	1.0	0.25 yr
	0.4	0.7	1.0	0.50 yr
	0.6	0.8	1.0	1.00 yr

Ad b. As generally structural analysis use the semi-probabilistic method, this means the load safety factor γ can be adjusted accordingly. In the NEN 6702, values for γ are given for three building safety classes. It is proposed to use these values of γ also for the demarcation of residual strength requirements.

A note should be added with regard to special actions A_{rep} . They may very well be governing in the case of glass constructions, but current codes usually do not provide an indication on their duration. These have to be determined. Specifically for the case of a

person haven fallen (e.g. on a glass roof or floor), it is suggested to maintain a time period of 30 minutes.⁵⁸

The use of codified ul-state loading combinations can cover all common applications of glass in construction. However, in some cases structural elements should not collapse even when they have reached initial failure and the ultimate limit state action is simultaneously applied (e.g. structural elements of which collapse would have severe consequences).⁵⁹ In those cases, the residual strength should exceed the ultimate limit state action. The size of that margin can be subject of debate. It is suggested that the material partial factor for glass⁶⁰ provides sufficient room to provide that margin.⁶¹

So, finally, the redundancy requirements should generally be formulated as a residual strength requirement for each model damage level, in the following format:

At model damage level n , the residual resistance should be equal to or higher than the governing ultimate limit state loading combination,

- with a time correction factor of $\psi_T = x$ (chosen from Table 6.2), and
- load safety factors γ corresponding with structure safety class y (1, 2, 3, as e.g. in Table 6.3),
- while considering a maximum duration $T_{D,n}$, to be determined from a combination of relevant time periods given in Table 6.1).

Table 6.3 Selectable values of γ and corresponding structure safety classes, taken from NEN 6702.

Combination	Structure safety class	$\gamma_{f;gu}$ (unfavourable)	$\gamma_{f;qu}$
Fundamental, as Eq. (6.15a)	1	1.2	1.2
	2	1.2	1.3
	3	1.2	1.5
Fundamental, as Eq. (6.15b)	1, 2, 3	1.35	-
Exceptional, as Eq. (6.15c)	1, 2, 3	1.0	1.0

Several suggested fully developed redundancy requirements for different applications are given in Appendix D, which also present an elaborated quantitative example of a glass beam supporting a glass roof. Table 6.4 lists the redundancy requirements from that example. It gives the time correction factor, safety class, and the maximum time period for each model level of damage. With these values and the actual project action data, the required resistances can be calculated, shown in an ESD in Figure 6.20. Several curves result with their own time-labels, corresponding with different loading

⁵⁸ As do the guidelines of the State of Hessen, Germany, discussed in Chapter 4, Section 5.1.

⁵⁹ Steel and reinforced concrete provide an extra hidden reserve to prevent failure and collapse from coinciding, provided by the fact that the tensile strength of steel is significantly higher than the yield strength. See previous discussion in Chapter 3, Section 6.

⁶⁰ Actually, a separate partial factor should be determined for each LTM. However, the glass material partial factor seems sufficient in case those data are lacking.

⁶¹ Note that the glass which at failure is not yet broken, is probably stronger because those are the places the governing defects apparently were *not*.

types: maintenance, snow, and permanent loads (wind was never governing in this example).

Table 6.4 Redundancy req. for an example beam presented extensively in Appendix D (based on Table G.10)

		Element Consequence Class							
		Medium							
Redundancy m	Level I: $R_{res,I}/S_{uls} \geq 1.0$			Level II: $R_{res,II}/S_{uls} \geq 1.0$			Level III: $R_{res,III}/S_{uls} \geq 1.0$		
	with:	Ψ_{T^*}	$T^* = 1.00$	with:	Ψ_{T^*}	$T^* = 0.50$	with:	Ψ_{T^*}	$T^* = 0.25$
		γ_{sc^*}	$sc^* = 3$		γ_{sc^*}	$sc^* = 2$		γ_{sc^*}	$sc^* = 1$
	for T	$\geq a+d$ $\approx d$	$= 90$ days	for T	$\geq a + c$	$= 96$ hrs	for T	$\geq a+b$ $\approx a$	$= 24$ hrs

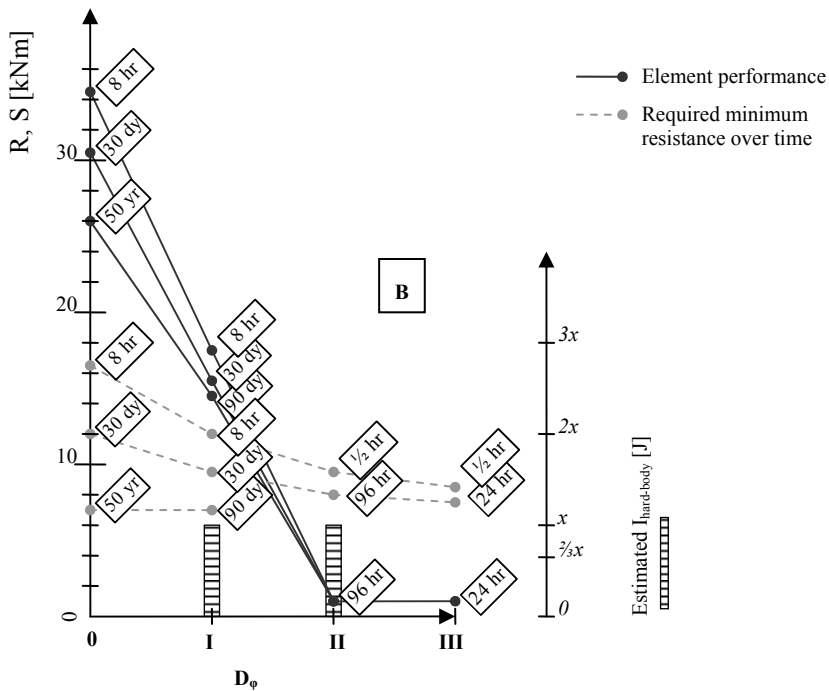


Fig. 6.20 ESD of the initial glass beam design, with the safety requirements and element performance. The dotted line marks the resistance of the 2nd LTM. This design fails to meet the redundancy requirements of Levels II and III (reprint of Fig. G.5).

5.3.3. Redundancy through Alternative Load Paths

The redundancy requirements are performance requirements. Thus, the demanded residual strength levels do not necessarily have to be provided by the element itself. When used in a construction, the actions may be carried through alternative load paths in case of damage or failure, as long as the required resistance (do not forget element

self weight) is somehow provided. Off course, the surrounding elements have to be calculated for this extra load, which may be considered a special action.

5.4. Fracture Mode at Failure

For structural application, the required fracture mode with regard to safety, is actually subordinate to the redundancy requirements. Modes A and C will only occur in single sheet elements without further reinforcement. These will not fulfil the redundancy requirements anyway, thus structural glass elements will always have to have fracture mode B. Modes A and C may be relevant for some glass in construction applications, but even then, for most applications, mode B is required (e.g. by the NEN 3569⁶²).

6. Element Categories

Off course, practically all glass in construction is applied as façade filling. Only a very small part is used for the main load bearing structure, but many intermediate uses exist. Although the integrated approach was primarily developed for structural glass applications, it could be applied for all glass in building construction. By formulating requirements in a consistent form, resemblances and differences become clear.

Principally, plastic failure behaviour with residual strength in the order of the original resistance should be pursued in any application which poses danger to humans in case of collapse, since failure can never be ruled out completely. However, in many cases this would be difficult to achieve and lead to requirements that are not in reasonable relation to the risk that is associated with them. Nevertheless, it should be the starting point. Because of the many ways in which glass is used in buildings, it is sensible to develop a classification with which it is possible to deviate from this principal starting point to greater or lesser extent, depending on the gravity of the consequences that may be associated with collapse of the element.

Such a classification should be based on the two sides of the cause-consequence diagram (Figure 6.1): the vulnerability of the element (determines the likelihood of damage and failure) and the severity (extent of injuries) of eventual collapse. This basic starting point holds, whether considering 'glass in construction' or 'structural glass'.

The vulnerability of an element may depend on:

- The quality of manufacturing and construction (the likelihood that an element is actually manufactured and used in the way it was designed),⁶³
- The degree of exposure.

The former is generally application independent, while the latter is highly dependent on the specific project. Exposure is determined by parameters such as inside/outside, possibility of collision, contact with degrading materials, contact with hard materials, possibility of vandalism, private or publicly accessibility, etc.

⁶² Nederlands Normalisatie Instituut, *NEN 3569: Safety glazing in buildings*, Delft, the Netherlands, 2001, p. 5.

⁶³ It should be noted that especially the manufacturing quality of heat treated glass should not be taken for granted. The author as well as other researchers at the TU Delft have occasionally been confronted with glass that turned out to be annealed when thermally tempered had been specified. The interview with Tim Macfarlane (Chapter 5, Section 3 and Appendix C, Section 4) testifies that these were not unique occurrences.

The severity of collapse depends on:

- The size of the area influenced by collapse,⁶⁴
- The degree of occupation of that area (including the frequency distribution),
- The indirect injury potential (fall-through, fall-on: e.g. overhead glazing, balustrades, etc.),
- The direct injury potential by shards in collision (i.e. the potential of colliding with the glass element).

Obviously, many different application classes could be formulated with the use of these parameters. Furthermore, such a classification could be expanded with sub-classes when the aspect of time (duration) for certain measures as introduced in Section 5.3.1. is incorporated.⁶⁵

In earlier publications⁶⁶, the author has introduced the concept of *Member Consequence Class* (MCC), derived from the concept of Consequence Class which applies to (complete) structures, as introduced in the NEN-EN 1991-7.⁶⁷ The MCC gives an indication of the consequences of collapse of that member. In those publications, a total of 6 MCCs was proposed, based on a classification according to accessibility of the building and function of the element in the structure. However, although that system provided insight in the way in which redundancy requirements can be differentiated, there was only a limited scientific foundation for the class definitions and the accompanying redundancy requirements – it was largely based on the judgement of the author.

To provide such a scientific foundation, much more extensive research is required, especially with regard to the relevant demarcations between element classes. This, unfortunately, could not be incorporated in this study. Nonetheless, the presented system of formulating requirements and the ESD could already be used in practice. Engineers and governing bodies could insert their own requirements based on the available research, their experience and priorities. This will at least make requirements insightful, comparable, and open to discussion.

Alternatively to stating a fully scientifically founded set of requirements, Appendix D presents some suggested requirements for different elements in different building types.

⁶⁴ In the case of fall-through barriers (e.g. balustrades), it is probably more appropriate to consider the area in terms of m length than m² surface area.

⁶⁵ Just the NEN 3569 already distinguishes 7 application classes. That code only relates to fall-through barriers and overhead glazing. It would have to be expanded with at least glass floors and structural glass applications.

⁶⁶ Bos, F.P., *Towards a Combined Probabilistic/Consequence-based safety approach of structural glass members*, HERON, Vol. 52, Is. 1/2, 2007, and Bos, F.P., Veer, F.A., *Consequence-based Safety Requirements for Structural Glass Members*, Proceedings of the Glass Performance Days, Tampere, Finland, June 2007.

⁶⁷ Nederlands Normalisatie Instituut, *NEN-EN 1991-1-7, Eurocode 1, Actions on Structures, Part 1-7: General actions – Accidental actions*, Delft, the Netherlands, 2006.

7. Required Further Research for Finalizing the Integrated Approach

The Integrated Approach to structural glass safety combines all relevant safety requirements in one diagram: the Element Safety Diagram (ESD). Thus, the demands can be assessed comprehensively. They have been quantified as much as possible, or at least the factors have been identified that should be used for quantification. This method of presenting makes a reasonably objective comparison between designs possible. Furthermore, it allows adjustment of requirements (e.g. due to advancing knowledge or varying assessment of the acceptability of certain risks) in an easy and insightful way, so that they can be subjected to discussion.

Many issues have been encountered that are in need of further research. Besides the general subjects relating to structural glass engineering,⁶⁸ the development of the Integrated Approach requires additional study of the issues listed below, grouped by relevancy.

To determine founded requirements for each element safety property:

- Development of application classes and safety requirements for each application class, as argued in the previous Section.
- Failure causes in reality. Much more extensively than in Chapter 5, the glass failure causes in practice will have to be inventorized and studied, so that some conclusions can be drawn towards governing impacts (type and magnitude), especially for structural elements like beams and columns (with regard to balustrades, floors, and roofs, a considerable amount of requirements have already been formulated).
- Actions and action histories, and the correlation between damage and actions. These data are required to determine correct residual strength requirements (to determine realistic values of γ , ψ , and ψ_t).

For the design of safe glass elements:

- The relation between physical and structural damage. Research on the resistance of damaged glass elements has only just started. It would be useful to know more about the consequences of certain impacts for the load carrying capacity of glass elements, to estimate the residual strength of elements with certain extents of physical damage.
- The relation between design parameters (e.g. glass thicknesses, heat treatment, laminates, aspect ratio) and damage sensitivity, so that a designer can actively work towards elements with lower damage sensitivity.
- Extensive comparative research on different designs for common glass elements to determine their ESDs. This should lead to an project-independent set of data that allows more conscious choices in element design. Chapter 7 and Appendix E provide a starting point by examining a large set of glass beams of various designs.
- The influence of connection designs on failure behaviour. Again, extensive comparative testing would provide valuable information for informed design decisions.

For evaluation of the Integrated Approach as a method, and its development:

⁶⁸ Such as the influence of thermal treatment of failure strength and fracture, sub-critical crack growth, the microscale fracture process, and so on; see Chapter 4.

- Practicality. Application of the Integrated Approach in practice should point out whether this method is suitable, e.g. whether it does decrease confusion, if it is not to elaborate, if it provides satisfying results, etc. Chapter 7 and Appendix E provide an analysis of glass beam failure behaviour based on the ESD and will give first conclusions of the suitability. However, experiences from practice will have to be collected and evaluated.
- Expansion of the Integrated Approach for complete structures.
- Expansion of the integrated approach to include manufacturing and construction processes, rather than just design.

Other relevant subjects:

- Injury potential of various types and sizes of collapsing glass elements and shards. An important unknown remains how significant the injury potential of thermally tempered glass compares to that of annealed and heat strengthened glass.

The subsequent Chapter explores the Integrated Approach by analyzing a considerable amount of experimental data of the failure of various glass beam designs. Conclusions towards the safety of different designs will be drawn and the suitability of the Integrated Approach will be evaluated.

7 The Integrated Approach Applied to the Safety Assessment of Glass Beams

This Chapter explores the Element Safety Diagram (ESD) as a tool to assess and compare the safety of structural elements. The ESDs of 14 glass beam designs have been constructed, based on experimental data extensively discussed in Appendices E and I. They are initially presented in absolute terms. Subsequently, relative ESDs are derived to allow for a comparison of the designs. Finally, the applicability of the ESD is evaluated. It is concluded that by using the ESD, quick insight is gained in the failure behaviour and safety of a glass element in comparison to requirements or in comparison to other designs. Although it would require extensive experimental research, it allows for the construction of a standard database of the failure behaviour and safety of glass element designs.

1. Constructing Element Safety Diagrams (ESDs) from Experimental Data

In the previous Chapter, the Integrated Approach to Structural Glass Safety was developed theoretically. Four element properties were identified which, together, determine its safety: damage sensitivity, relative resistance, redundancy, and fracture mode. The Element Safety Diagram was introduced, which combined these four properties into one diagram, thus providing a quick and relatively complete overview of all relevant safety properties and thereby the overall safety of the element. In this chapter, an attempt is made to construct actual ESDs of 14 glass beam designs from experimental data, compare them, and evaluate the ESD as a tool.

The beam designs differ by the most common design parameters: double- or triple-layer; annealed, heat strengthened, or thermally tempered; PVB or SG laminated. Additionally, the ESDs of two design concepts that have been developed within the Zappi Glass & Transparency framework, were determined: stainless steel reinforced glass beams bonded with Delo GB368 UV-curing adhesive and similarly reinforced beams laminated with SG.

The ESDs presented in this Chapter are based on the experiments described and discussed extensively in Appendices E and I.¹ Figure 7.1 shows the absolute ESD for a triple layer beam design. The different components of the Diagram are explained. Tables 7.1a and b indicate how the resistance, damage sensitivity and fracture mode figures were obtained for double and triple layer beams, respectively.

The ESDs presented in the subsequent section should be considered to be preliminary, basically because too few experimental results were available. To construct complete and statistically accurate diagrams, at least 10 specimens should be tested on each model damage level (3 or 4 – for double layer specimens, model damage level II = III),

¹ The reader is strongly recommended to study these Appendices before proceeding with this Chapter. They explain the experiments, provide the beam designs, and contain the experimental results on which the ESDs are based. The experimental results themselves will not be discussed further in this Chapter.

at three to four different relevant test durations and two to three relevant temperature levels – thus approximately $10 \times 4 \times 3 \times 2 = 240$ specimens.

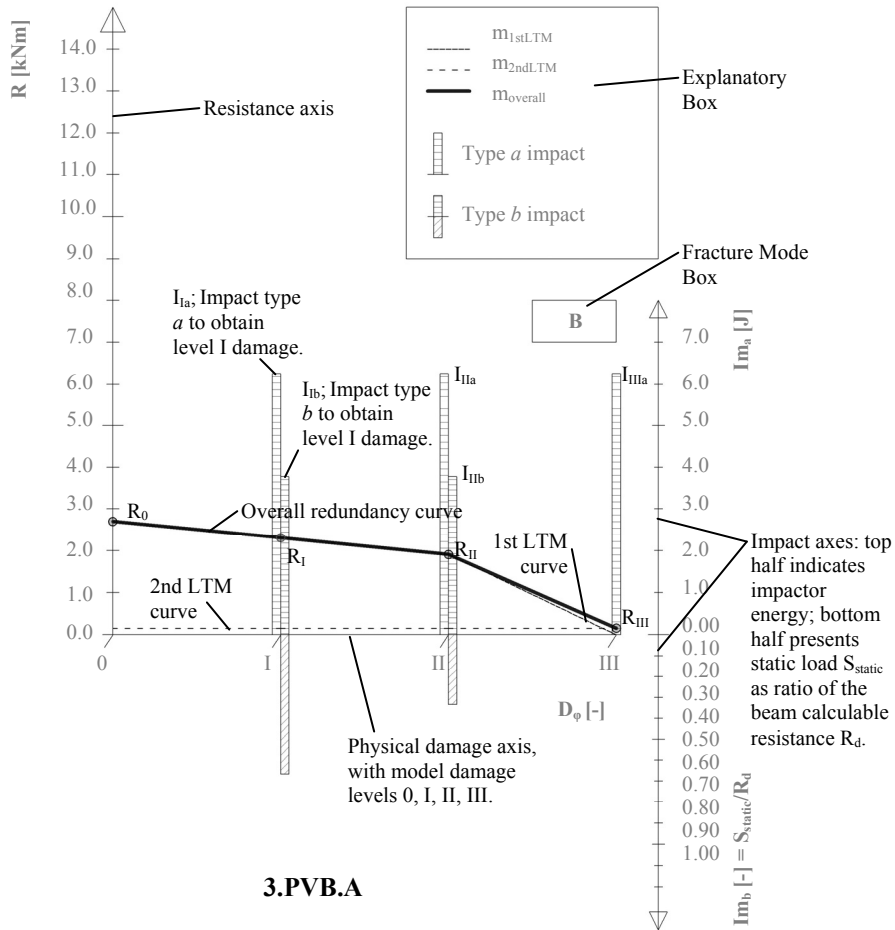


Fig. 7.1 Example ESD of triple layer ('3'), PVB laminated ('PVB'), annealed ('A') glass beam.

Through reasoning, this number may be significantly reduced,² but still extensive testing is required to obtain complete ESDs. Neither such numbers of specimens nor the time needed for testing were available.³ As a result, the time dependency of resistance was omitted in the presented diagrams. Furthermore, all figures are based on

² The initial resistance of the undamaged beams may be determined from existing research on glass strength, as well as the development of its resistance over time. Furthermore, it has been shown in Appendix E that for damaged (but not yet failed) elements, the assumption to apply only the resistance of the undamaged glass part in the calculation is valid (and with annealed glass slightly conservative). Thus, extensive testing on level I and/or II (if $II \neq III$) may neither be required. Therefore, only level III requires extensive testing over various time ranges and temperature levels.

³ For the purpose of this research it was deemed more relevant to determine preliminary diagrams for a large number of beam designs, then to construct one diagram with high statistical accuracy.

experiments executed at room temperature.⁴ However, notwithstanding the fact that more data would provide statistically more accurate resistance figures, the ESDs here presented certainly show the rough trend of the relation between structural and physical damage as well as the key differences between the failure behaviour of the various beam types presented.

The required magnitudes for two types of impact are presented to obtain the model damage levels I, and, for the triple layer specimens, II. For the top model damage level (II or III, depending on the design), only one impact type is presented. Type *a* Impact (left vertical bars) is a spring loaded, concentrated hard body impact on a glass sheet edge with the impact device described in Appendix E. Alternatively, the same physical damage can be obtained by a combination of a static load and a spring loaded impact, indicated as Type *b* Impact. Clearly, much less impact energy is required when a static load is present to obtain similar physical damage.

The Type *b* Impact was based on the assumption made in practice that a broken layer in a laminate beam can just be ignored in the resistance calculation of the damaged element. The applied static load was thus equal to the assumed calculable resistance of the remaining layers (those not affected by the impact). Thus the static load was a percentage < 100 % of the calculable resistance of the undamaged beam (e.g. 50 % in case of double layer specimens, and 67 % and 33 % in case of triple layer beams – as appears in Figure 7.1). Obviously, this impact method could not be applied to the highest damage level, as it would be unclear what static load should be present. In fact, the PVB laminated beams would have collapsed immediately with any significant static load present, as their post-failure strength was very low.

For resistance, average values of the test data, typically based on 1 – 3 specimens, were used.

It is important to note that the failure behaviour of glass beams is geometry dependent, as it is partially determined by the elastic strain energy content at failure. Thus, the ESDs presented in this Chapter are valid only for the investigated geometry. Although they may present an indication of the failure behaviour of differently sized beams, they may not be assumed to be generally valid for any geometry. The relation between failure behaviour and elastic strain energy is further discussed in Chapter 9 and also to various extent in Appendices E, F, G, H, and I.

The next section of this chapter discusses the absolute ESDs. Subsequently, the relative redundancy curves have been constructed in Section 3 to allow a comparison of the various designs.

⁴ The relevant temperature to consider in case of damage and failure is a difficult issue. The inner temperature of structural glass elements may be well above room temperature as they are often immediately behind glass roofs or façades. For elements that rely on the behaviour of polymers in their damaged or failed state, this may have important consequences for their resistance. On the other hand, at least in large parts of Europe, governing actions on structures (high wind loads, snow, etc.) are accompanied by bad weather (cold and/or overcast skies), reducing the likelihood of a high action coinciding with a high temperature. For wind loads in Germany, this has been proven by extensive statistical research in: Wellershoff, F., Nutzung der Verglasung zur Aussteifung von Gebäudehüllen, Ph.D. thesis, RWTH Aachen / Shaker Verlag, Germany, 2006.

Table 7.1a Origin of resistances and impact magnitudes of double layer glass beams in the Element Safety Diagrams of Section 2.

Resistance, Impact	Obtained from
R_0	Average initial failure load of directly tested specimens.
R_I	Average initial failure load of specimens tested after damage by static and impact load to level I ('static+impact' series).
R_{II}	Average maximum post-initial failure load of specimens tested after damage by impact load to level II = III ('predamaged' series).
R_{III}	= R_{II}
Im_{Ia}	Required impact energy on specimens without static load ('predamaged' series).
Im_{IIa}	= Im_{Ia}
Im_{IIIa}	= Im_{IIa}
Im_{Ib}	Required impact energy on specimens with static load ('static+impact' series).
Frac. Mode	Determined after initial failure of specimens predamaged to level II = III ('predamaged' series).

Table 7.1b Origin of resistances and impact magnitudes of triple layer glass beams in the Element Safety Diagrams of Section 2.

Resistance, Impact	Obtained from
R_0	Average initial failure load of directly tested specimens.
R_I	Linearly interpolated between R_0 and R_I .
R_{II}	Average initial failure load of specimens tested after damage by static and impact load to level II ('static+impact' series).
R_{III}	Average maximum post-initial failure load of specimens tested after damage by impact load to level III ('predamaged' series).
Im_{Ia}	Required impact energy on specimens without static load ('predamaged' series).
Im_{IIa}	= Im_{Ia}
Im_{IIIa}	= Im_{IIa}
Im_{Ib}	Required impact energy on specimens with static load ('static+impact' series).
Im_{IIb}	= Im_{Ib}
Frac. Mode	Determined after initial failure of specimens predamaged to level III ('predamaged' series).

2. Absolute ESDs for 14 Glass Beam Designs

The ESDs for each beam design are presented graphically in Figures 7.2 – 7.15. They have been based on the numerical data presented in Tables 7.2a, listing the impact values, and 7.2b, containing the average resistances as well as the number of specimens on which they were based. In some cases, there were insufficient experimental results to complete the ESD even without consideration of time dependency. The missing figures were then determined from argumentation and/or interpolation. Where applicable, the reasoning behind non-experimentally determined values is presented. Both tables appear at the end of this Section.

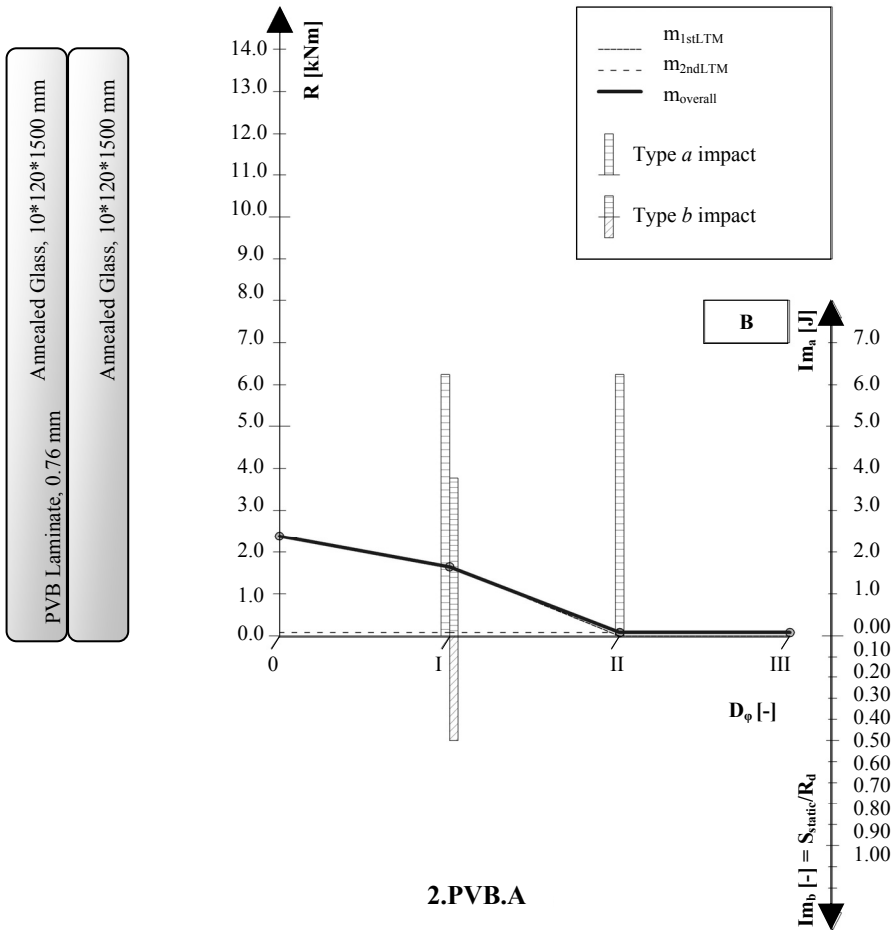


Fig 7.2a Element Safety Diagram for double layer, PVB laminated, annealed glass beams.



Fig 7.2b Typical model level I damage in 2.PVB.A specimen.

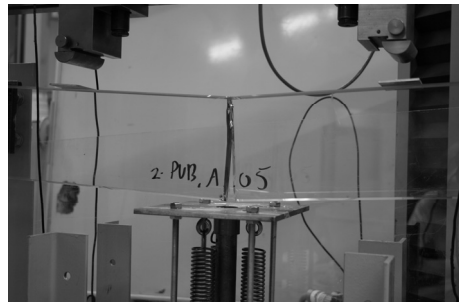


Fig 7.2c Typical final failure in 2.PVB.A specimen (after resistance test on specimen with model level II (=III) damage).

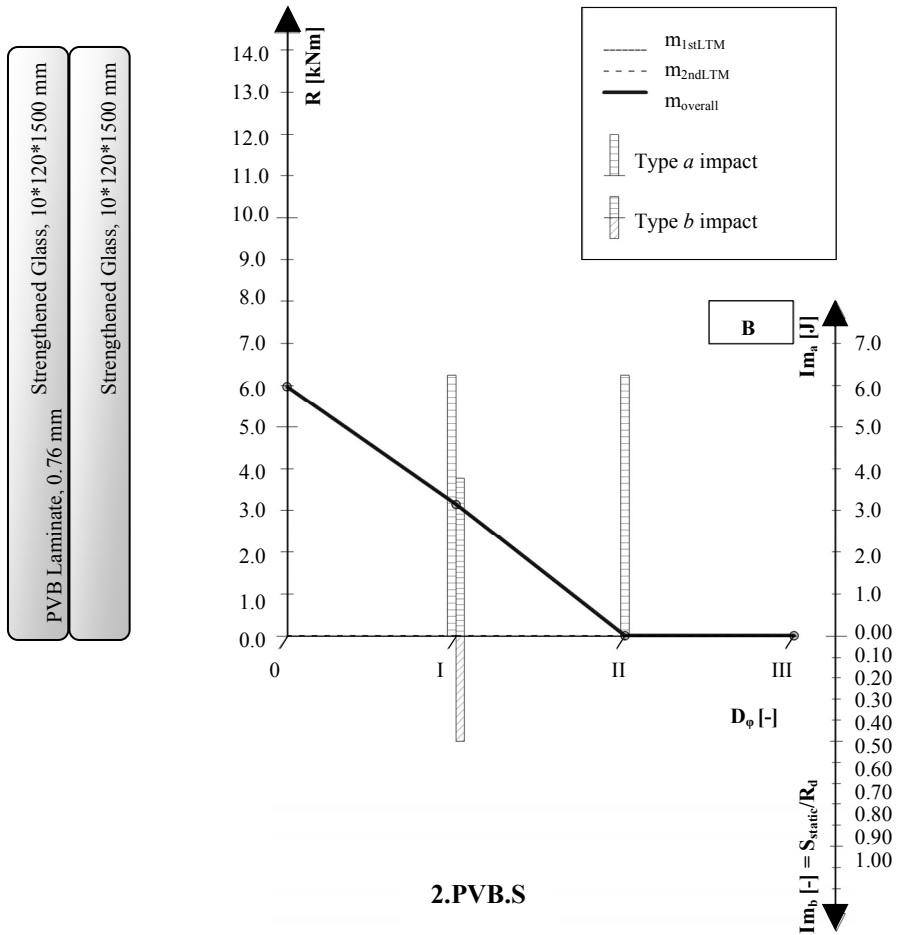


Fig 7.3a Element Safety Diagram for double layer, PVB laminated, heat strengthened glass beams.

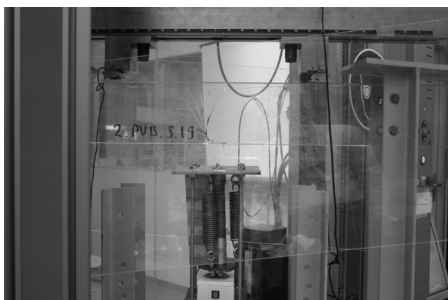


Fig 7.3b Typical model level I damage in 2.PVB.S specimen.

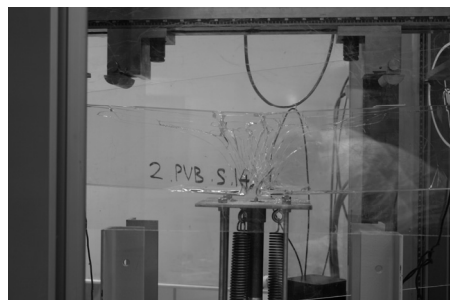


Fig 7.3c Typical final failure in 2.PVB.S specimen (after resistance test on specimen with model level II (=III) damage).

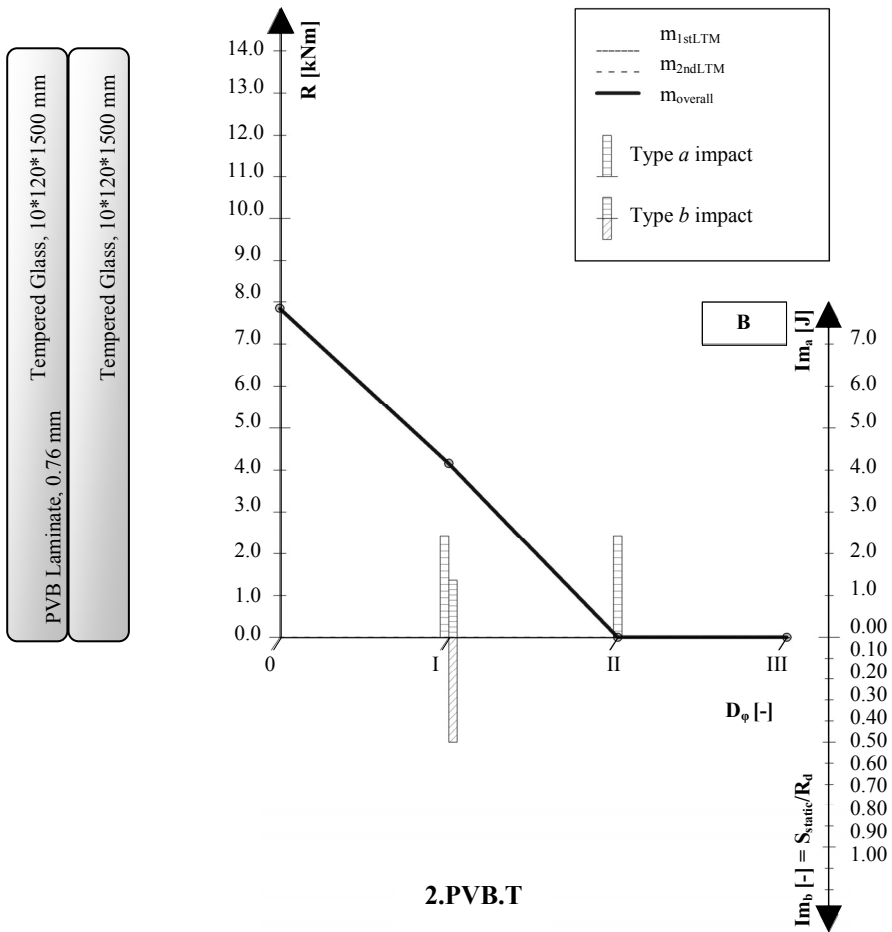


Fig 7.4a Element Safety Diagram for double layer, PVB laminated, thermally tempered glass beams.



Fig 7.4b Typical model level I damage in 2.PVB.T specimen.



Fig 7.4c Typical final failure in 2.PVB.T specimen (after resistance test on specimen with model level II (=III) damage).

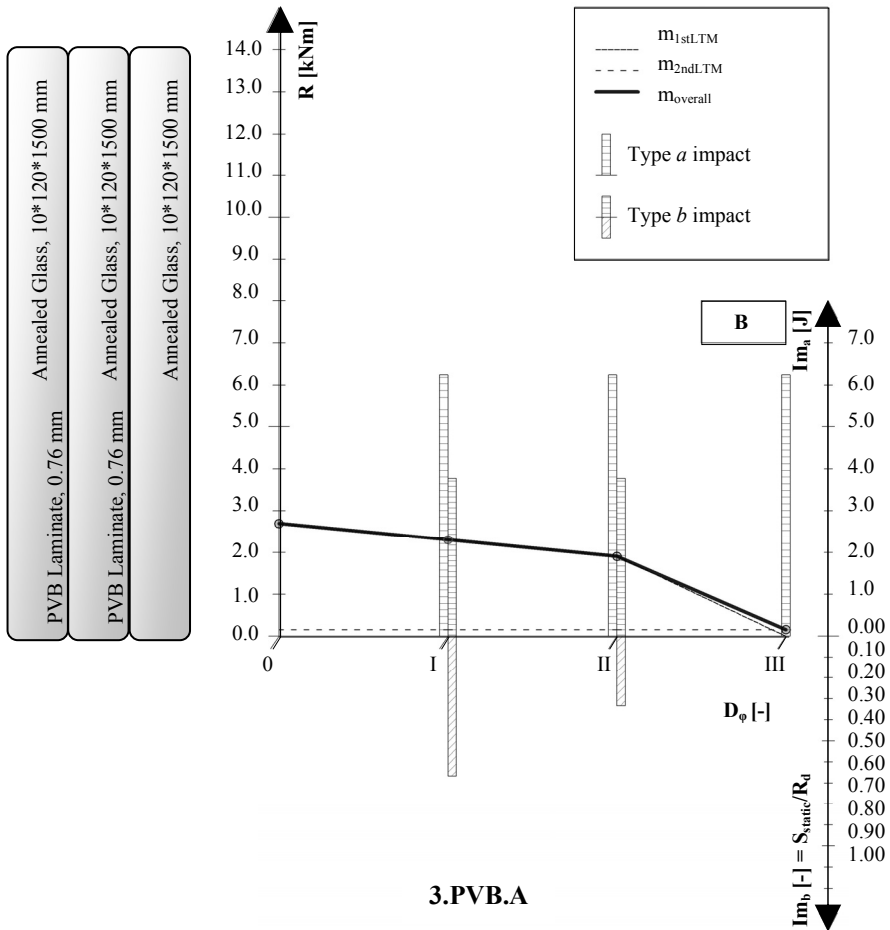


Fig 7.5a Element Safety Diagram for triple layer, PVB laminated, annealed glass beams.

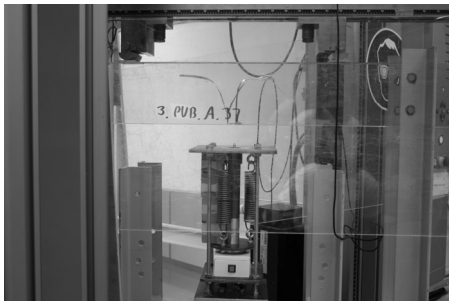


Fig 7.5b Typical model level II damage in 3.PVB.A specimen.

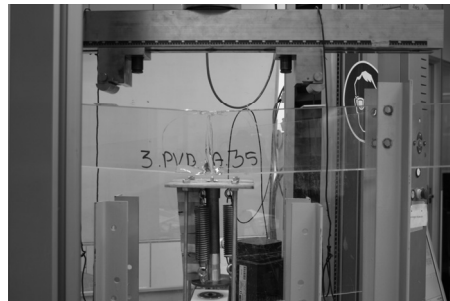


Fig 7.5c Typical final failure in 3.PVB.A specimen (after resistance test on specimen with model level III damage).

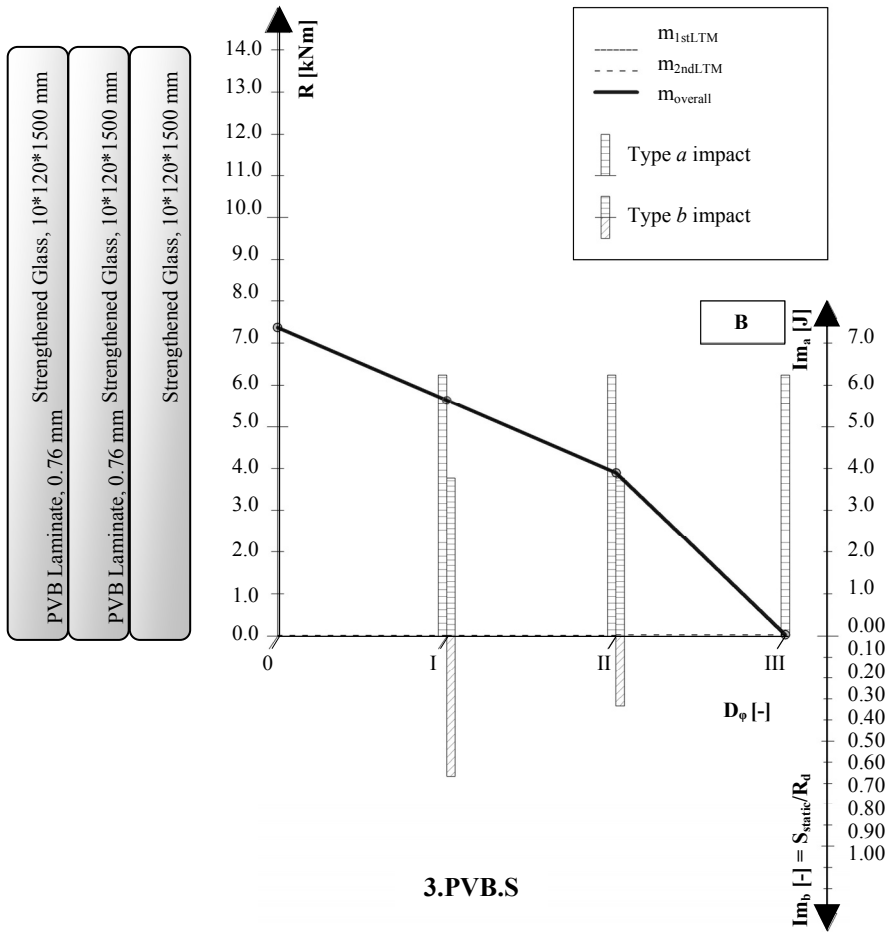


Fig 7.6a Element Safety Diagram for triple layer, PVB laminated, heat strengthened glass beams.

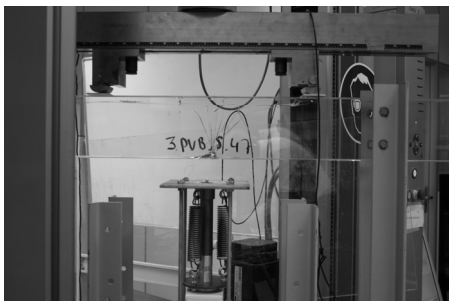


Fig 7.6b Typical model level II damage in 3.PVB.S specimen.

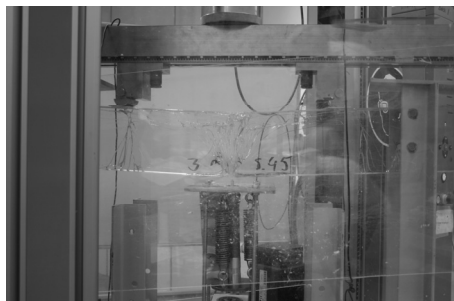


Fig 7.6c Typical final failure in 3.PVB.S specimen (after resistance test on specimen with model level III damage).

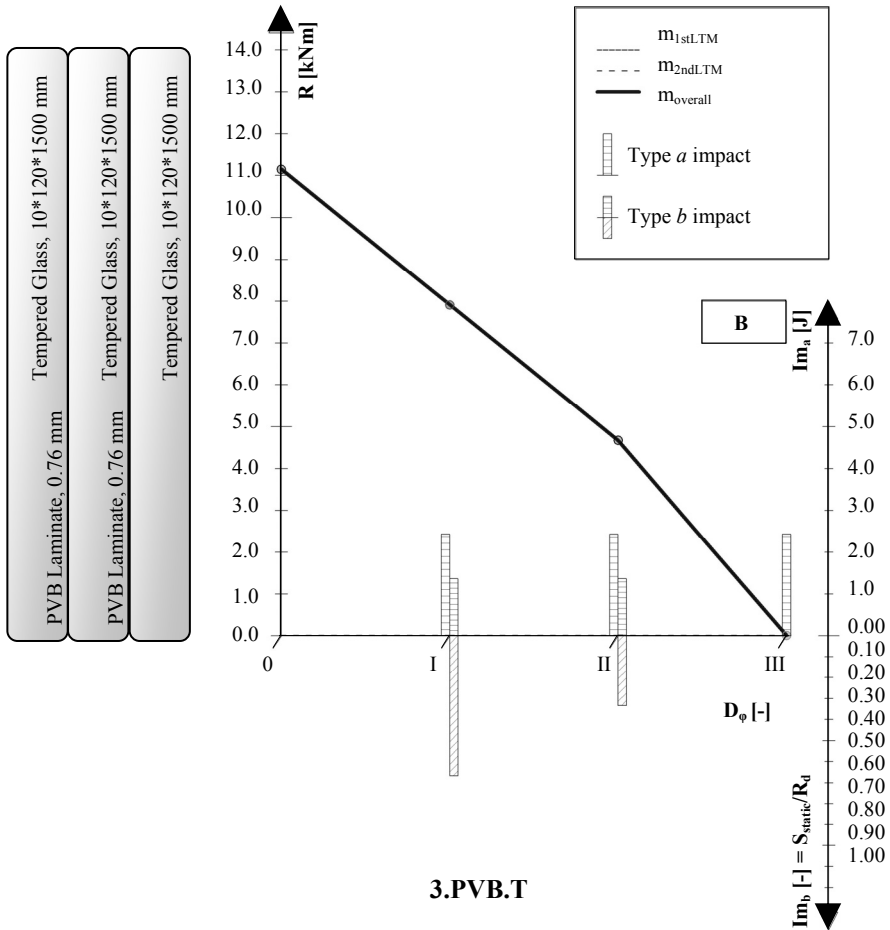


Fig 7.7a Element Safety Diagram for triple layer, PVB laminated, thermally tempered glass beams.

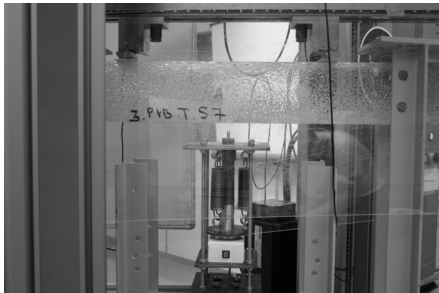


Fig 7.7b Typical model level II damage in 3.PVB.T specimen.

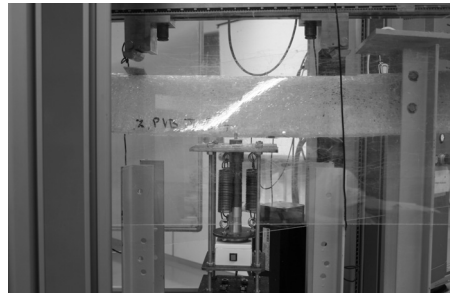
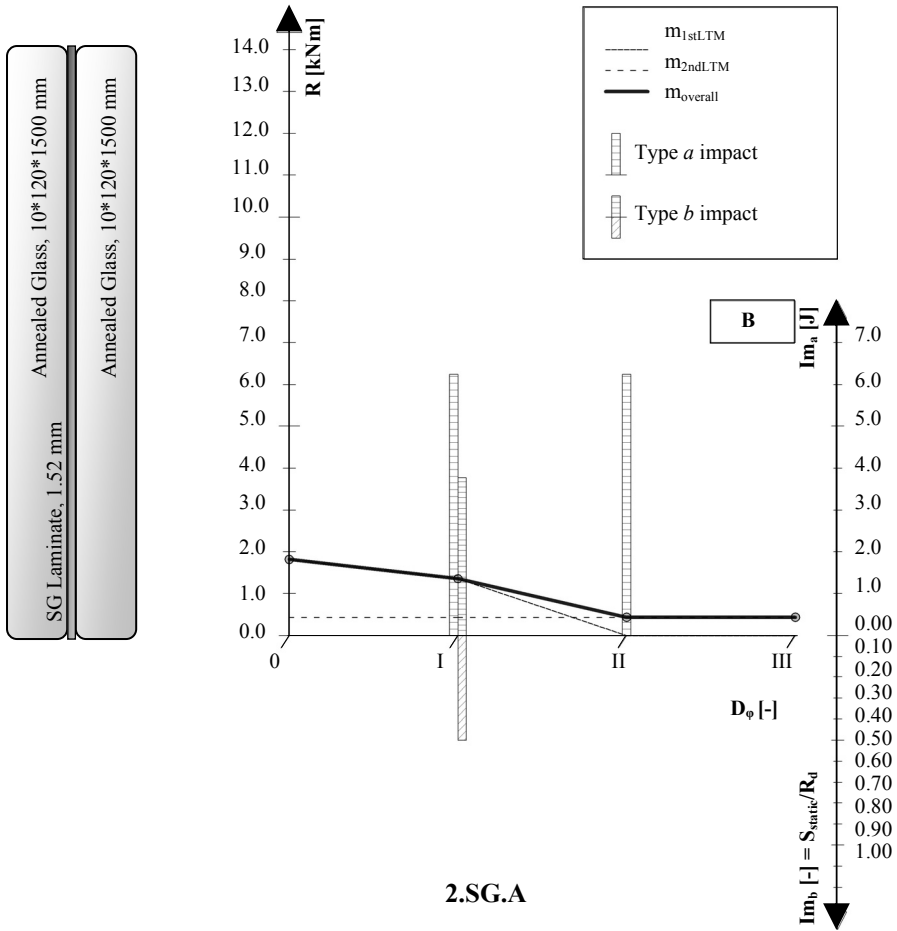


Fig 7.7c Typical final failure in 3.PVB.T specimen (after resistance test on specimen with model level III damage).



2.SG.A

Fig 7.8a Element Safety Diagram for double layer, SG laminated, annealed glass beams.



Fig 7.8b Typical model level I damage in 2.SG.A specimen.

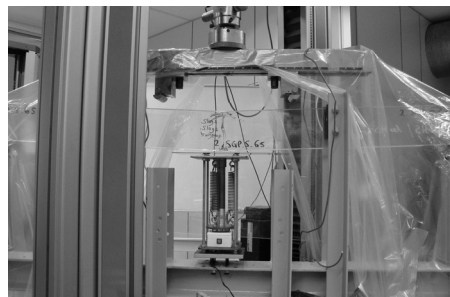
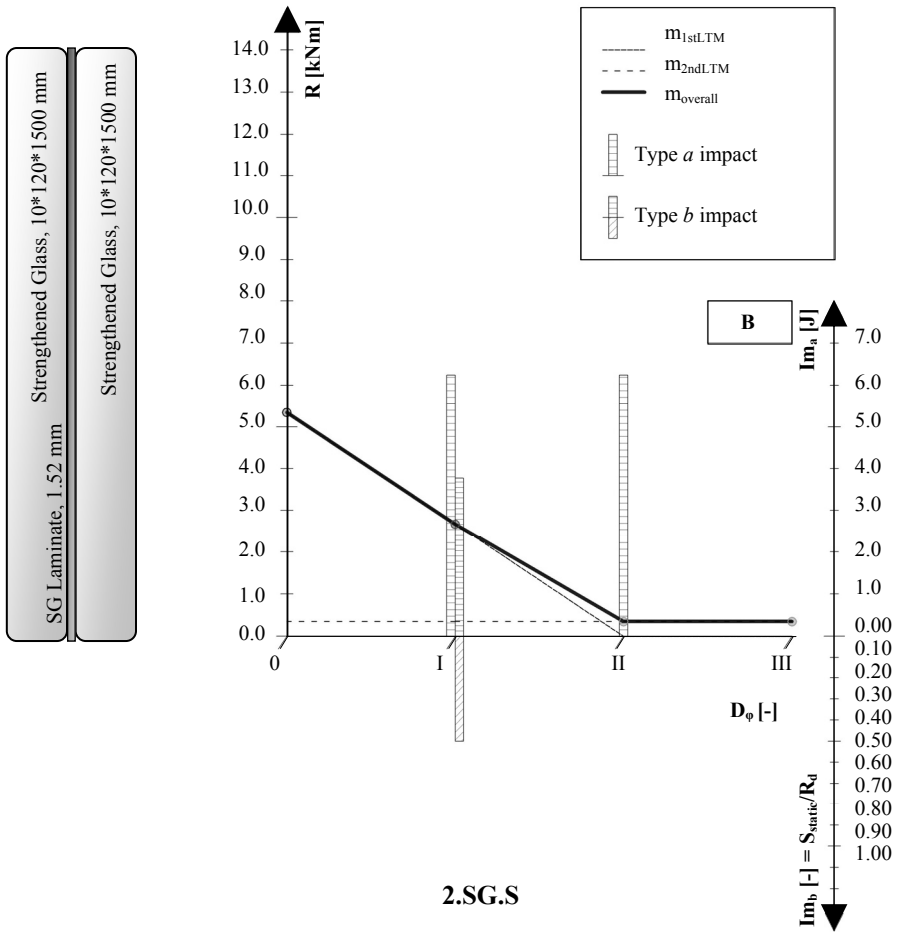


Fig 7.8c Typical final failure in 2.SG.A specimen (after resistance test on specimen with model level II (=III) damage).



2.SG.S

Fig 7.9a Element Safety Diagram for double layer, SG laminated, heat strengthened glass beams.

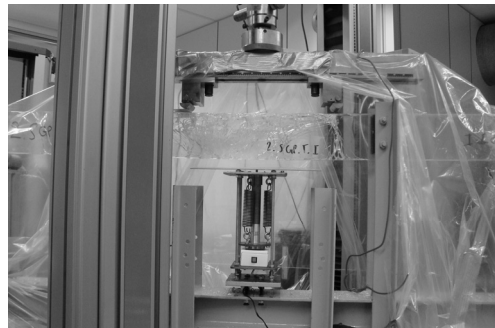
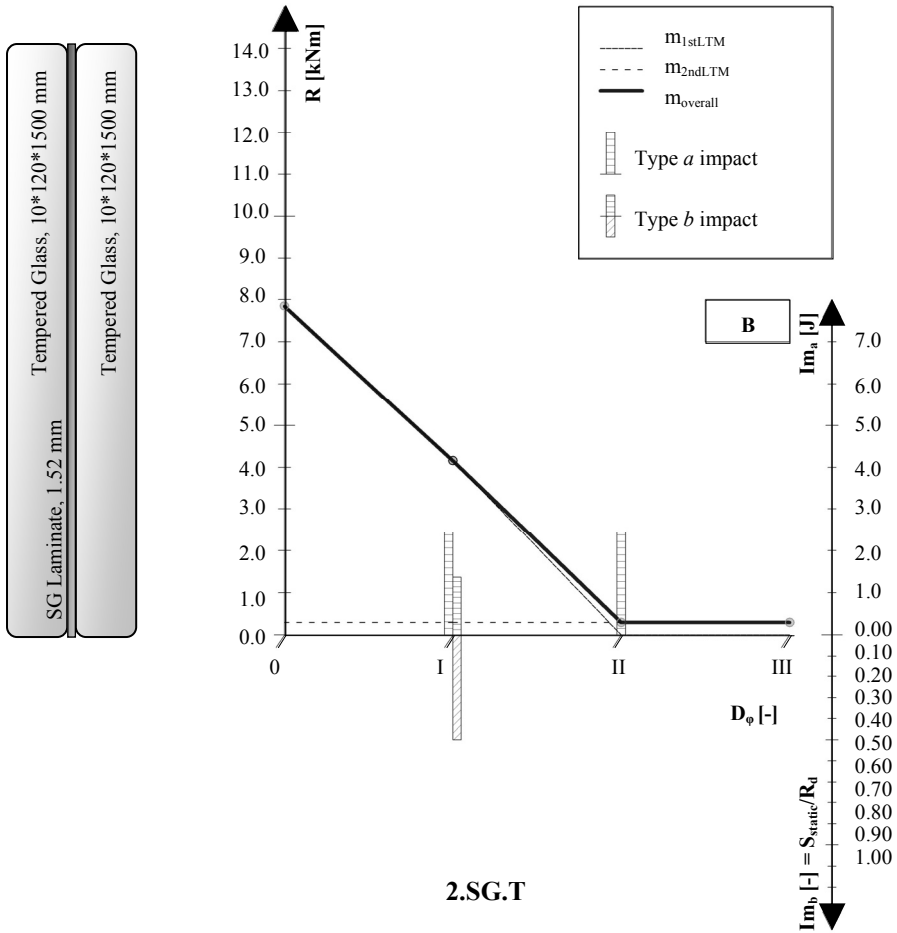


Fig 7.9b Initial failure in 2.SG.S specimen after direct overloading. The intense crack pattern suggests this element (from another badge than the PVB-laminated specimens and the annealed SG-specimens) came close to tempered glass.



2.SG.T

Fig 7.10a Element Safety Diagram for double layer, SG laminated, thermally tempered glass beams.



Fig 7.10b Typical final failure in 2.SG.T specimen (after resistance test on specimen with model level II (=III) damage).

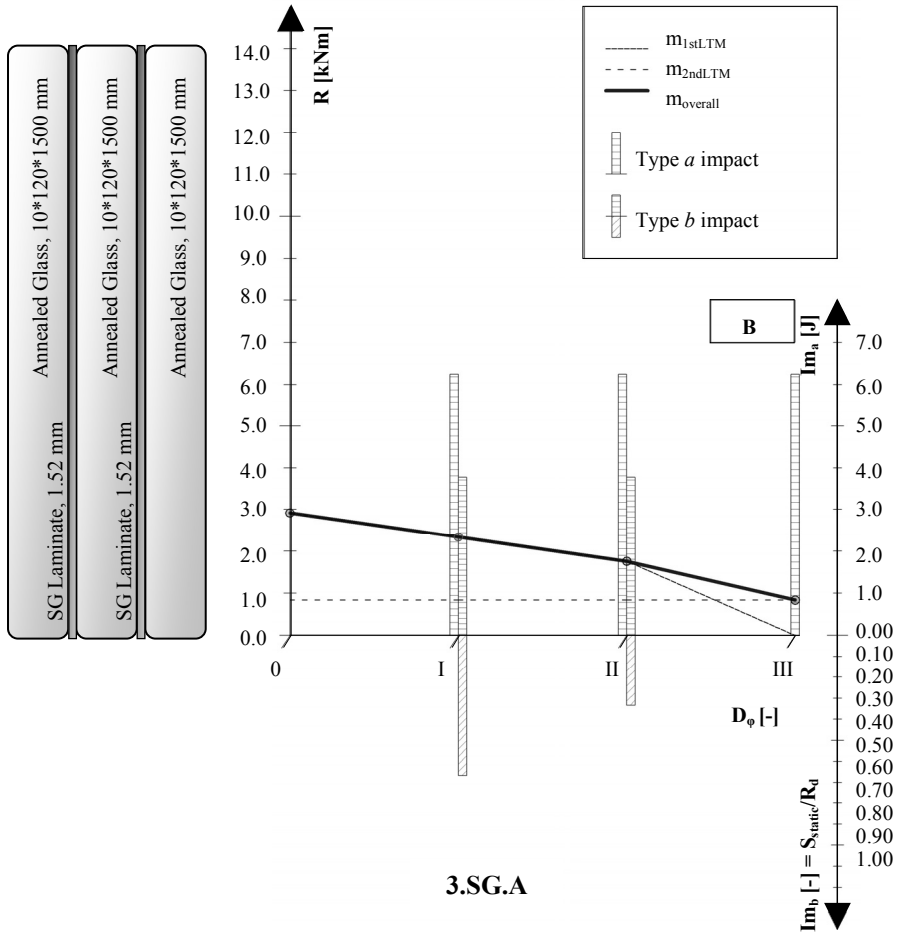


Fig 7.11a Element Safety Diagram for triple layer, SG laminated, annealed glass beams.



Fig 7.11b Typical model level II damage in 3.SG.A specimen.

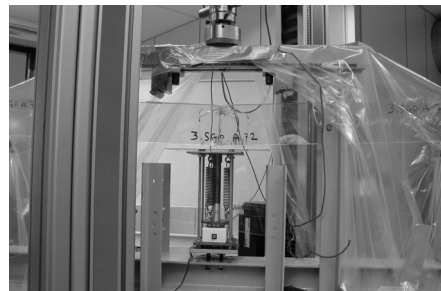


Fig 7.11c Typical final failure in 3.SG.A specimen (after resistance test on specimen with model level III damage).

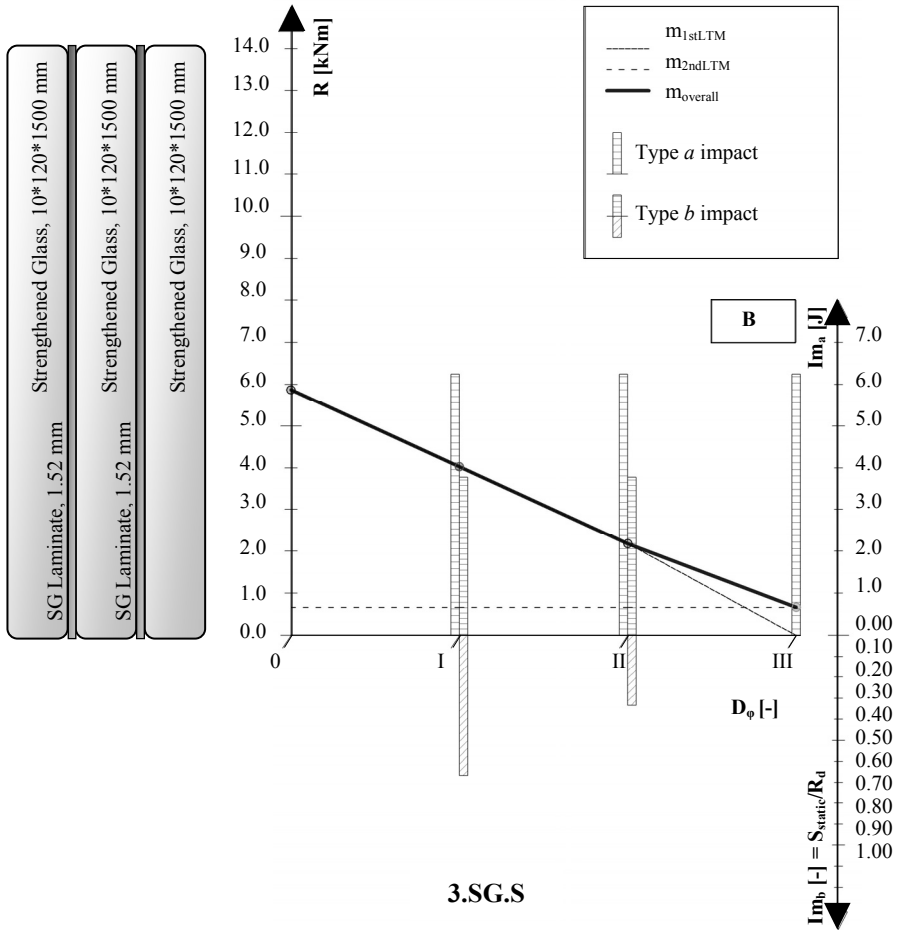


Fig 7.12a Element Safety Diagram for triple layer, SG laminated, heat strengthened glass beams.

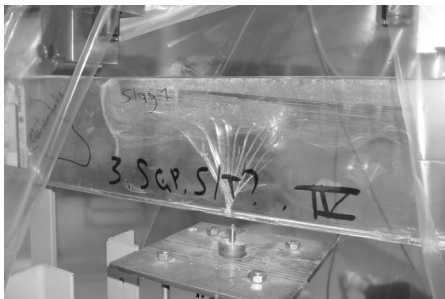


Fig 7.12b Typical model level II damage in 3.SG.S specimen.

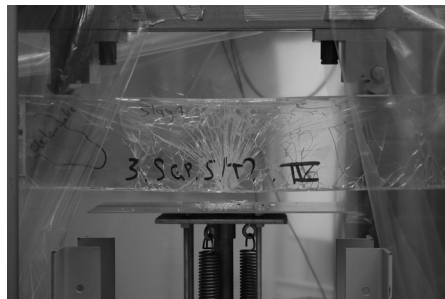


Fig 7.12c Final failure in 3.SG.S specimen, after resistance test on specimen with model level II damage.

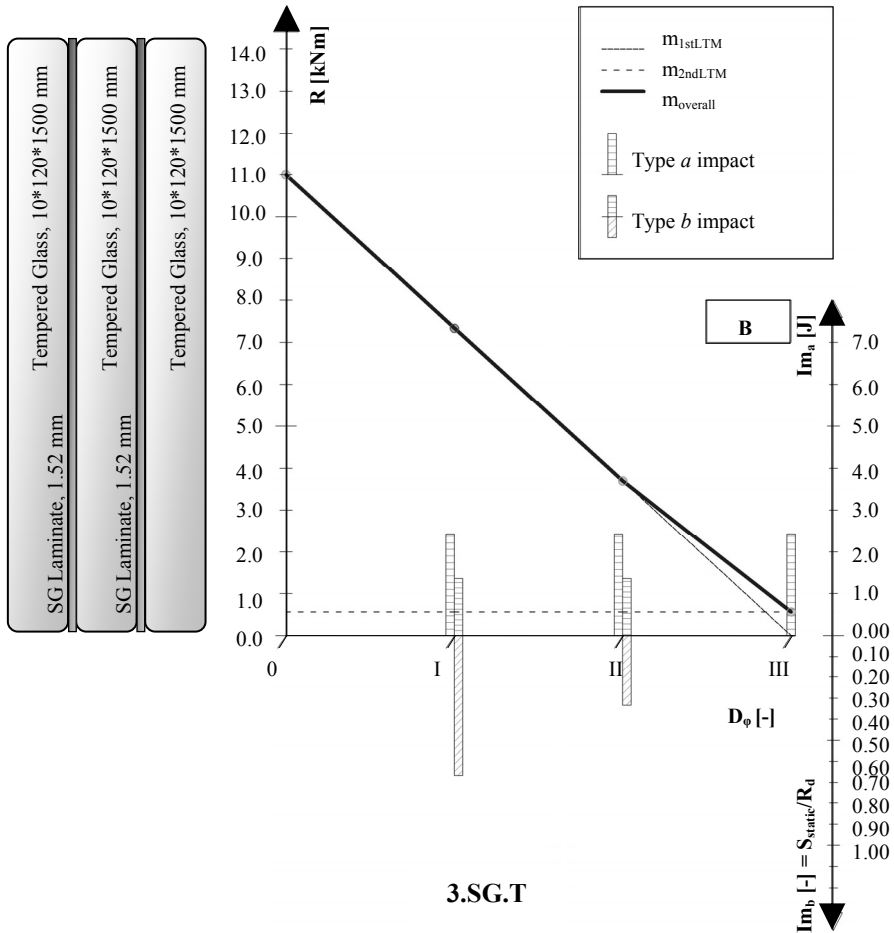


Fig 7.13a Element Safety Diagram for triple layer, SG laminated, thermally tempered glass beams.

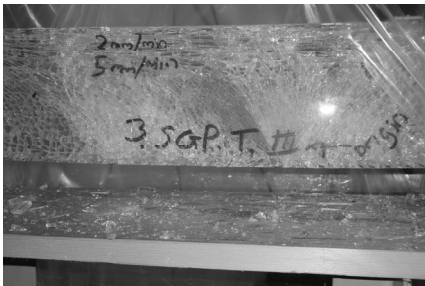
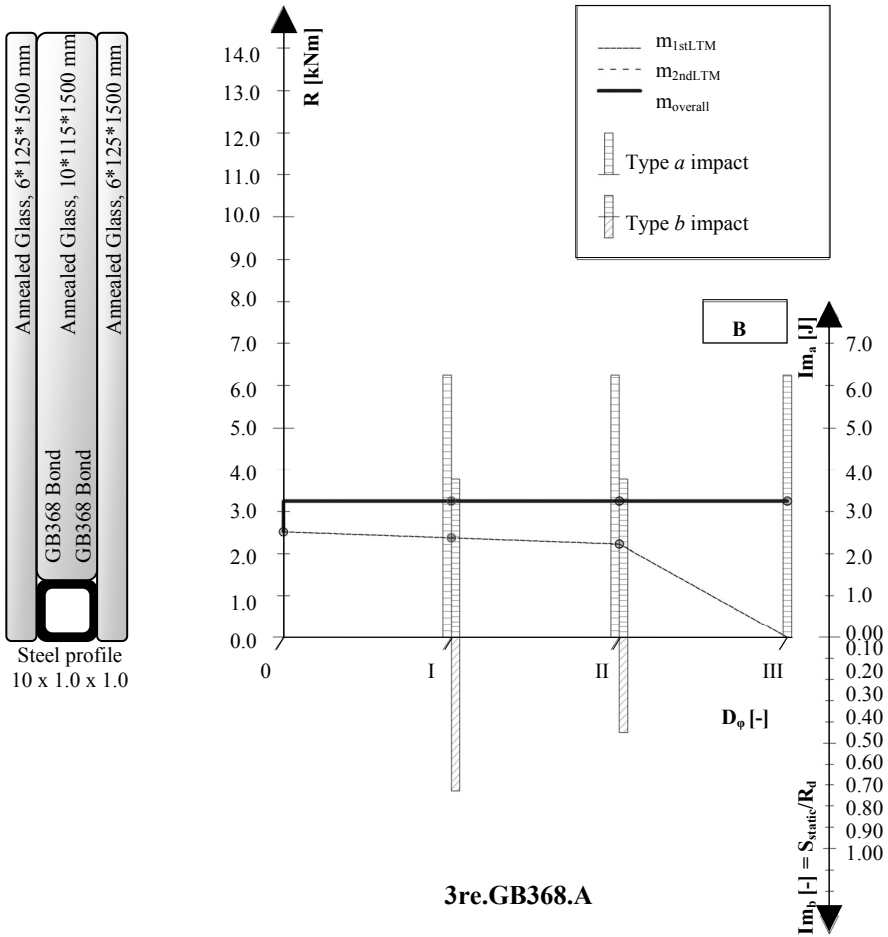


Fig 7.13b Fracture pattern and crack origin in 3.SG.T specimen after final failure through direct overloading.



Fig 7.13c Final failure in 3.SG.T specimen, after direct overloading.



3re.GB368.A

Fig 7.14a Element Safety Diagram for triple layer, reinforced, GB368 bonded, annealed glass beams.

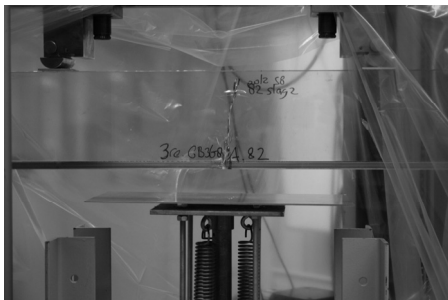


Fig 7.14b Typical model level II damage in 3re.GB368.A specimen.

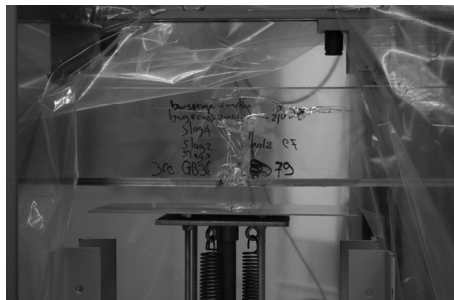


Fig 7.14c Typical final failure in 3re.GB368.A specimen (after resistance test on specimen with model level III damage).

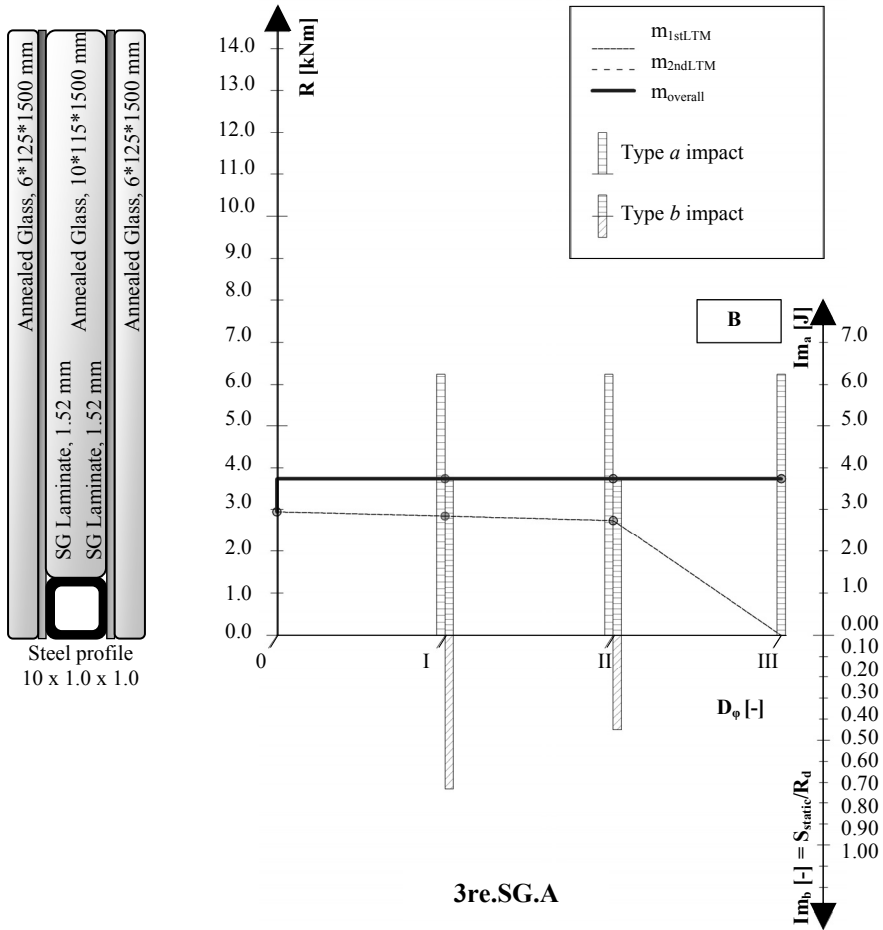


Fig 7.15a Element Safety Diagram for triple layer, reinforced, SG laminated, annealed glass beams.

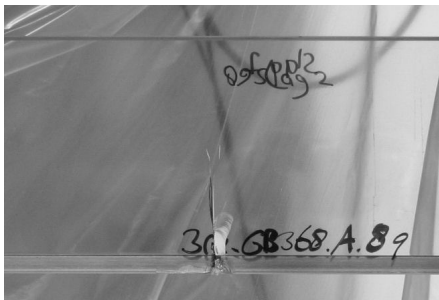


Fig 7.15b Typical model level II damage in 3re.SG.A specimen.



Fig 7.15c Typical final failure in 3re.SG.A specimen (after resistance test on specimen with model level III damage).

Table 7.2a Impact data for the Element Safety Diagrams. Type a Impact is a spring loaded, concentrated hard body impact on a glass sheet edge with the impactor described in Appendix E. Alternatively, the same physical damage can be obtained by a combination of a static load and a spring loaded impact, indicated as Type b Impact.

Beam Type	Im _{I,a} [J]	Im _{II,a} [J]	Im _{III,a} [J]	Im _{I,b}		Im _{II,b}	
				[J]	% R _d	[J]	% R _d
2.PVB.A	6.24	= Im _{I,a}	-	3.77	50	-	-
2.PVB.S	6.24	= Im _{I,a}	-	3.77	50	-	-
2.PVB.T	2.44	= Im _{I,a}	-	1.37	50	-	-
3.PVB.A	6.50	= Im _{I,a}	= Im _{II,a}	3.77	67	= Im _{I,b}	33
3.PVB.S	6.50	= Im _{I,a}	= Im _{II,a}	3.77	67	= Im _{I,b}	33
3.PVB.T	2.44	= Im _{I,a}	= Im _{II,a}	1.37	67	= Im _{I,b}	33
2.SG.A	6.24	= Im _{I,a}	-	3.77	50	-	-
2.SG.S	6.24	= Im _{I,a}	-	3.77	50	-	-
2.SG.T	2.44	= Im _{I,a}	-	1.37	50	-	-
3.SG.A	6.50	= Im _{I,a}	= Im _{II,a}	3.77	67	= Im _{I,b}	33
3.SG.S	6.50	= Im _{I,a}	= Im _{II,a}	3.77	67	= Im _{I,b}	33
3.SG.T	2.44	= Im _{I,a}	= Im _{II,a}	1.37	67	= Im _{I,b}	33
3re.GB368.A	6.24	= Im _{I,a}	= Im _{II,a}	3.77	73	= Im _{I,b}	45
3re.SG.A	6.24	= Im _{I,a}	= Im _{II,a}	3.77	73	= Im _{I,b}	45

Table 7.2b Resistance data for the Element Safety Diagrams. The number between brackets indicate the number of experimental results on which the average is based. Interpolated values have been determined by the preceding and following resistance values (e.g. an interpolated R_I is determined by linear interpolation between R_0 and R_{II}). They are indicated with a [#]. Values that have been determined by argumentation are indicated with asterisks. The reasoning is given at the bottom of the Table.

Beam Type	R_0 [kNm]	R_I [kNm]	R_{II} [kNm]	R_{III} [kNm]
2.PVB.A	2.39 (3)	1.65 (3)	0.086 (3)	= R_{II}
2.PVB.S	5.97 (3)	3.15 (3)	0.022 (3)	= R_{II}
2.PVB.T	7.85 (3)	4.16 (3)	0.010 (3)	= R_{II}
3.PVB.A	2.70 (3)	2.31 [#]	1.91 (3)	0.16
3.PVB.S	7.37 (2)	5.64 [#]	3.90 (1)	0.041
3.PVB.T	11.14 (3)	7.91 [#]	4.67 (3)	0.015* ⁵
2.SG.A	1.82 (3)	1.36 (3)	0.44 (2)	= R_{II}
2.SG.S	5.34 (1)	2.67 [#]	0.35* ²	= R_{II}
2.SG.T	7.50*	3.84 (1)	0.30* ³	= R_{II}
3.SG.A	2.92 (3)	2.34 [#]	1.76 (1)	0.84 (2)
3.SG.S	5.87 (1)	4.03 [#]	2.18	0.67* ⁶
3.SG.T	11.00*	7.33 [#]	3.70* ⁴	0.57* ⁷
3re.GB368.A	2.52 (6)	2.38 [#]	2.23 (3)	3.74 (2)
3re.SG.A	2.95 (5)	2.85 [#]	2.74 (2)	3.25 (3)

* From the experiments on annealed and heat strengthened specimens, it is clear the initial resistance R_0 is independent of laminate type, and therefore taken to be approximately equal to the 2.PVB.T and 3.PVB.T beams, respectively.

*² The ratio of R_{III} of 2.SG.A and 2.SG.S beams was considered to be equal to the ratio of R_{III} of 3.SG.A and 3.SG.S beams.

*³ The R_{III} value was determined from ‘static+impact’ tests, rather than from ‘predamaged’ tests (App. E).

*⁴ Assumed to be $\frac{1}{3}$ of R_0 . Based on the results of the PVB laminated beams, this seems a reasonable assumption.

*⁵ R_{III} of these beams was below self weight. The value could therefore not be determined, but was estimated at $\frac{2}{3}$ of the beam self weight.

*⁶ The R_{III} value was determined from ‘static+impact’ tests, rather than from ‘predamaged’ tests (App. E).

*⁷ The ratio of R_{III} of 3.SG.A and 3.SG.T beams was considered to be equal to the ratio of R_{III} of 2.SG.A and 2.SG.T beams.

2.1. Impact and Damage Sensitivity

The damage sensitivity of laminated glass beams is independent of laminate type for the impact types applied in the experiments on which these ESDs are based (compare Figure 7.2 to 7.8, or 7.5 to 7.11).⁵ There is no significant difference in fracture pattern between PVB- and SG-laminated beams.⁶ This is due to the very short duration of the impact which nullifies the time-dependency of the laminate stiffness. Unrecorded preliminary tests did show that the damage sensitivity of unlaminated, single sheet glass is much higher. The presence of a laminate restrains the glass and thereby slows down crack growth.⁷

On the other hand, damage sensitivity does depend on the thermal treatment of a glass sheet. Much less impact is required to shatter a thermally tempered glass sheet than an annealed or heat strengthened one (compare, e.g., Figure 7.4 to 7.3 and 7.2). This applies for both impact types applied, with and without the presence of a static load. The impact only needs to penetrate the compressive layer in the glass where after the sheet will disintegrate itself by release of internal strain energy. This confirms the observation sometimes made in practice,⁸ that tempered glass is actually more vulnerable to accidental damage than other glass types. Remarkably, the self-destructive mechanism does not occur with heat strengthened glass. As a result, heat strengthened glass and annealed glass have similar damage sensitivity.^{9, 10}

The presence of a static load significantly increases the physical damage an object impact induces (visible in all Figures ‘a’ of 7.2 – 7.15). The impact energy to obtain a certain level of damage is reduced by approximately 40 % when a static load equal to the calculable strength of the remaining layers is present.¹¹

Although the ESDs present similar impact values for the reinforced glass beams, they are in fact less damage sensitive, as their middle layers could actually not be damaged from the underside as the others were, because of the presence of the reinforcement. In the experiment, they were turned over and hit from the top. However, in practice this side will often be covered by glazing or profiles. Therefore, it will be very difficult to

⁵ In the remainder of this Section and Chapter, ‘damage sensitivity’ should be read as ‘damage sensitivity for the impact types applied in the experiments on which these ESDs are based’, unless noted otherwise.

⁶ Thus improvement of damage sensitivity of glass elements may not be expected from improvements of a laminate material (although that may improve redundancy). Rather, the only alterations to the glass itself or its surface may improve damage sensitivity.

⁷ More extensively discussed in Appendix E, Section 4.2.

⁸ Chapter 5, Section 3.2.

⁹ At least for the – very well made – heat strengthened glass applied in this experiment. The (lack of) quality control in practice may be an obstacle to assume general applicability of this conclusion to any piece of heat strengthened glass, which may be over- or understressed. Furthermore, it should be expected the fracture pattern is dependent on the strain energy release. In that case, the damage sensitivity of heat strengthened glass may also depend on the element size.

¹⁰ Further research should be carried out in order to explain why thermally tempered glass disintegrates when the compressive layer is penetrated, while heat strengthened glass does not. Apparently, some internal resistance is overcome at some degree of internal prestress, resulting in this behaviour and its distinctively different (from annealed and heat strengthened glass) cracking pattern.

¹¹ Note that in the ESDs, the static load component of impact type b is presented relatively, as a percentage of calculable strength of the beam. Thus, the static load applied on the heat strengthened and thermally tempered beams was significantly higher than on the annealed glass beams. However, since the actual external load is likely to be adjusted to the calculable strength, this is a reasonable approach.

actually damage the inner layer. The SG-laminated and GB368 bonded reinforced specimens behaved similarly, thus indicating no difference in damage sensitivity.

2.2. Resistances, Post-failure Strength, and Redundancy Curves

2.2.1. Resistances

The R_0 of the double layer, PVB laminated, heat strengthened and thermally tempered specimens was very high compared to previous experimental research and values listed in glass engineering codes (the given resistances correspond with $\sigma_{0,2,PVB,S} = 124.4$ MPa and $\sigma_{0,2,PVB,T} = 163.5$ MPa; Table 7.2b and Figures 7.3 and 7.4). Although some more detailed observations were made, the other initial resistances were generally in line with expected values and do not require further discussion here.¹² No resistance results below the representative strength values in the glass engineering codes were encountered in the experiment on which the ESDs have been based.¹³

2.2.2. Post-Failure Strength

The post-failure strength of the PVB laminated beams is small in all cases (Figures 7.2 – 7.7) Nevertheless, the annealed, heat strengthened, and thermally tempered beams present crucial differences. For all thermally tempered beams, the post-failure strength was less than their self weight.¹⁴ Heat strengthened beams could, on average, carry 1.5 times their self weight after failure, but, importantly, one of the three specimens on which this average was based had a post-failure strength lower than its self weight. Thus, it may be concluded that failed heat strengthened and thermally tempered PVB-laminated glass beams can carry practically no external loads.

Only with annealed glass, at least some surplus resistance remains (Figures 7.2 and 7.5). The post-failure strength of triple layer specimens is approximately twice that of double layer specimens, proportional with the increase of PVB layers in the section. Since the increase in glass is less than the increase in PVB (1.5 times versus 2 times), relatively more post-failure strength is available for carrying external loads. The average post-failure strength of double layer beams is approximately 5.7 times their self weight, while it is 7.3 times for triple layer ones. However, it is questionable whether this post-failure strength is relevant in practical applications. For small spans (e.g. the 1.4 m as applied in the experiment) and a relatively light roof covering, it may be just enough to carry the permanent external loads.¹⁵

However, with increasing spans, centre distances with other beams, or heavier roofing (e.g. insulated glass units), the permanent loads will soon exceed the post-failure strength. Failure will then be followed by collapse, even though the post-failure strength of annealed glass PVB-laminated beams is significantly higher than that of heat strengthened and thermally tempered ones.

¹² Appendix E, Section 3.1.

¹³ Although that has been observed occasionally in other experiments.

¹⁴ At least, within the deformation possibilities of the test set-up. It may be possible that with greater room for deformation, the beams would tilt and go (more or less) horizontal, into a state of membrane action. The strength of that state will probably be negligible.

¹⁵ If the post-failure strength would be just beneath the external permanent loads, specifying additional PVB-layers in the laminate may be a practical solution, as they are linearly proportional.

Contrary to PVB laminated beams, glass beams laminated with SG all possess 2nd LTMs with significant capacity (Figures 7.8 – 7.13). The post-failure strength is proportional to the amount of SG in the section, but also larger than could be expected based on the difference in thickness and tensile strength with PVB. The bending tensile stiffness of the laminate material plays a crucial role, as it determines the LTM that can develop after failure. A stiff laminate allows transfer of compressive stresses through the broken glass, while a weak one does not.¹⁶ This makes it possible to obtain considerable post-failure strength even when all glass layers in a beam are broken.

The differences in post-failure strength of annealed, heat strengthened, and thermally tempered, SG laminated beams, could not be extensively investigated because of a lack of specimens. It seems, however, something comparable to the PVB laminated specimens occurs: annealed glass specimens have the highest post-failure strength, thermally tempered ones the lowest. This should be attributed to the variety in crack pattern density, which probably influences the ability to transfer compressive stresses through the broken glass.

Unlike the more common laminated beam designs, the beams with steel reinforcement (Figures 7.14 and 7.15) have a post-failure strength that exceeds the initial resistance R_0 . This can be attributed to the 2nd LTM: composite action between the (broken) glass in compression and the steel in tension. The vastly superior stiffness and strength of stainless steel compared to polymer laminate materials accounts for the considerable difference in failure behaviour.

With the applied material proportions and (section) geometry, the post-failure strength is determined by the steel yield strength. It is likely even higher post-failure strengths can be obtained by applying more steel in a section. However, it should be questioned what the practical application of an element with an even greater difference between R_0 and R_{III} , would be.

Remarkably, the SG laminated reinforced specimens perform even better than the GB368 bonded ones. It is suggested that this is due to a difference in fracture pattern. Cracks in the SG laminated beams do not go through the thickness, as they do in GB368 bonded beams. This allows for a kind of shear-tension action in the overlapping pieces of broken glass which results in a higher tensile capacity of the failed beam. The 2nd LTM of the two reinforced beam designs is thus not completely equal.¹⁷

Finally, it should be noted that the post-failure strength highly depends on the elastic strain energy release upon failure, and thus on the applied test method. In the series of tests on which this Chapter is based, this was particularly apparent with the heat strengthened, PVB laminated beams. Plain overloading to failure led to complete breakage at failure, while loading after a predamage had been applied allowed at least some (though little) post-failure strength. The post-failure strength in annealed glass beams is less when overloading from the undamaged state, than when they had been

¹⁶ See Appendix E, Section 4.3.2, for a more extensive discussion on LTMs that develop in laminated glass beams after failure.

¹⁷ This has been extensively discussed in Appendix I, especially Section 4.

predamaged. The importance of elastic strain energy for the development of 2nd LTMs is extensively discussed in Chapter 9.

2.2.3. Redundancy Curves

Of all the annealed glass beams (both double and triple layer, both PVB and SG laminated; Figures 7.2, 7.5, 7.8, 7.11), the resistance at the intermediate damage levels¹⁸ is higher than would be expected based on linear interpolation between the initial resistance and 0 (by definition the 1st LTM resistance of the top damage level). This is shown by the change in slope in the redundancy curves. It should be attributed to compression transfer in the broken layer, which changes the effective section of the beam from rectangular into T-shaped.¹⁹ Thus, ignoring the broken layers in a resistance calculation of a damaged annealed glass beam seems safe and slightly conservative.

In triple layer, heat strengthened and thermally tempered, PVB laminated beams (Figures 7.6, 7.7), this happens as well, albeit not as obviously as in the annealed glass beams.

This effect does *not* occur with the double layer heat strengthened and thermally tempered, PVB laminated glass beams (Figures 7.3, 7.4). The intermediate resistance values in those beams is practically equal to the resistance of the undamaged part of the section. Ignoring the broken layers in a resistance calculation of a damaged strengthened or tempered glass beam still seems safe, but not as conservative as for the annealed glass beams.

Too few heat strengthened and thermally tempered SG laminated specimens were available to draw any definite conclusions on this issue for those designs.

The overall redundancy curves of the reinforced beams (Figures 7.14, 7.15) are fundamentally different from those of the laminated ones. Although their 2nd LTMs are not completely equal, their character is the same: they are dominated by the M_{2ndLTM} , which constantly exceeds M_{1stLTM} . This results in a horizontal line for $M_{overall}$, above the value of R_0 . The 1st LTM redundancy curve over the intermediate damage levels, therefore, has much less significance than in the laminated beams. Nevertheless, *it is noteworthy that the 1st LTM is only slightly affected by damage.*²⁰ It is suggested that the reinforcement reduces the stress concentrations along the bottom edge of the inner glass sheet, which results in a higher effective strength of that layer.²¹

2.3. Fracture Mode

As has been previously noted in Section 2.2.2, the failure behaviour of a glass beam depends on the test method applied. In some cases, this also influences the fracture pattern. Most beam designs failed in the same fracture mode, regardless of the test method. However, the PVB laminated heat strengthened beams broke in mode A when overloaded from the undamaged state, but in mode B when overloaded from a

¹⁸ For double layer ones: I; for triple layers: I and II.

¹⁹ Appendix E, Section 4.3.1.

²⁰ Note that at R_I and R_{II} , it is still the 1st LTM that is active since there is still a part of the glass section that carries the actions in linear elastic bending.

²¹ Appendix E, Section 3.3 (Figure E.27a, b). Further research would be required for a definite explanation for this phenomenon.

predamaged state. As simple overloading hardly ever causes failure in structural engineering practice, the latter fracture mode (B) is considered correct for these beams. However, it is not unimaginable that complete rupture upon failure occurs even in predamaged beams of other geometries, as the elastic strain energy released increases, while the PVB thickness may not. It should even be considered possible in annealed glass beams.

In any case, specifying the model impact type is essential to determine the safety of a glass element, as the failure behaviour (both post-failure strength and fracture mode) depends on it.

3. Relative Overall Redundancy Curves

In order to be able to compare the failure behaviour of the various beam designs, the redundancy curves have been made relative to R_0 , with Eq. (7.1). This is relevant because the calculable strength is also deducted from that value through the material partial factor ($R_d = R_{rep}/\gamma_M$) and it may, furthermore, be expected that dimensions of an element will be adjusted so that the actions will (almost) match the calculable strength (material efficiency). The relative resistance values have been shown in Figures 7.16 – 7.23 and listed in Table 7.4.

$$r_n = \frac{R_n}{R_0}, \text{ with } n = \text{model damage level I, II, III.} \tag{7.1}$$

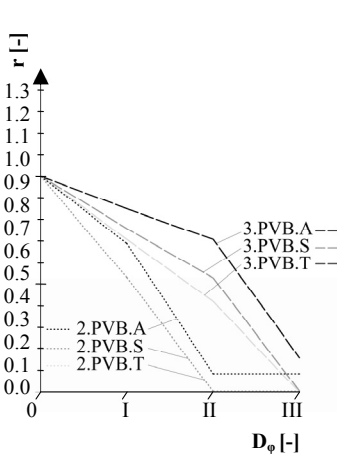


Fig 7.16 Relative redundancy curves for PVB laminated glass beams.

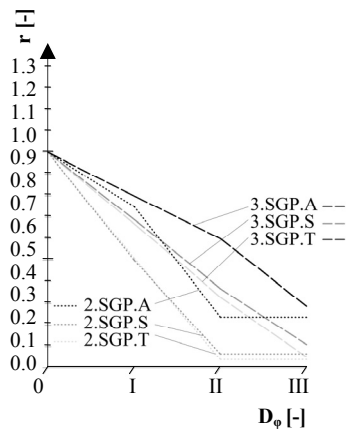


Fig 7.17 Relative redundancy curves for SG laminated glass beams.

Figure 7.16 shows the relative redundancy curves of the PVB laminated designs. The change in slope in the curves, as been noted previously in Section 2.2.3, indicating a non-linear relation between the reduction in unbroken layers and the resistance, also appears in the relative curves for 2.PVB.A, 3.PVB.A, 3.PVB.S, and 3.PVB.T. Only the

curves for 2.PVB.S and 2.PVB.T run straight – thus showing a linear relation between the broken layers and resistance decrease.

Of the heat strengthened and thermally tempered beams, R_{III} is low – but related to R_0 , it practically becomes negligible ($0.1 \% < r_{III,2/3,PVB,S/T} < 0.6 \%$). The annealed beams (especially the triple layer ones) on the other hand, show their r_{III} is not irrelevant.

The relative redundancy curves for the SG laminated beams are shown in Figure 7.17. The change in slope as observed with most of the PVB laminated specimens, here also occurs with the annealed specimens. Of the heat strengthened and thermally tempered beams, too few specimens were available to determine this. The intermediate resistance values were obtained by linear interpolation. All designs provided significant post-failure strength, but because of its lower initial resistance, the post-failure strength of the annealed beams is, relatively, much higher than of the strengthened and tempered ones. Such an amount of post-failure strength could be relevant in a range of practical applications.

As with the PVB laminated beams, the r_{III} of equally heat treated beams is higher for triple layer designs than for double layer ones, due to the increase of laminate in the section, which has little influence on R_0 .

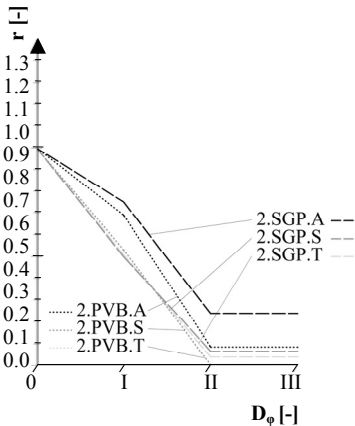


Fig 7.18 Relative redundancy curves for double layer glass beams.

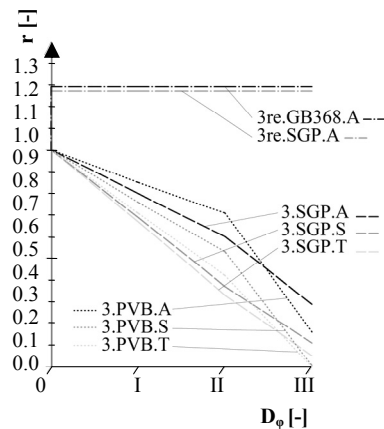


Fig 7.19 Relative redundancy curves for triple layer glass beams.

In Figure 7.18, the curves of the double layer beams are presented. Besides the fact that $r_{III,2,SG,A}$ clearly exceeds the r_{III} of the other designs, it is remarkable that $r_{III,2,PVB,A}$ is in the same order of magnitude (and even a bit larger) as $r_{III,2,SG,S}$ and $r_{III,2,SG,T}$ (also compare Figures 7.20 – 7.22).

Figure 7.19 shows the triple layer beam-curves. As with the double layer designs, the SG laminated, annealed glass beam has an r_{III} well above that of the other laminated beams. Here, also, $r_{III,3,PVB,A}$ exceeds $r_{III,2,SG,S/T}$. But none of these come close to r_{III} of the

reinforced beams. The difference between $r_{III,3re.GB368.A}$ and $r_{III,3re.SG.A}$ is small, and not very important for the overall safety of the design.²²

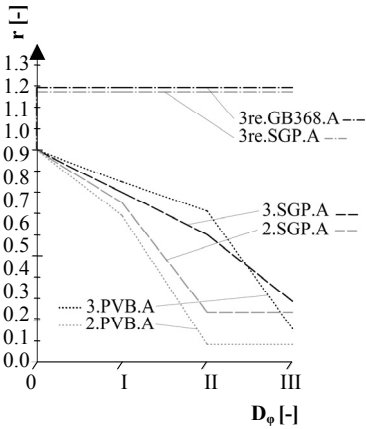


Fig 7.20 Relative redundancy curves for annealed glass beams.

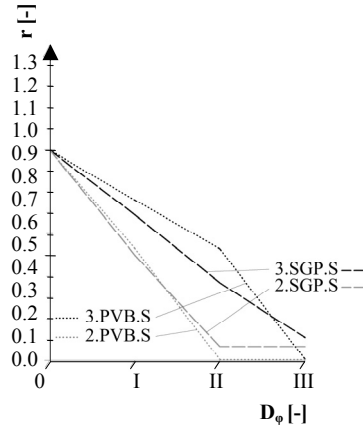


Fig 7.21 Relative redundancy curves for heat strengthened glass beams.

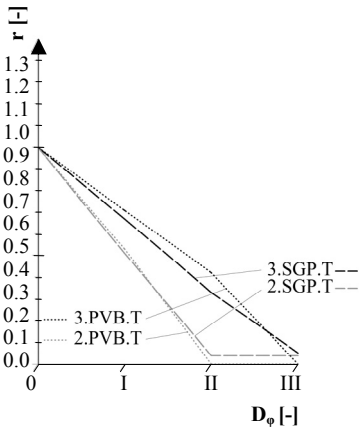


Fig 7.22 Relative redundancy curves for thermally tempered glass beams.

In Figures 7.20 – 7.22, the relative redundancy curves are shown per prestress treatment (annealed, heat strengthened, thermally tempered). They clearly show the potential of annealed glass in terms of residual strength, especially in comparison to tempered glass,

²² Although considerations with regard to production quality could influence a safety assessment. It should be noted that r_{III} values > 1 have also been observed for 3re.GB368.A type beams subjected to a variety of unfriendly environments. Louter, P.C., Veer, F.A., Belis, J., *Redundancy of Reinforced Glass Beams; temperature, moisture, and time dependant behaviour of the adhesive bond*, Proceedings of the Challenging Glass Conference, Delft, the Netherlands, May 2008.

but to lesser extent also to strengthened glass. The large difference in relative residual resistance stems not only from the higher absolute residual strength of annealed glass beams, but also importantly from their lower initial strength, which positively influences the ratio between pre- and post-failure strength.

For comprehensiveness, the relative redundancy curves of all designs are presented together in Figure 7.23.

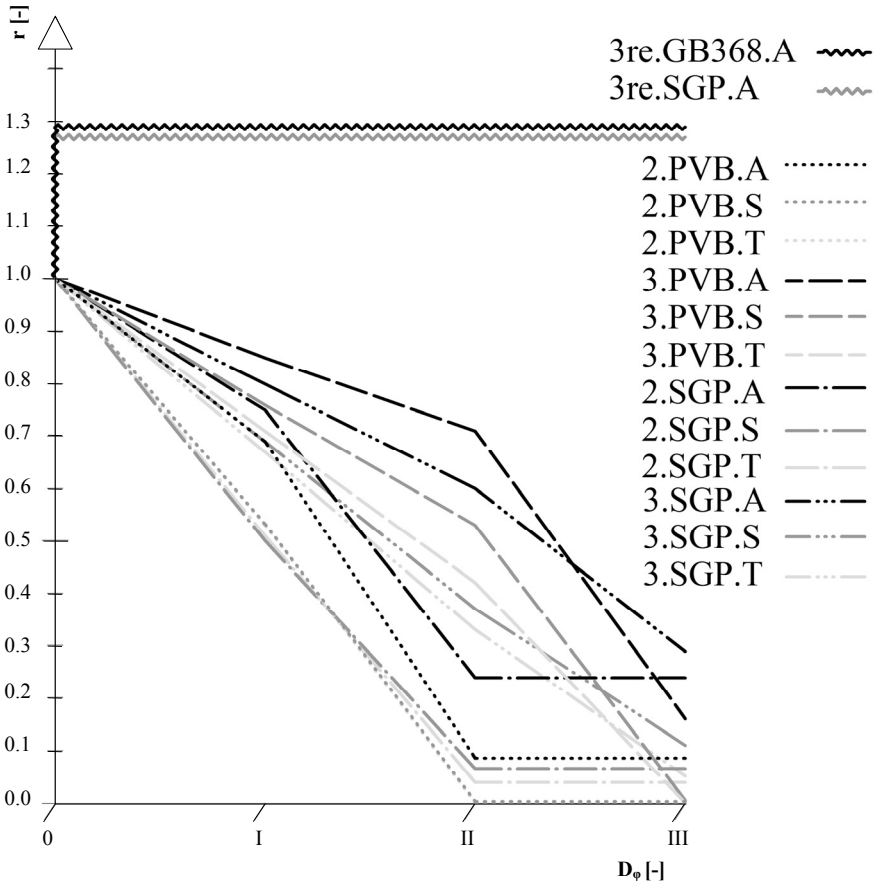


Fig 7.23 Relative redundancy curves for all glass beams presented in this Chapter.

Table 7.4 Relative resistance values of glass beam designs.

Beam design	r_0	r_I	r_{II}	r_{III}
2.PVB.A	1.00	0.69	0.036	0.036
2.PVB.S	1.00	0.53	0.004	0.004
2.PVB.T	1.00	0.53	0.001	0.001
3.PVB.A	1.00	0.85	0.707	0.059
3.PVB.S	1.00	0.76	0.529	0.006
3.PVB.T	1.00	0.71	0.419	0.001
2.SG.A	1.00	0.75	0.242	0.242
2.SG.S	1.00	0.50	0.066	0.066
2.SG.T	1.00	0.51	0.040	0.040
3.SG.A	1.00	0.80	0.603	0.288
3.SG.S	1.00	0.69	0.371	0.114
3.SG.T	1.00	0.67	0.333	0.052
3re.GB368.A	1.00	0.94*	0.885*	1.290
3re.SG.A	1.00	0.96*	0.929*	1.268

* 1st LTM

4. Safety Comparison

First of all, it should be noted that it is not particularly easy to induce significant physical damage in laminated glass – contrary to single sheet glass, which is much easier to break. Thus, even double layer beams are not nearly as vulnerable as a laymen may expect from his experience with dropping wine glasses on the floor – although it should be remembered that a certain amount of physical damage causes disproportional structural damage.

Obviously, from a safety point of view, the triple layer designs perform much better than the double layer ones. They are harder to damage to failure, as they require an extra impact. When a physical impact is considered to be governing, the fact that the inner layer is well protected by the outer ones should weigh heavily in the safety assessment. Receding the inner layer or protecting it with some kind of covering will make it even more difficult to cause damage. In a triple layer laminate, only erroneous manufacturing and handling or faulty joining then seem likely damage causes.

Besides the lower damage sensitivity, the redundancy of triple layer beams is also much better. At model damage level II, they can still rely on a portion of unbroken glass and thus much higher residual strength. At level III, they usually profit from more laminate material in the section, compared to double layer designs – although more layers than standard could be applied in double layer beams, nullifying this latter advantage.

As expected, the safety of the SG laminated beams is significantly higher than of the PVB laminated designs – even though their damage sensitivities are equal. Their safety

stems particularly from their post-failure strength, which exceeds that of PVB laminated beams even more than to be expected from the difference in laminate layer thickness and strength; its stiffness allows for a different LTM. The triple layer annealed glass beams laminated with SG have an r_{III} of close to 30 %. By doubling or tripling the number of SG layers, it may well be possible to arrive at r_{III} values close to 100 %. Furthermore, their fracture mode (in combination with heat strengthened glass) is probably less dependent on the failure cause.

Annealed and heat strengthened glass perform similarly with regard to damage sensitivity from physical impact. However, annealed glass provides higher post-failure strength, both relatively and absolutely. Annealed, PVB laminated beams even have a higher relative post-failure strength r_{III} than heat strengthened, SG laminated ones. Furthermore, its fracture mode is less dependent on the failure cause. On the other hand, heat strengthened glass is more resistant to some other impacts like thermal stress. Thermally tempered glass behaves poorly compared to annealed and heat strengthened glass. It has a much higher damage sensitivity and leads to less post-failure strength.

From a safety point of view, the reinforced beams outperform the other designs by far. They pair very low damage sensitivity with very high redundancy. Although their sensitivity to physical damage is comparable to that of the laminated beams, the model damage levels have little influence on the resistance, even of the 1st LTM. Furthermore, the presence of the reinforcement profile makes it very difficult to actually damage the inner layer. With the resistance of the 2nd LTM consistently above that of the 1st LTM, the amount of damage has practically no influence on the total load carrying capacity. Importantly, *this justifies effectively using the complete glass section in engineering calculations* (whereas with other beam designs, additional layers may have to be added). Provided the initial resistance $R_{0,1stLTM}$ exceeds the actions, $R_{III,2ndLTM}$ can never fail to meet the actions to be considered for higher model damage levels (in the worst case those actions are equal to the actions to be considered for level 0).

Finally, it should be noted that the safety assessment is highly dependent on the impact that is considered to be governing; some designs are less sensitive to one type of impact, while being more prone to another type.²³

5. Evaluation of the ESD as a Tool

Although a completely objective evaluation of the Element Safety Diagram as a tool for assessing and comparing the safety of glass elements by the author is impossible, – as he himself created it – some remarks may still be made on the subject.

This Chapter has shown that the ESD indeed provides a clear overview of the safety properties of a (structural) glass element. Combined with the possibilities to provide structural safety prerequisites, swift conclusions with regard to the suitability of a design can be drawn.

²³ Furthermore, including the time dependency of the resistance of annealed glass in structural glass calculations is still a subject of debate – even though this phenomenon has long been known (Chapter 4, Sections 1.2.2. and 1.3.). In the observations made above in this and the previous Chapter, it is assumed that the current modification factors reasonably account for this, but there is a possibility that further research requires the conclusions with regard to the safety of annealed glass to be revised.

By applying a relative redundancy curve, a comparison between the behaviour of different designs also becomes insightful, e.g. as has been shown by Figures 7.16 en 7.17 that remarkably showed $r_{III,2/3,PVB,A} > r_{III,2/3,SG,ST}$.

Although a number of values can be obtained from deduction and previously published research, the ESDs require a significant amount of tests on each individual design of which an ESD is constructed. However, such research would be required anyway if we were to fully understand failure behaviour of glass elements. The introduction of the ESD tool allows the gradual build up of databases of relevant glass element behaviour data that can be presented in a uniform method. This will enable more consistent and founded design choices.

Nevertheless, only use of the ESD in practice, by engineers and authorities, will allow for a proper evaluation.

8 Designing for Glass Element Safety

In the previous Chapters, the background to structural glass safety was investigated. The Integrated Approach was formulated. It identified four properties that, together, define the safety of a structural glass element. Subsequently, this chapter presents the fundamental design principles to obtain and optimize the safety performance, on three levels of scale: material, element, and structure. The effect on element safety of existing techniques like prestressing and laminating, as well as that of innovative concepts such as reinforcing, is discussed per element safety property. It will be put forward that the elastic strain energy content in a glass element at failure is an important parameter in further optimizing post-failure resistance, the primary safety parameter.

1. Element Safety Properties and Scale Levels of Approach

In the previous Chapters, the necessity of a comprehensive safety approach of structural glass was set forth. For the design of glass elements, the Integrated Approach was formulated to meet this need. The Element Safety Diagram (ESD) was presented as a tool to provide an overview of all relevant safety properties of a glass element. After the theoretical development of this approach, the ESDs for a number of glass beam designs were determined from experimental research. Although the Integrated Approach does not provide a single definite answer to the question ‘what is structural glass safety?’¹, it does offer a reasonably objective, clear, quantitative, and opposable method to assess and compare the safety of glass elements.

The development of the Integrated Approach already dropped some clues for the consequent research question: ‘how can structural glass safety be obtained?’. This question is generally treated in the subsequent sections. The basic design principles are presented for each element safety property and the effect on element safety of existing techniques like prestressing and laminating, as well as that of innovative concepts such as reinforcing, is discussed.

In Chapter 6, four element properties have been identified that determine the safety of a glass element: damage sensitivity, relative resistance, redundancy, and fracture mode. Structural glass safety is thus obtained by obtaining satisfying results for each property, and optimized by generating results as favourable as possible (i.e. more relative resistance, less damage sensitivity, more redundancy, and a coherent fracture mode).

When applying design measures to optimize safety, the properties damage sensitivity, relative resistance, and redundancy are the most relevant. Requirements with regard to fracture mode, will be fulfilled practically automatically in all cases that any post-failure strength is required. This property will therefore only be discussed briefly (Section 5).

Increasing relative resistance is not a very efficient and effective way to obtain safety. It requires adding more material than the actions in an undamaged state call for. It is thus

¹ Chapter 1, Section 2.

an inefficient method with regard to the use of material. Furthermore, it is flawed as a safety optimization approach as failure in practice is generally not caused by considered actions exceeding the considered resistance.² This property will still be discussed (Section 2), though, as the influence of some common safety enhancing techniques on the accuracy of the formal probability problem³ – and thus on the determination of relative resistance – may not be ignored.

Nevertheless, decreasing damage sensitivity and increasing redundancy remain as the key design objectives with which structural glass safety should be optimized. Both these properties can be altered by a wide range of engineering measures. In order to fully understand the possibilities, it is practical to roughly distinguish three levels of scale⁴ at which the safety properties can be influenced:

- Material Level (micro)
Altering the chemical composition and/or microstructure of a material to make it meet specific performance requirements.
- Element Level (meso)
Adjusting the element design, e.g. geometry, material selection, etc.
- Structure Level (macro)
Changing the overall structural composition, side constraints, and/or external influences.

The possibilities to decrease damage sensitivity and increase redundancy are discussed for each of the levels of scale (Sections 3 and 4, respectively).

2. Relative Resistance

The relative resistance r of an element is its resistance in the undamaged state divided by the calculable loads acting on it.⁵ As such, it is the inverse of the unity check (u.c.) usually required by codes. If $r = 1.0$, the probability of failure should be just small enough to be acceptable,⁶ if $r > 1.0$, the failure probability decreases (rapidly, i.e. not linearly with the increase of r) to lower levels. Thus, the higher r , the lower P_f and thus the safer the element is. The importance of r is likely to decrease with higher values of r , as overloading of the element by considered actions becomes less and less likely, while the probability of unconsidered failure causes will relatively increase. Notwithstanding this fact and the observation that failure in practice is generally not caused by

² Although it may be likely an increased resistance to the considered actions also results in a higher resistance to at least some of the unconsidered actions.

³ I.e. on the accurate prediction of the resistance of an element and thus on its failure probability. See also Chapter 3, Section 7.1. and Chapter 4, Section 4.

⁴ Off course, this distinction is somewhat arbitrary and the boundaries between can not be universally determined (e.g. a lattice truss may be considered an element, but also a (mini-) structure, composed of strut elements). This categorization more or less follows professional boundaries: the material level is the field of chemists and material scientists, the element level is that of manufacturing engineers and product developers, the structure level that of façade and structural engineers. Cross links between the latter two will probably be bountiful – much more so than between them and the first. Additionally, it should be noted that the material level can be further subdivided, e.g. into the atomic level, the molecular level, and the network level as proposed by Rouxel, T., *Designing Glasses to Meet Specific Mechanical Properties*, Proceedings of the Challenging Glass Conference, Delft, the Netherlands, May 2008.

⁵ Chapter 6, Section 4.2.

⁶ Codes require $u.c. \leq 1.0$. This corresponds to $r \geq 1.0$.

considered actions exceeding the considered resistance, it is obvious a stronger element is less likely to fail from the same actions⁷ than a weaker one, and is thus more safe.

Therefore, the accuracy of the formal probability analysis does influence the safety of an element. The problem of predicting glass strength was already discussed extensively in Chapter 4, Sections 1 and 2. But the two common safety enhancing techniques from practice, prestressing and laminating, both complicate this problem significantly.

2.1. Prestressing; Influence on the Formal Probability Analysis

The failure probability problem of glass, hosts a number of extra uncertainties for tempered glass. Most dimensioning methods consider the bending tensile strength of a glass sheet to be equal to the inherent strength⁸ plus the outer compressive surface strength (which has to be overcome before the inherent strength is called upon). This at least allows addressing some uncertainties particularly associated with thermal treatment in factors separate from those used for the inherent strength. However, two problems remain which leave such an approach to be somewhat flawed – though not as flawed as any approach that incorporates both inherent strength and the prestress contribution to it into one figure.

First, the prestress in a thermally treated glass piece is not as evenly distributed through the sheet, as is suggested by the single prestress figure and probably quite generally assumed. Using a SCALP-03 polariscopic measurement device, Nielsen et al.⁹ showed that even in simple square sheets of 300 x 300 mm² significant differences in prestress level could be found in x- and y-direction (thus often $\sigma_x \neq \sigma_y$; the stress state is not plane hydrostatic) and between various locations on the sheet, with higher variations nearer to the corners. The measured difference in prestress between the highest and lowest value could be as much as 35 MPa in a single 19 mm thick specimen. They concluded measuring the prestress level at a single location of a glass sheet would not give a sufficiently reliable determination of the specimen's prestress level. Imaginably, the actual prestress levels at edges, around bore holes and in glass sheets with more complicated shapes is even harder to predict accurately.

On a fundamental level, Veer et al.¹⁰ have even questioned the validity of the summation approach, i.e. that the bending tensile strength is obtained by adding the surface compression level to the inherent strength. For large series of annealed, heat strengthened and thermally tempered glass sheets, both standing up and lying flat, tested in four point bending, they found a considerable overlap between the weakest thermally tempered specimens and the strongest heat strengthened ones (the glass types were discerned by fracture pattern), see Figure 8.1. The overlap was too large to be explained by differences in inherent strength (which, due to defects, is variable). Thus, Veer et al.

⁷ Even though unconsidered actions generally cause failure, a stronger element is likely to be more resistant not only to considered actions, but also to unconsidered ones.

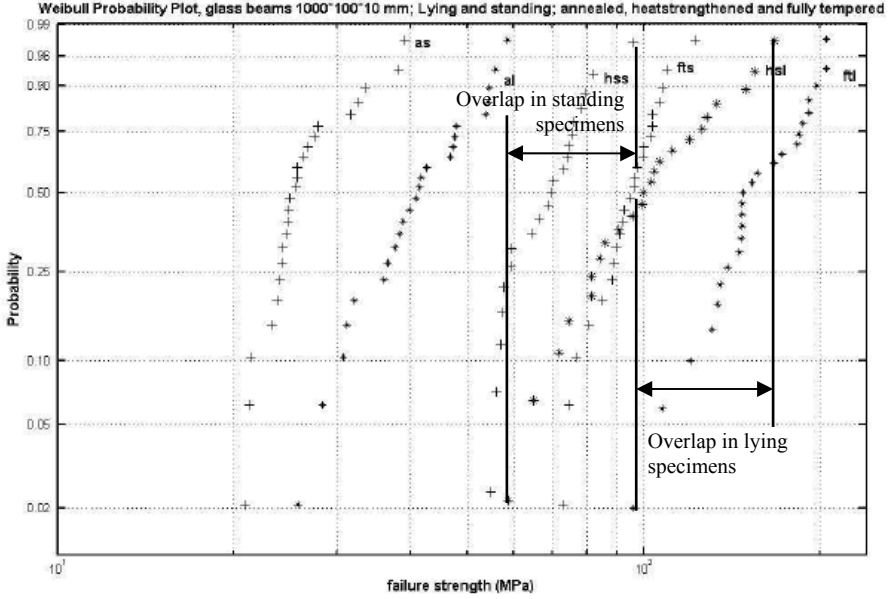
⁸ As should be clear by now, this is not a fixed value. Rather, the term is used here to indicate the resistance the material has to actions without (thermal) prestressing.

⁹ Nielsen, J.H., Olesen, J.F., Stang, H., *Experimental Investigation of Residual Stresses in Toughened Glass*, Proceedings of the Challenging Glass Conference, Delft, the Netherlands, May 2008.

¹⁰ Veer, F.A., Louter, P.C., Bos, F.P., Romein, T., Ginkel, H. van, Riemsdag, A.C., *The Strength of Architectural Glass*, Proceedings of the Challenging Glass Conference, Delft, the Netherlands, May 2008.

conclude a failure criterion based on Eq. (5.1), which is what the summation approach amounts to, has to be incorrect.

$$K = (\sigma_{inh} + \sigma_{res})Y\sqrt{\pi a} > K_C \tag{5.1}$$



as = annealed, standing hss = heat strengthened standing fts = fully tempered standing
 al = annealed, lying hsl = heat strengthened lying ftl = fully tempered lying

Fig. 8.1 Weibull plot for failure probability of annealed, heat strengthened, and thermally tempered glass sheets, lying and standing, in 4-point bending. Notice the overlap for heat strengthened and thermally tempered specimens.

Sglavo¹¹ stated the stress intensity K of prestressed glass is the sum of stress intensity associated with the external load K_{ext} and the stress intensity associated with the residual stress field K_{res} , Eq. 5.2. This approach is slightly different from the one with a summation of stresses as it allows discrimination of shape parameters Y and defect size a for the external load and residual stress field.

$$K = K_{inh} + K_{res} = \left(Y\sigma\sqrt{\pi a}\right)_{inh} + \left(Y\sigma\sqrt{\pi a}\right)_{res} \tag{5.2}$$

In consideration of the results obtained by Veer et al., this may lead to the suggestion that the defects in thermally tempered glass are somehow more severe than in heat strengthened glass (higher Y and/or a). But this is in contradiction with the observation

¹¹ Sglavo, V.M., *ESP (Engineered Stress Profile) Glass: High Strength Material, Insensitive to Surface Defects*, Proceedings of the 8th Glass Performance Days, Tampere, Finland, 2003.

of various authors¹² that thermal tempering actually also results in a crack healing effect. Thus one would expect *less* rather than *more* overlap between test results of heat strengthened and thermally tempered glass.

On the other hand, the views of Veer and Sglavo are supported by recently presented work of Rodichev & Tregubov.¹³ They found through microfractography analysis that, rather than crack healing, the initial cracks in glass which determine its inherent strength, are deteriorated by the heat treatment process. Thus, a summation approach to the strength of heat treated glass may be correct, but the inherent strength should *not* be considered to be equal to the strength of annealed glass, as is usually done. This could explain the experimental data found by Veer.

Clearly, this issue is yet unsolved and serious questions remain on how to model the strength of prestressed glass.

2.2. Laminating

Due to the statistical distribution of flaws, the average failure load for laminates is lower than that of the sum of the failure load of the individual sheets, when they are all loaded with the maximum failure load simultaneously.¹⁴ Whilst this is usually not the case in plane-loaded elements such as floors and windows, it is for the (standing) glass beams. Failure is namely governed by the weakest glass sheet.

On the contrary, Savineau¹⁵ has noted that laminated glass is at least as strong as monolithic glass of equivalent thickness. This seeming difference with the observations in the previous paragraph is probably due to the fact that the studies to which is referred use plate loaded specimens (not all layers in the laminate are simultaneously loaded with the maximum failure load). Furthermore, a laminate is slightly thicker than a monolithic glass plate of which the thickness equals the sum of the glass thicknesses in the laminate. Therefore, the bending stiffness is higher and the stresses are lower at equal loads. Finally, Veer¹⁶ has shown thin glass is stronger than thick glass because of the cutting process which introduces less severe defects in thin glass (a more 'clean cut edge' results). Thus, a laminate of two thin layers may be stronger than a monolithic glass sheet of equivalent thickness.

These effects are not included in any dimensioning method. Thus, when applied to laminated glass, they yield less accurate results in terms of failure probability.

¹² Haldimann, M., Luible, A., Overend, M., Ibid, p. 104, referring to:

- Bernard, F., *Sur le dimensionnement des structures en verre trempé: étude des zones de connexion*, Ph.D. thesis, LMT Cachan, France, 2001.
- Hand, R.J., *Stress intensity factors for surface flaws in toughened glass*, Fatigue and Fracture of Engineering Materials and Structures, 23(1): 73-80, 2000.

and: Nielsen, J.H., Olesen, J.F., Stang, H., Ibid.

¹³ Rodichev, Y., Tregubov, N., *The Challenge of Quality and Strength of the Hardened Architectural Glass*, Proceedings of the Glass Performance Days, Tampere, Finland, June 2009.

¹⁴ Hess, R., *Glasträger*, vdf Hochschulverlag AG an der ETH Zürich, Switzerland, 2000.

¹⁵ Savineau, G., *Durability and Postbreakage Behaviour of Laminated Safety Glass*, Proceedings of the Glass Processing Days, Tampere, Finland, 2001.

¹⁶ Veer, F.A., Zuidema, J., Berg, A. van den, Sluijs, M.M.A. van der, *Onderzoek naar de invloed van de dikte en het chemisch harden op de sterkte van glas*, december 2001 (unpublished).

The material characteristics of the laminate is another factor which makes an accurate failure probability prediction very difficult. Several types are used, but they are all polymers. Thus, their behaviour is complex, depending on load duration, temperature, moisture, and other environmental influences. Most importantly, this influences the shear modulus G and thereby the load distribution between the glass layers in the laminate, see Figures 8.2a – c. Structural glass engineering codes like the NEN-EN 2608-2 usually provide methods to determine an equivalent glass thickness to use in stress calculations. However, as the amount of coupling depends on the laminate shear modulus, the equivalent thickness in reality is not constant.

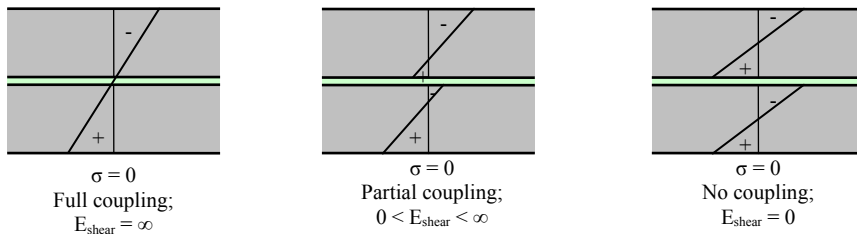


Fig. 8.2a – c Schematically representation of the stress distribution through a double layer glass laminate, depending on the extent of coupling (shear stiffness G of the interlayer).

Instead of working with an equivalent thickness codes usually also allow to assume either complete coupling or complete de-coupling, whichever is conservative for the case at hand. However, Gräf et al.¹⁷ stated that this, though easy to use, is inappropriate to describe the behaviour of laminates, although they admit the existing models to take laminate visco-elastic behaviour into account are too complex to be suitable for structural glass practice. An interesting point their research has shown is that the laminate action (effective shear modulus) is, among others, reduced with an increasing element stiffness. Thus short-span or four-side supported laminated glass will behave less like a monolithic sheet than long-span or two-side supported laminated glass. Wruk et al.¹⁸ noted that assuming complete decoupling for PVB laminated glass may be very conservative as significant coupling was observed for semi-long term loads (several days) even at 60 °C.

2.3. Improving Product Quality

Since glass failure is induced by surface defects, particularly those in the edges, it could be suggested that an improvement in the product quality of glass (and thus less defects) could bring an important improvement not only in strength but also a reduction in scatter of strength – and thus, perhaps, a more accurate failure probability determination. Uhm has suggested to flame polish edges. Although this indeed should improve the edge quality to a level comparable to that of the sheet surface, it may also introduce severe residual thermal stresses that, even during flame polishing, induce premature failure.

¹⁷ Gräf, H., Albrecht, G., Bucak, Ö., *The Influence of Various Support Conditions on the Structural Behaviour of Laminated Glass*, Proceedings of the 8th Glass Performance Days, Tampere, Finland, 2003.

¹⁸ Wruk, N., Schutte, A., Hanenkamp, W., *Load Bearing Behaviour of Laminated Glass Under Static and Dynamic Load*, Proceedings of the 6th Glass Performance Days, Tampere, Finland, 1999.

In experiments on more conventionally edge treated beams, Veer & Zuidema¹⁹ found proper edge finishing (grinding and polishing) could increase strength values to over that of tempered glass.²⁰ However, even though the average resistance increases, they concluded the engineering strength does not always follow this trend, because a fine edge finishing removes many defects, but not the most severe ones. Thus, in two groups of specimens, with and without fine edge treatment, the weakest specimens will have comparable strength. Therefore, until an edge treatment is found that also diminishes the effect of the most severe edge defects, product quality improvement may only marginally influence the failure probability accuracy.

3. Damage Sensitivity

Physical damage generally causes, usually by stress concentrations, a reduction in resistance compared to the nominal resistance, i.e. structural damage. It is a very diverse phenomenon with many different causes²¹, which may lead to many different symptoms, such as:

- Scratches, chippings, and other indentations – caused by (impact) contact with other materials,
- Micro and macro cracks – caused by (stress-driven) stable or unstable crack growth,
- Alterations to the chemical composition of the (surface of) the material – as a result of contact with reactive particles such as water (vapor) or alkalis (present in many building materials, like cement, concrete, and plaster) or by contaminations, e.g. NiS inclusions.

The formations of these damages are all complex processes that are still subject of research and debate. Decreasing damage sensitivity basically means making the formation of these damages more difficult. However, with the variety of damage causes and the complexity of damage phenomena, a comprehensive strategy to decrease damage sensitivity is difficult to develop and will require much more research in the future. Nevertheless, some options are discussed below.

3.1. Decreasing Damage Sensitivity on Material Level

3.1.1. Altering the Chemical Composition or Microstructure

A primary damage cause, especially to annealed glass, is stress corrosion under the influence of moisture. Glass damage sensitivity could be extremely improved if this effect – which, overtime, is responsible for a resistance reduction of approximately 70 %²² – could be neutralized. Perhaps it is possible to remove or reduce the number of reactive groups on the glass surface. However, since the process itself of moisture-

¹⁹ Veer, F.A., Zuidema, J., *The strength of glass, effect of edge quality*, Proceedings of the 8th glass processing days, Tampere, Finland 2003.

²⁰ Finally, it should be noted that some of the possibilities discussed in the next section on damage sensitivity, also influence the element resistance. However, since it has been argued decreasing damage sensitivity is a more fundamental safety enhancing approach, it was considered more appropriate to treat them there.

²¹ Chapter 4, Section 3.

²² Which can be deducted from the long term glass resistance reduction factor $k_{\text{mod}} = 0.29$.

driven stress corrosion is still subject of debate²³, it is unlikely a practical solution will arise soon.

Mechanical damage such as scratches are often caused by contact with other, harder materials. Rouxel²⁴ has shown there are significant differences in scratch formation behaviour of (silicate) glasses. He furthermore notes that the hardness of a material (e.g. as measured by Vickers indentation), although being a reasonable indicator, does not fully reflect its scratch behaviour. Rather, the hardness is determined by two complementary processes, shear flow and densification. The ratio in which each of these processes contributes to the hardness, determines the scratch formation behaviour. Shear flow and densification depend on the Poisson's ratio ν , high shear flow corresponds to a high value of ν , while high densification corresponds to a low value of ν . It turns out that both glasses with high shear flow and glasses with high densification (high and low ν , respectively) portray favourable scratch behaviour, while glasses with intermediate values of ν ($0.2 < \nu < 0.3$, as e.g. soda-lime silicate glass) show more severe scratching under contact pressure. Thus, damage sensitivity to scratching could likely be improved by applying glasses with either a high or low Poisson's ratio. As this ratio is correlated with the atomic packing density C_g ,²⁵ atomic or molecular alterations of this property should allow for the creation of more scratch resistant glasses. Rouxel²⁶ suggests cationic or anionic substitutions, or increasing the number of bridging oxygen atoms.²⁷

A third strategy, besides increasing chemical and scratch resistance, would be to augment crack growth resistance, i.e. making crack growth require more energy and thus increase fracture toughness. There may be several ways to achieve this. Introducing (elasto-)plastic or visco-elastic failure behaviour would be highly effective, not only with regard to damage sensitivity. It would also mean the introduction of a 2nd load transfer mechanism on material level, and thus dramatically increase redundancy.²⁸

Unfortunately, this is impossible. A crystal structure that is perhaps possible for glass through extremely slow solidification, would make the material opaque – and thus loose its *raison d'être* in buildings. Visco-elastic behaviour, on the other hand, requires long string molecules (e.g. polymers) that conflict with the basic building block of silicate glass.

Alternatively, Veer²⁹ has suggested that it may be theoretically possible to increase the fracture toughness of glass by introducing a second phase that acts as a crack stopper. However, he went on to conclude that it is questionable whether the obtainable increase

²³ Chapter 4, Section 1.2.2.

²⁴ Rouxel, T., *Designing Glasses to Meet Specific Mechanical Properties*, Proceedings of the Challenging Glass Conference, Delft, the Netherlands, May 2008.

²⁵ Rouxel, T., *Elastic Properties of Glasses: A Multiscale Approach*, Comptes Rendus Mecanique, August 2006. www.sciencedirect.com

²⁶ Rouxel, T., *Elastic Properties of Glasses: A Multiscale Approach*, Comptes Rendus Mecanique, August 2006. www.sciencedirect.com

²⁷ A suggestion which can also be found with: Dériano, S., Truyol, A., Sangleboeuf, J.-C., Rouxel, T., *Physical and Mechanical Properties of a New Borosilicate Glass*, Ann. Chim. Sci. Mat. 28, 2003. Pp. 55-62.

²⁸ See next Section (2.3).

²⁹ Veer, F.A., The limitations of current transparent sheet material in buildings, internal memo (not published), TU Delft, 1996.

in fracture toughness would be significant. In any case, it would not result in truly plastic behaviour.

The Young's Modulus of Elasticity E could be increased by alterations to the chemical composition similar to those required to increase the atom packing density. Thus, an increase in E is likely to go hand in hand with a decrease in ν . Side effects of such measures could not only include higher strength but also better post-failure behaviour as a stiffer material absorbs less energy and may produce less crack surface area upon fracture.³⁰ Alternatively, the E modulus could be reduced to about 35 – 40 MPa, increasing ν to approximately 0.35,³¹ thereby also decreased scratch sensitivity. The effectiveness of each E -related strategy is hard to predict.

Albeit opportunities to improve the structural and safety properties of (silicate) glasses, it is unlikely they can be implemented in any significant scale in the near future. Besides the fact that the improvement of glasses by material alterations is still in the field of scientific research, another complicating factor is the world-wide homogenized flat glass float production process. Its efficiency and continuous character make the manufacturing of specialty (custom) glasses extremely expensive in comparison to ordinary soda lime silicate glass. Even when the same production method would be possible, a float line is unable to change the composition of its product during its life time, because of the continuous nature of the production process. Unless a technical breakthrough occurs,³² custom specification of glass composition will be out of reach for the glass construction designer in practically any project.³³

3.1.2. Prestressing

Off course, the one strategy widely applied on material level to decrease damage sensitivity of a glass element, is thermal prestressing: tempering or strengthening, each with somewhat different effects on the damage sensitivity of glass. Tempered glass is less sensitive to a number of failure causes (soft-body impact, thermal stress, long term loading, general loading), but in the mean time it is more sensitive to some others (hard-body impact, deep scratches, chipping, and nickel sulfide inclusions), as has been shown by the impact tests presented in Appendix E and the Element Safety Diagrams in Chapter 7.³⁴ The net effect on damage sensitivity may be highly application dependent. Care should be taken especially during handling and construction to avoid chipping or similar damage as that may easily cause complete shattering of the glass sheet.

The damage sensitivity of heat strengthened glass, on the other hand, can more generally be said to be less than both that of annealed and thermally tempered glass, for it combines much of the advantages of tempered glass (thermal stress resistance, long

³⁰ The influence of strain energy content on failure behaviour is extensively discussed in Section 4 of this Chapter.

³¹ Veer, F.A., private discussion with the author, d.d. 26.06.2009.

³² A high-quality casting process, e.g. on polished stainless steel molds, would be desirable.

³³ Besides soda lime silicate glass, borosilicate glass is probably the only commercially available glass that is available flat and in relevant sizes. The damage sensitivity in comparison to soda lime silicate glass has not been investigated, but there are no indications it will behave significantly different in this respect, other than it is much less sensitive to thermal stress because of its low thermal expansion coefficient. However, borosilicate float glass is also much more expensive.

³⁴ It required about 60 – 65 % less energy to break a tempered glass sheet by concentrated hard-body impact on the edge.

term stress resistance) with those of annealed glass (impact/scratch resistance). It was shown in Appendix E and, consequently, Chapter 7 Section 2, the energy required to break a strengthened sheet by concentrated hard-body impact is as high as it is for an annealed glass sheet. Contrary to tempered glass, nickel sulphide failure is rare for heat strengthened glass.

Like heat treated glass, chemically strengthened glass is highly resistant to failure causes related to high stress concentrations such as impact or thermal stress. However, since the surface compressive layer is only very thin, it is susceptible to damages which go through it. Unlike heat treated glass, this does not result in immediate and complete failure, because the amount of stored energy is low. However, cracks which have gone into the tensile zone may be subjected to stable crack growth,³⁵ which can cause glass failure some time after the damage has been done. To stop cracks from growing through the compressive layer, Sglavo³⁶ has proposed to apply a two phase ion exchange process which results in a stress profile with a compressive maximum about half way in the compressive zone, rather than on the glass surface (Figure 8.3b). This may effectively stop cracks growing gradually from the surface, but it would not prevent crack growth of cracks that originate from damage (e.g. scratching) that goes through the outer layer immediately. Even if stable crack growth could be avoided, this would mean local weakening to the strength of annealed glass (only). It is thus questionable if the strength of chemically strengthened glass can be relied on in structural calculations. Consequently, it does not seem to have an overall advantage over annealed glass from a safety point of view.³⁷

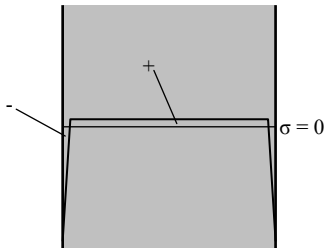


Fig. 8.3a Typical stress distribution through the glass sheet thickness from chemical strengthening.

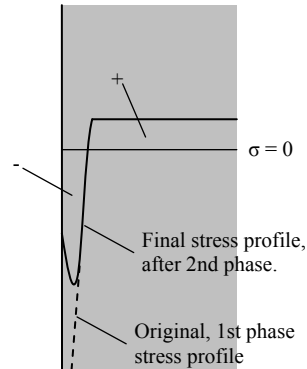


Fig. 8.3b Stress distribution near the glass sheet surface from a two phase chemical strengthening process, as proposed by Sglavo.

³⁵ Haldimann, M., Luible, A., Overend, M., *Structural Use of Glass*, Structural Engineering Documents 10, IABSE, Zurich, Switzerland, 2008.

³⁶ Sglavo, V.M., *Ibid.*

³⁷ Chemically strengthened glass is not usually applied in building constructions. More research is required into the damage sensitivity and the consequences for the load carrying capacity. Such research, unfortunately, could not be included in this study.

3.1.3. Coatings

Since the damage sensitivity of glass largely stems from stress concentrations that arise around surface defects, it should be considered whether coatings on the glass surface could help to decrease damage sensitivity. Basically, three types can be identified:

- Metallic coatings,
- Silica (sol-gel) coatings, for ‘self cleaning’ glasses and reduction of glare and reflectivity,
- Polymer coatings, applied as mechanical protection to glass fibers.

The use of a range of metallic coatings is actually wide spread. As they can alter heat and light transmission, they can play a considerable role in the climate performance of a façade.

Silica coatings (both single and dual systems exist) are applied to obtain ‘self cleaning’ glass. These coatings reduce the hydrophilic character of the glass surface thus reducing the contact angle of glass droplets, making them run off more easily and leaving less stains. In buildings, this may significantly cut cleaning costs, while in cars the main advantage is the glare reduction in dark, wet conditions (e.g. a rainy night).

Continuous glass fibres (e.g. as used for data transfer cables) are generally protected by polymer coatings. Several kinds of polymer coatings can also be applied to float glass in buildings, usually also to obtain a self-cleaning effect.

No comprehensive research exists considering the effect of various coatings on damage sensitivity or even strength of glass sheets, but some minor studies indicate improvements may be expected. Colvin³⁸ compared the strength and loading rate dependency of metallic coated glass and silica coated glass to annealed float glass. He found significant improvements of strength, especially for the silica coated glass. The loading rate dependency of the silica coated glass was slightly less than for uncoated glass, which he attributes to the fact that stress corrosion in pure silica is slower than in soda lime silicate glass. Notably, the metallic coated glass showed hardly any loading rate dependency owing to the absence of moisture related stress corrosion in the metallic layer. However, Colvin rightfully notes these advantages may be difficult to exploit in building engineering practice as loads on glass sheets may often be either one of two out-of-plane directions. Furthermore, the thin layer may be locally penetrated, thus nullifying the protective effect.

Tartival et al.³⁹ investigated the scratch resistance of sol-gel coated glass by subjecting a coated sample to a moving Vicker’s indenter under increasing pressure. In comparison to uncoated specimens, they found the three stages of scratch development (micro-ductility, micro-cracking, and micro-abrasion) each occurred at much higher load levels in the coated specimens. Additionally, the final scratch width was only about one third of that of the uncoated sample.

³⁸ Colvin, J.B., *The Effect of Coatings on the Bending Strength of Architectural Glass*, Proceedings of the Glass Performance Days, Tampere, Finland, 2007.

³⁹ Tartival, R., Reynaud, E., Grasset F., Sangleboeuf, J.-C., Rouxel, T., *Superscratch-resistant Glass by Means of a Transparent Nanostructured Inorganic Coating*, Journal of Non-Crystalline Solids, No. 353, 2007, pp. 108-110.

Kistner et al.⁴⁰ found a significantly smaller contact angle for glass treated with a specific polymeric coating. The angle of a glass sheet with the horizontal at which a droplet would start to run off was also reduced. Although the contact angle of water droplets on glass is not a direct indicator for damage sensitivity or even stress corrosion sensitivity, it does at least suggest reduced susceptibility.

A polymeric coating specifically for application to the edges of annealed glass was presented by Uhm et al.⁴¹ This resulted not only in a factor 2 increase of practical strength but also in a significant reduction in scatter, leading to a design stress more than 3 times as high as that of untreated annealed glass. They claim that ‘by filling, healing, and protecting the flaws, the coating minimizes any static fatigue effects related to humidity.’

The effect of the various coatings on damage sensitivity has not been comprehensively compared and proven. Nevertheless, there are important indications pointing towards decreased damage sensitivity, mainly from stress corrosion, but also from scratching. Edge coated sheets provide enhanced resistance particularly against thermal stress failure (which generally originates from the edges). Whether these advantages will persist when the coating is locally damaged, remains to be seen. The effectiveness of the protection provided by coating in relation to impacts that may be expected in various building practice applications, should also be subject of further research.

3.1.4. Transparent Polymers

Finally, it may be an option to, instead of altering the glass composition, choose another material altogether. The family of amorphous carbon-based polymers provide the only alternative.⁴² Attempts to apply polymers to create transparent structures were presented in Chapter 2, Sections 2.5.1. (as a material for the column-main beam joint in the All Transparent Pavilion) and 3.3.2.1. (as a material for both the joints and the general transfer of normal compressive and tensile stresses in the Transparent Façade Struts). From an extensive comparison of material properties,⁴³ it was concluded that, although at first glance many transparent polymers possess some favourable safety properties in comparison to glass, e.g. high fracture toughness and visco-elasticity, they also suffer from a range of drawbacks. The most crucial is their low Young’s modulus (ranging from 2 – 4 GPa at room temperature for the stiffer materials), which renders them unsuitable for most structural applications. Only in specific situations and designs in which the stiffness of an element is unimportant or otherwise provided (e.g. as by the glass tube in the façade struts), a transparent polymer can be the main structural material. Other disadvantages include temperature dependence, creep, sensitivity to moisture and other environmental influences, and surface softness (prone to scratches). Even when

⁴⁰ Kistner, D., Bretthauer, A., Kahles, H., *Using Polymers to Add Additional Functions to Toughened Glass*, Proceedings of the Glass Performance Days, Tampere, Finland, 1997.

⁴¹ Uhm, H., Bruce, L., Culp, T., Roger, C., *Glass Strengthening by Edge Coatings*, Proceedings of the Glass Processing Days, Tampere, Finland, 2001.

⁴² Veer, F.A., The limitations of current transparent sheet material in buildings, internal memo (not published), TU Delft, 1996.

⁴³ *AdDoc II: Transparent Polymers for Joint Applications in Glass Structures*, additional document to this PhD, www.glass.bk.tudelft.nl.

limiting the application of polymers to intermediate joint elements,⁴⁴ many questions remain with regard to the long-term behaviour and safety.

3.2. Decreasing Damage Sensitivity on Element Level

As the possibilities to decrease damage sensitivity on material level are limited, additional measures on a higher level of scale can be applied.

3.2.1. Laminating

The most widely applied safety enhancing technique for glass in construction, is *laminating*. Often, the outer layers are considered to be, at least partly, sacrificial, i.e. their contribution to the resistance capacity of the element is ignored. With the introduction of the Integrated Approach, it is suggested to abandon this rather artificial method (of pretending some layers just are not there), and obtain a clear perspective on the performance of laminated glass elements. With regard to damage sensitivity, laminating provides a highly effective protection for the inner/non-impacted layer(s). This was observed already in a case of vandalism on a glass bridge⁴⁵ and confirmed by the performance of side-impacted laminated glass beams discussed in Appendix E, Section 3.3., Table E.5e. Furthermore, the surface of the inner glass sheet in a laminate is probably well protected against stress corrosion as there is little or no moisture to attack the glass – although it should be noted that the edge, which may very well be governing, is not protected this way. Finally, it should be noted that the experimental results presented in Appendix E also showed that crack growth even in the outer, impacted layer is much less extensive in laminated (annealed) glass than in single sheet glass of equal thickness.

The influence of the laminate material on damage sensitivity is highly dependent on the impact type. In Chapter 7 and Appendix E, it was shown that for concentrated hard-body impact on the edge of a glass beam, no significant difference between PVB- and SG-laminated glass was found. However, that may not be the case for other impacts. Among others, the laminate material influences the element overall stiffness and therefore also the energy absorption, which may have both negative and positive effects.⁴⁶ Furthermore, the laminate material properties such as moisture absorption also has an impact on damage through e.g. delamination or stress corrosion.

Recently, studies⁴⁷ have been presented with regard to the behaviour of laminate glass reinforced by incorporating steel wire mesh or perforated sheet in the laminate layer (both PVB and SG). The focus was on post-breakage behaviour, rather than damage sensitivity. As the reinforcement increases the element stiffness, particularly at elevated temperatures (above $T_{g,lam}$), this may have effects on crack growth and energy

⁴⁴ As discussed in *AdDoc II: Transparent Polymers for Joint Applications in Glass Structures*, additional document to this PhD, www.glass.bk.tudelft.nl, Section 5.

⁴⁵ Chapter 5, Section 3.4.

⁴⁶ A high stiffness may lead to higher element resistance but to less impact energy absorption both at and after failure. Generally, this will positively influence the post-failure resistance (Chapter 9). However, in particular cases, such as explosive resistance, the higher energy absorption capacity obtained with a weak laminate may be more favourable as it will absorb more of the explosive energy, which is thus less likely to cause injury or failure in other parts of the structure. This is highly dependent on both the considered explosive load-time characteristic and the glass element design.

⁴⁷ Feirabend, S., Sobek, W., *Reinforced Laminated Glass*, Proceedings of the Challenging Glass Conference, Delft, the Netherlands, May 2008.

absorption. But in general, it does not seem to have much influence on the damage sensitivity of the glass element.

3.2.2. Design measures

Although no research has been published considering the influence of applying a *receding inner layer* in laminated glass elements (e.g. beams and columns) on the damage sensitivity, it should obviously be expected the sensitivity of the inner layer to mechanical impact is significantly reduced. This strategy has been applied, among others, in a design for crucifix glass columns for a town hall in France⁴⁸ (Figure 8.4a and b). In beams (as opposed to columns) the tensile stresses in the edge of the receded layer will furthermore be lower than those in the outer ones. The inner layer will thus suffer less from stress corrosion, which provides an additional damage sensitivity improvement.

Impact tests on glass beams reinforced with stainless steel profiles (Appendix E) have shown a form of *metal protective covering* is very effective in reducing damage sensitivity. Furthermore, those tests showed the edge strength of glass sheets with steel covering were significantly higher than those not protected. This seems to indicate the covering helps to avoid local peak stresses around defects – and thus provide an additional type of damage sensitivity control (Figure 8.5a, b).⁴⁹

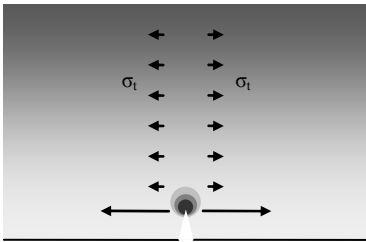


Fig. 8.5a Stress concentrations around a defect tip in a glass sheet.

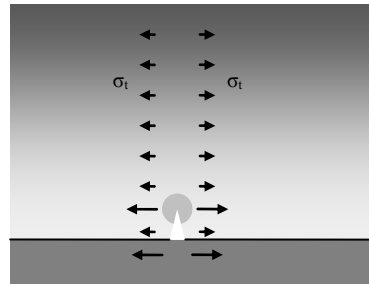


Fig. 8.5b Suggested effect of reinforcement as micro scale crack bridge: de-intensification of the stress concentration.

A protective covering also protects the edge against moisture induced stress corrosion, although no quantitative studies to this respect are known. A decrease of element transparency may be a disadvantage of applying protective covering, but compared to a receding inner layer it is questionable which measure is more visually invasive (especially when the covering is highly polished).

3.3. Decreasing Damage Sensitivity on Structure Level

As argued in Chapter 6, Section 2.2., a comprehensive treatment of safety on the level of the complete structure, falls outside the scope of this research. Nevertheless, some possibilities to decrease structure damage sensitivity are discussed to clarify the wide range of options open to the designer.

⁴⁸ Figure 5.5a, b, Chapter 5, Section 1.3.

⁴⁹ See also Appendix E, Section 3.3.

3.3.1. Compound members

Two basic design strategies are usually followed to obtain safe failure behaviour in structures: providing *alternative load paths* and *compartmentalization*.⁵⁰ The latter, often applied to horizontally orientated structures like multi-span bridges, aims at localizing failure by allowing one compartment to collapse while leaving the rest of the structure relatively unscathed. This strategy could also be applied on smaller scale – actually an intermediate level between that of elements and complete structures – to glass constructions. Consider for instance the canopy described by Techen in the interview presented in Appendix C, Section 5.3.2. As this canopy was repetitively damaged by collision with unloading trucks, the damage sensitivity of the complete canopy could be significantly reduced by limiting the size of glass sheets⁵¹ of which it consists, so that upon collision only a part of the canopy would break. Limiting the size of glass panels could also be effective for e.g. balustrades.

The *compound design of elements* has approximately the same effect on damage sensitivity: glass breakage remains localized to one segment. Especially when working with tempered glass, this may be important. With this strategy, a structural element is divided into multiple parts, effectively turning it into a miniature structure, with the appropriate consequences for the failure probability.⁵² Two (remarkably similar) examples are shown in Figure 8.6 and 8.7. In each section of these compound beams, there are at least two parts present.



Fig. 8.6: Subway Entrance Canopy, Tokio, Japan. Total span 10.8 m, 4 segments (3 of which double), two 19 mm thermally tempered glass layers, with an acrylic layer in between, 1996. Structural glass engineer: Dewhurst Macfarlane, London, UK.



Fig. 8.7: Atrium roof of the Chamber of Commerce, Munich, Germany. Total span 14 m, 5 segments (2 double, 3 triple), double and triple layers, PVB laminated, thermally tempered and heat strengthened, 2002. Structural glass engineer: Ludwиг und Weiler, Germany.

In order to avoid failure of the whole element when one segment fails, this strategy is only effective in a parallel system, i.e. in combination with an alternative load path provision (in the designs in Figures 8.6 and 8.7 provided by a doubling/tripling of the compound elements).

⁵⁰ Starossek, U., *Progressive Collapse of Structures; Nomenclature and Procedures*, Structural Engineering International, 2/2006, pp. 113 – 117.

⁵¹ And indeed they probably are.

⁵² A serial structure will have a failure probability in the order of the sum of the failure probabilities of the individual components, while a parallel structure will have one in the order of their product.

3.3.2. *Alternative Load Paths*

Introducing *alternative load paths* into a structure decreases its damage sensitivity, despite not that of its individual elements. It does increase redundancy of the elements, though (and will thus be discussed in Section 4).

3.3.3. *Specific Design Measures*

Additionally, damage sensitivity of the structure can be reduced by providing protective measures which make it less likely damage occurs. These will be highly application dependent, but could consist of anti-collision measures (e.g. concrete blocks between façades and heavy traffic roads), railings, thresholds, etc.

3.4. *Conclusions with Regard to Minimizing Damage Sensitivity*

A systematic treatment of strategies to minimize damage sensitivity is extremely difficult as there is a very wide range of possible impacts, of which the relative importance is largely unknown (what impact occurs how often and on which parameters does it depend?).⁵³ A variety of measures has been discussed on different levels of scale. However, very little is quantitatively known about the effectiveness on different types of impact.

The absence of these two parameters (what impacts are relevant and what is the effectiveness of measures to counter them) makes it virtually impossible to develop a general strategy to minimize damage sensitivity. Much more research in this area is required.

It should be noted though, that the interviews⁵⁴ with glass engineering experts seem to indicate the majority of glass damages and failures can be attributed to errors in production, transport, or construction – not in design or causes during life time. The design measures presented above will not alter this. Rather, damage sensitivity optimization should therefore encompass quality control at all stages (manufacturing, treatment, transport, construction) before anything.⁵⁵

Along with the fact that there can always be unexpected damage causes,⁵⁶ it follows that optimizing redundancy is therefore the fundamental approach to provide maximum safety for glass in construction.

4. **Redundancy and Post-Failure Strength**

Redundancy was defined as the development of residual resistance over increasing levels of physical damage, from 0 to 1.⁵⁷ Two fundamentally different stages of damage were recognized: partial damage ($0 < D_{\phi} < 1$) and full damage or failure ($D_{\phi} = 1$). The active LTM forms the discerning criterion. In a partially damaged element, the 1st LTM is still active although with less than its original capacity; in a failed element, the 1st LTM is no longer active and superseded by another load carrying mechanism, the 2nd LTM. Optimizing redundancy requires fundamentally different strategies for these two stages, and will therefore be treated separately.

⁵³ As argued in Chapter 4, Section 3.

⁵⁴ Chapter 5, Section 3.3., and Appendix D.

⁵⁵ This, however, falls outside the scope of this research, as argued in Chapter 6, Section 2.2.

⁵⁶ Chapter 3, Section 7, and Chapter 5, Section 3.3.

⁵⁷ Chapter 6, Section 4.3.

4.1. Optimizing Redundancy in the Stage of Partial Damage

For this stage, the (only) point of interest is the resistance ratios of the undamaged versus the damaged parts at the model (partial) damage levels.⁵⁸ By altering these ratios in the direction of more resistance for the undamaged parts, the redundancy will increase, as shown in Figure 8.8.⁵⁹

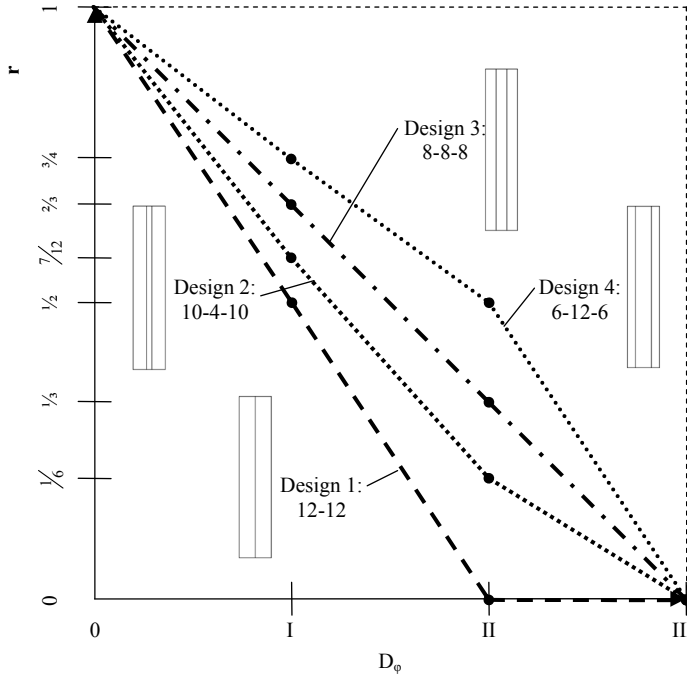


Fig. 8.8 1st LTM redundancy curves for four different beam section designs of equal total thickness.

Various strategies are open to increase the resistance of undamaged parts. In the example of Figure 8.8,⁶⁰ this is obtained by introducing a third layer (so that model damage levels II and III do not coincide anymore; design 1 and 2) and consequently by changing the thickness ratios of the glass layers. Some other methods can also be considered:

- On material level:⁶¹
 - Alterations to the composition or microstructure of the material,
 - Introducing prestress by thermal or chemical treatment,
 - Improving edge quality,

⁵⁸ The concept of model damage levels was introduced in Chapter 6, Section 3.3.2.

⁵⁹ This example was already introduced in Chapter 6, Section 3.3.2. (Figure 6.9). However, in this reprint, the vertical structural damage axis was replaced by a relative residual resistance axis (compare also Figure 6.10), which provides a more naturally understandable curve development (the highest curve now shows the most redundancy).

⁶⁰ Previously introduced in Chapter 6, Section 3.3.2, as Figure 6.9.

⁶¹ Section 2.1 of this Chapter.

- On Element level:⁶²
 - o Protective, strength increasing (edge) coatings – especially to avoid resistance reductions through stress corrosion when long term loads are governing,
 - o Defect bridging reinforcement or covering,⁶³
 - o Limit crack growth in the broken parts, to profit from compression transfer in broken parts (this leads to a shift of the neutral axis, effectively increasing the (tensile) resistance of the unbroken layer).⁶⁴

To increase partial damage redundancy, these measures should *not* be applied to all layers, but rather to the unbroken ones (according to the model damage levels) in order to alter to resistance *ratios*. However, care should be taken not to make the strengths differences too large.⁶⁵ If, for whatever reason, the actual damage sequence should divert from the model damage sequence (which should be the most probable one), this would result in redundancy development significantly different from that which was expected.

4.1.1. Laminating

Laminating is the technique that actually provided the possibility of introducing the concepts of partial and full damage. The laminate material provides a crack growth barrier which allows to discern between various levels of damage. Numerous pendulum-, drop- and other tests⁶⁶ have proven the effectiveness of this approach to keep breakage localized to fewer sheets than the laminate thickness. Many publications on post-breakage behaviour of laminated glass focus on the resistance to a variety of impact tests and consequently if a damaged pane stays in place⁶⁷ (i.e. if it can carry its self weight). The maximum post-failure resistance is rarely investigated.

4.2. Optimizing Redundancy in the Stage of Full Damage (Generating Post-Failure Resistance); Material Level

When Full Damage occurs, the load transfer mechanism (LTM) initially responsible for the resistance capacity of an element, is no longer capable of transferring forces.⁶⁸ If there is no 2nd LTM present in the element, the post-failure resistance equals 0 and collapse occurs. To optimize redundancy in the Full Damage Stage, a 2nd LTM must be generated and optimized. Like damage sensitivity, this problem can be tackled on different levels of scale: material, element, and structure. These are discussed in this and subsequent sections.

The introduction of a 2nd LTM on material level, means that a subsequent (elasto-) plastic or visco-elastic stage should be added to the (uni-linear) elastic failure behaviour

⁶² Section 2.2 of this Chapter.

⁶³ As observed in tests on reinforced glass beams, see Appendix E, Section 3.3., and specifically Figure E.27.

⁶⁴ As observed in the ESDs of several beams presented in Chapter 7, specifically: 2.PVB.A (Figure 7.2), 3.PVB.A (Figure 7.5), 3.PVB.S (Figure 7.6), 3.PVB.T (Figure 7.7), 2.SG.A (Figure 7.8), 3.SG.A (Figure 7.11).

⁶⁵ This is an arbitrary criterium, but the author would suggest a maximum factor of 2.

⁶⁶ E.g. Nourry, E., Nugue, J.-C., *Impact on Laminated Glass: Post-breakage behaviour assessment*, Proceedings of the 9th Glass Performance Days, Tampere, Finland, 2005.

⁶⁷ This has also been noted by Delincé, D., Callewaert, D., Belis, J., Impe, R. van, *Post-breakage Behaviour of Laminated Glass in Structural Applications*, Proceedings of the Challenging Glass Conference, Delft, the Netherlands, May 2008.

⁶⁸ By definition, see Chapter 6, Section 3.3.1.

of glass. However, as previously argued,⁶⁹ this is not possible without the introduction of a crystal structure, rendering the material opaque.

Only in some specific cases (full-framed, small to medium sized plates), may prestress have an influence on post-failure strength of single sheet glass. Because, whereas tempered glass will disintegrate completely upon breakage and not stick in a frame,⁷⁰ annealed and strengthened glass may still do so after breakage and thus effectively provide some post-failure resistance.

As transparent polymers (the only other significant group of materials with the property of transparency) suffer from a range of other drawbacks,⁷¹ redundancy in the full damage state can not be obtained (or optimized) through measures taken on material level.

4.3. Element Level

4.3.1. Principles of Designing Secondary Load Transfer Mechanisms

An example of secondary LTMs in a glass element was already shown in Chapter 6, Section 3.1. The concept of 2nd LTMs was further applied to the analysis of post-failure resistance of glass beams in Appendices E and I. This limited number of applications already indicates there may be many ways to achieve secondary LTMs in glass elements – and that they are highly dependent on element and loading type. It should be noted that the loading type on one element may even change between one LTM and the next (e.g. plate bending that is superseded by tension membrane action). Nevertheless, three starting points govern the design of any 2nd LTM into a glass element:

- The stiffness (either bending $E_b I_{\text{eff}}$, compressive $E_c A_{\text{eff}}$, or tensile $E_t A_{\text{eff}}$) of the 2nd LTM is, by definition, lower than that of the 1st LTM, as the stiffness determines which LTM will carry a load on an element.
- Failed glass layers are considered to be broken; broken glass can not carry any tensile loads.⁷² Therefore, a complementary component will have to be present in any glass element with post-failure resistance, to carry the post-failure tensile loads. This is even the case in compression loaded elements as there will always occur complementary tensile stresses perpendicular to the main loading direction. Furthermore, compression loaded elements will often be prone to stability failure⁷³ like buckling. As this is a form of bending, it is accompanied by tensile stresses.

⁶⁹ Section 3.1.1. of this Chapter. Actually, the material would, by definition, no longer be a glass if plasticity were to be introduced by a crystal structure.

⁷⁰ Although exceptions exist to this rule, see Figure 5.33, Chapter 5, Section 3.2.

⁷¹ Section 3.1.4. of this Chapter.

⁷² Actually, experimental research indicated that glass beams damaged with serious dents already showed severe resistance reductions (Appendix E, Section 4.2., Figure E.29), so that it should be expected that glass sheets can carry practically no tensile forces even when not completely broken, but ‘only’ highly cracked (e.g. > 50 % of a section).

⁷³ Which results in bending and thus also in tensile stresses.

- Failed, broken glass layers can still transfer compressive loads. Although theoretically not strictly necessary,⁷⁴ this ability can be used to obtain relatively high post-failure resistances.⁷⁵

From these starting points it follows that any glass element with post-failure resistance will have to be a composite, i.e. glass with a complementary component to transfer tensile stresses after glass breakage.

An LTM on element level is represented by a (statics) mechanics model. Its maximum resistance may thus be determined by material and geometrical properties. Failure may be induced either by:

- insufficient strength (material failure) or
- instability (stability failure).

4.3.1.1. Strength Governed Failure

Tension, compression, and bending are probably the most common loading types in construction.⁷⁶

Tension

The post-failure resistance of a tension-loaded glass element is fully determined by the tensile failure stress $\sigma_{t,max}$ and the section area A of the complementary component. Based on a sole consideration of the post-failure statics model, it would be concluded that the post-failure resistance is independent of the impact type causing failure (other than the effect the impact may directly have on the complementary component), as it does not rely on any post-failure behaviour of the (broken) glass.

Importantly though, the element post-failure behaviour does *not* solely depend on the post-failure statics model. Rather, the process in which the active LTM in the element shifts from the 1st to the 2nd plays a – in cases decisive – role in the post-failure behaviour. As will be discussed to a greater extent in Section 4, this process highly depends on the energy released during failure of the 1st LTM, and thus on the impact type as well as the relative stiffnesses of the 1st and 2nd LTM. As a result, an experimental investigation of an element's failure behaviour is always recommendable, even though the capacity of the post-failure statics model can usually be determined quite easily.

⁷⁴ E.g. in the double layer, PVB-laminated glass beams discussed in Chapter 7, Section 2 (Figures 7.2, 7.3, 7.4) and Appendix E, Section 4.3.2, the complementary component (PVB) is not stiff enough to allow any compressive stresses to build up in the broken glass, and the post-failure resistance is completely determined by the linear elastic bending in the PVB (and therefore also very low compared to the initial resistance of those beams).

⁷⁵ It is, off course, efficient to do so and probably even difficult to avoid when significant post-failure resistance is aimed at. The compressive strength of (broken) glass is unlikely to be a restrictive parameter in glass element post-failure performance. It was observed only once within the Zappi research project, in a post-tensioned glass beam (see also Section 4.3.4.1. of this Chapter). It has never occurred in any of the stainless steel reinforced glass beams tested over the years. Generally, it will be more likely, that it will be governed by tensile strength or stiffness of the complementary components transferring the tensile strength and/or keeping the glass together.

⁷⁶ Shear and torsion may also be recognized. Furthermore, distinction could be made between one- and two-dimensional tension, compression, and/or bending.

Compression

Glass elements whose failure behaviour is theoretically governed by compressive failure will be rare in practice. More likely, failure of such elements will be stability governed (i.e. buckling will occur before breakage by compressive stresses), especially since the compressive strength of glass is much higher than its (practical) tensile stress.⁷⁷ Care should be taken, though, to properly introduce compressive loads into a glass element to avoid premature failure from stress concentrations at the joints, and effectively utilize the actual compressive capacity of the glass.

The post-failure resistance is determined by the compressive strength of broken glass, of which little is yet qualitatively known. It has been shown⁷⁸ that it depends highly on the crack pattern density and the (tensile) stiffness of the complementary components keeping the glass together, as will be further discussed in Section 4 of this Chapter.

Finally, it should be noted that stability may not be governing for initial failure, but, since cracking causes decreased bending stiffness or, effectively, hinges, it may be governing for final failure.

Bending

Bending is arguably the most common loading case in building construction and structures. As it is the effect of a combination of compression, tension, and their mutual distance, the post-failure capacity of a bending-loaded glass element depends on the parameters listed above for each of those loading components individually. For failure, either the compressive or the tensile capacity may be governing – and the same comments with regard to impact dependence, compressive capacity, tensile stiffness, and stability, apply.

4.3.1.2. Stability Governed Failure

Contrary to the strength governed elements, elements whose failure behaviour is governed by instability derive their maximum resistance from:

- their bending stiffness and
- support conditions (which determine e.g. the buckling length).

It is important to realize that, since the stiffness also decides which LTM is active, it is impossible to create a purely stability failure governed glass element with a relative post-failure resistance greater than 1 ($r_{\text{res,III}} \leq 1$). If a $r_{\text{res,III}} > 1$ is required, this can only be obtained by introducing alternative load paths, or altering the geometry so that initial failure is no longer stability governed, but strength governed.

Often failure stems from a combination of loss of stability and exceeding of the material strength as a consequence. This happened, among others, with the buckling/

⁷⁷ The actual compressive failure stress of glass is not mentioned in any code, as it is not the checked property. Antonelli et al. list a compressive failure stress of 221 MPa, under reference to: Royer-Carfagni, G., Silvestri, M., *A proposal for an arch footbridge in Venice made of structural glass masonry*, Engineering Structures, Vol. 29, No. 11, 2007, pp. 3015-3025. Antonelli, A., Cagnacci, E., Giordano, S., Orlando, M., Spinelli, P., *Experimental and Theoretical Analysis of C-FRP Reinforced Glass Beams*, Proceedings of the 3rd International Symposium on the Application of Architectural Glass (ISAAG), Munich, October, 2008.

⁷⁸ Appendix E.

compression tests on welded glass tubes, see Figure 8.9.⁷⁹ Contrary to pure stability failure cases, it is not theoretically impossible to obtain post-failure resistances of > 100 %. As with bending governed cases, it requires a 2nd LTM with lower stiffness but higher resistance.⁸⁰

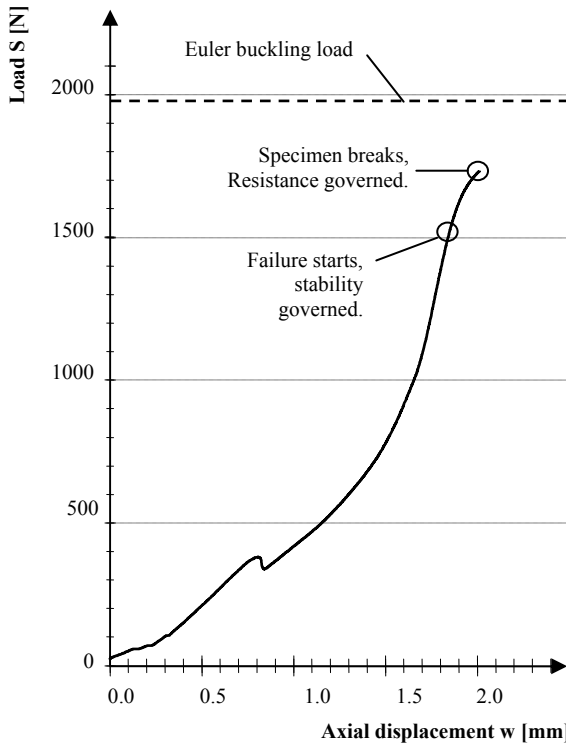


Fig. 8.9 Typical load-displacement graph for compression loaded specimen.

4.3.2. Laminating

The post-failure resistance of laminated elements, is highly dependent on load conditions, support conditions, aspect ratio, relative glass sheet thicknesses, glass type, and laminate type.⁸¹ While project specific tests have been regularly published⁸², no systematic investigation of the influence of all these parameters has yet been published, although some first steps were taken by Kott and Vogel, who introduced a distinction between three stages of failure in their investigation of post-failure behaviour of double layer laminated glass.⁸³ Nevertheless, from a range of published studies on impact

⁷⁹ *AdDoc III: Welding and Hot-Shaping Borosilicate Glass Tubes; Possibilities, Strength and Reliability*, additional document to this PhD, www.glass.bk.tudelft.nl, Section 3.4.

⁸⁰ In the redesign of the ATP columns (Chapter 10, Section 2.3.1), this has been attempted by applying glass fibre strands in the resin filled cavity between two glass tubes.

⁸¹ And thus also on environmental conditions that govern laminate behaviour.

⁸² E.g. Beer, B., *Structural Glass Engineering – a Review of Project Specific Testing*, Proceedings of the 9th Glass Performance Days, Tampere, Finland, 2005.

⁸³ Stage I corresponds with the undamaged state (not yet failed), stage II with one layer on the tensile side broken (partial glass failure), and finally stage III with both layers broken (full glass failure). In stage II, loads are mainly carried by the unbroken sheet, but somewhat stiffened by the particles of the broken sheet. In stage

resistance and residual strength of laminated glass, several observations can be made. Generally speaking, the overall stiffness of the element after failure determines the remaining load capacity.

4.3.2.1. Load Condition

For plate elements laminated with resins and soft foils, usually no residual strength can be obtained when the element strength is exceeded in (semi) static loading conditions. A bending test on a laminated element with continuously increasing load will yield linear elastic behaviour until complete failure and (almost) direct collapse.⁸⁴ Kott and Vogel observed this was independent of glass type. Even in annealed float glass, a direct loading test will cause so many cracks in a small region, effectively a hinge results which leads to instability and failure of the element.

However, when failure was caused by incidental actions, significant residual strength can remain. The extent of residual strength is again dependent on all factors mentioned above, but Kott and Vogel⁸⁵ found for annealed PVB-laminated double layer float glass values of around 25 % of the ultimate failure load.

The difference with direct loading stems from the number of overlapping cracks in the glass sheets. When two crack lines sheets coincide, they form a plastic hinge⁸⁶ with a certain maximum moment capacity determined by the strength of the laminate, the compressive strength of the (broken) glass and the inner moment arm. Such a plastic hinge also has a certain stiffness, i.e. for the given moment capacity to develop, it will deform (rotate) to a certain extent. The rotational stiffness of the plastic hinge is determined by the stiffnesses of the laminate and the (broken) glass. Now, the global deformation of the lamination may be limited if only one plastic hinge occurs. However, when, because of a more dense cracking pattern, a number of plastic hinges occurs closely together, the deformation will get very large. This will cause a gradual change in load carrying principle from plate bending into membrane action (Figures 8.10a – d). As the broken glass has no tensile capacity, this means increasing loads on the laminate foil which, in turn, will cause collapse. Also, other side effects, such as slipping from supports (membrane action requires horizontal force reactions in the supports) may cause collapse.

III, the laminate foil acts as reinforcement and carries tension, while the broken glass transfers compressive loads.

- Kott, A., Vogel, T., *Structural Behaviour of Broken Laminated Safety Glass*, in: Crisinel, M., Eekhout, M., Haldimann, M., Visser, R. (Eds.), *EU Cost C13 Final Report. Glass & Interactive Building Envelopes*, Research in Architectural Engineering Series, Volume 1, IOS Press, Amsterdam, the Netherlands, 2007, pp. 123 – 132.
- Kott, A., Vogel, T., *Remaining Structural Capacity of Broken Laminated Safety Glass*, Proceedings of the 8th Glass Performance Days, Tampere, Finland, 2003.

⁸⁴ This has been shown for plate-loaded panels by Kott and Vogel (Ibid), and for both plate loaded panels as well as (standing) beams by Hess, R., *Glasträger. Forschungsbericht*, ETH Zürich, Switzerland, 2000. However, these observations do not completely agree with the experimental results in Appendix E. Rather, the author found very small residual resistances in PVB laminated annealed glass beams after overloading. Nevertheless, these residual resistances were so small, they could be ignored practically just as well.

⁸⁵ Kott, A., Vogel, T., *Remaining Structural Capacity of Broken Laminated Safety Glass*, Proceedings of the 8th Glass Processing Days, Tampere, Finland, 2003.

⁸⁶ Kott and Vogel refer to this as a *yield line*.

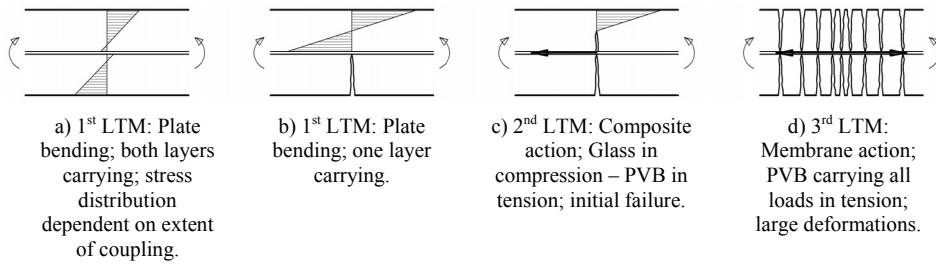


Fig. 8.10a – d Load transfer mechanisms in a laminated glass sheet, loaded in plate bending and developing into membrane action.

For laminated beams, a similar difference in post-failure resistance of directly overloaded specimens and specimens overloaded after impact damage, was found (Appendix E). Here, too, a significant difference in crack pattern density was observed, which stems from the difference in elastic strain energy stored in the element and released upon failure.⁸⁷ For impact load, this is usually much lower (the impactor may carry much more kinetic energy upon impact, but only transmits a portion of this to the glass panel) than for static overloading.

4.3.2.2. Support Conditions

The support conditions greatly influence the element stiffness and load carrying mechanisms. Normally, four-side supported panels perform better than two-side supported ones, which in turn may perform better than point supported panels. More extensive supports will make it less likely that a crack pattern will cause instability through the formation of (plastic) hinges.

Besides the influence on the element stiffness, the supports themselves may also play a crucial role in the failure process. When the broken element develops membrane stresses, reaction forces are required in the supports, or the element will slide off. Furthermore, when the support is designed so that reaction forces *can* be resisted, the laminate may be overstressed itself and tear near or around the support. Nugue and Savinea⁸⁸ have claimed this would not happen for PVB laminated point supported glass loaded in self weight after full glass breakage, but this has been disputed, for instance, by Neugebauer⁸⁹, who developed a special reinforcement to prevent laminated glass to tear from point supports. Unfortunately, extensive comparative studies are lacking.

⁸⁷ See also Chapter 9.

⁸⁸ Nugue, J.-C., Savineau, G., *Safe Post-Breakage Behaviour of Point Fixed Glazing Systems – More Than a Case Study a Real Breakthrough*, Proceedings of the Glass Performance Days, Tampere, Finland, 2003.

⁸⁹ Neugebauer, J., *A Special Fixation With Which the Broken Laminated Safety Glass Is Prevent From Falling Down*, Proceedings of the 9th Glass Performance Days, Tampere, Finland, 2005. He shows an example photo of broken laminated thermally tempered glass, torn from one of its point fixings, taken from: Wirtschaftsministerium Baden-Württemberg, *Bauen mit Glas, Information für den Bauherrn, Architekten und Ingenieure*, Germany, 2002.

4.3.2.3. Relative Glass Sheet Thicknesses

For plates, Kott and Vogel⁹⁰ found that the residual strength is approximately proportionally higher when the compressive layer is thicker than the tensile layer. This is caused by an increase in internal moment arm.

4.3.2.4. Glass Prestress

Again, no systematic comparisons exist. It is generally assumed that thermally tempered glass after full glass failure turns into a ‘wet towel’, i.e. a shape that is practically completely dominated by the laminate behaviour (usually PVB). Heat strengthened and annealed glass are supposed to fracture in a such a pattern that they can still contribute to the element stiffness.

Some nuancing remarks have to be made, however. When loading PVB laminated double layer annealed, heat strengthened and thermally tempered specimens to model damage level I (bottom layer broken)⁹¹, Kott and Vogel found all specimens suffered some permanent deformation. The thermally tempered specimens most; the annealed specimens least; the heat strengthened specimens in between. Hence, the broken glass layer contributes to the element stiffness also after breakage, but to varying extent depending on crack pattern density. On the other hand, experimental research by Weller & Weimar⁹² on polyurethane glued glass-polycarbonate (PC) laminates showed that the element stiffness after glass breakage was independent on glass type – results were practically equal for broken annealed and broken thermally tempered glass. Thus, the post-failure element stiffness not only depends on the crack pattern density, but also on how well the glass fragments are held together. The PC obviously holds them together much better than a PVB layer. Post-failure behaviour of heat treated glass can therefore be improved by improving the stiffness of the laminate layer.

4.3.2.5. Laminate Material

The material behaviour of PVB, the most used laminate material, has been extensively investigated. Belis et al.⁹³ note reliable material laws (e.g. for FE analysis) can be found with several authors. Other laminate materials have received significantly less attention. Cast resins have a low tear resistance and are generally considered not to be sufficiently cohesive to carry any significant (tensile) loads themselves after glass breakage. Thus

⁹⁰ Kott, A., Vogel, T., *Structural Behaviour of Broken Laminated Safety Glass*, in: Crisinel, M., Eekhout, M., Haldimann, M., Visser, R. (Eds.), *Ibid*.

⁹¹ Kott and Vogel refer to this as stage II.

⁹² Weller, B., Weimar, T., *Glass-Polycarbonate-Sandwich-Elements as Overhead Glazing*, Proceedings of the 10th Glass Performance Days, Tampere, Finland, 2007.

⁹³ Belis, J., Beken, J. vander, Impe, R. van, Callewaert, D., *Performance of Glass-Ionoplast Laminates Above Room Temperature*, Proceedings of the 10th Glass Performance Days, Tampere, Finland, 2007. They list:

- D’Haene, Pol, *Structural Glazing – Creep Deformation of PVB in Architectural Applications*, Proceedings of the 7th Glass Performance Days, Tampere, Finland, 2001.
- Schuler, C., *Einfluss des Materialverhaltens von Polyvinylbutiral auf das Tragverhalten von Verbund sicherheitsglas in Abhängigkeit von Temperatur und Belastung*, Berichte aus dem Konstruktiven Ingenieurbau, Technische Universität München, Germany, 2003.
- Sobek, W., Kutterer, M., Messmer, R., *Rheologisches Verhalten von PVB im Schubverbund*, Forschungsbericht, Universität Stuttgart, Germany, 1998.
- Duser, A. van, Jagota, A., Bennisson, S.J., *Analysis of Glass/PVB Laminates Subjected to Uniform Pressure*, Journal of Engineering Mechanics, Vol. 125, No. 4, April 1999.

they are often (at least in Germany, see e.g. Wruk et al.⁹⁴) not allowed to use as laminated safety glass (e.g. for overhead glazing).

Like cast resins, EVA is often not allowed for laminated safety glass. However, a comparison between PVB and EVA made by Weller et al.,⁹⁵ indicates that EVA with an appropriate acetate content⁹⁶ has a tensile strength comparable to PVB (approximately 20 MPa for PVB vs 10 – 25 MPa for EVA). The shear stiffness is higher for temperatures above 25 °C and somewhat lower for temperatures below 10 °C. This seems to indicate EVA could perform just as well as PVB in post-failure situations, although Weller et al. do indicate further research in this area is required.

Research results on SG can be found with Belis,⁹⁷ Belis et al.,⁹⁸ Delincé et al.,⁹⁹ Bucak & Meissner,¹⁰⁰ and Sackmann & Meissner.¹⁰¹ Its stress-strain behaviour deviates significantly from that of PVB at room temperature, due to the higher glass transition temperature. The modulus of elasticity is thus more than 15 times higher (0.3 MPa versus 0.018 MPa). The difference in shear modulus¹⁰² is significant for loading times between 10^{-2} and 10^{12} seconds and can vary almost as much as a factor 100. At 34.5 MPa, its tensile strength is also considerably higher. Not only does this imply the reinforcing properties of the laminate are much better than that of PVB, the increased stiffness will also better allow broken glass to transfer compressive forces (as argued above). Thus, a failed SG-laminated glass plate can longer rely on a plate bending load carrying mechanism (broken glass for compression and SG for tension) before switching to a membrane mechanism (only tensile forces, transferred by SG) than PVB laminated glass.

As shown in Appendix E, the relevance of the laminate material stiffness to the compressive capacity of the broken glass part also applies to beams. The difference in post-failure resistance between PVB- and SG-laminated beams was more than could be expected based on the difference in laminate tensile strength and thickness alone. The SG stiffness actually allowed another 2nd LTM to develop (Figures 8.11 a and b).

Despite increasing numbers of publications on SG, it should be noted the quantity of available data on SG behaviour is considered to be still quite low by glass engineering

⁹⁴ Wruk, N., Schutte, A., Hanenkamp, W., *Load Bearing Behaviour of Laminated Glass Under Static and Dynamic Load*, Proceedings of the 6th Glass Performance Days, Tampere, Finland, 1999.

⁹⁵ Weller, B., Wünsch, J., Härth, K., *Experimental Study on Different Interlayer Materials for Laminated Glass*, Proceedings of the 9th Glass Performance Days, Tampere, Finland, 2005.

⁹⁶ The acetate content strongly influences the mechanical behaviour of EVA. Generally speaking, a higher acetate content increases the tear resistance and elongation at fracture but lowers the melting temperature. Weller et al. used an EVA with 32 % acetate content.

⁹⁷ Belis, J., *Kipsterkte van monolithische en gelamineerde glazen liggers*, Dissertation, Laboratory for Research on Structural Models, Ghent University, Ghent, Belgium, 2005.

⁹⁸ Belis, J., Beken, J. vander, Impe, R. van, Callewaert, D., *Performance of Glass-Ionoplast Laminates Above Room Temperature*, Proceedings of the 10th Glass Performance Days, Tampere, Finland, 2007

⁹⁹ Delincé, D., Callewaert, D., Belis, J., Impe, R. van, *Post-breakage Behaviour of Laminated Glass in Structural Applications*, Proceedings of the Challenging Glass Conference, Delft, the Netherlands, May 2008.

¹⁰⁰ Bucak, Ö., Meissner, M., *Trag- und Resttragfähigkeitsuntersuchungen an Verbundglas mit der Zwischenschicht "Sentry Glas Plus"*, Abschlussbericht AiF-Forschungsprojekt, Munich, Germany, 2005.

¹⁰¹ Sackmann, V., Meissner, M., *On the Effect of Artificial Weathering on the Shear Bond and the Tear Strength of two Different Interlayers of Laminated Glass*, Proceedings of the 2nd International Symposium on the Application of Architectural Glass (ISAAG), Munich, Germany, 2006.

¹⁰² Delincé, D., Callewaert, D., Belis, J., Impe, R. van, Ibid.

practitioners.¹⁰³ Furthermore, there are some doubts about the consistency of the quality of the laminated product because the laminating process is more difficult than that of PVB.

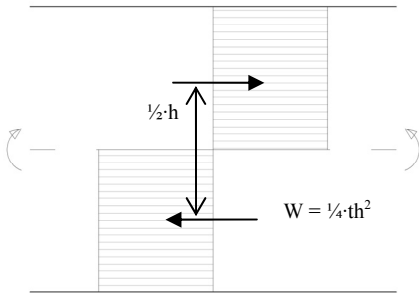


Fig. 8.11a Load transfer mechanism in a double layer PVB laminated glass beam, after overloading: only the PVB is active in (approximate) linear elastic bending.

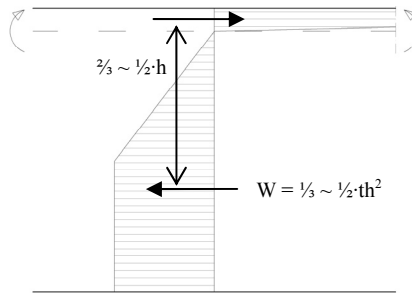


Fig. 8.11b Load transfer mechanism in a double layer SG laminated glass beam, after overloading: composite action between the glass in compression and the SG partially in elastic, partially in plastic bending.

4.3.2.6. Laminate Plates with Reinforcement

Since both PVB and SG adhere well to several metals, it is possible to incorporate a layer of steel-wire mesh or perforated sheet in a laminated glass plate, between two layers of laminate material. As both the strength and the tensile stiffness of these materials are considerably larger than those of polymer laminates, a significant increase in post-failure resistance may be expected. Feirabend & Sobek¹⁰⁴ presented a study on the pre- and post-failure performance of such laminates (Figure 8.12). They found significant post-failure resistance improvements, particularly for temperatures above $T_{g,lam}$ of the laminate. Table 8.1 lists some of their results.¹⁰⁵

Contrary to expectation, the post-failure resistance is not solely governed by the steel-wire mesh behaviour. The laminate material shear stiffness is still crucial, as can be deduced from the significant differences between the post-failure resistance of PVB- and SG steel-wire mesh laminate plates.

¹⁰³ Based on survey results in Chapter 5, Sections 2.2.6. Since the survey (2007), a steady stream of publications on SG has been produced. Thus, this obstacle may have been overcome by now.

¹⁰⁴ Feirabend, S., Sobek, W., *Reinforced Laminated Glass*, Proceedings of the Challenging Glass Conference, Delft, the Netherlands, May 2008. Figure 8.12 is taken from this publication.

¹⁰⁵ Unfortunately, Feirabend & Sobek do not present pre-failure resistances. Thus, only a limited comparison is possible. Furthermore, although noting the importance of the impact type causing failure (e.g. direct overloading, glass cutter, punch) for the post-failure performance (see observations made in Appendix E), they do not state clearly which impact was applied to the specimens tested for post-failure resistance, or comment on which impact should be preferred in testing.

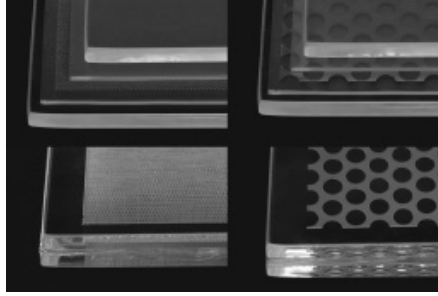


Fig. 8.12 Laminated glass with steel-wire mesh and perforated sheet incorporated between two layers of laminate material.

Table 8.1 Approximate maximum post-failure resistances of laminated glass plates with and without steel-wire mesh reinforcement, at different temperature levels. Composed from data presented by Feirabend & Sobek.

Laminate and reinforcement	Maximum post-failure resistance [N]		
	at 23 °C	at 40 °C	at 70 °C
PVB	n/a	n/a	n/a
PVB and steel-wire mesh	600	500	200
SG	425	125	0
SG and steel-wire mesh	1500	1000	700

4.3.3. Additional Transparent Polymer Sheets

Occasionally, a combination of glass and polymer sheets has been applied.

The structural glass design of many staircases by Eva Jiricna (Fig. 8.13) was done by Macfarlane (Appendix C, Section 4). To obtain treads with safe failure behaviour, he simply added an acrylic sheet underneath the (annealed) glass tread – without laminating it to the glass. The one time such a glass tread has broken, the assembly behaved exactly as one would expect: the acrylic took the loads under rather large deformations. The post-failure resistance was equal to the resistance of the acrylic sheet.

In the cantilevering entrance canopy to the Yurakucho subway station in Tokio, Japan (Figure 8.6), acrylic sheets were added to the glass laminate to ensure safe failure behaviour on instigation of the client. Macfarlane did not feel this was absolutely necessary.¹⁰⁶ Several earthquakes have shook the area since completion, but no failures have yet occurred.

¹⁰⁶ Appendix D, Section 4.

Glass-PC laminates are used as bullet-proof glazing, but some time ago, Veer et al.¹⁰⁷ already showed glued glass-PC laminates can also present considerable post-failure resistance. For plates, the maximum post-failure resistances could not be determined because the maximum displacement within the experimental set-up was reached, but could be expected to be in the order of $r_{res,III} > 100\%$. Post-failure resistances of approximately $r_{res,III} \approx 80\%$ were found for beam specimens ranging from 420 mm to 2 m in length.¹⁰⁸ With the PC thickness only approximately one-third or less of the glass thickness, it is obvious the residual strength is not solely provided by the PC, but rather by the glass-PC composite action, with glass in compression still playing a vital role.

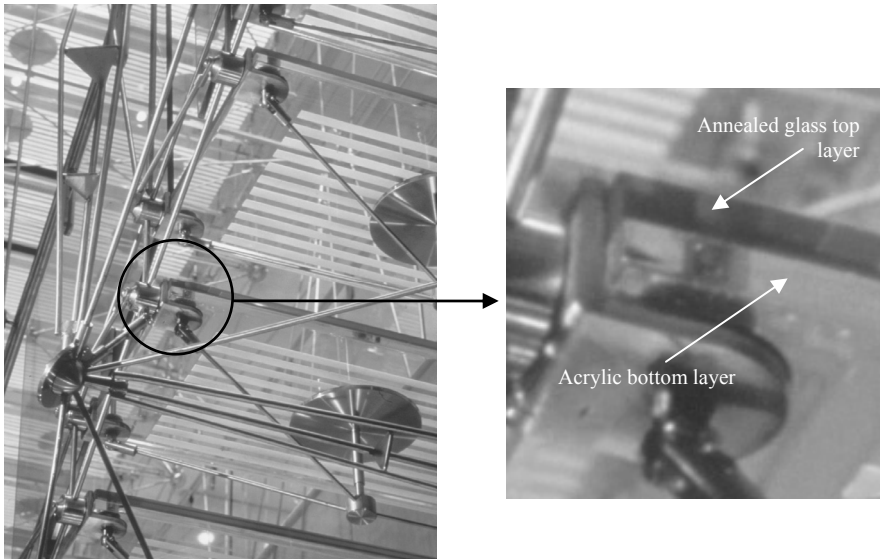


Fig. 8.13a, b Glass staircase. Architectural design: Eva Jiricna. Structural Glass design: Tim Macfarlane.

In the 2 m beams, the PC often ruptured at failure, causing collapse. This should be attributed to elastic strain energy release (the failure stress is comparable to that in the small samples), see Chapter 9.

The post-failure performance of glass-PC laminates was globally confirmed by more recent research by Weller et al.¹⁰⁹, although their study focused on pre- and post-failure stiffness rather than resistance.

Despite its favourable performance, glass-PC laminates are seldom (if ever) applied in practice. In Section 2 of Chapter 5, it was shown there is considerable doubt with

¹⁰⁷ For (standing) beams: Veer, F.A., Liebergen, M.A.C. van, Vries, de S.M., *Designing and engineering transparent building components with high residual strength*, Proceedings 5th glass processing days, Tampere, Finland, 1997, and later publications. For plates: Veer, F.A., Vries, S.M. de, *Transparent laminated composites for novel architectural structures*, Proceedings 9th European Conference on Composite Materials, Brighton, UK, 2000.

¹⁰⁸ Post-failure resistances obtained by direct overloading in four-point bending tests.

¹⁰⁹ Weller, B., Weimar, T., *Glass-Polycarbonate-Sandwich-Elements as Overhead Glazing*, Proceedings of the 10th Glass Performance Days, Tampere, Finland, 2007.

structural glass engineers about the added value of PC in laminates (in relation to the price and difficulty of manufacture), and the long term behaviour and quality of both the PC and the PC-Glass adhesive bond.

4.3.4. Reinforced Glass Beams

A hitherto rarely in practice applied, but highly effective method of obtaining post-failure strength, is reinforcing beams with a strand of another, stronger and more stiff material. Concepts with two materials, steel and carbon-fibre reinforced polymers (CFRP) have been developed at several institutes and engineering offices.

4.3.4.1. Steel reinforcement

The concept of stainless steel reinforced beams was initially presented by Veer et al.¹¹⁰ in 2003, in a beam design in which it was combined the previously developed glass-PC laminate. After evaluation, it was felt the steel reinforcement actually made the PC obsolete, and was therefore omitted in subsequent designs. Since then, the Zappi research group has presented a range of studies on the failure behaviour reinforced glass beams.^{111, 112, 113} The research focus has mainly been to experimentally prove the feasibility of the concept both with regard to mechanical functionality, economy, and durability. Investigated parameters included glass section geometries and spans, reinforcement sections, adhesive bond geometries, adhesive types, effect of load duration, temperature and other environmental conditions,¹¹⁴ stress distribution in the post-failure condition, and manufacturing methods. Typically, post-failure resistances of $r_{res,III} = 120 - 150 \%$ can be expected. A typical section consists of 3 layers of annealed glass, with a receding middle layer to create a groove in which the reinforcement profile is placed (see e.g. Chapter 7, and Appendices H and I).

A beam with additional post-tensioning by a rod through the reinforcement box profile has also been tested.¹¹⁵ This was the only prototype ever observed by the group to collapse by compressive failure of the glass part (Figure 8.14a, b), at a post-failure resistance of 117 %.

¹¹⁰ Veer, F.A., H. Rijgersberg, D. Ruytenbeek, P.C. Louter, J. Zuidema, *Composite glass beams, the third chapter*, Proceedings of the 8th international conference on Architectural and Automotive Glass (GPD), Tampere, Finland, 2003.

¹¹¹ E.g.: Louter, P.C., J. Belis, F.P. Bos, F.A. Veer, G.J. Hobbelman, *Reinforced glass cantilever beams*, Proceedings of the Glass Processing Days, Tampere, Finland, 2005; J. Belis, R. van Impe, P.C. Louter, F.A. Veer, F.P. Bos, *Design and Testing of Glass Purlins for a 100 m² Transparent Pavilion*, Proceedings Glass Processing Days, Tampere, Finland, June 2005; Veer, F.A., Gross, S., Hobbelman, G.J., Vredeling, M., Janssen, M.J.H.C., Berg, R. van den, Rijgersberg, H., *Spanning structures in glass*, Proceedings Glass Processing Days, Tampere, Finland, 2003.

¹¹² A particularly extensive discussion can be found in: Louter, P.C., *Adhesively bonded reinforced glass beams*, HERON Volume 52 (2007) issue 1/2 special issue: Structural glass, <http://heron.tudelft.nl>.

¹¹³ Appendices H and I.

¹¹⁴ Louter, P.C., Veer, F.A., Belis, J., *Redundancy of Reinforced Glass Beams: Temperature, Moisture, and Time Dependent Behaviour of the Adhesive Bond*, Proceedings of the Challenging Glass Conference, Delft, the Netherlands, May 2008.

¹¹⁵ Bos, F.P., F.A. Veer, G.J. Hobbelman, P.C. Louter, *Stainless steel reinforced and post-tensioned glass beams*, Proceedings of the 12th International Conference of Experimental Mechanics (ICEM12), Bari, Italy, 2004.

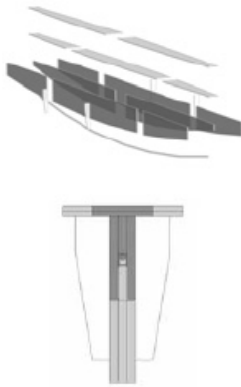


Fig. 8.14a Design of reinforced, post-tensioned, T-shaped glass beam.



Fig. 8.14b Explosive final failure of the compression zone in a reinforced, post-tensioned T-shaped glass beam.

Several adhesives have been tried to combine the components together. Usually, a UV-curing acrylate is used for both the glass-glass and glass-steel bonds. Recently, an alternative using SG was developed (Figure 8.15a, b).¹¹⁶ The experimental results have not (yet) been used in developing a predictive model for the post-failure strength, although the simple static model as applied e.g. in Appendix I (reproduced here in Figure 8.16) provides a rough estimate of what may be expected.

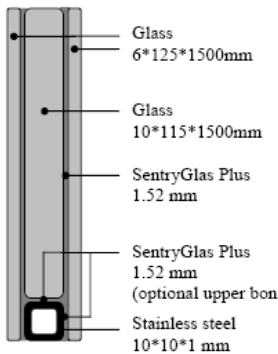


Fig. 8.15a Section design of SG-laminated, stainless steel reinforced glass beam.

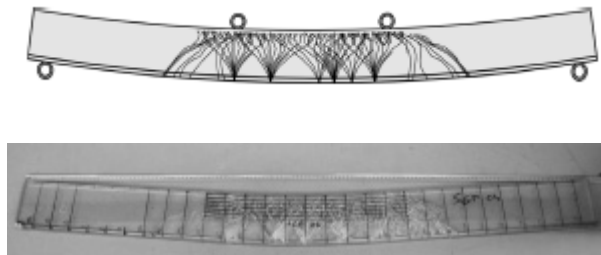


Fig. 8.15b Crack pattern in SG laminated, reinforced glass beam: schematic and picture.

¹¹⁶ Appendix I, and: Louter, P.C., Bos, F.P., Veer, F.A., *Performance of SGP and adhesively bonded metal reinforced glass beams*, Proceedings of the International Symposium on the Architectural Application of Glass, Munich, Germany, 2008.

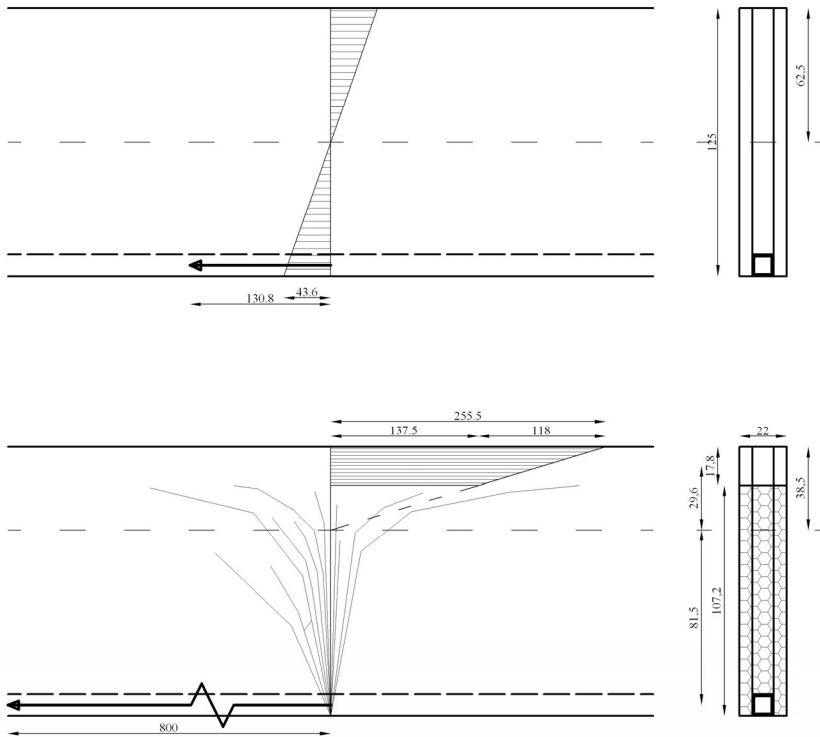


Fig. 8.16 Approximate load transfer mechanism of reinforced glass beam in pre- and post-initial failure stage (reprint of Figure L.10).

It has been assumed the crack patterns of heat strengthened and thermally tempered glass would be too dense to obtain significant post-failure strengths with this concept. However, the experimental results presented in Appendix E, as well as e.g. the research of Weller et al. on glass-PC laminates, seem to indicate that when the tensile component is sufficiently stiff (and it may be expected the steel profile is), the crack pattern density is of less consequence to the maximum post-failure resistance. The manufacturing obstacle related to thermally treated glass, i.e. that it is hard to bond with acrylate adhesives with little filling capacity, is overcome by the introduction of SG-laminated, reinforced glass beams. Thus, beams with high strength, little stress corrosion, and high post-failure strength without over sizing may very well be developed in the near future.

Researchers from the Technical University of Denmark have also explored the concept of steel reinforced glass beams. The specimen section design is given in Figure 8.17. Annealed float glass was used. Contrary to most of the beams developed in Delft, the glass layers are laminated with PVB. The reinforcement is bonded to the glass with a two component epoxy. Nielsen & Olesen¹¹⁷ found post-failure resistances of $r_{res,III} \approx 120 - 170\%$ depending on the reinforcement section (120 or 240 mm²). Although no predictive post-failure resistance model was developed, the failure behaviour was

¹¹⁷ Nielsen, J.H., Olesen, J.F., *Mechanically Reinforced Glass Beams*, Proceedings of the third international conference on Structural Engineering, Mechanics, and Computation (SEMC), Cape Town, South Africa, 2007.

modelled using FEA. The cracks were modelled by a reduction of E from 70 to 0.5 GPa when a predefined failure stress was exceeded. Weak spots (with a defined failure stress lower than the rest) were introduced at 30 mm intervals. According to the Nielsen & Olesen, this allowed for reasonable modelling of the crack development. Too few experiments (only 4 specimens) were conducted to conclude whether or not this method provides a reliable post-failure resistance prediction. It may be questioned whether the dynamic (energy driven) effects of crack growth are properly taken into account this way.

Despite its promising failure behaviour, steel reinforced glass beams have not been widely applied in practice. Perhaps the only example is provided by the glass roof of the Thermal Spa in Badenweiler, Germany (Fig. 8.18) which contains glass beams of three layer laminated, thermally tempered glass¹¹⁸. The middle ply is recessed. In the groove thus created, an aluminium U-profile has been placed and a stainless steel cable has been fed through the profile. The cable has been post tensioned. The profile and cable should keep the glass together in case of glass failure. Unlike the concepts developed at the universities, the glass was fully tempered. According to unpublished research by the FH Munich,¹¹⁹ considerable post-failure resistance was still possible – in line with the argument given above.

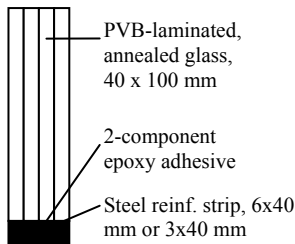


Fig. 8.17 Section of reinforce annealed glass beams investigated by Nielsen & Olesen.



Fig. 8.18 Glass beam (detail) at the Spa Thermen in Badenweiler.

4.3.4.2. CFRP Reinforcement

Around the time the concept of steel-reinforced glass beams was introduced, another reinforcement scheme was applied in a reconstruction project in Arquà Petrarca, Italy (Fig. 8.19a, b).¹²⁰ Here, beams from PVB-laminated annealed glass are reinforced with a rectangular strand of CFRP, adhesively bonded to the beams bottom edge. These were developed by Vetrostrutturale and the Politecnico in Brescia. The applied beams span approximately 12 m in a tri-hinged frame structure. Each individual beam is 6 m long, 500 mm high, and 4 layers thick. A rectangular profile CFRP strip is adhesively bonded

¹¹⁸ Schober, H., H. Gerber, J. Schneider, *Ein Glashaus für die Therme in Badenweiler*, Stahlbau 73, Heft 11, 2004, pp. 886-892.

¹¹⁹ Bucak, Ö., *Gutachterliche Stellungnahme zur Glasdachkonstruktion beim Bauvorhaben Therme Badenweiler*, 06/2003.

¹²⁰ Palumbo, M., *A new roof for the XIIIth Century "Loggia de Vicari" (Arquà Petrarca –PD, Italy) based on structural glass trusses: a case study*, Proceedings of the 9th international conference on Architectural and Automotive Glass (GPD), Tampere, Finland, 2005.

to the beams bottom edge. The outer layers are sacrificial, i.e. they have not been considered in the resistance calculations. Experimental tests on smaller specimen gave a very high post-failure resistance of $r_{res,III} \approx 180\%$. Like the Zappi Research group, Palumbo assumed the use of annealed glass was necessary to allow sufficient compression to build up in the broken glass. For reasons discussed above, heat strengthened glass and thermally tempered glass may work as well.



Fig. 8.19a Loggia dei Vicari, Arquà Petrarca (PA), Italy.

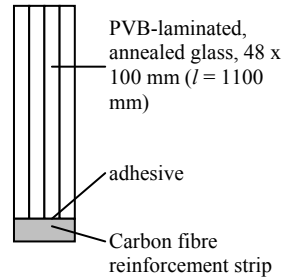


Fig. 8.19b Section of the CFRP reinforced glass beams applied at the Loggia dei Vicari.

More recently, Antonelli et al.¹²¹ and Cagnacci et al.¹²² presented results on CFRP-reinforced glass façade fins. The inner layer of the triple layer, PVB-laminated, annealed glass fin was recessed on both sides to create grooves in which round section CFRP bars were placed (Figure 8.20). Reinforcement on two sides was required because wind loads may act in either direction. Several types of adhesive were applied to fill the cavity between the glass and the reinforcement bar. Smooth and ribbed bars were used, to investigate the effect on adhesive bonding and beam failure behaviour.

Antonelli et al. present a simple mechanical model to predict the post-failure resistance, similar to the method applied in Appendices H and I. This yields $r_{res,III} \approx 188\%$. Such values, however, were not obtained in testing. The smooth bar prototypes have $r_{res,III} \approx 20\%$. Out of three ribbed bar specimens, one broke by adhesive failure at $r_{res,III} \approx 60\%$, while the other two collapsed through failure of the reinforcement at $r_{res,III} \approx 75\%$ and $r_{res,III} \approx 83\%$, respectively. Obviously, the adhesive bond governs failure in most specimens and would thus need improvement. The premature failure of the reinforcement, though, is remarkable and unfortunately not specifically discussed. In general, Antonelli et al. attribute the early failures to dynamic effects at failure, i.e. strain energy release.

¹²¹ Antonelli, A., Cagnacci, E., Giordano, S., Orlando, M., Spinelli, P., *Experimental and Theoretical Analysis of C-FRP Reinforced Glass Beams*, Proceedings of the 3rd International Symposium on the Architectural Application of Glass (ISAAG), October 2008, Munich, Germany.

¹²² Cagnacci, E., Orlando, M., Pecora, M. L., Spinelli, P., *Application of C-FRP Strengthened Glass Beams in Façade Design*, Proceedings of the 3rd International Symposium on the Architectural Application of Glass (ISAAG), October 2008, Munich, Germany.

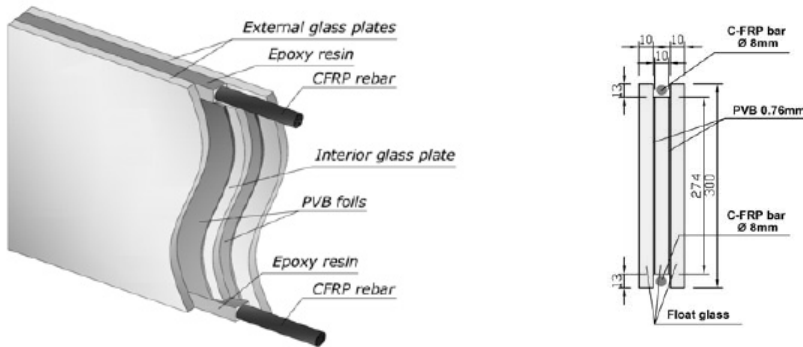


Fig. 8.20a, b CFRP reinforced facade fins, proposed by Antonelli et al. and Cagnacci et al.

Cagnacci et al. present an FE-model to predict crack growth and post-failure resistance. The method applied is similar to that of Nielsen & Olesen: the Young's modulus of the element that reaches its failure stress is reduced by $1/100^{\text{th}}$ of its original value. However, as applied this reduction manually controlled, it was very time consuming, thus they only modelled the first three steps. Contrary to the analytical model presented by Antonelli et al., this results in a predicted post-failure resistance of approximately $r_{\text{res,III}} \approx 100\%$, which is much closer to the experimental results. They, too, attribute the remaining gap to the effects of energy release, which were not incorporated in the FE-model.

4.3.5. Hybrid Elements

4.3.5.1. Glass-Wood Elements

The development of glass-wood hybrid elements seems to be driven not just by a search for increased safety, but at least as much from an aesthetic desire. Such elements have been extensively investigated at the EPFL by Hamm¹²³ and Kreher.¹²⁴

Hamm investigated in- and out-of-plane loaded panels as well as I-section beams, consisting of four timber sections and a single annealed glass sheet. For beams, post-failure resistances of up to $r_{\text{res,III}} \approx 250\%$ were found. An analytical model was developed to calculate the initial failure resistance (found to be in good agreement with experimental results), both for an annealed glass and a thermally tempered glass web. The model did not include the post-failure resistance. Based on the analytical model and experimental results, Hamm also presented a dimensioning concept (*Bemessungskonzept*). For a thermally tempered web, he proposed to dimension a beam so that the calculable material strength is equal to or exceeds the ultimate limit state (uls) action – on the argument that glass failure would cause immediate collapse as the disintegration of the web would make a 2nd LTM impossible. For annealed glass, a beam would have to be dimensioned so that the calculable material strength is equal to

¹²³ Hamm, J., *Tragverhalten von Holz und Holzwerkstoffen im Statischen Verbund mit Glas*, PhD Thesis Nr. 2065, IBOIS/EPFL, Lausanne, Switzerland, 1999.

¹²⁴ Kreher, K., *Tragverhalten und Bemessung von Holz-Glas-Verbundträgern unter Berücksichtigung der Eigenspannungen im Glas*, PhD Thesis Nr. 2999, IBOIS/EPFL, Lausanne, Switzerland, 2004. See also: Kreher, K., Natterer, J., Natterer, J., *Timber-Glass-Composite Girders for a Hotel in Switzerland*, Structural Engineering International, No. 2, 2004, pp. 149-151.

or exceeds the serviceability limit state action (sls). The absence of a specific post-failure requirement is a fundamental mistake in both proposals. Because of the many possible glass failure causes, a system relying on a single sheet of thermally tempered glass is extremely dangerous. With a post-failure resistance of approximately 250 %, the annealed glass variant is in itself not unsafe, even when dimensioned to the sls, but applying such an approach is generally risky as other designs (e.g. with smaller timber components) may not boost the same post-failure resistance. As a rule, dimensioning for failure should never be related to sls-actions as they are by definition not related to (acceptable) structural failure probabilities.¹²⁵

Kreher also worked on in-plane loaded panels and further developed the I-beam concept investigated by Hamm. He was involved in their application in a hotel in Switzerland (Fig. 8.21a, b).¹²⁶ Kreher extended the dimensioning model and tested beams with annealed glass, several strengths (ranging from 25 to 70 MPa) of heat strengthened glass, and thermally tempered glass. He found relative post-failure resistances of $r_{\text{res,III}} \approx 300\%$ for annealed glass webs, $r_{\text{res,III}} \approx 200\%$ for low strength heat strengthened glass webs, $r_{\text{res,III}} \approx 100\%$ for medium strength heat strengthened glass webs, and $r_{\text{res,III}} = 0\%$ for thermally tempered glass webs. For the annealed and heat strengthened beams it is not clear whether the reduction in $r_{\text{res,III}}$ is caused solely by the higher initial failure resistance or also by a lower absolute post-failure resistance. Importantly, final failure in some of the heat strengthened and most of the annealed glass beams was caused by shear failure of the glass. Thus, a simple bending-based mechanics model for the section overestimates the post-failure resistance. Like Hamm, Kreher proposed a dimensioning concept in which he discerned between glass-wood beams with glass with a surface prestress of < 50 MPa and > 50 MPa. To the latter, he would apply existing glass dimensioning methods (e.g. Shen, GÜsgen, EN 13474), similar to Hamm. For the low prestress beams, he proposed to apply the existing glass dimensioning methods with altered material partial factors: $\gamma_M = 1.0$ and $\gamma_V = 1.0 - 1.1$ for prestresses of 25 – 50 MPa. As discussed above, this approach to the high-stress glass beams must be considered rather dangerous. For low-stress glass beams, this approach also has significant weaknesses. Reducing the material factor from $\gamma_M = 1.8$ to 1.0, means the post-failure resistance should be at least approximately 1.8 in order to maintain the same level of safety. Since the approach does not include any post-failure requirements, there is no guarantee this is actually achieved. Furthermore, reducing the material factor with this number may lead to many costly replacements, which should be deemed undesirable even if they are not accompanied by actual collapses. Fundamentally, the initial resistance requirements should not be decreased without adding post-failure requirements.

¹²⁵ See extensive discussion in Chapter 6, Section 5.3.2.

¹²⁶ Perhaps adversely to the possibilities presented by the glass-wood beam concept, thermally tempered glass was used in the beams applied at the Palafitte Hotel. Post-failure resistance was thus not obtained by composite glass-wood action. Rather, the section of the wooden upper flange was enlarged to provide sufficient post-failure strength.



Fig. 8.21a Hotel Palafitte, Monruz (NE), Switzerland, 2002. Structural glass engineer: IBOIS Institute, EPFL, Lausanne, Switzerland.

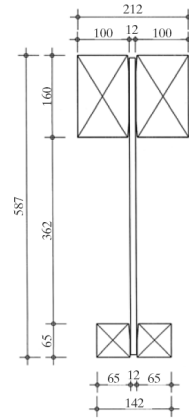


Fig. 8.21b Section of the glass-wood beams applied at the Hotel Palafitte. A thermally tempered 12 mm single sheet of glass was used.

Lately, glass-wood beams and glass-wood panels have also been presented by Cruz & Pequeno (Figure 8.22).¹²⁷ For beams, they have obtained post-failure resistances of $r_{res,III} \approx 135\%$ (box sections) – 185% (I-sections).

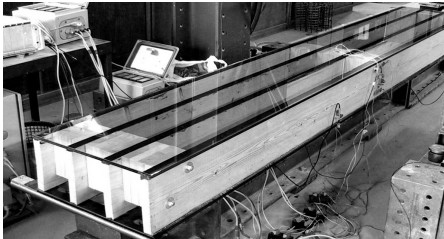


Fig. 8.22 Glass-wood panels (Cruz et al.).

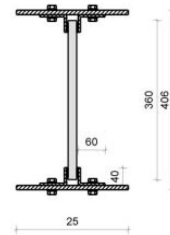


Fig. 8.23 Glass-steel beams (section), by Wellershof & Sedlacek.

4.3.5.2. Glass-Steel Elements

An I-section beam with steel flanges and a glass web was presented by Wellershof & Sedlacek¹²⁸ (Figure 8.23), particularly to increase the lateral torsional buckling resistance, mentioned to often be governing in the dimensioning of glass façade fins. Unfortunately, the pre- and post-failure resistance was not discussed.

¹²⁷ Cruz, P., Pequeno, J., *Timber-Glass Composite Beams: Mechanical Behaviour & Architectural Solutions*, Proceedings of the Challenging Glass Conference, Delft, the Netherlands, 2008; and: Cruz, P., Pequeno, J., *Timber-Glass Composite Structural Panels: Experimental Studies & Architectural Applications*, Proceedings of the Challenging Glass Conference, Delft, the Netherlands, 2008.

¹²⁸ Wellershof, F., Sedlacek, G., *Structural Use of Glass in Hybrid Elements: Steel-Glass-Beams, Glass-GFRP-Plates*, Proceedings of GPD 2003.

Another hybrid glass-steel design was presented by Froli & Lani (Figure 8.24).¹²⁹ This interesting concept consisted of steel bars in a lattice truss layout. The triangular voids between the bars were filled with PVB-laminated, chemically prestressed sheets. The steel rods were post-tensioned, to obtain compressive stress in the glass. The steel rods were dimensioned so that they would yield before glass fracture. A single specimen was tested this way, and behaved accordingly. However, for such designs it is crucial to also consider failure behaviour in case of glass breakage. In this case, specifically the release of post-tension in the steel rods could be cause for concern.

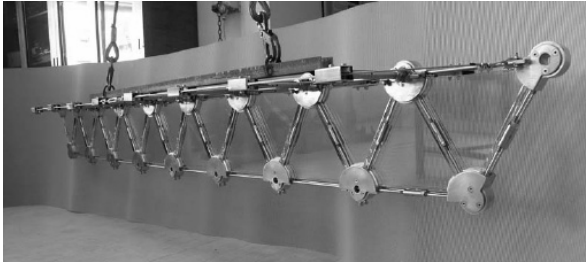


Fig. 8.24 Glass-filled post-tensioned steel lattice truss, presented by Froli & Lani.

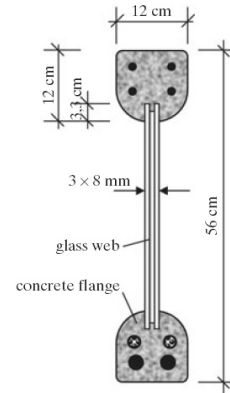


Fig. 8.25 Glass-Reinforced Concrete beam (section), proposed by Freytag.

4.3.5.3. Glass-Reinforced Concrete Elements

A beam design with flanges of high strength concrete with reinforcement bars and a glass web, was presented by Freytag (Figure 8.25).¹³⁰ The web consists of a 3x8 mm, PVB laminated annealed glass sheet. It has been segmented over the length of the beam. The concrete is directly poured onto the glass, which is treated with an enamel coating for better adhesion. The inner layer of the laminate is recessed to obtain more adhesive surface area.

When subjected to four point bending, the outer glass layers break first as they are much weaker because of the enamel coating. After failure of the inner layer, a post-failure resistance of approximately $r_{res,III} \approx 75\%$ is obtained. Final failure occurs by shear failure in the glass web, at the overlap joints in the web.¹³¹ The failure behaviour is examined quite extensively both analytically and numerically, but no predictive model is presented.

¹²⁹ Froli, M., Lani, L., *Towards Ductile Glass Beams*, Proceedings of the IASS Symposium, Venice, Italy, 2007.

¹³⁰ Freytag, B., *Glass-Concrete Composite Technology*, Structural Engineering International, No. 2, 2004, pp. 111-117.

¹³¹ Compare observations in glass-wood beams by Kreher.

4.4. Structure Level; Alternative Load Paths

The one design measure available at structure level to provide redundancy for an element (not necessarily for the complete structure) is to provide alternative load paths. This approach is widely used. An example was already shown in Chapter 5, Section 1.3. Figure 8.26 presents a similarly obtained alternative load path: it is provided by catenary action in the roof plates perpendicular to the main beam direction, thus transferring loads to the beams adjacent to the one supposedly failed.



Fig. 8.26 Alternative load path in the Wolfson Building glass roof, Glasgow, UK. In case one beam loses all load transfer capacity (1), loads can be redistributed to the adjacent beams (3) through catenary action (perpendicular to the beam length axis) in the roof panels (2).

An often copied method of providing alternative load paths was first applied in the hanging façades of the Serres at la Villette (Figure 8.27). The cross-shaped joint components allow the weight of a lower panel to be carried by the upper panels in the neighbouring columns, in case the one directly above it has failed.

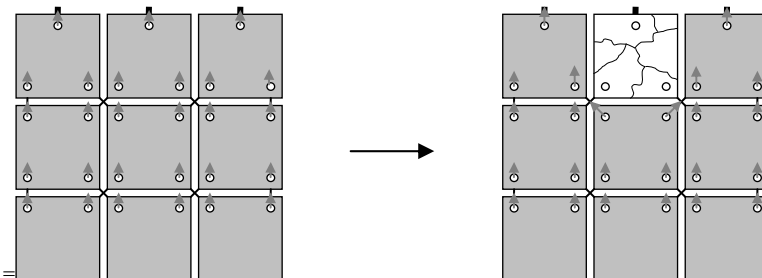


Fig. 8.27a, b, c Principle of the alternative load path design in the hanging glass façades of the Serres at La Villette: the panels are joined with cross shaped connectors, allowing a redistribution of loads through adjacent panels in case one should break.

Of course, in order for such an approach to be effective, the adjacent elements need to be sufficiently strong to carry the loads of the failed element as an incidental extra

action. Whether this will require additional structural mass is highly dependent on project requirements, the overall structural design, as well as the design of the individual elements. In the example presented in Appendix D, Section 2.5, no additional material in the adjacent beams was necessary.

More crucially though, the structural joints also need to be designed in a way that they can accommodate alternative load transfer. It is likely they will be governing in the determination of the alternative load path capacity, as they are e.g. in the AIB glass roof design.¹³²

5. Comments

In Section 1.3 of Chapter 5, it was noted that none of the publications concerning the innovative safety enhancing design concepts mention specific quantitative performance goals. When analysing those concepts with the Integrated Safety Approach, it is obvious they aim at enhancing the redundancy in full damage stage $r_{res,III}$, i.e. the post-failure resistance. On the other hand, none of the concepts aim at minimizing damage sensitivity, although in some concepts this comes as a by-product (the edges are often protected by reinforcement components).

As previously argued (Section 3.4 of this Chapter), providing a high post-failure resistance is indeed the most effective strategy to enhance safety, as it altogether bypasses the question of whether an impact (damage cause) could occur, as well as the question of how many broken layers should be considered to be realistic in a damage scenario. Additionally, another side-effect of the effort to increase $r_{res,III}$ may in some cases be an increase in $r_{res,I}$ and $r_{res,II}$ as well, as occurred with the reinforced beams discussed in Appendix E.

Without clear *a priori* performance criteria, it is difficult to see how the presented concepts could progress fundamentally.¹³³ The Integrated Approach, however, provides the opportunity to work towards specific goals. From the arguments presented in Section 4 of Chapter 7, it can be concluded that it is not necessary to aim at post-failure resistances well over 100 %. Rather, a consistently proven post-failure resistance of 100 %, should suffice for any application.¹³⁴ But the ESD and the Integrated Approach also allow to require lower post-failure resistances (see e.g. examples in Appendix D as well as redesign of the case study projects, Chapter 10) – actually, most common applications of glass in construction will not require $r_{res,III} \geq 1.0$. In those cases, however, the requirements will be application dependent and the design will be suitable in a limited number of situations.

With a post-failure resistance of 100 % guaranteed (or less, but sufficient for a specific application), there is actually little reason from a strictly safety point of view to apply further measures to minimize damage sensitivity. Because in case of failure, however

¹³² Chapter 5, Section 1.3, Figures 5.8a and b.

¹³³ Hence this research.

¹³⁴ Preferably, the scatter in post-failure resistance of the 2nd LTM as well as its damage sensitivity should be lower than that of glass. If this is not the case, additional probability analyses should ensure that $r_{res,III}$ is likely actually to exceed 1.0. Scatter and damage sensitivity should be analyzed with scrutiny in design concepts that depend on the functionality of adhesive bonds (as many are), as they may be more vulnerable to environment and execution quality than other methods of connection.

likely or unlikely, sufficient residual resistance will remain.¹³⁵ Rather, economical (and perhaps aesthetical) arguments will govern the application of damage sensitivity decreasing instruments.¹³⁶ Thus, the application of two sacrificial layers in the CFRP reinforced glass beams applied in the Loggia de Vicari (Figure 8.19; total 4 layers), seems quite conservative¹³⁷ when considering experiments (on smaller specimens) had shown post-failure resistances of over 180 %.

Many of the concepts being developed have shown post-failure resistances of 100 % are obtainable, even under extreme environmental conditions.¹³⁸ Therefore, with the help of the Integrated Approach and the ESD to set performance criteria, it is now possible to optimize those concepts (e.g. with regard to material efficiency, transparency, cost, etc.) and expand them with hitherto neglected elements such as columns.

All the innovative concepts apply the starting points mentioned above (Section 3.2.2) to introduce a 2nd LTM in a glass element: broken glass is loaded in compression, the reinforcement in tension. In most cases, their behaviour has also been modelled with FE analysis, with results that generally agree quite well with experiments. Particularly with complex hybrid elements such as the glass-wood and glass-reinforced concrete beams, this has provided valuable insight in their failure mechanisms, which may not always be governed by bending tensile failure (in fact, the mentioned beams fail by shear failure of the glass web).

Various FE models and crack simulation methods have been presented. They are usually (semi-) static in character. They apply a stress-based failure criterion together with stiffness reductions to predict crack growth, rather than include dynamic (energy-driven) crack growth modelling. Although this provides valuable insight in the distribution of stresses in the post-failure state of elements and such models may serve as an indicative tool to design glass elements, it is questionable whether this is sufficient to constitute a predictive method which failure behaviour can be determined and post-failure resistance assessed. Rather, it will be shown in the next chapter that elastic strain energy release at initial failure is an important, but hitherto underestimated, parameter that, among others, determines failure behaviour.

¹³⁵ Note that this argument does not work the other way around: damage sensitivity can never be minimized to a point that it is no longer necessary from a safety point of view to omit post-failure resistance, because potential failure causes can never be completely banned.

¹³⁶ On the other hand, when sufficient post-failure resistance is not provided by the 2nd LTM, decreasing damage sensitivity should be a priority to avoid the probability of failure from causes not considered by the actions-on-structures codes.

¹³⁷ Although understandable considering the fact that such beams had never been applied in practice.

¹³⁸ Louter, P.C., Veer, F.A., Belis, J., *Redundancy of Reinforced Glass Beams: Temperature, Moisture, and Time Dependent Behaviour of the Adhesive Bond*, Proceedings of the Challenging Glass Conference, Delft, the Netherlands, May 2008.

9 Elastic Strain Energy and Glass Element Failure Behaviour

In this chapter it will be shown elastic strain energy release is a key parameter for the post-failure resistance of an element, as it influences both the post-failure compressive capacity through the crack pattern, and the post-failure tensile capacity, through shock loading of the tensile component at initial failure. First, theory is discussed. A simple relation between crack growth and energy release in glass beams will be disclosed next. The complex relation between elastic strain energy and other parameters will then be discussed extensively, considering extensive experimental research on a range of beam designs subjected to 4-point bending after the application of different levels of predamage, and comparative investigations involving reinforced glass beams with different section properties. It will be concluded the initial hypothesis has to be nuanced, most importantly with the remark that the relative importance of crack pattern density decreases with increasing stiffness of the tensile components. The relevance of this matter is then explained and (design) methods are presented to avoid premature failure caused by elastic strain energy release.

1. Introduction

Contrary to most (innovative) glass elements, the Transparent Façade Struts presented in Chapter 2, Section 3, were tested under the three most common loading conditions: tension, compression, and bending. When comparing the results of the bending (Figure 9.1a) and compression/buckling tests (Figure 9.2a), an important difference in post-failure stiffness was noted. Whereas the secondary load transfer mechanism (LTM) stiffness is approximately $1/6^{\text{th}}$ of the 1^{st} LTM in bending, it is just $1/16^{\text{th}}$ in compression/buckling. In compression/buckling, the bending stiffness is practically solely provided by the PMMA outer tube, while in tension, the broken glass inner tube still contributes significantly to the 2^{nd} LTM.

From pictures of both tests, Figure 9.1b and 9.2b and c, it is obvious the fracture pattern in the compression/buckling tested prototype is much more extensive than in the bend tested specimen. The latter is broken only once laterally, while the former has suffered numerous such fractures. It can easily be seen why one can still add to the element bending stiffness, while the other can not.

The cause for this significant difference, however, is not immediately obvious, as both failed in bending at, which most likely have been,¹ similar stress levels. In the discussion of the experimental results in Chapter 2, Section 3.5., no explanation was yet offered.

¹ Several studies on failure stresses of glass tubes indicated no particularly high scatter (relative standard deviation was found to be in the order of 4 – 6 %). Bos, F.P., Veer, F.A., *Bending and buckling strength of butt-welded borosilicate glass tubes*, 3rd International Conference on Structural Engineering, Mechanics and Computation, Cape Town, South Africa, September 10-12, 2007; and: More extensively published as Bos, F.P., Giezen, C., Veer, F.A., *Opportunities for the Welding and Hot-Shaping of Borosilicate Glass Tubes in Building Structural Applications*, Proceedings of the Challenging Glass Conference, Delft, the Netherlands, May 2008.

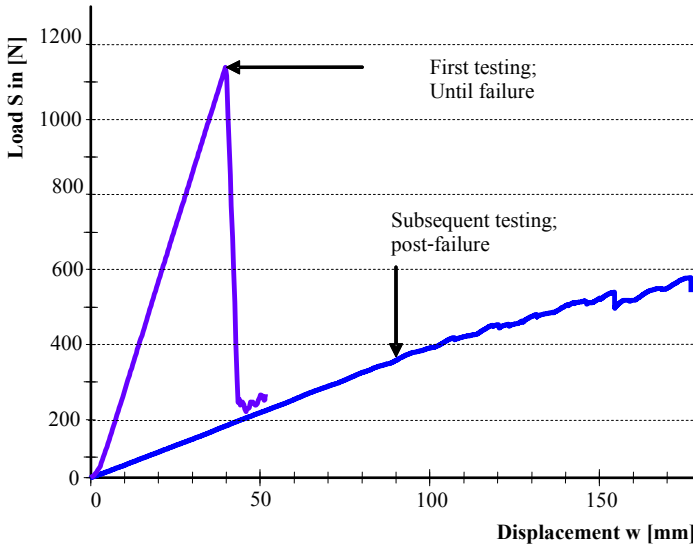


Fig. 9.1a Force-displacement graph of the impact/bending test on a TFS prototype (reprint of Fig. 2.43).

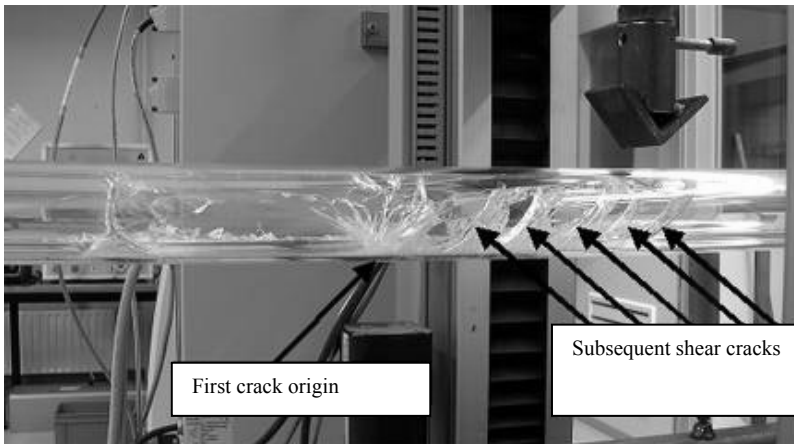


Fig 9.3 Fracture pattern in bending loaded TFS prototype, after initial failure.

It is now suggested that the difference in fracture pattern density – and thus post-failure resistance – should be attributed to the release of elastic strain energy,² which is much higher for the compression/buckling case than for the bending case.³ Several other

² The theoretical background to this concept is explained in Section 2.

³ The energy in the complete element was about 40 times higher in the compression loaded element, as it was in the bending loaded element (determined from area under load-displacement graphs). This distribution is not necessarily completely proportional to the energy in the glass tube, but it does provide an impression of the energy differences. See section 2 and Appendix D on theory how to calculate elastic strain energy content.

incidents suggest that this influences the post-failure state and its load carrying capacity, not only of these prototypes, but of glass elements in general.

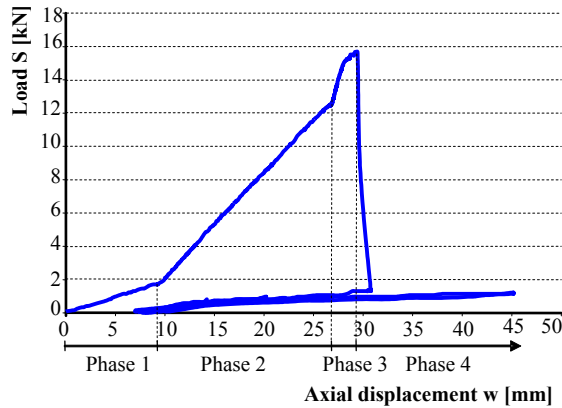


Fig. 9.2a Force-displacement graph of the compression/buckling test on a TFS prototype (reprint of Fig. 2.37).

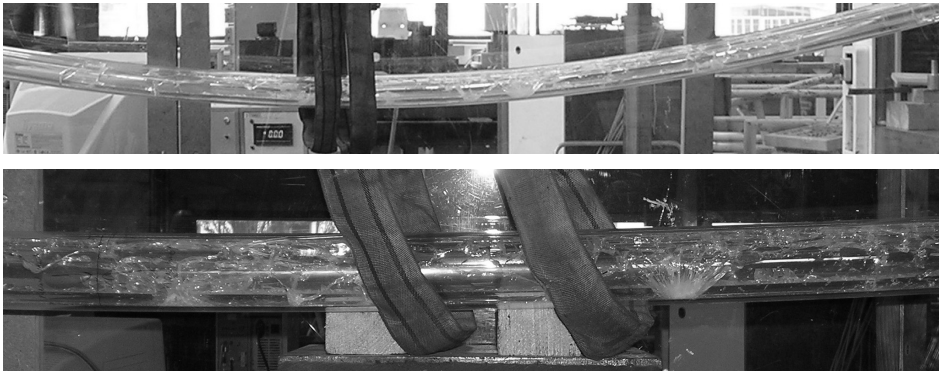


Fig 9.2b, c Pictures of the fracture pattern in compression/buckling loaded TFS prototype, after initial failure.

A number of observations seem to point to this relation being two-sided. First, as shown by the TFS project sketched above, the energy release seems to determine the extensiveness of crack growth in glass, which in turn, plays a role in the compressive strength and stiffness of the post-failure state. The other side is illustrated by these events:

- For the initial tests on the Zappi Glass-PC concept, specimens of 400 mm length and 40 mm height were used. Glass-PC composite action after glass fracture provided post-failure resistances of $r_{\text{res,III}} \approx 80\%$. When the concept was scaled to a more realistic size of 3000 mm length, however, many specimens suffered immediate collapse at initial failure (glass fracture) because

the PC layers were torn.⁴ This could not be attributed to the average failure stress, as it was generally lower than in the smaller specimens.

- The CFRP reinforced glass beams presented by Antonelli et al.⁵ and Cagnacci et al.⁶ suffered premature adhesive failure. They, too, attributed this to elastic strain energy release.

Apparently, the energy release relates directly to the shock load on the element's tensile components at initial failure, which may lead to premature failure of the element.

This chapter seeks to establish more definitely the hypothesis that:

The elastic strain energy release at initial failure of a glass element influences the maximum post-failure resistance, in a way that a release of more energy generally results in less post-failure resistance, either by premature failure of the tensile component as a cause of the shock load or through the extent of crack growth, which allows less compressive stresses to build up.⁷

Therefore,

- Section 2 treats the theoretical background to the concept of elastic strain energy,
- Section 3 presents experimental results from standing, single sheet annealed glass beams, revealing a simple linear relation between elastic strain energy release, some geometry parameters, and total crack length – which could not be found for failure stress or strain energy density,
- Section 4 refers to the analysis in Appendix E of the experiments on laminated and reinforced glass beams which have also been used to create ESDs in Chapter 7, in order to show: 1) for laminated beams, the post-failure strength depends on experiment type (but not for reinforced glass beams), 2) post-failure resistance depends on the type of heat treatment of the glass, and 3) premature collapse can occur through excess shock loading on the laminate at initial failure,
- Section 5 evaluates experiments on reinforced glass beams (extensively discussed in Appendix H) with different bending stiffness, and thus varying strain energy content, to demonstrate for the time being,⁸ that the post-failure

⁴ Ting, C.N., Zappi – onderzoek naar transparante liggerconstructies, Graduation project, Faculty of Architecture TU Delft, October 2000 (not published).

⁵ Antonelli, A., Cagnacci, E., Giordano, S., Orlando, M., Spinelli, P., *Experimental and Theoretical Analysis of C-FRP Reinforced Glass Beams*, Proceedings of the 3rd International Symposium on the Architectural Application of Glass (ISAAG), October 2008, Munich, Germany.

⁶ Cagnacci, E., Orlando, M., Pecora, M. L., Spinelli, P., *Application of C-FRP Strengthened Glass Beams in Façade Design*, Proceedings of the 3rd International Symposium on the Architectural Application of Glass (ISAAG), October 2008, Munich, Germany.

⁷ The premise being that the maximum capacity of the 2nd LTM is determined by a combination of the maximum compressive and the maximum tensile capacity, on which the elastic strain energy release both has an effect.

⁸ The results were difficult to interpret because of errors in the experimental set-up. See discussion in Section 4 of Appendix H.

resistance in this type of element hardly depends on energy release, but rather on other, geometrical parameters,

- Section 6 discusses the results obtained to conclude that the hypothesis is, in general, established, but should be expanded with the notion that the relative importance of energy release reduces when the 2nd LTM tensile stiffness increases.

Subsequently,

- the relevancy of this matter is discussed in Section 7,
- and Section 8, finally, presents design strategies to avoid premature failure or sub-standard post-failure resistance by excessive energy release. It shows how the use of a more shock resistant adhesive in reinforced glass beams (Appendix I) allows a different 2nd LTM to develop, resulting in more post-failure strength.

2. Elastic Strain Energy and Crack Growth

When a load is exerted on a linear elastic body, this body will deform proportionally to the load (Figure 9.5a). The amount of work W_o [$J = 10^3 \text{ Nmm}$] performed by the load is the load-displacement function integrated over the displacement, Eq. (9.1) (or the area under the load-displacement graph, Figure 9.5a). It is stored in the body as an equal amount of elastic strain energy U_e (1st law of thermodynamics; Eq. 9.2) which is released when the load is removed. This principle can be made useful, e.g. to fire an arrow from a bow or in other spring loaded mechanisms.

$$W_o = \int S(w)dw ; \text{ for linear elastic materials: } W_o = \frac{1}{2} S_{\max} w_{\max} \quad (9.1)$$

$$dW_o = dU_e \quad (9.2)$$

The elastic strain energy is distributed through the body proportionally with the strain distribution (as the strains determine the deformations). The amount of strain energy at a certain point in a body is known as the strain energy density χ [Nmm^{-2}], and the result of integrating the stress at that point over the strain. For materials following Hooke's Law, this yields Eqs. (9.3a and b) (see also Figure 9.5b). The total elastic strain energy in the body can now also be obtained from integrating the strain energy density over the body volume, Eq. (9.4). Thus, when the stress pattern and Young's modulus are known, the total elastic strain energy in the body can be calculated.

$$\chi_{x,y,z} = \int_{\varepsilon_{el,\max}} \sigma_{x,y,z}(\varepsilon) d\varepsilon ; \quad (9.3a)$$

$$\text{for linear elastic materials: } \chi = \frac{1}{2} \sigma \varepsilon = \frac{1}{2} \varepsilon^2 E \quad (9.3b)$$

$$U_e = \int_B \chi(x, y, z) dx dy dz \quad (9.4)$$

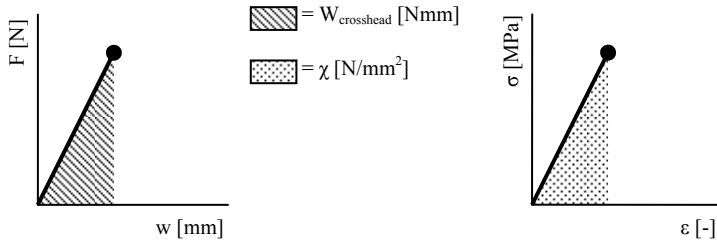
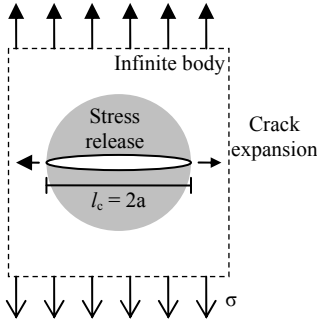


Fig. 9.5a Work is the load-displacement function integrated over the displacement.

Fig. 9.5b Strain energy density is the stress-strain function integrated over the strain.

Appendix F shows how the elastic strain energy in a beam can be determined, applying these principles. Three example calculations have been made: a beam in three point bending (calculated in three different ways), one loaded in four point bending, and finally the elastic strain energy introduced into a glass sheet by thermal prestress. Although the exact ratio is highly geometry dependent, these example calculations have shown there are 1 to 2 orders of magnitude between the energy introduced to failure by external loads and the energy introduced by thermal tempering. At a failure stress of 45 MPa, an annealed single sheet glass beam of $l_s \times h \times t = 1400 \times 120 \times 10$ mm in three point bending will contain 2.75 J strain energy at failure, while an equal sheet thermally prestressed to a compressive surface stress of 70 MPa will contain 199.6 J.

The fact that crack growth requires energy to form new surfaces is well known in the field of fracture mechanics, see Eq. (9.5a and b). This subject was previously discussed more extensively in Chapter 4, Section 1.1.1. The surface energy U_v is provided by the release of strain energy around the growing crack, Eq. (9.6a and b) and Figures 9.6a and b. However, it will be shown that upon glass failure, only a small portion of the elastic strain energy is consumed by crack formation (several percent). The rest is dissipated by other forms of energy, most notably kinetic energy. Thus, it is not necessarily obvious that there is a constant relation between the elastic strain content in a glass sheet and the total crack area (as suggested by the hypothesis).



Crack area :

$$A_{vol-crack} = l_c t = 2at$$

Crack surface energy :

$$U_v = 2l_c t v_s = 4atv_s \quad (9.5a)$$

Strain energy release around crack:

$$U_a = \frac{1}{2}(\sigma^2 / E)\pi a^2 t \quad (9.6a)$$

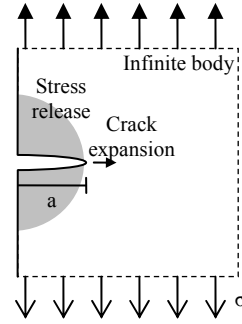
$$\pi a^2 t$$

Volume released of strain energy

$$\frac{1}{2}(\sigma^2 / E) = \frac{1}{2}\epsilon^2 E = \chi$$

Elastic Strain Energy Density, i.e. the Elastic Strain Energy stored per unit volume; [Nmm/mm³] = [N/mm²].

Fig. 9.6a Volume crack and required fracture energy.



Crack area :

$$A_{surf-crack} = at$$

Crack surface energy :

$$U_v = 2atv_s \quad (9.5b)$$

Strain energy release around crack:

$$U_a = \frac{1}{4}(\sigma^2 / E)\pi a^2 t \quad (9.6b)$$

Fig. 9.6b Surface crack and required fracture energy.

As we have seen in Chapter 4, energy-based considerations in relation to glass fracture are not at all new. Griffith formulated the glass fracture criterion in terms of an energy balance. This balance was later expanded by Irwin and Mott to Eq. (9.7). However, it was developed as a fracture and fracture propagation criterion, but provides little information with regard to macroscopic crack growth.

$$U = U_\epsilon + U_\gamma + U_K \quad (9.7)$$

3. Experimental Determination of an Energy Release-Crack Growth Relation

It is well known similar sheets of glass may break at rather varying stress levels. Usually the density of the cracking pattern, which results from failure, increases with increasing stress levels. Therefore, it can be tempting to assert that the total crack surface area depends directly on the failure stress at the crack origin. However, considering the observations on the TFS prototypes recalled in Section 1, the author suggests that the crack area is a function of the elastic strain energy stored in the glass element upon failure, rather than of the failure stress (although they are related properties). It is crucial to the hypothesis to establish this.

This section briefly summarizes the results and conclusions of an experimental study⁹ in which stress, strain energy density and total strain energy content¹⁰ have been compared as predictive indicators for the total crack area in standing single sheet annealed glass beams. It will be shown that, at least for such specimens, the total strain energy content predicts the total crack area best – and the failure stress predicts it worst.

3.1. Experimental Method

A large series of over 50 single sheet annealed glass beams of various geometries has been subjected to 3- and 4p-bending tests in different load configurations. The total crack length in each specimen was determined by photographing the specimens after failure, importing the pictures into AutoCad and drawing lines over all cracks. The elastic strain energy content of each specimen at failure was calculated based on the nominal dimensions of the specimens and the specimen failure stress with a specially prepared spreadsheet.

3.2. Investigated Relations

Subsequently, a number of hypothetical constant relations between specimen and failure parameters was investigated. Their validity was assessed through the relative standard deviation (RSD; the standard deviation as a percentage of the mean) of the constant C_n (with n the number of the relation) which results from them, taken over all specimens, as well as over sets of groups. Ideally, a constant relation would yield equal results for C_n for all specimens and $RSD = 0$.

In total, 15 relations were examined, divided into three sets of five each. Each set takes similar shape and is based on the basic variables failure stress σ_f , failure strain energy density χ_f , and total elastic strain energy at failure $U_{e,f}$ ¹¹ respectively. Within one group the relations vary by the number and kind of geometry parameters that have been applied, e.g. beam height, and thickness. The proposed relations and parameters, specifically the load configuration factor, are explained in Appendix G.

Two groups, one based on failure stress and the other on strain energy density respectively, are independent of specimen geometry and load configuration. The other, based on the total strain energy content, is highly dependent both on specimen geometry and load configuration.

3.3. Results and Discussion

The, rather extensive, numerical results¹² have all been presented in Appendix G.

Comparison of the results for the individual specimen groups (i.e. specimens with the same geometry), showed the χ - and U_e -based relations provided much higher

⁹ Appendix G. Please refer to this appendix for a full and extensive report on the method, results, and discussion.

¹⁰ Both concepts have been introduced in Appendix F, along with example calculations.

¹¹ For the determination of the relations, the *total* elastic strain energy in the beam was used. The author finds no reason to ignore the compressive strain energy, as was done by Gulati when studying the frangibility of thermally tempered glass (Gulati, S.T., *Frangibility of Soda Lime Tempered Glass Sheet*, Proceedings of the Glass Processing Days, Tampere, Finland, 1997).

¹² Consisting of a C_n for each specimen, for each relation, as well as the average C_n s and RSDs for sets of specimens and all specimens together. The energy dissipation as a percentage of the total stored strain energy at failure was also determined, assuming a surface energy of $\nu = 3 \text{ J/m}^2$.

consistency than the σ -based ones. However, a simple relation between crack length l_{cr} and either χ or U_ε (as R6 and R11) did not hold when comparing different groups of specimens with varying geometry and loading configuration.¹³ Therefore, geometry and loading configuration parameters were introduced to find a constant value for the crack factor C_n for different specimen groups. In the end, the χ - and U_ε -based relations predict the failure stress *much better* than the σ -based relations.

A fairly accurate prediction of failure stress from determining the crack length, specimen geometry and loading configuration, with a RSD of only 8.7%, is provided by Eq. (9.8). The value for the constant, which the author proposes to call the (*elastic strain energy*) *cracking constant*, is $C_{U_{\varepsilon,f}} = 27.1 \cdot 10^3 \text{ mm/N} = 27.1 \text{ m}^2/\text{J}$ ¹⁴.

$$U_{\varepsilon,f} = \frac{A_{fr}}{C_{U_{\varepsilon,f}} h \alpha_{config}} = \frac{A_{fr}}{27.1 \frac{\text{m}^2}{\text{J}} \cdot h \alpha_{config}} \quad (9.8)$$

With: $U_{\varepsilon,f}$ Elastic Strain Energy content at failure [J] = [Nm]
 A_{fr} Fracture surface area [mm²]
 $C_{U_{\varepsilon,f}}$ Elastic Strain Energy Cracking Constant [m²/J]
 h Beam Height [mm]
 α_{config} Load Configuration Factor [m⁻¹]

3.3.1. Energy Dissipation by Crack Growth

It is noteworthy that in all specimens, only a small portion of 3.4 % on average of the stored strain energy is dissipated by crack surface formation. A small amount of energy is released by means of sound, but most is transformed into kinetic energy. This explains the fact that glass shards tend to fly away from the broken specimen, rather than to just fall on the floor. For the development of glass elements with residual strength (and thus second load carrying mechanisms) it is important to realize that this energy has to be dissipated by the other materials (e.g. adhesive layers and/or reinforcement) in a composite glass element at the moment of failure. This may lead to premature tearing or adhesive failure, especially when brittle materials are used, as will be shown in Section 4 of this Chapter.

3.4. Conclusions

The amount of crack growth through a glass beam loaded in 3- or 4-point bending is linearly related to the total strain energy at failure through a constant and several geometry and loading configuration parameters, as presented by Eq. (9.8).

Attempts at finding a similar linear relation between crack length and failure stress have not produced satisfying results. Thus, it is concluded that crack length is not directly dependent on failure stress, but only indirectly through its influence on the total strain energy and strain energy density.

¹³ I.e. the RSD of C_n obtains high values (40 % or more) that do not reasonably indicate any consistency.

¹⁴ The unit of the cracking constant $U_{\varepsilon,f}$ [m²/J] is not to be read as a crack surface area created per amount of strain energy stored in the beam at failure, as the unit may suggest. For now, no physical meaning is suggested. Further (theoretical) research is required. The similarity of unit of $U_{\varepsilon,f}$ with that of the surface energy ν [J/m²] may be coincidental because the units of beam height h and loading configuration α_{config} cancel each other out.

4. Effect of Energy Release on the Failure Behaviour of Glass Beams

Now that a relation between elastic strain energy release and crack growth in glass has been established, it is time to investigate the relation between elastic strain energy release and failure behaviour.¹⁵ This subject is more complex as it is much more multi-sided. For a start, the hypothesis already includes two different ways in which energy release may influence failure behaviour: through a) the crack pattern density and thus the compressive capacity, and b) through shock loading on the tensile component. Furthermore, the failure behaviour, naturally, is also determined to a considerable extent by other parameters, namely material and geometrical properties (strength, stiffness).

Additionally, the concept ‘elastic strain energy’ is not necessarily unambiguous. In the failure process of a glass element, at least three types of energy may be involved:

- Elastic strain energy induced by (semi-)static external action (as in a 4-point bending test). Its release causes a redistribution of stresses and thus a shock load on the tensile component.
- A dynamic load may also transfer energy onto a glass element, that may be absorbed by e.g. crack growth. Principally, the effect is the same as with the energy release from static load, but material properties may be load speed dependent. Thus the element may respond differently to dynamic (e.g. shock impact) and static loads.
- Elastic strain energy caused by heat treatment, can be released from individual glass sheets. This has consequences for the fracture pattern in that particular sheet, but has little influence on the tensile component in a composed glass element (e.g. a laminated beam), because there is no external load to transfer at initial failure.

The analysis in this chapter is focused on the first form of elastic strain energy (caused by (semi-)static load; henceforth referred to as ‘external elastic strain energy’), with some attention also to the third one (caused by heat treatment; henceforth named ‘internal elastic strain energy’). Too little data are available to relate the hypothesis to dynamic elastic strain energy.

4.1. Elastic Strain Energy Release and Failure Behaviour of Glass Beams with Different Levels of Damage

In Appendix E, a large number of glass beam designs were subjected to three different test methods. The specimens had been damaged to different levels before being subjected to a 4-point bending test, firstly to the point of initial failure and subsequently to the point of final failure/collapse. With increasing levels of damage, the load to initial failure decreases. Therefore, the elastic strain energy release from external load also decreases.

¹⁵ ‘Failure behaviour’ should be understood as the whole trajectory from initial failure of the element (i.e. the 1st LTM losing its capacity) to final failure. The maximum post-failure resistance R_{III} is thus one aspect of failure behaviour.

Table 9.1 Initial- and post-failure strengths of glass beams (4-p. bending), after different levels of predamage.

Beam Type	Predamage (model damage level)	Average initial failure resistance $R_{dir/st+i/pd}$ [kNm]	Average post-failure resistance $R_{II,dir/st+i/pd}$ [kNm]
2.PVB.A	No	2.39	0.025
	Partial (I)	1.65	0.041
	Full (II = III)	0	0.086
2.PVB.S	No	5.97	0
	Partial (I)	3.15	0
	Full (II = III)	1.48*	0.022
2.PVB.T	No	7.85	0.010**
	Partial (I)	4.16	0.010**
	Full (II = III)	0	0.010**
3.PVB.A	No	2.70	0.082
	Partial (II)	1.91	0.095
	Full (III)	0	0.130
3.PVB.S	No	7.37	0
	Partial (II)	3.90	0
	Full (III)	2.02*	0.041
3.PVB.T	No	11.14	0.015**
	Partial (II)	4.67	0.015**
	Full (III)	0	0.015**
2.SG.A	No	1.82	0.33
	Partial (I)	1.36	0.33
	Full (II = III)	0	0.44
3.SG.A	No	2.92	0.66
	Partial (II)	1.76	0.70
	Full (III)	0	0.84
3re.GB368.A	No	2.52	3.50
	Partial (II)	2.11	3.25
	Full (III)	2.23	3.19
3re.SG.A	No	2.95	4.38
	Partial (II)	3.24	3.74
	Full (III)	3.39	3.79

** These beams were not fully predamaged by impact because the right set-up of the impact device was still experimented with. Therefore, they had to loaded in 4-point bending to first obtain initial failure (as in the specimens with no or partial damage).

*** Estimate ($2/3^{\text{rd}}$ of self weight). The post-failure resistance was $0 < R_{res,III} < s.w.$

The applied damage levels applied to each beam design, were:

- Model damage level 0 (no damage),
- For double layer beams: Model damage level I, or
For triple layer beams: Model damage level II,
- Model damage level III (=initial failure, the 1st LTM has no capacity anymore, a 2nd LTM is activated).¹⁶

The initial failure strength and maximum post-failure strength were recorded. Table 9.1 lists these values per beam design and predamage level. Figures 9.5a and b present the post-failure resistances per predamage level again, in bar diagrams.

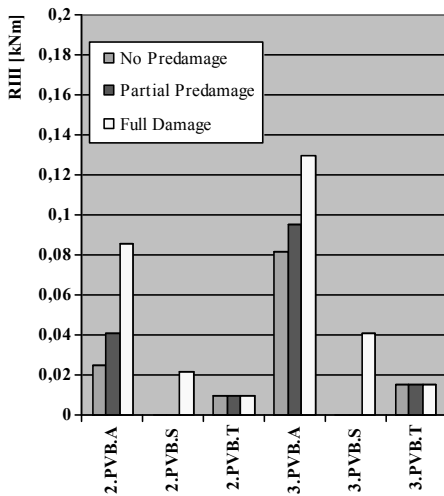


Fig. 9.5a Post-failure resistances of PVB laminated glass beams tested in 4-point bending, after different levels of predamage.

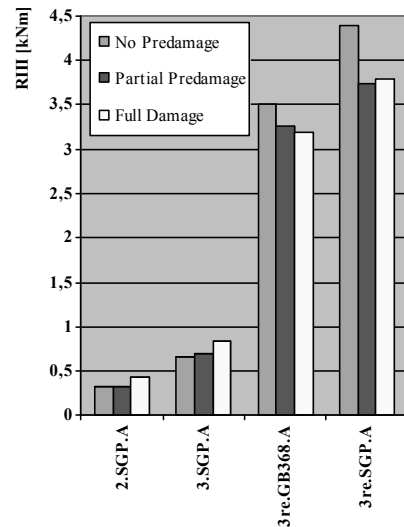


Fig. 9.5b Post-failure resistances of SG laminated and reinforced glass beams tested in 4-point bending, after different levels of predamage.

4.1.1. Double and Triple Layer PVB Laminated Annealed Glass Beams

Both the double and triple layer PVB laminated annealed glass beams (2.PVB.A and 3.PVB.A) showed a considerable dependency of post-failure resistance on damage level: the less pre-test damage, the more energy release, the less post-failure strength. The relation, however, is not linear. There is a particularly great difference between post-failure resistance from full damage (model damage level III = initial failure), and the post-failure resistances obtained after no or partial damage (although also between the latter two, the difference in post-failure resistance is significant). Figures 9.6a, b, and c, show typical fracture patterns in 2.PVB.A beams after initial failure under the three different predamage levels. There is an obvious increase in crack pattern density

¹⁶ In principal, these specimens do not need to be loaded to initial failure in the 4-point bending test, as they have already reached initial failure. However, in some of the heat strengthened beams, this damage level was not fully reached with the impact device because it was still being tested what the the right set up was. In those cases, an initial load was still needed in 4-point bending to reached initial failure. See also Table 9.1.

from the beams with full pre-test damage, through the one with partial pre-test damage, to the one without pre-test damage. Similar observations were made with the 3.PVB.A beams.

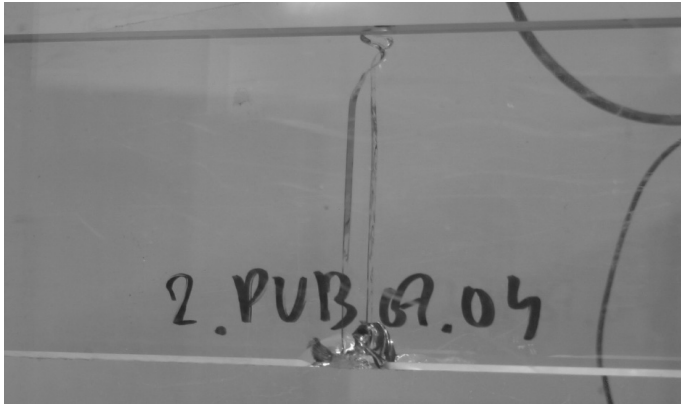


Fig. 9.6a Fracture pattern at initial failure in a double layer annealed glass beam tested in 4-point bending, with full predamage (level II = III).

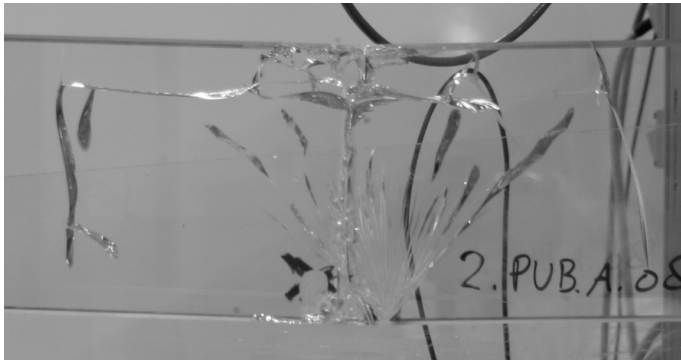


Fig. 9.6b Fracture pattern at initial failure in a double layer annealed glass beam tested in 4-point bending, with partial predamage (level I).



Fig. 9.6c Fracture pattern at initial failure in a double layer annealed glass beam tested in 4-point bending, with no predamage (level 0).

There were no observations indicating a reduction in the tensile capacity of the PVB (e.g. tearing or delamination). It thus appears the differences in post-failure strength are caused by the fracture pattern density, and therefore also by the extent of elastic strain energy release.

4.1.2. Double and Triple Layer PVB Laminated Heat Strengthened Glass Beams

With the double and triple layer PVB heat strengthened beams, a correlation between post-failure resistance and pre-test damage can also be observed, albeit of a different nature. Only the fully damaged specimens (damaged to initial failure) actually exhibited post-failure resistance (Figure 9.7a). The beams with no or partial damage break instantly at initial failure through tearing of the PVB foil (Figure 9.7b), an occurrence which shows similarities with the rupture of PC experienced in past research.¹⁷



Fig. 9.7a Only in fully predamaged double layer PVB laminated heat strengthened glass beams some post-initial failure resistance remains.

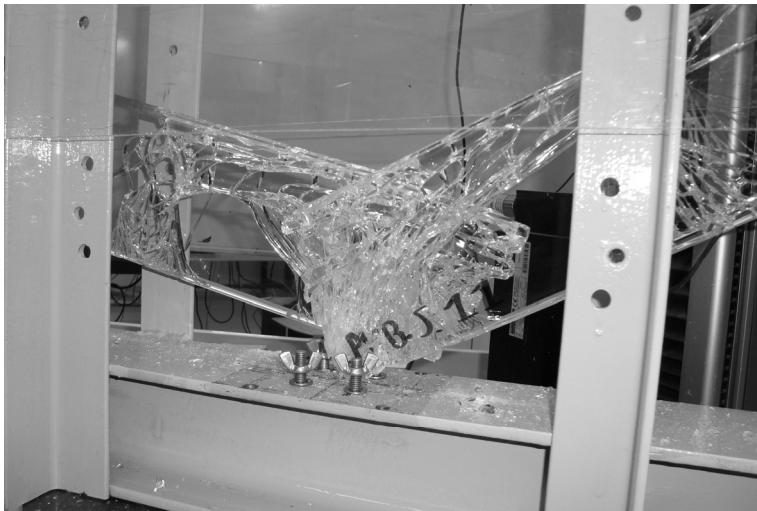


Fig. 9.7b Collapse occurs immediately at initial failure in double layer PVB laminated heat strengthened glass beams tested in 4-point bending after no or partial predamage (this picture: no predamage), because of tearing of the PVB foil.

¹⁷ Ting, C.N., Zappi – onderzoek naar transparante liggerconstructies, Graduation project, Faculty of Architecture, TU Delft, October 2000 (not published).

In comparison to the annealed beams, this raises the question whether the PVB tears because of exceeding the material strength (under (semi-)static load) or as a result of a shock load greater than the energy absorption capability (as is implied by the hypothesis). The first explanation (exceeding material strength) is actually highly unlikely: the stress in the PVB is determined by the strain in the glass and the stiffness ratio between both materials. Since approximately $E_{\text{PVB}} / E_{\text{glass}} = 18 / 70\,000 = 2.57 \cdot 10^{-4}$, the stress in the PVB at an initial failure load of (average for 2.PVB.S), is only 0.032 MPa. Although this is higher than the value in annealed glass beams (which would be 0.013 MPa for 2.PVB.A), it is far below the material strength ($> 20 \text{ MPa}^{18}$). This can not be the cause of rupture. This argument is further supported by the results of the thermally tempered beams, where the average maximum tensile stress in the PVB is 0.042 MPa, and no PVB rupture has occurred in any of those beams. It is therefore preliminarily concluded that the PVB rupture is caused by excessive external energy release (shock loading). One would then perhaps expect PVB rupture also to occur in tempered glass beams, as the external energy, like the initial failure stress, is higher. The reasons why this does not occur are explained in the next section, where the behaviour of the tempered glass beams is discussed.

Because of PVB rupture in both the partially and undamaged beams, the possible influence of fracture pattern density differences could not be investigated.

In comparison to the annealed specimens, it is remarkable that the post-failure resistance of the fully damaged heat strengthened beam double layer beam is similar to the undamaged annealed beam. For the fully damaged triple layer heat strengthened beam, the post-failure strength is even significantly lower than for the undamaged annealed one. Since the compressive strength of annealed and heat strengthened glass should be comparable and the tensile strength and stiffness of the PVB are equal in both cases, the observed crack pattern differences explain the differences between annealed and heat strengthened glass beams.¹⁹ Compare e.g. Figures 9.6c and 9.7a. Specifically

¹⁸ Belis, J., *Kipsterkte van monolithische en gelamineerde glazen liggers*, Ph.D. Thesis, Ghent University, Belgium, 2005.

¹⁹ There are some interesting points to make with regard to the fracture pattern in annealed, heat strengthened, and thermally tempered glass. Since the fracture pattern of heat strengthened glass is similar to that of annealed glass, only somewhat more dense or extensive, it seems only a small portion of the internal energy is released through crack growth. The difference in pattern density between annealed and heat strengthened glass can not be explained by external energy release, as the external energy with the undamaged annealed specimens was higher (see Table 9.1) than with the 'fully' predamaged heat strengthened beams (see also foot note 16). On the other hand, the great difference in crack pattern density between strengthened and tempered glass, while the internal energy content only varies by a factor of approximately 4, indicates most of the internal energy remains in the glass, and thus most of the prestress must also remain.

This goes against the common notion that suggests the fracture density in heat treated glass stems from a loss of equilibrium between compressive and tensile stresses after a crack penetrates the compressive layer (this would also lead to disintegration in heat treated glass, while it is now shown that it not necessarily does). Careful consideration of this notion also leads to the conclusion that it is mistaken: even without a surrounding compressive layer, a glass section with a typical parabolic stress distribution can be in equilibrium.

Especially considering Section 3 of this Chapter, it should be concluded the present internal energy drives a crack once it has started. The large quantity of energy results in a high crack growth speed and extreme branching. Highly interesting is the demarcation point between the prestress that only leads to minor energy release (heat strengthened) and the level that results in all (or most) energy to be released. This should be subject of further research, e.g. with photoelastic measuring equipment.

the wide branching in the top of the heat strengthened beams limits the possibility to transfer compressive stresses.

4.1.3. Double and Triple Layer PVB Laminated Thermally Tempered Glass Beams

Contrary to the annealed glass beams, the PVB laminated thermally tempered ones did not show any pre-test damage dependency. Their behaviour thus seems independent of external elastic strain energy release. The crack pattern density is comparable in all cases, although a typical V-pattern can be discerned at the initial crack origin in beams without pre-test damage. In combination with the PVB, no significant post-failure stiffness remains after initial failure, and the beams slowly sag from their supports under their self weight. The post-failure strength, therefore, is estimated to be higher than 0, but smaller than the self weight ($0 < R_{\text{res,III}} < \text{s.w.}$).

A remarkable difference between the heat strengthened and thermally tempered glass is that while a large portion of internal elastic strain energy seems to remain in the glass after fracture²⁰ in the former, all or most of it seems to be released in the latter. Since this generally involves much more energy than the energy caused by external loads (typically between 1 and 2 orders of magnitude, see example calculations in Appendix G), its influence on the crack pattern density completely overrules that of the external energy.

Remarkably, the post-failure resistance of the tempered beams is higher than that of the heat strengthened beams with no or partial pre-test damage,²¹ namely $0 < r_{\text{res,III,PVB,T}} < \text{s.w.}$, while $r_{\text{res,III,PVB,S}} = 0$. In spite of the higher release of both external and internal energy, the PVB did not rupture. To explain this, consider the process of rupture in the PVB: it occurs when the variation in displacements over time becomes too large to be accommodated by local plastic deformation, or in other words: when the energy release is too large to be absorbed by the material around the crack. Now, the differences between the annealed, heat strengthened, and tempered glass beams are explained as follows:

- When the energy release is low, as in the annealed beams, the PVB can dissipate the energy release by (elasto-)plastic deformation.
- When the energy release is higher, as in the heat strengthened beams, the PVB can not absorb enough energy by plastic deformation, and ruptures.
- In the tempered beams, the external energy release is even higher, but also a large quantity of internal energy is released. This causes a dense fracture pattern, but *no additional shock load* on the PVB.²² The dense fracture pattern allows much more volume of PVB to be available for plastic deformation and thus energy absorption. As the increase in crack pattern density in comparison to heat strengthened glass is much greater than the increase in total *external* elastic strain energy, the net result is that the PVB in these beams does not rupture.

²⁰ See previous foot note.

²¹ Not than that of the fully predamaged beams.

²² As it is not caused by an external load that is shifted from one component (i.e. glass) to another (i.e. PVB) in the element.

4.1.4. Double and Triple Layer SG Laminated Annealed Glass Beams

The influence of the amount of predamage in the double and triple layer, SG-laminated annealed glass beams is smaller than in the PVB-laminated annealed glass beams. The fully damaged specimens have a higher failure strength than the other ones (approximately 1.3 times), but this difference is less than with the PVB-laminated specimens (3.4 times between no and full predamage). The specimens with no and partial pre-test damage had almost equal residual strength. Apparently, the influence of the crack pattern density on the compressive capacity of the broken glass *reduces* when the stiffness of the tensile component (i.e. the laminate) *increases* (the broken glass is held together better).

4.1.5. Triple Layer GB368 Bonded, Steel Reinforced, Annealed Glass Beams

The reinforced specimens seem to be hardly influenced by the amount of pre-test damage, both in pre- and post-failure resistance. This supports the notion in the previous section, indicating an *increase* in post-failure tensile stiffness causes a *decrease* of crack pattern density influence.

Remarkably, the average post-failure resistance of the partially and fully damaged beams is somewhat lower (contrary to other specimens) than of the directly tested specimens. This may be attributed to the fact that they came from different batches.

Before reaching conclusions with regard to the hypothesis, another experiment is discussed in the subsequent section.

5. Failure Behaviour of Reinforced Glass Beams with Varying Energy Content

The influence of elastic strain energy release from (semi-)static loads has been investigated further by comparing the failure behaviour of two reinforced glass beam designs: a stocky beam with relatively low bending stiffness which stores a high amount of strain energy during loading, and a slim beam with high bending stiffness which contracts relatively little energy during loading (Figures 9.8a and b). The experiment and its results have been extensively reported in Appendix H.

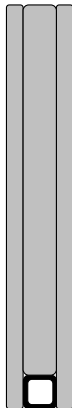


Fig. 9.8a Section design of the slim glass beam: high stiffness, low energy absorption ($h \times t = 155 \times 22$ (6 – 10 – 6) mm).

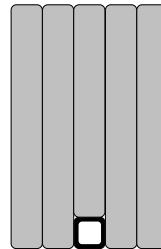


Fig. 9.8b Section design of the stocky glass beam: high stiffness, low energy absorption ($h \times t = 95 \times 58$ (12 – 12 – 10 – 12 – 12) mm).

5.1. Experimental Method

Two reinforced glass beams were designed and subject to 4-point bending. They were both 1.5 m long, but had different section dimensions (width and height), so that their moments of resistance were approximately equal ($88.1 \cdot 10^3 \text{ mm}^3$ and $87.2 \cdot 10^3 \text{ mm}^3$) while their moments of inertia varied by a factor 1.6 ($6.83 \cdot 10^6 \text{ mm}^4$ and $4.14 \cdot 10^6 \text{ mm}^4$). Thus, when they are loaded with an equal load, the displacement as well as the elastic strain energy content of both beams would also vary by a factor 1.6 (see Appendix F).

Like the beams previously discussed in Section 4, the bending tests were executed in two stages: first to initial failure, and subsequently to final failure (after unloading).

5.2. Results

Table 9.2 lists the average maximum initial and post-initial failure loads, the initial glass tensile failure stress, the uncorrected maximum initial and post-initial displacements, the relative residual strength, and the final failure cause. Table 9.3 gives the data related to energy release.

Table 9.2 Direct experimental results (taken from Table K.1).

Beam Type		R_{ini} [kN] = R_0	σ_{ini} [MPa]	$R_{\text{post,max}}$ [kN] = R_{III}	Rel. Res. Strength $r_{\text{III}} = R_{\text{III}} / R_0$
Slim beam: high stiffness, low energy absorption.	Ave. (6 spec)	15.2	43.1	16.8	1.12
	St. Dev.	1.99	5.66	1.68	0.20
	Rel. St. Dev.	13.1 %	13.1 %	10.0 %	17.9 %
Stocky beam: low stiffness, high energy absorption.	Ave. (5 spec)	14.8	42.5	11.2	0.76
	St. Dev.	1.26	5.66	1.01	0.10
	Rel. St. Dev.	8.5 %	8.5 %	9.1 %	13.7 %

Table 9.3 Elastic strain energy related results (taken from Table K.2).

Beam Type		$U_{\text{e,ini}}$ [J]*	$U_{\text{e,post@w,ini}}$ [J]**	$U_{\text{e,released}}$ [J]***	Rel. $U_{\text{e,released}}$ [%] = $U_{\text{e,released}} / U_{\text{e,ini}}$
Slim beam: high stiffness, low energy absorption.	Ave. (6 spec)	27.6	18.9	8.8	31.0
	St. Dev.	6.30	3.72	3.01	5.20
	Rel. St. Dev.	22.8 %	19.7 %	34.3 %	16.8 %
Stocky beam: low stiffness, high energy absorption.	Ave. (5 spec)	30.6	15.6	15.0	48.1
	St. Dev.	5.31	0.62	4.94	7.15
	Rel. St. Dev.	17.4 %	4.0 %	33.0 %	14.9 %

* The elastic strain energy in the beam at initial failure.

** The elastic strain energy in the beam after initial failure, at the same displacement as the initial failure.

*** The elastic strain energy released from the beam at initial failure. Calculated from: $U_{\text{e,released}} = U_{\text{e,ini}} - U_{\text{e,post@w,ini}}$.

5.3. Discussion

As expected, both beam types showed similar initial failure strengths, averaging at 15.2 and 14.8 kN for the slim and stocky beams, respectively (Table 9.2). In the post-initial failure stage, however, an important difference in residual strength was encountered. For type I, this averaged on 16.8 kN or 112 %, while for type II it was only 11.2 kN or 75.9 %. This would seem to justify a conclusion that low energy content beams indeed perform much better in the post-initial failure stage than high energy content beams. However, this line of thought would be erroneous.

Consider, therefore, the load transfer mechanisms in the beam before and after initial failure, as presented in Figures 9.9a and b. In the post-initial failure stage, the external moment is counteracted by a couple of internal forces multiplied by the internal moment arm z : compression in the top part of the glass section and tension in the steel reinforcement. The exact magnitude of the internal moment arm is hard to estimate as it is not directly obvious what the height of the active glass compression zone is, but it seems reasonable to assume the internal moment arm z is approximately proportional to the beam height h ($z_I / z_{II} \approx h_I / h_{II}$). Thus, the moment capacity of the section depends on the steel tensile strength, the glass compressive strength and the internal moment arm.

Using the geometrical values as presented in Figures 9.9a and b, the internal moment capacity of a slim beam (average) is 4.1 kNm, which corresponds to a crosshead load of 16.3 kN. For a stocky beam, the internal moment capacity is 2.5 kNm, corresponding to 10.1 kN crosshead load. These values are governed by yielding of the reinforcement and correspond relatively well to the obtained experimental values of $R_{\text{post,max,I,ave}} = 16.8$ kN and $R_{\text{post,max,II,ave}} = 11.2$ kN, respectively.

Since $R_{\text{post,max,ave,I}} / R_{\text{post,max,ave,II}} = 16.8 \text{ kN} / 11.2 \text{ kN} = 1.5$ and $h_I / h_{II} = 155 \text{ mm} / 95 \text{ mm} = 1.63$, it can now easily be seen that the difference in maximum post-initial failure strength is likely to be caused primarily by the difference in beam height, rather than by the difference in elastic strain energy release. The beam height h and elastic strain energy U_e are not independent properties, but in this argument, the relation between internal moment capacity directly depends on beam height, while the relation with elastic strain energy is only indirect.²³

Apparently, the tensile stiffness of both beam types is sufficiently high to render the extensiveness of the crack pattern (which is greater in the stocky beams than in the slim ones; compare Figures 9.10a and b) irrelevant in determining the maximum post-failure resistance. Therefore, the elastic strain energy release is also of subordinate importance. This is consistent with the conclusions from the previous section: the relevance of elastic strain energy release decreases with increasing post-failure tensile stiffness in the element.

²³ There are some important additional comments to be made. Most importantly, due to errors in the experimental setup, the differences in energy content in both beam types were not as big as they should have been. See Appendix H for further discussion.

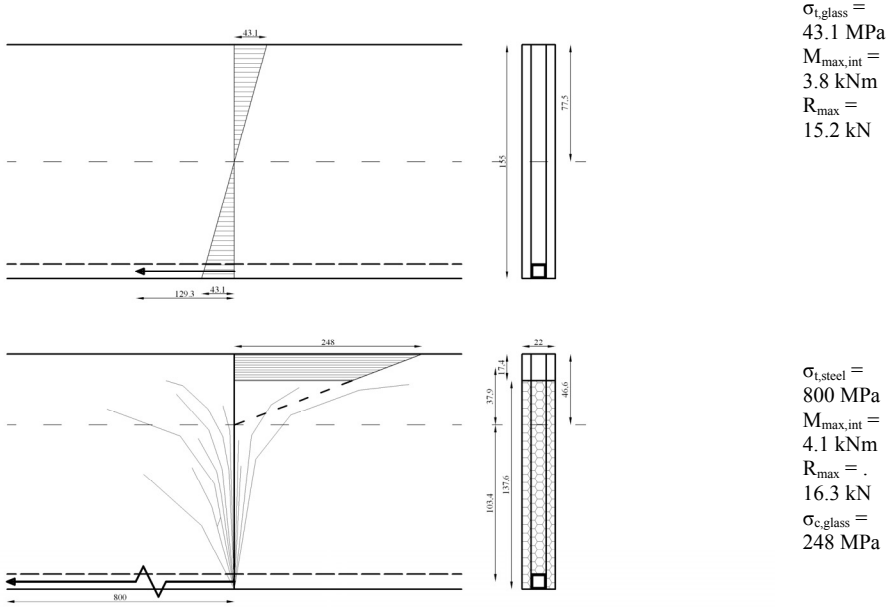


Fig. 9.9a Load transfer mechanism of slim beams specimens in pre- and post-initial failure stage (top and bottom, respectively) (reprint of Fig. K.10a).

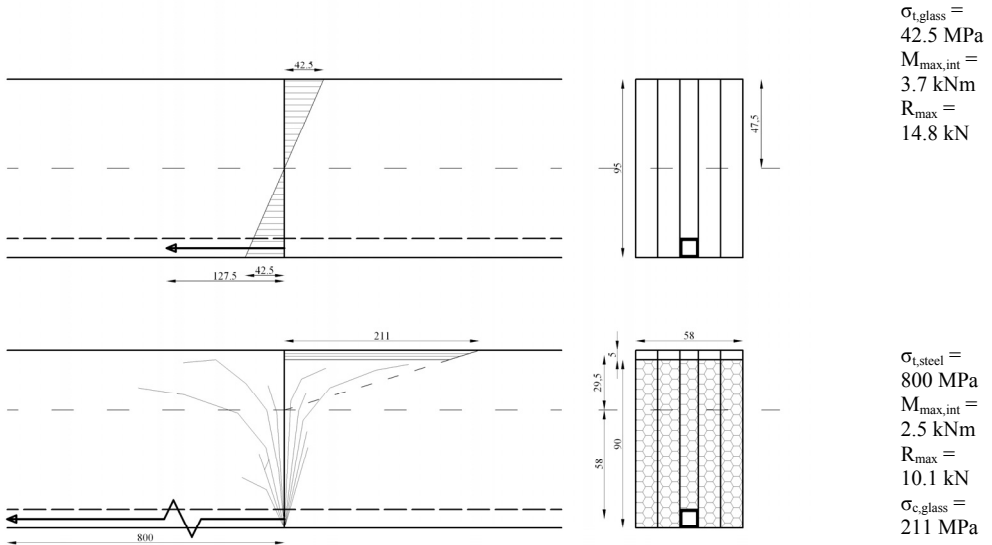


Fig. 9.9b Load transfer mechanism of stocky beams in pre- and post-initial failure stage (top and bottom, respectively) (reprint of Fig. K.10b).



Fig. 9.10a Typical fracture pattern in slim beam after initial failure. A portion of the beam (at the top) remains unbroken.

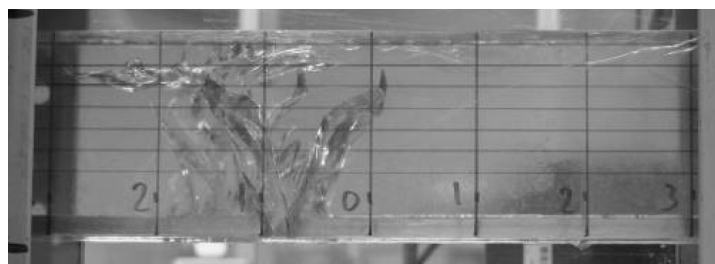


Fig. 9.10b Typical fracture pattern in stocky beam after initial failure. The cracks run almost completely to the top of the beam.

Nevertheless, it remains possible that the elastic strain energy release causes direct collapse through shock loading of the tensile component upon initial failure (e.g. in the case of the reinforced glass beams through failure of the adhesive layer between the glass and the reinforcement). That relation between elastic strain energy release and failure behaviour, however, is more of a pass/fail nature, rather than a gradual one,²⁴ and did not occur in this experiment. In relation to this, it should furthermore be noted that the shock load on the tensile component will reduce with increasing tensile component stiffness, as it will contract more stresses before initial failure. Hence the stress difference between the pre- and post-failure states will be smaller.

6. Conclusions

From Sections 3, 4, and 5, it may be concluded that, at least for standing glass beams, the initial hypothesis, despite being principally correct, needs to be extended and nuanced :

The *external* elastic strain energy release at the moment of initial failure of a glass element, influences the maximum post-failure resistance, in a way that a release of more energy generally results in less post-failure

²⁴ I.e. the elastic strain energy release either does or does not cause immediate collapse at initial failure through shock-induced failure of the element tensile component (as with the PVB laminated, heat strengthened beams, Section 4 of this chapter), whereas an increasing elastic strain energy release causes a gradual increase in crack pattern density, and thus a gradual decrease in post-failure compressive capacity.

resistance, either by premature failure of the tensile component as a cause of the shock load or through the extent of crack growth/branching. The following points should be noted:

- o **The importance of the extent of crack growth reduces with increasing tensile stiffness of the 2nd LTM. The fracture pattern density may become irrelevant with high stiffness elements, such as steel reinforced glass beams.** [see the comparison between the behaviour of PVB- and SG-laminated annealed glass beams and the reinforced glass beams in Sections 4.1.4. and 4.1.5., and the comparison between high and low stiffness reinforced glass beams in Section 5]
- o **The differences in crack growth between annealed, heat strengthened, and thermally tempered glass, as a result of internal elastic strain energy release, govern over those caused by external elastic strain energy release.** [see comparison between annealed, heat strengthened, and thermally tempered, PVB-laminated beams in Sections 4.1.1. – 4.1.3.]
- o **When the release of internal elastic strain energy is sufficient to disintegrate the glass, this may effectively distribute the shock load over the tensile element, thus avoiding direct rupture and improving post-failure resistance (over a condition in which the tensile element ruptures).** [see the results of the PVB-laminated thermally tempered beams compared to those of the heat strengthened beams with no or partial predamage, Section 4.1.3.]

Thus, the relation between the external elastic strain energy release and the post-failure resistance is part of a more complex set of relations between geometry, material properties, heat treatment and external actions. These other parameters not only influence failure behaviour directly, but also the energy absorption in the element and the distribution of shock load at initial failure. This has schematically been summarized in Figure 9.11.

Specifically the element post-failure tensile stiffness plays an important role in determining the relevance of elastic strain energy release. The effect of crack pattern density on the post-failure compressive capacity may be reduced or even nullified with increasing post-failure tensile stiffness. Nevertheless, as a parameter partially responsible for determining the maximum post-failure resistance, it should not be ignored.

7. Relevance

In Chapter 1, the question was raised how the safety of structural glass should be defined – and, subsequently, how it may be ensured. Four properties were introduced in Chapter 6, with which the various aspects of the safety of a glass element can be described. For each element safety property, Chapter 8 showed how safety can be achieved and optimized.

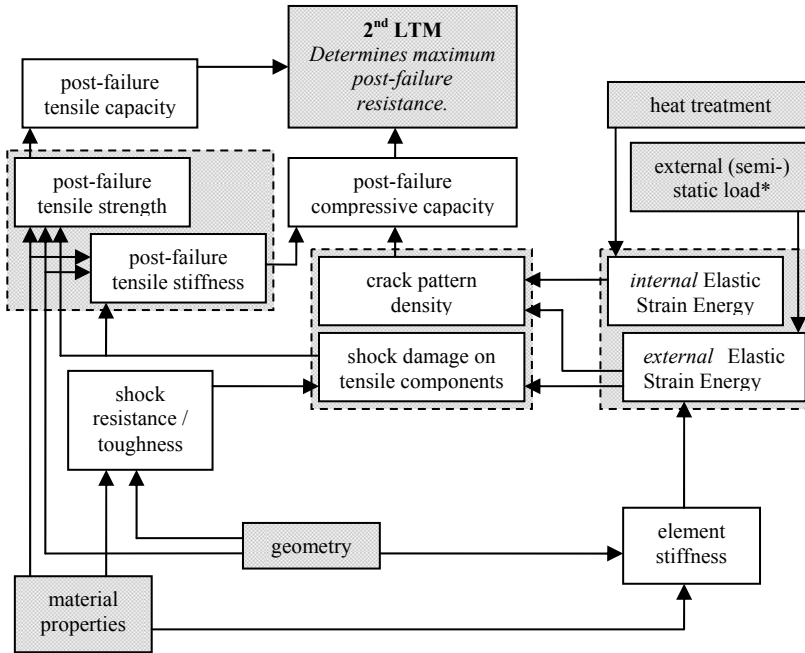


Fig. 9.11 Schematic summary parameters influencing the maximum post-failure resistance of the 2nd LTM.

Realizing a 2nd LTM was argued²⁵ to be the most fundamental step in obtaining glass element safety. As it introduces residual strength even at a level of full damage, it is a key parameter in the overall redundancy of the element.

A 2nd LTM is usually presented as a static analytical mechanics model (as e.g. Figure 9.9a and b, or Figures 8.10a – d in Chapter 8) or calculated from (semi-)static FE models, based on the application of a stress-based failure criterion together with stiffness reductions to predict crack growth (rather than include dynamic (energy-driven) crack growth modelling).²⁶ In spite of the role of elastic strain energy release on the post-failure resistance as indicated in Figure 9.11, its influence is never incorporated in the analytical or FE modelling of 2nd LTMs. However, by looking again at the experimental results on glass beams as described in Appendix E, it will be shown the release of external and internal elastic strain energy may actually determine what 2nd LTM develops and how it should be calculated.

7.1. Elastic Strain Energy Release and The Effective 2nd LTM

In the laminated specimens, the laminate must carry the tensile loads after failure. In some cases the cracking pattern is too dense or the laminate is not stiff enough to allow compressive stresses in the (broken) glass, and the interlayer thus remains the only active material. In others, the laminate works in composite action: the glass in

²⁵ Sections 3.4 and 5 in Chapter 8.

²⁶ See also Chapter 8, Section 5. Crack growth in those models is based on stiffness reduction after exceedence of a failure stress criterion.

compression and the interlayer in tension. Four 2nd LTMs have been proposed,²⁷ Figure 9.12a – d. Ranked according to capacity, they are:

- 1: linear elastic bending of the laminate,
- 2: plastic bending of the laminate,
- 3: composite action with laminate in elastic bending and glass in compression,
- and 4: composite action with laminate in plastic bending and glass in compression.

The theoretical capacity of each 2nd LTM was calculated, and, based on the experimental results, it was determined which one is applicable to each beam design and level of pre-test damage. The results are listed in Table 9.4.

This clearly shows the elastic strain energy release affects the 2nd LTM that develops after initial failure, and thus relates directly to one of the most important safety parameters of a glass element. Additionally, it is important to realize that the post-failure resistance of an element can thus not be established without specifically indicating the impact type (and thus the energy release) with which failure is to be obtained.

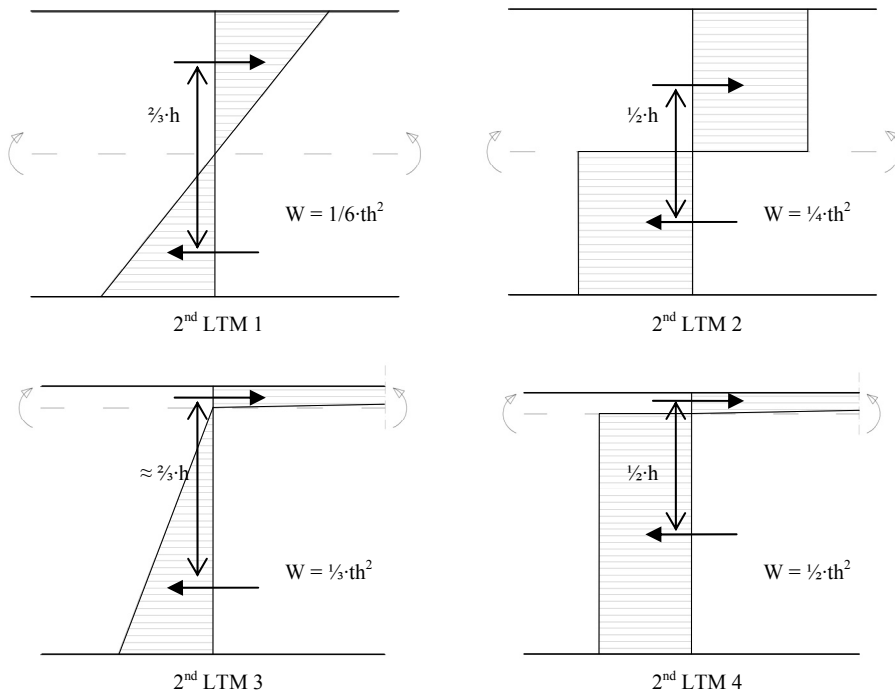


Fig. 9.12a – d Four alternative 2nd LTMs that may develop in a double or triple layer laminated glass beams.

²⁷ Appendix E, Section 4.3.2.

Table 9.4 2nd Load Transfer Mechanism per specimen type, per predamage level – sorted by beam type. A ‘0’ means there is no 2nd LTM is present; ‘0-1’ indicates the fracture pattern is too dense to allow LTM I to fully develop (to reach laminate tensile strength); ‘3-4’ points to an intermediate situation as in Figure H.32.

2nd LTM			
Specimen Type	Predamage level		
	0	I / II*	III
	(relative) Elastic Strain Energy release at initial failure		
	high	medium	low/zero
2.PVB.A	0 – 1	1	3
2.PVB.S	0	0	0 – 1
2.PVB.T	0 – 1	0 – 1	0 – 1
3.PVB.A	1	1	3
3.PVB.S	0	0	0 – 1
3.PVB.T	0 – 1	0 – 1	0 – 1
2.SG.A	3 – 4	3 – 4	4
3.SG.A	3 – 4	3 – 4	4

* I for double layer beams, II for triple layer beams.

7.2. Consequences of the Elastic Strain Energy Release Parameter

Because of its crucial influence on the 2nd LTM in a glass element, the elastic strain energy release at initial failure in a glass element is critical to the question of how to obtain safety, and should not be ignored. This has consequences for the appreciation of existing methods to calculate post-failure resistance as well as the interpretation of experimental results and the development of glass elements with safe failure behaviour.

First, it should be concluded that the FE-models quoted in Chapter 8, should be fundamentally questioned as methods to predict crack growth. Agreements with observations made in experiments may be (partially) accidental. Although valuable insights in the distribution of stresses in the post-failure state of elements is provided, they do not constitute a predictive method with which failure behaviour can be determined and post-failure resistance predicted. They can, therefore, only be indicative tools to design and determine the dimensions of glass elements. Much more research is required in this field so that predictive models for failure behaviour and post-failure resistance can be developed.

Furthermore, the geometry dependency of elastic strain energy²⁸ raises a number of issues that should be considered regarding the further development of safe glass elements:

²⁸ With a constant thickness and a constant l/h ratio, the energy content quadruples when the span and total load carrying capacity (only) doubles.

- Negative scaling effects can be expected when increasing the size of (innovative) elements, as e.g. proposed by Louter & Veer²⁹. Because of the stiffness of the tensile component, increased crack pattern density is not so much likely to become a problem. However, the shock load on the tensile system, particularly on the glass-to-steel adhesive, may induce collapse at initial failure or premature final failure. When alternative brittle reinforcement materials are used, such as CFRP profiles, or carbon or glass fibres³⁰ this could also cause premature collapse.
- Test results on smaller size specimens can not be safely extrapolated to larger sizes without further consideration. Full-scale testing should be preferred, especially when tensile components with relatively low stiffness are applied.
- Although PVB rupture at initial failure was only witnessed in directly tested heat strengthened glass beams,³¹ it could also occur:
 - o In larger size annealed glass beams. Even at lower failure stresses, the total energy content could quickly grow above that of the 2.PVB.S beams tested in Appendix E.
 - o In larger size heat strengthened beams which do not fail by overloading, but by e.g. a combination of static and impact load. When the span doubles, only half the external load will induce the same amount of energy – and therefore possibly the same catastrophic collapse when some unexpected failure cause occurs.
 - o In larger size SG-laminated beams. Although the toughness is considerably higher than that of PVB (both through the higher thickness and the material properties), it may still succumb to shock load when the energy release is increased sufficiently (as has been witnessed in glass-PC laminates in the past).

8. Elastic Strain Energy and Structural Design

The previous Sections 1 – 7 have made clear that the elastic strain energy content in a structural glass element is a parameter that deserves consideration, especially when optimizing structural performance. In order to avoid excessive energy release inducing premature failure or sub standard post-failure resistance, two strategies are basically available: minimize elastic strain energy content in structural elements, and counteract the effects of energy release – also see Figure 9.11.

8.1. Minimizing Elastic Strain Energy Content in Structural Elements

For elements behaving linear elastically to failure, the total strain energy content U_e depends on the strain energy density χ distribution over the element body, Eq. (9.4). The strain energy density, in turn, is the stress integrated over the strain at a point, Eq. (9.3a), which, for linear elastic materials, yielded Eq. (9.3b). This last equation can be rewritten into Eq. (9.10), to show χ depends on σ^2 and E_{eff} .³² Subsequently, the stress is obviously

²⁹ Louter, P.C., Veer, F.A., *Experimental Research on 1:4 Scale Models of an 18 m Reinforced Glass Beam, Part I*, Proceedings of the Glass Performance Days, Tampere, Finland, 2007.

³⁰ Louter, P.C., *High-strength Fibre Rods as Embedded Reinforcement in SentryGlas-laminated glass beams*, Glass Performance Days, Tampere, Finland, June 2009.

³¹ Appendix E.

³² The effective elastic modulus, as used to determine the elasticity of composite sections.

determined by the well known relations Eqs. (9.11) and (9.12), for bending and normal loads.³³

$$\chi = \frac{1}{2}\sigma\varepsilon = \frac{1}{2}\frac{\sigma^2}{E_{eff}} \quad (9.10)$$

$$\text{For bending: } \sigma = \frac{M}{W} \quad (9.11)$$

$$\text{For normal loads: } \sigma = \frac{S}{A} \quad (9.12)$$

From these equations, the strategies to limit strain energy content can be deduced:

- Increase the effective elastic modulus ($E \uparrow$)
- Decrease the stress ($\sigma \downarrow$), by:
 - Reducing the failure stress ($\sigma_{max} \downarrow$),
 - Reducing the external moment ($M \downarrow$),
 - Reducing the external load ($S \downarrow$),
 - Increasing the section surface area or the moment of resistance ($A \uparrow$; $W \uparrow$)

Each of these strategies will be briefly discussed.

The effective modulus of elasticity can be increased by raising the glass Young's modulus through alteration of the composition. Options for this have been discussed in Chapter 8, Section 3.1.1. It is not likely transparent high Young's modulus glasses will be commercially available for application in building construction in the near future. Alternatively, therefore, complementary components (e.g. reinforcement profiles) with a high Young's modulus could be applied. Steel or CFRP³⁴ may therefore be more effective as reinforcement than, for instance, aluminium.³⁵ However, since the complementary components are generally only a small part of a glass element section, it is questionable whether this would significantly alter the E_{eff} . Furthermore, alterations in E_{eff} only linearly affect the elastic strain energy content. It is therefore more effective to consider stress reducing options.

There is a number of possibilities to reduce the stress at failure and thus the energy release. Perhaps trivial, but the first option is to reduce the failure stress of the material.

³³ In Appendix F, Section 2.1., it was shown that shear stresses, at least in ordinary bending cases, hardly contribute to the deformations and stresses. They are thus further ignored in this analyses, but similar observations and strategies will apply to cases where shear stresses do form an important part of the total stress, as e.g. in beams with very high h/l ratios (which will not act as a bending element, but as a shear element).

³⁴ The CFRP sections applied by Antonelli et al. had a $E = 218.6$ GPa. Antonelli, A., Cagnacci, E., Giordano, S., Orlando, M., Spinelli, P., *Experimental and Theoretical Analysis of C-FRP Reinforced Glass Beams*, Proceedings of the 3rd International Symposium on the Architectural Application of Glass (ISAAG), October 2008, Munich, Germany.

³⁵ As applied in the purlins of the ATP discussed in Chapter 2, Section 2. (specifically 2.4.3.).

The effect of this was shown by the difference in failure behaviour of *directly*³⁶ tested 2.PVB.S and 2.PVB.A glass beams presented in Appendix E: while the former collapsed by PVB tearing at failure, the latter could still retain some resistance after initial failure. However, in practice this option will not be of much use, as it simultaneously means a reduction in load carrying capacity.

Reduction of the moment in an element, on the other hand, may be a more realistic option. There are several ways to achieve this. A possibility that should not be overlooked for bending governed elements, is altering the support conditions. The moment integrated over a beam length can be reduced by almost $2/3^{\text{rds}}$ when changing the system from freely supported to rigid connections on both sides, as shown in Figures 9.11a and b. A disadvantage of this strategy could be that the possibility of unpredictable stresses in the glass (especially near the supports) may drastically increase and, depending on the design and type of element it may also be difficult to design a rigid connection capable of properly transferring loads between the glass and the substructure (without unintended stress concentrations).



Fig 9.11a Moment distribution in a freely supported beam.



Fig 9.11b Moment distribution in a rigidly connected beam.

The moment can also be reduced by limiting the span or the external load. This may be done by designing finer structures, e.g. with smaller centre distances (this may decrease the span of roof plates and reduce the load on roof beams).

Finally, the geometrical sections properties may be changed. For bending governed elements, the moment of resistance can be increased. This will automatically also increase the load carrying capacity (assuming the failure stress remains unchanged). To obtain an element with equal resistance but less energy content, the moment of inertia can be changed by adjusting the t/h ratio, as done with the two beam types presented in Appendix H. This approach may be limited by stability considerations (e.g. lateral torsional buckling), but may therefore also spawn the development of more complex sections such as I-, H- and T-profiles.³⁷

For elements of which failure is governed by normal loads, the section area A may be increased, although this can not be done without simultaneously also altering the load carrying capacity.

³⁶ Note that the data in Table 9.1 are not based on directly tested specimens, but rather on pre-damaged ones.

³⁷ Several manufacturing obstacles may be expected, but a T-profile was already successfully built and tested by Louter, several years ago. See: Louter, Christian, Constructief glazen overkapping – verslag 2e peiling, november 2003, Graduation project, Faculty of Architecture TU Delft, November 2003 (not published); and: Bos, F.P., Veer, F.A., Hobbelman, G.J., Louter, P.C., *Stainless Steel Reinforced and Post-Tensioned Glass Beams*, Proceedings of the 12th International Conference on Experimental Mechanics (ICEM12), Bari, Italy, 2004.

For stability governed elements (e.g. buckling), geometrical adaptations similar to those that can be used for bending governed elements, can be applied.³⁸

8.2. Reducing the Effects of Strain Energy Release on a Structural Element

Instead of minimizing the strain energy content at failure, the influence of the energy release may be reduced. Three strategies are available:

- Increase the shock absorption capacity of the complementary component – either its material fracture toughness or its geometry (e.g. laminate thickness). This property determines whether collapse may occur at initial failure (e.g. by premature reinforcement rupture). In reinforced concepts³⁹ the application of non-rigid adhesive systems may help to avoid premature failure.
- Increase the stiffness ($E_{\text{eff}}I$ or $E_{\text{eff}}A$) of the 2nd LTM. In Appendix H, it is shown that the sturdy beams (low I , high energy content), release more energy (both absolutely and relatively) than the slim beams (high I , low energy content). The energy release was determined from the difference in pre- and post-failure bending stiffness.
- Distribute the energy release over a larger area of the complementary component. As discussed before, the sudden PVB-rupture in directly loaded heat strengthened beams did not occur in thermally tempered ones, despite their significantly higher failure load and energy.⁴⁰

8.3. Application of Effect-Reducing Measure: SG-Laminated Reinforced Glass Beams

The strategy of reducing the effects of energy release was successfully applied in a further development of the reinforced glass beams. Previously, they had all been bonded by GB368 UV-curing acrylate adhesive. Final failure has regularly been caused by failure of the adhesive layer which is damaged (debonded) around the initial crack origin and subsequently debonds outwards in the post-failure stage, until the remaining adhesive layer is insufficient to carry the loads and breaks, resulting in final failure. An improved beam design uses SG as a laminate and bonding material. With both a higher fracture toughness⁴¹ and layer thickness, this adhesive/interlayer system can absorb much more shock energy than the GB368 bond. An experimental comparison between both designs is presented in Appendix I.

The SG bonded reinforced glass beams showed consistently higher levels of residual strength and displacement than those bonded with GB368. This should be attributed to the development of a *different 2nd load transfer mechanism* in the post-initial failure stage, made possible by a) the transverse crack stopping properties of the interlayer, and b) the elastic strain energy absorbance capacity of the interlayer.

The post-initial failure strength of the GB368 bonded specimens was governed by the moment capacity of one or two plastic hinges which occurred along the beam length

³⁸ Although this may be more complex as bending around multiple axes may have to be considered.

³⁹ Chapter 8, Section 4.3.4.

⁴⁰ Note that there may be other safety reasons (e.g. damage sensitivity, redundancy) not to opt for thermally tempered glass.

⁴¹ Although no fracture toughness data, the 'elongation at tear [%]' provides an indication: it is 17 % for GB368 (Delo Glassbond Selection Chart, www.delo.de) but 400 % for SG (Belis, J., [Kipsterkte van monolithische en gelamineerde glazen liggers](#), Ph.D. Thesis, Ghent University, Belgium, 2005).

(Figure 9.13a), like those discussed earlier, e.g. in Sections 4 and 5 (Figure 9.9a and b) of this Chapter, and Appendix H. These plastic hinges consist of a compressive glass zone in the top and a tensile steel zone at the bottom. The capacity of these hinges can be determined by quite simple two-dimensional analytical calculations.



Figure 9.13a Plastic hinge determines 2nd LTM in GB368 bonded reinforced glass beams. Maximum theoretical capacity is 3.59 kNm.

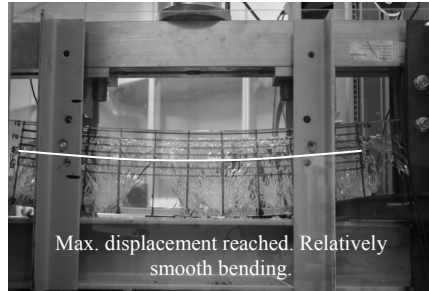


Figure 9.13b A more complex system involving overlapping glass segments and shear loads, determines the 2nd LTM in SG laminated reinforced glass beams.

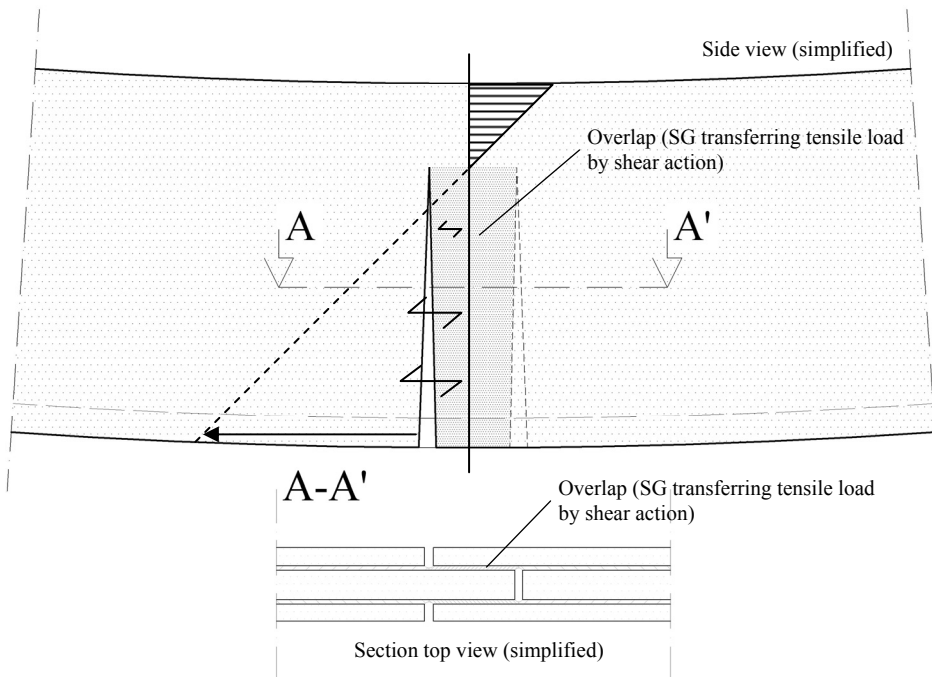


Fig. 9.14 Simplified representation of the extra tensile capacity provided by shear loaded SG (reprint of Figure L.12).

The SG bonded beams however, showed post-failure resistances well above what can be maximally obtained through this mechanism (namely $r_{res,III,ave} = 4.38$ kNm, while $r_{res,III,max}$ theoretically = 3.59 kNm). This can be explained by the presence of an additional

tensile capacity provided by overlapping glass segments transferring tensile actions through shear loaded glass-SG-glass bonds (Figure 9.14) – thus resulting in a different 2nd LTM.

For this mechanism to work, the non-coincidence of glass cracks in the various layers, is crucial. In transverse direction, this is ensured by the crack stopping properties of the SG laminate. In the longitudinal direction, the higher energy absorbance compared to GB368 plays a crucial role: less delamination results in shorter cracks and less concentration of cracks (Compare Figures 9.13a and b). The natural variation of bending tensile strength along the edges of glass sheets also provides a ‘natural’ spread of crack origins.

So, the application of a more shock resistant adhesive layer improved the performance of the element in post-failure both on the tensile side (no adhesive failure) and compressive side (more favourable crack pattern development).

10 Case Studies Revisited

In this pre-final Chapter, the ATP and TFS designs are re-analyzed using the Integrated Approach and Element Safety Diagrams. Also considering the many technical problems, it was concluded the ATP elements needed to be redesigned. For so far relevant to the safety evaluation, the redesign of ATP elements is presented in this chapter. The TFS did not need to be redesigned.

1. Introduction

In Chapter 2, the design and prototypes of two case study projects were presented: the All Transparent Pavilion (ATP; Figures 10.1a and b) and the Transparent Façade Struts (TFS; Figure 10.2a, b, c). These served to explore the possibilities of the concepts that had been developed within the framework of the Zappi Glass & Transparency research and to formulate new research goals.

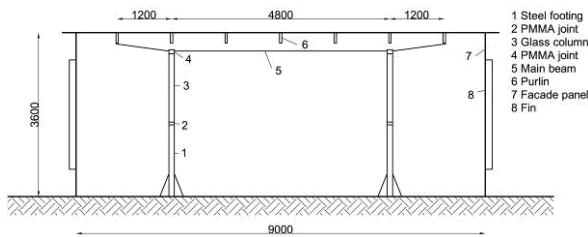


Fig. 10.1a All Transparent Pavilion; section (reprint of Fig. 2.4).

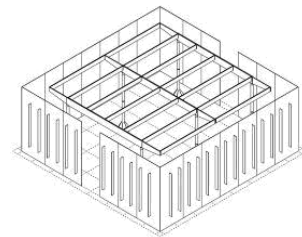


Fig. 10.1b ATP; 3d view of the structure, without roof (reprint of Fig. 2.3c).



Fig. 10.2a Transparent Façade Struts; impression (reprint of Fig. 2.2).

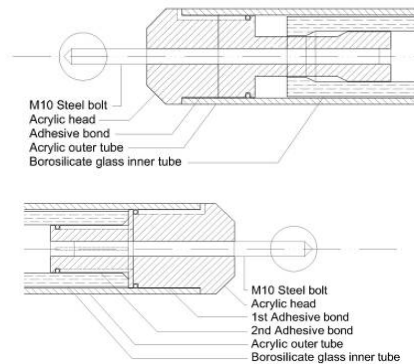


Fig. 10.2b (top), c (bottom) TFS; design of the joints (reprints of Figures 2.35a and b).

Two problem areas were identified:

- Joints. It proved difficult to design transparent, safe joints that enable the structure to act as it was designed.
- Safety definition. Although elements performed in a manner that was intuitively perceived to be safe, there were no *a priori* requirements to which their behaviour could be checked or optimized. Nor was there a fundamental understanding of how safe elements were to be designed.

The study presented in the preceding Chapters 3 – 9 focused on the latter problem. In this pre-final Chapter, the ATP and TFS designs are re-analyzed using the Integrated Approach and Element Safety Diagrams. Also considering the many technical problems, it was concluded the ATP elements needed to be redesigned. For so far relevant to the safety evaluation, the redesign of ATP elements is presented in this Chapter. Section 1.6 of Appendix A provides the rest of the redesign. The TFS did not need to be redesigned.

2. All Transparent Pavilion Revisited

2.1. Specification of Use, Load Cases, and Ultimate Limit State Actions

In the ATP design, a range of measures was applied to ensure the safety of the structure. They all aimed particularly at providing post-failure strength in case of failure of one or more elements, and included:

- Resin laminated columns with significant post-failure resistance ($r_{\text{res,III}} = 200 - 343 \%$),
- Steel reinforced glass cantilever main beams with $r_{\text{res,III,mid-span}} \approx 150 \%$ and $r_{\text{res,III,cantilever}} \approx 66 - 75 \%$,
- Aluminium reinforced, PVB laminated, ‘double’ purlins with $r_{\text{res,III}} \approx 50 \%$,
- PVB laminated roof plates spanning two fields,
- PVB laminated façade panels with a shifted grid respective to the roof plate grid,
- Steel clamp back-up provision in the main beam-purlin joints.

All these measures were applied intuitively, without a priori stated requirements with regard to failure behaviour of the structure and its elements. The main reason was that no method was available to construct a set of such requirements. However, the Integrated Safety Approach and the Element Safety Diagram which have been developed over the previous Chapters, now allow the formulation of failure behaviour requirements and to adjust the design accordingly – at least for the individual elements. In the subsequent sections, ESDs will be constructed for each separate element, and the original design will be checked against it.

Although no definite set of rules was yet presented, it was proposed in Chapter 6, Section 6, that the determination of safety requirements of a structural glass element should depend on its vulnerability and the severity of an eventual collapse. Both will depend to a significant extent on the intended use of the structure. It will determine the exposure of the structure, as well as its occupation frequency and density. In Chapter 2, no specific use has been specified for the ATP. For further discussion in this Chapter, it

is assumed the pavilion will serve as a waiting room at a bus station. Hence, it may be densely occupied (especially in bad weather conditions) and publicly accessible – but closed off at night (i.e. the interior will hardly ever be completely unattended). Thus, rather strict requirements will have to imposed.¹

To determine the required residual strength at increasing model damage levels, selectable values for the time correction factor ψ_T and action partial safety factors γ were introduced in Chapter 6. They are repeated here in Tables 10.1a and b.

To calculate actual figures for resistance and redundancy requirements, the calculable actions on each of the elements have been determined and listed in Table 10.2b from the load cases and durations given in Table 10.2a – both based on the Dutch general code for actions on structures, NEN 6702.²

Table 10.1a Selectable values for the time correction factor ψ_T .

ψ	0.0	0.5	1.0	Corresponding T*
ψ_T	0.3	0.6	1.0	0.25 yr
	0.4	0.7	1.0	0.50 yr
	0.6	0.8	1.0	1.00 yr

Table 10.1b Selectable values for the action partial safety factors γ .

Combination	Structure safety class	$\gamma_{f;g,u}$ (unfavourable)	$\gamma_{f;q,u}$
Fundamental	1	1.2	1.2
	2	1.2	1.3
	3	1.2	1.5
Fundamental	1, 2, 3	1.35	-
Exceptional	1, 2, 3	1.0	1.0

Table 10.2a Load cases and durations.

	Description	Specification	duration
LC1	Permanent actions and variable loads	Cleaning & maintenance	8 hours*
LC2	Permanent actions and variable loads	Snow	30 days
LC3	Permanent actions	Self weight	50 years
LC4	Permanent actions and variable loads	Wind (upwards)	5 seconds

* suggested; not specified in NEN 6702.

¹ Contrary to, for instance, use as an art pavilion in a closed off museum garden.

² Nederlands Normalisatie Instituut, NEN 6702 Technische grondslagen voor bouwconstructies – TGB 1990 – Belastingen en vervormingen, Delft, the Netherlands, 2007.

Table 10.2b Calculable actions R_d on elements of the ATP structure (for $D_\phi = 0$)

Element	Load case				
	R_d type and unit	LC1	LC2	LC3	LC4
Column	F_d [kN]	-24.6	-21.9	-10.8	6.77
Main Beam	$M_{d,mid\ span}$ [kNm]	-20.8	-13.9	-5.16	-0.40
	$M_{d,support}$ [kNm]	10.7	7.25	2.90	-2.34
Purlin	$M_{d,midspan}$ [kNm]*	-3.93	-2.65	-1.14	1.20

* assuming freely supported beams. For rigid connections, the moment maximums shift their sign and location (from mid span to the connections); but their absolute magnitude remains the same (see Section 2.1.3.).

2.2. Columns

2.2.1. Element Safety Diagram

Being free standing elements in a room, the columns should be considered rather vulnerable to all kinds of contact damage.

The exact consequence of the eventual collapse of one of the six columns is hard to predict. Theoretically (just from the statics model), it may be possible new stable mechanisms develop through the disc function of the roof and façades, but it seems risky to rely on this. First, it is questionable whether the remaining elements and joints are strong enough and, second, the dynamic effects of such a collapse will probably play a crucial, but difficult to predict, role. It should be assumed at least half of the pavilion would collapse, but perhaps the whole pavilion would.

A suggestion of relevant time components for the ESD is listed in Table 10.3 (for all discussed ATP structural elements). As a bus station waiting room, it is likely to be used daily, thus severe damages (level II, III) will not go unnoticed for more than 24 hours (component *a*). Smaller damages (level I), however, may not be recognized as such by the general public when they do not lead to immediate collapse. Although evacuation of the pavilion should be possible in a matter of minutes, it may take some more time to close the structure off from the public, hence component *b* is estimated at 2 hours. It should not be very difficult to put up temporary supports for a damaged column, thus component *c* is estimated at 24 hours. Replacement (component *d*) may be much more time consuming, as the design requires custom manufacturing (welding, resin laminating³). This may very well take up to 6 months. The reference life time (component *e*) is 50 years.

The model damage levels are defined as generally proposed in Chapter 6:⁴

- I: Physical damage to the extent that *one outer glass layer* does not transfer principal tensile stresses related to the governing load case anymore in at least one section of the element.
- II: Physical damage to the extent that *all outer glass layers* do not transfer principal tensile stresses related to the governing load case anymore in at least one section of the element.

³ See Chapter 2, Section 2.4.1 for the original design, and Section 2.3.1. of this Chapter for the redesign.

⁴ Chapter 6, Section 3.3.2.

- III: Physical damage to the extent that *all glass layers* do not transfer principal tensile stresses related to the governing load case anymore in at least one section of the element.

Table 10.3 Relevant time components for ATP elements.

		DURATIONS					
		Column		Main Beam		Purlin	
	Description	T [s]	other	T [s]	other	T [s]	other
a	Time-to-discovery	86 400	24 hrs	86 400	24 hrs	86 400	24 hrs
b	Time-to-evacuate	7 200	2 hrs	7 200	2 hrs	7 200	2 hrs
c	Time-to-support	86 400	24 hrs	86 400	24 hrs	21 600	6 hrs
d	Time-to-replace	$15.8 \cdot 10^6$	6 months (183 days)	$15.8 \cdot 10^6$	6 months (183 days)	$5.18 \cdot 10^6$	2 months (60 days)
e	Reference Life Time	$1.58 \cdot 10^9$	50 years	$1.58 \cdot 10^9$	50 years	$1.58 \cdot 10^9$	50 years

From considerations of use, vulnerability, consequence of collapse, and time components, the element safety requirements may be constructed. Table 10.4 provides a general overview of proposed requirements with regard to relative resistance, damage sensitivity, redundancy, and fracture mode, based on the format as used in Appendix D (Tables D.5, D.8, and D.10). Together with the results of the calculable actions for $D_{\phi} = 0$ presented in Table 10.2b, the residual strength requirements can be determined for each model damage level, Table 10.5, and applied in an ESD for the columns, Figure 10.3. The ESD also contains the redundancy curves of the original column design and the redesign, which will be discussed below in this Section and in Section 2.3.1, respectively.

The requirements with regard to resistance and fracture mode are self explanatory. With regard to damage sensitivity, it is considered that accidental collision with falling people may very well be possible in relation to the intended use. Therefore, a soft-body pendulum impact test is required for levels I and II (a drop height of 450 mm should not cause level I damage, while a drop height of 1200 mm should not cause level II damage).⁵ For level III, some resistance to vandalism should also be required. Although being closed off when not in use implies that there will be little possibility for vandals to take their time in doing damage, the structure should be resistant to a particularly aggressive person active even when other people are around. Thus it is suggested to require 10 or more hits with an axe according to NEN-ISO 16936-2⁶ before damage level III may occur.

The vital role the column plays in the overall integrity of the structure call for quite strict redundancy requirements. As limited damage may not even go noticed, the level I

⁵ Note that with the current design, levels I and II coincide, thus the level II requirement is governing for damage sensitivity.

⁶ Nederlands Normalisatie Instituut, NEN-ISO 16936-2 Glas voor gebouwen - Beveiligingsbeglazing - Deel 2: Beproeving en classificatie door herhaalde impact van een hamer en bijl bij kamertemperatuur, Delft, the Netherlands, 2005.

requirements are equal to those in the undamaged situation. For levels II and III, only a minor reduction in requirements (with regard to time and resistance) is allowed. At level II, it is required the resistance is sufficient to allow column replacement without the need of additional supports during the manufacturing time of a new column. For level III, two days are allowed to set up a supporting construction, but during that period, the requirements are such that the structure can be entered and used (the safety class remains 3 at all damage levels).

Table 10.4 General safety requirements for ATP column.

Relative Resistance r	$r = R_d/S_{uls} \geq 1.0$ (sc = 3, $T_{ref} = e = 50$ yrs)	
Damage Sensitivity Σ	Level I: soft body pendulum impact test on undamaged element according to NEN-EN 12600; Σ_{drop} height soft body ≥ 450 mm	
	Level II: soft body pendulum impact test on undamaged element according to NEN-EN 12600; Σ_{drop} height soft body ≥ 1200 mm	
	Level III: - soft body pendulum impact test on undamaged element according to NEN-EN 12600; Σ_{drop} height soft body ≥ 1200 mm - repetitive impact by axe (vandalism) according to NEN-ISO 16936-2, impact applied orthogonally to column length axis in combination with the governing momentary load*; $\Sigma_{min.}$ no impacts before level III damage ≥ 10 - average speed collision with a cleaning vehicle (to be determined).	
Redundancy m	Level I: $R_{res,I}/S_{uls,I} \geq 1.0$	
	with:	Ψ_{T^*} $T^* = T_{ref}$
		γ_{sc^*} $sc^* = 3$
	for T	$\geq e$ $= 50$ yrs ($k_{mod} = 0.29$)
	Level II: $R_{res,II}/S_{uls,II} \geq 1.0$	
	with:	Ψ_{T^*} $T^* = 1.00$
		γ_{sc^*} $sc^* = 3$
	for T	$\geq a+b+c+d \approx d$ $= 183$ dys ($k_{mod} = 0.39$)
	Level III: $R_{res,III}/S_{uls,III} \geq 1.0$	
with:	Ψ_{T^*} $T^* = 0.50$	
	γ_{sc^*} $sc^* = 3$	
for T	$\geq a+b+c \approx a+b$ 48 hrs ($k_{mod} = 0.52$)	
Fracture Mode	B	

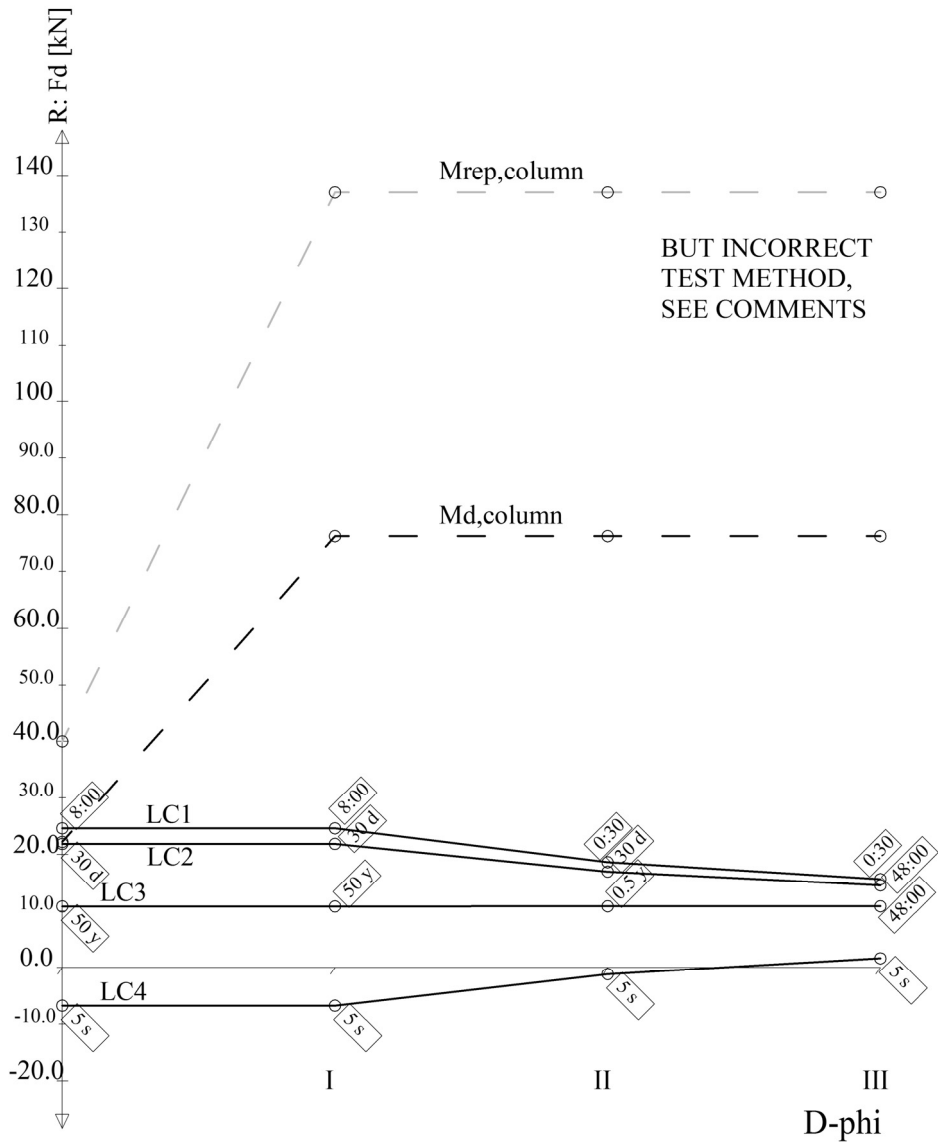


Fig. 10.3 Required Element Safety Diagram for ATP column.^{7,8}

⁷ Note that, contrary to the ESDs presented in Chapter 7, this one refers to a column. As it may be loaded in either compression or tension, the resistance axis has both a positive and negative part.

⁸ Note that the failure behaviour of the tested ATP column prototypes (Chapter 2, Section 2.4.1) was resistance governed, rather than stability governed.

Table 10.5 Calculable actions R_d on ATP column for each model damage level.

D_ϕ	Load case			
	LC1 [kN]	LC2 [kN]	LC3 [kN]	LC4 [kN]
0	-24.6	-21.9	-10.8	6.77
I	-24.6	-21.9	-10.8	6.77
II	-18.6	-17.0	-10.8	1.17
III	-15.6	-14.5	-10.8	-1.63

2.2.2. Safety Evaluation of Original Design

First, it should be noted that, because of the design, the model damage levels I ('one outer layer broken') and II ('all outer layers broken'), coincide. Thus, the redundancy requirements for level I should be met also for level II and the damage sensitivity requirements for level II should be met also for level I.

In the practical application of the Element Safety Diagram, as extensively discussed in Chapter 7, it became clear that a full safety evaluation of a structural glass element design, extensive prototype testing is required at different model damage levels under conditions that simulate both the model impact type and, off course, the support method.

For the ATP column, only a limited number of specimens were subjected to experimental testing:⁹ six small models ($d = 40$ mm, $l = 150$ mm), and three larger ones ($d = 120$ mm, $l = 1200$ and 1500 mm). The small specimens were tested in displacement controlled compression, the larger ones in force-controlled compression.

The redundancy curve of the worst performing large prototype is shown in Figure 10.3,¹⁰ and a calculable redundancy curve is determined by dividing the residual strength values by 1.8 (as a material partial factor).¹¹

Besides the insufficient number of specimens tested, the results do not provide the data required for a conclusive evaluation of the safety of the column design, despite providing important indications with regard to failure behaviour.

The tests did not provide any information for the intermediate damage stage I (= II). As the joints play a crucial role in the initial failure loads, it is likely considering the compressive strength of the element is proportional to the undamaged glass section area (i.e. the inner tube, when the outer one is considered broken) is a conservative, but not very accurate approach.

⁹ Nieuwenhuijzen, E.J. van, Bos, F.P., Veer, F.A., *The Laminated Glass Column*, Proceedings of the Glass Processing Days, Tampere, Finland, 2005.

¹⁰ Determining a 5%-fractile value over 3 results does not make much sense, thus the worst performing specimen is considered governing.

¹¹ Actually, the material partial factor of the 2nd LTM should be determined by testing a large range of prototypes and determining the scatter of the post-failure resistance. However, since such data are not available, the glass material partial factor is maintained. Especially for the metal reinforced elements discussed in the subsequent sections, this may be rather conservative.

For the tested large prototypes, initial failure started at very low nominal stresses (11.8 to 28.9 MPa, whereas earlier studies¹² reported values of around 300 MPa), probably due to stress concentrations caused by imperfections in the tube end geometry and/or irregular deformation of the PMMA connection element.¹³ Due to the low initial strength, the column does not meet the initial resistance requirement when applying $\gamma_M = 1.8$ to the worst performing prototype. This should be solved by improving the joint design to obtain compressive strength values closer to the values obtained in other studies.

As a result of the low initial failure stress, the energy stored at failure is still relatively low, resulting in limited crack growth.¹⁴ If the initial failure stress is increased by improvements of the force transfer into the column, not only the relative post-failure strength $r_{res,III}$ (obtained values: 200 – 343 %) will be reduced drastically, the absolute post-failure strength $R_{res,III}$ may also drop.^{15,16}

This may lead one to conclude it may be an option *not* to try to improve quality of force introduction and actually rely on a low initial failure stress, so that a high post-failure strength can be benefited from. This line of thought should not be pursued, though. A bad quality connection is likely to behave less predictable and show more scatter in strength. Furthermore, the experimental results (compressive initial failure loads of 40, 61, and 73 kN) are hardly sufficient for the initial resistance requirement (short term: 24.6 kN).¹⁷ Finally, the test method (compression on undamaged specimen) failure from the connections is not in line with the impact type by the damage sensitivity requirements. Thus, a post-failure resistance analysis based on simple compression testing is flawed. Rather, a combination of static load and horizontal impact should be applied to assess the post-failure behaviour. As these impacts will cause horizontal deflections, it is likely buckling rather than compressive failure will become governing¹⁸ – thereby changing the failure process altogether.

Thus, with regard to the safety of the glass column design, it may be concluded that although favourable post-failure resistances were obtained in compression,¹⁹ it should

¹² Veer, F.A., Pastunink, J.R., *Developing a transparent tubular laminated column*, Glass Technology International, vol 11, no. 6, p. 134, november 2000; and: Swart, P., Zappi ontwerp van een transparante kolom met voet, Graduation project, Faculty of Architecture TU Delft, July 2002.

¹³ Nieuwenhuijzen, E. van, Bos, F.P., Veer, F.A., *The laminated glass column for the All Transparent Pavilion*, Proceedings 9th Glass Processing Days, Tampere, Finland, June 2005.

¹⁴ Chapter 9, Appendix F.

¹⁵ The influence of initial failure load on post-failure behaviour in glass beams was abundantly clear in tests presented in Appendix E.

¹⁶ Actually, collapse at initial failure was observed in some non-published experiments on small specimens.

¹⁷ Determining a 5%-fractile value over 3 results does not make much sense, but when the lowest value is divided by the material partial factor usually applied for glass, an initial resistance of $40/1.8 = 22.2$ kN is obtained, where 24.6 kN is required.

¹⁸ The Euler buckling load of the undamaged glass column is $F_{b,E} = 306$ kN (assuming $I_{b,E} = 3200$ mm; $E_{borosilicate\ glass} = 64000$ MPa). The recorded initial failure loads (40, 61, 73 kN) were well below this. Even if it should prove to be possible to increase the average initial failure stress by a factor 6 by better joint design and manufacturing, compressive stress would govern failure over buckling. However, when horizontal displacements are introduced and concentrated damage in both glass tubes, e.g. by vandalism (axis test as required for damage sensitivity), both the actual buckling load and the bending resistance of the failed element may decrease rapidly.

¹⁹ Not only in the research discussed here, but also in previous studies with higher initial compressive failure stresses. See: Veer, F.A., Pastunink, J.R., *Developing a transparent tubular laminated column*, Glass

be doubted whether these could be maintained for the required impact types (that introduce horizontal forces). Rather, the design should be enhanced to provide post-failure bending resistance (the applied resin has a very low stiffness and therefore practically ineffective as reinforcement), or an alternative load path should be developed.²⁰

2.2.3. Redesign

The redesigned column is shown in Figures 10.4a – c. The general concept of two glass tubes, one laminated within the other with a clear resin, has been maintained.

An important addition in the form of six reinforcement glass fibres has been applied. This concept is rather new, but preliminary tests on glass beams reinforced with glass fibres have shown favourable results as to their effectiveness.²¹ The effect of the fibres should be a significant residual moment capacity after failure (to avoid buckling). The post-failure moment capacity $M_{\max, \text{post-failure}} \approx 3.77$ kNm (based on the $f_{\text{glass fibre}} = 3400$ MPa, $A_{\text{glass fibre}} = 3.14$ mm²), while the pre-failure moment capacity $M_{\max, \text{pre-failure}} \approx 2.89$ kNm. This would result in a relative residual resistance of $r_{\text{res, III}} = 130$ %. However, the actual post-failure behaviour can not be determined by simple analytical calculations because properties (effective stiffness and effective buckling length) required to determine the buckling load can not be established easily. Thus, a redundancy curve for the redesign could not be given.

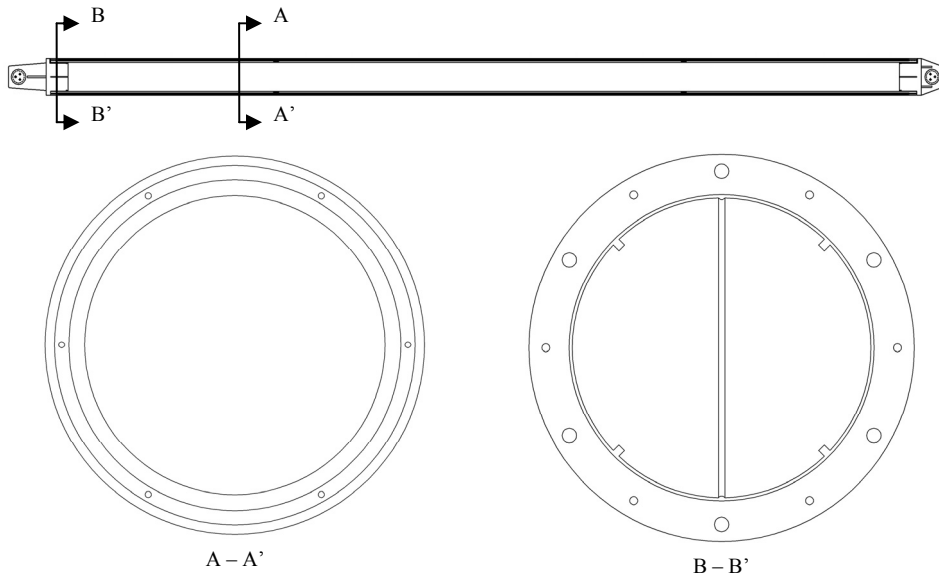


Fig. 10.4a – c ATP glass column: longitudinal section and two transverse sections.

Technology International, vol 11, no. 6, p. 134, november 2000; and: Swart, P., Zappi ontwerp van een transparante kolom met voet, Graduation project, Faculty of Architecture TU Delft, July 2002.

²⁰ Importantly though, the process developed for resin laminating glass tubes was successful and may be applied in a developed design

²¹ Louter, P.C., *High-Strength Fibre Rods as Embedded Reinforcement in SentryGlas-Laminated Glass Beams*, Glass Performance Days, Tampere, Finland, June, 2009.

2.3. Main Beams

2.3.1. Element Safety Diagram

With their bottom edge approximately 3.2 m above the ground, the ATP main beams are not very vulnerable to contact damage. Some may occur during construction and (during its life time) by cleaning, but these are unlikely to cause extensive cracking. Nevertheless, these damages could also cause premature failure over time in combination with static loads through sub critical crack growth.

The consequence of a collapse of a main beam is likely to be similar to that of a column: collapse of the whole, or at least half, of the structure.

It is suggested to use time components equal to those applied for the columns as similar considerations are valid for the main beams. Although it may be a bit more difficult to put up a support structure, it should be possible to do so within 24 hours.

The model damage levels are defined as generally proposed in Chapter 6 and repeated in the previous Section.

Table 10.6 provides a general overview of proposed safety requirements. Table 10.7 lists absolute numbers. Because of the cantilevers, the load distribution (from the purlins) influences the governing moment. Therefore, two load distributions have been considered for each load case (Figure 10.5). Figures 10.6a and b present the ESDs for the beam mid span and above the supports, respectively.

To assess damage sensitivity, it is suggested to perform impact testing on the bottom edge while simultaneously applying a static load.²² Reasonable required impact energies will have to be determined from further research. As the beams are located well above man height, they are unlikely to encounter collision with people. Vandalism in the form of thrown objects may occur, but as the inner layers of a laminate will not likely be influenced by such actions, the ‘static+impact’ impact type is more likely governing.

As the consequence of a collapse of a main beam is similar to that of the collapse of a column, the redundancy requirements are the same.

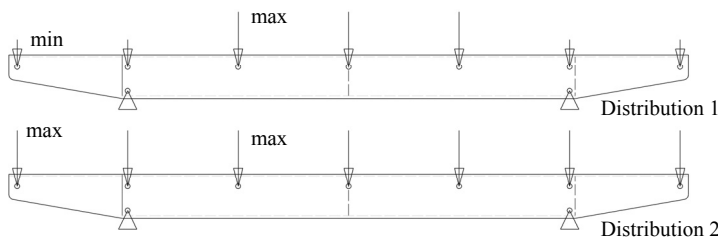


Fig. 10.5 Considered load distributions for ATP main beam.

²² As in Appendix E, method ‘static+impact’.

Table 10.6 General safety requirements for ATP main beam.

Element Safety Property	Element Consequence Class	
	High	
Relative Resistance r	$r = R_d/S_{uls} \geq 1.0$ ($sc = 3, T_{ref} = e = 50$ yrs)	
Damage Sensitivity Σ	Level I: concentrated hard body impact test on the tensile loaded edge of a single sheet (the one considered to be broken at this damage level), in combination with a static load; $\Sigma_{impact} \geq$ to be determined [J]	
	Level II: concentrated hard body impact test on the tensile loaded edge of a single sheet, in combination with a static load; $\Sigma_{impact} \geq$ to be determined [J]	
	Level III: concentrated hard body impact test on the tensile loaded edge of a single sheet, in combination with a static load; $\Sigma_{impact} \geq$ to be determined [J]	
Redundancy m	Level I: $R_{res,I}/S_{uls,I} \geq 1.0$	
	with:	ψ_{T^*} $T^* = T_{ref}$
		γ_{sc^*} $sc^* = 3$
	for T	$\geq e$ $= 50$ yrs ($k_{mod} = 0.29$)
	Level II: $R_{res,II}/S_{uls,II} \geq 1.0$	
	with:	ψ_{T^*} $T^* = 1.00$
		γ_{sc^*} $sc^* = 3$
	for T	$\geq a+b+c+d \approx d$ $= 183$ dys ($k_{mod} = 0.39$)
	Level III: $R_{res,III}/S_{uls,III} \geq 1.0$	
	with:	ψ_{T^*} $T^* = 0.50$
	γ_{sc^*} $sc^* = 3$	
for T	$\geq a+b+c \approx a+b$ 48 hrs ($k_{mod} = 0.52$)	
Fracture Mode	B	

Table 10.7 Calculable actions R_d on ATP main beam for each model damage level. Distribution 1 gives the a maximum moment at the beam mid span, whereas distribution 2 results in a maximum moment above the supports.

D_ϕ	Load case							
	LC1 [kNm]		LC2 [kNm]		LC3 [kNm]		LC4 [kNm]	
	Dis. 1	Dis. 2	Dis. 1	Dis. 2	Dis. 1	Dis. 2	Dis. 1	Dis. 2
0	-20.7	10.7	-13.9	7.25	-5.16	2.90	-0.40	-2.34
I	-20.7	10.7	-13.9	7.25	-5.16	2.90	-0.40	-2.34
II	-14.5	7.56	-10.4	5.51	-5.16	2.90	-2.01	-0.25
III	-11.4	6.01	-8.64	4.64	-5.16	2.90	-2.82	0.80

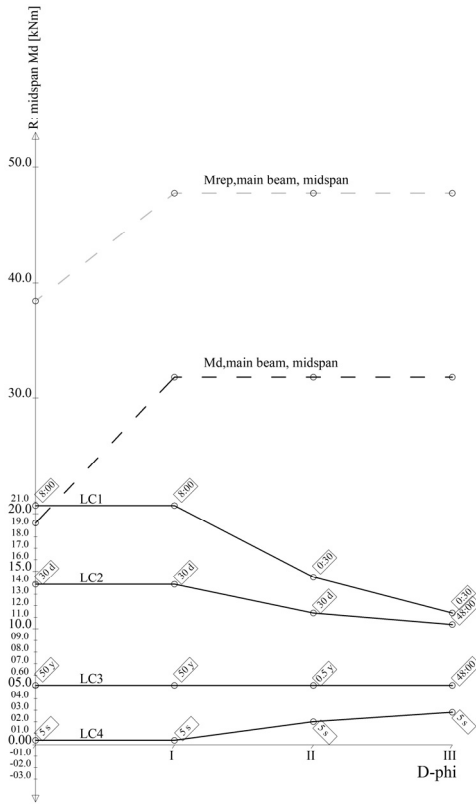


Fig. 10.6a Element Safety Diagram for ATP main beam mid span, with requirements and performance curves (experimental result and calculable; duration unspecified).

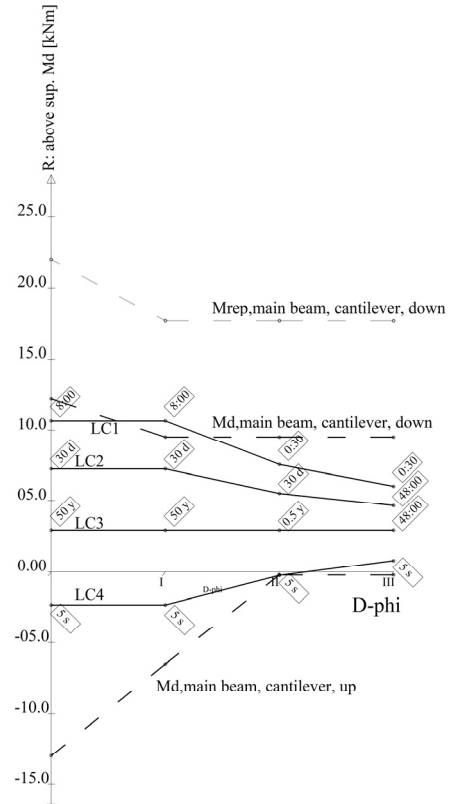


Fig. 10.6b Element Safety Diagram for ATP main beam above the support (tested: cantilever), with requirements and performance curves (experimental result and calculable; duration unspecified).

2.3.2. Safety Evaluation of Original Design

Only one main beam prototype was tested (in three consecutive tests, one on each cantilever and one on the mid span).²³ The mid span section had a relative post-failure strength of $r_{res,III,midspan} = 149.1\%$. From cantilevers, varying results were obtained: one end had a $r_{res,III,cantilever B} = 80.3\%$, but on the other end the adhesive bond between the reinforcement and the glass failed, causing $r_{res,III,cantilever A}$ to sag from 67.0 % directly after failure to $r_{res,III,cantilever A} < 47.6\%$, at which point the test was stopped. The final $r_{res,III,cantilever A}$ was thus not established. The resulting redundancy curves (experimentally established and calculable) for the mid span section and cantilever B are given in Figures 10.6a and b.

Again, the amount of experimental data is far too little to provide a definite comprehensive determination of the safety of this element. Nevertheless, on the failure

²³ Louter, P.C., Belis, J., Bos, F.P., Veer, F.A., Hobbelman, G.J., *Reinforced Glass Cantilever Beams*, Proceedings of the Glass Processings Days, Tampere, Finland, June 2005.

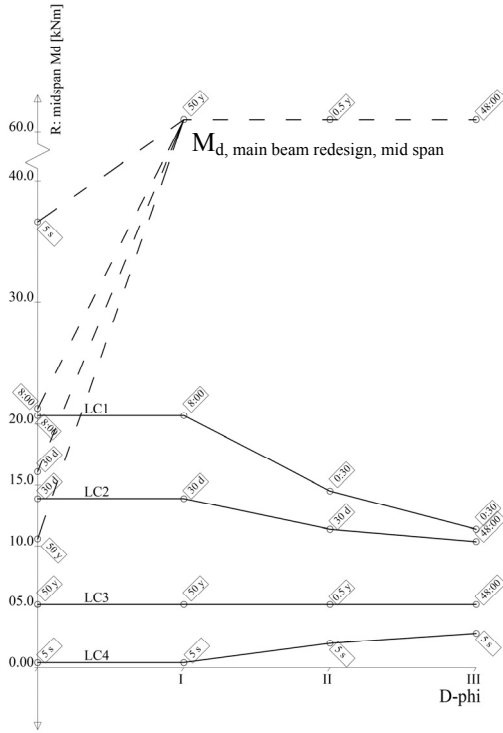


Fig. 10.6c Element Safety Diagram with redundancy requirements for ATP main beam mid span, and estimated redundancy curves of redesign.

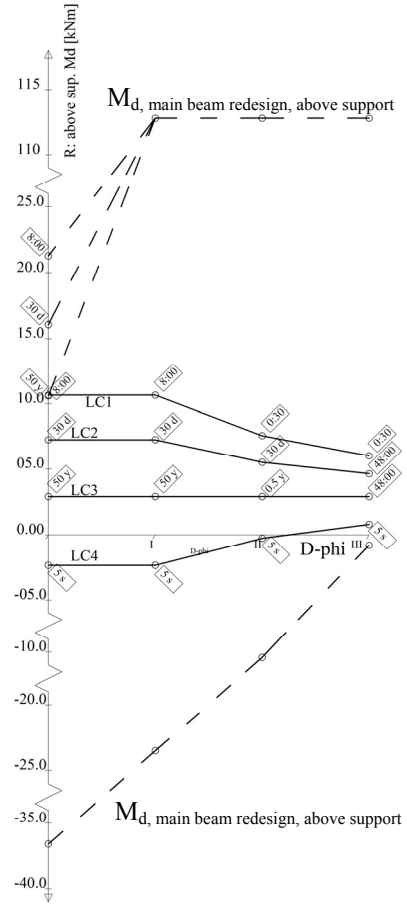


Fig. 10.6d Element Safety Diagram with redundancy requirements for ATP main beam above the support, and estimated redundancy curves of redesign.

behaviour of the concept of stainless steel reinforced glass beams, much more is known.²⁴ From a range of experimental test results on this concept and the internal post-failure moment capacity calculation shown in Figure 10.7a, it may be concluded the post-failure resistance of the mid span section will consistently provide $R_{res,III,midspan} \approx 49.2$ kNm (experimental result: 47.7 kN). Although the prototype test did not feature the governing impact type, it was shown in Appendix E, the impact type has little influence on the post-failure behaviour of this type of reinforced beam.

The adhesive failure witnessed in cantilever A though, does casts some doubts on the safety of that section of the beam. When considering the theoretically possible internal post-failure moment of the cantilever of $R_{res,III,cantilever} \approx 49.2$ (experimental result

²⁴ See Appendices H, J and K, Section 4.3.4.1 of Chapter 8, as well as numerous publications by P.C. Louter and F.A. Veer.

cantilever B: 18.4 kN), as determined in Figure 10.7b, it must be concluded cantilever B also fails prematurely, despite not as drastically as cantilever A.

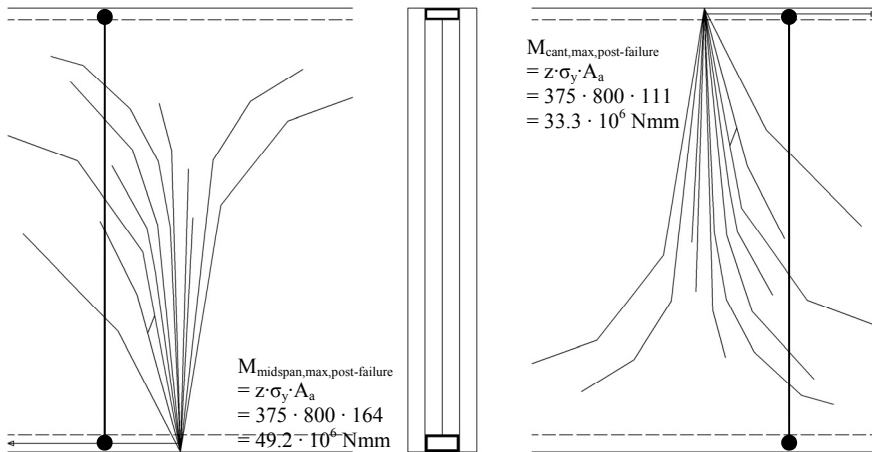


Fig. 10.7a and b Theoretical post-failure moment capacity of original ATP main beam (left: mid span; right: cantilever).

The damage sensitivity of the cantilever parts, having only two layers which, in addition, are also unprotected at the bottom edge, is significantly larger than that of the mid span section. However, for the redundancy for load cases with a net downward action, this will have little effect as cracks will be in the compressive section of the beam. As shown in Figure 10.6b, however, problems occur at model damage level II for LC4 (wind lift). When considering both glass layers broken, the cantilever resistance is provided purely by bending of the reinforcement profile (no compressive action in the glass). This could cause bending stresses in excess of 1242 MPa, which would result in (unacceptable) steel rupture.

A redesign should focus on the cantilever behaviour. The residual strength for LC4 at model damage level II needs to be increased. Furthermore, the resistance of the reinforcement-glass adhesive bond should be increased by either applying a more shock resistant adhesive bond (through bond geometry or adhesive type) or energy release at failure should be significantly reduced.

2.3.3. Redesign

Figures 10.8a – c present the main beam redesign. In comparison to the original design, the beam dimensions and layer layout have been changed. The height h was increased to 480 mm, resulting in a mid span h/l ratio of 1/10. In section, three layers were applied along the total beam length, instead of four in the mid span section, and two at the cantilevers. Although it is nowadays possible to manufacture and laminate glass sheets of over 6 m length, the original starting point that the design should be producible from standard jumbo size float glass sheets was maintained. Thus segments according to Figure 10.9 were applied. Because of the consistently high post-failure resistance of reinforced glass beams,²⁵ the segmentations were not considered in the pre-failure

²⁵ See e.g. appendices H, J, and K.

resistance calculations (i.e. they were assumed to be as strong as not segmented sections). Besides easier manufacturing, the main advantage of applying three layers over the main beam length is the increase in adhesive surface area between the reinforcement and the glass – which was considered governing in the final failure of the cantilever parts of the beam (Section 2.1.2). The estimated redundancy curves of the redesign are given Figure 10.6c and d.

To allow for a mechanical joint between the main beams and the roof plates (because of stability issues), the upper reinforcement profile has been replaced by a massive square rod (see Section 2.3.4). The lower reinforcement profile was rotated 90 degrees in order for it to fit in the three layer section layout.

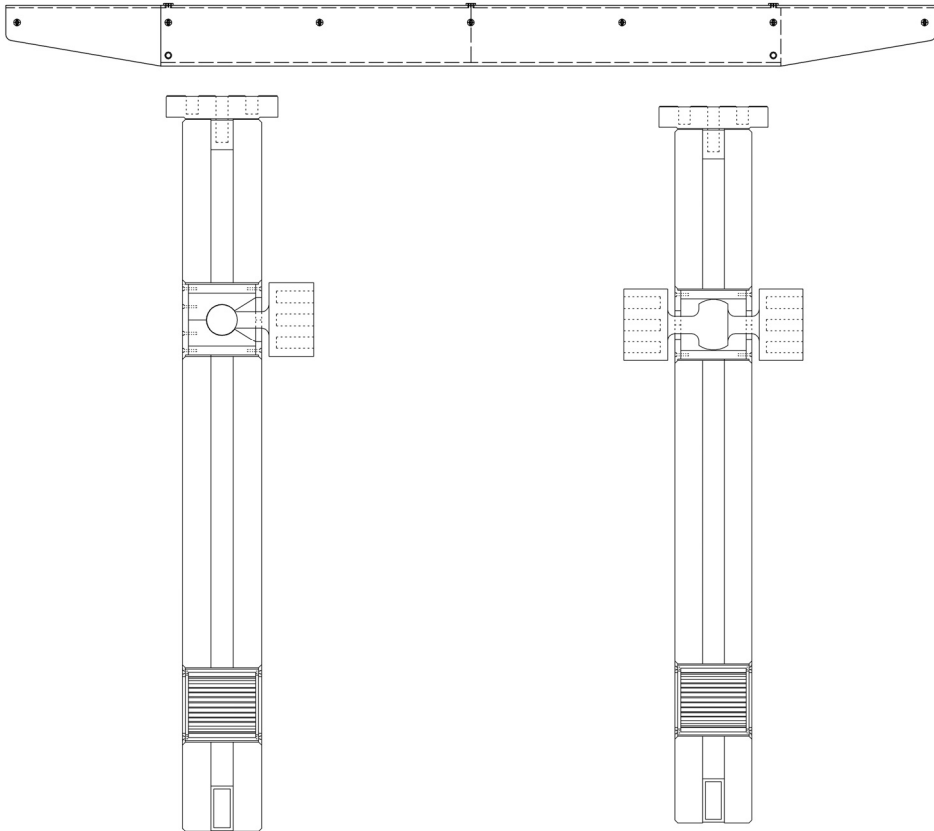


Fig. 10.8a – c ATP main beam: longitudinal view of end beam, section of end beam, section of mid beam.

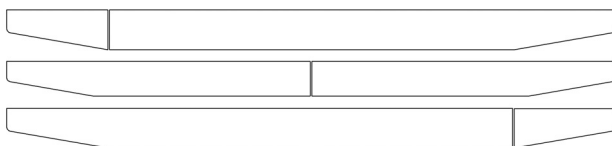


Fig. 10.9 ATP main beam: glass segmentation pattern.

2.4. Purlins

2.4.1. Element Safety Diagram

The vulnerability of the purlins is similar to, or even somewhat less than, the main beams. The consequences of collapse are much less. In the worst case, a 2.4 by 3.6 m² section of the roof could collapse, but stability of the overall structure will not be endangered. Thus, the redundancy requirements – both in terms of resistance and time requirements – are much less severe than for the main beams and columns. They are listed in Table 10.8, along with the other safety requirements. Absolute numbers are given in Table 10.9.

2.4.2. Safety Evaluation of Original Design

The ESD presented in Figure 10.10a is based on freely supported purlins. The experimentally determined and calculable redundancy curves are given as well.²⁶ Although the element passes the redundancy requirements, it should be noted the post-failure resistance, at $r_{\text{res,III,ave}} = 50\%$, is rather low compared to the steel reinforced beams. This is due to the fact that aluminium was used as reinforcement. Its yield strength is more than three times lower than that of stainless steel. When considering the post-failure results that have been obtained with SG laminated beams (Chapter 7 and Appendix E: $r_{\text{res,III,3,SG,A,ave}} = 28.8\%$), it could be questioned whether the aluminium reinforcement is really effective.

Importantly, the chosen rigid support conditions for the purlins alters the stress distribution considerably (Figure 10.11). The maximum moments and stresses remain equal, but their location changes from mid-span to support, and, even more crucial, the orientation turns around – the tensile stresses are at the top. This results in an ESD as Figure 10.7b. As there is no reinforcement at the purlin top, the redundancy curve drastically alters, and is reduced to practically 0 for damage level III. Thus, the design does not meet the safety requirements for this situation. This may be solved either by adjusting the purlin design or the support conditions.²⁷

2.4.3. Redesign

The purlin redesign consists of a three-layer, SG laminated beam (Figures 10.12a – c). The advantage of the rather elaborate initial design with aluminium reinforcement was considered minimal. Actually, the specified safety requirements do not call for metal reinforcement at all – which is thus omitted to obtain maximum transparency. The estimated redundancy curves of the redesign are given Figure 10.10c.

²⁶ Based on experimental data published in: Belis, J., Impe, R. van, Louter, P.C., Veer, F.A., Bos, F.P., *Design and Testing of Glass Purlins for a 100 m² Glass Pavilion*, Proceedings of the Glass Processing Days, Tampere, Finland, June 2005.

²⁷ Although then another way of stabilizing the main beams from tilting should be incorporated.

Table 10.8 General safety requirements for ATP purlin.

Element Safety Property	Element Consequence Class		
	Medium-Low		
Relative Resistance r	$r = R_d/S_{uls} \geq 1.0$ ($sc = 3, t_{ref} = e = 50$ yrs)		
Damage Sensitivity Σ	Level I: concentrated hard body impact test on the tensile loaded edge of a single sheet (the one considered to be broken at this damage level), in combination with a static load; $\Sigma_{impact} \geq$ to be determined [J]		
	Level II: concentrated hard body impact test on the tensile loaded edge of a single sheet, in combination with a static load; $\Sigma_{impact} \geq$ to be determined [J]		
	Level III: concentrated hard body impact test on the tensile loaded edge of a single sheet, in combination with a static load; $\Sigma_{impact} \geq$ to be determined [J]		
Redundancy m	Level I: $R_{res,I}/S_{uls,I} \geq 1.0$		
	with:	Ψ_{T^*}	$T^* = 1.00$
		γ_{sc^*}	$sc^* = 3$
	for T	$A+b+c+d \approx d$	$= 2 \text{ mnd} = 60 \text{ dys}$ ($k_{mod} = 0.42$)
	Level II: $R_{res,II}/S_{uls,II} \geq 1.0$		
	with:	Ψ_{T^*}	$T^* = 0.50$
		γ_{sc^*}	$sc^* = 3$
	for T	$\geq a+b+c$	$= 32 \text{ hr}$ ($k_{mod} = 0.53$)
	Level III: $R_{res,III}/S_{uls,III} \geq 1.0$		
	with:	Ψ_{T^*}	$T^* = 0.25$
		γ_{sc^*}	$sc^* = 2$
	for T	$\geq a+b$	26 hrs ($k_{mod} = 0.54$)
Fracture Mode	B		

Table 10.9 Calculable actions R_d on ATP purlin for each model damage level.

D_ϕ	Load case			
	LC1 [kNm]	LC2 [kNm]	LC3 [kNm]	LC4 [kNm]
0	3.93	2.65	1.14	-1.20
I	2.76	2.00	1.14	-0.42
II	2.18	1.67	1.14	-0.02
III	1.77	1.44	1.14	0.25

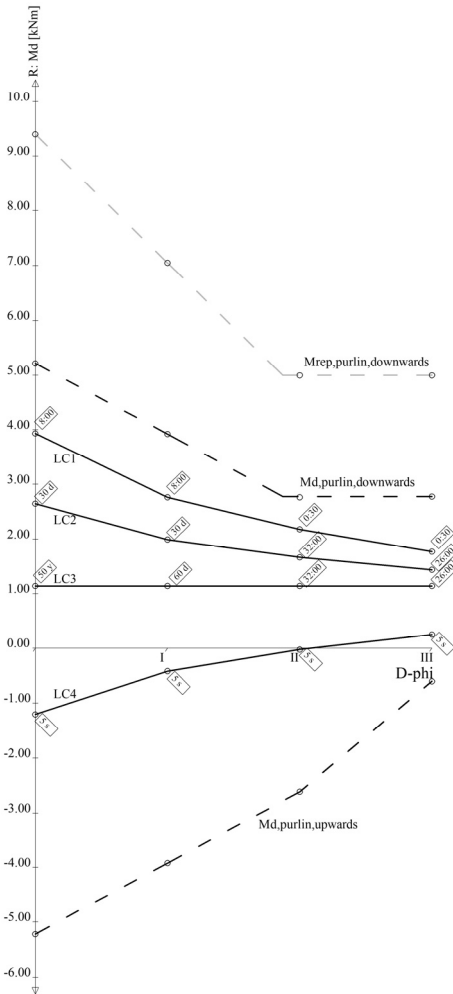


Fig. 10.10a Required Element Safety Diagram and redundancy performance curves for ATP purlin, assuming free supports.

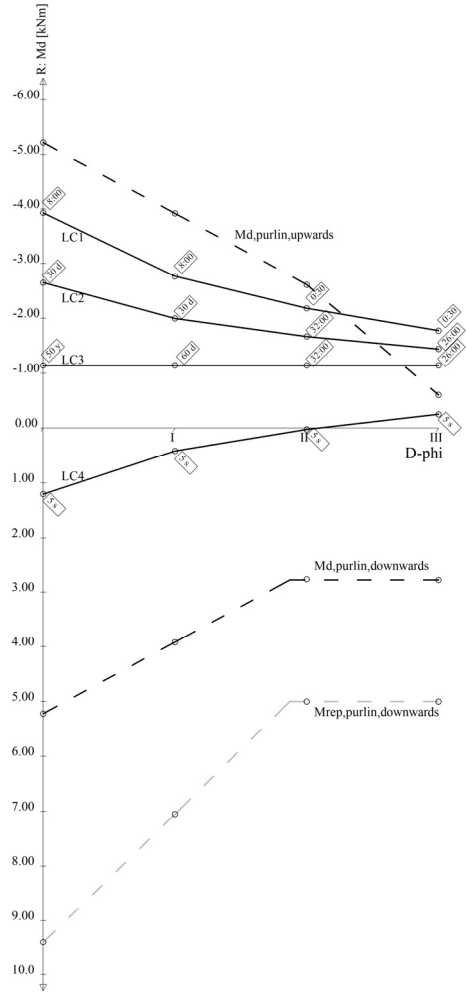


Fig. 10.10b Required Element Safety Diagram and redundancy performance curves for ATP purlin, for rigid connections.

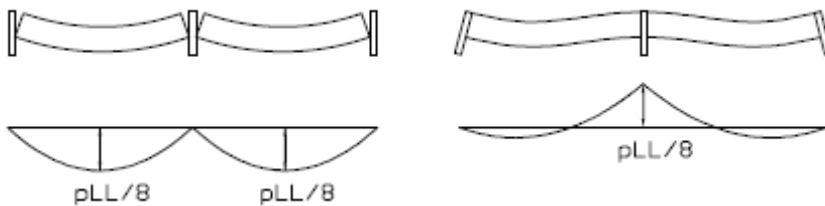


Fig. 10.11 Stress distribution in ATP purlin, for free supports (left) and rigid (right) connections.

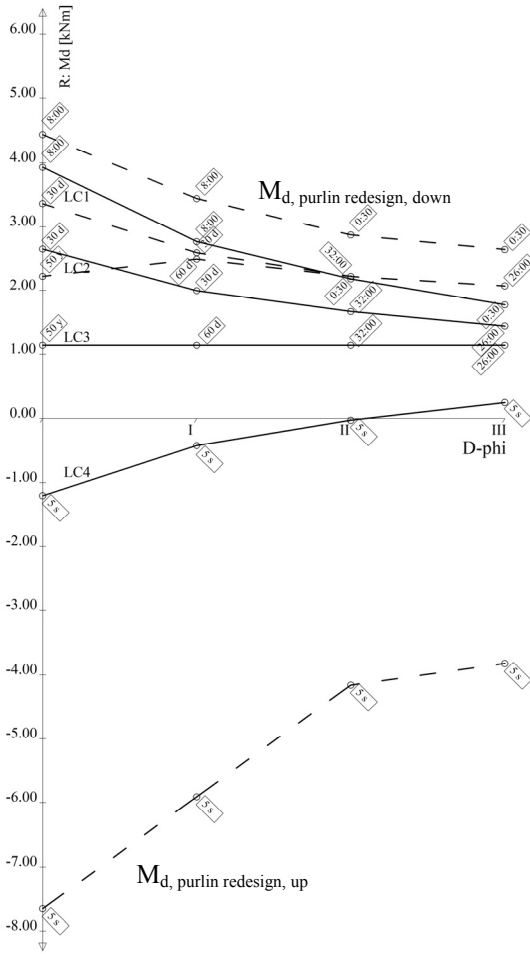


Fig. 10.10c Element Safety Diagram with redundancy requirements for ATP purlin (free supports), and estimated redundancy curves of redesign.

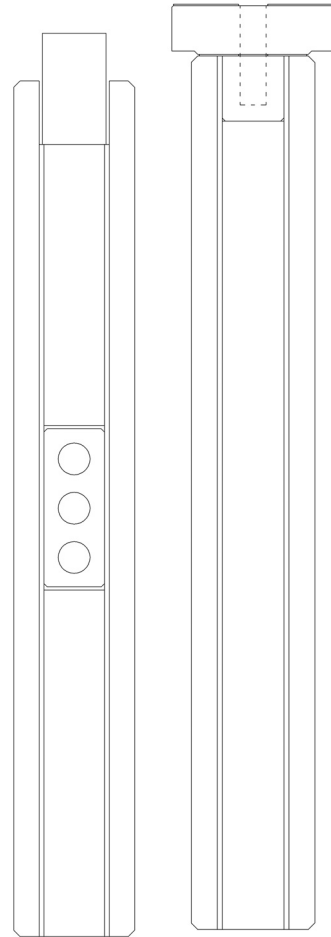


Fig. 10.12a, b ATP purlin: section of near the end, section of at mid span.



Fig. 10.12c ATP purlin: longitudinal view.

3. Transparent Façade Struts Revisited

3.1. Specification of Use, Load Cases, and Ultimate Limit State Actions, and ESD

Contrary to the ATP project, the Transparent Façade Struts (TFS) did not suffer from unsolvable technical problems. However, like the ATP, it was unclear what (quantitative) performance requirements were to be maintained to evaluate the TFS failure behaviour. This became particularly clear when the destructive tension, compression, and bending tests on TFS prototypes were assessed.²⁸

To enable a proper assessment of the TFS designs and determine whether a redesign is necessary, Table 10.12 lists the safety requirements that are proposed for this element and application. They are based on Tables 10.10a, b, and 10.11, that present the load cases, calculable actions and time components, respectively. Absolute resistance requirements are tabulated in Table 10.13. The requirements have been developed into an ESD shown in Figure 10.13. In comparison to the ATP ESDs, the redundancy curves are relatively simple as the load case ‘wind’ only requires residual strength checks for a single time period, namely 5 seconds.

Table 10.10a Load cases and durations.

	description	specification	Duration
LC1	Wind	Pressure	5 seconds
LC2	Wind	Suction	5 seconds

Table 10.10b Calculable actions R_d on elements of the ATP structure.

Element	Load case		
	R_d type and unit	LC1	LC2
Façade Strut	F_d [kN]	-3.6	3.9

Table 10.11 Relevant time components for TFS element.

description	Durations	
	T [s]	other
a Time-to-discovery	86 400	24 hrs
b Time-to-evacuate	1 800	30 min
c Time-to-support	21 600	6 hrs
d Time-to-replace	$15.8 \cdot 10^6$	6 months (183 days)
e Reference Life Time	$1.58 \cdot 10^9$	50 years

²⁸ Chapter 2, Section 3.4. The post-failure resistances in each case were significantly different, ranging from $r_{res,III,compression} = 118\%$ to $r_{res,III,tension} = 9.7\%$.

Table 10.12 General safety requirements for TFS.

Element Safety Property	Element Consequence Class	
	Medium-Low	
Relative Resistance r	$r = R_d/S_{uls} \geq 1.0$ ($sc = 3$, $t_{ref} = e = 50$ yrs)	
Damage Sensitivity Σ	Level I: none.	
	Level II: none.	
	Level III: drop test with a 4.1 kg steel sphere, as specified in structural glass guidelines from Hessen, Germany; $\Sigma_{impact} \geq 1$ m.	
Redundancy m	Level I: $R_{res,I}/S_{uls,I} \geq 1.0$	
	with:	Ψ_{T^*} $T^* = 1.00$
		γ_{sc^*} $sc^* = 3$
	for T	$\geq a+b+c+d \approx d$ $= 6$ mnd = 183 dys ($k_{mod} = 0.39$)
	Level II: $R_{res,II}/S_{uls,II} \geq 1.0$	
	with:	Ψ_{T^*} $T^* = 0.50$
		γ_{sc^*} $sc^* = 3$
	for T	$\geq a+b+c \approx a + c$ $= 30$ hr ($k_{mod} = 0.54$)
	Level III: $R_{res,III}/S_{uls,III} \geq 1.0$	
	with:	Ψ_{T^*} $T^* = 0.25$
	γ_{sc^*} $sc^* = 2$	
for T	$\geq b$ $0:30$ ($k_{mod} = 0.69$)	
Fracture Mode	B	

Table 10.13 Calculable actions R_d on TFS for each model damage level.

D_ϕ	Load case	
	LC1 [kN]	LC2 [kN]
0	-3.60	3.90
I	-2.16	2.34
II	-1.44	1.56
III	-0.94	1.01

Contrary to the (envisaged) use of the ATP, the TFS will not be very exposed to damage. Although the smoking room was²⁹ semi-publicly accessible, the building security and constant presence of people make vandalism highly unlikely. The lower TFS were applied at a height of 3.70 m, thus accidental impact was also improbable. Although the

²⁹ The building was destroyed by fire on May 13th 2008.

smoking room was heavily used from time to time, the area directly affected by a collapse of a strut and the façade area it immediately supported, was small (estimated at about 4 m²).

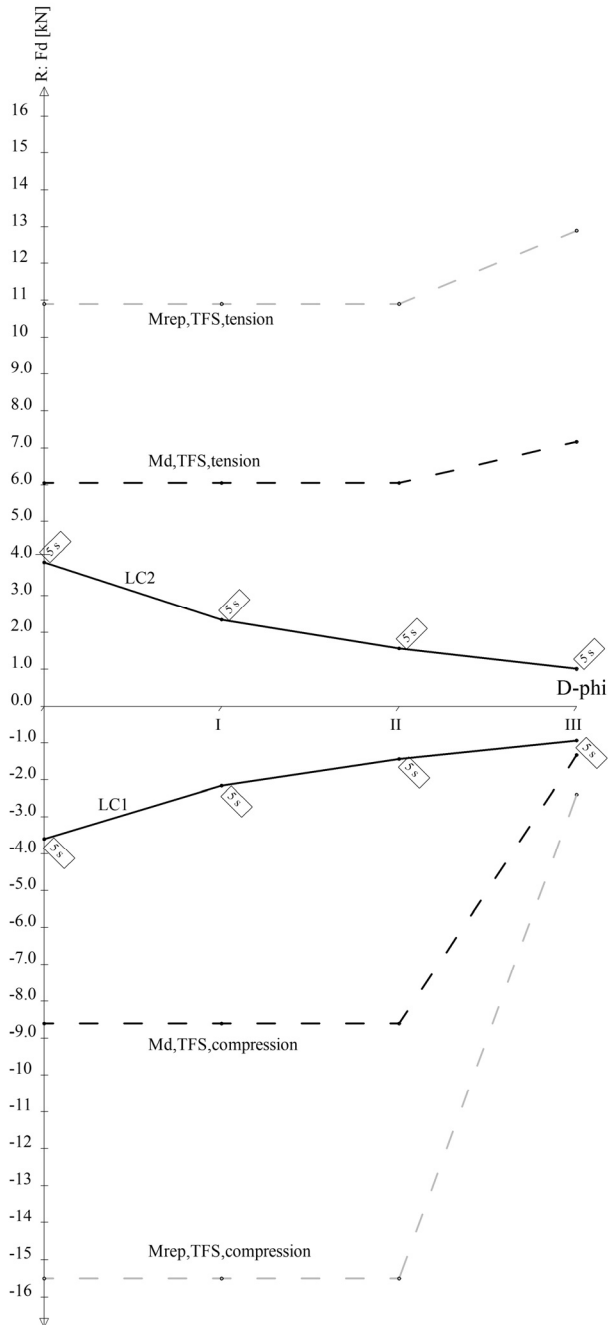


Fig. 10.13 Element Safety Diagram for TFS.

Therefore, both the damage sensitivity and redundancy requirements are proposed to be rather lenient (compared to those proposed for the ATP elements earlier). No specific damage sensitivity requirements are formulated for damage levels I and II. For level III, damage sensitivity could be formulated as a combination of a hard body impact (simulating a falling object, e.g. as the steel sphere test specified in glass construction guidelines from Hessen³⁰) with a certain static load. A reasonable magnitude of a static load should be determined from an expected wind load at an arbitrary point in time.

The redundancy requirements quickly drop over the increasing model damage levels, to almost the lowest value possible within the system of the Integrated Approach: $T^* = 0.25$, $sc^* = 2$, for the duration of b (in this case estimated at 30 minutes).

3.2. Safety Evaluation of the Original Design

The particular design with a glass tube inside an acrylic one, makes the definition of model damage levels I, II, and III less obvious than in the previously presented element designs. Since the glass tube is completely protected and not even directly loaded, it seems reasonable to define levels I and II (one and all outer layers broken, respectively) as equal to level 0 for this particular design. Breakage of the glass tube should be considered model level III damage. It could be discussed whether breakage of the glass tube (with a limited cracking pattern density, so that the broken tube still contributes to the element stiffness), actually induces another LTM, thus whether glass breakage actually means failure for this element. The ambiguity encountered here is the result of the hybrid character of the element design: glass is actually not the primary load transferring material. Nevertheless, it seems the definitions of residual strength and model level damage can be used to define redundancy requirements also for this hybrid element.

The damage sensitivity of the TFS design has not been investigated according to the method proposed here. However, the bending tests (using a steel angle profile as loading point) indicated the glass inner tube is not easily damaged (nor is the PMMA outer one) by mechanical impact. Besides the effective protection by the PMMA, the tubular shape makes falling objects bounce off, transferring less impact energy than they would to rectangular section elements. Thus, the TFS is likely to meet the damage sensitivity requirements.

The calculable redundancy curves for tension and compression have been introduced in the ESD in Figure 10.13. The tensile curve is based on the results of the tensile test, divided by the material partial factor of $\gamma_M = 1.8$. The application of this factor is rather arbitrary based on a single test, but this is inevitable as more test data to determine a material partial factor are just not available.

Perhaps contrary to expectation, the compression redundancy curve is only partially based on the compression test. The level 0 (= I = II) resistance is determined from the

³⁰ Hessisches Ministerium für Wirtschaft, Verkehr und Landesentwicklung, *Anwendung nicht geregelter Bauarten nach § 20 der Hessischen Bauordnung (HBO) im Bereich der Glaskonstruktionen, Anforderungen an Bauarten im Zustimmungsverfahren und Freistellung vom Erfordernis der Zustimmung im Einzelfall nach § 20 Abs. 1 HBO*, Erlass vom 26. Juni 2001, Wiesbaden, Germany, 2001.

initial failure load, divided by $\gamma_M = 1.8$. However, the level III resistance has *not* been taken from the compression test. The compression induced failure results in extensive cracking of the glass tube due to the high energy release.³¹ This influences $R_{res,III}$ in an unreasonably negative way. The shattered glass tube does not contribute to the element bending stiffness anymore, whereas a broken glass tube with limited amount of cracking still would provide residual stiffness, as shown by the bending experiment. Overloading, as simulated by the compression test, is an unrealistic failure cause,³² especially since the relative resistance is high ($r_{d,compression} = R_{0,d} / S_d = (15.5/1.8)/3.6 = 2.4$). The cracking to be induced by the required impact type (object drop test) is likely to be much less severe. Thus, it is more reasonable to determine the $r_{res,III}$ based on the ratio of the (buckling governing) pre- and post-failure effective bending stiffness $(EI)_{eff}$ obtained from the *bending* test. The bending test gave $(EI)_{eff,pre-failure} / (EI)_{eff,post-failure} = 6.5$, thus the calculable post-failure TFS resistance in compression is estimated at $(15.5/1.8) / 6.5 = 1.33$ kN.

When now considering the redundancy requirements, it can be concluded the TFS design provides sufficient redundancy. Additionally, it should be noted the contribution of alternative load paths through the façade plates has been ignored in this assessment. Including that would give an even more positive result.

Since the TFS meets the safety requirements and all major technical problems have been solved in the design,³³ a redesign of the TFS is not necessary.

Although the application of a polymer with plastic failure behaviour (at room temperature) would allow a less elaborate design, this is not strictly essential. The results of the study into the suitability of transparent polymers³⁴ do not justify the application of another polymer. Besides the glass temperature, the availability of products is usually insufficient to actually manufacture the TFS design.

4. Evaluation of ATP en TFS Revisited

Remarkably, the reduction in resistance required over increasing damage levels is often limited when quantified. This is due to the considerable proportion of permanent loads in the total calculable actions, which relatively increases at higher damage levels. The absolute residual resistance therefore rarely reduces below 50 % for elements with permanent loads.

A subtle aspect when formulating the safety requirements is that they should be detached completely from the already developed (preliminary) design. It may be tempting, for instance, with the TFS to estimate the consequence of their collapse as practically zero because the façade panels they support will not collapse when one strut does. In fact, the large façade panels ‘span’ more struts and thus provide an alternative load path for the TFS – and should therefore be assessed as such (whether it provides sufficient redundancy). It should *not* be used as an argument to reduce the safety

³¹ Chapter 9.

³² Chapters 3 and 4.

³³ Most notably obtaining sufficient glass tube length by welding and designing a proper adhesive joint between the PMMA strut heads and the glass inner tube.

³⁴ *AdDoc II: Transparent Polymers for Joint Applications in Glass Structures*, additional document to this PhD, www.glass.bk.tudelft.nl.

requirements on for hand. The consequence class of an element should be determined by the area it supports, not by whether or not alternative load paths are available.

If this trap is sufficiently recognized, the Integrated Approach and ESD provide valuable insight in the failure behaviour required for structural glass elements in certain applications and consequence classes. The designs can be adjusted accordingly.

11 Conclusions and Outlook

1. Conclusion

A solely probabilistic approach, in which the material resistance is compared to a limited number of actions, is principally insufficient to determine the safety of glass structures and structural glass elements. It would not heed considerable uncertainties in the formal probability problem caused by the still debated statistical description of glass strength, disregard the vulnerability of glass to many potential failure causes not considered as actions in the probability analysis, overlook the fact that – unlike other materials – glass is likely to directly collapse upon failure, and ignore the injury potential of glass shards.

In spite of this being generally recognized by glass engineering specialists, this issue is only addressed to a limited extent both in codes and guidelines, as well as in scientific treatises. A comprehensive approach, in which all relevant factors are observed simultaneously, is lacking. Thus, it is often unclear what part of the failure process safety requirements address. Furthermore, safety requirements for different parts of the failure process are unrelated, and they may not be suitable for all structural elements. They are usually independent of the role of the element within the structure. Often, they also have a very general and/or non-quantitative nature. Finally, safety requirements are not described in terms of continuous structural performance properties, but merely as single value pass/fail criteria.

Additional safety measures are taken in practice projects, based on the (single) commonly held presumption that ‘residual strength’ should be provided in any glass structure. However, as there is no generally accepted, quantitative definition of this concept, the extent and type of measures applied, varies widely. A gradual development towards explicit resistance requirements at predefined levels of damage of an element, and thus a more conscious application of safety measures, can be discerned. But this is yet far from being common practice.

The proposed *Integrated Approach to Structural Glass Safety* introduces four element safety properties, with which element behaviour can be characterized and safety can be assessed. The properties *damage sensitivity*, *relative resistance*, *redundancy*, and *fracture mode* each address a specific part of the chain of events from failure cause(s) to the final consequence: injury.

The element safety properties can be combined into an *Element Safety Diagram* (ESD), presenting a letter to indicate fracture mode and a graph of damage versus (residual) resistance. The resulting *redundancy curve* indicates both the impact magnitude required to create a certain amount of damage (and is thus a measure for damage sensitivity) and the residual resistance at that amount of damage. Time-dependency can be incorporated by a third axis or time-tags.

Too little data are available to formulate definite safety requirements for glass elements in their various applications, specifically concerning governing impact types (and magnitudes), short period time correction factors for general actions, and the correlation between failures and actions histories. It is, in any case, clear that safety requirements should be diversified by application category, based on the vulnerability (exposure) of an element and the severity of its collapse. As they are related to failure, residual resistance requirements should always be based on ultimate limit states rather than serviceability limit states. It is theoretically more correct to diversify them through the structure safety classification (and thus γ) and/or the action time correction factor ψ_t , than through omission of the partial safety factors (approach of ‘unfactored loads’).

The Integrated Approach makes it possible to build a body of knowledge on glass element safety by project-independent testing, as well as to compare reasonably objectively between designs and material selections. Furthermore, it allows adjustment of requirements in an easy and insightful way, so that they can be subjected to discussion.

Experimental testing to create ESDs for a range of glass beam designs has shown the presence of a static load during impact greatly enhances the physical damage caused by that impact. Furthermore, in laminated glass beams, the post-failure strength depends on the fracture pattern density, the laminate stiffness and the laminate tensile strength. The elastic strain energy released at failure, which, among others, depends on the failure cause, determines the post-failure load transfer mechanism (LTM). *Therefore, requirements with regard to residual resistance should be formulated with consideration of the failure cause.*

The damage sensitivity and redundancy of triple layer beams is (far) better than that of double layer ones. SG laminated beams have higher redundancy than PVB laminated ones, but comparable damage sensitivity. Annealed and heat strengthened glass perform similarly with regard to damage sensitivity from physical impact. However, annealed glass provides higher post-failure strength, both relatively and absolutely. Thermally tempered glass behaves poorly compared to annealed and heat strengthened glass. It only requires approximately a third of the energy to completely fracture a sheet with a hard-body impact to the glass edge, compared to annealed and heat strengthened glass. Its fracture pattern results in less post-failure resistance.

From a safety point of view, the reinforced beams out perform the other designs by far. They pair very low damage sensitivity with very high redundancy. The amount of damage has practically no influence on the total load transfer capacity. Importantly, this justifies effectively using the *complete glass section* in engineering calculations (instead of applying sacrificial sheets).

From an evaluation of common as well as innovative safety enhancing options and their effects on the element safety properties, it may be concluded that increasing redundancy by introducing/improving post-failure LTMs is the most effective strategy.

Elastic strain energy release is an important parameter for the determination of post-failure resistance by its influence on the crack pattern density and shock load on tensile

components. Negative scaling effects may be expected when increasing the size of (innovative) elements.

There is a linear relation between total crack length, the elastic strain energy released at failure, and some geometry parameters in single sheet, standing, annealed glass beams. With increasing post-failure element stiffness, the relative influence of elastic strain energy release on the post-failure resistance decreases. In order to avoid excessive energy release to induce premature failure or sub standard post-failure resistance, two strategies are basically available: minimize elastic strain energy content or counteract the effects of energy release (e.g. by increasing fracture toughness of the tensile component or the bending stiffness of the post-failure LTM).

Application of the Integrated Approach and ESD on two case study projects, have shown they are valuable tools in understanding glass element safety and adjusting element design to specific requirements.

2. Outlook

As recent large structural glass projects have shown, it is likely architects and their clients will desire ever more, greater, and more complex glass structures. A comprehensive, explicit, and objective approach to assess their safety, already dearly missed, will become indispensable. Further development of probabilistic dimensioning methods will not provide this, and is, furthermore, futile until there is a better understanding of the physio-chemical processes governing glass failure.

The Integrated Approach, on the other hand, provides a step towards the development of a comprehensive safety method for glass in construction. After exploration of the Integrated Approach through the classification of glass beams (Chapter 7) and the implementation in the ATP and TFS case study designs (Chapter 10), the next step should be the pilot-application and evaluation by engineers and building authorities in actual structural glass projects.

Laying down preliminary safety requirements for different classes of structural glass elements by building authorities should be possible, based on their knowledge and experience. Further extensive research into failure causes in reality, actions and action histories, and correlation between damage and actions, should facilitate the development of final application classes and safety requirements for structural glass elements.

There will be an increasing demand for project independent data on glass element failure behaviour to allow for a more conscious selection of element designs. The Integrated Approach provides an opportunity to present such data in a uniform manner. Together with universities and/or other research institutes, the glass industry should instigate an extensive program of glass element testing aimed at failure behaviour, rather than failure stress, to supply these data.

The expected growth of the number of glass projects will also call for reliable predictive analytical and FE-modelling of pre- and post-failure resistances of glass elements. This will be aided by the conscious design of primary and secondary load transfer mechanisms, which make the determination of the resistances relatively easy. However,

the relevance of elastic strain energy release to the post-failure LTM should not be neglected, specifically for low stiffness 2nd LTMs. This should be subject of further research. Hopefully, this will also provide a more fundamental understanding of the relation between impact and physical damage, as well as the relation between physical and structural damage.

The increasingly daring structural applications of glass will continue to drive the development of structural glass elements with high post-failure resistances, e.g. the reinforced concepts. It is likely such elements will become common place in the coming years. Optimization with regard to structural performance and aesthetical appearance (transparency) may be expected.

In the end, everybody will know about glass: it is transparent ... but it doesn't just break!

12 Bibliography

1. Books, Theses

- **Anderson, T.L.**, Fracture Mechanics, Fundamentals and Applications, 3rd Edition, CRC Press, Taylor & Francis, Boca Raton, USA, 2005.
- **Belis, J.**, Kipsterkte van monolithische en gelamineerde glazen liggers, Ph.D. Thesis, Ghent University, Belgium, 2005.
- **Bernard, F.**, Sur le dimensionnement des structures en verre trempé: etude des zones de connexion, Ph.D. thesis, LMT Cachan, France, 2001.
- **Bucak, Ö., Meissner, M.**, Trag- und Resttragfähigkeitsuntersuchungen an Verbundglas mit der Zwischenlage "Sentry Glas Plus", Abschlussbericht AiF-Forschungsprojekt, Munich, Germany, 2005.
- **Cottrell, A.H.**, The Mechanical Properties of Matter, Robert E. Krieger Publishing Company, Huntington NY, USA, 1981.
- **Cowie, A.P. (Ed.)**, Oxford Advanced Learner's Dictionary of Current English, 4th Edition, Oxford University Press, Oxford, UK, 1989.
- **CUR Bouw en Infra, Kenniscentrum Glas**, Construeren met glas, stand der techniek, CUR rapport 2007-1, Gouda, the Netherlands, 2007.
- **Doremus, R.H.**, Glass Science, 2nd Edition, John Wiley & Sons Inc., New York, USA, 1994.
- **Haldimann, M.**, Fracture Strength of Structural Glass Elements – Analytical and numerical modeling, testing and design, Thèse No 3671, Ecole polytechnique fédérale de Lausanne (EPFL), Switzerland, 2006.
- **Haldimann, M., Luible, A., Overend, M.**, Structural Use of Glass, Structural Engineering Documents 10, IABSE, Zurich, Switzerland, 2008.
- **Hamm, J.**, Tragverhalten von Holz und Holzwerkstoffen im statischen Verbund mit Glas, PhD Thesis Nr. 2065, IBOIS/EPFL, Lausanne, Switzerland, 2000.
- **Hess, R.**, Glasträger, vdf Hochschulverlag AG an der ETH Zürich, Switzerland, 2000.
- **Knaack, U.**, Konstruktiver Glasbau 1, Rudolf Müller Verlag, Cologne, Germany, 1998.
- **Knaack, U., Führer, W., Wurm, J.**, Konstruktiver Glasbau 2, Rudolf Müller Verlag, Cologne, Germany, 2000.
- **Kottogoda, N.T., Rosso, R.**, Applied Statistics for Civil and Environmental Engineers, 2nd edition, Blackwell Publishing, Oxford, United Kingdom, 2008.

- **Kreher, K.**, Tragverhalten und Bemessung von Holz-Glas Verbundträgern unter Berücksichtigung der Eigenspannungen im Glas, PhD Thesis Nr. 2999, IBOIS/EPFL, Lausanne, Switzerland, 2004.
- **Loughran, P.**, Falling Glass, Birkhäuser, Basel, Switzerland, 2003.
- **Luible, A.**, Stabilität vor Tragelementen aus Glas, PhD Thesis Nr. 3014, EPFL, Lausanne, Switzerland, 2004.
- **Nghiem, B.**, Fracture du verre et heterogeneites a l'echelle sub-micronique, Ph.D. Thesis Nr 98 PA06 6260, Université Paris-VI, 1998.
- **Nijse, R.**, Glass in Structures, Birkhäuser, Basel, Switzerland, 2003.
- **Rice, P. Dutton, H.**, Structural Glass, E&FN Spon, London, UK, 1995.
- **Sedlacek, G., Blank, K., Laufs, W., Güssen, J.**, Glas im Konstruktiven Ingenieurbau, Ernst & Sohn Verlag, Berlin, Germany, 1999.
- **Scheerbart, P.**, Glasarchitektur, Germany, 1914.
- **Schittich, C.**, Glass Construction Manual, 2nd Edition, Birkhäuser, Basel, Switzerland, 2007.
- **Schneider, J.**, Introduction to Safety and Reliability of Structures, Structural Engineering Document 5, IABSE, Zurich, Switzerland, 1997.
- **Schuler, C.**, Einfluss des Materialverhaltens von Polyvinylbutirial auf das Tragverhalten von Verbundsicherheitsglas in Abhängigkeit von Temperatur und Belastung, Berichte aus dem Konstruktiven Ingenieurbau, Technische Universität München, Germany, 2003.
- **Shand, E.B.**, Glass Engineering Handbook, 2nd edition, McGraw-Hill, New York, USA, 1958.
- **Shelby, J.E.**, Introduction to Glass Science and Technology, 2nd Edition, The Royal Society of Chemistry, Cambridge, United Kingdom, 2005.
- **Shen, X.**, Entwicklung eines Bemessungs- und Sicherheitskonzeptes für den Glasbau, Ph.D. thesis, Technische Hochschule Darmstadt, Germany, 1997.
- **Siebert, G.**, Beitrag zum Einsatz von Glas als tragendes Bauteil im konstruktiven Ingenieurbau, Ph.D. thesis, Technische Universität München, Germany, 1999.
- **Sobek, W., Kutterer, M., Messmer, R.**, Rheologisches Verhalten von PVB im Schubverbund, Forschungsbericht, Universität Stuttgart, Germany, 1998.
- **Standing Committee on Structural Safety**, Structural Safety 1996-99: Review and recommendations, SETO, London, UK, 1999.
- **Vrouwenvelder, A.C.W.M., Vrijling, J.K.**, Probabilistisch Ontwerpen (b3), TU Delft, the Netherlands.
- **Wagner, E.**, Glasschades – Oppervlaktebeschadigingen, glasbreuk in theorie en praktijk, Kenniscentrum Glas, Gouda, the Netherlands, 2006. Original (German) title: Glasschäden – Oberflächenbeschädigungen, Glasbrüche in Theorie und Praxis, Verlag Karl Hofman, Schorndorf, Germany, 2002.
- **Wellershoff, F.**, Nutzung der Verglasung zur Aussteifung von Gebäudehüllen, Ph.D. thesis, RWTH Aachen / Shaker Verlag, Germany, 2006.

- **Wigginton, M.**, *Glass in Architecture*, Phaidon, London, UK, 1996.
- 2. Articles, Papers, Chapters**
- **Achenbach, J., Behling, S., Doenitz, F.-D., Jung, H.**, *Konstruktive Elementen aus Glasrohrprofilen*. Glas: Architektur und Technik. Vol. 5, 2002, pp. 5-10.
 - **Antonelli, A., Cagnacci, E., Giordano, S., Orlando, M., Spinelli, P.**, *Experimental and Theoretical Analysis of C-FRP Reinforced Glass Beams*, Proceedings of the 3rd International Symposium on the Application of Architectural Glass (ISAAG), Munich, October, 2008.
 - **Bando, Y., Ito, S., Tomozawa, M.**, *Direct observation of crack tip geometry of SiO₂ glass by high-resolution electron microscopy*, Journal of the American Ceramic Society, 67 (3):C36-C37, 1984.
 - **Beason, W.L.**, *A failure prediction model for window glass*, NTIS Accession no. PB81-148421, Texas Tech University, Institute for Disaster Research, USA, 1980.
 - **Beason, W.L., Morgan, J.R.**, *Glass Failure Prediction Model*, Journal of Structural Engineering, 110(2): 197-212, 1984.
 - **Beer, B.**, *Structural Glass Engineering – a Review of Project Specific Testing*, Proceedings of the 9th Glass Performance Days, Tampere, Finland, 2005.
 - **Belis, J., Impe, R. van, Louter, P.C., Veer, F.A., Bos, F.P.**, *Design and Testing of Glass Purlins for a 100 m² Transparent Pavilion*, Proceedings 9th Glass Processing Days, Tampere, Finland, June 2005.
 - **Belis, J., Beken, J. vander, Impe, R. van, Callewaert, D.**, *Performance of Glass-Ionoplast Laminates Above Room Temperature*, Proceedings of the 10th Glass Performance Days, Tampere, Finland, 2007.
 - **Belis, J., Depauw, J., Callewaert, D., Delincé, D., Impe, R. van**, *Failure Mechanisms and Residual Capacity of Annealed glass/SGP Laminated Beams at Room Temperature*, Engineering Failure Analysis, 2008.
 - **Biondini, F., Frangopol, D.M., Restelli, S.**, *On Structural Robustnes, Redundancy and Static Indeterminacy*, Proceedings of the Structures 2008 Congress: Crossing Borders, of the ASCE, Vancouver, April, 2008.
 - **Bos, F.P., Veer, F.A., Hobbelman, G.J., Louter, P.C.**, *Stainless steel reinforced and post-tensioned glass beams*, Proceedings of the 12th International Conference of Experimental Mechanics (ICEM12), Bari, Italy, 2004.
 - **Freek, F.P., Veer, F.A., Hobbelman, G.J., Romein, T., Nijssse, R., Belis, J., Louter, P.C., Nieuwenhuijzen, E.J. van**, *Designing and planning the world's biggest experimental glass structure*, Proceedings of the 9th 9th Glass Processing Days, Tampere, Finland, June 2005.
 - **Bos, F.P., Veer, F.A., Romein, T., Nijssse, R.**, *The evaluation of the All Transparent Pavilion project*, Proceedings 9th Glass Processing Days, Tampere, Finland, June 2005.

- **Bos, F.P., Veer, F.A., Belis, J., Nieuwenhuijzen, E.J. van, Louter, P.C.,** *The Joints for the All Transparent Pavilion*, Proceedings 9th Glass Processing Days, Tampere, Finland, June 2005.
- **Bos, F.P.,** Maak een buiging, het warm en koud vervormen van glas, DAX, nr. 10, October 2006.
- **Bos, F.P.,** *Glass-to-Acrylic and Acrylic-to-Acrylic Cylindrical Adhesive Bonds*, 2nd International Symposium on the Application of Architectural Glass, Munich, Germany, October, 2006.
- **Bos, F.P., Veer, F.A., Heidweiller, A.,** *Using Plastics in the Design of Joints in Transparent Structures*, Proceedings of the 2nd International Symposium on the Architectural Application of Glass, Munich, Germany, October 2006.
- **Bos, F.P.,** *Towards a Combined Probabilistic/Consequence-based safety approach of structural glass members*, HERON, Vol. 52, Is. 1/2, 2007.
- **Bos, F.P., Veer, F.A.,** *Transparent Polymer Joints in Glass Structures*, Proceedings 10th Glass Performance Days, Tampere, Finland, June 2007.
- **Bos, F.P.,** *Hybrid Glass-Acrylic Façade Struts*, Proceedings of the 10th Glass Performance Days, Tampere, Finland, June 2007.
- **Bos, F.P., Veer, F.A.,** *Consequence-based Safety Requirements for Structural Glass Members*, Proceedings of the 10th Glass Performance Days, Tampere, Finland, June 2007.
- **Bos, F.P., Veer, F.A.,** *Bending and buckling strength of butt-welded borosilicate glass tubes*, 3rd International Conference on Structural Engineering, Mechanics and Computation, Cape Town, South Africa, September 10-12, 2007.
- **Bos, F.P., Giezen, C., Veer, F.A.,** *Opportunities for the Welding and Hot-Shaping of Borosilicate Glass Tubes in Building Structural Applications*, Proceedings of the 1st Challenging Glass Conference, Delft, the Netherlands, May 2008.
- **Budden, P.J., Sharples, J.K., Dowling, A.R.,** *The R6 procedure: recent developments and comparison with alternative approaches*, International Journal of Pressure Vessels and Piping 77, 2000, pp. 895-903.
- **Cagnacci, E., Orlando, M., Pecora, M.L., Spinelli, P.,** *Application of C-FRP Strengthened Glass Beams in Façade Design*, Proceedings of the 3rd International Symposium on the Application of Architectural Glass (ISAAG), Munich, October, 2008.
- **Calderone, I., Jacob, L.,** *The Fallacy of the Weibull Distribution for Window Glass Design*, Proceedings of the 7th Glass Processing Days, Tampere, Finland, June 2001.
- **Callewaert, D., Belis, J., Impe, R. van, Lagae, G., Beule, M. de,** *Glued and preloaded bolted connections for laminated float glass*, Proceedings of the 10th Glass Performance Days, Tampere, Finland, June 2007.
- **Colvin, J.B.,** *The Effect of Coatings on the Bending Strength of Architectural Glass*, Proceedings of the Glass Performance Days, Tampere, Finland, 2007.

- **Charles, R.J., Hillig, W.B.**, *The kinetics of glass failure by stress corrosion*, Symposium on Mechanical Strength of Glass and Ways of Improving it, Charleroi, Belgium, 1962.
- **Cruz, P., Pequeno, J.**, *Timber-Glass Composite Beams: Mechanical Behaviour & Architectural Solutions*, Proceedings of the Challenging Glass Conference, Delft, the Netherlands, 2008..
- **Cruz, P., Pequeno, J.**, *Timber-Glass Composite Structural Panels: Experimental Studies & Architectural Applications*, Proceedings of the Challenging Glass Conference, Delft, the Netherlands, 2008.
- **Delincé, D., Callewaert, D., Belis, J., Impe, R. van**, *Post-breakage Behaviour of Laminated Glass in Structural Applications*, Proceedings of the Challenging Glass Conference, Delft, the Netherlands, May 2008.
- **Dériano, S., Truyol, A., Sangleboeuf, J.-C., Rouxel, T.**, *Physical and Mechanical Properties of a New Borosilicate Glass*, Ann. Chim. Sci. Mat. 28, 2003, pp. 55-62.
- **Doenitz, F.-D., Jung, H., Behling, S., Achenbach, J.**, *Laminated glass tubes as structural elements in building industry*, Proceedings 8th Glass Processing Days, Tampere, Finland, 2003.
- **Duser, A. van, Jagota, A., Bennison, S.J.**, *Analysis of Glass/PVB Laminates Subjected to Uniform Pressure*, Journal of Engineering Mechanics, Vol. 125, No. 4, April 1999.
- **Evans, A.G.**, *A Method for Evaluating the Time-Dependent Failure Characteristics of Brittle Materials – and its Application to Polycrystalline Alumina*, Journal of Materials Science, no. 7, 1972, pp. 1137 – 1146.
- **Feirabend, S., Sobek, W.**, *Reinforced Laminated Glass*, Proceedings of the Challenging Glass Conference, Delft, the Netherlands, May 2008.
- **Freytag, B.**, *Glass-Concrete Composite Technology*, Structural Engineering International, 2/2004, pp. 111-117.
- **Frischat, G.-H.**, *Glas – Struktur und Eigenschaften*. In: Lohmeyer, S., Werkstoff Glas I: Sachgerechte Auswahl, optimaler Einsatz, Gestaltung und Pflege, 2. Aufl., Ehningen bei Böblingen: expert Verlag, 1987.
- **Froli, M., Lani, L.**, *Towards Ductile Glass Beams*, Proceedings of the IASS Symposium, Venice, Italy, 2007.
- **Gehrke, E., Ullner, C., Hähnert, M.**, *Fatigue limit and crack arrest in alkali-containing silicate glasses*, Journal of Materials Science, 26:5445-5455, 1991.
- **Gehrke, E., Ullner, C., Hähnert, M.**, *Effect of corrosive media on crack growth of model glasses and commercial silicate glasses*, Glastechnische Berichte, 63(9):255–265, 1990.
- *Glass-Cube SS 1996*, Glas; Architektur und Technik, issue 6/1996.
- **Gräf, H., Albrecht, G., Bucak, Ö.**, *The Influence of Various Support Conditions on the Structural Behaviour of Laminated Glass*, Proceedings of the 8th Glass Performance Days, Tampere, Finland, 2003.

- **Grenet, L.**, *Mechanical Strength of Glass*, Enc. Industr. Nat. Paris, 5 (4): 838 – 848, 1899.
- **Griffith, A.A.**, *The Phenomenon of Rupture and Flow in Solids*, Philosophical Transactions of the Royal Society of London, Vol. A221, 1921, pp. 163-198.
- **Guin, J.-P., Wiederhorn, S.**, *Crack growth threshold in soda-lime silicate glass: role of hold-time*, Journal of Non-Crystalline Solids, 316 (1):1-11, 2003.
- **Hand, R.J.**, *Stress intensity factors for surface flaws in toughened glass*, Fatigue and Fracture of Engineering Materials and Structures, 23(1): 73-80, 2000.
- **Inglis, C.E.**, *Stresses in a plate due to the presence of cracks and sharp corners*, Transactions of the Institution of Naval Architects, 55 (219), 1913.
- **Isselmans, C.**, *Schadegevallen met Glas*, in: Stichting Postacademisch Onderwijs in Civiele Techniek en Bouwtechniek, Bouwkundige en constructieve toepassingen met glas, professional post-academic course, Delft, the Netherlands, 2007.
- **Irwin, G.R.**, *Onset of Fast Crack Propagation in High Strength Steel and Aluminium Alloys*, Sagamore Research Conference Proceedings, Vol. 2, 1956, pp. 289 – 305.
- **Jacob, L., Davies, P.S., Munz, N.**, *Fracture Characteristics of Heat Treated Glass – Safety Classification Characteristics*, Proceedings of the Glass Performance Days, Tampere, Finland, June 2009.
- **Kistner, D., Bretthauer, A., Kahles, H.**, *Using Polymers to Add Additional Functions to Toughened Glass*, Proceedings of the Glass Performance Days, Tampere, Finland, 1997.
- **Kott, A., Vogel, T.**, *Remaining Structural Capacity of Broken Laminated Safety Glass*, Proceedings of the 8th Glass Performance Days, Tampere, Finland, 2003.
- **Kott, A., Vogel, T.**, *Structural Behaviour of Broken Laminated Safety Glass*, in: Crisinel, M., Eekhout, M., Haldimann, M., Visser, R. (Eds.), EU Cost C13 Final Report, Glass & Interactive Building Envelopes, Research in Architectural Engineering Series, Volume 1, IOS Press, Amsterdam, the Netherlands, 2007, pp. 123 – 132.
- **Kreher, K., Natterer, J., Natterer, J.**, *Timber-Glass-Composite Girders for a Hotel in Switzerland*, Structural Engineering International, 2/2004, pp. 149-151.
- **Lamers, E., Derkink, M.**, *Towards Design Rules for Structures with Glass Panels During Impact*, Proceedings of the Challenging Glass Conference, Delft, The Netherlands, May 2008.
- **Ledbetter, S.R., Walker, A.R., Keiller, A.P.**, *Structural Use of Glass*, Journal of Architectural Engineering (ASCE), Vol. 12, no.3, September 1, 2006, pp. 137 – 149.
- **Louter, P.C., Belis, J., Bos, F.P., Veer, F.A., Hobbelman, G.J.**, *Reinforced Glass Cantilever Beams*, Proceedings 9th Glass Processing Days, Tampere, Finland, June 2005.
- **Louter, P.C.**, *Adhesively bonded reinforced glass beams*, HERON, Vol. 52, Is. 1/2, 2007.

- **Louter, P.C., Veer, F.A., Belis, J.**, *Redundancy of Reinforced Glass Beams; temperature, moisture, and time dependant behaviour of the adhesive bond*, Proceedings of the Challenging Glass Conference, Delft, the Netherlands, May 2008.
- **Louter, P.C., Bos, F.P., Veer, F.A.**, *Performance of SGP and adhesively bonded metal reinforced glass beams*, Proceedings of the International Symposium on the Architectural Application of Glass, Munich, Germany, 2008.
- **Louter, P.C., Bos, F.P., Callewaert, D., Veer, F.A.**, *Performance of SentryGlas-Laminated Metal-reinforced Glass Beams at 23, -20, and 60 °C*, Proceedings of the Glass Performance Days, Tampere, Finland, June 2009.
- **Maes, M.A., Fritszons, K.E., Glowienka, S.**, *Structural Robustness in the Light of Risk and Consequence Analysis*, Structural Engineering International, No. 2, 2006, pp. 101 – 107.
- **Matousek, M., Schneider, J.**, *Untersuchungen zur Struktur des Sicherheitsproblems bei Bauwerken*, Institut für Baustatik und Konstruktion an der ETH Zürich, Bericht no. 59, Switzerland, 1976.
- **Menzies, J.**, *Hazards and controlling the risks to structures*, , In: IABSE (Ed.), Proceedings of the International Conference on Safety, Risk and Reliability – Trends in Engineering, Malta, 2001.
- **Mott, N.F.**, *Brittle Fracture in Mild Steel Plates*, Engineering 165 (16), 1948.
- **Neugebauer, J.**, *A Special Fixation With Which the Broken Laminated Safety Glass Is Prevent From Falling Down*, Proceedings of the 9th Glass Performance Days, Tampere, Finland, 2005.
- **Nielsen, J.-H., Olesen, J.F.**, *Mechanically Reinforced Glass Beams*, Proceedings of the 3rd International Conference on Structural Engineering, Mechanics, and Computation, Cape Town, South Africa, 2007.
- **Nielsen, J.H., Olesen, J.F., Stang, H.**, *Experimental Investigation of Residual Stresses in Toughened Glass*, Proceedings of the Challenging Glass Conference, Delft, the Netherlands, May 2008.
- **Nieuwenhuijzen, E.J. van, Bos, F.P., Veer, F.A.**, *The Laminated Glass Column*, Proceedings of the 9th Glass Performance Days, Tampere, Finland, June 2005.
- **Nugue, J.-C., Savineau, G.**, *Safe Post-Breakage Behaviour of Point Fixed Glazing Systems – More Than a Case Study a Real Breakthrough*, Proceedings of the Glass Performance Days, Tampere, Finland, 2003.
- **Overend, M., Gaetano, S. de, Haldimann, M.**, *Diagnostic Interpretation of Glass Failure*, Structural Engineering International, no. 2, 2007, pp. 151-158.,
- **Palumbo, M.**, *A new roof fort he XIIIth Century “Loggia de Vicari” (Arquà Petrarca –PD, Italy) based on structural glass trusses: a case study*, Proceedings of the 9th international conference on Architectural and Automotive Glass (GPD), Tampere, Finland, 2005.

- **Popovic, P.L., Nugent, W.J.**, *Common causes of structural collapses*, In: IABSE (Ed.), Proceedings of the International conference on Safety, Risk and Reliability – Trends in Engineering, Malta, 2001.
- **Porter, M.I., Hously, G.T.**, *Development of scrack size and limit state design methods for edge-abraded glass members*, The Structural Engineer, Volume 79, No. 8.17 (April 2001), pp. 29-35.
- **Rodichev, Y., Tregubov, N.**, *The Challenge of Quality and Strength of the Hardened Architectural Glass*, Proceedings of the Glass Performance Days, Tampere, Finland, June 2009.
- **Rouxel, T.**, *Elastic Properties of Glasses: A Multiscale Approach*, Comptes Rendus Mecanique, August 2006.
- **Rouxel, T.**, *Designing Glasses to Meet Specific Mechanical Properties*, Proceedings of the Challenging Glass Conference, Delft, the Netherlands, May 2008.
- **Royer-Carfagni, G., Silvestri, M.**, *A proposal for an arch footbridge in Venice made of structural glass masonry*, Engineering Structures, Vol. 29, No. 11, 2007, pp. 3015-3025.
- **Sackmann, V., Meissner, M.**, *On the Effect of Artificial Weathering on the Shear Bond and the Tear Strength of two Different Interlayers of Laminated Glass*, Proceedings of the 2nd International Symposium on the Application of Architectural Glass (ISAAG), Munich, Germany, 2006.
- **Savineau, G.**, *Durability and Postbreakage Behaviour of Laminated Safety Glass*, Proceedings of the Glass Processing Days, Tampere, Finland, 2001.
- **Schober, H., Gerber, H., Schneider, J.**, *Ein Glashaus für die Therme in Badenweiler*, Stahlbau 73, Heft 11, 2004, pp. 886-892.
- **Sglavo, V.M.**, *ESP (Engineered Stress Profile) Glass: High Strength Material, Insensitive to Surface Defects*, Proceedings of the 8th Glass Performance Days, Tampere, Finland, 2003.
- **Sglavo, V., Bertoldi, M.**, *Vickers indentation: A powerful tool for the analysis of fatigue behaviour on glass*, Ceramic Transactions, 156:13–22, 2004.
- **Simmons, C. J., Freiman, S. W.**, *Effect of corrosion processes on subcritical crack growth in glass*, Journal of the American Ceramic Society, 64, 1981.
- **Starossek, U.**, *Progressive Collapse of Structures: Nomenclature and Procedures*, Structural Engineering International, No. 2, 2006, pp. 113 – 117.
- **Starossek, U., Haberland, M.**, *Measures of Structural Robustness – Requirements & Applications*, Proceedings of the Structures 2008 Congress: Crossing Borders, of the ASCE, Vancouver, April, 2008.
- **Tartival, R., Reynaud, E., Grasset F., Sangleboeuf, J.-C., Rouxel, T.**, *Superscratch-resistant Glass by Means of a Transparent Nanostructured Inorganic Coating*, Journal of Non-Crystalline Solids, No. 353, 2007, pp. 108-110.
- **Uhm, H., Bruce, L., Culp, T., Roger, C.**, *Glass Strengthening by Edge Coatings*, Proceedings of the Glass Processing Days, Tampere, Finland, 2001.

- **Veer, F.A.; Liebergen, M.A.C. van; Vries, S. de**, *Designing and engineering transparent building components with high residual strength*, Proceedings 5th Glass Processing Days, Tampere, Finland, June 1997.
- **Veer, F.A., Pastunink, J.R.**, *Developing a transparent tubular laminated column*, Proceedings 5th Glass Processing Days, Tampere Finland, 1999.
- **Veer, F.A., Vries, S.M. de**, *Transparent laminated composites for novel architectural structures*, Proceedings 9th European Conference on Composite Materials, Brighton, UK, 2000.
- **Veer, F.A., Rijgersberg, H., Ruytenbeek, D., Louter, P.C., Zuidema, J.**, *Composite glass beams, the third chapter*, Proceedings of the Glass Processing Days, Tampere, Finland, 2003.
- **Veer, F.A., Zuidema, J.**, *The strength of glass, effect of edge quality*, Proceedings of the 8th glass processing days, Tampere, Finland 2003.
- **Veer, F.A., Gross, S., Hobbelman, G.J., Vredeling, M., Janssen, M.J.H.C., Berg, R. van den, Rijgersberg, H.**, *Spanning structures in glass*, Proceedings Glass Processing Days, Tampere, Finland, 2003.
- **Veer, F.A., Bos, F.P., Zuidema, J., Romein, T.**, *Strength and Fracture Behaviour of Annealed and Tempered Float Glass*, Proceedings of the 11th International Conference on Fracture (ICF), Turin, Italy, 2005.
- **Veer, F.A.; Janssen, M.J.H.C.; Nägele, T.**, *The possibilities of glass bond adhesives*, Proceedings 9th Glass Processing Days, Tampere, Finland, June 2005.
- **Veer, F.A.**, *The Strength of Glass; a Non-Transparent Value*, HERON, Vol. 52, Is. 1/2, 2007, pp. 87-104.
- **Veer, F.A., Louter, P.C., Bos, F.P., Romein, T., Ginkel, H. van, Rienslag, A.C.**, *The Strength of Architectural Glass*, Proceedings of the Challenging Glass Conference, IOS Press, Delft, the Netherlands, May 2008.
- *Verbundsicherheitsglas mit SentryGlas Plus erstmals in Europa eingesetzt*, Glas; Architektur und Technik, issue 4/2002, pp 51-53.
- **Vlek, C.A.J., Stallen, P.J.M.**, *Beoordeling van riskante activiteiten: een psychometrische analyse*, De Ingenieur, 29 November 1979.
- **Weller, B., Wünsch, J., Härth, K.**, *Experimental Study on Different Interlayer Materials for Laminated Glass*, Proceedings of the 9th Glass Performance Days, Tampere, Finland, 2005.
- **Weller, B., Weimar, T.**, *Glass-Polycarbonate-Sandwich-Elements as Overhead Glazing*, Proceedings of the 10th Glass Performance Days, Tampere, Finland, 2007.
- **Wellershof, F., Sedlacek, G.**, *Structural Use of Glass in Hybrid Elements: Steel-Glass Beams, Glass-GFRP Plates*, Proceedings of the Glass Processing Days, Tampere, Finland, 2003.
- **Wiederhorn, S. M., Bolz, L. H.**, *Stress corrosion and static fatigue of glass*, Journal of the American Ceramic Society, 53(10):543-548, 1970.

- **Wruk, N., Schutte, A., Hanenkamp, W.,** *Load Bearing Behaviour of Laminated Glass Under Static and Dynamic Load*, Proceedings of the 6th Glass Performance Days, Tampere, Finland, 1999.

3. Codes, Guidelines

- **American Society for Testing of Materials**, ASTM C 1048-04, Standard Specification for Heat-Treated Flat Glass—Kind HS, Kind FT Coated and Uncoated Glass, USA, 2004.
- **Centraal Overleg Bouwconstructies (COBc)**, Constructief glas, toetsingshulpmiddel voor Bouwtoezichten, 1999. In Dutch; not publicly published.
- **Centre for Window & Cladding Technology (CWCT)**, Glass Breakage, Technical Note No. 13, Bath, UK, 2000.
- **Deutsches Institut für Bautechnik (DIBt)**, DIBt 04.17 Anforderungen an begehbbare Verglasungen; Empfehlungen für das Zustimmungsverfahren, Fassung März 2000, Berlin, Germany, 2000.
- **Deutsches Institut für Bautechnik (DIBt)**, Technische Regeln für Verwendung von linienförmig gelagerten Verglasungen (TRLV), Entwurfsfassung September 2005, Technische Regeln für die Bemessung und Ausführung punktförmig gelagerten Verglasungen (TRPV), Entwurfsfassung August 2005, and Technische Regeln für die Verwendung von Absturzsichernden Verglasungen (TRAV), Fassung Januar 2003, Berlin, Germany.
- **Deutsches Institut für Normung**, DIN 18008-1 Entwurf: Glas im Bauwesen – Bemessungs- und Konstruktionsregeln – Teil 1: Begriffe und allgemeine Grundlagen, Berlin, Germany, 2006.
- **Deutsches Institut für Normung**, DIN 18008-2 Entwurf: Glas im Bauwesen – Bemessungs- und Konstruktionsregeln – Teil 1: Linienförmig gelagerten Verglasungen, Berlin, Germany, 2006.
- **Health and Safety Executive (HSE)**, The Construction (Design and Management) Regulations 2007, Statutory Instrument 2007 No. 320, UK, 2007.
- **Hessisches Ministerium für Wirtschaft, Verkehr und Landesentwicklung**, Anwendung nicht geregelter Bauarten nach § 20 der Hessischen Bauordnung (HBO) im Bereich der Glaskonstruktionen, Anforderungen an Bauarten im Zustimmungsverfahren und Freistellung vom Erfordernis der Zustimmung im Einzelfall nach § 20 Abs. 1 HBO, Erlass vom 26. Juni 2001, Wiesbaden, Germany, 2001.
- **Hessisches Ministerium für Wirtschaft, Verkehr und Landesentwicklung**, Anwendung nicht geregelter Bauarten §20 der Hessischen Bauordnung (HBO) im Bereich der Glaskonstruktionen, VII 2-2 – 64 b 16/01 – 8/2003, 17. Januar 2003.
- **Nederlands Normalisatie Instituut**, NEN-EN 12150-1, Glass in building - Thermally toughened soda lime silicate safety glass - Part 1: Definition and description, Delft, the Netherlands, 2000.
- **Nederlands Normalisatie Instituut**, NEN-EN 12337-1, Glass in building - Chemically strengthened soda lime silicate glass - Part 1: Definition and description, Delft, the Netherlands, 2000.

- **Nederlands Normalisatie Instituut**, NEN EN 12600: Glass in building - Pendulum test - Impact test method and classification for flat glass, Delft, the Netherlands, 2003.
- **Nederlands Normalisatie Instituut**, NEN-EN 13474-1 Ontw.: Glass in building - Design of glass panes - Part 1: General basis of design, Delft, the Netherlands, 1999.
- **Nederlands Normalisatie Instituut**, NEN-EN 1748-1-1 Glas voor gebouwen – Bijzondere basisproducten - Borosilicaatglas - Deel 1-1: Definitie en algemene fysische en mechanische eigenschappen, Delft, the Netherlands, 2004.
- **Nederlands Normalisatie Instituut**, NEN-ISO 16936, Forced Entry Security Glazing, Delft, the Netherlands.
- **Nederlands Normalisatie Instituut**, NEN-EN 1863-1, Glass in building - Heat strengthened soda lime silicate glass - Part 1 : Definition and description, Delft, the Netherlands, 2000.
- **Nederlands Normalisatie Instituut**, NEN-EN 1990 Eurocode – Grondslag van het constructief ontwerp, Delft, the Netherlands, 2006.
- **Nederlands Normalisatie Instituut**, NEN-EN 1991 Eurocode 1: Actions on Structures, (various parts), Delft, the Netherlands.
- **Nederlands Normalisatie Instituut**, NEN-EN 1991-1-7, Eurocode 1, Actions on Structures, Part 1-7: General actions – Accidental actions, Delft, the Netherlands, 2006.
- **Nederlands Normalisatie Instituut**, NEN-EN 1991-1-7 Eurocode 1: Belastingen op constructies – Deel 1-7: Algemene belastingen – Buitengewone belastingen: stootbelastingen en ontploffingen, Delft, the Netherlands, 2006.
- **Nederlands Normalisatie Instituut**, NEN 2608-1: Glass in building - Resistance against windload - Requirements and determination method, Delft, the Netherlands, 1997.
- **Nederlands Normalisatie Instituut**, NEN 2608-2:2000 2° Ontw. Vlakglas voor gebouwen – Deel 2: Niet-verticaal geplaatst glas – Weerstand tegen windbelasting, sneeuw, eigen gewicht – Eisen en bepalingsmethode, Delft, the Netherlands, 2000.
- **Nederlands Normalisatie Instituut**, NEN 2608-2: Vlakglas voor gebouwen - Deel 2: Niet-verticaal geplaatst glas - Weerstand tegen eigen gewicht, wind- en sneeuwbelasting en isochore druk - Eisen en bepalingsmethode, Delft, the Netherlands, 2007.
- **Nederlands Normalisatie Instituut**, NEN 3569: Safety glazing in buildings, Delft, the Netherlands, 2001.
- **Nederlands Normalisatie Instituut**, NEN-EN 572-1:2004 Glas voor gebouwen - Basisproducten van natronkalkglas - Deel 1: Definities en algemene fysische en mechanische eigenschappen, Delft, the Netherlands, 2004.
- **Nederlands Normalisatie Instituut**, NEN 6700 Technische grondslagen voor bouwconstructies – TGB 1990 – Algemene basiseisen, Delft, the Netherlands, 2005.

- **Nederlands Normalisatie Instituut**, NEN 6702 Technische grondslagen voor bouwconstructies – TGB 1990 – Belastingen en vervormingen, Delft, the Netherlands, 2007.
- **Nederlands Normalisatie Instituut**, NEN 6702, Technical principles for building structures - TGB 1990 - Loadings and deformations, Delft, the Netherlands, 2007.

4. Other Documents

- 3rd International Workshop on Flow and Fracture in Advanced Glasses (FFAG), Pennsylvania State University, USA, October 2005.
- **Bos, F.P.**, *AdDoc I: Zappi, 1996 – February 2004*, (unpublished), TU Delft, the Netherlands, www.bk.tudelft.nl/glass.
- **Bos, F.P.**, *AdDoc II: Transparent Polymers for Joint Applications in Glass Structures*, (unpublished), TU Delft, the Netherlands, www.bk.tudelft.nl/glass.
- **Bos, F.P.**, *AdDoc III: Welding and Hot-Shaping Borosilicate Glass Tubes; Possibilities, Strength and Reliability*, (unpublished), TU Delft, the Netherlands, www.bk.tudelft.nl/glass.
- **Bos, F.P.**, *AdDoc IV: Glass-to-Acrylic and Acrylic-to-Acrylic Cylindrical Adhesive Bonds*, (unpublished), TU Delft, the Netherlands, www.bk.tudelft.nl/glass.
- **Bucak, Ö.**, Gutachterliche Stellungnahme zur Glasdachkonstruktion beim Bauvorhaben Therme Badenweiler, 06/2003.
- **Granta Design Limited**, *CES Edupack 2007, version 4.7.0*, Database Architecture & Structural Sections.
- **Veer, F.A.**, *The Limitations of Current Transparent Sheet Material in Buildings*, internal memo (unpublished), TU Delft, the Netherlands, 1996.
- **Veer, F.A., Zuidema, J., Berg, A. van den, Sluijs, M.M.A. van der**, *Onderzoek naar de invloed van de dikte en het chemisch harden op de sterkte van glas*, (unpublished), Delft, the Netherlands, December 2001.

5. Websites

- www.sv.vt.edu/classes/MSE2094_NoteBook/97ClassProj/anal/yue/energy.html
- www.basf.de
- www.glass.bk.tudelft.nl
- www.glassfiles.com
- www.louwers.nl
- www.matbase.com
- www.matweb.com
- www.wikipedia.org
- www.sciencedirect.com

6. Illustration Credits

Fig. 1.1a www.flickr.com/photos/stevecadman/753459212, **Fig. 1.1b** www.flickr.com/photos/giacomo/3473812295, **Fig. 1.2a** www.flickr.com/photos/benbawden/3789320739, **Fig. 1.2b** www.flickr.com/photos/stevecadman/2786634171, **Fig. 1.2c** www.flickr.com/photos/koltregaskes/776564142, **Fig. 1.3** www.london-architecture.info, **Fig. 1.4** Mies van der Rohe, **Fig. 1.5a** Unknown, **Fig. 1.5b** www.flickr.com/photos/piet_musterd/1355435495, **Fig. 1.5c** www.flickr.com/photos/bartvandamme/3391516943, **Fig. 1.6** B.H.G. Peters, **Fig. 1.7** www.flickr.com/photos/sebastiagiralt/503535787, **Fig. 1.11** www.flickr.com/photos/kittymghee/2538715425, **Fig. 1.12a** R. Nijssse / ABT, **Fig. 1.12b** N. Baldassini / RFR, **Fig. 1.13** unknown, **Fig. 1.14** www.flickr.com/photos/niecieden/3011958650, **Fig. 1.15a** www.flickr.com/photos/1gl/2711898158, **Fig. 1.15b** www.flickr.com/photos/harryharris/304528697, **Fig. 1.16 – 1.19** T. Macfarlane / Dewhurst Macfarlane and Partners, **Fig. 1.20, 1.21** R. Nijssse / ABT, **Fig. 1.22** P.C. Louter, **Fig. 1.23** R. Nijssse / ABT, **Fig. 1.24** U. Knaack, **Fig. 1.25** A.C.J.M. Eekhout, **Fig. 1.26** P.C. Louter, **Fig. 1.27** U. Knaack, **Fig. 1.33a, b** F.A. Veer.

Fig. 2.1 H.W. Kruse, **Fig. 2.3a** E.J. van Nieuwenhuijzen, **Fig. 2.3b – d, 2.4** ATP Team, **Fig. 2.7** F.A. Veer, **Fig. 2.8 xxx** **Fig. 2.9, 2.10, 2.11** ATP Team, **Fig. 2.12, 2.13a – c** P.C. Louter, J. Belis, F.P. Bos, F.A. Veer, G.J., Hobbelman, **Fig. 2.14a, b** ATP Team, **Fig. 2.15, 2.16a – c** J. Belis, R. van Impe, P.C. Louter, F.A. Veer, F.P. Bos, **Fig. 2.17** H.W. Kruse.

Fig. 5.1 T. Macfarlane / Dewhurst Macfarlane and Partners, **Fig. 5.2** U. Knaack, **Fig. 5.3** R. Nijssse / ABT, **Fig. 5.5a, b** U. Knaack, **Fig. 5.6** T. Macfarlane / Dewhurst Macfarlane and Partners, **Fig. 5.8a, b** F. Wellershoff / Gartner Steel and Glass, **Fig. 5.9** F.A. Veer, **Fig. 5.10** T. Macfarlane / Dewhurst Macfarlane and Partners, **Fig. 5.11** S. Feirabend, W. Sobek, **Fig. 5.12** P.C. Louter, F.P. Bos, D. Callewaert, F.A. Veer, **Fig. 5.14a** M. Rasche, **Fig. 5.14b** J. Schneider, **Fig. 5.15a** M. Palumbo, **Fig. 5.16a, b** K. Kreher, J. Natterer, J. Natterer, **Fig. 5.17** P. Cruz, J. Pequeno, **Fig. 5.18** F. Wellershof, G. Sedlacek, **Fig. 5.19** M. Froli, L. Lani, **Fig. 5.20** B. Freytag, **Fig. 5.30** C. Isselmans / Köhler Peutz, **Fig. 5.31** R. Nijssse / ABT.

Fig. 8.1 F.A. Veer, **Fig. 8.6** T. Macfarlane / Dewhurst Macfarlane and Partners, **Fig. 8.12** S. Feirabend, W. Sobek, **Fig. 8.13a, b** T. Macfarlane / Dewhurst Macfarlane and Partners, **Fig. 8.14a, b** F.P. Bos, F.A. Veer, G.J. Hobbelman, P.C. Louter, **Fig. 8.15a, b** P.C. Louter, F.P. Bos, D. Callewaert, F.A. Veer, **Fig. 8.18** J. Schneider, **Fig. 8.19a** M. Palumbo, **Fig. 8.20a, b** A. Antonelli, E. Cagnacci, S. Giordano, M., Orlando, P. Spinelli, **Fig. 8.21a, b** K. Kreher, J. Natterer, J. Natterer, **Fig. 8.22** P. Cruz, J. Pequeno, **Fig. 8.23** F. Wellershof, G. Sedlacek, **Fig. 8.24** M. Froli, L. Lani, **Fig. 8.25** B. Freytag.

Fig. 10.1a, b ATP Team, **Fig. 10.11** J. Belis, R. van Impe, P.C. Louter, F.A. Veer, F.P. Bos.

Fig. A.3, A.4, A.5a, b, A.6a, b c P.C. Louter, J. Belis, F.P. Bos, F.A. Veer, G.J. Hobbelman, **Fig. A.7, A.8a, b, c** J. Belis, R. van Impe, P.C. Louter, F.A. Veer, F.P. Bos, **Fig. A.11** ATP Team, **Fig. A.12a, b** E.J. van Nieuwenhuijzen, F.P. Bos, F.A. Veer, **Fig. A.13, A.14a, b, A.17, b** ATP Team, **Fig. A.18a – d** H.W. Kruse, **Fig. A.20** ATP Team.

Fig. C.2, C.3 F. Wellershoff / Gartner Steel and Glass.

All other images (drawings, graphs, photographs) have been produced by the author. The author gratefully acknowledges all those who have contributed illustrations.

Veiligheidsconcepten bij het constructief gebruik van glas – naar een geïntegreerde aanpak

Nederlandse samenvatting

Naar aanleiding van twee case-study projecten op het gebied van constructief glas (een paviljoen en pendelstaven voor een gevelconstructie), had dit onderzoek tot doel:

- Het toepasbaar definiëren van kwantificeerbare criteria waarmee het constructieve risico voor verschillende toepassingen van glas in bouwconstructies kan worden bepaald.
- Het bepalen van de ontwerpparameters die relevant zijn voor het minimaliseren van het constructieve risico van toepassingen van glas in gebouwen.

Een enkel probabilistische aanpak, waarin de materiaalweerstand wordt vergeleken met een beperkt aantal belastingen, is principieel ontoereikend om de veiligheid van glasconstructies en glazen constructie-elementen vast te stellen. Zo'n benadering zou a) geen rekening houden met de aanzienlijke onzekerheden in de formele waarschijnlijkheidsberekening, die worden veroorzaakt doordat de statistische sterkteverdeling van glas nog steeds onderwerp van discussie is, b) de kwetsbaarheid van glas negeren voor vele potentiële faalorzaken die niet in de formele waarschijnlijkheidsberekening worden meegenomen, c) over het hoofd zien dat bij glas – in tegenstelling tot veel andere materialen – falen en bezwijken vrijwel samenvallen, en d) het verwondingspotentieel van glasscherven verwaarlozen.

Alhoewel dit algemeen onderkend wordt door specialisten op het gebied van constructief glas, wordt er zowel in normen, richtlijnen als wetenschappelijke publicaties slechts zeer beperkt aandacht aan besteed. Een overkoepelende aanpak, waarin alle relevante factoren simultaan worden meegenomen, ontbreekt. Daardoor is het dikwijls onduidelijk op welk gedeelte van het faalproces bepaalde veiligheidseisen betrekking hebben. Bovendien zijn veiligheidseisen voor verschillende delen van het faalproces doorgaans niet aan elkaar gerelateerd. Soms zijn ze niet toepasbaar voor alle typen constructieve elementen. De eisen zijn meestal onafhankelijk van de rol van een element in de constructie. Vaak hebben ze een nogal algemeen en/of niet-kwantitatief karakter. Tot slot worden veiligheidseisen niet geformuleerd als continue constructieve prestatie-eigenschappen, maar slechts als enkelvoudige zak-/slaagcriteria.

In de praktijk worden bijkomende veiligheidsmaatregelen genomen op basis van het (enige) algemeen gehanteerde uitgangspunt, namelijk dat 'reststerkte' gegarandeerd moet zijn in iedere glasconstructie. Omdat er echter geen universeel geaccepteerde, kwantitatieve definitie van dit begrip is, varieert de mate en het soort van maatregelen

die worden toegepast, aanzienlijk van project tot project. Een langzame ontwikkeling is waar te nemen richting het expliciet formuleren van sterkte-eisen per vooraf gedefinieerd schadeniveau – en daarmee naar een meer bewuste toepassing van veiligheidsmaatregelen. Dit is echter voorlopig nog geen algemene gewoonte.

De voorgestelde *Geïntegreerde Aanpak voor de Veiligheid van Constructief Glas* introduceert vier element-veiligheidseigenschappen, waarmee het gedrag van een element kan worden gekarakteriseerd en de veiligheid kan worden bepaald. De eigenschappen *schadegevoeligheid*, *relatieve weerstand*, *redundantie* en *breukpatroon* zijn allen gerelateerd aan een specifiek deel van de ketting van gebeurtenissen die leidt van faaloorzaak tot het uiteindelijke gevolg: verwonding.

De element veiligheids-eigenschappen kunnen worden gecombineerd tot een Element Veiligheidsdiagram (EVD), die bestaat uit een letter die het breukpatroon aangeeft en een grafiek van schade tegen (rest-)sterkte. De *redundantiecurve* die daaruit resulteert geeft zowel de grote van de benodigde invloed aan om een bepaalde schade te creëren (en is daarmee dus een maat voor de schadegevoeligheid), als de reststerkte bij dat schadeniveau. Tijdsafhankelijkheid kan worden meegenomen door middel van een derde as of tijdlabellen.

Er zijn te weinig gegevens beschikbaar om definitieve veiligheidseisen for glazen elementen in hun verschillende toepassingen te formuleren, met name met betrekking tot het type en de grootte van maatgevende schade-invloeden, tijdscorrectiefactoren voor korte periodes, en de correlatie tussen gevallen van falen en belastingsgeschiedenissen. Het is, hoe dan ook, duidelijk dat veiligheidseisen gevarieerd dienen te worden per toepassingscategorie, gebaseerd op de kwetsbaarheid (mate van blootstelling) van een element en de gevolgen van een eventueel bezwijken. Omdat ze gerelateerd zijn aan falen, dienen reststerkte eisen altijd gebaseerd te zijn op uiterste grenstoestanden, en niet op gebruiksgrenstoestanden. Het is theoretisch correcter om in eisen te variëren door de veiligheidsclassificatie van de constructie (en dus door middel van γ) en/of de tijdscorrectiefactor ψ_t aan te passen, dan door het weglaten van veiligheidsfactoren.

De *Geïntegreerde Aanpak* maakt het mogelijk een ‘body of knowledge’ omtrent de veiligheid van glazen elementen op te bouwen door het uitvoeren van project-onafhankelijke testen. Ook het redelijk objectief vergelijken van ontwerpen en materiaalkeuzes behoort ermee tot de mogelijkheden. Bovendien laat de aanpak toe de gestelde eisen op een eenvoudige en inzichtelijke aan te passen. Daarmee kunnen ze ook onderwerp worden van open discussie.

Experimenten uitgevoerd om EVDs te creëren voor een reeks glazen liggerontwerpen, toonde aan dat de aanwezigheid van een statische belasting de fysieke schade die een impact van een hard voorwerp achterlaat, aanzienlijk groter maakt. In gelamineerd glas is de post-faal sterkte afhankelijk van scheurpatroondichtheid, de stijfheid van de tussenlaag en de treksterkte van de tussenlaag. De elastische rekenergie die vrijkomt bij falen en onder andere van de faaloorzaak afhangt, bepaalt het secundaire draagmechanisme dat zich na falen kan ontwikkelen. *Eisen met betrekking tot reststerkte kunnen daarom niet worden geformuleerd zonder een faaloorzaak aan te geven.*

De schadegevoeligheid en redundantie van drielaagse liggers is (veel) beter dan dat van dubbellaagse. SentryGlas gelamineerde liggers hebben een hogere redundantie dan PVB gelamineerde liggers, maar hun schadegevoeligheid is vergelijkbaar. Ongehard en thermisch versterkt glas gedragen zich vergelijkbaar met betrekking tot schadegevoeligheid voor fysieke impact. Ongehard glas echter, biedt zowel absoluut als relatief, een hogere post-faal sterkte. Thermisch gehard glas presteert matig in vergelijking tot ongehard en thermisch versterkt glas. Er is slechts ongeveer een derde van de energie nodig om met een fysieke impact op de rand volledige breuk te bereiken, in vergelijking met de andere twee typen. Het breukpatroon resulteert in een lagere post-faal sterkte.

Vanuit een oogpunt van veiligheid, presteren de gewapende liggers veel beter dan de andere ontwerpen. Ze koppelen een lage schadegevoeligheid aan een zeer hoge redundantie. De hoeveelheid schade heeft nauwelijks invloed op de totale belastingscapaciteit. Dit rechtvaardigt het effectieve gebruik van de *gehele glasdoorsnede* in constructieve berekeningen, in plaats van de toepassing van opofferingslagen.

Uit een analyse van zowel gewone als innovatieve veiligheidsvergroten opties en hun effect op de element-veiligheidseigenschappen, is gebleken dat het verhogen van de redundantie door het toevoegen/verbeteren van post-faal draagmechanismen, de meest effectieve strategie is.

De vrijkomende elastische rekenergie is een belangrijke parameter die de post-faal sterkte mede bepaald door haar invloed op de scheurpatroon dichtheid en schokbelasting op de trekcomponenten. Er moet daarom rekening worden gehouden met negatieve schaaffecten wanneer de afmeting van (innovatieve) elementen worden vergroot.

Er is een lineaire relatie tussen totale scheurlengte, de vrijkomende elastische rekenergie bij falen, en enkele geometrische parameters, in enkellaagse, staande, ongehard glazen liggers. Met toenemende post-faal stijfheid, neemt de relatieve invloed van de vrijkomende elastische rekenergie af. Om ervoor te zorgen dat overmatige vrijkomende energie niet leidt tot voortijdig bezwijken of ondermaatse post-faal sterkte, zijn er in principe twee strategieën beschikbaar: het minimaliseren van de vrijkomende elastische rekenergie of het tegengaan van de effecten van vrijkomende energie (bijvoorbeeld door de breuktaaiheid van de trekcomponent of de buigstijfheid van het post-faal draagmechanisme, te verhogen).

Toepassing van de Geïntegreerde Aanpak en het Element Veiligheidsdiagram op de herevaluatie van de case-study projecten, heeft laten zien dat dit waardevolle instrumenten kunnen zijn om de veiligheid van glazen elementen te begrijpen en hun ontwerp aan te passen om aan specifieke eisen tegemoet te komen.

Appendix A: Case Studies

The design considerations, experimental research and construction – the issues not directly related to this thesis' research questions, but which are nevertheless important to a structural design – of the two case study projects presented in Chapter 2 (ATP and TFS), are presented. Based on the technical evaluation in this Appendix and the safety review in Chapter 10, a redesign for the All Transparent Pavilion is proposed. This was not required for the TFS project.

1. All Transparent Pavilion

1.1. Team

The ATP project was the result of intensive team work. The idea for an all glass pavilion was hatched by the Zappi research program coordinator Fred Veer around January 2004, some three months after the author started his research. The available manpower at the time however, was too small to seriously work on such a project. That changed by March when Elke van Nieuwenhuijzen started her graduation project under the supervision of Veer and the author, and the decision was made to start the project while searching for more extensions to the team. In August, Jan Belis and Christian Louter joined the project. The former was working on his own PhD on lateral torsional buckling behaviour of glass beams at the University of Ghent and came over as a guest researcher until November 2004. The latter had finished his graduation project on reinforced glass beams with Veer earlier that year and continued his work on that as a PhD researcher after the ATP project, working closely together with the author on a great number of occasions. The team was expanded with a group of M.Sc. students from September onward. They did a lot of work in manufacturing of structural components as well as some detail design and experimental testing. Gerrie Hobbelman advised us on several structural mechanics issues such as stability. Finally, we were supported by Kees Baardolf, the workshop manager and Henk Rijgersberg, both experienced craftsmen proficient in many construction and machining processes. The structure was mounted by the glass sponsor, the Van Noordenne Groep, under supervision of Ton Romein, in close consult with the ATP team.

Although the project was intensive team work, there was a rough division of the responsibilities over the team members as shown in Table A.1. Table A.2 provides an overview of the time schedule of the project and the involvement of the team members. The All Transparent Pavilion was presented on November 23rd 2004, during the international symposium There / Not there, on architectural and structural applications of glass.

1.2. Design Stress and Safety Factors

An important issue in any structural design is the stresses that can be allowed. When designing a structure in glass, the failure stress is very much dependent on the way the glass is loaded. In the All Transparent Pavilion, four different situations were recognized: plate bending in roof and façade panels, mid-field stress concentrations

around the fin tips in façade panels, bending stresses in beams, and compression stresses in borosilicate columns. These were labeled with separate design stresses.

Table A.1 Division of duties and responsibilities during the ATP project

Name	Responsibilities, duties.
Fred Veer	Project supervision, supervision graduation project E. van Nieuwenhuijzen, supervision M.Sc. students.
Freek Bos	Day-to-day project coordination, design integration, joints, supervision graduation project E. van Nieuwenhuijzen, organization symposium There / Not there.
Christian Louter	Main beams
Jan Belis	Purlins
Elke van Nieuwenhuijzen	(graduation student) Pavilion overall design, Columns.
Gerrie Hobbelman	Mechanics consultation.
Kees Baardolf and Henk Rijgersberg	Various manufacturing.
Julian Hoogmans, Huub Metsch, Jordy de Raay, Sabine de Richemont, Desirée Schouten, Remko Siemerink, Marten Valk, Thijs Welman, Wijnand Wesselink.	(M.Sc. students) various design, testing, manufacturing.

Table A.2 ATP project time schedule and team member involvement.

Period (all 2004)	Stage	Team involvement
January	Initial ideas	Veer, Bos
April – July	Project start, preliminary design, research into columns	Veer, Bos, van Nieuwenhuijzen.
August – September	Definite design, structural member design, details.	Veer, Bos, van Nieuwenhuijzen, Louter, Belis, Hobbelman.
October	Experimental testing, construction preparation.	Veer, Bos, van Nieuwenhuijzen, Louter, Belis, Hobbelman, Baardolf, M.Sc. students.
November	Construction	Veer, Bos, van Nieuwenhuijzen, Louter, Belis, Hobbelman, Baardolf, Rijgersberg, M.Sc. students.
November – December	Exhibition	-
December	Demounting	Veer, Bos, van Nieuwenhuijzen, Louter, Belis, Hobbelman, Baardolf, M.Sc. students.

1.2.1. Plate bending in roof and façade panels

By 2004, the national Dutch codes had been developed to a stage that they provided a reasonable starting point for checking stresses in glass structures. The Dutch code NEN 2608-2 (design)¹ allowed a (short term) representative bending tensile stress of 46.2 N/mm² in annealed glass. This number had to be divided by a material factor 1.8 to obtain the calculable stress of 25.7 N/mm². Short term wind loading was the governing stress situation.

1.2.2. Mid-field stress concentrations

A specific situation occurs in the façade panels with the glued on fins. Under bending loads, stress concentrations occur at the fin tips. According to FEM analysis, these can

¹ Nederlands Normalisatie Instituut, *NEN 2608-2:2000 2^e Ontw. Vlakglas voor gebouwen – Deel 2: Niet-verticaal geplaatst glas – Weerstand tegen windbelasting, sneeuw, eigen gewicht – Eisen en bepalingsmethode*, Delft, the Netherlands, 2000. Currently, there is a definite version of this code which lists a slightly different characteristic bending strength for annealed glass, namely 45 N/mm² (NEN-EN 2608-2:2007).

rise up to 55.2 MPa (Figure A.1). According to the codes, this would be far from acceptable. However, the failure stress of glass is very much dependent on the place where the stress occurs. It is generally known that glass does not actually fail at the mentioned (nominal) stresses, but at much higher peak stresses that are caused by surface defect. The nominal stress is only an indication of a stress that could produce local peak stresses leading to failure. Now, the surface defects in the mid-field (Griffith flaws) are much smaller than the edge defects caused by the cutting of the glass. Because the peak stress occurs in such a small area, where the probability of a large flaw is small, and the peak stress does not occur at the edge, it was assumed a higher bending tensile stress could be allowed. The lowest result on three experimental specimens² was a failure peak stress of 108 N/mm². Divided by 1.8, this gave a maximum allowable stress of 60 N/mm².

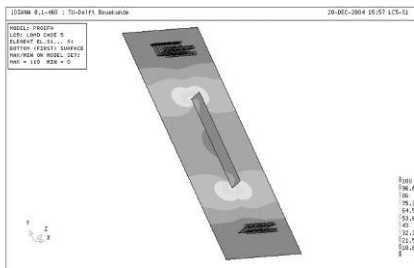


Fig. A.1 Stress concentrations around the fin tips in the façade panels, according to FEM analysis.



Fig. A.2 Possible shape distortions in the ends of glass tubes (exaggerated).

1.2.3. Bending stresses in glass sheet edges in beams and purlins

The bending stresses allowed in plate bending loaded sheets can not simply be applied to upright standing sheets like those in glass beams. In bending loaded beams, the maximum bending tensile stresses occur in the (bottom) glass edge. As has been shown by Hess³, this leads to early failure. He therefore proposes to multiply the calculable bending tensile stress for float glass with a factor of 0.75, resulting in an allowable stress of 18 N/mm². As this factor was approximately corroborated by our own research⁴, this number was wielded. Because of the safe failure behaviour of the beams, no extra material (sacrificial sheets) was added. The complete section was taken into account when checking the stresses.

1.2.4. Compression stresses in borosilicate glass columns

No codes exist for the compressive strength of borosilicate glass. Compressive strengths as high as 400 N/mm² even up to 800 N/mm² have been reported⁵. However, in our own experiments, nominal initial cracking stresses as low as 11.8 MPa were recorded (complete failure of this specific specimen occurred at 40.6 MPa). This immense difference rises from the manufacturing and post-treatment of the tubes and the joints

² See Section 2.4.4 of this Chapter, or Bos, Freek; Veer, Fred; Romein, Ton; Nijssse, Rob, *The evaluation of the All Transparent Pavilion project*, Proceedings 9th Glass Processing Days, Tampere, Finland, June 2005.

³ Hess, R., *Glasträger*, vdf Hochschulverlag AG an der ETH Zürich, Switzerland, 2000.

⁴ Veer, F.A., Bos, F.P., Zuidema, J., Romein, T., *Strength and Fracture Behaviour of Annealed and Tempered Float Glass*, Proceedings of the 11th International Conference on Fracture (ICF), Turin, Italy, 2005.

⁵ Doenitz, Fritz-Dieter; Jung, Herbert; Behling, Stefan; Achenbach, Joachim, *Laminated glass tubes as structural elements in building industry*, Proceedings 8th Glass Processing Days, Tampere, Finland, 2003.

that introduce the loads into the glass. Nonetheless, even these low initial crack stresses still exceeded the maximum design load by 20%.

1.3. Individual Members

1.3.1. Columns⁶

The design of the columns had to meet strict requirements for transparency, strength and safety. During previous Zappi research, a concept had been developed of tubular glass columns consisting of two glass tubes laminated together with a clear resin⁷. It assumes the resin to slow down crack growth and keep the fragments of broken glass together, thereby allowing them to keep transferring compressive loads. This concept had been tested and shown to work on small scale specimens and was consequently also adopted for the ATP columns.

Although the concept is relatively straight forward, producing such components without defects caused by the curing of the resin proved to be a repetitive difficulty from the first experimental specimens in 1997 onward. Heat production, swelling and shrinkage resulted in occasional cracking of the glass, bubbles in the resin, delamination and other defects. Besides the few specimens in which the glass cracked, this did not influence the structural capacity. However, it did seriously compromise the aesthetical quality of those specimens.

The problems are caused by the cylindrical shape of the cavity which prohibits stress free volume changes⁸. To overcome these difficulties, van Nieuwenhuijzen⁹ developed a carefully controlled curing process in which the cavity was gradually filled while the specimen was slowly turning on a turn table. The shrinkage that occurs under these conditions is only in the vertical direction and can thus be filled up with new resin. By using the right pumping rate the top of ring i meets the bottom of ring $i+1$ before it is fully cured thus ensuring a physicochemical continuous joint. A low shrinkage, slow UV-curing resin was developed together with the industry especially for this project. This resulted in consistently faultless curing of the resin in the columns and gave an aesthetically satisfying result.

A series of small scale specimens ($\varnothing_{\text{outer}} = 40 \text{ mm}$, $l = 400 \text{ mm}$) was tested in compression tests, followed by a 1.2 m and two 1.5 m long specimens ($\varnothing_{\text{outer}} = 110$ and 120 mm, respectively). All specimens showed considerable residual strength. The ultimate failure loads ranged from 200 to 300 % of the initial crack strength. Thus their structural behaviour can be considered very safe.

The initial crack strength appeared to be highly dependent on the load introduction into the glass tube. On the larger three specimens, the initial crack strength ranged from 11.8 to 28.9 N/mm². As indicated above, this is very low compared to other studies. However,

⁶ An extensive discussion on the column design, manufacturing and testing can be found in: Nieuwenhuijzen, E. van, Bos, F.P., Veer, F.A., *The laminated glass column for the All Transparent Pavilion*, Proceedings 9th Glass Processing Days, Tampere, Finland, June 2005. This section is based on that paper.

⁷ F.A.Veer, J.R. Pastunink, *Developing a transparent tubular laminated column*, Proceedings 5th Glass Processing Days, Tampere Finland, 1999.

⁸ Similar problems were encountered with cylindrical adhesive joints in the TFS project, see Section 2.3 of this Chapter.

⁹ During her graduation project under supervision of dr. Veer and the author.

the tubes reported by Doenitz et al. have probably been very carefully grinded until the ends were completely flat. Not only are bending stresses avoided this way, it also allows for a precisely fitting joint piece, which evenly spreads the compression stresses. The tubes used for the ATP however, were off-the-shelf products with no special post-treatment. Due to the manufacturing process, the ends of the tubes were not completely flat and not completely straight (Figure A.2). This introduces highly unfavourable bending stresses when the column ends are loaded. Furthermore, the joint design, a block of PMMA with a silicone rubber ring between the glass and the PMMA, proved not to be capable of evenly spreading the stresses. The silicone ring was too soft and got punctured unevenly causing stress concentrations leading to premature initial cracking. The ultimate failure loads showed similar differences and ranged from 40.6 to 57.9 N/mm².

1.3.2. Main Beams¹⁰

The ATP features three main beams. Although the outer ones carry less load, they were all equal due mainly to manufacturing reasons¹¹. The main beam design was based on the reinforced glass beam concept which had been developed from 2001 onwards within the Zappi research¹². Such beams consist of annealed glass layers, glued together with UV-curing acrylate adhesives and provided with a stainless steel section or profile in the tensile zone. Up until the ATP project, only single span beams had been tested. To obtain lengths beyond the standard glass sheet length (6.00 m), the glass layers can be segmented in longitudinal direction. Upon failure, the steel profile starts to act as a crack-bridge, both slowing further crack growth and taking tensile loads. The top glass section remains unbroken and carries compressive loads¹³, resulting in a closed system comparable to reinforced concrete.

The full-section glass main beams for the ATP were 7.2 m long, with a mid-span of 4.8 m and two additional tapered cantilever ends of 1.2 m each (Figure A.3). The cantilevers allow a more favourable bending moment distribution and thereby reduce the height and weight. The mid-span section consists of four 15 mm float glass layers bonded together. Only the two inner layers continue beyond the supports to form two tapered cantilever ends. Thus the main beams have section dimensions of 385 x 60 mm² in the middle; at the tapered ends this is reduced to 230 x 30 mm². Due to the cantilevers, tensile stresses will locally occur on both the top and the bottom part of the beam thus requiring steel reinforcement on either side. At the top, a 30 x 10 x 1.5 mm section was used, while at the bottom a 30 x 15 x 2 mm section was applied. At the cantilevers the upper steel box section continues and is bonded to the top of the (inner) sheets. To obtain the 7.2 m length, the inner layers of the beams were segmented in three parts; two parts of 2 m long and one part of 3.2 m long. The seams are covered by the outer sheets which have a length of 5 m, and located 80 cm inwards from the supports, where in normal loading conditions the bending moments are theoretically zero (Figure A. 4).

¹⁰ An extensive discussion on the main beam design, manufacturing and testing can be found in: Christian Louter, Jan Belis, Freek Bos, Fred Veer, Gerrie Hobbelman, *Reinforced Glass Cantilever Beams*, Proceedings 9th Glass Processing Days, Tampere, Finland, June 2005.

¹¹ Using three equal beams allows for less different glass sheets and easier exchange in case of glass breakage.

¹² *AdDoc I: Zappi, 1996 – February 2004*, additional document to this PhD, www.glass.bk.tudelft.nl.

¹³ Sometimes the top part of the beam was also (partly) cracked; the cracked glass then also carries compressive loads.

One full scale prototype has been subjected to three 3-point bending tests to validate its structural behaviour. The first two tests investigate failure behaviour of the cantilevers, while the final test provided insight into the failure behaviour of the mid-span (Figure A.5).

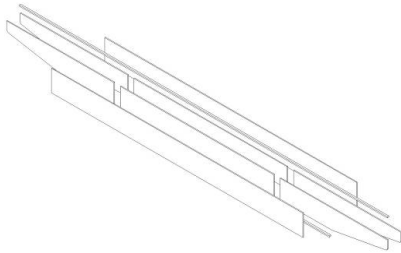


Fig. A.3 ATP main beam design.

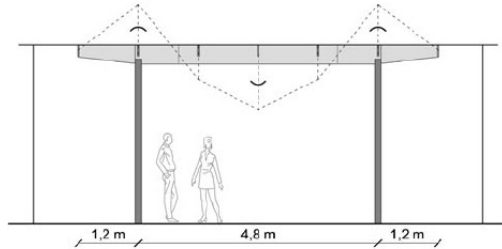


Fig. A.4 Moment distribution on ATP main beam, in evenly loaded condition.

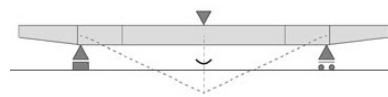


Fig. A.5a, b Experimental set-up for cantilever test (a, left) and centre span test (b, right).

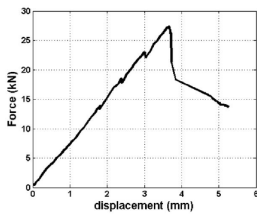


Fig. A.6a Load-displacement curve of first cantilever test.

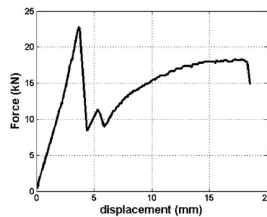


Fig. A.6b Load-displacement curve of second cantilever test.

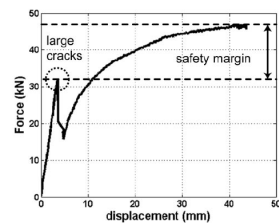


Fig. A.6c Load-displacement curve of centre span test.

Figures A.6a, b and c show the load-displacement curves of the respective tests. Although in principle they showed failure behaviour similar to previous tests on reinforced glass beams, there is a significant difference between the first two tests on the cantilevers and the final test on the mid-span. Where the latter reaches a residual strength of approximately 150 % of the initial crack strength, the former ones only reach about 66 - 75 %¹⁴. In terms of safety, this difference is fundamental as the latter would not fail upon overloading the initial crack strength, whereas the former two would. They would only survive if (part of) the load would be removed.

Several causes have been identified to explain this difference. Perhaps most significantly, the reinforcement profile on the cantilevers was bonded to the glass on

¹⁴ The residual strength as percentage of the initial crack strength varies because the initial crack strength varies. The residual strength absolute however, is remarkably constant at 18.4 kN on each side.

only one side, whereas the profile in mid-span on the under side was bonded at three sides. Indeed, the profile had broken loose over quite some distance on the cantilevers. Furthermore, it was discovered the adhesive on the top profile had not cured completely and that the edges of the glass sheets had not been in line completely.

1.3.3. Purlins¹⁵

Fourteen purlins carry the roof panels of the ATP, spanning 3.6 m. An important paradox of the purlin geometry is that an optimal economic design aims at a minimal glass section, while at the same time quite some thickness is required in order to assure enough support for two meeting/adjacent roof plates, especially when tolerances on final cut sizes have to be taken into consideration. Some solutions have been investigated. Finally, a solution consisting of two two-layer PVB-laminated glass sheets joined by an aluminium profile at the bottom was adopted (Figure A.7). The profile serves both as a spacer as well as reinforcement similar to that in the stainless steel glass beams and is bonded to the glass with Blue light/UV-curing adhesive¹⁶.

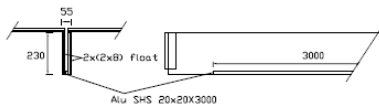


Fig. A.7 ATP purlin design.

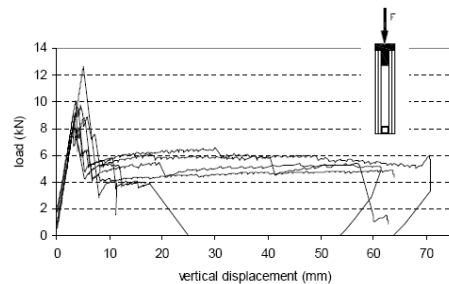


Fig. A.8a Load-displacement curves of centrally loaded specimens (load case 1).

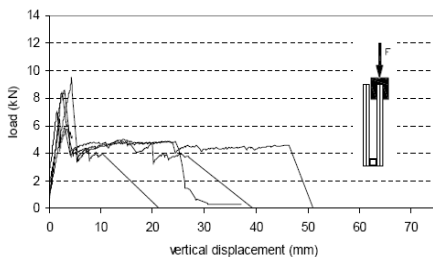


Fig. A.8b Load-displacement curves of specimens loaded asymmetrically on one laminate (load case 2).

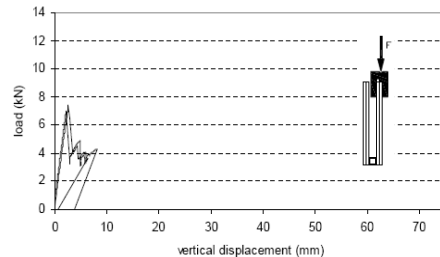


Fig. A.8c Load-displacement curves of specimens loaded asymmetrically on one sheet (load case 3).

After the pavilion was demounted, all 14 purlins have been tested in a lateral torsional buckling installation developed at Ghent University. The purlins have been subjected to

¹⁵ An extensive discussion on the purlin design, manufacturing and testing can be found in: J. Belis, R. van Impe, P.C. Louter, F.A. Veer, F.P. Bos, *Design and Testing of Glass Purlins for a 100 m² Transparent Pavilion*, Proceedings 9th Glass Processing Days, Tampere, Finland, June 2005.

¹⁶ The blue light initiator in this adhesive was essential because lighting the adhesive occurred through PVB foil, which blocks UV light.

three different loading cases to study the effect of asymmetrical loading on failure behaviour. The load-displacement curves are given in Figures A.8a, b, and c.

As could be expected, the average initial strength of the centrally loaded purlins is the highest. The difference however, is not very big. The residual strength is also quite close, about 4 kN for load case 3, 4-5 kN for load case 2 and 4-6 kN for load case 1. With residual strengths varying from 33 – 66 % of the initial crack strength, the purlins behave somewhat similarly to the main beam cantilever ends. It is significant to note none of the purlins obtained residual strength anywhere near the initial crack strength.

The most striking difference between the loading cases is the deformation capacity after initial cracking. That decreases rapidly with increasing asymmetry of the loading. This is explained by the fact that the loaded sheet in cases 2 and 3 begins to buckle, thereby exerting a peeling stress on the adhesive between the glass and the aluminium resulting in increasingly early complete adhesive failure. In load case 1 however, the adhesive failed gradually from the cracking area outwards but never completely debonded.

1.3.4. Roof and Façade Panels

The roof was considered to be accessible only for occasional cleaning or replacement, in which case it would be advisable to use some kind of wooden lattice to walk on in order to avoid damaging the glass. When determining the panel section dimensions, the bending stiffness turned out to be governing over the glass strength, thus 2 x 8 mm PVB laminated annealed glass panels sufficed.

The façade panels, however, had to carry significant vertical loads as well as horizontal wind loads and were thus prone to buckling. Therefore horizontal fins were added to increase the panel's bending stiffness over the mid-area of the panel (Figure A.9). They were glued to the panel face with UV-curing adhesive. This solution has several advantages over introducing wind fins as separate, new structural components. It requires less mass and results in a less complicated structural system. More importantly, many extra structural joints were avoided. It was also an aesthetical novelty.

The durability of the adhesive joint between the fin and the façade panel may raise some questions. If a fin would break loose from a façade panel, the panel's bending stiffness would be significantly reduced. But as soon as it would start to buckle, the vertical load is redirected to the neighbouring façade panels because of the segmentation scheme (see Section 2.2.2.). It would then only have to carry wind loads, for which it is strong enough even without fin, albeit exceeding the usual serviceability displacements limits. It would thus require the fins of at least two adjacent façade panels failing combined with significant vertical loading, before there is risk of part of the roof collapsing.

FEM calculations suggested the glued-on fin might cause considerable peak stresses in the façade face around the fin tips. Three small scale specimens with similar geometry¹⁷ have been subjected to four-point bending tests to show such peak stresses would not be a severe problem. First, the actual peak stress is probably somewhat lower because the fin was modeled as with 2D shell elements. Furthermore, they only occur locally, thus seriously decreasing the risk of coinciding with a critical defect. Finally, they only occur

¹⁷ Plates of 2 x 6 mm laminated 300 x 1000 mm float glass with glued on fins, 8 mm thick, 52 mm high and 500 mm long.

in the glass face, in which flaws are generally less critical than in the edge of the glass. Failure loads corresponding with stresses between 108 and 148 N/mm² were recorded. The intense cracking patterns supported the assumption that the failure stress was very high (Figure A.10).



Fig. A.9 ATP façade panel design.



Fig. A.10 Scale model of ATP façade panel design crack pattern after four-point bending test.

1.4. Joints

Joints perform a crucial role in building structures. Within them, problems of connection, adjustment, thermal expansion, strength, stiffness, static functioning, mounting and demounting meet. This usually requires components with a certain geometrical complexity not attainable in float glass. Stainless steel pin joints have proved to effectively deal with these aspects simultaneously in glass structures. However, it may be desired that, like the rest of the structure, the joints are transparent. Obviously, these connections are not. Furthermore, it was common perception they can only be applied in strengthened or toughened glass, as they lead to stress concentrations around the pins. In the ATP design, several innovative joints have been applied. Optimizing transparency and developing methods to connect annealed glass components were the main objectives.

1.4.1. Column to Main Beam

In a quest to optimize the transparency of the ATP structure, PMMA (polymethylmethacrylate, a transparent polymer popularly known as acrylic) was selected as material for the transition components instead of steel. The idea behind using a transparent polymer is that, like steel, they behave plastically and are thus unlikely to initiate failure in a glass structure. Contrary to most transparent polymers however, PMMA is brittle. It was nevertheless chosen because it is readily available, it can be machined and polished afterwards, thus a highly transparent result is possible (Figure A.11). Although being brittle, it is less sensitive to impact and crack propagation than glass, because of its long molecular chains. Other polymers often have to be injection moulded, which is not economical for these small series. They may also be less transparent¹⁸.

¹⁸ I have discussed the possibilities of using transparent polymer joint in glass structures extensively in two publications, dealing with specific structural problems, polymer properties and material selection. See: Bos, F.P., Veer, F.A., Heidweiller, A., *Using Plastics in the Design of Joints in Transparent Structures*,



Fig. A.11 Flame polished (left) and machined (right) PMMA joint components.

The joint design is straightforward: a cylindrical piece of PMMA with an outer diameter equal to that of the glass column, with a groove on the top side in which the main beam is placed and a decreased diameter at the bottom to fit into the glass column (Figure A.12a). The PMMA piece is glued into the glass column with silicone adhesive, only to fix it. The joint should only be loaded in compression. A strip of silicone rubber would be placed between the PMMA head and the main beam, again fixed with silicone adhesive.

Five experimental specimens of this joint were tested in force controlled compression tests. With two, a silicone rubber ring was placed between the PMMA and the glass, while this was omitted with the other three. Remarkably, the former two failed significantly earlier than the latter three (Figure A.12b). The silicone ring is too soft and pressed out of the joint unevenly, leading to an uneven stress distribution and premature failure.

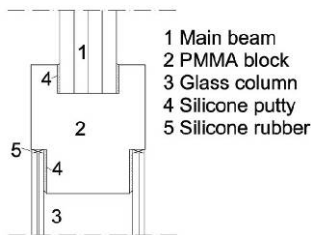


Fig. A.12a Design of column-main beam joint.

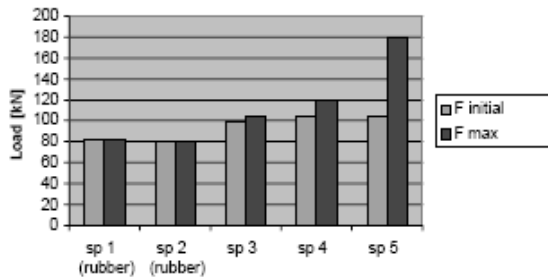


Fig. A.12b Results of compression test on five PMMA column-main beam joint specimens.

Only one specimen showed considerable residual strength, beginning failure (cracking) at 100 kN and finally collapsing at 170 kN. This was due to gradual cracking, not to

plastic behaviour. The other specimens showed this could not be relied on as they collapsed much sooner after initial cracking.

1.4.2. Main Beam to Purlin

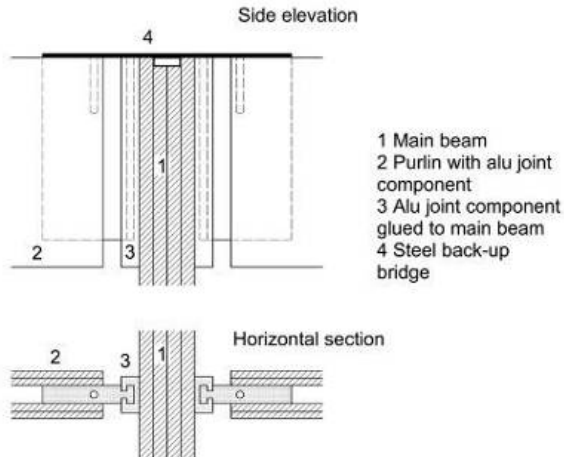


Fig. A.13 Design of the joint between the main beam and the purlins.



Fig. A.14a, b Aluminium transitional components glued to the main beam (a, left) and to the purlins (b, right).

The joint between the main beam and the purlins plays an important part in the overall stability of the pavilion. It is rigid not only in order to prevent the main beams from tilting (the column to main beam joint gives no rotational restraint), but also to prohibit the creation of a rotation axis in the top of the main beam, where it is connected to the roof panel. This would lead to global instability. Polymers could not be used as the transition material because of the required stiffness and the difficulty of obtaining high strength adhesive polymer to glass bonds. Aluminium was chosen instead.

The joint consists of two transitional components, one glued to the side of the main beam, the other connected to the purlin (Figures A.13 and A.14a, b). A steel bridge served as back-up to prevent the purlins coming down in case of adhesive layer failure. The aluminium pieces slide into each other in a kind of swallow tail design.

1.4.3. Roof to Façade Panel

The minimal facade to roof panel-joint design is shown in Figure A.15. Although there was little doubt about the strength of this joint in longitudinal direction, the lateral strength could be questioned. In this direction, the joint has to transfer horizontal wind loads and shock loads caused by persons or objects bumping into the walls.

Therefore a specific specimen was designed (Figure A.16) to be able to test this joint in a displacement controlled shear test. Five such specimens were tested. In direct loading, the strength was well above the required minimum, but cyclic testing indicated the fatigue strength was slightly too little¹⁹. Thus the principle of the design was accepted (the ATP would be built inside and only remain standing for a month), but in reality it would need some optimization, e.g. by increasing the bond width and decreasing the bond height to width (h/w) ratio.

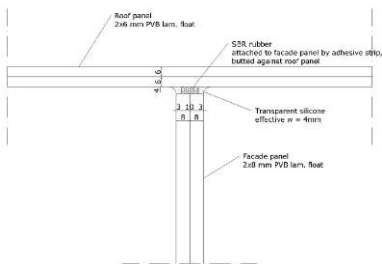


Fig. A.15 ATP roof-to-façade panel joint.

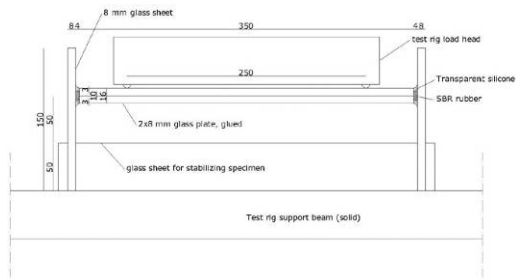


Fig. A.16 Specimen geometry for roof-to-façade joint testing.

1.5. Realisation

Due to several practical problems described below, and the time available, the ATP was only partly constructed (Figures A.17a, b and A.18a – d).

¹⁹ For a more extensive report of the experimental results, see: Bos, F.P., Veer, F.A., Belis, J., Nieuwenhuijzen, E.J. van, Louter, P.C., *The Joints for the All Transparent Pavilion*, Proceedings 9th Glass Processing Days, Tampere, Finland, June 2005.



Fig. A.17a ,b ATP during construction. An attempt was made to place the glass columns.

The realized structure consisted of the roof grid of main beams and purlins and the roof panels. The main beams were laid upon acrylic joints which are placed in steel tube footings. In comparison to the design, the glass columns had to be left out. This was mainly due to the lack of availability of sufficiently long glass tubes. Originally, the ATP design contained 3 m high glass columns out of one piece, with hinged connections on either side. However, the standard maximum trade length of borosilicate glass tubes is only 1.5 m. At the time, the possibility of welding tubes together was briefly discussed, but we had doubts about the strength and reliability as well as the practical feasibility of that proposal. Since there was no time to extensively investigate that option²⁰, we chose to place the glass columns on 1.5 m high steel footings. The footings had to be rigidly joined with the floor in order to obtain a stable static scheme (Figures A.19a and b). But as the first phase of the pavilion was mounted inside the faculty building, we could not bolt the footings to the floor. Still, an attempt was made to mount the glass column (Figures A.17a, b). But the footings could move too easily, so we concluded the structure was not stable enough and decided to build the pavilion at half-height, leaving out the glass columns and façades. The structure was stabilized with diagonal steel cables.

²⁰ Subsequent research has shown welding actually would have been a suitable solution. See e.g. Bos, F.P., Veer, F.A., *Bending and buckling strength of butt-welded borosilicate glass tubes*, 3rd International Conference on Structural Engineering, Mechanics and Computation, Cape Town, South Africa, September 10-12, 2007, or (more extensively): *AdDoc III: Welding and Hot-Shaping Borosilicate Glass Tubes; Possibilities, Strength and Reliability*, additional document to this PhD, www.glass.bk.tudelft.nl.

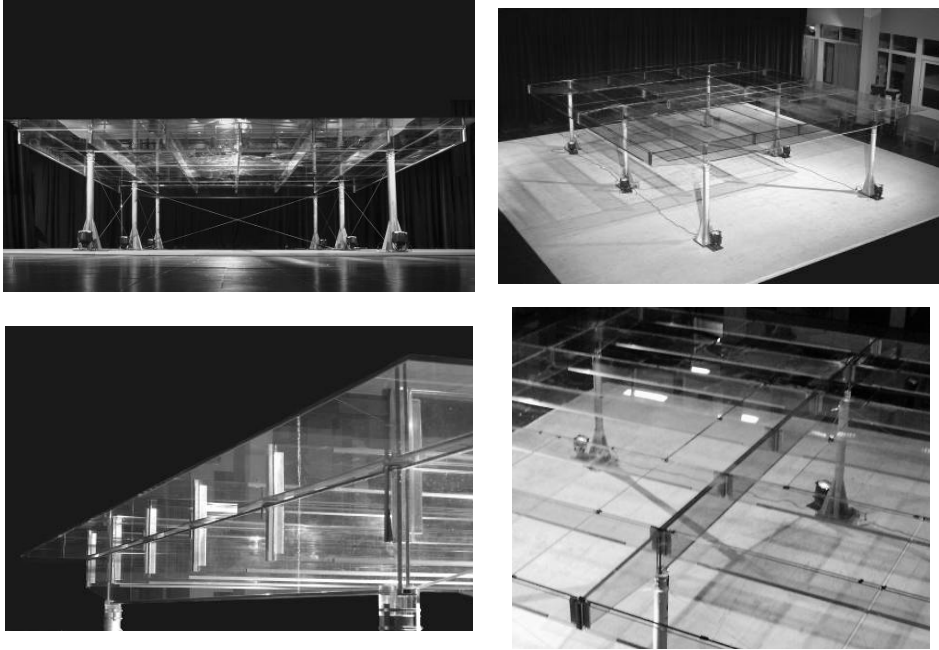


Fig. A.18a, b, c, d Realized result: the ATP roof structure.

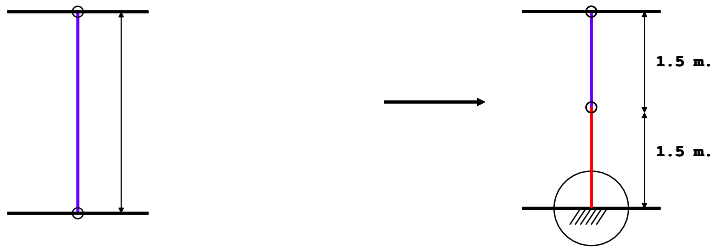


Fig. A.19a, b Static scheme for the ATP in the original design (a, left) and after the design alteration due to lack of sufficiently long glass tubes.

Already in the design stage, but even more so during mounting, it became apparent the joints within this structure are critical for the stability of the structure. In a glass structure, a transition component of some other material is virtually always needed because the glass components can not be connected together directly.²¹ The transition component fulfills several functions:

- Provide a way to connect it to the rest of the structure or to some other transition component. In this particular case it was also required that the structure could be demounted.
- Provide an adjustment possibility and room to absorb dimensional inaccuracies.

²¹ An exception can be made for the finger joints that are sometimes possible between a column and a beam. However, this is only possible when both the sheets of the beam and of the column are in the same plane.

- Ensure that the joint behaves according to the static model of the structure (e.g. as a roller bearing, pin hinge, or rigid restraint).
- Absorb shock waves to keep damage localized.

The transition material in glass structures is usually stainless steel, fitted by bolted pin joints through drilled holes or glued onto the glass surface. This technique has been developed ever since the Serres at la Villette and are common practice. A large number of manufacturers offer these kinds of joints, that are quite able to meet the demands described above.

Since we assumed such joints could not be used in annealed glass and only annealed glass was used in the ATP, joining was a specific problem that required alternative solutions, such as surface- or line-shaped joints. Because it is difficult to create such joints mechanically, chemical connections with adhesives were necessary.

The column to main beam joint was designed as a pin hinge. Therefore the stiffness requirements of the joint were limited, which allowed the use of a polymer transition component, instead of a metal one. Because of the shape distortions at the tube ends and the round shape that does not allow the parts to be pressed together, the PMMA components could not be glued with a rigid adhesive to the column. A small cavity was filled with silicone instead. The shape of the PMMA component and the demand for adjustment space also prohibited rigid gluing to the main beam. Again, silicone was used.

Because the glass columns were not used, the acrylic blocks were placed directly in the steel footing (Figure A.20). The steel tube had a larger inner diameter than the glass column. Therefore, the components were not connected to the steel tube by silicone. As there were no uplift wind loads inside the faculty building, this was allowable. Nevertheless, there were several reasons to further develop this joint. First of all, the average experimental failure strength was less than 4 times the design stress, which is usually considered too little for brittle polymers. Furthermore, the connection to the glass column was not completely thought through. Just using silicone is not only aesthetically displeasing, it also results in a joint with little tensile capacity, insufficient in case of wind suction on the roof combined with an asymmetrical roof loading.

The main beam to purlin-joint plays an important part in the overall stability of the pavilion. During mounting, it turned out that the joint did not allow for dimensional inaccuracies larger than approximately ± 1 mm. Unfortunately, in this experimental stage it proved to be impossible to manufacture the purlins and mount the pavilion to such an accuracy. Partially due to a lack of communication between designers and the working crew, the purlins were hammered into place, exerting shock loads and forced deformations on the adhesive layer between the aluminium transition piece and the main beam.

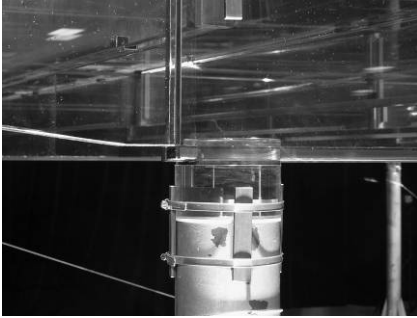


Fig. A.20 Because the glass columns were left out, the main beams were put on acrylic blocks which were directly placed on the steel footings.

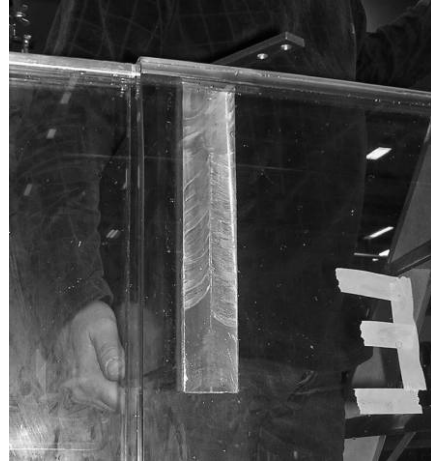


Fig. A.21 Many aluminium-glass adhesive bonds on the main beams showed significant visual damage after the purlins had been put into place.

Extensive research on the static strength and fatigue behaviour of the applied adhesive (Delo GB368)²² led us to have considerable faith in this joint. Shear strengths of 23 MPa have been observed (both in glass-glass and glass-aluminium joints), far more than was required here. However, about 50% of these adhesive layers failed under the applied loading. Even more showed significant visual damage (Figure A.21).



Fig. A.22 Damage in this purlin did not induce complete element failure because annealed glass was used.

The back-up bridge held the purlins in place, but obviously this joint had to be reengineered. More specifically, the joint geometry should allow stress free mounting and an adhesive with a higher damage tolerance should be used.

Accidentally, the mounting problems of the purlins did prove the advantages of the use of annealed glass. During the process several purlins got damaged (Figure A.22). But instead of failing completely – which would have happened had we used tempered glass – the damage remains localized.

²² Veer, F.A.; Janssen, M.J.H.C.; Nägele, T., *The possibilities of glass bond adhesives*, Proceedings 9th Glass Processing Days, Tampere, Finland, June 2005.

The technical and practical problems have been summarized in Table A.3.

Table A.3 Inventory of technical and practical problems in the ATP project.

Structural part / element	Brief description of the problem(s)
Overall structure	The global static system of the structure, which features an almost complete separation between the load carrying elements (purlins, main beams, and columns) and the stabilizing elements (walls and roof), relies heavily on the performance of the silicone joints, (particularly those between the façade panels and roof plates, in between the roof plates, and between the roof plates and the purlins).
	Possible tilting of the main beam. A solution to this problem will affect the whole stability scheme of the structure.
Column	Available trade length size (max. 1.5 m).
	Developing joints around the circular ends of the glass tubes.
	The method to introduce loads into the glass tube, without causing uneven stress concentrations and early failure.
Main beam	The relative post-failure strength $r_{res,III}$ of the outrigger part of the beam was significantly less than for the mid-span section.
	As it was assumed no pin-joints could be applied in the annealed glass of the main beams, it was difficult to develop properly performing joints to connect them to the columns and purlins.
Purlin	With regard to joining, similar problems as with the main beam ('no pin-joints in annealed glass') were encountered.
Roof plate	-
Façade panel	-
Column-main beam joint	The long-term performance (shape stability; consider long term actions and possible high temperatures under the glass roof) of the PMMA connection element has been insufficiently investigated.
	In lateral direction, it is actually more like a roller bearing than a hinge. Horizontal reaction forces can only be transferred through friction between the beam and the PMMA connection element. This should not be relied upon (especially with a net upward (wind) action being possible).
	By allowing the structural elements to rotate around the lateral axis, tilting of the main beams has to be prevented in another way (in steel structures this is usually not possible). This has proven to be difficult.
	The joint cannot transfer net upwards wind actions that could be expected in an outside situation.
	The connection of the PMMA element to the top of the tubular glass column was not properly designed. The just-fit solution as designed can not transfer tensile actions and may cause incompatibility problems through unequal thermal expansion. Furthermore, in practice it proved impossible to manufacture just-fit elements due to irregularities in the glass tube end geometry. The finally applied silicone bonded solution was aesthetically unpleasant and its structural quality doubtful.
Main beam-purlin joint	By applying a rigid connection, the highest stress levels move from mid-span of the purlin (as with a freely supported beam), to the joints. This makes it more difficult to predict stress distributions, and to make to joint demountable and adjustable to dimensional inaccuracies.

	Selection of an adhesive bond to the main beam. The rigid connection resulted in a peeling action on the bond, which is the most severe loading type on an adhesive.
	Insufficient adjustability of the joint to dimensional inaccuracies. In the construction phase this resulted in purlins being hammered in place. The adhesive proved very sensitive to this kind of shock loading, which caused extensive damage to the bond and therefore premature failure.
Façade panel-roof plate joint.	Although the short term resistance was adequate, there can be doubts about the long term performance.

1.6. Redesign

Based on the fundamental issues related to safety and failure behaviour of the ATP elements as well as the practical and technical problems that were encountered during design and construction, a redesign is proposed in this Section. The architectural scheme has been maintained as much as possible, but the designs of the elements and joints have all been redone. Besides meeting the safety requirements formulated in Chapter 10 and solving the technical problems described in the previous Section, the original starting points were upheld: the structure should be demountable and as transparent as possible. As the application of transparent polymers was insufficiently trusted, the latter (aesthetical) requirement translated into minimal amounts of steel, shaped as smoothly as possible.

Figures A.23 and A.24 present the ATP redesign in plan, sections, side views, and (exploded) 3d. The structural scheme still relies on the roof and façade planes to provide stability, while the central column-main beam-purlin structure carries most of the vertical loads. However, one major modification has been applied: the purlins are now freely supported instead of rigidly fixed on both sides. The connection to the outer main beams acts as a hinge, while the one to the central main beam is a roller bearing. Therefore, the main beam can not rely on the beam-purlin grid to prevent it from tilting. Rather, the column-main beam joint has been redesigned as well to work as a fork. Since the purlin-main beam connection will no longer induce horizontal actions on the main beam and the external horizontal actions on the structure are directly diverted to the facades through the roof, this should not introduce unacceptable stresses in the column head.

This modification has the further advantage that the stress distribution through the purlins is better predictable and the governing stresses will not occur in the joints. This makes it easier to design minimal, demountable connections. In the redesign, the effective axis of the support is inside the main beam, so additional torsional actions are minimized.

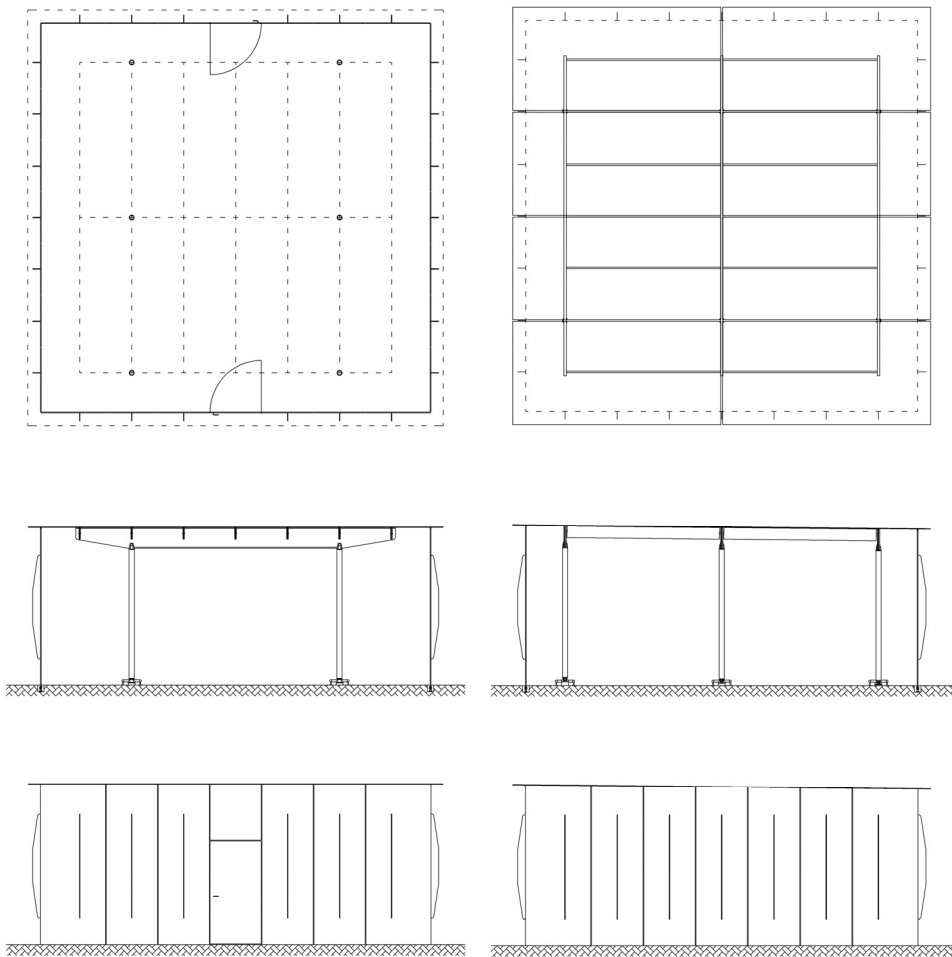


Fig. A.23 Plans, sections, and side views of the redesigned ATP.

As with the original design, all glass is annealed. The redesign shows that no thermal treatment is necessary to design such a glass structure. Some important advantages are the optical quality and the options to grind and polish as well as drill holes, after laminating (thus ensuring perfect alignment).

Finally, the roof panel size has been maximized to 4.8 by 2.4 m (centre distance measures). Since the overall stability of the structure relies heavily on the in-plane stiffness of the roof, this was deemed desirable.

1.6.1. Columns

The redesigned column is shown in Figures A.25a - c. The general concept of two glass tubes, one laminated within the other with a clear resin, has been maintained. Sufficient tube length can be obtained from butt-welding shorter tubes together, with a 1.4 m centre piece, a 0.8 m piece on one side, and a variable piece on the other (to obtain the roof angle for water run off). Several studies (e.g. related to the TFS project) have

proven the feasibility of this solution).²³ At the tube ends, the outer and inner tubes can be welded together. Thus, the resin is automatically in an enclosed space and there is a larger surface area to introduce external actions. After joining the tubes, the heads should be grinded and polished to ensure a perfectly smooth surface. The design specifically avoids using the ends of as-delivered tubes, as they may have geometrical distortions leading to stress concentrations.

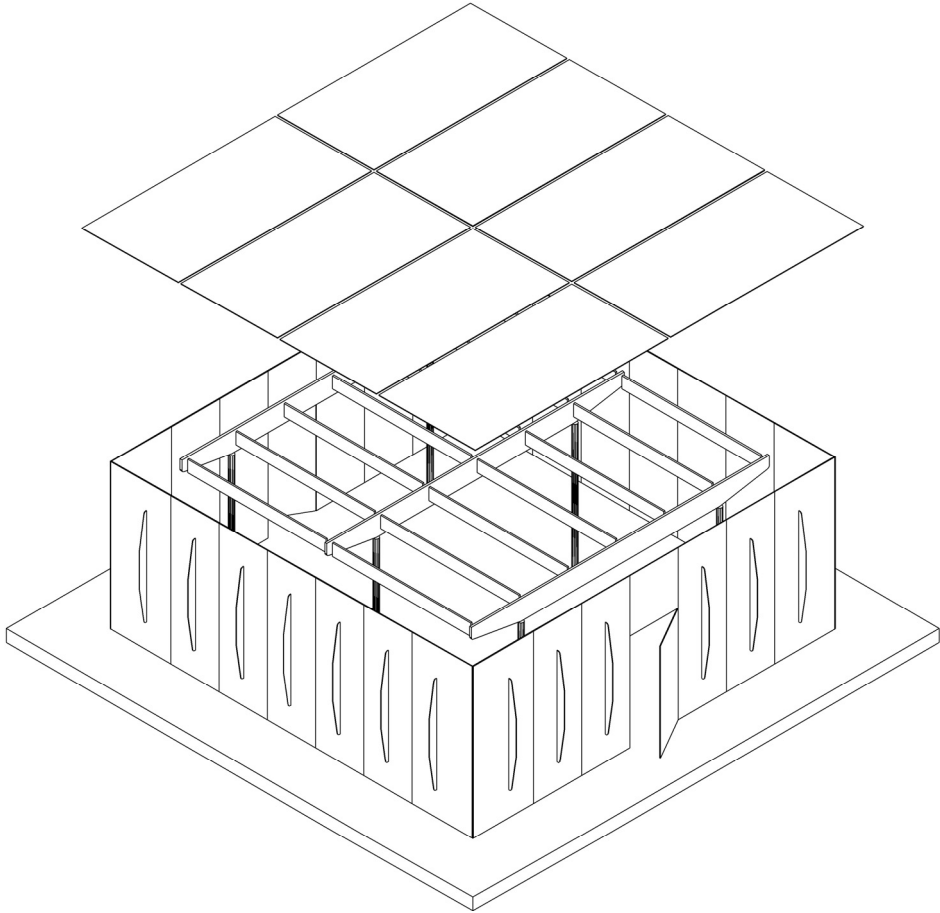


Fig. A.24 ATP redesign in 3d exploded view.

An important addition in the form of six reinforcement glass fibres has been applied. This concept is rather new, but preliminary tests on glass beams reinforced with glass

²³ Bos, F.P., Veer, F.A., *Bending and buckling strength of butt-welded borosilicate glass tubes*, 3rd International Conference on Structural Engineering, Mechanics and Computation, Cape Town, South Africa, September 10-12, 2007; More extensively published as Bos, F.P., Giezen, C., Veer, F.A., *Opportunities for the Welding and Hot-Shaping of Borosilicate Glass Tubes in Building Structural Applications*, Proceedings of the 1st Challenging Glass Conference, Delft, the Netherlands, May 2008; Bos, F.P., *Hybrid Glass-Acrylic Façade Struts*, 10th Glass Performance Days, Tampere, Finland, June 15-18, 2007.

fibres have shown favourable results as to their effectiveness.²⁴ The effect of the fibres should be a significant residual moment capacity after failure (to avoid buckling). The post-failure moment capacity $M_{\max, \text{post-failure}} \approx 3.77 \text{ kNm}$ (based on the $f_{\text{glass fibre}} = 3400 \text{ MPa}$, $A = 3.14 \text{ mm}^2$), while the pre-failure moment capacity $M_{\max, \text{pre-failure}} \approx 2.89 \text{ kNm}$. This results in a relative residual resistance of $r_{\text{res,III}} = 130 \%$. Naturally, further experimental research would be prudent to prove these calculations.

To allow significant room for the fibres, the outer tube thickness was reduced from 5 to 3 mm. Although this decreases the glass column section area, and thus increases the compressive stress to $\sigma_{\text{d,comp,short term}} = 9.2 \text{ N/mm}^2$ (from 7.3 N/mm^2), the improved design of the glass tube ends should make this order of stresses allowable.

At each end of the columns, a stainless steel element is inserted and glued to the column head, e.g. with Delo GB368 UV-curing acrylate adhesive. The method and design developed for the TFS (PMMA pin in a glass tube) could be used.²⁵ The actions are introduced into the glass tubes primarily through normal forces at the tube end. This results in the most even stress distribution. When both the steel elements and the glass tube ends are properly flattened this need not cause premature failure. A very thin aluminium strip between the stainless steel and the glass further minimize undesired stress concentrations through contact.

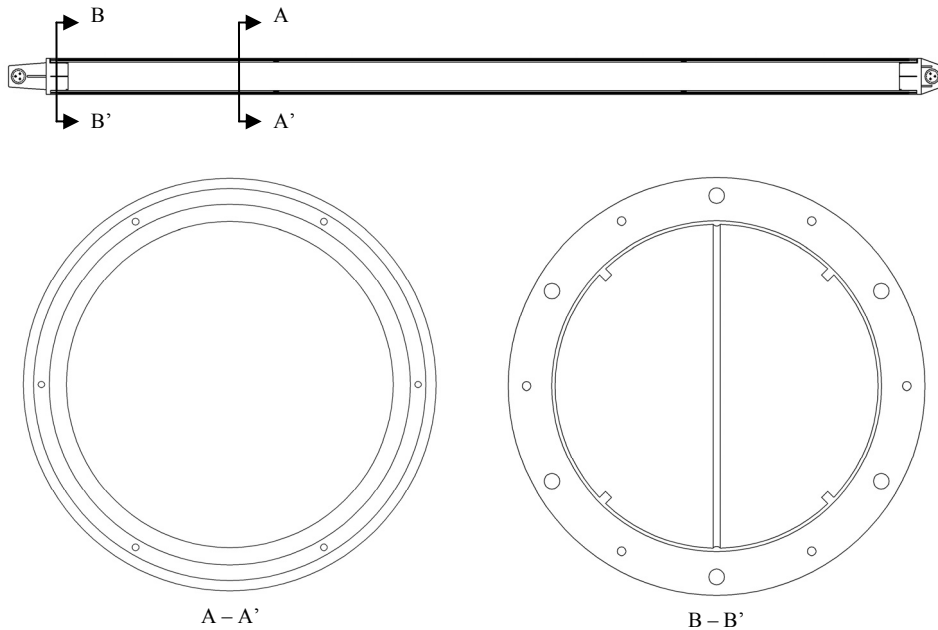


Fig. A.25a – c ATP glass column: longitudinal section and two transverse sections.

²⁴ Louter, P.C., *High-Strength Fibre Rods as Embedded Reinforcement in SentryGlas-Laminated Glass Beams*, Glass Performance Days, Tampere, Finland, June, 2009.

²⁵ Bos, F.P., *Glass-to-Acrylic and Acrylic-to-Acrylic Cylindrical Adhesive Bonds*, Proceedings of the 2nd International Symposium on the Architectural Application of Glass (ISAAG), Munich, Germany, October 2006.

The column-foundation joint (Figure A.26a, b) is rather standard. It features a rotating pin, axis perpendicular to the main beam. The connection can be adjusted in three directions to allow for inaccuracies (horizontally by shifting the floor plate or the column along the support pin; vertically along the protruding foundation reinforcement bars). A small railing is placed at approximately 100 mm height around the column, to accidental collision impact with e.g. a cleaning vehicle.

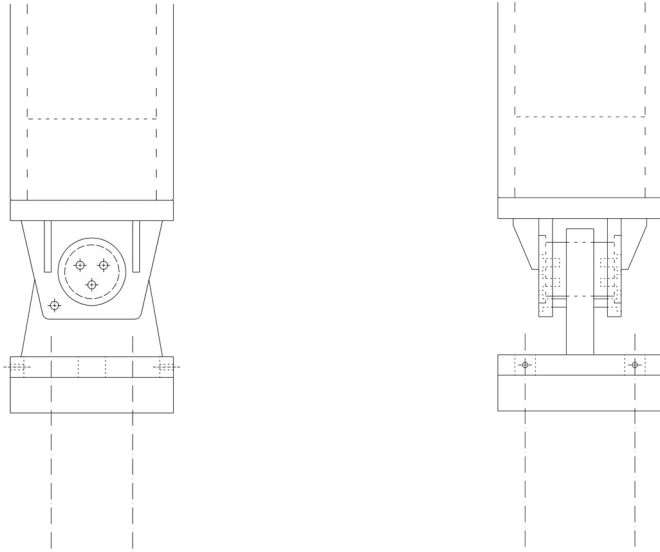


Fig. A.26a, b ATP foundation – column joint.

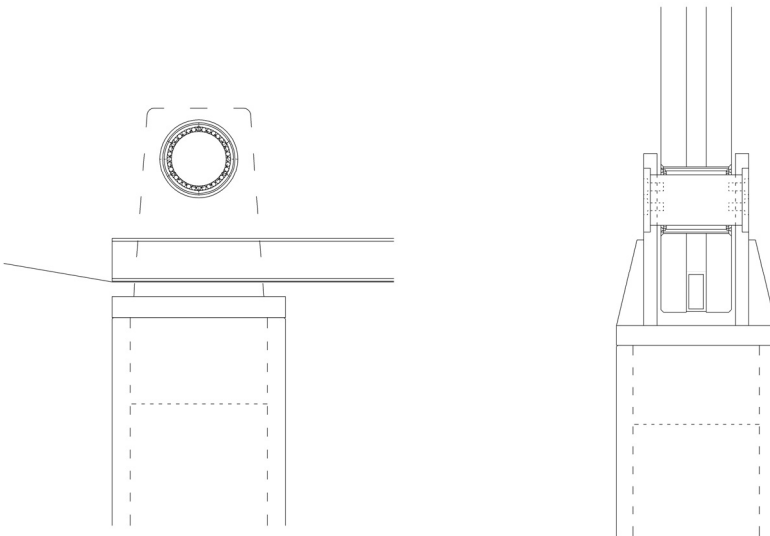


Fig. A.27a, b ATP column – main beam joint.

The column-main beam joint (Figure A.27a, b) has been redesigned to act as a fork. The original joint pieces were PMMA. Although this provided a beautifully transparent joint, the long term properties (under permanent load and varying temperature) is considered by the author to be insufficiently known to apply again in the redesign (especially given the severe safety requirements). Therefore, the redesign features stainless steel. This allows for minimal dimensions. The connection to the main beam is provided by a carrying pin, through a roller bearing adhesively bonded to the inside of a 50 mm diameter drilled and polished hole in the beam. Contrary to common perception, this does not necessarily result in unacceptable stress concentrations along the hole rim (see some further discussion in the next Section). The roller bearing ensures the connection can not transfer any moment in the plane of the beam (e.g. by friction). Together with the main pin, two bolts at the underside of the beam prevent the main beam from rotating around its longitudinal axis (tilting).

1.6.2. Main beams

Figures A.28a – c present the main beam redesign. In comparison to the original design, the beam dimensions and layer layout have been changed. The height h was increased to 480 mm, resulting in a mid span h/l ratio of 1/10. In section, three layers were applied along the total beam length, instead of four in the mid span section, and two at the cantilevers. Although it is nowadays possible to manufacture and laminate glass sheets of over 6 m length, the original starting point that the design should be producible from standard jumbo size float glass sheets was maintained. Thus segments according to Figure A.29 were applied. Because of the consistently high post-failure resistance of reinforced glass beams,²⁶ the segmentations were not considered in the pre-failure resistance calculations (i.e. they were assumed to be as strong as not segmented sections). Besides easier manufacturing, the main advantage of applying three layers over the main beam length is the increase in adhesive surface area between the reinforcement and the glass – which was considered governing in the final failure of the cantilever parts of the beam.

To allow for a mechanical joint between the main beams and the roof plates (because of stability issues), the upper reinforcement profile has been replaced by a massive square rod. The lower reinforcement profile was rotated 90 degrees in order for it to fit in the three layer section layout.

Like the column-main beam joints, the main beam-purlin joints (Figures A.30a and b) are based on circular elements glued into drilled holes in the main beam. The inner diameter is 50 mm to allow for polishing. An FE-analysis (Figure A.31)²⁷ shows that,

²⁶ See e.g. appendices H, J, and K.

²⁷ This analysis was based on the original main beam dimensions and was part of a more elaborate, but unpublished parameter study on the relation between glass beam dimensions and stress concentrations around bore holes. The study concluded that stress concentrations around the bore hole area are unlikely to be governing over the maximum stresses along a beam edge in normal beam dimensions. The inner bore hole edge strength was considered equal to that along the outer edge. This requires that the inner edge is polished – but then it will likely be even higher than the outer edge strength as it is less vulnerable and much shorter (thus less possibility of severe surface defects).

The general misunderstanding of the unacceptability of bore hole connections in annealed glass probably stems from the application at the corners of plates. The non-linear stress distribution in plates is such that the maximum stresses occur at the corners, and are then magnified by the presence of bore holes. In those cases,

contrary to common perception, the stress concentration around the bore hole area are *not* governing with regard to failure. They occur very locally and have smaller magnitudes than the maximum stresses occurring along the beam bottom edge. The glued-in steel elements may be expected to act as reinforcement for cracks that do start from the bore hole (though unlikely).

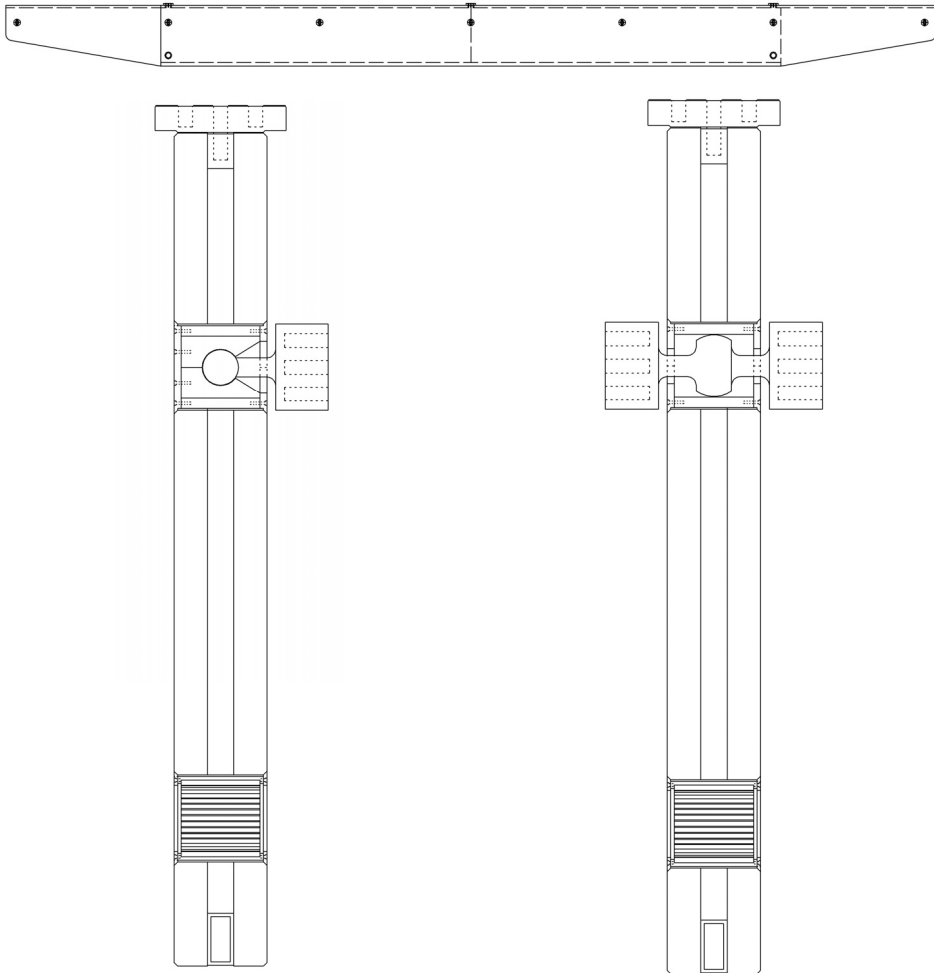


Fig. A.28a – c ATP main beam: longitudinal view of end beam, section of end beam, section of mid beam.

the stress concentrations around the bore hole edges *are* likely to be governing, and may easily exceed the strength of annealed glass. But it is important to realize that this is not the case in any element.

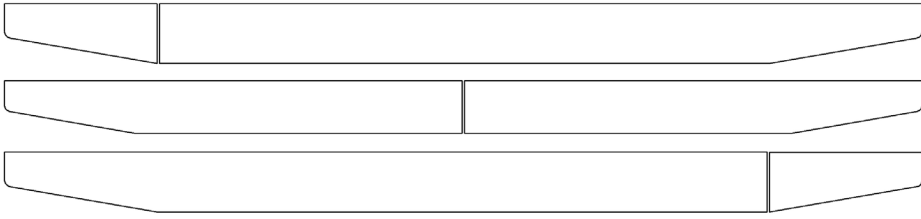


Fig. A.29 ATP main beam: glass segmentation pattern.

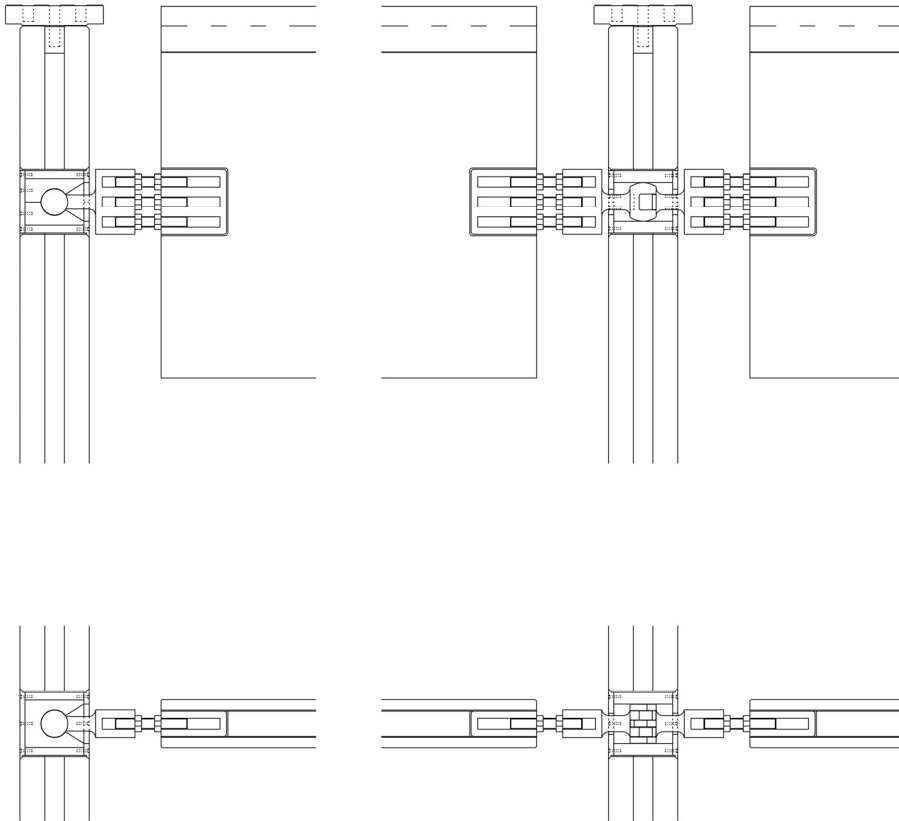
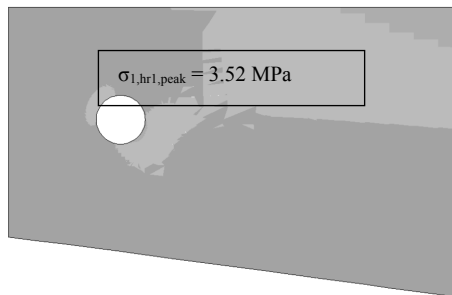
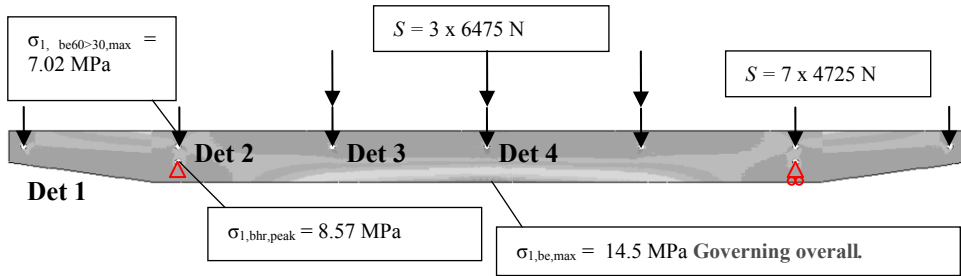


Fig. A.30a, b ATP main beam – purlin joint; vertical section and horizontal section, respectively.

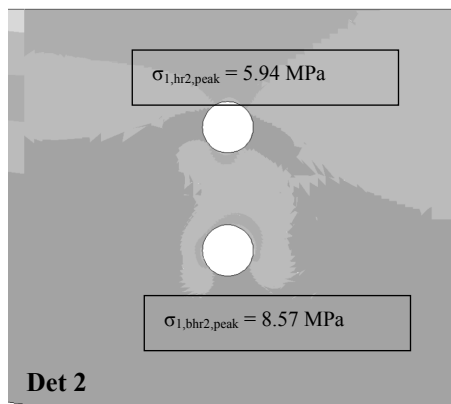
The holes should be drilled carefully from one side after all beam glass sheets have been bonded together. Chamfer should be applied from either side and the inside of the hole needs to be polished.

The side beams feature rotating connection pieces. In the central main beam, connection pieces may slide somewhat. Thus horizontal reaction forces in all of the main beams are avoided. They also have some rotational capability. Together, this allows to absorb some dimensional inaccuracies and to slightly incline the roof for water run-off.

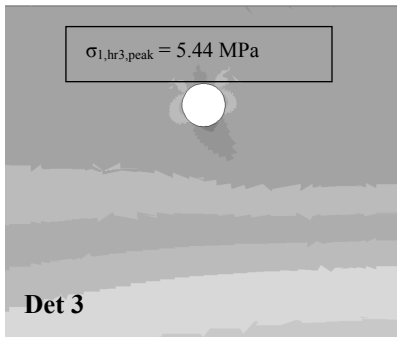
As a result of the joint design, the actions from the purlins are transferred in the centre of the main beam, thus avoiding additional torsional stresses. It also means the adhesive bonds are only minimally loaded – and mostly in compression – thus avoiding catastrophic adhesive failure as occurred in the original project.



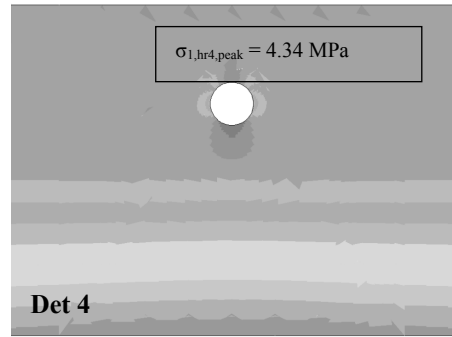
Det 1



Det 2



Det 3



Det 4

Fig. A.31 FE analysis of ATP main beam with bore holes for the connections to the purlins and columns (based original main beam glass dimensions). The governing stresses do not occur around the bore hole edges, but along the beam bottom edge.

The main beams are connected to the roof plates at three points (the seams between the roof plates) for stability reasons (Figures A.32a and b). A circular stainless steel disc with rubber profiles is bolted to the upper reinforcement profile. The roof plates are placed on the disc. The steel plates laminated into the roof plates are bend slightly to fit

over each other. Holes are drilled in these (thin) plates on site to guarantee a perfect fit. Bolts with circular fixing discs are applied through the holes. The connection is provided with a closing cap and sealed with silicone.

In between these mechanical main-beam roof plate connections, a silicone line joint backed with a PMMA strip is applied to connect the main beams to the roof plates along their entire length.

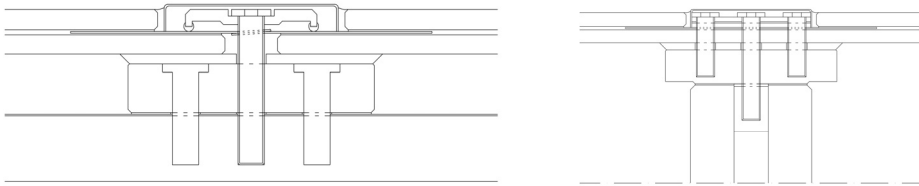


Fig. A.32a, b ATP main beam – roof plate joint; vertical sections in two perpendicular directions.

1.6.3. Purlins

The purlin redesign consists of a three-layer, SG laminated beam (Figures A.33a – c). The advantage of the rather elaborate initial design with aluminium reinforcement was considered minimal. Actually, the specified safety requirements do not call for metal reinforcement at all – which is thus omitted to obtain maximum transparency.

Two types of purlins are applied. Those that coincide with the roof plate joint lines have receding inner layers at the top of the purlin to allow for inlaminated stainless steel blocks to connect the roof plates. The in-between purlins do not require such a recession. In both types, cut outs on either short side of the purlin middle layer allow for blocks for the main beam-purlin joints.

The mechanical purlin-roof plate joints are similar to those between the main beam and the roof plates, but somewhat smaller (Figure A.34a and b). As the longitudinal axes of the purlins are in line with those of the roof plates, the bolt layout is simpler. In between the mechanical joints, a double-sided transparent silicone kit joint along a strip of PMMA is applied. For the in-between purlins, this is the only connection to the roof plates.

1.6.4. Roof Plates and Façade Panels

An important addition to the roof plates (Figures A.35a and b), is the in-laminated steel strips. These allow for mechanical (dismountable) connections to each other, the façade panels, the purlins, and the main beams. As the overall stability of the structure relies on the in-plane stiffness of the roof, the option of applying only silicone joints between the plates was rejected. The applied transparent silicone was not considered reliable enough. As shown by Blandini,²⁸ some silicones may be used in (permanent) structural applications, but those are opaque (black). Furthermore, they may be difficult to remove, thus reducing the demountability of the structure (and eventual damaged elements).

²⁸ Blandini, L., *Structural Use of Adhesives in Glass Shells*, PhD Thesis University of Stuttgart, Verlag Grauer, Beuren/Stuttgart, Germany, 2005.

The façade panels (Figures A.36a, b) were altered from a 2x8 mm section to 3x6 mm, to allow opportunity at both the top and bottom for connections based on in-laminated steel blocks, similar to those applied in the main beams and purlins (Figures A.37a, b). The glued-on fins were maintained for bending stiffness.

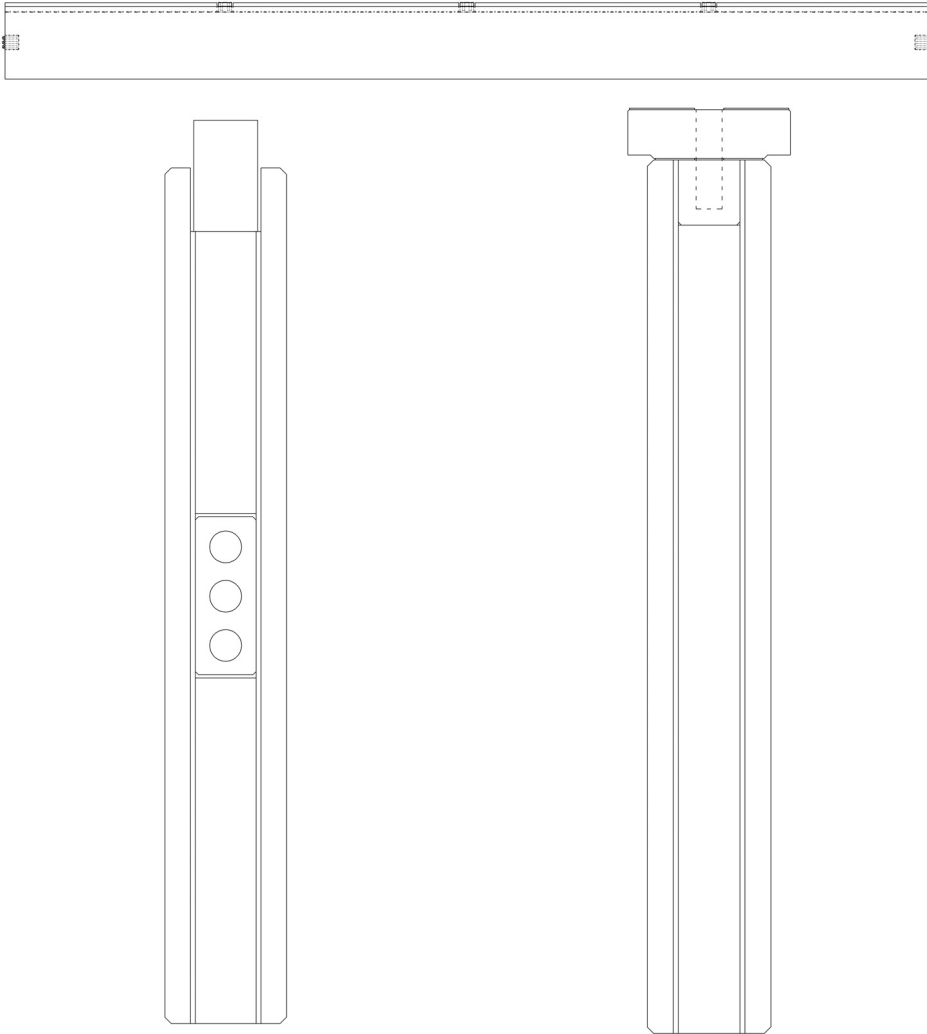


Fig. A.33a – c ATP purlin: longitudinal view, section of near the end, section of at mid span.



Fig. A.34a, b ATP purlin – roof plate joint; vertical sections in two perpendicular directions.

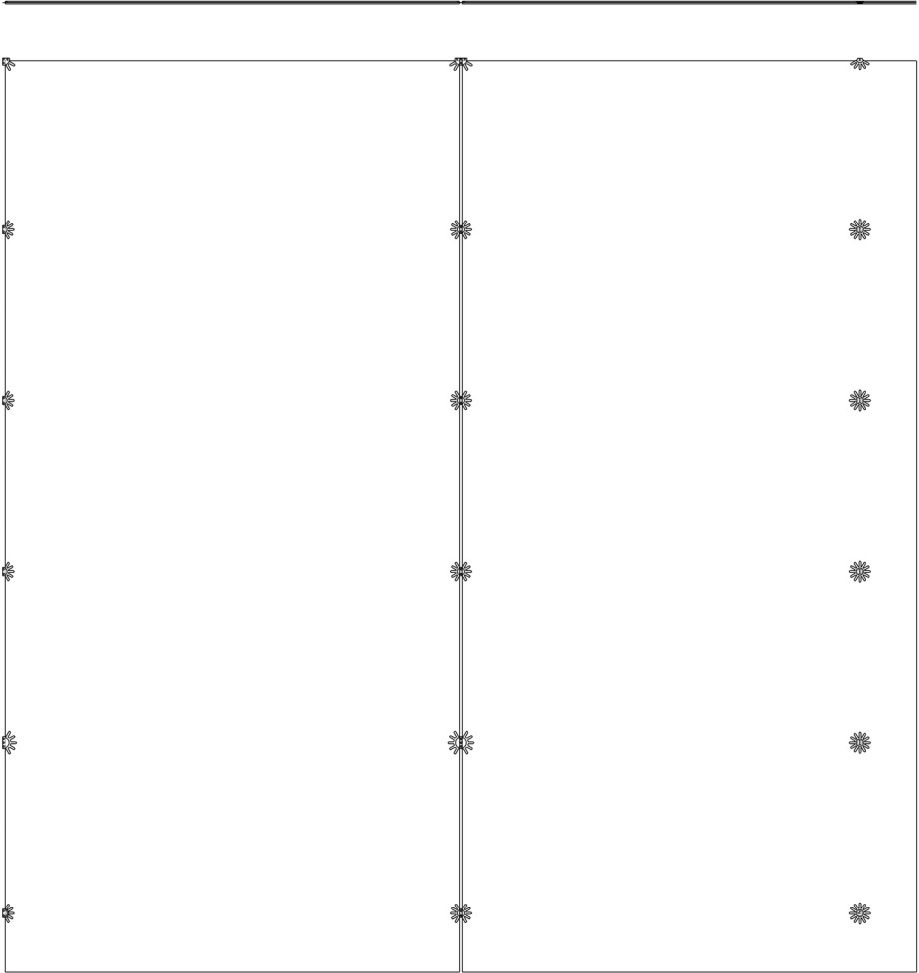


Fig. A.35a, b ATP roof plate: top view and transverse section.

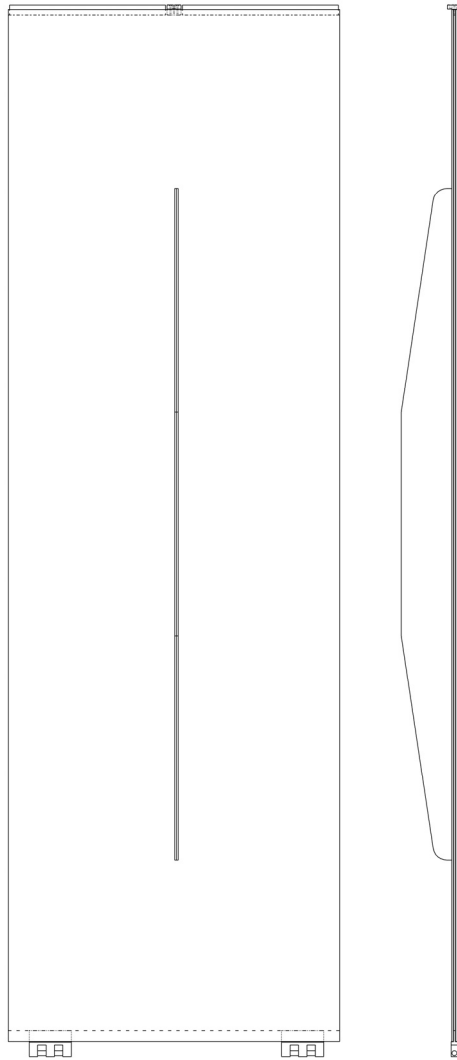


Fig. A.36a, b ATP façade panel: front and side views.



Fig. A.37a, b ATP façade panel – roof plate joint; vertical sections in two perpendicular directions.

2. Transparent Façade Struts²⁹

The ATP project brought several practical and fundamental problems to the attention, but it also pointed to opportunities that might be explored further, such as:

- The use of transparent polymers for joints,
- Creating glass tubes beyond the standard trade length by welding or other techniques,
- Creating (tubular) structural members with safe failure behaviour in tension or a combination of compression and tension.

A possibility to address these possibilities arose in 2006, when some steel façade struts could be replaced with glass ones in a new addition to the Architecture Faculty building. This resulted in the Transparent Façade Struts (TFS) project,³⁰ in which the opportunities mentioned above have been extensively investigated. The struts were unfortunately never actually mounted, due to time and financial limitations. Nevertheless, several 1:1 scale prototypes have been tested.

2.1. Existing façade structure



Fig. A.38 The Faculty of Architecture has been extended with a smoking room; essentially a glass box added to the existing glass façade (picture taken from inside the Faculty building). The two steel struts which are to be replaced are visible in the centre of the picture.

At the end of 2005, a small extension to the Architecture faculty building at the TU Delft was built by Octatube bv. It was essentially a glass box with structural glazing all around (Figure A.38). The glass sheets were connected to each other by stainless steel

²⁹ This section is a slightly altered version of Bos, F.P., *Hybrid Glass-Acrylic Façade Struts*, Proceedings of the 10th Glass Performance Days, Tampere, Finland, June 2007.

³⁰ Contrary to the ATP project, the TFS case was a solo project by the author.

point fixings. Their self weight was transferred directly to the concrete floor on which the walls stand. Steel struts ($d \times t = 40 \times 4 \text{ mm}^2$) carried wind loads to the previously existing structure. Their span was 2.7 m and the design actions on these members were 3.6 kN (compression) and 3.9 kN (tension). For these struts, an alternative was devised during the TFS project. To maintain a consistent architectural image, the Transparent Façade Struts had to have a tubular section.

2.2. Transparent Façade Struts Design

2.2.1. Material Selection

2.2.1.1. Transparent Polymer

There are over a 100 different transparent polymers in existence. Most of them do not match the transparency of glass and do not possess sufficient strength and stiffness. Contrary to the ATP project, an extensive investigation was conducted to compare them to PMMA (which had been used for the ATP) and to conclude which one would be most suitable for glass structural applications in general and the TFS project in particular.³¹ Basically, the quest was for a polymer with the aesthetical and practical qualities of PMMA combined with more favourable mechanical and failure behaviour. This resulted in a short list of 9 transparent polymers.

After considering properties related to manufacturing, machining, polishing, scratch resistance, impact strength, plasticity, availability, flammability, UV- and chemical resistance, it was concluded that four polymers had credible potential for structural glass joints:

- Polyetherimide (PEI)
- Impact modified Polymethylmetacrylate (i.m. PMMA)
- Polycarbonate (PC)
- Glycol modified Polyethylene Terephthalate (PET-G)

Their properties are summarized in Table A.4. Polyetherimide (PEI) is a high performance polymer used for airplane parts, cockpit glazing in fighter jets and medical instruments. PEI is injection moulded at high temperatures, but it is well machinable. PEI is available in different grades and would be the best option from a technical point of view. However, it is extremely expensive compared to the other polymers. Although price is not the first issue in most glass structures, this would probably be unacceptable in most projects.

In terms of mechanical properties, impact modified (i.m.) PMMA is somewhat inferior to PEI, PC and PET-G. Although its failure behavior is not completely brittle, the

³¹ The results were published in two papers: Bos, F.P., Veer, F.A., Heidweiller, A., *Using Plastics in the Design of Joints in Transparent Structures*, Proceedings of the 2nd International Symposium on the Architectural Application of Glass, Munich, Germany, October 2006, and: Bos, F.P., Veer, F.A., *Transparent Polymer Joints in Glass Structures*, Proceedings 10th Glass Performance Days, Tampere, Finland, June 2007. The contents of those papers have been collected in: *AdDoc II: Transparent Polymers for Joint Applications in Glass Structures*, additional document to this PhD, www.glass.bk.tudelft.nl, which also provides a more extensive explanation of the selection criteria.

amount plastic deformation is highly dependent on loading speed³² and the presence of notches (stress concentrators). The main advantages of impact modified PMMA are its processing properties. Unlike PEI, PC and PET-G it can be cast instead of injection molded. On the other hand, impact modified PMMA is not readily available in many shapes. For joint components, resin would have to be obtained. Another advantage is that impact modified PMMA can be flame polished.

Table A.4 Characteristics of short-listed transparent plastics, #1 - #5.

Material ▶	Impact modified PMMA	PET-G	PC	PEI	
▼ Property					
Mechanical	E [GPa]	2.1	1.9-2	2.3	3.0
	σ_y [MPa]	48.7	50-51	62	100-110
	σ_{ul} [MPa]	48.4	40	64	90-100
	ϵ_y [%]	4.7	3.9-4.1	6.1	6.8-7.2
	ϵ_{ul} [%]	22.2	50	97.9	59-60
	K_{1C} [MPa \sqrt{m}]	1.8-2.2	2.1-2.5	2.1-2.3	2.0-4.0
Various	λ [%]	89.3	88-91	87.9	-
	Θ_g [°C]	80-103	81-91	142-158	215-217
	Water absorption @24 hrs	0.19-0.8	0.118-0.143	0.135-0.165	0.227-0.275
Durability&processing	Flammability	Low	Low	No*	No
	Resistance to other substances	Mostly average to very good.	Mostly average to very good.	Mostly average to very good.	Generally very good.
	Castability	3-5	1-2	1-2	-
	Polishing	Flame	Flame	Vapor	Vapor
	Price €/kg	2.01-2.21	2.09-2.29	2.99-3.72	14.58-16.04

* Self-extinguishing.

The mechanical properties of PC are very good and it has a high glass temperature. The plasticity behavior of PC is not significantly influenced by loading speed, but is notch-dependent in a way similar to i.m. PMMA. One of the reasons that PC is being used as a carrier for CDs, is that it is extremely transparent. However, it is also quite soft and can thus be scratched quite easily. As a result, the transparency of available PC items is highly dependent upon the manufacturing method. Sheets usually have highly transparent surfaces, but gray translucent edges. The surface of rods and tubes produced by extrusion is usually full of tiny scratches, which results in less clear sight when

³² See *AdDoc II: Transparent Polymers for Joint Applications in Glass Structures*, additional document to this PhD, www.glass.bk.tudelft.nl, or Bos, F.P., Veer, F.A., *Transparent Polymer Joints in Glass Structures*, Proceedings 10th Glass Performance Days, Tampere, Finland, June 2007.

looking through them, in comparison to glass or PMMA. PC can be vapor polished, but only if a surface is not heavily scratched. A machined edge can probably not be polished to an acceptable transparency. Therefore, if joint components were to be produced from PC, they should be injection molded without further machining (also to avoid stress cracking) and coated with a protective, scratch resistant layer.

PET-G, probably known best for its application as water or soda bottles, behaves plastically and can be easily nailed, cut, bend, welded and glued. Although it can not be cast, PET-G can be flame polished³³. This makes it possible to machine parts from large blocks, making the injection moulding less of an obstacle. Its most serious drawback is its low glass temperature of approximately 80 °C. The Young's modulus of polymers decreases seriously when approaching the glass temperature. When opting for PET-G as joint component material, a thorough estimation of the temperature range that may be expected in the structure is therefore necessary. The failure behaviour of PET-G is highly plastic. It does not seem to be influenced by loading speed and the presence of a notch does not necessarily localize plastic flow.

Although PC, PET-G, and i.m. PMMA were all reasonable alternatives to PMMA, none of these were available in the trade sizes required for this project (tube length and block sizes for the strut heads). Furthermore, they would all require more extensive material research to obtain more insight into their behaviour. Unfortunately, the time and budget required for obtaining resins, performing material research and custom casting or injection moulding, was not available for this very small scale project (requiring only 4 joints in total). Therefore, using PMMA again remained the only option. However, future development of transparent polymer structural joints should start from further investigating these materials as they theoretically possess the best combination of mechanical, practical and aesthetical properties.

Working with PMMA meant the disadvantage of its brittleness had to be neutralized by specific design measures. First of all it called for a joint design that would allow the inner glass tube to serve as a back-up provision in case of failure of the acrylic tube, even though it is much less sensitive to impact than glass. Second, it required specific attention to make sure the strut heads which join the struts to the external structure could not subside to brittle failure.³⁴

2.2.1.2. Glass

The necessary length of the inner glass tube was to be obtained by butt-welding glass tubes together.³⁵ Borosilicate glass was therefore the obvious choice. The strength and reliability properties of butt-welded glass tubes had been experimentally investigated on small welded glass tube specimens.³⁶

A total of 30 specimen tubes ($d_{\text{outer}} = 12 \text{ mm}$; $l = 450 \text{ mm}$) had been subjected to two kinds of tests: a four-point bending test and a compression/buckling test. Ten specimens

³³ www.basf.de

³⁴ This is explained further in Section 3.3.3 of this Chapter.

³⁵ Glass welding was conducted by Louwers Glastechniek in Hapert, the Netherlands, www.louwers.nl.

³⁶ The experimental specimens had been prepared by the technical glass workshop of the Faculty of Applied Physics of the Delft University of Technology.

were singular glass tubes without a weld; the other twenty had a weld in the middle or at one third of their length. Some had been annealed after welding, and others had not.

The experimental results indicated that butt-welded borosilicate glass tubes, either annealed or non-annealed, are not importantly weaker than tubes without weld. The weld behaves to a large extent (both strength and stiffness) similar to the main material. It should also be noted that, in comparison to annealed soda-lime float glass, very high failure stresses were recorded (Table A.5) Finally, the butt-welds did not produce unacceptable aesthetical results. No principal objection to applying welded borosilicate glass in building structures were found³⁷.

Table A.5 Summarized experimental results of 4-point bending test on small butt-welded borosilicate glass tubes.

Series	Description	R [N]			σ [MPa]		
		Ave	SD	Rel SD	Ave	SD	Rel SD
1-5	Single piece	272.21	49.22	18.08%	127.64	23.45	18.38%
6-10	Weld at $1/2l$, not annealed	327.38	87.06	26.59%	152.33	40.79	26.78%
11-15	Weld at $1/2l$, annealed	251.42	35.73	14.21%	116.41	17.5463	15.07%

The relative standard deviation (Rel SD) for failure load and failure stress are not equal because geometrical variations influence the relative standard deviation of stress, but not that of failure load.

2.2.2. Section dimensions and strut head design

The strut section consists of an acrylic tube of $d \times t = 60 \times 4 \text{ mm}^2$ and a borosilicate glass tube of $d \times t = 50 \times 9 \text{ mm}^2$. There is a 1 mm wide cavity between both tubes. The PMMA tube, with a length of 2500 mm, had been custom cast³⁸ (most available trade lengths go up to 2 m). The glass tube was welded in two points, with one standard 1.5 m length in between. Two 440 mm long pieces were welded to each side.

At the ends of the acrylic tube, massive acrylic pins are inserted and bonded adhesively (Figures A.39a and b). They have been machined from a solid 60 mm diameter rod. The particular problem of adhesive curing in a cylindrical cavity had also been encountered in the development of resin laminated tubular glass columns and the column-main beam joint for the ATP. Thus, further research was done to devise methods to apply adhesive

³⁷ Bos, F.P., Veer, F.A., *Bending and buckling strength of butt-welded borosilicate glass tubes*, 3rd International Conference on Structural Engineering, Mechanics and Computation, Cape Town, South Africa, September 10-12, 2007.

Subsequent research into the possibilities of welding borosilicate glass tubes was done by Cecile Giezen during her M.Sc. graduation project, supervised by Fred Veer and the author. She tested larger butt-welded and T-shaped specimens, based on tubes $d_{\text{outer}} = 80 \text{ mm}$; $t = 5.0 \text{ mm}$; $l = 600 \text{ mm}$ and $d_{\text{outer}} = 40 \text{ mm}$; $t = 3.2 \text{ mm}$; $l = 600/350 \text{ mm}$, in various experimental set-ups. In this study, failure stresses were found that were closer to those normally encountered in annealed soda-lime float glass. But again, there was no convincing indication the welds were significant weak points in the specimens. The experimental results were used to design a spectacular cable-stayed façade structure in which the compression members were 3D cross-shaped elements produced from welding glass tubes together. This study was published as Bos, F.P., Giezen, C., Veer, F.A., *Opportunities for the Welding and Hot-Shaping of Borosilicate Glass Tubes in Building Structural Applications*, Proceedings of the 1st Challenging Glass Conference, Delft, the Netherlands, May 2008.

The results of various investigations into welding borosilicate glass tubes have been collected in *AdDoc III: Welding and Hot-Shaping Borosilicate Glass Tubes; Possibilities, Strength and Reliability*, additional document to this PhD, www.glass.bk.tudelft.nl.

³⁸ By Stanley Plastics Ltd., Midhurst, West Sussex, UK, www.stanleyplastics.co.uk.

to such a joint and obtain defect free curing³⁹. Applying the adhesive under pressure at three points through small tubes in grooves proved to provide acceptable results.

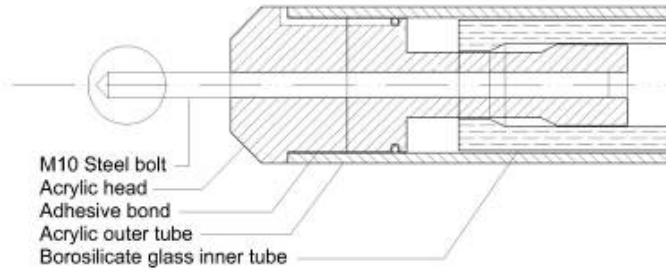


Fig. A.39a Joint design of the A-side of the TFS.

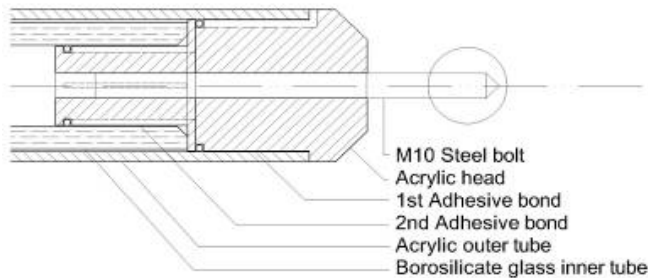


Fig. A.39b Joint design of the B-side of the TFS.

To connect the strut heads to the external structure, steel M10 bolts with a spherical head are screwed into the acrylic. At the tip of the bolt, peak stresses occur in the acrylic because the steel bolt has a much higher tensile stiffness than the acrylic section. As acrylic is brittle, this may cause breakage of the strut head from perpendicular cracks originating at the bolt tip – thus instigating complete collapse of the strut. Experimental research (unpublished) had shown failure behaviour of such joints with axially loaded bolts would be completely different if a plastic polymer is used. In that case the joint would fail from the inner thread within the polymer peeling off. This results in gradual failure. From FEM research it was concluded brittle failure from the bolt tip can be avoided by specific design measures to the strut head. Essentially, the bolt tip should be inserted further than the point of impact of the load which the acrylic transfers to the bolt. It can then no longer cause peak stresses around its tip. Figures A.40a, b, and c clarify this.

³⁹ Bos, F.P., *Glass-to-Acrylic and Acrylic-to-Acrylic Cylindrical Adhesive Bonds*, 2nd International Symposium on the Application of Architectural Glass, Munich, Germany, October, 2006. This paper has been reproduced as *AdDoc IV: Glass-to-Acrylic and Acrylic-to-Acrylic Cylindrical Adhesive Bonds*, additional document to this PhD, www.glass.bk.tudelft.nl.

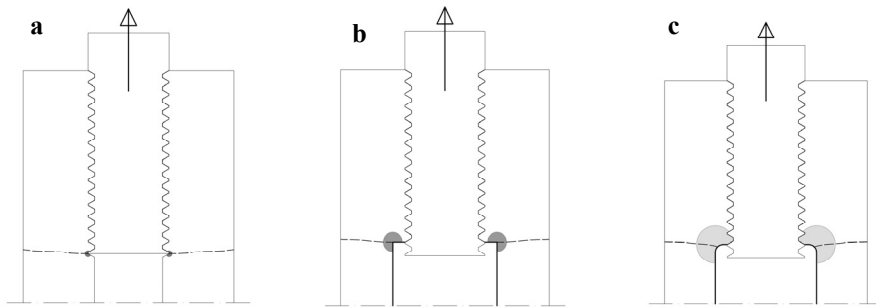


Fig. A.40a, b, c Stress concentrations at the tip of the bolt may cause complete failure in brittle materials (a, left). By inserting the bolt through the acrylic completely, the impact point of the load shifts away from the bolt tip, thus avoiding peak stresses at the tip (b, middle). By further applying a fillet, stress concentrations away from the bolt can be minimized (c, right).

Together, the acrylic tube and strut heads form the primary load path. For safety reasons, a secondary load path is obtained by activating the glass tube in case of breakage of the acrylic one. On the B-side (Figure 2.39a), the acrylic pin protrudes again into the glass tube. An adhesive bond similar to the previous one, connects the acrylic to the glass. A slice has been cut out of the acrylic so that thermal expansion of the pin joint will go inwards instead of outwards, which might break the glass. To avoid peak stresses at the top of the adhesive cylinder, the edges of the glass tube were tapered in a hot-shaping process. UV-curing Delo Glassbond GB368 was used in both adhesive bonds. The adhesive joints were cured slowly by lighting the bonds from a distance from all sides.

On the A-side (Fig A.39a), such an adhesive connection could not be used, because it would not allow for the difference in thermal expansion of the glass and the acrylic tube or for the elastic strain caused by loads. Therefore, a sliding joint was designed. The glass tube end has been thickened by hot shaping. Subsequently, an acrylic rod with a wide end has been inserted from the other end of the glass tube, and screwed to the primary acrylic pin on this side. Thus, the head piece can slide ± 20 mm, before being blocked by the glass tube end.

2.3. Conclusions

A hybrid design for Transparent Façade Struts has been presented, in which the favourable properties of a transparent polymer have been combined with those of borosilicate glass. An acrylic tube is the primary load carrying component, while an inner glass tube provides stiffness. This stability concept provides satisfactory buckling resistance. In combination with acrylic joint pieces on the strut heads, this produces a completely transparent structural member with impact resistance as well as safe failure behaviour in bending, tension and compression.

Three 1:1 scale prototypes have been tested. All showed significant post-failure strength, thus providing structural redundancy. Because the specimens also retained glass shards, the prototypes furthermore provided no risk of personal injury.

The glass inner tube was welded to obtain the appropriate length from standard sizes. This proved to be an economical solution that did not influence the strength of the member negatively. Meanwhile, altering the tube end geometry by hot shaping gave the opportunity to make complex joints which activate the glass tube as alternative load path in case of breakage of the acrylic tube under tension.

Several innovations were successfully brought together in the Transparent Façade Strut design. By obviating the need for auxiliary steel components for joining purposes and safety, this opens up the road to truly transparent structures.

Appendix B: Short Survey on Material and Design Specifications in Structural Glass Components

The results of a survey conducted in 2006 and 2007 among structural engineers working with glass are presented. The survey inquired about material and design specifications on some common structural glass components: a beam, a façade fin, and a roof plate. The contents of this appendix have previously been distributed among the survey participants.

1. Introduction

Because of its material properties, (soda lime silicate) glass is an inherently unsafe material to use in building structures. This is universally recognized by engineers and researchers. Several techniques have been developed to limit the risks associated with structural glass, of which laminating and thermal stressing are the primary. However, it is unclear to what extent these techniques should be used. Questions that may arise are:

- Should a glass member consist of multiple layers, and if so, how many?
- Should thermally toughened, heat strengthened or annealed glass be used, or perhaps a combination of these?
- Should glass breakage be reckoned with, and if so, of what part of the section?
- Which actions should be reckoned with after glass breakage? At which temperature and for what time?
- To which extent are these choices dependent on the application of the member in question?

A variety of solutions is applied in practice. As existing structural glass codes and guidelines provide very little generally accepted guidance on these issues, it seems that the individual experiences and opinions of the parties involved in an individual project play a major role in determining the design specifications of glass members. Their premises and to which extent they are achieved, however, usually remain unknown. It is therefore also unknown if there is much consensus on the premises, or if they vary widely.

To gain insight into this, a short survey has been conducted among structural engineers and researchers working with glass about their opinions on material and design specifications for structural glass members.

The survey has yielded 21 responses. Although this number is quite small, the results certainly show significant tendencies. The need to provide some form of redundancy is universally recognized. However, views on how residual strength should be obtained in practical designs vary. Thus, there seems to be no quantitative elaboration of this concept. Especially for beams and fins, this leads to different views on the minimum

number of layers needed, although a majority can be found for three layers. For floors, the opinions are less divided. Of PVB not only the properties are valued but also the fact that there is a considerable amount of knowledge available on that material. More than the other investigated parameters the level of required prestress seems to be very dependent on project specific parameters.

2. Method

2.1. Survey questions

A proper balance was sought between the number and kind of questions (and thus the time required to fill out the survey) on one hand and the relevance and usefulness of the response on the other. This resulted in a five question survey, three of which also contain sub questions. Table B.1 lists the survey questions.

The opening question inquires about the general premises of the respondent with regard to safety in glass structures. In the consecutive questions 2 through 4, the respondent is asked to consider three specific structural elements: a beam, a façade fin and a floor panel. The sub questions a through d deal with the material- and design specifications for these elements, particularly with regard to the number of layers in laminate, the required level of thermal stressing, the laminate type and other measures. Thus, these questions try to shed light on the way general premises are translated into practice solutions. Finally, question five gives room for further comments by the respondent.

2.2. Distribution

The survey was distributed among engineers and researchers known to have experience with the structural use of glass, more specifically the members of several professional organizations as well as a number of personal contacts of the author. The organizations are:

- The CUR-KCG Committee *Constructief Glas* (Structural Glass) in the Netherlands,
- The Fachverband Konstruktiver Glasbau with mainly German members,
- The IABSE Working Group Structural Glass.

Furthermore, the survey was put to the discussions sections of the Glassfiles website (www.glassfiles.com) as well as the website of the author's research group (www.glass.bk.tudelft.nl).

The survey has been made available in three languages: English, German and Dutch. Unfortunately, during the analysis of the results it was discovered there is a translation error in the German version. Question 3 should be about a glass façade fin. In the German version, this has been translated into '*Glasfassade*', which just means 'glass façade'. Therefore, the answers to question 3 of 7 respondents who have used the German version, had to be ignored. Therefore, the number of useable answers to that question was significantly lower than that of the other questions. Of course, the German answers to the other results were taken into account normally.

Table B.1 Survey questions.

#	Question
1	Could you briefly describe your premises with regard to safety, when you're working on a project involving structural glass?
2	Consider a <u>GLASS BEAM</u> (span approx. 5 m):
2a	- How many layers of glass would you prescribe? Explanation (if dependent on the situation, please identify the most important considerations):
2b	- What type of prestressing, if any, would you prescribe? (chemical/thermal, toughened/strengthened/annealed) Explanation:
2c	- What kind of laminate material would you prescribe? (PVB, EVA, ionomer (e.g. Sentry Glass Plus), resin, other) Explanation:
2d	- Would you prescribe any other special measures, like a layer of Polycarbonate in the laminate, etc? Explanation:
3	Consider a <u>GLASS FAÇADE FIN</u> :
3a	- How many layers of glass would you prescribe? Explanation:
3b	- What type, if any, of prestressing would you prescribe? Explanation:
3c	- What kind of laminate material would you prescribe? Explanation:
3d	- Would you prescribe any other special measures? Explanation:
4	Consider a <u>GLASS FLOOR PANEL</u> :
4a	- How many layers of glass would you prescribe? Explanation:
4b	- What type, if any, of prestressing would you prescribe? Explanation:
4c	- What kind of laminate material would you prescribe? Explanation:
4d	- Would you prescribe any other special measures? Explanation:
5	Is there any other comment you would like to add?

3. Results

It has proven difficult to obtain a substantial number of responses. Finally, 21 responses were collected in a time period of approximately 1 year. No responses came to the survey put to the discussion section of the glassfiles website.

3.1. Respondents

The respondents are active in various professions within the field of structural glass. In this survey, distinction is made between A) engineers at consulting offices (i.e. firms that do not actually construct glass structures), B) engineers at façade or construction firms (i.e. firms that construct glass structures themselves), C) researchers at university and other institutions. Occasionally, respondents hold positions in more than one of these professions. In those cases, they are listed in the profession in which they spent the major part of their time. Also, some respondents are active in one field, but also have been active in another. In those cases, only the current profession is considered. Table B.2 provides an overview of respondent professions. The survey was held at an international level, the respondents are active in seven different countries shown in Table B.3.

Table B.2 Respondents profession.

Respondent profession	# resp.
A engineer at consulting office	12
B engineer at construction/façade firm	5
C researcher at university or institute	4
TOTAL	21

Table B.3 Respondent's country of practice

Country of practice	# resp.
France	1
Germany	8
the Netherlands	7
Switzerland	1
United Kingdom	3
United States of America	1
TOTAL	21

One of the problems of the analysis of the survey responses, is that the engineering skills and experience will inevitably vary between respondents. It could thus be tempting to value the responses of one respondent higher than those of another. However, since there is no objective ground to discriminate between the quality of respondents and their responses, all responses were valued equally.

The survey results are presented here completely anonymous, as this was desired by most of the respondents.

3.2. Responses

Not all questions were answered by each respondent. Therefore, Table B.4 lists the number of responses per question.

Table B.4 Number of responses per question.

Question	1	2a	2b	2c	2d	3a	3b	3c	3d	4a	4b	4c	4d	5
# of responses	18	19	19	19	18	13	11	12	12	18	18	17	18	8

3.2.1. Responses to question 1: *Could you briefly describe your premises with regard to safety, when you're working on a project involving structural glass?*

Eighteen respondents answered this question, mostly in a qualitative way. The necessity for residual strength in case of glass breakage was named numerous times. Different formulations were used but they amount to the same: glass breakage in some form should be considered and some form of residual strength should be present after glass breakage. Some of the formulations were:

- 'Don't ask if the glass will break, but when and how': 1 time.
- Guarantee a safe failure mechanism and consider what would happen in case of glass failure: 1 time.
- 'The glass structure shall be designed to ensure stability even in case of glass breakage of a certain percentage of the glass panes': 1 time.
- Residual strength has to be proven in case of glass breakage: 7 times. Glass breakage was quantified as being to breakage of 1 layer of glass by 1 respondent.
- Another respondent indicated he used a 'belt and suspenders' approach and required breakage of 1 layer not to harm the structural integrity.

- ‘...the question of failure scenarios should be considered, in which case sufficient residual strength should always be present.’: 1 time.
- ‘Belt and suspenders approach’: 1 time.

Two respondents specified the post-breakage behaviour should be dependent on the application. One of them made a distinction between application in the primary load-carrying structure (Dutch: *Hoofddraagconstructie*) and application in a secondary structure, while the other named the consequence of failure of that particular element or structure a criterion for the amount of residual strength required.

In an elaborate answer, one respondent indicated that he assumes that any glass component may break at any time and that the system should remain safe in that condition. He furthermore would consider multiple panes of a laminated panel breaking. The number of layers would depend on location, application and type of glass. Finally, for structures where glass provides the entire supporting structure, he applies the principle that it should not be possible to knock down a building with a ‘centre punch, i.e. continued vandalism ... must not lead to structural collapse’.

One respondent recommended always to use laminated glass in structural applications. It is assumed that this recommendation also stems from the necessity to provide residual strength in case of glass breakage.

Another respondent claimed an extensive risk analysis concentrated on the specific application is necessary in each case. While this is reasonable, it is also very general. Since this respondent did not fill out any of the other questions, it is unclear how this should translate into practice.

A number of other comments were given, most of them appearing only once or twice, such as:

- ‘Proper joints and the glass element composition are important in determining the residual strength.’
- ‘Create residual strength by laminating.’
- ‘Joints should also be able to carry the loads and deformations.’
- ‘Pay attention to proper detailing. Careful construction. Use high safety factors because of large scatter. Detailed, local stress analysis because of brittle behavior. Extensive checking.’
- ‘Use personal knowledge of the material as well as common sense’.
- ‘Prove safety in undamaged state by 3D finite element analysis and fracture mechanics. Proving residual strength in damaged stage is usually only possible by experimental testing, although there are some experiential data for common, small span structures. Also prove the joints. Do not forget movements in the supporting structure; often complete modeling of the glass and supporting structure is necessary.’
- ‘The mathematical safety level should be chosen based on the redundancy of individual members of the structural system, the redundancy of the complete system, and the consequences of damage. The choice of safety level can be based on EN 1990. Also consider non-calculable actions like stress

concentrations caused by sharp impact objects. This can be either willful (vandalism) or accidental (collision).’

- ‘Structural boundary constraints, such as avoiding contact with hard bodies, should be fulfilled.’
- ‘Material partial factor on glass 2.5; the partial factor on thermal treatment 1.8 – 2.5.’

3.2.2. Responses to question 2: Consider a **GLASS BEAM** (span approx. 5 m)

3.2.2.1. 2a: **How many layers of glass would you prescribe?**

This question was answered by 19 respondents. The results, specified per professional group, are summarized in Table B.5 and Figure B.1.

3.2.2.2. 2b: **What type of prestressing, if any, would you prescribe?**

This question was answered by 19 respondents. The results, specified per professional group, are summarized in Table B.6 and Figure B.2. The following abbreviations were used: A = annealed glass, S = heat strengthened glass, T = thermally toughened glass.

Table B.5 Answer summary to question 2a.

Min. # of layers in laminate	Answer frequency				
	Professional group			Total	
	A	B	C	#	%
1	1 ^a	0	0	1	05.3 %
2	3 ^{c,g,h}	2 ^j	1 ^b	6	31.6 %
3	6 ^{f,k}	2 ^e	3 ^{d,i}	11	57.9 %
4	1	0	0	1	05.3 %
5 or more	0	0	0	0	00.0 %
TOTAL		19			100.0 %

^a A respondent answered that 1 layer suffices if the consequences of collapse are insignificant, but that 3 layers is sensible in many cases.

^b A respondent noted that the minimum should be 2 or 3 layers, depending on the possibilities of damage.

^c A respondent noted that it could be anything between 2 and 5 layers, depending on available thicknesses, cost, bearing requirements of glass panels supported by the beam, etc.

^d A respondent stated that the beam should be able to carry the representative actions with a safety factor of 1.1 after glass breakage.

ⁱ Another indicated that there should be structural continuity of at least 2 layers at any given section and that each layer should be able to carry the representative (=unfactored) loads.

^e A respondent declared that two out of three layers should be considered in the structural calculation (so one is reserve).

^f A respondent noted that the edge of the middle ply should be moved back a little in comparison to the edges of the outer plies, so that it will be protected when the outer plies sustain damage.

^g A respondent indicated 2 layers can be used when a kind of catenary action can be relied on. If no alternative load path is available, 3 layers should be used.

^h A respondent noted 2 layers can be used in combination with tempered glass and ionomer interlayer. Three layers are necessary with a PVB laminate.

^j A respondent indicated the minimum number of layers is dependent on the vulnerability to vandalism. Two layers suffice if this vandalism can be ruled out, three layers plus edge protection are required for applications prone to vandalism.

^k According to a respondent, the middle layer should be the main structural layer, the other two serve as protection. In case of the middle layer breaking, the others should take over the load carrying function.

Notes a, b and c all point out that, although in general there may be several options, there are specific cases causing stress concentrations that make the use of thermally

toughened glass the only remaining option. None of the respondents opted for chemically prestressed glass. Some respondents identified the small depth of compressive layer as a potential hazard for premature failure.

3.2.2.3. 2c: **What kind of laminate material would you prescribe?**

This question was answered by 19 respondents. The results, specified per professional group, are summarized in Table B.7 and Figure B.3.

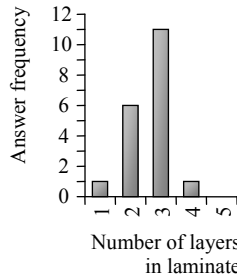


Fig. B.1 Responses to question 2a.

Table B.6 Answer summary to question 2b.

Prestress Treatment	Answer frequency			Total	
	Professional group			#	%
	A	B	C		
A	1 ^f	1	0	2	10.5 %
S	4 ^{a, h}	1 ^h	2 ^{b, h}	7	36.8 %
T	0	0	0	0	00.0 %
S or T	1 ^g	0	1	2	10.5 %
Any	3 ^c	2 ^d	1 ^c	6	31.6 %
Comb. S+T	2	0	0	2	10.5 %
TOTAL		19			100.0 %

^a A respondent noted that in general he prefers heat strengthened glass, but thermally tempered glass is necessary in cases where the edge can not be polished (e.g. in holes).

^b This respondent noted that prestressing is necessary because of the stress concentrations at the point where the actions are transferred into the glass.

^c A respondent noted that thermally toughened glass is necessary when point fixings are used. Otherwise annealed glass is also possible.

^d A respondent noted that he considered a combination of heat strengthened and thermally toughened glass to be the most safe, although annealed glass is possible.

^e A respondent noted that the choice for prestress is principally independent of span, but that a 5 m span would probably require prestressing. The respondent suggested a combination of heat strengthened and thermally toughened glass.

^f A respondent noted he would prefer annealed because of optical quality, edge work and economy. Heat strengthened would be a second choice.

^g A respondent indicated that thermally toughened glass should be used in combination with an ionomer laminate (presumably to guarantee stiffness in case of glass breakage -author) while heat strengthened glass should be used when the interlayer is PVB.

^h Three respondents choose heat strengthened glass because of the combination of relatively high impact strength and favourable cracking pattern (for residual strength).

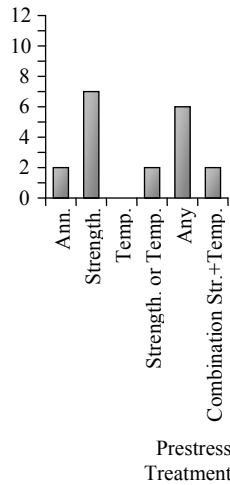


Fig. B.2 Responses to question 2b.

Table B.7 Answer summary to question 2c.

Type of laminate	Answer frequency			#	Total %
	Professional group				
	A	B	C		
PVB	2 ^{g, h}	0	2 ^f	4	21.1 %
Ionomer	0	1	0	1	5.3 %
PVB or Ionomer	7 ^{b, j, k}	2 ^{e, l}	1	10	52.6 %
Any/other	2 ^{a, d}	1 ⁱ	1 ^c	4	21.1 %
TOTAL	19				100.0 %

^a A respondent noted that the choice should be based on calculations of desired post-failure behavior.

^b A respondent preferred SG, but considered PVB more realistic from a commercial point of view.

^c A respondent noted that the laminate material should at least have a good resistance to tearing, e.g. PVB.

^d A respondent noted that the behavior of the laminate material itself is not particularly critical.

^e A respondent claimed that EVA foil and resins are not sufficiently resistant to fall-through. Furthermore, SG is only sensible when a 100 % cooperation between the glass sheets is required.

^f A respondent instructed not to use resin, and added that SG could delaminate at low temperatures.

^g A respondent notes that PVB is best known and causes the least problems. For SG, sufficient experiential values are still lacking. In some cases, other foils may be required, but these possess inferior residual strength.

^h A respondent noted that SG should only be applied durability has been proven and resins should not be used.

ⁱ A respondent noted that the shear modulus G, which may be different for each loading case since it is time and temperature dependent, is of primary importance. Residual strength experiments for each application are necessary.

^j A respondent noted that he preferred PVB, with ionomer being second choice if essential for post-breakage integrity.

^k A respondent indicated the choice for PVB or ionomer would depend on required post-breakage stability.

^l A respondent indicated that PVB is readily accepted by building authorities. Relying on increased cooperation between SG laminated glass layers can requires early consultation with the authorities. He would only use resin if there is no other option.

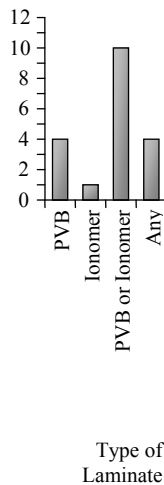


Fig. B.3 Responses to question 2c.

3.2.2.4. 2d: *Would you prescribe any other special measures, like a layer of Polycarbonate in the laminate, etc?*

This question was answered by 18 respondents. The answers were more diverging in nature than those to the previous questions and are therefore not summarized in one table and one figure.

Four respondents answered ‘no’ to this question.

In total, twelve respondents particularly reacted to the suggestion of adding Polycarbonate (PC) within the laminate. Three of them remarked that PC or another solid polymer interlayer should only be added in case of bulletproof or burglar proof glass. This is not likely to be necessary for a glass beam. Another one indicated it can be useful in case of specific requirements. Two others noted that it would not be useful in the Netherlands (one of those added it adds much complexity but it could be required in seismic areas). Another respondent also indicated PC might be used in seismic or vandalism prone areas.

Two respondents commented that there are many questions concerning a glass-PC laminate, such as durability and glass-PC bond quality, and that it should therefore not be used. One said PC should not be used as redundancy can be obtained in other ways, while another mentioned that it is certainly a possibility to laminate PC if it is the only way to obtain a fail safe structure, but that it is very well possible to obtain safe failure behavior without PC. Finally, one respondent remarked it is good to have polymer with a section suitable to carry the loads.

Some other remarks were:

- Complementary steel elements can be helpful.

- Distinguish between strength and stiffness in different scenarios (presumably pre- and post-failure).
- Other measures are dependent on the danger potential of the application.
- Edges should be grinded.

3.2.3. To question 3: **Consider a GLASS FACADE FIN:**

3.2.3.1. 3a: **How many layers of glass would you prescribe?**

This question was answered by 13 respondents. The results are summarized in Table B.8 and Figure B.4.

3.2.3.2. 3b: **What type, if any, of prestressing would you prescribe?**

This question was answered by 11 respondents. The results are summarized in Table B.9 and Figure B.5.

3.2.3.3. 3c: **What kind of laminate material would you prescribe?**

This question was answered by 12 respondents. The results are summarized in Table B.10 and Figure B.6.

Table B.8 Answer summary to question 3a.

Min. # of layers in laminate	Answer frequency				
	Professional group				Total
	A	B	C	#	%
1	4 ^{a, b, c}	1 ^b	1 ^f	6	46.2 %
2	4 ^e	0	0	4	30.8 %
3	1 ^d	2	0	3	23.1 %
4	0	0	0	0	00.0 %
5 or more	0	0	0	0	00.0 %
TOTAL		13			100.0 %

^a A respondent answered that there is no fundamental difference between beams and façade fins.

^b Two respondents answered 1-3 layers.

^c Two respondents stated that one layer is minimum, but two layers is preferable.

^d A respondent declared that two out of three layers should be considered in the structural calculation (so one is reserve).

^e A respondent indicated that two would be minimum unless the area below the wall was not accessible to people.

^f A respondent answered 1-2 layers, depending on the presence of an alternative load path.

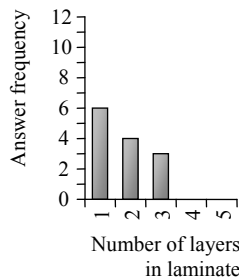


Fig. B.4 Responses to question 3a.

Table B.9 Answer summary to question 3b.

Prestress treatment	Answer frequency				
	Professional group				Total
	A	B	C	#	%
A	0	1	0	1	08.3 %
S	1	0	0	1	08.3 %
T	1 ^a	0	1	2	16.7 %
S or T	1	0	0	1	08.3 %
Any	5 ^{b, d, e, f, g}	2 ^c	0	7	58.3 %
Comb. S + T	0	0	0	0	00.0 %
TOTAL		12			100.0 %

^a A respondent preferred thermally toughened glass in case of one layer, in case of three layers the thermally toughened layer should be joined by two layers of heat strengthened glass.

^b A respondent preferred annealed glass, unless the fin is supported by point fixings.

^c A respondent answered that annealed glass ok, but thermally toughened glass is necessary when point fixings or peak stresses are present. Heat strengthened glass should be used when there is risk of collision by persons.

^d A respondent indicated he preferred annealed or heat strengthened glass, but would allow heat soaked tempered glass if that would be required because of the high loading to depth ratio, common in fins.

^e A respondent indicated that thermally toughened glass should be used in combination with an ionomer laminate while heat strengthened glass should be used when the interlayer is PVB.

^f A respondent noted annealed is usually insufficient, also because of point fixings.

^g Another one indicated the contrary, stating prestress is usually not required.

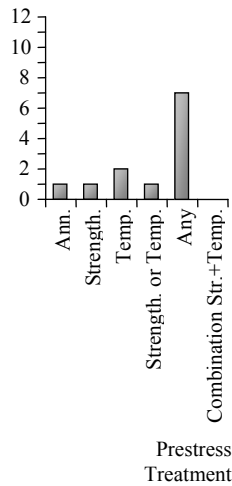


Fig. B.5 Responses to question 3b.

Table B.10 Answer summary to question 3c.

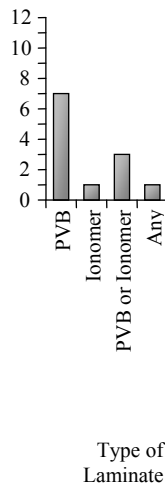
Type of laminate	Answer frequency				
	Professional group				Total
	A	B	C	#	
PVB	3 ^b	2 ^a	2	7	58.3 %
Ionomer	0	1	0	1	08.3 %
PVB or Ionomer	3 ^{c, d}	0	0	3	25.0 %
Any	1	0	0	1	08.3 %
TOTAL			12		100.0 %

^a A respondent claimed that EVA foil and resins are not sufficiently resistant to fall-through. Furthermore, SG is only sensible when a 100 % cooperation between the glass sheets is required.

^b A respondent noted that SG should only be applied durability has been proven and resins should not be used.

^c A respondent noted that he preferred PVB, with ionomer being second choice if essential for post-breakage integrity.

^d A respondent indicated the choice for PVB or ionomer would depend on required post-breakage stability.

**Fig. B.6** Responses to question 3c.

3.2.3.4. 3d: *Would you prescribe any other special measures?*

This question was answered by 12 respondents. The answers were more diverging in nature and are therefore not summarized in one table and one figure.

Six respondents answered 'no' to this question.

Some remarks were:

- Pay attention to forced stresses during mounting.
- Heed the deformation of the higher floor or roof.
- Pay extra attention to joint details.

- Edges should be grinded.
- Would consider safety cables on long (> 10 m) fins.
- Measures to avoid lateral torsional buckling could be required.

3.2.4. To question 4: **Consider a GLASS FLOOR PANEL**

3.2.4.1. 4a: **How many layers of glass would you prescribe?**

This question was answered by 18 respondents. The results are summarized in Table B.11 and Figure B.7.

Table B.11 Answer summary to question 4a.

Min. # of layers in laminate	Answer frequency				
	Professional group			Total	
	A	B	C	#	%
1	0	0	0	0	00.0 %
2	2	1 ^d	1 ^e	4	22.2 %
3	8 ^{a, b, c}	3 ^{a, b}	3 ^a	14	77.8 %
4	0	0	0	0	00.0 %
5 or more	0	0	0	0	00.0 %
TOTAL	18				100.0 %

^a Four respondents noted that the top layer is for wear and tear, while the bottom two should be considered as load carrying sheets.

^b Two respondents noted that the minimum number of layers for a frequently used floor should be three, while for incidentally accessible glazing, two layers suffice.

^c A respondent stated that in public areas, four might be minimum and that the aim should be to keep avoid breakage of at least one pane from hard body impact.

^d A respondent specified a minimum of 2 layers for annealed and heat strengthened glass and 3 layers for thermally tempered glass.

^e A respondent specified a minimum of 2 layers for domestic applications and 3 for public applications.

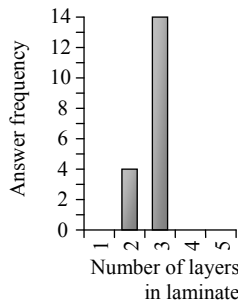


Fig. B.7 Responses to question 4a.

3.2.4.2. 4b: **What type, if any, of prestressing would you prescribe?**

This question was answered by 18 respondents, six of whom made an explicit distinction between the top sheet (for wear & tear), and the bottom, load carrying sheets. Table B.12 and Figure B.8 therefore summarize the results for the load carrying layers, while Table B.13 and Figure B.9 present the results for the top layer.

Table B.12 Answer summary to question 4b.

Prestress treatment for load carrying layers	Answer frequency				
	Professional group				Total
	A	B	C	#	%
A	2 ^{a, g}	0	0	2	11.1 %
S	2 ^f	1	0	3	16.7 %
T	0	1	0	1	05.6 %
A or S	1	0	1	2	11.1 %
S or T	1	0	2	3	16.7 %
Any	3 ^{b, d}	2	1 ^c	6	33.3 %
Comb. A or S + T	1 ^e	0	0	1	05.6 %
TOTAL		18			100.0 %

^a A respondent stated that annealed glass is usually the best option; the bending stiffness is usually governing in determining the dimensions.

^b A respondent preferred annealed glass, unless there are point fixings.

^c A respondent noted that thermally toughened glass is necessary when there are point fixings, but in other cases annealed glass or heat strengthened glass can be used.

^d A respondent stated that the top layer should always be prestressed (S or T), and that for the load carrying layers all kinds of combinations are possible, like: H-S-S, S-S-S. When the span is small and there are line supports, T-A-A or S-A-A are also conceivable.

^e A respondent explained that the bottom layer should be thermally toughened because of the maximum tensile stresses, while the top two layers should be annealed or heat strengthened.

^f A respondent indicated heat strengthened glass would provide the best combination of strength and crack pattern.

^g A respondent indicated he would prefer annealed glass with an SG interlayer, but that in reality often thermally tempered glass with PVB laminate is used.

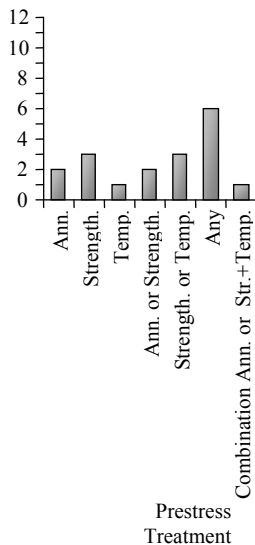


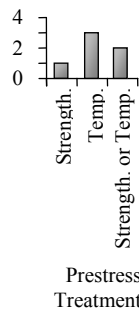
Fig. B.8 Responses to question 4b; for load carrying layers.

Table B.13 Answer summary for question 4b, specified for top layer.

Prestress treatment for top layer	Answer frequency				
	Professional group			Total	
	A	B	C	#	%
S	0	1 ^b	0	1	16.7 %
T	1	1 ^a	1	3	50.0 %
S or T	2	0	0	2	33.3 %
TOTAL			6		100.0 %

^a A respondent noted that the top layer should be thermally toughened, among other reasons to make failure clearly visible.

^b A respondent indicated the top layer should be heat strengthened, while the other layers would probably have to be thermally tempered.

**Fig. B.9** Responses to question 4b; for top layer.

3.2.4.3. 4c: *What kind of laminate material would you prescribe?*

This question was answered by 17 respondents. The results are summarized in Table B.14 and Figure B.10.

3.2.4.4. *Would you prescribe any other special measures?*

This question was answered by 18 respondents. The answers were more diverging in nature and are therefore not summarized in one table and one figure.

Five respondents answered 'no' to this question.

With regard to residual strength, some remarks were made. According to three respondents, residual strength tests should be carried out (one of whom specified a torpedo drop test). Another (German) respondent noted that in Germany, there are guidelines from glass manufacturers for standard glass floor applications. In case of non-standard applications, the residual strength should be proven by experiments. Finally, one respondent indicated that in most cases, the perimeter should be bonded to the (sub) frame to prevent the panel from sliding off the support when broken.

A (Dutch) respondent remarked that perhaps the German guidelines should be adopted in the Netherlands as well.

Some other remarks were:

- Use mechanical supports.
- Apply an anti-slip coating
- Pay attention to detailing.
- Edges should be grinded.
- Drain the perimeter to avoid water accumulation from rain or floor cleaning when seal fails.
- The administrator should take measures upon glass breakage.

Table B.14 Answer summary for question 4c.

Type of laminate	Answer frequency				
	Professional group			#	Total
	A	B	C		
PVB	3 ^{c, f}	3 ^c	4 ^d	10	58.8 %
Ionomer	1 ^b	0	0	1	5.9 %
PVB or Ionomer	5 ^{a, g}	0	0	5	29.4 %
Any	1 ^h	0	0	1	5.9 %
TOTAL			17		100.0 %

^a A respondent preferred SG, but considered PVB more realistic from a commercial point of view.

^b A respondent preferred SG, but recommended that the design is always tested experimentally.

^c A respondent claimed that EVA foil and resins are not sufficiently resistant to fall-through. The technical specifications of SG should be mentioned in the codes.

^d A respondent instructed not to use resin, and added that SG could delaminate at low temperatures.

^e A respondent chose PVB because although SG seems to have advantages over PVB, there are still many questions about the material.

^f A respondent noted that SG should only be applied durability has been proven and resins should not be used.

^g A respondent noted he would prefer SG, but accepted PVB.

^h A respondent noted he would require ionomer in case of a uni-direction stress state, but any other laminate in other cases.

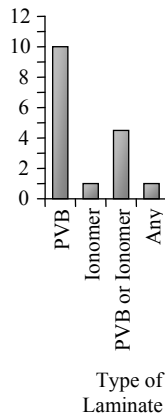


Fig. B.10 Responses to question 4c.

3.2.5. To question 5: **Is there any other comment you would like to add?**

Eight respondents gave further comments. Most of those related to the relevance and correctness of the questions.

One respondent considered that to prescribe (German: *Vorschreiben*; Dutch: *Voorschrijven*) would be a technically and scientifically incorrect way to go. Another respondent agreed, by stating that the applied way of questioning would lead to a catalogue of solutions, while a generally accepted dimensioning norm is what is actually needed. This norm should contain:

- which aspects with regard to use, danger and safety should be considered,
- what has to be proved and which glass properties should be heeded for the proving,
- which material strength properties are to be used,
- which general equations should be used for dimensioning,
- easy-to-use equations for common situations,
- *a possibility to use other ways of proving, by accepted scientific methods relevant to the application.*

A third respondent argued in the same direction. In his opinion, as little as possible should be prescribed definitely. In some common applications it may be sensible to prescribe some definite material- and design specifications, if this would obviate the need for experimental testing. But the road to proof by experimental testing should always be open. According to a fourth respondent, readymade solutions can be dangerous. Different solutions are usually possible and may depend on applied actions, residual strength, use of the structure, climate, possible damage scenarios, type of supports, kind of materials, etc.

Related to these comments, is one from another respondent who stated that the classical structural members are not the problem. The important issues rather, are those not often encountered in common steel or concrete structures, like cavity air pressure, identifying stress concentrations and tension zones, specifications of glass surface area, differential temperature stresses, influence of deflection on stresses, time dependent effects in glass and plastics, issues of robustness, replacement and post failure behavior.

According to another respondent, the factors influencing the design are many and interlinked. Therefore, it is sometimes necessary to diverge from the starting rules. This respondent furthermore warned that we are reaching a stage where many engineers start to design with glass without proper heed to the dangers, because they see so many built examples. To articulate clear rules that achieve reliability whilst also allowing for innovative engineering will be difficult.

Another remark was that supports, actions and detailing are very important to consider for the elements described in questions 2, 3 and 4. Finally, one respondent also indicated that it is hard to give general recommendations for PVB or Ionomer interlayers, as they each have their pro's and con's.

3.3. Analysis

3.3.1. Analysis of Question 1: **Could you briefly describe your premises with regard to safety, when you're working on a project involving structural glass?**

Realizing residual strength is by far the most important point of attention when using glass for structures. In 17 out of 18 answers with regard to the premises for a structural glass project, this is mentioned in one way or another. However, seems to be significant differences in the level of detail this principle is carried through in the design. While a few consider multiple stages of damage of a member, most others simply indicate residual strength needs to be realized. The type or area of application is mentioned by some to be of influence on the level of residual strength required.

In most cases, the level of required residual strength is not quantified further. Only one respondent states he uses a safety factor of 1.1 in case of failure, while another said to use three layers in a beam, and count only two in the calculations. Yet another indicated to work with lower safety factors when considering glass breakage, depending on the location and application.

Thus, although the necessity for residual strength is commonly felt, there seems to be no clear idea what 'residual strength' actually is in quantifiable terms and on which factors it may depend. Therefore, there can also be no common agreement on how much residual strength is needed in which application.

3.4. Analysis of question 2: **Consider a GLASS BEAM (span approx. 5 m)**

3.4.1. 2a: **How many layers of glass would you prescribe?**

A small majority (57.9 %) has developed in favour of a three layer minimum for glass beams of 5 m span. In one case, the choice for two or three layers was made dependent on the presence of an alternative load carrying mechanism. The general idea seems that in a three layer beam, there is a reasonable probability that both outer layers will break, but the inner layer is so well protected, it should not fail. In some cases, design measures (like a retreating the inner sheet or covering the edges with a protective strip of some kind) are suggested to guarantee this. Nevertheless, a large minority of 31.6 % finds two layers can be acceptable in some cases, especially in applications where the probability of willful damage is minimal.

3.4.2. 2b: **What type, if any, of prestressing would you prescribe?**

The responses to this question gave a more diffuse picture. Most respondents (36.8 %) would prescribe heat strengthened glass, but an almost equally large group (31.6 %, a difference of 1 respondent) indicated that any type of prestress is in principle possible. Heat strengthened glass is generally valued for its combination of reasonable impact resistance and favourable cracking pattern (and thus ability to obtain residual strength). It should, however, be questioned what the value of the breakage pattern is: as long as not all layers are broken, the breakage pattern is of little significance since the intact layer will be carrying the forces; when all layers are broken, a PVB laminated glass member will probably not be able to carry much forces, although there may be some shear-lock effect of large overlapping pieces of glass. This will be subject of further research.

Another remarkable result was that a considerable group suggested a combination of heat strengthened and thermally toughened glass (2 made it their preferred choice, while 2 others suggested it), while this is not applied much in practice (to the knowledge of the author). In such combinations, the outer layers are suggested to be heat strengthened, while the inner layer is thermally toughened. The outer layers are then weaker, and thus more prone to breakage, but the inner layer is stronger. When that finally breaks, an interlocking effect of the heat strengthened layers (similar to all HS variants) is hoped for. The difference between calculable strength of heat strengthened and thermally toughened glass also provides an extra reserve.

When point fixings are needed, most respondents indicate thermally toughened glass is compulsory. On the other hand, none of the respondents indicated thermally toughened glass in general should be preferred above other variants. Although this glass is accepted as an option, the tendency is rather not to use thermally toughened, unless this is necessary because of expected peak stresses. Hence, its breakage pattern is considered a drawback with regard to safety.

3.5. 2c: What kind of laminate material would you prescribe?

Again, a significant group considered any laminate material possible (21.1 %), but the majority indicated that it would have to be either PVB or Ionomer (52.6 %). Together with the 21.1 % group specifically requiring PVB and the one respondent requiring Ionomer, these two interlayer types are by far the most appreciated ones, at least from a structural safety point of view. The consensus on the issue of laminate material seems to be somewhat larger than on prestress treatment, but there are still considerable differences.

An important note by one respondent was, that the behaviour of the laminate material actually is not very important. This is true as long as at least one layer of glass is not broken (since $E_{\text{glass}} \gg E_{\text{laminate}}$) and there are no stability issues.

Others claim EVA and resins are not sufficiently safe against falling through. For beams, this may not be very relevant. However, it probably also means it has a low tearing resistance which may be relevant for the residual strength in case all glass layers break. It is thus noted that these respondents seem to consider some kind of residual strength necessary even when all glass is broken.

Although ionomer interlayers like Sentry Glass Plus claim superior strength and stiffness properties over PVB, there is no general preference for this material. Only one respondent claimed ionomer would be required for the 5 m beam. On the other hand, a group of 21.1 % specifically excluded ionomer by prescribing (only) PVB.

Apparently, there are still significant doubts about the performance of ionomer interlayers. One respondent pointed out that it may delaminate at low temperatures, while others just found there are too little experiential values available. Non-technical issues such as price and availability may also play a role.

3.5.1. 2d: Would you prescribe any other special measures?

This question yielded a host of varying answers. No clear picture emerged with regard to other/special measures that might be required. Adding Polycarbonate (PC; an explicit

suggestion made in the question) was met with varying response, ranging from approval (presumably because of safe, ductile failure behavior) through indignity to disapproval because of unanswered questions with regard to durability (both of PC itself and the PC-glass bond).

3.6. Analysis of question 3: Consider a **GLASS FACADE FIN**:

3.6.1. 3a: ***How many layers of glass would you prescribe?***

Almost half of the respondents (46.2 %) found a one-layer solution suitable in cases where there is no risk of people bouncing into the fins. However, one of those noted he would prefer a two layer solution, although they did not find that the absolute minimum. A slight majority of 53.8 % specified a multi-layer (2-3) solution in any case. Therefore, opinions on using single- or multilayer solutions for façade fins are momentarily practically tied, but there seems to be a slight preference for multilayer solutions.

3.6.2. 3b: ***What type, if any, of prestressing would you prescribe?***

A large majority considers any type of prestressing possible, depending on parameters such as the presence of point fixings, required strength, maximum weight and price. Annealed glass is accepted or preferred by some, but those respondents also all required a multi-layer solution in question 3a. The other way around, other respondents instructed to use thermally toughened glass if a single layer solution is opted for.

3.6.3. 3c: ***What kind of laminate material would you prescribe?***

Contrary to the similar question with regard to 5 m beams, there is a considerable consensus on the use of laminate in fins. Seven respondents (58.3 %) chose PVB, three PVB or Ionomer, one Ionomer, and only two did not make a definite choice. However, since a large part of the respondents suggested one layer as a minimum for fins, the question of what laminate should be used, becomes less important.

3.6.4. 3d: ***Would you prescribe any other special measures?***

Some general heeds were given regarding detailing, but there is no generally felt need for further measures.

3.7. Analysis of question 4: Consider a **GLASS FLOOR PANEL**

This question yielded the most agreement in the answers. Especially question 4a gave a clear picture.

3.7.1. 4a: ***How many layers of glass would you prescribe?***

Fourteen respondents (77.8 %) opted for at least three layers, while four (22.2 %) choose two layers. Many of the first group specified that the top layer is for wear and tear, and should not be considered load-carrying. Some furthermore explained that if the surface were only to be accessible for cleaning and maintenance, two layers would suffice. Of the second group, some nuanced that 2 layers would be required for private floors and 3 would be the minimum for publicly accessible floors.

3.7.2. 4b: ***What type, if any, of prestressing would you prescribe?***

As with questions 2b and 3b, the largest group (33.3 %) felt any prestress treatment could be possible. The rest was quite evenly spread over the other options. However, since heat strengthened glass is included in several options ('Any', 'S', 'S or T', and 'A or S'), this seems again to be the prestress type of choice.

Only one respondent noted that annealed glass is usually best because of its breakage pattern and, since stiffness is usually governing over strength in these applications, heat strengthened or thermally toughened is not necessary.

Six respondents specifically mentioned that the top layer should be prestressed: thermally toughened according to three respondents of them. One respondent required the bottom layer to be prestressed because that is where the highest stresses occur.

3.7.3. 4c: *What kind of laminate material would you prescribe?*

Again, a high preference for PVB was found. Although ionomer laminates are specifically known for their high stiffness and shear modulus, which would be an advantage in floor applications both in terms of deformations and residual strength, it is not generally considered necessary by any but one of the respondents.

It is furthermore worthwhile to note that, contrary to previous questions, no other options besides PVB and ionomer are suggested. This may be related to the inferior fall-through and residual strength properties mentioned earlier (in the comments to questions 2c and 3c).

3.7.4. 4d: *Would you prescribe any other special measures?*

Some general remarks concerning detailing were given. However, four respondents explicitly required residual strength tests (although one of those found this only needs to be done in cases which divert from standard applications for which glass floor suppliers provide guidelines).

3.8. *Analysis of question 5: Is there any other comment you would like to add?*

Most answers to question 5 contained the notion that there should not be a definite design and/or material prescription for certain applications, but rather that clear criteria are necessary to which designs can be checked.

It was not the intention of this survey to arrive at definite member designs by inventorizing what the majority of the field thinks of certain design issues. Rather, the goal was to find out a) how certain premises work out in practical design and b) how big opinion differences are on these issues in the field of structural glass specialists. In the framework of this survey, the word choice in the questions ('prescribe') was perhaps misleading. Maybe a more neutral word like 'use' would have been more suitable.

Several respondents also noted that the questions were too general and that many design specifications would depend on the project specifics. However, a detailed design problem was consciously avoided because it might have resulted in a tedious fill in exercise and would not yield general results.

By formulating the questions in a general manner, some insight was gained as to which issues are (to which extent) project independent, and which are project dependent. The number of layers, for instance, especially for a floor application yielded quite clear results, while the prestress treatment is apparently heavily project specific.

3.9. *General*

In the results section, answers were specified according to professional group. No clear differences per professional group were found. However, with only around eighteen

useable answers per question, it is impossible to draw reliable conclusions per professional group because the answer frequency specified per group becomes too small. The same holds for an analysis per country.

This survey sought to find out a) how big opinion differences are on these issues in the field of structural glass specialists and b) how certain premises work out in practical design.

Ad a: The number of layers and laminate material yielded quite clear results. For floors, there is hardly any discussion: three layers is minimum according to most. For beams and fins there is more discussion. Small majorities require 3 layers for beams and a multi-layer solution (2 or 3 layers) for fins. But there were also considerable minorities for other options.

The required prestress treatment is much more project specific. Judging from several remarks and suggested prestress levels, both annealed and heat strengthened glass are appreciated for their breakage pattern and thus post-failure behavior, while tempered glass is mainly required in case of stress concentrations. Hence, the strongest material is not generally considered the most safe.

With regard to the laminate, it can be said there is a great appreciation for the properties of PVB and the body of knowledge available for that material. This leads to a wide spread preference for this material over other laminates. There is not much discussion on its suitability especially for floors, but also for fins. It is also favorite for beams, but has more competition from ionomer layers like SG because of the residual strength.

Ad b: The most clearly stated premise is residual strength. It translates into practice mostly by requiring multi-layer solutions, although that is less required for façade fins. Apparently, residual strength is not as important for those members. This may be explained from the fact that they rarely carry people and failure of a fin usually leads to large façade deflections, but not necessarily to extensive collapse. Furthermore, they are usually not above people, and are thus less likely to inflict injury.

Three layers is generally considered enough to provide residual strength, in any of the proposed structural members. The premise is probably that the inner layer is always sufficiently protected and the probability of inner layer failure is acceptably small. Outer layers may be sacrificed, although sometimes lower actions are taken into account in case of breakage of two layers. Some also consider the probability of two layers breaking acceptably small in some applications.

The premise of residual strength also leads to a preference (by some respondents) for annealed or heat strengthened glass.

Finally, careful detail design is also an important aspect in controlling the risk of failure, as is pointed out by the numerous remarks with regard to detailing in the d-questions.

4. Conclusions

The need for some form of residual strength in structural glass projects is generally recognized by professionals in the field. However, views on how residual strength should be obtained in practical designs vary. There seems to be no quantitative elaboration of this concept. No other generally carried premise with regard to the safety of structural glass was encountered.

In practice, residual strength is provided by multi-layer designs in beams and floors. For both these types of members, a majority finds three layers to be the minimum (regardless of project specifics), but for floors this majority is more significant than for beams (over 75 % vs approximately 55 %). However, there is no generally accepted view on what extent of glass breakage should be taken into account (1, 2, or all layers broken) and what loads should be considered in those cases. The level of detail in which such scenarios are considered, also seem to vary widely, although this impression may be depend on the amount of time and effort put in the survey by the individual respondents.

More than three layers are not necessary from a safety point of view, neither for beams nor for floors.

Fins are judged differently. Almost half of the respondents finds one layer to be the minimum, although some prefer two layers. The rest half requires a multi-layer solution. That group can again be approximately equally split between respondents requiring 2 and those requiring 3 layers. Residual strength for this type of members is thus not as important.

Residual strength is also provided by using annealed or heat strengthened glass which has favourable cracking patterns. Thermally tempered glass is appreciated for point fixings and other peak stress applications, but its breakage pattern is a major disadvantage for the safety. Possibly as a result, the level of prestress required in structural glass members is highly dependent on the specific project details, much more so than the other investigated parameters. Relevant project specifics may include presence of point fixings / type of support, risk of bumping into, actions on the member, required maximum weight, etc.

The large body of knowledge on PVB, both in terms of scientifically acquired data and practical experience, is greatly appreciated and is one of the reasons why it is often preferred to ionomer interlayers.

Finally, piled together from a number of general as well as detailed remarks, it can be argued that a guideline for the structural use of glass should (at least) contain:

- A method for calculating and checking dimensions (stresses),
- A qualitative and quantitative method for determining residual strength,
- Provide specific opportunity for experimentally proving the strength and residual strength of structural glass as well as some guidelines on how the proving may be executed.

- A set of detailing and finishing rules or suggestions to minimize the probability of premature failure.

5. Acknowledgements

I would like to express my sincere gratitude to all the respondents who have taken the time to fill out this survey, as well as to prof. Rob Nijse, with whom I have drawn up the survey questions.

Appendix C: Interviews on Structural Glass and Safety

Following the survey presented in Appendix B, six structural glass specialists have been interviewed, to probe the questions raised in the survey more in depth. The interviews were conducted in the summer of 2007 with Rob Nijse, Graham Dodd, Tim Macfarlane, Holger Techen, Jens Schneider, and Frank Wellershof. This appendix contains an introduction into the subjects which were discussed, as well as the reports of each of the six conversations. They have been checked with and approved by the interviewees.

1. Explanatory Notes to the Interview

For the interviews, a general agenda was determined, as given in Figure C.1. The agenda was made available to the interviewees prior to the interview, along with some explanatory notes, reproduced below.

<p>Agenda:</p> <ol style="list-style-type: none"> 1. INTRODUCTION by interviewer 2. BACKGROUND AND EXPERIENCE of the interviewee <ol style="list-style-type: none"> a. Present profession and company b. Education and working experience c. Structural glass projects 3. EXPERIENCES WITH STRUCTURAL GLASS <ol style="list-style-type: none"> a. General premises b. Project specific parameters c. How premises translate into practice d. Failure experiences 4. GENERAL SAFETY ISSUES <ol style="list-style-type: none"> a. Residual strength b. Load requirements in case of failure c. Time requirements in case of failure d. Testing procedures 5. CODES AND GUIDELINES 6. PAST AND FUTURE DEVELOPMENTS 7. POSSIBLE OTHER ISSUES raised by the interviewee 8. CONCLUSION
<p>Fig. C.1 Interview agenda.</p>

Ad 1: Introduction

A recurring problem which has to be solved for each glass structure, is how to make it safe. Surprisingly enough, the amount of codes, guidelines and literature on this subject

has remained extremely limited, even though the number of realised glass structures is steadily rising.

Several techniques are used in practice to increase the safety of structural glass, like laminating and prestressing. Opinions on the extent to which these techniques should be used however, vary significantly. This can be deduced from comparing various projects and has also been shown by a survey on design- and material specifications of structural glass members, conducted previously by the interviewer. That survey has yielded some interesting results with regard to the premises generally held by engineers working with structural glass and the way these are translated into practice. To gain some more in-depth understanding of the issues raised in the survey, a number of respondents, each highly respected professionals in the field of structural glass engineering, have been approached for an interview. They are:

- Rob Nijse,
- Graham Dodd,
- Tim Macfarlane,
- Jens Schneider,
- Holger Techen,
- Frank Wellershof.

Specifically, the interviews should:

- provide elucidation on several important general concepts and issues such as residual strength, post-failure strength requirements, and testing procedures,
- provide insight into the influence of project specific parameters such as accessibility on the structural design,
- clarify what a structural glass code or guideline should and should not contain.

This interview should have the character of an open discussion. The agenda proposes a number of subjects to be discussed in a logical order. However, the interview itself may develop along other lines, and the interviewee is encouraged to bring up any subject that he feels relevant, at any time.

After the interview, a report will be made up and send to the interviewee for checking and correction. The interviewee will have the possibility to add further comments if necessary. Both the survey and these interviews are part of the PhD research of the interviewer. By agreeing to these interviews, the interviewees are assumed to have agreed with publication of the results in the PhD dissertation of the interviewer. If preferred by the interviewee, this can be done anonymously. Furthermore, the results may be interesting enough to publish in professional or scientific journals and/or to bring them up at meetings such as those of the IABSE WG Structural Glass. The interviewees will be asked for their permission to use the results in those cases.

Ad 2: Background of the interviewee

For the report which will be made of the interviews, it is necessary to have some background information on the interviewees. Therefore, inquiries will be made with regard to education, working experience and the number and kind of glass projects the

interviewee has been involved in. It is the intention of the interviewer not to spend too much time on this point because most of it can be filled in before or after the interview.

Ad 3: Experiences with structural glass

The actual discussion could start with the way the interviewee handles structural glass projects in practice. Issues to be discussed are the general safety premises or reference frame of the interviewee when he gets started on a structural glass project. It is highly likely that the discussion will also come across subjects listed under point 4, but that should not be a problem.

Many survey respondents indicated a lot of safety design decisions are dependent on project specific parameters. A next issue could therefore be what those issues are and how they relate to general premises.

Finally, it would be interesting to discuss failure experiences of the interviewee. It is known that a lot can go wrong, but what does actually go wrong in practice? What are the causes and the consequences of failures?

Ad 4: General safety issues

Based on the survey results, there are several issues and concepts with regard to structural glass safety which deserve further elaboration (if not yet discussed under 3), such as:

a. Residual strength

The necessity of residual strength is generally recognized, but there seems to be no definite idea of what that is.

b. Load requirements in case of failure

What loads would be reasonable to expect in case of failure? How would this relate to building type of structure type?

c. Time requirements in case of failure

How long should a glass structure be able to transfer loads after failure?

d. Testing procedures

Experiments are generally deemed necessary to prove certain structural glass behaviour, but failure of glass is not only highly test dependent but also statistically difficult to interpret.

Ad 5: Codes and guidelines

Codes on structural glass seem to develop slowly and with difficulty. The European prEN13474 has been withdrawn. Under this point, the interviewer would like to discuss the requirements for a new code or guideline. What should be in it and what should not?

Furthermore, it seems a sound 'basis for design' is needed, but what should such a document contain?

Ad 6: Past and future developments

Developments in structural glass have started some 30 years ago. At this point, the interviewer would like to discuss if the interviewee has noticed significant changes in the way the issues of structural glass and safety are approached. Furthermore, it will be interesting to discuss what developments may or should lie ahead.

Ad 7: Possible other issues raised by the interviewee

Besides the possibility of introducing an issue to the discussion at any time, the interviewee will be asked specifically if there are any other issues that should be discussed before rounding up.

Ad 8: Conclusion

The interviewer will summarize the discussion and draw some conclusions (if possible).

2. Report of the Interview with Rob Nijse

Interviewee: prof. ir. Rob Nijse (RN); Interviewer: ir. F.P. Bos (FB); Date & time: Thursday, July 26th, 2007, 14:00-15:20 hrs.¹

2.1. Introduction by Interviewer

FB starts the interview with a short introduction, giving the reasons for keeping this interview (see explanatory notes to the interview).

2.2. Background and Experience of the Interviewee

RN's profession is structural engineer. He graduated at the Civil Engineering Faculty of the TU Delft, at the department of 'Utiliteitsbouw'. Furthermore, he is director and partner of the engineering firm ABT and professor in structural engineering at the TU Delft Faculty of Architecture.

2.3. Experiences with Structural Glass and General Safety Issues

His experience with structural glass started when he was asked to act as a structural engineer for the temporary Sonsbeek pavilion (1986) by architect Benthem & Crouwel, in which pieces of art were to be displayed. This essentially stretched box contained glass columns, glass walls and a glass roof. At that time, there were several pioneering projects going on with structural glass. Most notable were the hanging glass façades which Peter Rice was working on and glass façades supported by glass fins of the Willis Faber Dumas building and the Sainsbury Centre. These developments were made possible by the development of affordable laminating techniques. Laminated glass provided the necessary redundancy to create safe structures. RN kept to the principle that one sheet of glass should be able to break without collapse.

In the mid-1980's there was very little information available on the strength of glass (for the structural calculations). Inquiries at major glass manufacturers yielded little result. A limited amount of available test data indicated a tensile strength of approximately 40 MPa. RN used a safety factor of 5 over that value to obtain the maximum design strength for the glass.

The first glass beams by his firm (ABT) were realized in the ING Vastgoed-office building in Budapest, Hungary in the early 1990's (architect: Mecanoo). They consisted of three layers of glass with a span of approximately 4 m. The outer ones were annealed, the inner one thermally toughened. The outer sheets were also thinner than the inner one; their function is to protect the inner, load carrying sheet. The beams were

¹ Because of the open character of the interview, it did not strictly follow the lines of the agenda that was set out, and therefore neither does this report. Nevertheless, most subjects on the agenda have been covered. This applies to all interviews.

supported by point fixings, but the holes in the outer sheets were oversized, so that only the inner sheet is load carrying.

The beams were manufactured and mounted by the Belgian firm Portal. Prototypes were tested in direct bending tests (i.e. loaded in a bending test at moderate speed until failure) at the Free University of Brussels, Belgium. According to the design, the outer sheets would transfer the loads in case of failure of the inner pane. This situation, however, has not been experimentally tested. As with the Sonsbeek pavilion, a safety factor of 5 was applied to the load carrying inner sheet.

The subsequent structural glass projects continued on this theme; always laminating is used to provide redundancy. In practice, the discussion arose which type of glass was safer to use: annealed or thermally toughened. This discussion still has not subsided completely today, but RN's conclusion was that in principle annealed should be applied because of its favourable cracking pattern (provided the edge quality is excellent and the holes have been polished), unless use is made of bolt hole connections or when, for whatever reason, high stress levels occur. The stress concentrations around those holes call for thermally toughened glass.

2.3.1. Experiences with failure cases

One of the most important lessons RN has learned over the years was the key role a careful manufacturing and mounting process plays. In one project, all 2-layer laminate beams broke during mounting. The annealed glass beams were centrally supported and cantilevering on two sides. Although the beams themselves were not supported with bolt hole joints, there were bolt holes in the top of the beam to connect the glass roof. The beams broke through the holes in the middle, where the tensile stresses are in the top of the beam, and thus around the bolt holes. This need not have been a problem, but inspection of the failed beams showed that the inside edges in the hole had not been polished and that the holes had been drilled from two sides, resulting in misalignment. Together, these defects caused catastrophic stress concentrations.

A comprehensive safety approach should therefore pay specific attention to manufacturing, handling, transport and mounting in order to avoid premature failures. Unfortunately, quality improving treatments such as polishing are still not a matter of course.

RN has had no experiences with inexplicable (mysterious) failures. Relatively common failures are thermal stress breakage or breakage caused by damage to the glass. Another situation on which RN is increasingly alert, is the combination of glass and free flowing water. This can occur, off course, in outdoor situations but also with cleaning. Water collected in scratches in the glass is also a common failure cause. The cleaning process itself can also be a cause of failure due to scratching. Cleaning in general decreases the long term glass strength.

Another failure occurred in the glass wall of an aquarium in a large zoo in the Netherlands. The cause was suspected to be cleaning with scourers (to remove algae), in combination with the salt water, high water pressure and high water temperature of approximately 30 °C.

For glass creep, or the idea that glass is not a solid but actually a highly viscous fluid (a popular myth), RN has not found any evidence over the years, either from scientific research or practical experience. The reduction of glass strength over the years is primarily caused by accrued damage and the influence of water.

From a safety point of view, the development of heat strengthened glass, the use of which became common from the mid 1990's onward, was an important improvement as it combined a relatively high impact resistance with a favourable cracking pattern. RN has used heat strengthened glass in many projects, especially for balustrades. In his experience, the level of prestress may indeed vary between 30 and 70% of thermally toughened glass, but even at 70% prestress the cracking pattern is still more similar to that of annealed glass than to that of thermally toughened glass. Somewhere around 80% of prestress there is a quite sudden transition to the typical dice pattern of thermally tempered glass. Off course, the level of prestress can be checked by polarized light. Glass manufacturers are increasingly able to control the tempering process and it is now possible to order glass thermally prestressed to a custom level from Saint Gobain.

2.3.2. General premises and project specific parameters

Perhaps surprisingly, minimizing a glass structure often is not a goal set by the architect. Most architects want a glass structure to be transparent, but not invisible. Therefore, structural glass members usually have a certain massiveness, which is also desirable from a structural point of view, because it provides some robustness. This can also be favourable to the mounting process, because large glass sheets (used in glass stairs for example) tend to sway considerably which increases the risk of failure incidents during handling and makes mounting more difficult.

RN nowadays advises contractors that are building glass structures, to start out with a wooden 1:1 scale prototype on site. This can bring all kinds of unexpected problems to light at a stage in which it is still easy to adapt the design and thus avoid costly delays and damage/glass breakage. In a project of a glass staircase in Amsterdam, this method has proved extremely insightful.

In general, when getting started on a structural glass project, the first thing RN considers is the size of glass components. Basically the structure is cut in pieces with a size dictated by the available maximum size of laminated glass for that project. Although there are developments towards sizes of 10 m length, approximately 4.5 m is still a common maximum size that can be delivered by an average glass laminator. The actual design of the structure starts after this cutting up, with determining loads, designing joints, etc.

2.3.3. Residual strength, load and time requirements

Contrary to a result of the structural glass survey, RN feels there are actually not many project specific parameters with regard to the safety design of a glass structure. He uses an approach quite similar in all projects, which amounts to:

- Applying a material partial factor of 1.8 for short term loads (resulting in a design stress of approximately 25 MPa), and maintaining a design stress of approximately 8 MPa for long term loads. RN is quite satisfied with the present NEN 2608-2 which by and large is along the lines he usually works. It contains a clear glass strength formula which takes all important aspects into account.

- Using laminated glass to provide residual strength. RN usually considers the possibility of one sheet breaking at any time, or two outer ones if there is risk of vandalism. The remaining sheet(s) should be able keep transferring loads. RN does not specify a particular length of time for this residual strength requirement.

A consideration that is project specific is the chance of damage to the glass. What RN particularly looks for in his structural glass designs is where critical zones of tensile stress may coincide with elevated risk of damage. For instance, a multi-field glass floor plate would have zones of high tensile stress in the top sheet above the middle supports. This may be a particularly dangerous combination with small sharp stones in the soles of shoes of people walking over these floors. But apart from such considerations, the safety design is not very project dependent.

According to RN, the residual strength of the structural glass component should be sufficient to carry the load on an arbitrary point in time (Dutch: *momentaanbelasting*) multiplied by a safety factor of 1.1. In cases where the arbitrary point in time factor according to Dutch codes equals 0 (like wind, rain, snow or variable loads by persons on a roof), RN picks a reasonable strength requirement himself, based on experience. This is usually around 25% of the serviceability limit state. Requiring a significantly higher residual strength, for instance equal to the serviceability limit state, he considers excessive in most cases.

2.4. Codes and Guidelines

The recently published NEN 2608-2² is quite satisfactory to RN. It does not contain requirements with regard to residual strength, but RN notices that the discussions on how to define and quantify this are new to the field of structural engineering in general, also in relation to common structural materials such as steel and reinforced concrete. For now, providing sufficient residual strength is up to the individual engineer. Nevertheless, the issue of how to define and quantify residual strength requirements is an interesting one and one of the new challenges for structural designers, together with the susceptibility of structures to terrorist attacks. RN feels this should also become a design criterium in the future.

Although RN recognizes that codes may suffocate innovations (the absence of strict building codes in Hungary in the early 1990's was actually helpful in getting the roof with glass beams realized), this should not be an excuse not to develop them. Rather, it should be an incentive for the profession to formulate codes in a clever way, so that they provide useful rules without blocking innovation.

² Nederlands Normalisatie Instituut, *NEN 2608-1: Glass in building - Resistance against windload - Requirements and determination method*, Delft, the Netherlands, 1997; and: *NEN 2608-2: Vlakglas voor gebouwen - Deel 2: Niet-verticaal geplaatst glas - Weerstand tegen eigen gewicht, wind- en sneeuwbelasting en isochore druk - Eisen en bepalingmethode*, Delft, the Netherlands, 2007. A new preliminary version of the NEN 2608 is planned for publication around September 2009. It will combine and replace the earlier parts 1 and 2. The new NEN 2608 will include further requirements with regard to residual resistance and fracture mode. As such it will also replace much of NEN 3569.

2.5. Future Developments

A development RN would really applaud is improving the glass composition and manufacturing process to make it more suitable for structural applications. Compare window glass to an average glass ovenproof plate, for instance. The difference in fire resistance is incredible. From a fire safety point of view, we should be using borosilicate glass instead of soda lime. RN also expects improvements in the manufacturing and handling process could significantly decrease the number of surface defects in glass, and thus avoid premature failure. It is, however, questionable to what extent such developments are likely to happen – even though they are desirable. It would require a lot of commitment from large glass manufacturing companies and RN does not see this happening anytime soon, as it is uncertain if that would increase their profit.

Another development mentioned by RN is the increased use of curved glass in structural applications. He is currently working on a project with glass walls from corrugated sheet. The large waves, with a centre distance of some 1800 mm, provide enough out of plane stiffness.

2.6. Conclusion

Careful manufacturing, transport, mounting and detailing are key aspects in avoiding glass failures which are frequently overlooked. Nevertheless, structural glass engineering has come a long way since RN's first projects in the mid-1980's. 'At that time you were practically declared certifiable if you wanted to use glass as a structural material'. Fortunately, those days are long gone.

3. Report of the Interview with Graham Dodd

Interviewee: Graham Dodd (GD); Interviewer: Freek Bos (FB); Date & time: Wednesday, August 8th, 2007, 15:50-16:30 hrs.

3.1. Introduction by Interviewer

FB starts the interview with a short introduction, giving the reasons for keeping this interview (see explanatory notes to the interview).

3.2. Background and Experience of the Interviewee

GD studied engineering science at Liverpool University. Chartered as a mechanical engineer, he started his professional career in household product engineering. He consequently worked at a material selection consultancy before moving to Pilkington Glass in 1988. There, he became the 'nuts and bolts' man, working on the design of point-fixed glazing. In the end, he was responsible for the design team for the Pilkington Planar system. In 1994 he left Pilkington to join Arup's Façade Engineering Group, and he is now Design Leader of Arup Materials Consulting. Despite having no education in architecture or structural engineering, GD now has almost 20 years of experience in structural glass and building façades.

3.3. Experiences with Structural Glass and General Safety Issues

At Pilkington, GD did his first glass projects. These included the skylight of the BBC television centre (double-glazed units supported by a tension rod system), a façade

supported by large glass fins at Bordeaux airport and the glass roof of the Birmingham Convention Centre.

A cantilevering, point supported glass canopy at the entrance of the Beyerle Art Museum in Switzerland was one of his first glass projects for Arup. Since the end glass plate of the canopy is cantilevering in two directions, the challenge here was to prevent it from falling down in case of glass breakage. This was resolved by applying a laminate plate with a 12 mm thick thermally tempered layer underneath a 6 mm thick heat strengthened top layer. The thickness ratio between both plates results in the lower sheet carrying most of the loads in normal conditions. Should the bottom layer break, it can still transfer significant compressive forces, while the top sheet will carry the tensile loads. This has been proven in experiments showing that such a damaged plate could still carry the required snow load. In case of both layers breaking, fold lines may occur in the laminate, but the stepped friction joint design (friction is applied to each layer separately) ensures that the plate will not sag out of its fixings. Through the friction joint design, peak stresses along the edge of the hole are also avoided.

3.3.1. General Approach to Safety in Structural Glass Projects

In the Beyerle Art Museum project, GD had specific requirements set for each stage of failure. These requirements were defined in terms of residual strength required for a certain period of time, at different stages of failure. This is exemplary for his approach to safety of structural glass in general. First, the post-failure requirements are set. Consequently, an experimental testing procedure and fail/pass criteria are defined. This precedes the structural and detail design. When asked, GD agrees that few glass engineers seem to follow such an explicit approach. It not only forces the engineer to think about the kind of behavior he expects from a glass structure, but also acts as a clear performance reference in discussions with the (sub-)contractor responsible for building the structure.

The value of this is illustrated by the National Glass Centre in Sunderland. It features a 1000 m² glass roof over a glass production facility. The roof is accessible to the public from the street (as the building is on a slope, the roof on one end of the building is at street level). Arup initially suggested four side supported glass panels consisting of three layers of 10 mm heat strengthened glass. The contractor however, wanted to use 8 mm thick glass, and proposed a 3x8 mm laminate instead. Arup found this to be insufficient and suggested to use 4x8 mm panels. The issue was resolved by testing both proposals according to the prescribed testing method (involving multiple hard body impacts), to find if the construction would meet the preset residual strength criteria. Since one of the three 3x8 mm specimens failed prematurely, that construction failed the test. All three 4x8 mm specimens on the other hand, passed the test, leaving no room for discussion as to which design should be applied.

Being completed in 1996, GD reckons this is the first glass floor making use of heat strengthened glass. The reason for not using annealed was the risk of thermal cracking which may occur when part of the roof would remain cool because of an object accidentally placed on it.

The flying saucer project 'Big Blue' at Canary Wharf by sculptor Ron Arad, was met with the same explicit approach. It features a huge glass fiber reinforced shell supported

by a 7 m diameter circular glass wall. The saucer hovers over an underground shopping mall. The 12 wall panels consist of 2x15 mm thermally tempered glass. In this case there was no disagreement with the contractor and given the extensive glass experience of the engineers, experimental testing was restricted to tensile tests of bearing connections in samples of toughened glass. Although several panels have been damaged over the years, none of them have collapsed

The procedure to arrive at the performance requirements is as follows:

1. First, the issues defined by codes (most notably actions on the structure) are inventoried.
2. This is followed by a process of thinking through different scenarios that may occur and cause damage. There is a wide range of scenarios thinkable. Some common considerations may include someone dropping a toolbox, vandalism or NiS inclusions. For the Big Blue project, a runaway lawnmower was a specific possibility while AK47 gun fire (either accidental or purposeful) was certainly not unthinkable for the glass walls of the 300 m high panorama bridge of the Kingdom Centre in Riyadh.
3. Finally, the requirements and testing procedures are defined based on the results from step 1 and 2.

3.3.2. Consistency

Using an explicit safety approach helps maintaining a consistent safety level in different projects, which according to GD is very important. People should not be exposed to unnecessary risk. However, the nature of step 2 makes it difficult even in an explicit approach, to maintain consistency. Generally speaking, an engineer should consider the design options and the risks related to a project and consequently analyze which risks can reasonably be eliminated (or minimized). Through the CDM (Construction Design Management) regulations, engineers in the UK are obliged by law to perform a risk assessment. This results in a fairly consistent approach to safety, provided a constant professional attitude is maintained.

With some 150 Arup engineers working on façades world wide, this is relatively difficult. Two basic policies are communicated throughout Arup Façade Engineering. First of all, you have to assume that any piece of glass may break one day. In laminated glass, GD is always suspicious of designs relying on at least one layer remaining in tact, although he recognizes that it is sometimes inevitable (e.g. in aquarium design). Rather, you should always reckon with the (perhaps slight) possibility of all layers breaking, although your performance requirements at such a stage may be light. Secondly, thermally tempered glass falling on a person after breakage presents a significant safety hazard. The idea that the small fragments are not harmful is outdated.

3.4. Codes and Guidelines

Obtaining a consistent approach to structural glass safety by different engineers in different projects would be a distinct advantage of developing common rules. However, because there are such big differences in projects, it is unlikely that such rules could be prescriptive codes. Furthermore, simply following codes does not provide safety – one of the reasons to develop the CDM regulations. Rather, such rules should be guidelines on what is reasonable and at what point residual risk is acceptable.

One of the difficulties that will come up in such a guide is that safety can be obtained at different levels. You could use a material with inherently safe failure behaviour, but you could also provide safety through structural measures (i.e. providing alternative load paths). FB argues that both will be needed to some extent (even steel can fail in a brittle manner), but with structural glass, the emphasis is more likely to be on providing structural measures as it is difficult to obtain inherently safe failure behaviour from a glass member alone. GD agrees.

Another advantage of the development of codes or guidelines may be that it will ease the commercial pressure by contractors on engineers to approve of minimal designs. Avoiding erosion of the safety of a design is one of the main reasons for Arup to provide such specifications, including testing specifications (which are not always actually invoked).

At the moment, the UK is well behind other countries in the development of codes for structural applications of glass. It is still allowed to use single sheet thermally tempered glass as a fall through barrier, something not accepted in most neighbouring European countries and indeed not accepted by Arup. However, the fact that it is allowed by the codes can give rise to extensive discussions with contractors. Generally however, the idea held in the past that thermally tempered glass practically could not break and could therefore be used in single sheet solutions, has given way. It should also be remembered this view was held in a time it was still very difficult to laminate tempered glass.

Glass floors is another subject not yet covered by the codes. While this is liberating in the sense that the absence of such a code gives intellectual freedom to design as the engineer sees fit instead of just blindly following what is in the codes, it off course also provides a risk.

3.5. Future Developments

Stimulated by the steadily increasing number of realized structural glass projects, more and more engineers enter the field of structural glass. This poses an increasing risk of faulty copies. Especially structural measures applied to provide safety may not necessarily be obvious. Copies may therefore miss the point of the original structure. Structural glass engineering is going through a dangerous phase. It has passed the initial pioneering stage in which the pioneers had to be extremely careful and thorough because nobody yet knew how to do it, but has not yet arrived at the point were all difficulties of glass are generally understood and laid down in guidelines or codes.

3.6. Other Subjects

Confronted with one of the prime points made by Rob Nijse in a previous interview in this series, namely that their should be a lot of attention for handling, transport, mounting etc because a lot of failure could be avoided this way, GD agrees wholeheartedly. But it should also be realized that you simply can not banish errors being made. Besides accidental mistakes, errors can be caused by financial and/or time pressure, lack of communication or just ignorance. ‘What happens if it is built the wrong way?’ is therefore one of the scenarios you have to design for.

GD gives an example of a failure case caused by somebody replacing a polymer bush in a point fixing by the cap of a soda bottle. In another case, a glass panel designed to be

hung from a point fixing, was supported by glass setting blocks at the bottom side instead, because the right bolt size for the point fixing was temporarily unavailable at the building site. An important way to minimize such errors is to design less complex and more tolerant constructions.

3.7. Conclusion

By specifying performance criteria for different stages of glass failure as well as providing rules for experimental testing, an acceptable and fairly constant safety level can be obtained in each project. This method provides a clear reference in discussion with contractors and other parties and stimulates active thought about possible failure causes and the required reaction of the structure.

4. Report of the Interview with Tim Macfarlane

Interviewee: Tim Macfarlane (TM); Interviewer: Freek Bos (FB); Date & time: Thursday, August 9th, 2007, 9:30-11:30 hrs.

4.1. Introduction by Interviewer

FB starts the interview with a short introduction, giving the reasons for conducting this interview (see explanatory notes to the interview).

4.2. Background and Experience of the Interviewee

TM graduated from Strathclyde University, Glasgow, as a civil engineer. He has worked in two different consulting practices in London doing conventional projects, before starting his own firm in 1981. In 1985 he teamed up with Laurence Dewhurst to form a partnership which he has headed up until this day.

At university, TM already came into contact with structural glass. His graduation project was on glass fibre reinforced structures. From J. Gordon's *The new science of strong materials*, which, among other things, discusses glass as a structural material, he learned of the inherent strength of glass, being much higher than that of steel. At the same time, a friend of his graduating in architecture wanted to know if it was possible to use glass columns in his design. At the time, that was still a far-fetched idea, but both introductions to glass kept playing in the back of TM's head.

4.3. Experiences with Structural Glass and General Safety Issues

In the second half of the 1980's, TM first became involved in structural glass. After having built a name as an architect-friendly structural engineering firm, TM came in contact with Eva Jiricna. The Joseph Shop glass staircase in Sloane Street, London, built in 1990, was the first in a series of over 30 glass staircases they did together. This staircase was the first project in which TM actively had to think about what would happen in case of glass failure. To provide a safe failure mechanism, the treads consisted of 19 mm annealed float glass which acts as the load carrying sheet, and a 15 mm clear acrylic layer underneath, serving as a back-up provision in case of glass breakage. Using a thick annealed glass had the distinct advantage that failure would likely result in a single crack developing through the glass sheet. Therefore, the risk of loose shards flying around was limited and there was no need to laminate both sheets together. Since the large difference in thermal expansion coefficient could furthermore cause difficulty with laminating, it was omitted.

The tread bending stiffness was governing in determining the dimensions. Thus the higher tensile strength of thermally tempered glass could not have been used anyway. From an aesthetic point of view, annealed glass also has advantages. It has a better appearance and can be polished and sand-blasted to give an anti-slip grip. The sand-blasting may cause scratching and chipping of the glass but those problems are all underpinned by the fail safe mechanism. Actually, only one tread in all these stairs has ever broken, and it did so in exactly the way predicted: by a crack through the middle, and the acrylic taking the loads.

4.3.1. Glass strength

At the time, it was very difficult to obtain data with regard to the glass strength that could be used in the structural analysis. TM ended up using a figure of 7 N/mm^2 for long-term loading, based on a mean value of approximately 70 N/mm^2 he found in *Mark's Handbook*, an engineering handbook from 1941, divided by rather arbitrary safety factor of 10 (which TM aptly dubbed the ignorance factor). Later, TM came across the *Glass Engineering Handbook* (2nd edition 1958 by E.B. Shand), which features a glass strength versus time graph. According to that book, a 3 s load gives a 70 N/mm^2 mean failure stress. The hyperbolic strength graph rapidly decreases to a lower bound limit of approximately 40 N/mm^2 . TM increased the calculable stress figure to 13 N/mm^2 when designing the beam elements for the Keats Grove Conservatory in 1992, arguing the increased failure probability was reasonable because of the safe failure mechanisms built into his structural glass designs.

A consequent structural glass project was a large glass floor, on the external frontage of Now and Zen's restaurant on St. Marlines lane (London). The design uniformly distributed load was 5 kN/m^2 . For several reasons, TM opted for a $2 \times 19 \text{ mm}$ annealed glass laminate. This was cheaper and stiffer than a glass-acrylic combination. Using a calculable stress of 7 N/mm^2 , each individual sheet could take the calculable load. Again, the cracking pattern of annealed glass was considered an important advantage over thermally tempered glass. Even in case of both sheets breaking, the cracks are unlikely to be completely aligned, and thus considerable residual strength should remain by residual action between the laminated, broken sheets.

At a later stage, TM got involved in larger span staircases (i.e. those of the Apple flagship stores in New York and other major cities in the USA). There, he had to start using laminated glass to provide sufficient stiffness. This obviated the need for an acrylic underlayer, as the annealed glass laminate provides sufficient residual strength. Using annealed glass allowed the edges to be polished after lamination. The completely smooth edge thus obtained, could not have been produced with thermally treated glass.

Concluding, it is TM's opinion that for floors and stairs, annealed glass provides a good relation between strength, stiffness and cracking pattern, and there is no reason to do otherwise.

The extension of a private house in Keats Grove, Hampstead, in 1992, was TM's first project with glass beams and columns. The insulated glass panels, which had glass edge spacers instead of aluminium, were made by the German company Hahn Glas. Here, TM specified the beams to consist of three layers of thermally tempered glass, which

each individual layer capable of carrying the design load. This was deemed necessary because the beams were supported on one side by point fixings through drilled holes which were not polished on the inside edge. However, when inspecting on site, TM encountered a small crack in one of the beams. In thermally tempered glass this should not be possible. So, TM confronted the contractor who admitted he had not had enough time to have the beams tempered, but he thought it would be all right to use annealed glass. TM then redid the calculations to be sure the stresses around the hole would not exceed admissible values. To evaluate stresses around holes, TM uses the rule of thumb that the highest peak stress will be approximately 3 times the general stress at the bearing based on the bearing load. Thus the allowable long term general stress at the bearing would be $13:3 \approx 4.4 \text{ N/mm}^2$. The structure met this requirement, so TM and the contractor agreed that the latter could install the annealed glass beams, provided he would take responsibility in case of failure. Fortunately, the beams have been problem free for the last 15 years.

One of the best known structural glass projects by TM is the canopy over the Yurakucho subway entrance in Tokyo, built in 1996. This was the first project for which TM did extensive experimental testing. Initially, the failure load for the bearing holes was determined by crudely testing a small sample in a simple loading frame. Since the client had a considerable budget, simple tensile tests were consequently executed as well as a full scale prototype test. Although the bearing holes were relatively close to the edge (about 1.5t, with t being 19 mm, whereas the hole diameter d was 40 mm, thus approximately twice t), this did not induce premature failure. To the tempered glass laminate, acrylic sheets were added, as requested by the client although TM did not feel this was necessary. No failures have occurred.

4.3.2. *Thermally tempered glass*

In a previous interview with Graham Dodd, it came up that according to UK codes, it is still acceptable to use single layer thermally tempered glass as fall-through proof barriers (e.g. as external floor to floor glazing in high rise buildings, without handrails). When asked, TM notes that there are still companies wanting to use single sheet tempered glass, but that it is a flawed idea of safety. In the first place, it is certainly not unbreakable and it disintegrates completely upon failure, thus providing no residual strength whatsoever (whereas the large shards of an annealed glass sheet may still be able to transfer some loads to its supports). Furthermore, having broken tempered glass falling on someone's head is not ok. It may be less dangerous than the large shards into which annealed glass breaks, but it can still cause serious injury and should therefore not be relied upon.

4.3.3. *Design procedure and consistency*

TM's working method on a structural glass project is quite straight forward. Basically, it comes down to 'doing the numbers' (i.e. calculating loads and stresses) and, for the safety aspect, consider what can go wrong and adjust the design so that those situations will not cause damage or injury. This method requires acute awareness of general engineering principles and a responsible attitude.

TM does not specify specific safety requirements beforehand, as this would lead to general statements that may not be relevant to a particular design problem. The question of residual strength depends to a great degree on project specific factors, for instance the structural nature of the element, if it is a floor, a roof beam, etc. TM has never had

problems with contractors wanting to alter the glass design in a way he could not agree with from a safety point of view. He reckons this maybe due to the fact that he usually works on small projects with genuinely interested firms with whom he develops solutions in open discussion.

As a result, there is no quantitative consistency in the safety of TM's structural glass projects, other than that resulting from maintaining a consistent attitude. Basically, there is no consistency in different scenarios, but this is not necessarily a problem because in daily life you are constantly subjected to varying levels of risk. Furthermore, safety thinking develops as you go along and is therefore not consistent. The general problem in providing safety is that there are always 'unknown unknowns' (i.e. unpredictable situations you can not even imagine). Thus, a universal equation for safety is impossible. Because of the unknown unknowns, the basic attitude should be 'assume that any piece of glass may break'. When that happens, the structure should not fall down. Furthermore, the broken glass must be replaceable and the failure should not bankrupt the client (so there are other issues besides safety which make it important to limit the consequences of failure).

4.4. Codes and Guidelines

The principle goal of a structural glass code should be to provide a common set of numbers (most notably strength) to design by. Furthermore, it should describe general principles and minimal requirements for safety.

4.5. Future Developments

TM feels the development of ionomer interlayers like SG can be helpful to provide safe failure behaviour. Furthermore it will allow using the full glass thickness in calculations, rather than separate layers.

Using laser jet cutting for holes is another development TM would like to try in future projects because of the enhanced cut surface quality.

4.6. Conclusion

The key to a safe structural glass design is a conscious attitude towards failure possibilities and providing safe failure behaviour, because there may always be unexpected failure causes.

5. Report of the Interview with Holger Techen

Interviewee: Prof. dr.-ing. Holger Techen (HT); **Interviewer:** Freek Bos (FB); **Date & time:** Wednesday, August 22nd, 2007, 17:10-18:30 hrs.

5.1. Introduction by Interviewer

FB starts the interview with a short introduction, giving the reasons for keeping this interview (see explanatory notes to the interview).

5.2. Background and Experience of the Interviewee

HT graduated from the TU Darmstadt as a structural engineer in 1989, on a study on ductility improvement of glass by gluing fabrics on it. Thus, HT came into contact with glass early in his career. He consequently worked at the structural engineering firm

König und Heunisch, where he was a colleague of prof. Wörner, with whom he had done his graduation project. During that time he was also a representative for the institute of 'Konstruktiver Glasbau' in Gelsenkirchen, a knowledge centre to which different companies turned with all kinds of questions regarding glass design, calculation and properties. HT was first confronted with the issue of the problems concerning glass failure and safety when working on the trade hall glass roof in Leipzig.

HT then returned to the TU Darmstadt to do his PhD on bolted joints and other glass connections, again under prof. Wörner. Together they explored the vast range of research questions concerning structural glass and produced some early guidelines. A lot of the consequent PhD research at the TU Darmstadt focused on the various research topics that came up during that time, such as PVB interlayers, resins, etc. One of HT's students was Jens Schneider, who filled his position as research assistant after HT had finished his PhD. They did a lot of work on point fixings together.

After his promotion, HT first worked for an engineering firm in Hamburg before switching to Bollinger Grohmann in Frankfurt a.M., where he worked on different glass structures. His latest structural glass project with B+G was the new Nordkettebahn stations in Innsbruck (arch. Zaha Hadid), featuring double curved, single sheet annealed glass glued to the support structure by PU.

5.3. Experiences with Structural Glass and General Safety Issues

5.3.1. General premises

Generally, a structural glass project starts with discussions with the architect on matters such as glass size, façade grid, type of fixing (point supported, line supported), etc. All these points are discussed before, in an iterative process, working to a solution, first for the overall situation and then step wise to detailed solutions. To obtain an optimal result, close cooperation between the architect, structural engineer and façade engineer is of paramount importance.

Based on his experience with experimental testing of glass, there are two points HT always keeps in mind in a structural glass project. One is the protection of the edges of glass sheets, because most failures originate there. The other is the flexibility of glass. Due to the relatively small thickness of large sheets of glass (compared to their length and width), they can actually behave very wobbly. Therefore, HT prefers not to use glass with a thickness < 8 mm. Such thin sheets are too sensible to forced deformations and possess little robustness. Forced deformations are something to watch out for in any case. HT has never heard of glass structures failing from stresses in the bolt holes, but always from the inability of the glass to accommodate forced deformations.

HT is most comfortable with using 8 – 15 mm thick glass. Thicker glass (19 mm) has a number of disadvantages. From experiments conducted together with Jens Schneider, HT knows 19 mm thermally tempered or heat strengthened glass contains so much energy that it will explode upon breakage, which is rather unsafe. It is also expensive (prices are not linear with thickness). Furthermore, sheets of this thickness tend to be very heavy (depending off course on the other dimensions as well). This makes them difficult to handle during construction (thus they get damaged quite easily) and hard to

replace. It is HT's experience that damaged glass which is hard to replace is often just left in place, which is a cause for future failures.

5.3.2. Time requirements

The time a broken glass pane should be able to remain in place, should depend on the usage of the structure (public space, company, private) but also on the level of maintenance. HT illustrated this with two examples. The first was a glass canopy, across the street from his office while he was working in Hamburg. It was in front of a store being supplied by trucks approximately every 3 weeks. Glass panes got damaged almost on a regular basis by trucks hitting the edge of the glass, but the panes were always replaced within a day or two. The other was a parking garage in Dresden with a glass entrance, which was hardly maintained at all. HT encountered a broken glass pane there, but never saw any action to have it replaced. It may still be there.

In an enactment of the Hessisches Ministerium für Wirtschaft, Verkehr und Landesentwicklung³, it is specified that overhead glazing under certain loads must remain in place after breakage for:

- 30 minutes, if the area underneath the glass not accessible or
- 24 hrs, if the area underneath is accessible.

5.3.3. Load requirements

There is much discussion on what loads should be designed for in a failed state (how high should the residual strength be?). HT's personal view is that only small loads need to be reckoned with. The failure will usually be discovered quickly, so it is unlikely high loads will occur during the failed state. Again, this should also be dependent on the level of maintenance.

The number of layers that may be broken is, for a large part, dependent on the question if the edge is protected. If it is not protected, then two sheets may very well break simultaneously upon impact on the edge. However, if it is protected, it may be highly unlikely both sheets break. Project testing for a glass roof (\pm 2001) required a steel ball drop test on the glazing. The test specifications required residual strength of the glass in case it would break, but no residual strength if the glazing would survive the ball drop tests without breakage.

5.3.4. Annealed, Heat Strengthened and Thermally Tempered glass

The type of glass (annealed/heat strengthened/thermally tempered) to be used really depends on the project specifics. In balustrades, HT prefers thermally tempered glass with protected edges, because of the high impact resistance. But, along with previous interviewees Graham Dodd and Tim Macfarlane, HT agrees the classical safety philosophy of thermally tempered glass ('the shards are so small they will not hurt you') is absolutely mistaken. For a green house project, HT has done experiments with puppets covered with leather, situated beneath a heavily tempered (150 MPa) 4 mm thick glass pane, and then break the glass. The test showed the glass falls down in large pieces which only break into small ones upon hitting an object (i.e. the puppets). The leather skin was punctured numerous times.

³ Hessisches Ministerium für Wirtschaft, Verkehr und Landesentwicklung, *Anwendung nicht geregelter Bauarten §20 der Hessischen Bauordnung (HBO) im Bereich der Glaskonstruktionen*, VII 2-2 – 64 b 16/01 – 8/2003, 17. Januar 2003. (erlass-hessen-17.01-2003.pdf)

For overhead glazing, heat strengthened glass is the best choice because of its combination of impact resistance and cracking pattern (resulting in residual strength). In both situations, the glass would also have to be laminated. Annealed glass could be used in the lower part of façades, or in the load carrying layers of glass floor panels (with the top layer being tempered).

Consistency in all projects should be obtained by brainstorming for failure scenarios in each project. Nonetheless, you can never be sure you do not overlook something and there will always be a remaining risk. Also, it is not always feasible to design for every scenario you can think of. Far-fetched scenarios should be discussed with the client, so he can decide if he wants his structure designed for it.

5.4. Codes and Guidelines

For structural glass, it is essential not to ‘think’ in codes, and not to blindly follow the rules that may be in them. Rather, for the safety it is important to think in terms of scenarios: what may happen that can damage the glass, to what extent? Consequently the structure should be designed in a way that there will be no catastrophic consequences to such a scenario. Thinking in terms of scenarios requires an active, open mind. Many clients and authorities just hold on to regulations, slowing down innovations. A serious drawback of codes is that they are adjusted to low-quality companies (even they should be able to meet the code requirements), partly because they are drawn up by companies from practice. Effectively, this makes it very difficult for high-quality companies realize profit from their quality.

Thus, glass codes are desirable to the extent that they deal with standard problems. For innovative structures, they should provide a hand hold (e.g. for stress checking, etc) without blocking an open-minded approach. It should not regulate everything in detail.

To HT, the Swiss codes are a good example. They are limited in size and place a lot of responsibility at the engineer. This allows for innovative structures. In France, however, the situation is rather the opposite. Being anxious about everything which is not in the codes has resulted in a lack of structural glass innovations.

5.5. Past and Future Developments

Several changes have occurred in structural glass engineering over the years, some of which are still developing:

- Calculation methods have improved significantly, especially for (FE) modelling of glass.
- Glass is increasingly used for stability of façades and structures. The main problem there is the load transition from one plane to another.
- More interlayers, such as SG, have become available, increasing the flexibility of the designer.

For the future, HT would like to see more developments in the field of joints, especially adhesive connections. HT feels this method would do most justice to the material properties of glass, although he recognizes such joints require a high level of quality control to guarantee reliability. Another main problem of adhesive glass joints though,

is the difference in thermal expansion coefficients. In his opinion this problem, which he already encountered during his graduation project, is still not solved satisfactorily. The result may be that glass breaks when you put a glass-adhesive joint through temperature cycles.

5.6. Further Subjects

Perhaps not very obvious, but glass in interior partitioning walls (as in offices or shopping malls) pose a specific risk when the glass panes are close together but not silicone joined. When a person leans on one pane, a gap between that pane and the next emerges. If somebody (e.g. a child) puts his fingers in, they could be snapped off when the pane recovers its original shape. Accidents like these actually happen, and underline the importance of active thinking about the risks of structures and constructions. However, a code should not be so detailed as to handle this kind of problems. Rather, it is important that such accidents are communicated clearly throughout the building industry. A worked out report on glass damages and failure causes would therefore also be very useful.

5.7. Conclusion

Thinking in terms of scenarios is the single most important thing in glass engineering. This sets it apart from engineering with more common materials such as steel, for which you can suffice with 'doing' the codes. In glass engineering there are more steps in the process. Dynamic forces should be reckoned with and thought should be given as to how the damages from them may be avoided or minimized.

6. Report of the Interview with Jens Schneider

Interviewee: Prof. dr.-ing. Jens Schneider (JS); Interviewer: Freek Bos (FB); Date & time: Wednesday, August 22nd, 2007.⁴

6.1. Introduction by Interviewer

FB starts the interview with a short introduction, giving the reasons for keeping this interview (see explanatory notes to the interview).

6.2. Background and Experience of the Interviewee

Jens Schneider obtained his PhD on structural glass from the Darmstadt University of Technology in 2001. He has worked for Schlaich Bergermann und Partner, where his main working field was glass structures and structural glass.

His special fields are structural analysis and structural dynamics of glass, safety aspects, test procedures, research and development on glass structures and fittings, standards and regulations, and numerical modelling.

Schneider has written 30 publications on glass within the last 5 years and he is a Co-author of "Glasbau", a book in Springer-Verlag on glass structures. He was a professor at the FH in Frankfurt am Main, before switching to the TU Darmstadt in 2009.

⁴ The time available for this interview was limited. Therefore, not all subjects have been covered.

6.3. Experiences with Structural Glass and General Safety Issues

6.3.1. General premises

JS divides glass structures into three categories: façades, overhead glazing, and ‘special stuff’ (columns, beams, etc). Besides the category, there are basically three important issues to think of when getting started on a structural glass project. The first is sizes, which is an important parameter in the structural system and connections. Second is thickness (stress check) and third are safety issues. A safe structure needs to provide redundancy. This means that the local failure of one component should not lead to collapse of the structure.

In laminated glass, it depends on the application whether or not you should consider situations with more than one layer broken. In four side supported overhead glazing, it is highly unlikely both layers will break simultaneously, thus this need not be considered. In cases where the glass edge is unprotected though, such as glass staircases, at least three layers should be used. A situation with two sheets broken should be reckoned with. Three layers broken seems a very severe condition. A paradox then arises: if you would use a 2 layer laminate, you only have to consider two layers broken, but when you use a 3 layer laminate, you have to reckon with three layers broken.

6.3.2. Time requirements

The issue of how much time a failed piece of structural glass should be able to carry a certain load is a difficult one. For stairs, JS maintains 30 minutes. For overhead glazing, the German TRÜV guideline requires 24 hrs. This seems reasonable, for one thing because it is a duration that can still reasonably be tested, without unreasonably delaying the building process. Furthermore, the critical phase is usually between 0 – 2 hrs after failure. If a structure holds a load for 24 hrs, it is likely it will also hold for 2 months.

Nevertheless, the 24 hr, although sounding reasonable, is also quite arbitrary. There is no objective justification. Furthermore, JS has noticed people have a tendency not to replace broken glass if it does not fall down quickly. Although this is, off course, not a pledge for designing structures in a way they fall down after failure, it has made JS realize this is a complicated issue.

6.3.3. Temperature requirements

JS would not require specific temperatures for residual strength. This would make experimental testing complicated and expensive. Most severe loads like snow or high wind loading coincide with low temperatures anyway. Therefore, testing at room temperature is usually already conservative because the shear modulus of laminates will increase with decreasing temperature.

Nevertheless, many German building authorities require elevated temperature testing. Those requirements are not based on codes, and may lead to ridiculous demands such as testing at 50 °C with a snow load on the glass. Another over the top requirement JS was once faced with was to consider a 25 cm layer of dust on a roof.

6.3.4. DIN 18008 and testing requirements

In the new DIN 18008⁵ code, which is being developed at the moment, more unity will be brought into testing requirements. Basically, it will require a glass structure always to be tested, unless you apply a code-defined standard solution within certain boundary conditions. Specific testing methods defining testing time, load speed and minimum number of specimens, have been defined for the sections ‘*absturz-sichernde Verglasungen*’ (fall-through safe glazing) and ‘*begehbares Glas*’ (accessible glass⁶, e.g. staircases, floors, etc.). For façades and overhead glazing, this is undesirable as it raised endless discussions on questions of safety factors and redundancy. Thus, it was agreed to just require laminated glass which breaks in larger pieces in combination with some constructional restraints. Neither has a universal testing procedure been defined, as nobody has been able to formulate a procedure which is generally applicable to all glass structures.

6.3.5. Construction

As noted by other interviewees, JS agrees that the construction of structural glass, resulting in unwanted forces in the glass, is the most pressing problem. Even if you would maintain very low stresses in the glass, you will not be protected from failures by construction errors.

6.3.6. Annealed, Heat Strengthened and Thermally Tempered glass

Annealed glass should not be used for structural applications. JS likes annealed glass for façades because the new generation soft coatings can not be applied to thermally treated glass. In a project JS did in Dubai with Schlaich Bergermann, they originally designed 10.10 laminated thermally tempered glass sheet had to be replaced by a 8.12 laminate because the desired coating was not available on 10 mm tempered glass.

Annealed glass is also much flatter than heat strengthened or thermally tempered glass. According to Luible’s PhD thesis on glass buckling⁷, the bow of an annealed glass sheet is around $1/1000 \cdot \text{length}$, while that of a strengthened or tempered sheet is typically $1/400 \cdot \text{length}$.

Heat strengthened or thermally tempered glass can be used in a façade if it is heat-soaked. If the sheets do not function as a fall-through barrier but only carry wind loads (e.g. the outside sheet of an insulated glass unit-panel), they need not be laminated.

JS is also not convinced that, because of the cracking pattern, heat strengthened glass in a reinforced beam is much better than thermally tempered glass. Experiments executed on beams for the Therme extension in Badenweiller, consisting of three layers of tempered glass reinforced and slightly prestressed by a steel cable, yielded considerable residual strength even in case all three layers were broken. Actually, local buckling of

⁵ Provisional (*Entwurf*) versions have been published of part 1 and 2:

- DIN Deutsches Institut für Normung, *DIN 18008-1:2006-03 Glas im Bauwesen – Bemessungs- und Konstruktionsregeln – Teil 1: Begriffe und allgemeine Grundlagen*, March 2006.
- DIN Deutsches Institut für Normung, *DIN 18008-2:2006-03 Glas im Bauwesen – Bemessungs- und Konstruktionsregeln – Teil 2: Linienförmig gelagerte Verglasungen*, March 2006.

⁶ In German guidelines, a distinction is made between *begehbares Glas* (generally accessible glass) and ‘*betretbares Glas*’ (incidentally accessible glass, e.g. for cleaning and maintenance).

⁷ Luible, A., *Stability of Load Carrying Elements in Glass*, Dissertation at the EPFL, Lausanne, Switzerland, 2004.

the completely broken beam was not the biggest problem. Toppling over of the complete beam was the key issue to resolve. This was independent on glass type.

6.3.7. Residual Strength and Safety Factors

When asked if JS feels that using a lower material partial factor γ_M is justified if a structural glass component has safe failure behaviour, he responds that is the core problem of laminated glass with post-breakage behaviour and how to quantify redundancy. This also has to do with the definition of what is 'safe'.

First, JS wouldn't refer to the partial safety factor of the material glass itself. Principally, a lower partial safety factor of the glass is possible, if the scattering of the material is low (e.g. the failure of glass in the hole area scatters little because the glass is already drilled and the scratches are evenly distributed and you can calculate the needed safety factor with regard to the scattering).

If you look at the composite glass - PVB - glass with a 'safe failure behaviour', one could estimate the needed safety factor of the composite (which of course will be lower than of not laminated glass). But for a quantifiable calculation you would need either:

- The load resistance of the broken glass for regular loads (e.g. snow, wind, etc.) and for a given temperature scenario which acts at the same time (e.g. like Frank Wellershoff calculated for PVB which was wind and temperature at the same time). The problem is that broken glass is seldom behaves consistently in a series of tests.
- Or the probability of irregular actions (e.g. a pistol shot, thunder storm debris, etc.), which are statistically not available.

Therefore, we maintain an engineering approach to calculate the glass as if it would have to sustain the regular loads fully (no composite) and had no post-breakage behaviour, and at the same time add some redundancy for the unforeseeable events. However, how the redundancy can be quantified to reduce the safety factor, JS does not know. It would also be an interesting issue for structural systems consisting of other materials.

6.3.8. Structural vs other safety issues

With regard to safety, JS points out that an overemphasis on structural safety may introduce other undesired risks. He mentions that in a fire at the Düsseldorf Airport some 12 years ago, several people were unnecessarily killed. The glazing of the room they were in consisted of laminated tempered glass, which they could not break before being overcome by smoke. Had it been single glazing, they could have just smashed the window and flee.

(at this point Katrin Havemann, also present, adds that she knew of a case where the firemen could not enter a building because of the laminated glazing).

In most buildings, the probability of a fire is actually much higher than that of a structural failure. Therefore, safety measures should be taken cohesively.

7. Report of the Interview with Frank Wellershof

Interviewee: Dr.-ing. Frank Wellershof (FW); Interviewer: Freek Bos (FB); Date & time: Thursday, August 23rd, 2007, 11.00 – 12.45 hrs.⁸

7.1. Introduction by Interviewer

An introduction to the interview has been provided by FB in the form of explanatory notes prior to the interview. There was no necessity for further explanations.

7.2. Background and Experience of the Interviewee

- born 1967
- received his civil engineering degree from the University of Bochum 1994
- engineer in the consulting office CSK (Bochum) 1994 – 1997
- scientific assistant at the institute of steel construction, RWTH Aachen, 1997 – 2005
- research fields: wind engineering and the structural use of glass in building
- doctorate degree 2006
- since 2005 at Permasteelisa⁹
- team leader engineering at Permasteelisa Central Europe, Würzburg
- member of R&D team at Permasteelisa Group of Companies

7.3. The Allied Irish Bank (AIB), PLC, Bankcentre, Dublin.

7.3.1. Short project description

The entrance to the AIB Bank in Dublin is a glass structure. The roof, consisting of insulated glass units with 8 mm tempered glass on top and 2*10 mm strengthened glass underneath, is supported by 8 m long glass beams of 3*12 mm strengthened glass (Figure C.2). The beams are connected to the main building structure on one side and on the other side hung from an external steel structure which also carries the vertical glass façade. The beams carry part of the wind loading on the façade as well as the roof load. They consist of two pieces which have been bolted together.

7.3.2. The structural analysis report

The report contains six chapters. Chapters 2 (Safety concept) and 6 (Residual Strength) were particularly interesting for the authors research, and have thus been discussed thoroughly.

7.3.2.1. The start of a project

A structural glass project starts with the question of how residual strength can be implemented in the structural system. Suitable measures to provide residual strength are devised on a conceptual level, before starting the structural calculations of the

⁸ This interview proceeded along different lines than the previous ones. Rather than discussing the proposed agenda, FW discussed his approach to structural glass safety on the basis of a project he has done for Permasteelisa, namely the AIB Bank glass entrance in Dublin. He presented FB with the structural analysis report for the glass beams. Near the end of the interview, he also showed the report on the experimental tests on the columns for the Rheinbach pavilion, which he did while doing his PhD at the RWTH Aachen. Furthermore, FW has read the paper ‘Consequence-based safety requirements for structural glass members’ (GPD07) by FB and gave his view on it. FW has offered to add further comments to this report, which was highly appreciated.

⁹ The company branch in which Wellershoff is working was renamed to Gartner Steel and Glass in 2009.

undamaged glass. For the calculations, FW uses a probability approach with all stresses, based on Permasteelisa's own test data, or the partial safety factor method provided by the codes. If the probability approach is used, EN 1990 Annex D (basis for structural design) gives rules how to determine a design stress value from the test results mean value and standard deviations.

In the AIB project, the design strength for the bolt splice joints between both parts of the beam, has been determined experimentally by tensile tests. This is discussed in chapter 5 of the structural analysis report.

7.3.2.2. Chapter 2: Safety concept

The safety of a structural glass design is not only determined by the residual strength provided by the system but obviously also by the applied safety factors. In chapter 2, a comparison has been made between partial safety factors for the steel parts according to the German DIN codes and the BS codes which are valid in Ireland. There are differences of around 10% between the partial factors in the different codes. FW applied the partial load factors of the BS and the partial material factors of the DIN. He consequently multiplied these to check if this was a safe combination, compared to the BS and DIN.

7.3.2.3. Chapter 6: Residual Strength

After having determined the dimensions based on the undamaged state, an argumentation is presented on the residual strength of the system (concisely presented in Chapter 6). Both a qualitative explanation and an explicit residual strength calculation should be given. In the AIB project, three stages are considered:

1. Undamaged state
2. Damaged state; 2 outer plies broken
3. Damages state; all plies (of one beam) broken

Ad 2: The tensile bolt-splice joint specimens were also tested with two layers broken, and loaded with 25 kN for 6 hrs. This coincides with a load caused by the self weight plus an additional 0.35 kN/m² of roof load. None of the 3 specimens showed additional damage after the test, and thus were considered to be able to carry significant loads for considerable time.

Ad 3: If all three layers of a beam should break, the beam is considered not to be able to carry any significant load (including self weight) anymore. To provide residual strength even in this case, a perpendicular catenary reaction in the roof plates is activated (illustrated in Figure C.3). This system requires a certain amount of sagging before reaching equilibrium. The sag or angle rotation is a measure for the force applied on the silicone sealing which becomes the crucial link in the alternative load carrying system. FW calculated the silicone sealing stresses for two different load cases: self weight and self weight + imposed load of 1.60 kN/m (per m in direction of beam axis). He found the silicone would be loaded to 50 % and 68 % of it's characteristic strength, respectively. Although the partial safety factor on silicones is 6 (thus the design value is only 17 % of the characteristic strength), this was deemed acceptable for this very extraordinary case. One argument for this could be that even if some part of the silicone sealing is weaker, it will deform and redistribute stresses to other parts. Since there was no target value for the partial safety factor of silicone in a glass failure situation, this judgment call, based on experience, had to be made.

7.3.2.4. Scenario thinking

In the design and test process, debate often arises (between the façade contractor, structural engineering consultant and/or building authorities) on the issue of residual strength. There are no quantitative target values in codes or guidelines for residual strength. Often, failure scenarios are considered: ‘what can happen that would damage the structure, and to what extent?’. However, it will be clear that such questions are very difficult to answer objectively. It is difficult to debate what scenario would be reasonable, and what would not. As a consequence, the required scenarios can vary widely from project to project, even if the projects themselves are similar. To avoid having to do the scenario discussion over and over again as well as to prevent arbitrariness, FW pleads for explicit residual strength requirements instead of a scenario approach (even though the requirements may be derived from scenarios).

7.4. Discussion of the ‘Consequence-based Safety Requirements for Structural Glass Members’, GPD2007 paper by the author.

7.4.1. Time requirement

The German authorities often ask for a guaranteed residual strength during 24 hrs or 72 hrs for buildings usually closed during weekends. However, the manufacturer may demand more extensive time requirements for other reasons. FW himself discerns three important points in time related to glass failure.

1. The time needed for the damage to be discovered.
2. The time needed to erect a supporting structure.
3. The time needed to replace the component.

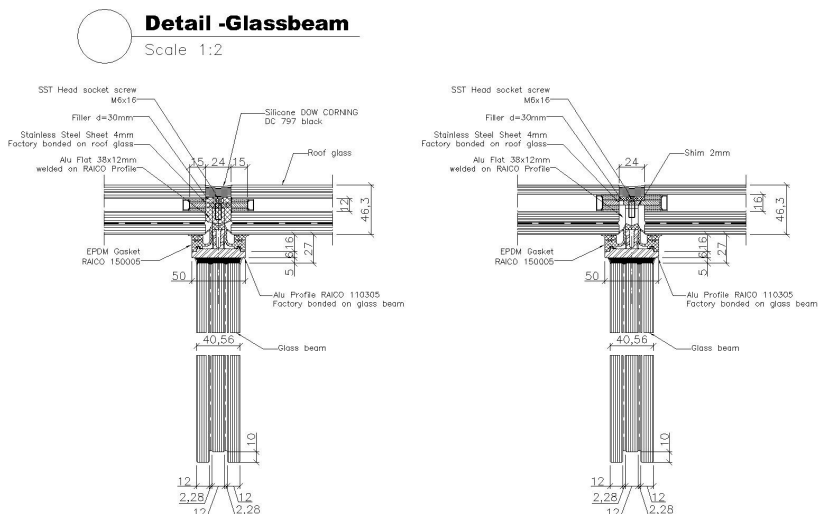


Fig. C.2 Details of the glass beam and connection to the roof plates.

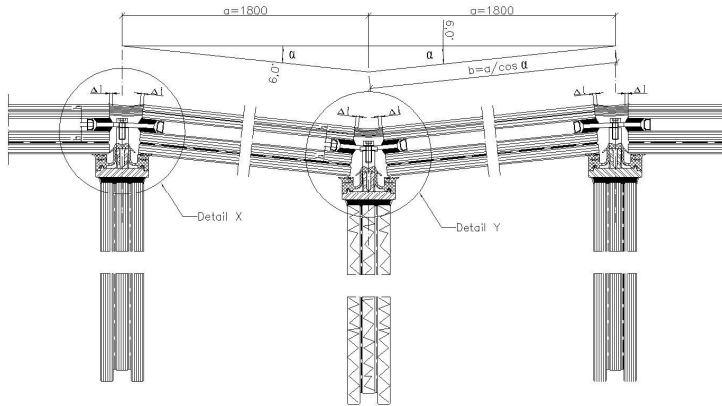


Fig. C.3 Catenary action in the roof plates if the complete glass beam section would fail.

Ad 1. This is usually a day or several days.

Ad 2. This can usually also be done relatively quickly.

Ad 3. Complex structural glass components may take several months to manufacture. This would require the supporting structure to be present for a long period of time. Since glass structures are usually applied in high-profile buildings, this is often not desired by the client. Therefore, if a long term supporting structure is not acceptable, the damaged structure itself should be able to provide residual strength for a longer period of time.

In case of the AIB Bank, the structure can remain in place unsupported for an infinite amount of time as long as it is loaded in wind and self weight. Only in the rather unlikely scenario of heavy snowfall would a supporting structure have to be erected. In the rare case all layers would break, a supporting structure would have to be put up until the beam is replaced. So, this is a balanced approach towards time requirements in relation to residual strength.

Generally, FW would leave the time requirement spaces open in table 2 of the paper (presenting all Member Consequence Class requirements), or only provide a recommendation. The client or authorities can fill these in, according to their desires.

7.4.2. Residual strength

To avoid endless discussion on scenarios, there should be a basic rule or definition on residual strength. The paper provides an attempt to describe such a rule. The quantitative interpretation can be left to the individual authority, client or consultant – within a consistent concept, this can be discussed. Furthermore, it would be useful to

add a catalogue with structural glass applications and proposals for required residual strength and replacement time.

Miscellaneous remarks

- Provide examples to elucidate the categorization.
- The serviceability limit state does not sound like a very logical demarcation on the strength axis, because you would not bother with serviceability requirements in case of failure.

7.5. Conclusion

It is important to develop explicit residual strength requirements based on a consistent concept of what residual strength actually is. Such requirements should contain required levels of strength at specific levels of damage. Although it is important to consider what may happen to a structure, endless scenario discussions should thus be avoided.

Appendix D: Suggested Safety Requirements and Example Application

Chapter 6 presents a new comprehensive approach to structural glass safety, the Integrated Approach. It identifies four glass element properties that determine its safety: relative resistance, damage sensitivity, redundancy, and fracture mode. It was explained how quantitative requirements for each property could be formulated, but, due to a lack of scientific evidence, provided no definite set of requirements for each glass application. The first section of this appendix provides a number of suggested performance criteria for three types of glass elements (floor plate, façade fin, beam) in three degrees of consequence (of collapse), totaling nine sets of performance criteria. The second section provides an elaborated example of a glass beam. It is checked to the performance criteria and concluded to fail. Subsequently, two redesigns are proposed which do meet the requirements. Together, the suggested performance criteria and elaborated example serve to give an impression of the way the Integrated Approach might work.

1. Some Suggested Performance Criteria

A lack of scientific evidence prohibits the presentation of a definite set of quantitative safety requirements in this publication.¹ Alternatively, performance criteria are suggested for three types of glass elements, similar to those considered in the structural glass survey²: a floor plate, a façade fin, and a glass beam.³ Three consequence classes are considered for every element: low, medium, and high. Thus, nine sets of performance requirements are proposed.

For each consequence class, some indicative characteristics are listed. However, for an element to qualify in a certain class, it does not necessarily possess all of those characteristics and the classification is inevitably rather arbitrary.

The requirements for redundancy are based on the ultimate limit state actions. However, rather than applying the load safety factors γ and reference life time correction factors ψ_t applicable to the undamaged structure, the values for these factors should be determined from Tables D.1 and D.2. Thus, the calculable value of the ultimate limit state action S_{uls} can decrease significantly, which is appropriate for the unusualness of the situation as well as the fact that specific action to control further damage, failure, and injury is likely to be taken. The background to this selection has been extensively argued in Chapter 6, Section 5.3.2.

The applicable reference life time correction factor is presented as ψ_{t^*} , referring to the life time t the values theoretically correspond to – in reality though, the formula for ψ_t is not valid for values of $t < 1$ yr. The asterisk is meant to indicate this. Similarly, the load safety factor is presented as γ_{ssc^*} . The subscript ssc^* indicates the values of γ should be

¹ Chapter 6, Sections 5 and 6.

² Chapter 5, Section 2 and Appendix B.

³ Off course, many other element types exist, such as roof plates, fall through barriers, and columns, which could all require different performance criteria.

used that belong to building safety class 1, 2, or 3, to incorporate the fact that a higher collapse probability may be accepted in the (rare) case of damage or failure – even though this does not mean the actual safety class of the structure has changed. The corresponding loading combinations, taken from NEN 6702, are reproduced as Eqs. (G.1a, b, c).

Table D.1 Values of ψ_{T^*} to use with redundancy requirements.

T* [yr]	Ψ_{T^*}		
	$\psi = 0.0$	$\psi = 0.5$	$\psi = 1.0$
0.25	0.3	0.6	1.0
0.50	0.4	0.7	1.0
1.00	0.6	0.8	1.0
≥ 1.00	As active code for actions on structures indicates.		

Table D.2 Values of γ_{ssc^*} to use with redundancy requirements.

Combination	ssc*	$\gamma_{fg;u}$ (unfavourable)	$\gamma_{fq;u}$
Fundamental, as Eq. (G.1a)	1	1.2	1.2
	2	1.2	1.3
	3	1.2	1.5
Fundamental, as Eq. (G.1b)	1, 2, 3	1.35	-
Exceptional, as Eq. (G.1c)	1, 2, 3	1.0	1.0

Fundamental combinations:

$$S_{f;u;d} = \gamma_{f;g;u} S_{perm,rep} + \gamma_{f;q;u} \psi_t S_{var,1;rep} + \sum_{i \geq 2}^n \gamma_{f;q;u} \psi_i S_{var,i;rep} \quad (G.1a)$$

$$S_{f;u;d} = \gamma_{f;g;u} S_{perm,rep} \quad (G.1b)$$

Exceptional combinations:

$$S_{a;u;d} = \gamma_{f;g;u} S_{perm,rep} + \gamma_{f;a;u} S_{inc,rep} + \sum_{i \geq 1}^n \gamma_{f;q;u} \psi_i S_{var,i;rep} \quad (G.1c)$$

1.1. Glass Façade Fin

Glass façade fins as schematically presented in Figure D.1 are becoming quite common elements to stiffen glass façades. Additionally to horizontal wind loads, some also carry the façade self weight. They may be hung from the ceiling or stacked on the floor.

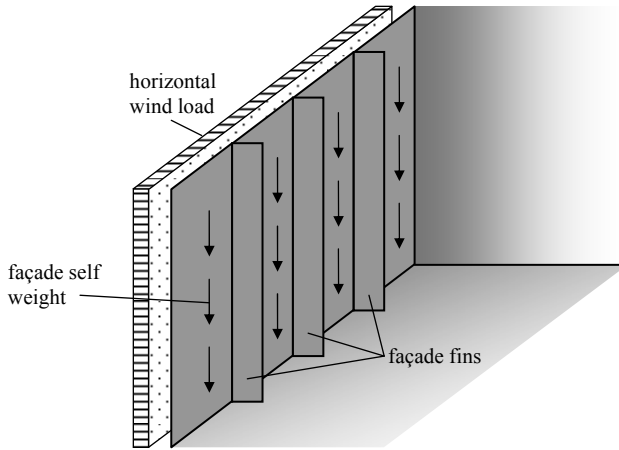


Fig. D.1 Façade fins, schematically.

Table D.3 Characteristics for the Element Consequence Classes (ECC) of façade fins and indicative time components.

ECC	Characteristics		Approximate Time Components	
Low	Application:	Interior	a	n/a
	Size:	$< \pm 2$ m	b	n/a
	Actions:	Only horizontal wind loads and self weight.	c	n/a
	Collision:	People: low; vehicles: none.	d	n/a
	Occupation density and frequency:	Low	e	T_{ref}
Medium	Application:	Interior or exterior but not publicly accessible.	a	24 hrs
	Size:	$2 < h < 6$ m	b	0:30 hrs
	Actions:	Only horizontal wind loads and self weight.	c	24 hrs
	Collision:	People: medium; vehicles: none.	d	60 days
	Occupation density and frequency:	Medium	e	T_{ref}
High	Application:	Exterior, publicly accessible.	a	24 hrs
	Size:	$> \pm 6$ m	b	2:00 hrs
	Actions:	May carry wind loads as well as façade self weight.	c	72 hrs
	Collision:	People: high; vehicles: low to medium.	d	180 days
	Occupation density and frequency:	High	e	T_{ref}

Façade fins are applied in a range of sizes, from around 2 m to over 10 m high. Table D.3 gives some characteristics for an element consequence classification as well as indicative quantification of the redundancy time components a, b, c, d, and e.⁴ The

⁴ See Chapter 6, Section 5.3.1. The time components are: a- time-to-discovery; b- time-to-evacuate; c- time-to-support; d- time-to-replace; e- reference life time.

proposed model damage levels are given in Table D.4. They correspond with the descriptions given in Chapter 6, Section 3.3.2. The suggested safety requirements for each element safety property are listed in Table D.5.

Table D.4 Description of Model Damage Levels for façade fins.

Description	
$D_{\phi,I}$	Physical damage to the extent that <i>one outer glass layer</i> does not transfer principal tensile stresses related to the governing load case anymore in at least one section of the element.
$D_{\phi,II}$	Physical damage to the extent that <i>all outer glass layer</i> does not transfer principal tensile stresses related to the governing load case anymore in at least one section of the element.
$D_{\phi,III}$	Physical damage to the extent that <i>all glass layer</i> do not transfer principal tensile stresses related to the governing load case anymore in at least one section of the element.

1.2. Glass Floor Plate

Like façade fins, glass floor plates (Figure D.2) are fairly common. An important difference with other horizontally applied glass elements is that floor plates are intended for regular and/or continuous actions, rather than incidental ones (e.g. roof plates).⁵ Glass floor generally carry their self weight and traffic loads (either as distributed or point load), but can also be subjected to semi-permanent variable loads caused by e.g. furniture.

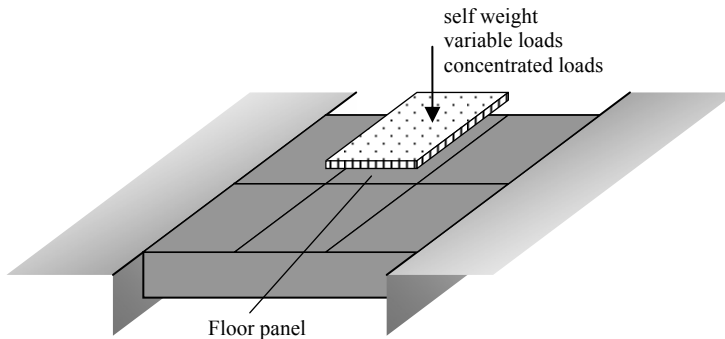


Fig. D.2 Glass floor plates, schematically.

Glass floor plates are applied in a range of sizes, from tile-size to around $2 \times 2 \text{ m}^2$. The panel stiffness often prohibits larger sizes. Table D.6 gives some characteristics for an element consequence classification as well as indicative quantification of the redundancy time components a, b, c, d, and e. The proposed model damage levels are given in Table D.7. They deviate somewhat from the descriptions given in Chapter 6, Section 3.3.2. The suggested safety requirements for each element safety property are listed in Table D.8.

⁵ See for instance the distinction between ‘betretbares Glas’ (incidentally accessible) and ‘begehbbares Glas’ (generally accessible) made in several German guidelines (Chapter 4, Section 5.1).

Table D.5 Safety requirements for façade fins.

Element Consequence Class		
Low	Medium	High
Relative Resistance r		
$r = R_d/S_{uls} \geq 1.0$	$r = R_d/S_{uls} \geq 1.0$	$r = R_d/S_{uls} \geq 1.0$
Damage Sensitivity Σ		
Level I: none.	Level I: = soft body pendulum impact test on undamaged element (e.g. according to NEN-EN 12600) and/or a hard body impact test (e.g. a falling bookcase). Research will have to point out which test is governing. $\Sigma_{\text{drop height soft body}} \geq 450 \text{ mm}$ $\Sigma_{\text{drop height hard body}} \geq (\text{to be determined})$	Level I: soft body pendulum impact test on undamaged element (e.g. according to NEN-EN 12600) and/or a hard body impact test (e.g. a falling bookcase). Research will have to point out which test is governing. $\Sigma_{\text{drop height soft body}} \geq 1200 \text{ mm}$ $\Sigma_{\text{drop height hard body}} \geq (\text{to be determined})$
Level II: none.	Level II: as level I.	Level II: as level I.
Level III: soft body pendulum impact test on undamaged element, e.g. according to NEN-EN 12600. $\Sigma_{\text{drop height soft body}} \geq 1200 \text{ mm}$	Level III: as level I, but with higher minimum values. $\Sigma_{\text{drop height soft body}} \geq 1200 \text{ mm}$ $\Sigma_{\text{drop height hard body}} \geq (\text{to be determined})$	Level III: as level I, but with higher minimum values (e.g. double weight). $\Sigma_{\text{drop height } 2x \text{ soft body}} \geq 1200 \text{ mm}$ $\Sigma_{\text{drop height } 2x \text{ hard body}} \geq (\text{to be determined})$
Redundancy m		
Level I: $R_{\text{res,I}}/S_{uls} \geq 1.0$	Level I: $R_{\text{res,I}}/S_{uls} \geq 1.0$	Level I: $R_{\text{res,I}}/S_{uls} \geq 1.0$
with: ψ_{T^*} -	with: ψ_{T^*} $t^* = 0.50$	with: ψ_{T^*} $T^* = 1.00$
γ_{ssc^*} -	γ_{ssc^*} $\text{ssc}^* = 2$	γ_{ssc^*} $\text{ssc}^* = 3$
for T - -	for T $\geq a+d \approx d = 60 \text{ days}$	for T $\geq a+d \approx d = 180 \text{ days}$
Level II: none ($R_{\text{res,II}} \geq 0$)	Level II: $R_{\text{res,II}}/S_{uls} \geq 1.0$	Level II: $R_{\text{res,II}}/S_{uls} \geq 1.0$
with: ψ_{T^*} -	with: ψ_{T^*} $T^* = 0.25$	with: ψ_{T^*} $T^* = 0.50$
γ_{ssc^*} -	γ_{ssc^*} $\text{ssc}^* = 1$	γ_{ssc^*} $\text{ssc}^* = 3$
for T - -	for T $\geq a + c = 48 \text{ hrs}$	for T $\geq a+d \approx d = 180 \text{ days}$
Level III: none ($R_{\text{res,III}} \geq 0$)	Level III: $R_{\text{res,III}}/S_{uls} \geq 1.0$	Level III: $R_{\text{res,III}}/S_{uls} \geq 1.0$
with: ψ_{T^*} -	with: ψ_{T^*} $T^* = 0.25$	with: ψ_{T^*} $T^* = 0.25$
γ_{ssc^*} -	γ_{ssc^*} $\text{ssc}^* = 1$	γ_{ssc^*} $\text{ssc}^* = 3$
for T - -	for T $\geq b = 0:30 \text{ hrs}$	for T $\geq a+c = 144 \text{ hrs}$
Fracture Mode		
B/C	B	B

Table D.6 Characteristics for the Element Consequence Classes (ECC) of floor plates and indicative time components.

ECC	Characteristics		Approximate Time Components		
Low	Accessibility:	Controlled (e.g. private, office, etc.)		a	24 hrs
	Size:	< ± 1.5 m ² .		b	0:15 hrs
	Drop height in case of collapse	< 3 m. (expected consequence of fall: mild injuries)	c	24 hrs	
			d	30 days	
	Occupation density and frequency:	On floor: Low; Underneath floor: Low		e	T _{ref}
Medium	Accessibility:	Uncontrolled (e.g. outside)		a	30 days
	Size:	1.5 – 4.0 m ²		b	0:30 hrs
	Drop height in case of collapse	3 – 13 m. (expected consequence of fall: severe injuries)	c	24 hrs	
			d	60 days	
	Occupation density and frequency:	On floor: Medium; Underneath floor: Medium		e	T _{ref}
High	Application:	Uncontrolled (e.g. outside)		a	30 days
	Size:	4 – 9 m ² .		b	1:00 hrs
	Drop height in case of collapse	>13 m (expected consequence of fall: death)	c	72 hrs	
			d	60 days	
	Occupation density and frequency:	On floor: High; Underneath floor: High		e	T _{ref}

Table D.7 Description of Model Damage Levels for floor plates.

	Description
D _{φ,I}	Physical damage to the extent that <i>the top glass layer</i> would not transfer principal tensile stresses anymore in at least one section of the element, if the direction of the governing load case would be inverted.
D _{φ,II}	Physical damage to the <i>top glass layer</i> as for level I, and to <i>the bottom glass layer</i> to the extent that it does not transfer principal tensile stresses related to the governing load case anymore in at least one section of the element.
D _{φ,III}	Physical damage to the extent that <i>all glass layers</i> do not transfer principal tensile stresses related to the governing load case anymore in at least one section of the element.

Table D.8 Safety requirements for floor plates.

Element Consequence Class		
Low	Medium	High
Relative resistance r		
$r = R_d/S_{uls} \geq 1.0$	$r = R_d/S_{uls} \geq 1.0$	$r = R_d/S_{uls} \geq 1.0$
Damage Sensitivity Σ		
Level I: Crack applied with a glasscutter, if necessary effectuated through bending. $\Sigma_{\text{bend. stress to eff. glass cut}} \geq 0 \text{ MPa}$	Level I: Crack applied with a glasscutter, if necessary effectuated through bending. $\Sigma_{\text{bend. stress to eff. glass cut}} \geq 0 \text{ MPa}$	Level I: Crack applied with a glasscutter, if necessary effectuated through bending. $\Sigma_{\text{bend. stress to eff. glass cut}} \geq 0 \text{ MPa}$
Level II: soft body drop impact test on Level I damaged element and/or hard body impact test, from smaller drop height (e.g. both similar to the glass construction guideline from Hessen, Germany). $\Sigma_{\text{drop h. 50 kg soft body}} \geq 900 \text{ mm}$ $\Sigma_{\text{drop h. 40 kg hard body}} \geq 450 \text{ mm}$	Level II: soft body drop impact test on Level I damaged element and/or hard body impact test, from smaller drop height (e.g. both similar to the glass construction guideline from Hessen, Germany). $\Sigma_{\text{drop h. 50 kg soft body}} \geq 900 \text{ mm}$ $\Sigma_{\text{drop h. 40 kg hard body}} \geq 450 \text{ mm}$	Level II: soft body drop impact test on Level I damaged element and/or hard body impact test, from heavy bodies, from smaller drop height (e.g. both similar to the glass construction guideline from Hessen, Germany). $\Sigma_{\text{drop h. 80 kg soft body}} \geq 900 \text{ mm}$ $\Sigma_{\text{drop h. 60 kg hard body}} \geq 450 \text{ mm}$
Level III: soft body drop impact test on Level I damaged element and/or hard body impact test (e.g. both similar to the glass construction guideline from Hessen, Germany). $\Sigma_{\text{drop h. 50 kg soft body}} \geq 1200 \text{ mm}$ $\Sigma_{\text{drop h. 40 kg hard body}} \geq 800 \text{ mm}$	Level III: soft body drop impact test on Level I damaged element and/or hard body impact test (e.g. both similar to the glass construction guideline from Hessen, Germany). $\Sigma_{\text{drop h. 50 kg soft body}} \geq 1200 \text{ mm}$ $\Sigma_{\text{drop h. 40 kg hard body}} \geq 800 \text{ mm}$	Level III: soft body drop impact test on Level I damaged element and/or hard body impact test with heavy bodies (e.g. both similar to the glass construction guideline from Hessen, Germany). $\Sigma_{\text{drop h. 80 kg soft body}} \geq 1200 \text{ mm}$ $\Sigma_{\text{drop h. 60 kg hard body}} \geq 800 \text{ mm}$
Redundancy m		
Level I: $R_{\text{res,I}}/S_{uls} \geq 1.0$	Level I: $R_{\text{res,I}}/S_{uls} \geq 1.0$	Level I: $R_{\text{res,I}}/S_{uls} \geq 1.0$
with ψ_{T^*} $T^* = 0.50$	with: ψ_{T^*} $T^* = t_{\text{ref}}$	with: ψ_{T^*} $T^* = T_{\text{ref}}$
γ_{sc^*} $sc^* = 2$	γ_{sc^*} $sc^* = 3$	γ_{sc^*} $sc^* = 3$
for $T \geq a+c = 48 \text{ hrs}$	for $t \geq e = T_{\text{ref}}$	for $t \geq e = T_{\text{ref}}$

Level II: none ($R_{res,II} \geq 0$)			Level II: $R_{res,II}/S_{uls} \geq 1.0$			Level II: $R_{res,II}/S_{uls} \geq 1.0$		
with:	ψ_{T^*}	$T^* = 0.50$	with:	ψ_{T^*}	$T^* = 0.50$	with:	ψ_{T^*}	$T^* = T_{ref}$
	γ_{sc^*}	$sc^* = 1$		γ_{sc^*}	$sc^* = 3$		γ_{sc^*}	$sc^* = 3$
			and	A_{rep}	0.5 kN	and	A_{rep}	0.8 kN
				t_{Arep}	0:30 hrs		t_{Arep}	1:00 hrs
for T	$\geq a+b$ $\approx a$	= 24 hrs	for T	$\geq a+c$ $\approx a$	≈ 30 days	for T	$\geq e$	= t_{ref}
Level III: none ($R_{res,III} \geq 0$)			Level III: $R_{res,III}/S_{uls} \geq 1.0$			Level III: $R_{res,III}/S_{uls} \geq 1.0$		
with:	ψ_{T^*}	$T^* = 0.25$	with:	ψ_{T^*}	$T^* = 0.25$	with:	ψ_{T^*}	$T^* = 1.00$
	γ_{sc^*}	$sc^* = 1$		γ_{sc^*}	$sc^* = 2$		γ_{sc^*}	$sc^* = 3$
and ⁶	A_{rep}		and	A_{rep}	0.5 kN	and	A_{rep}	0.8 kN
	T_{Arep}			T_{Arep}	0:30 hrs		T_{Arep}	1:00 hrs
for T	$\geq b$	0:15 hrs	for T	$\geq a+b$ $\approx a$	≈ 30 days	for T	$\geq a+d$	= 90 days
Fracture Mode								
	B			B			B	

Extra classes may be introduced for floor plates with one or more free edge. These could have specific redundancy and damage sensitivity requirements (e.g. by demanding an impact test on the free edge).

1.3. Glass Beam

Glass beams are less common than façade fins and floor plates, but enjoy increasing popularity. Although also applicable for floors, they are usually applied for roofs (although some glass bridges also use glass beams). Thus, besides the self weight of the structure they support, they are likely loaded with variable environmental loads such as wind, rain water, snow, and incidental persons for maintenance and cleaning.

Glass beams often span 3 – 6 m, but built examples exist that go beyond 15 m. Their centre distance usually ranges from 0.5 – 2 m. Table D.9 gives some characteristics for an element consequence classification as well as indicative quantification of the redundancy time components a, b, c, d, and e. The proposed model damage levels are identical to those for façade fins, and given in Table D.4. The suggested safety requirements for each element safety property are listed in Table D.10.

⁶ For glass floors in some cases of model damage, an exceptional load A_{rep} has to be considered that may correspond with a person or object lying on the floor (e.g. unconscious) for a short period of time.

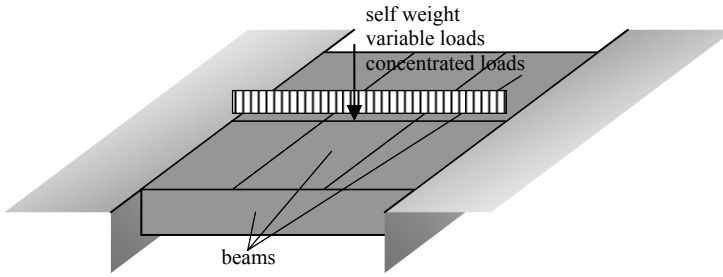


Fig. D.3 Glass beams, schematically.

Table D.9 Characteristics for the Element Consequence Classes (ECC) of glass beams and indicative time components.

ECC	Characteristics	Approximate Time Components	
Low	Accessibility: Very controlled (e.g. private)	a	24 hrs
	Span and area carrying: $< \pm 3 \text{ m}; < \pm 6 \text{ m}^2$.	b	0:15 hrs
	Drop height: $< \pm 3 \text{ m}$.	c	24 hrs
	Structural function: Roof beam.	d	90 days
	Occupation density and frequency: On roof: Very Low; Underneath roof: Low	e	T_{ref}
Medium	Accessibility: Controlled (e.g. office)	a	24 hrs
	Span and area carrying: $3 - 6 \text{ m}; 6 - 24 \text{ m}^2$	b	0:30 hrs
	Drop height: $3 - 6 \text{ m}$.	c	72 hrs
	Structural function: Roof beam.	d	90 days
	Occupation density and frequency: On roof: Very Low; Underneath roof: Medium	e	T_{ref}
High	Accessibility: Controlled, but publicly accessible.	a	24 hrs
	Span and area carrying: $> \pm 6 \text{ m}; > \pm 24 \text{ m}^2$	b	2:00 hrs
	Drop height: $> 6 \text{ m}$.	c	72 hrs
	Structural function: Floor beam.	d	180 days
	Occupation density and frequency: On floor: High; Underneath floor: High	e	T_{ref}

Table D.10 Safety requirements for glass beams.

Element Consequence Class		
Low	Medium	High
Relative Resistance r		
$r = R_d/S_{uls} \geq 1.0$	$r = R_d/S_{uls} \geq 1.0$	$r = R_d/S_{uls} \geq 1.0$
Damage Sensitivity Σ		
Level I: Hard-body concentrated impact on edge of one outer layer, in combination with a static load equal to $S_{res,I}$ (e.g. as experiments in App. I). $\Sigma_{conc. \text{ hard impact} + \text{static}} \geq$ (to be determined)	Level I: Hard-body concentrated impact on edge of one outer layer, in combination with a static load equal to $S_{res,I}$ (e.g. as experiments in App. I). $\Sigma_{conc. \text{ hard impact} + \text{static}} \geq$ (to be determined)	Level I: Hard-body concentrated impact on edge of one outer layer, in combination with a static load equal to $S_{res,I}$ (e.g. as experiments in App. I). $\Sigma_{conc. \text{ hard impact} + \text{static}} \geq$ (to be determined)
Level II: Hard-body concentrated impact on edge of other outer layer(s), in combination with a static load equal to $S_{res,II}$. $\Sigma_{conc. \text{ hard impact} + \text{static}} \geq$ (to be determined)	Level II: Hard-body concentrated impact on edge of other outer layer(s), in combination with a static load equal to $S_{res,II}$. $\Sigma_{conc. \text{ hard impact} + \text{static}} \geq$ (to be determined)	Level II: Hard-body concentrated impact on edge of other outer layer(s), in combination with a static load equal to $S_{res,II}$. $\Sigma_{conc. \text{ hard impact} + \text{static}} \geq$ (to be determined)
Level III: Hard-body concentrated impact on edge of inner layer(s), in combination with a static load equal to $S_{res,III}$. $\Sigma_{conc. \text{ hard impact} + \text{static}} \geq$ (to be determined)	Level III: Hard-body concentrated impact on edge of inner layer(s), in combination with a static load equal to $S_{res,III}$. $\Sigma_{conc. \text{ hard impact} + \text{static}} \geq$ (to be determined)	Level III: Overloading from undamaged state. $\Sigma_{conc. \text{ hard impact} + \text{static}} \geq S_{res,III}$ (to be determined) ⁷
Redundancy m		
Level I: $R_{res,I}/S_{uls} \geq 1.0$	Level I: $R_{res,I}/S_{uls} \geq 1.0$	Level I: $R_{res,I}/S_{uls} \geq 1.0$
with: $\psi_{T^*} \quad T^* = 1.00$	with: $\psi_{T^*} \quad T^* = 1.00$	with: $\psi_{T^*} \quad T^* = T_{ref}$
$\gamma_{sc^*} \quad sc^* = 3$	$\gamma_{sc^*} \quad sc^* = 3$	$\gamma_{sc^*} \quad sc^* = 3$
for T $\geq a+d \approx d = 90 \text{ days}$	for T $\geq a+d \approx d = 90 \text{ days}$	for T $\geq e = t_{ref}$
Level II: $R_{res,II}/S_{uls} \geq 1.0$	Level II: $R_{res,II}/S_{uls} \geq 1.0$	Level II: $R_{res,II}/S_{uls} \geq 1.0$
with: $\psi_{T^*} \quad T^* = 0.25$	with: $\psi_{T^*} \quad T^* = 0.50$	with: $\psi_{T^*} \quad T^* = T_{ref}$
$\gamma_{sc^*} \quad sc^* = 2$	$\gamma_{sc^*} \quad sc^* = 2$	$\gamma_{sc^*} \quad sc^* = 3$
for T $\geq b = 0:15 \text{ hrs}$	for T $\geq a + c = 96 \text{ hrs}$	for T $\geq e = t_{ref}$

⁷ Due to the redundancy requirements, this test makes the tests for levels I and II superfluous. The test for level III will be governing as it will result in more energy at failure than at levels I and II, while requiring the same residual strength.

Level III: none ($R_{res,III} \geq 0$)	Level III: $R_{res,III}/S_{uls} \geq 1.0$	Level III: $R_{res,III}/S_{uls} \geq 1.0$
with: ψ_{T^*} -	with: ψ_{T^*} $T^* = 0.25$	with: ψ_{T^*} $T^* = T_{ref}$
γ_{sc^*} -	γ_{sc^*} $sc^* = 1$	γ_{sc^*} $sc^* = 3$
for T - -	for t $\geq a+b \approx$ a = 24 hrs	for T $\geq e$ = T_{ref}
Fracture Mode		
B	B	B

2. Example Application of the Integrated Approach and ESD: a Glass Beam

An elaborated example of a glass roof beam will explicate how the Integrated Approach and the ESD works. The actions on the structure have been based on the NEN 6702. The allowable stresses on glass have been taken from NEN 2608-2. Some additional data from various publications have been used.

2.1. Initial Design

Consider a glass beam, e.g. as in Figure D.3, and assume the ECC is Medium. The initial design consists of a two-layer, heat strengthened, PVB-laminated glass beam as given in Figure D.4. Some beam properties are listed in Table D.11. Table D.12 presents the actions and their durations. It will be determined whether this design is suitable, and redesigns will be proposed and evaluated if necessary.

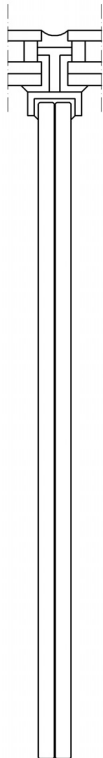


Table D.11 Glass and Beam properties.		
Glass Density	ρ	25 kN/m ³
Glass Young's Modulus	E	70 000 MPa
Heat treatment	Heat Strengthened	
Laminate	PVB*	
Span	l_s	4800 mm
Height	h	500 mm
Thickness	t	$2 \cdot 12 = 24$ mm
Glass Section Area	A_{glass}	12000 mm ²
Moment of Resistance	W	$1.0 \cdot 10^6$ mm ³
Centre distance	l_{cd}	2400 mm

Fig. D.4 Section of the initial glass beam design.

* PVB strength and stiffness have been ignored in the calculations.

Table D.12 Actions on Glass Beam.

Type	Description	t	ψ	S _{var,rep}
Permanent	Self weight roof plates	50 years	1.0	$S_{var,rep} = p_{rep} \cdot l_{cd} = t \cdot \rho \cdot l_{cd} = 0.024 \cdot 25 \cdot 2.4 = 1.44 \text{ kN/m}$
	Self weight glass beam	50 years	1.0	$S_{var,rep} = t \cdot h \cdot \rho = 0.024 \cdot 0.5 \cdot 25 = 0.30 \text{ kN/m}$
Variable	Maintenance, etc.	8 hrs; 0:30 hrs*	0.0	$S_{var,rep} = p_{rep} \cdot l_{cd} = 1.0 \cdot 2.4 = 2.4 \text{ kN/m}$ $S_{rep} = 2 \text{ kN}$ $S_{var,rep,line} = 2 \text{ kN/m, for 1 m.}$
				Wind
	Snow	1 month	0.0	$S_{var,rep} = p_{rep} \cdot l_{cd} = C_i \cdot p_{sn} = 0.8 \cdot 0.7 \cdot 2.4 = 1.34 \text{ kN/m}$

* No duration is specified for this action in NEN 6702. It is proposed to maintain 8 hours for level 0 and I (a working day) and 0:30 hrs for level II and III.

2.2. Safety Requirements

The safety requirements for a glass beam of Medium ECC have generally been formulated in Table D.10. For so far as possible, they have been quantified and calculated below. The results have been summarized in Figure D.5.

The actions from which the ultimate limit state loading combinations have to be determined were given in Table D.12. The required resistances and time durations for the undamaged state (level 0) have been determined from the fundamental combinations given in NEN 6702. The results are tabulated in terms of internal moment capacity, in Table D.13.

Table D.13 Governing ultimate limit state actions S_{uls}, presented in terms on internal moment.

LEVEL 0		
T	Governing Loading Combination	S _{uls}
0 – 8 hrs	Permanent + Variable: Maintenance	$M_{uls} = \frac{1}{8} \cdot q_d \cdot l_s^2 = \frac{1}{8} \cdot (\gamma_{f,gu} \cdot S_{perm,rep} + \gamma_{f,gu} \cdot \psi_T \cdot Q_{1,rep}) \cdot l_s^2 = \frac{1}{8} \cdot (1.2 \cdot (1.44 + 0.30) + 1.5 \cdot 1.0 \cdot 2.4) \cdot 4.8^2 = \mathbf{16.38 \text{ kNm}}$
8 hrs – 1 month	Permanent + Variable: Snow	$M_{uls} = \frac{1}{8} \cdot q_d \cdot l_s^2 = \frac{1}{8} \cdot (\gamma_{f,gu} \cdot S_{perm,rep} + \gamma_{f,gu} \cdot \psi_T \cdot Q_{1,rep}) \cdot l_s^2 = \frac{1}{8} \cdot (1.2 \cdot (1.44 + 0.30) + 1.5 \cdot 1.0 \cdot 1.34) \cdot 4.8^2 = \mathbf{11.80 \text{ kNm}}$
1 month – 50 years	Permanent	$M_{uls} = \frac{1}{8} \cdot q_d \cdot l_s^2 = \frac{1}{8} \cdot (\gamma_{f,gu} \cdot S_{perm,rep}) \cdot l_s^2 = \frac{1}{8} \cdot (1.35 \cdot (1.44 + 0.30)) \cdot 4.8^2 = \mathbf{6.77 \text{ kNm}}$

As indicated before, too little experimental data exists to specify quantitative requirements for damage sensitivity. Therefore, only a dimensionless horizontal axis has been used in the ESD.

The required redundancy (resistances and time durations for the model damage levels I, II, and III) have been determined from the fundamental combinations given in NEN

6702 and requirements formulated in Table D.10. The results are tabulated in terms of internal moment capacity, in Table D.14a, b, and c.

The required fracture mode is B.

Table D.14a Governing ultimate limit state actions S_{uls} for model damage level I.

LEVEL I, $t^* = 1.00$, $sc^* = 3$		
T	Governing Loading Combination	S_{uls}
0 – 8 hrs	Permanent + Variable: Maintenance	$M_{uls} = \frac{1}{8} \cdot S_{var,d} \cdot l_s^2 = \frac{1}{8} \cdot (\gamma_{f,gu} \cdot S_{perm,rep} + \gamma_{f,gu} \cdot \Psi_T \cdot S_{var,1,rep}) \cdot l_s^2 = \frac{1}{8} \cdot (1.2 \cdot (1.44 + 0.30) + 1.5 \cdot 0.6 \cdot 2.4) \cdot 4.8^2 = \mathbf{12.23 \text{ kNm}}$
8 hrs – 1 month	Permanent + Variable: Snow	$M_{uls} = \frac{1}{8} \cdot S_{var,d} \cdot l_s^2 = \frac{1}{8} \cdot (\gamma_{f,gu} \cdot S_{perm,rep} + \gamma_{f,gu} \cdot \Psi_T \cdot S_{var,1,rep}) \cdot l_s^2 = \frac{1}{8} \cdot (1.2 \cdot (1.44 + 0.30) + 1.5 \cdot 0.6 \cdot 1.34) \cdot 4.8^2 = \mathbf{9.49 \text{ kNm}}$
1 month – 90 days	Permanent	$M_{uls} = \frac{1}{8} \cdot S_{var,d} \cdot l_s^2 = \frac{1}{8} \cdot (\gamma_{f,gu} \cdot S_{perm,rep}) \cdot l_s^2 = \frac{1}{8} \cdot (1.35 \cdot (1.44 + 0.30)) \cdot 4.8^2 = \mathbf{6.77 \text{ kNm}}$

Table D.14b Governing ultimate limit state actions S_{uls} for model damage level II.

LEVEL II, $t^* = 0.50$, $sc^* = 2$		
T	Governing Loading Combination	S_{uls}
0 – 0:30 hrs	Permanent + Variable: Maintenance	$M_{uls} = \frac{1}{8} \cdot S_{var,d} \cdot l_s^2 = \frac{1}{8} \cdot (\gamma_{f,gu} \cdot S_{perm,rep} + \gamma_{f,gu} \cdot \Psi_T \cdot S_{var,1,rep}) \cdot l_s^2 = \frac{1}{8} \cdot (1.2 \cdot (1.44 + 0.30) + 1.3 \cdot 0.4 \cdot 2.4) \cdot 4.8^2 = \mathbf{9.61 \text{ kNm}}$
0:30 hrs – 96 hrs	Permanent + Variable: Snow	$M_{uls} = \frac{1}{8} \cdot S_{var,d} \cdot l_s^2 = \frac{1}{8} \cdot (\gamma_{f,gu} \cdot S_{perm,rep} + \gamma_{f,gu} \cdot \Psi_T \cdot S_{var,1,rep}) \cdot l_s^2 = \frac{1}{8} \cdot (1.2 \cdot (1.44 + 0.30) + 1.3 \cdot 0.4 \cdot 1.34) \cdot 4.8^2 = \mathbf{8.02 \text{ kNm}}$

Table D.14c Governing ultimate limit state actions S_{uls} for model damage level III.

LEVEL III, $t^* = 0.25$, $sc^* = 1$		
T	Governing Loading Combination	S_{uls}
0 – 0:30 hrs	Permanent + Variable: Maintenance	$M_{uls} = \frac{1}{8} \cdot S_{var,d} \cdot l_s^2 = \frac{1}{8} \cdot (\gamma_{f,gu} \cdot S_{perm,rep} + \gamma_{f,gu} \cdot \Psi_T \cdot S_{var,1,rep}) \cdot l_s^2 = \frac{1}{8} \cdot (1.2 \cdot (1.44 + 0.30) + 1.2 \cdot 0.3 \cdot 2.4) \cdot 4.8^2 = \mathbf{8.50 \text{ kNm}}$
0:30 hrs – 24 hrs	Permanent + Variable: Snow	$M_{uls} = \frac{1}{8} \cdot S_{var,d} \cdot l_s^2 = \frac{1}{8} \cdot (\gamma_{f,gu} \cdot S_{perm,rep} + \gamma_{f,gu} \cdot \Psi_T \cdot S_{var,1,rep}) \cdot l_s^2 = \frac{1}{8} \cdot (1.2 \cdot (1.44 + 0.30) + 1.2 \cdot 0.3 \cdot 1.34) \cdot 4.8^2 = \mathbf{7.40 \text{ kNm}}$

2.3. Evaluation of the Initial Design

The beam resistances for the undamaged state have been determined from the calculable glass strength according Eq. (G.2) based on Eq. (9b) taken from NEN 2608-2, multiplied by a factor of 0.8 which incorporates the fact that the peak stresses occur along the beam bottom edge.⁸ The relevant values of k_{mod} are determined by Eq. (G.3)⁹ and given in Table D.15. Table D.16 provides the element resistances (expressed as f_d

⁸ Various studies have shown the bending tensile strength of a piece of glass to be lower when it the peak stresses occur on the edge (i.e. when the glass plate is loaded as a standing beam).

⁹ Presented as Eq. (10) (general) and Eq. (11) (linear elastic calculations) in NEN 2608-2.

and M_d) and unity checks for the governing loading combinations. The design passes all checks.

$$\sigma_d = \frac{\sigma_{g;k} k_b k_e k_{mod}}{\gamma_M} + \frac{\sigma_{b;k} - \sigma_{g;k}}{\gamma_V} \quad (G.2)$$

with the representative inherent strength of annealed glass $\sigma_{g;k} = 45$ MPa, the representative strength of heat strengthened glass $\sigma_{b;k} = 70$ MPa, the fracture mode factor $k_b = 1.15$, the edge quality factor $k_e = 1.0$, the loading duration correction factor k_{mod} to be determined from Table D.15, the material partial factor $\gamma_M = 1.8$, and the heat treatment partial factor $\gamma_V = 1.4$.

$$k_{mod} = m_T \sqrt{\frac{T_0}{T}} \quad (G.3)$$

with the corrosion constant $m_T = 16$, and the reference time $T_0 = 5$ s.

Table D.15 Values for k_{mod} for the relevant time durations.

T		k_{mod}
0:30 hrs	= 1800 s	0.69
8 hrs	= 28 800 s	0.58
24 hrs	= 86 400 s	0.54
96 hrs	= 345 600 s	0.50
1 month (30 days)	= $2.59 \cdot 10^6$ s	0.44
90 days	= $7.78 \cdot 10^6$ s	0.41
50 years	= $1.58 \cdot 10^9$ s	0.29

Table D.16 Glass beam resistances for the undamaged state.

Resistances, Level 0					
T	σ_d	$M_d = \sigma_d \cdot W$	M_{ult}	Unity Check	Pass/Fail
0 – 8 hrs	34.53 MPa	34.53 kNm	16.38 kNm	0.474	Pass
8 hrs – 1 month	30.51 MPa	30.51 kNm	11.80 kNm	0.386	Pass
1 month – 50 years	26.19 MPa	26.19 kNm	6.77 kNm	0.258	Pass

The damage sensitivity of the design is unknown.

To determine the redundancy, the residual resistances for each model damage level have been calculated. For level I, it was assumed the contribution of one damaged layer could be ignored to calculate the remaining resistance.

In this design, Level II = Level III (since only two layers were used). For level II = III, it was assumed the residual strength is approximately equal to the self weight of the

beam (not including the weight from the roof plates). Experimental research¹⁰ has shown these assumptions to be realistic.

Tables D.17a and b show the element resistances (expressed as f_d and M_d) and unity checks for the governing loading combinations. The design passes the checks for level I, but fails on level II.

Table D.17a Glass beam resistances for the model damage level I.

Resistances, Level I					
T	$\sigma_{d,I}$	$M_{d,I} = \sigma_{d,I} \cdot W_I$	$M_{uls,I}$	Unity Check	Pass/Fail
0 – 8 hrs	34.53 MPa	17.27 kNm	12.23 kNm	0.709	Pass
8 hrs – 1 month	30.51 MPa	15.25 kNm	9.49 kNm	0.621	Pass
1 month – 90 days	29.64 MPa	14.82 kNm	6.77 kNm	0.457	Pass

Table D.17b Glass beam resistances for the model damage level II (= III).

Resistances, Level II (=III)					
t	$M_{d,eff,II}^{11} = \frac{1}{8} \cdot s_{var,d} \cdot l_s^2 =$	$M_{uls,II}$	Unity Check	Pass/Fail	
0 – 0:30 hrs	$\frac{1}{8} \cdot 1.35 \cdot 0.3 \cdot 4.8^2 = 1.17$ kNm	9.61 kNm	8.33	Fail	
0:30 hrs – 96 hrs	$\frac{1}{8} \cdot 1.35 \cdot 0.3 \cdot 4.8^2 = 1.17$ kNm	8.02 kNm	6.67	Fail	

Research¹² has shown the fracture mode of PVB-laminated, heat strengthened beams depends on the experiment type. In direct overloading, the foil will tear upon failure and the beam will break into two pieces. On the other hand, when loaded after initial damages have been applied, the laminate will not tear as the energy release is lower upon failure. As this latter method is the one required to obtain the model damage levels, heat strengthened glass beams should be considered to behave as fracture mode B.

The safety requirements and element behaviour have been summarized in Figure D.5.

The element fails to meet the redundancy requirements. Specifically, the residual strength at model damage levels II and III is insufficient. Therefore, two alternative designs, presented in the subsequent Sections, may be suggested.

¹⁰ Appendix E.

¹¹ Research (Appendix E) has shown the residual moment capacity is approximately equal to that required to carry the element self weight. The time dependency was not established and here ignored.

¹² Appendix E.

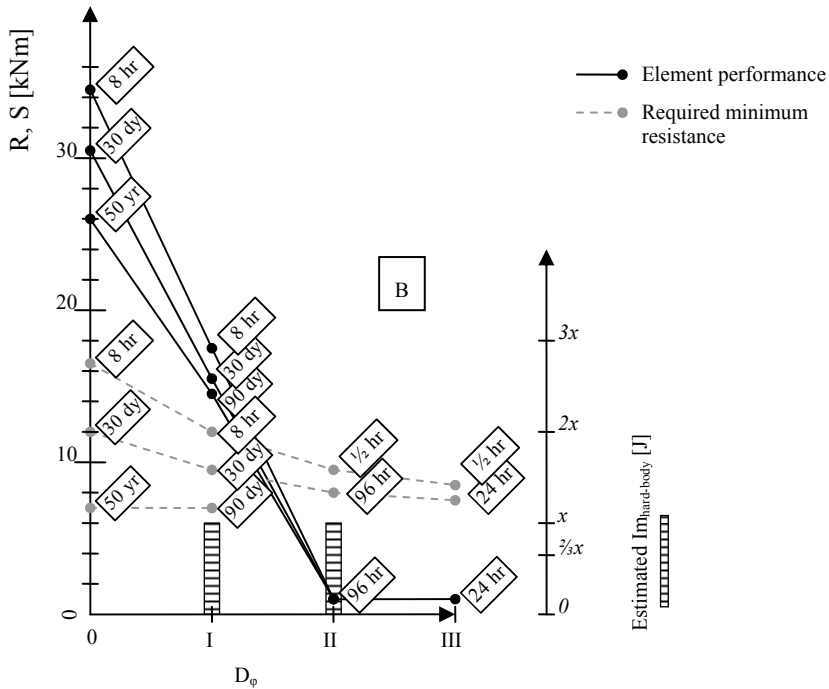


Fig. D.5 ESD of the initial glass beam design, with the safety requirements and element performance. The dotted line marks the resistance of the 2nd LTM. This design fails to meet the redundancy requirements of Levels II and III.

2.4. Redesign 1: Three-layer SG Laminate Beam

Figure D.6 and Table D.18 describe redesign 1. The number of layers has been increased by one, but the total nominal glass thickness has remained equal. The laminate material has been changed, from PVB to SG. Double layers of SG (i.e. 3.04 mm) have been applied to obtain sufficient residual strength at level III.

Table D.19 provides the element resistances (expressed as f_d and M_d) and unity checks for the governing loading combinations. The design passes all checks.

The damage sensitivity of the design is unknown.

To determine the redundancy, the residual resistances for each model damage level have been calculated. For level I, it was assumed the contribution of one, damaged layer could be ignored to calculate the remaining resistance. Similarly, the contribution of the two outer layers was ignored for level II.

In level III, the load carrying mechanism in the beam changes. Research has shown,¹³ bending loads are transferred by a composite bending mechanism with the broken glass in compression and the SG laminate in tension. It is assumed the moment capacity can approximately be determined by the considering the complete SG section to be in plastic tension, as in Figure D.7.¹⁴ The moment capacity can then be determined by Eq. (H.3).

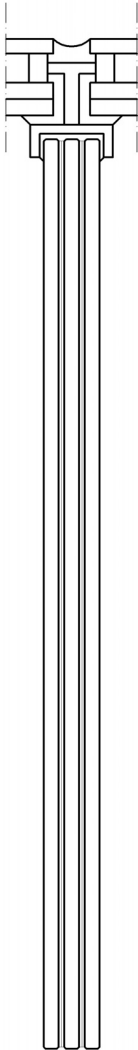


Fig. D.6 Section of the glass beam design; redesign 1.

Table D.18 Beam properties; redesign 1.

Heat treatment		Heat Strengthened
Laminate		SG*
Span	l_s	4800 mm
Height	h	500 mm
Glass thickness	t_{glass}	$3 \cdot 8 = 24$ mm
Glass Section Area	A_{glass}	12000 mm ²
Moment of Resistance	W	$1.0 \cdot 10^6$ mm ³
Centre distance	l_{cd}	2400 mm
SG thickness	t_{SG}	$2 \cdot (2 \cdot 1.52) = 6.08$ mm

* SG strength and stiffness have been ignored in Level I and II calculations.

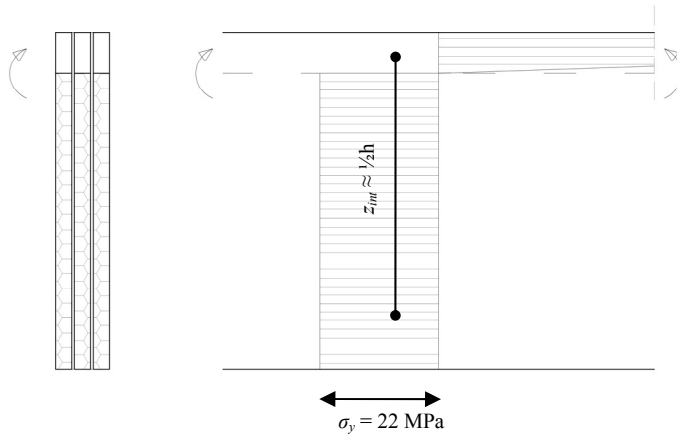


Fig. D.7 2nd LTM in an SG laminated glass beam: composite action between SG (tension) and glass (compression).

¹³ Appendix E.

¹⁴ Based on experimental research presented in Appendix E.

$$M_{d,III,SGPlam} = \sigma_{y,SGP} \left(\frac{1}{2} t h^2 \right) \quad (\text{H.3})$$

With the SG yield strength $\sigma_y \approx 22.0$ MPa.¹⁵

Tables D.20a, b and c show the element resistances (expressed as σ_d and M_d) and unity checks for the governing loading combinations.

Table D.19 Glass beam resistances for the undamaged state; redesign 1.

Resistances, Level 0					
T	σ_d	$M_d = \sigma_d \cdot W$	M_{uls}	Unity Check	Pass/Fail
0 – 8 hrs	34.53 MPa	34.53 kNm	16.38 kNm	0.474	Pass
8 hrs – 1 month	30.51 MPa	30.51 kNm	11.80 kNm	0.386	Pass
1 month – 50 years	26.19 MPa	26.19 kNm	6.77 kNm	0.258	Pass

Table D.20a Glass beam resistances for the model damage level I; redesign 1.

Resistances, Level I					
T	$\sigma_{d,I}$	$M_{d,I} = \sigma_{d,I} \cdot W_I$	$M_{uls,I}$	Unity Check	Pass/Fail
0 – 8 hrs	34.53 MPa	22.79 kNm	12.23 kNm	0.538	Pass
8 hrs – 1 month	30.51 MPa	20.13 kNm	9.49 kNm	0.472	Pass
1 month – 90 days	29.64 MPa	19.57 kNm	6.77 kNm	0.346	Pass

Table D.20b Glass beam resistances for the model damage level II; redesign 1.

Resistances, Level II					
T	$\sigma_{d,II}$	$M_{d,II} = \sigma_{d,II} \cdot W_{II}$	$M_{uls,II}$	Unity Check	Pass/Fail
0 – 0:30 hrs	37.69 MPa	12.44 kNm	9.61 kNm	0.775	Pass
0:30 hrs – 96 hrs	32.23 MPa	10.64 kNm	8.02 kNm	0.752	Pass

Table D.20c Glass beam resistances for the model damage level III; redesign 1.

Resistances, Level III					
T	$M_{d,eff,III} = \frac{1}{2} \cdot \sigma_y \cdot t_{SG} \cdot h^2 =$	$M_{uls,III}$	Unity Check	Pass/Fail	
0 – 0:30 hrs	$\frac{1}{2} \cdot 22 \cdot 6.08 \cdot 500^2 = 11.12$ kNm	9.61 kNm	0.862	Pass	
0:30 hrs – 24 hrs	$\frac{1}{2} \cdot 22 \cdot 6.08 \cdot 500^2 = 11.12$ kNm	8.02 kNm	0.730	Pass	

¹⁵ The yield stress of SG is strain rate dependent. Delincé et al. found values ranging from 20.97 to 25.09 MPa. Delincé, D., Callewaert, D., Belis, J., Impe, R. van, *Post-breakage behaviour of laminated glass in structural applications*, Proceedings of the Challenging Glass Conference, Delft, the Netherlands, May 2008.

The fracture mode of this element is considered to be B (see previous remarks).

The safety requirements and element behaviour have been summarized in Figure D.8. This redesign meets all safety requirements for this application.

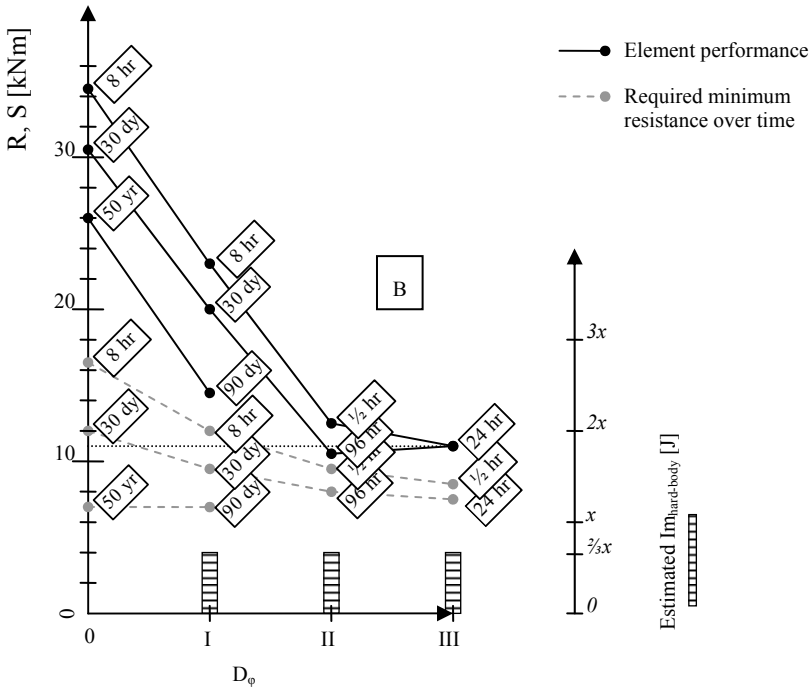


Fig. D.8 ESD of the glass beam design, redesign 1, with the safety requirements and element performance. The dotted line marks the resistance of the 2nd LTM. This design meets all resistance and redundancy requirements.

2.5. Redesign 2: Alternative Load Path

Instead of designing an element which itself can meet all redundancy requirements, it is also possible to adjust the structure to introduce alternative load paths that may be activated in case of failure. Redesign 2 is presented in Figure D.9 and Table D.21. In this case, an alternative load path was created by introducing a catenary reaction perpendicular to the main load axis. Similar solutions have been applied in realized projects such as the Allied Irish Bank in Dublin and the Wolfson Medical Building in Glasgow.¹⁶ In this case, the catenary loads are transferred by in-laminated steel strips.

The element resistances are equal to those of the initial design. Thus, it passes the resistance checks (Tabl H.22).

¹⁶ See Chapter 5, Section 1.1.3, and Appendix C, Sections 3 and 7.

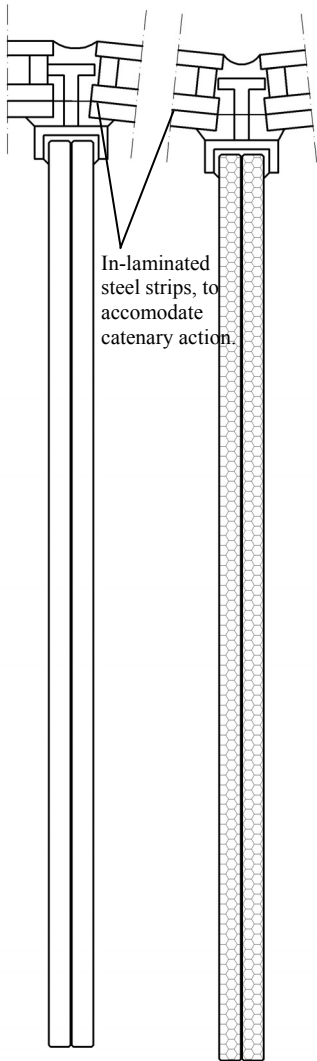


Fig. D.9 Section of the construction design; redesign 2.

Table D.21 Beam properties.

Heat treatment	Heat Strengthened	
Laminate	PVB*	
Span	l_s	4800 mm
Height	h	500 mm
Thickness	t	$2 \cdot 12 = 24$ mm
Glass Section Area	A_{glass}	12000 mm ²
Moment of Resistance	W	$1.0 \cdot 10^6$ mm ³
Centre distance	l_{cd}	2400 mm

* PVB strength and stiffness have been ignored in the calculations.

Table D.22 Glass beam resistances for the undamaged state; redesign 2.

Resistances, Level 0					
T	σ_d	$M_d = \sigma_d \cdot W$	M_{uls}	Unity Check	Pass/Fail
0 – 8 hrs	34.53 MPa	34.53 kNm	16.38 kNm	0.474	Pass
8 hrs – 1 month	30.51 MPa	30.51 kNm	11.80 kNm	0.386	Pass
1 month – 50 years	26.19 MPa	26.19 kNm	6.77 kNm	0.258	Pass

Table D.23a Glass beam resistances for the model damage level I; redesign 2.

Resistances, Level I					
T	$\sigma_{d,I}$	$M_{d,I} = \sigma_{d,I} \cdot W_I$	$M_{uls,I}$	Unity Check	Pass/Fail
0 – 8 hrs	34.53 MPa	17.27 kNm	12.23 kNm	0.709	Pass
8 hrs – 1 month	30.51 MPa	15.25 kNm	9.49 kNm	0.621	Pass
1 month – 90 days	29.64 MPa	14.82 kNm	6.77 kNm	0.457	Pass

Table D.23b Adjacent glass beam resistances (undamaged state) for model damage level II in considered beam; redesign 2.

Resistances, Level II				
T	Reserve capacity in adjacent beam $M_{d,0} - M_{uls,II}$	Additional load $0.5 \cdot M_{uls,II}$	Check ($M_{d,0} - M_{uls,II} / (0.5 \cdot M_{uls,II})$)	Pass/Fail
0 – 0:30 hrs	37.69 - 9.61 = 28.08 kNm	4.81 kNm	0.171	Pass
0:30 hrs – 96 hrs	32.23 - 8.02 = 24.21 kNm	4.01 kNm	0.166	Pass

Table D.23c Adjacent glass beam resistances (undamaged state) for model damage level III in considered beam; redesign 2.

Resistances, Level III				
T	Reserve capacity in adjacent beam $M_{d,0} - M_{uls,III}$	Additional load $0.5 \cdot M_{uls,III}$	Check ($M_{d,0} - M_{uls,III} / (0.5 \cdot M_{uls,III})$)	Pass/Fail
0 – 0:30 hrs	37.69 – 8.50 = 29.19 kNm ¹⁷	4.25 kNm	0.146	Pass
0:30 hrs – 24 hrs	33.38 – 7.40 = 25.98 kNm	3.70 kNm	0.142	Pass

The damage sensitivity of the design is unknown.

The redundancy for Level I is equal to that of the initial design (Table D.23a). For level II = III, the alternative load path is activated. It is assumed the roof plate construction is sufficiently resistant. Then, the residual strength is determined by the reserve capacity of the adjacent beams (they are considered to be of equal design, and likely to be subjected to similar loads at the same time). The reserve capacity is $M_{d,0} - M_{uls,II}$. The

¹⁷ Considering this result, the load carrying capacity of the adjacent beams is probably not governing.

alternative load path provides sufficient residual strength when $M_{d,0} - M_{uls,II} \geq 0.5M_{uls,II}$ (assuming each adjacent beam will carry half the loads on the failed beam). Tables D.23b and c provide the reserve capacities and checks. The design passes the redundancy requirements.

The fracture mode of this element is considered to be B (see previous remarks).

The safety requirements and element behaviour have been summarized in Figure D.10. This redesign meets all safety requirements for this application.

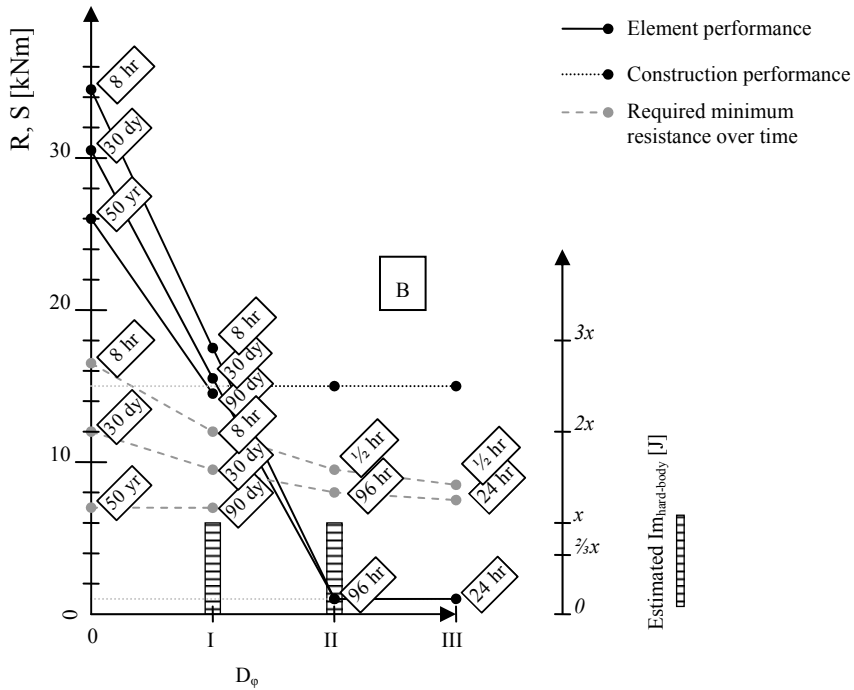


Fig. D.10 ESD of the initial glass beam design, with an enhanced construction to allow for an alternative load path by catenary action. In table D.23c, it was shown the capacity of the adjacent beams is sufficient, but probably not governing. The resistance of the alternative load path will depend on the structural behaviour of the beam-glass plate joints. It is assumed here they will have a time-independent resistance of 15 kNm. The dotted line marks the resistance of the 2nd LTM. This design meets all resistance and redundancy requirements.

Appendix E: Failure Behaviour of Glass Beams

A large quantity of glass beams has been subjected to three different test methods based on 4-point bending. Specimens were either tested directly or after having been damaged by a spring-loaded impact device. The latter group was subdivided in a set that was damaged to level III without external load and a set being damaged to level I or II, while simultaneously being subjected to a static load. The specimen variables included the most important commonly available design- and material specifications: two or three layers, PVB or SG laminated, annealed, heat strengthened or thermally tempered. Furthermore, stainless steel reinforced beams bonded with GB368 adhesive or laminated with SG, were also tested. The influence of damage on resistance and post-failure resistance was analyzed and a number of common assumptions was investigated. Conclusions were drawn with regard to impact and damage sensitivity as well as to initial and post-failure behaviour. The results have been used in Chapter 7 to construct Element Safety Diagrams and assess the safety of the designs.

1. Introduction

A large set of glass beams has been subjected to experimental testing to investigate failure behaviour and safety. A range of beam designs was applied, differing by the most common design parameters: double- or triple-layer; annealed, heat strengthened, or thermally tempered; PVB or SG laminated. Additionally, two design concepts that have been developed within the Zappi Glass & Transparency framework, were tested: stainless steel reinforced glass beams bonded with Delo GB368 uv-curing adhesive or SG laminated.¹

Three test methods were applied: 4-point bending ('direct', 'dir'), 4-point bending after damage by hard-body concentrated impact to all edges ('predamaged', 'pd'), and 4-point bending after damage by simultaneous static load and hard-body concentrated impact on one or two layers ('static+impact', 'st+i'). These methods were custom developed to obtain the relevant data to be used in Chapter 7 to determine construct preliminary Element Safety Diagrams (ESD)² for each design. Specifically, this meant constructing a method and apparatus ('impact device') to acquire the relevant model damage levels and test their resistance.

Besides generating data to construct ESDs, this study served to clarify a number of issues related to failure behaviour of glass beams in relation to impact damage:

¹ The failure behaviour of SG-laminated and GB368-bonded reinforced glass beams in direct 4-point bending has been extensively analysed and discussed in Appendix I. Some experimental data were borrowed from that study to complete the analysis presented here.

² A number of new concepts are used in this appendix, such as physical and structural damage, impact, Element Safety Diagram (ESD), model damage level, load transfer mechanism (LTM), etc. These have been introduced and explained in Chapter 6.

- Is the general assumption valid that one broken layer in a laminate with other layers still unbroken, can be ignored when calculating the resistance, or may it still contribute (significantly) to the overall resistance e.g. by carrying compressive loads?
- Does impact damage that originates in a single layer spread through to other layers (e.g. by shock waves), or can it be considered to provide a reasonable protection for other layers?
- Is there a significant difference in the failure behaviour of undamaged and damaged specimens (other than, off course, the maximum resistance)?
- Is there significant difference in the damage sensitivity of annealed, heat strengthened, and thermally tempered glass, and is there such a difference between PVB- and SG-laminated glass?
- What is the influence of the presence of a static load during impact on the physical damage created by that impact?
- May the presence of a static load equal to the calculable resistance of an undamaged layer, at the moment of impact on another layer, cause premature failure?
- Can conclusions be drawn concerning the relation between physical and structural damage?
- What resistance may be expected of 2nd LTMs in the various designs (what is the influence of the design parameters)?

2. Experimental Method

2.1. Specimens

Specimens of 13 different designs were tested. They are listed and described in Table E.1. Three test methods have been applied. These are further explained in the subsequent Sections. The quantity of specimens per test method is summarized in Table E.2. Unfortunately, only a few heat strengthened and thermally tempered SG-laminated specimens were available. Figures H.1a – f present sections of the specimen types.

Table E.1 Specimen designs.

Specimen Type	Beam design description					
	Geometry			Laminate / Bond	Heat Treatment	W [10^3 mm^3]
	t_{glass} [mm]	h [mm]	l [mm]			
2.PVB.A	2x10 = 20	120	1500	PVB	Annealed	48.0
2.PVB.S	2x10 = 20	120	1500	PVB	Heat Strengthened	48.0
2.PVB.T	2x10 = 20	120	1500	PVB	Thermally Tempered	48.0
3.PVB.A	3x10 = 30	120	1500	PVB	Annealed	72.0
3.PVB.S	3x10 = 30	120	1500	PVB	Heat Strengthened	72.0
3.PVB.T	3x10 = 30	120	1500	PVB	Thermally Tempered	72.0
2.SG.A	2x10 = 20	120	1500	SG	Annealed	48.0
2.SG.S	2x10 = 20	120	1500	SG	Heat Strengthened	48.0

2.SG.T	2x10 = 20	120	1500	SG	Thermally Tempered	48.0
3.SG.A	3x10 = 30	120	1500	SG	Annealed	72.0
3.SG.S	3x10 = 30	120	1500	SG	Heat Strengthened	72.0
3re.GB368.A	6-10-6 = 22	125	1500	GB368, reinforced	Annealed	57.3
3re.SG.A	6-10-6 = 22	125	1500	SG, reinforced	Annealed	57.3

Table E.2 Quantity of tested specimens per type, per method.

Specimen Type	Test Method	Qty.	Specimen Type	Test Method	Qty.
2.PVB.A	Direct	3	2.SG.A	Direct	3
	Predamaged*	4		Predamaged	2
	Static+Impact	3		Static+Impact	3
2.PVB.S	Direct	3	2.SG.S	Direct	1
	Predamaged	3		Predamaged	-
	Static+Impact	3		Static+Impact	-
2.PVB.T	Direct	3	2.SG.T	Direct	-
	Predamaged	3		Predamaged	-
	Static+Impact	3		Static+Impact	1
3.PVB.A	Direct	4	3.SG.A	Direct	3
	Predamaged	2		Predamaged	2
	Static+Impact	3		Static+Impact	2
3.PVB.S	Direct	2	3.SG.S	Direct	1
	Predamaged	2		Predamaged	-
	Static+Impact	2		Static+Impact	1
3.PVB.T	Direct	3			
	Predamaged	-			
	Static+Impact	3			
3re.GB368.A	Direct**	6	3re.SG.A	Direct**	5
	Predamaged*	4		Predamaged	2
	Static+Impact	3		Static+Impact	2
TOTAL					90

* One of these specimens was damaged on the side (see Section 2.2.2.)

** results imported from Appendix I.

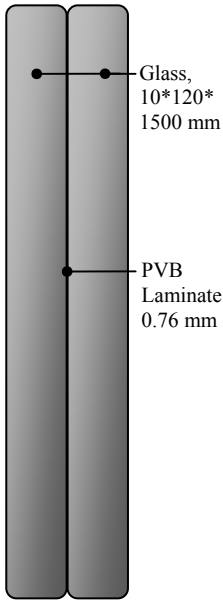


Fig. E.1a Specimen Types: 2.PVB.A, 2.PVB.S, 2.PVB.T

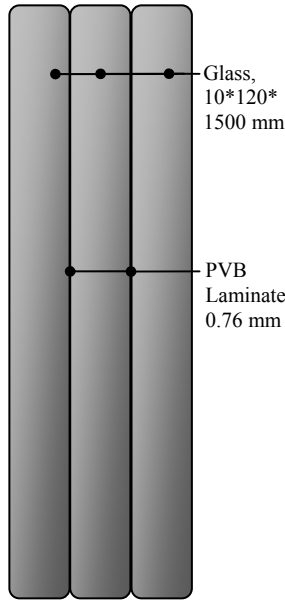


Fig. E.1b Specimen Types: 3.PVB.A, 3.PVB.S, 3.PVB.T

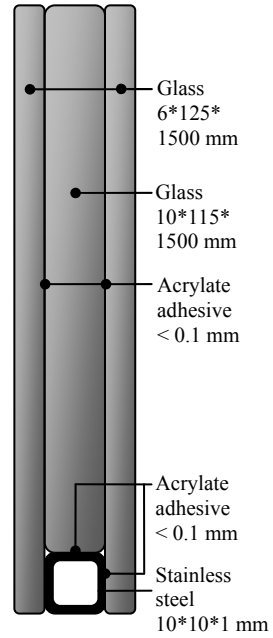


Fig. E.1c Specimen Type: 3re.GB368.A

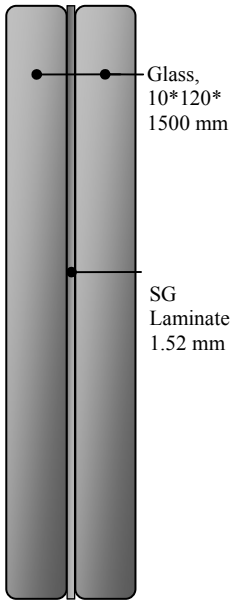


Fig. E.1d Specimen Types: 2.PVB.A, 2.PVB.S, 2.PVB.T

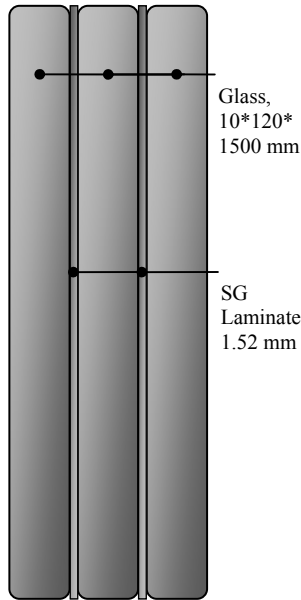


Fig. E.1e Specimen Types: 3.SG.A, 3.SG.S

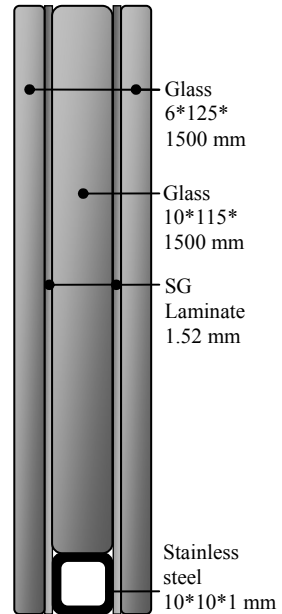


Fig. E.1f Specimen Type: 3re.SG.A

2.2. Test Methods

2.2.1. Direct

A number of 37 specimens was tested directly in displacement-controlled 4-point bending. The load span was 400 mm; the support span 1400 mm (Figure E.2). Initially, the specimens were tested at a displacement speed of 2 mm/min. The tests were stopped at initial failure (e.g. when the primary load transfer mechanism ceases to be active). Specimens with significant post-failure strength were subsequently tested at an increased displacement speed of 5 mm/min. The double layer specimens were supported laterally to avoid lateral torsional buckling at approximately 400 mm from each support point. For the triple layer specimens, this was deemed unnecessary.

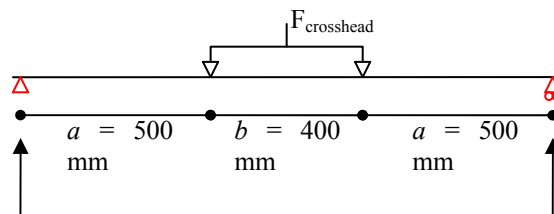


Fig. E.2 Lay-out of four-point bending test.

2.2.2. Pre-damaged

A group of 24 specimens was damaged previously to being subjected to a four-point bending test as described in Section 2.2.1. The damage was applied by consecutive impact to, first, the bottom edge of the front sheet and, second, the rear sheet (in double layer specimens), or to, first, the bottom edge of the rear sheet, second, the front sheet, and, third, the middle sheet (triple layer specimens). The damages were applied at mid-span with the specimen in the bending set-up (Figure E.3). The goal of the impacts was to create model level III damage to a specimen by creating vertical cracks through the width, over the height of the beam (Figure E.4). To create the damage, a custom-made spring-loaded impact device with an impact tip from hardened tool steel was used, described in detail in Section 2.3.

Not all specimens proved to be able to carry their self-weight after having been damaged in this fashion, but the specimens which did have significant post-failure strength were subjected to four-point bending as described in Section 2.2.1 after application of the damage.

It proved impossible to crack the inner layer of the reinforced specimens in the fashion described above. Therefore, instead of applying the impact on the bottom edge, the specimens were turned and the impact was applied to the top edge of the inner sheet.

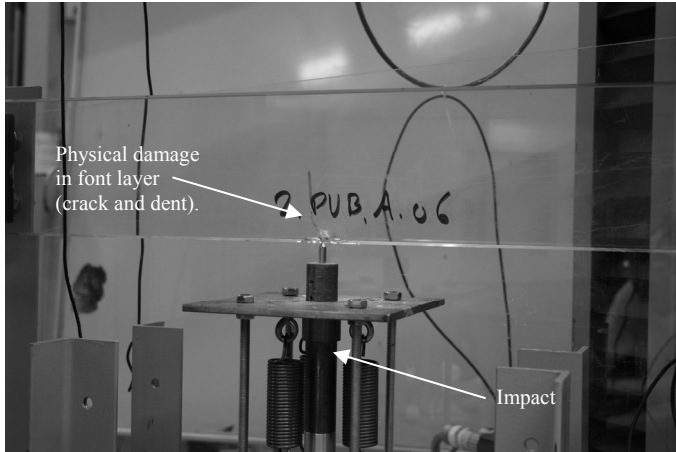


Fig. E.3 Double layer, annealed glass specimen in 4-point bending set-up, after first impact (in front layer).

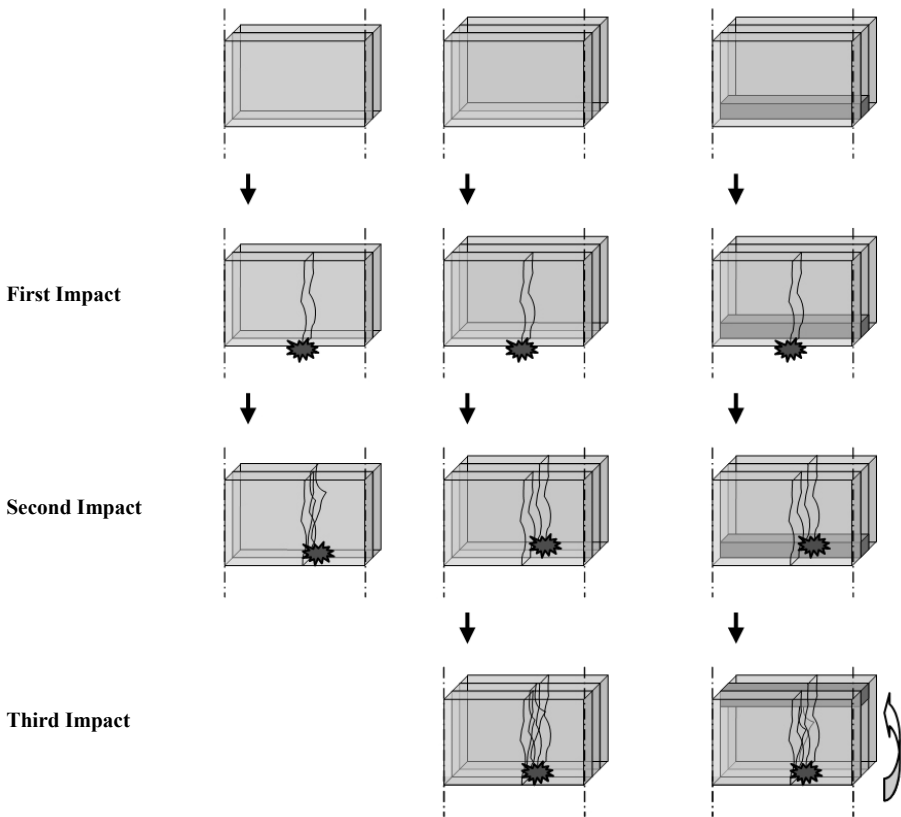


Fig. E.4 Impact sequence to create model level III damage in (from left to right) double layer, triple layer, and reinforced specimens.

Additionally to the edge-impacted specimens, two specimens (one of type 2.PVB.A and one of type 3re.GB368.A) were impacted from one side before 4-point bending, at mid span and mid height of the beam, specifically to investigate whether the GB368-bonded, reinforced specimens would be more susceptible to side damage than to edge damage (Figure E.5a and b).



Fig. E.5a, b 2.PVB.A specimen before being subjected to side impact, and after side impact in 4-point bending test set-up.

2.2.3. Static and Impact Load

Another set of 29 specimens was damaged by a combination of impact and a simultaneous static load. As with the specimens in the previous group, the impact was applied consecutively to the bottom edge of the glass layers in specimens with the use of the impact device described in Section 2.3. However, the damage was only applied to one outer layer in the double layer specimens, or both outer layers in the triple layer specimens, and thus to create model level I and model level II damage, respectively (instead of model level III).

During the impact, the specimens were subjected to a constant, force controlled, 4-point bending load (Figure E.6). It was applied at 50 N/s. The impact was always applied within 60 s after reaching the maximum load. For the double layer specimens, the constant load was one half of the calculable resistance ($0.50 \cdot R_d$) applied for 600 s. Triple layer specimens were first loaded for two-thirds of their calculable resistance ($0.67 \cdot R_d$) for 300 s. The first impact was delivered. Subsequently, they were loaded to one-third of their calculable resistance ($0.33 \cdot R_d$), again for 300 s, before the second impact hit.

This presence of a static load stimulated crack growth in the desired direction (to create model damage levels).

After the damage had been applied, the specimens were subjected to destructive 4-point bending as described in Section 2.2.1.

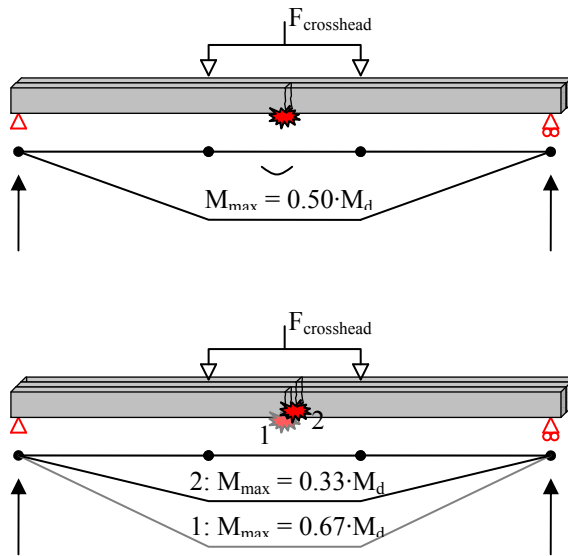


Fig. E.6 Impact sequence and static load on double (top) and triple (bottom) layer specimens.

2.3. Impact Device

The damages were created using a custom-made impact device (Figure E.7). Some other options have been considered, but proved unsuitable: the impact created with a hammer and chisel could not be measured and would not be equal in repetitive blows, a fall-tower or similar set-up would make it difficult to apply static loads, standard centre-punches do not yield enough force to create the desired damages, and working with small explosives proved very elaborate and also gave dubious results with regard to the cracking pattern.

The head of the impact device consists of a thin, flat hardened steel tip (similar to a screwdriver) on a steel shaft. The flat is oriented perpendicularly to the glass sheet edge. The shaft is connected through a steel disk to three tension springs (Alcomex T1930; $d_{\text{thread}} = 2.5 \text{ mm}$; $d_{\text{spring,centre}} = 25.5 \text{ mm}$). The springs can be strained by pressing the steel disk to an electromagnet (Maasland Security DH502A). By shifting the electromagnet along four M10 threads, the force and energy of the impact can be controlled. The springs are released simply by pressing a button on the electromagnet.

The force-displacement relation of the impact device springs has been determined by a simple compression test on the shaft of the impact device (Figure E.8). The energy content is determined by the equation in Figure E.9. Table E.3 gives the forces and corresponding spring energy values for the displacements used in the experiments.

Although the force-displacement and energy-displacement relations could be established relatively easily, it could not be determined what quantity of the impact energy is transferred into the glass at the moment of impact. The stored energy before release was considered a sufficiently reliable measure for comparison purposes and to determine a preliminary damage sensitivity.

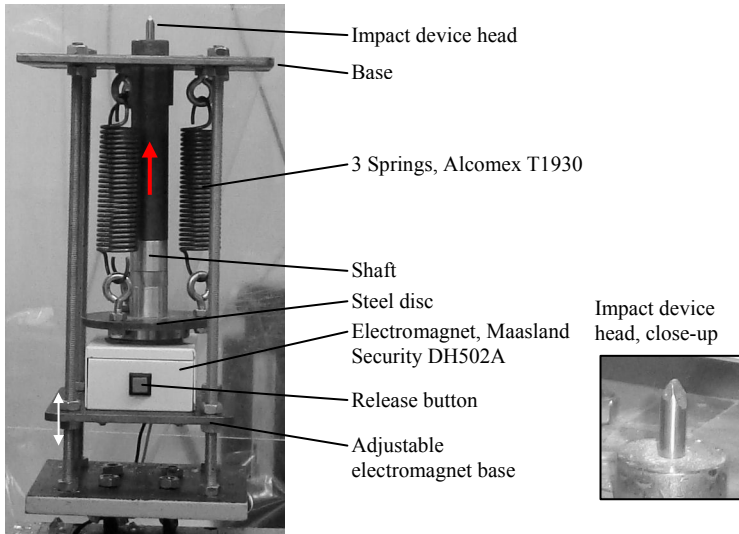


Fig. E.7 The impact device.

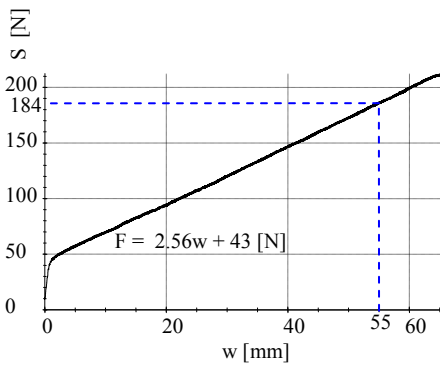


Fig. E.8 Load-displacement graph of the impact device. The maximum in service displacement is 55 mm, which requires 184 N.

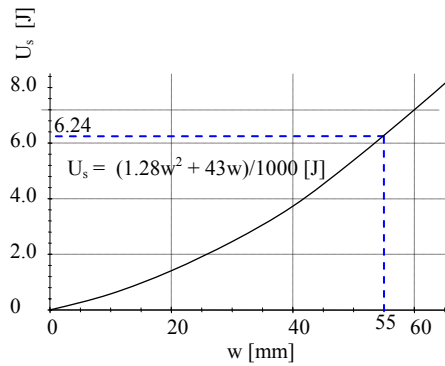


Fig. E.9 Spring energy-displacement graph of the impact device. At $w = 55$ mm, $U_s = 6.24$ J.

Table E.3 Displacements, forces, and spring energies for the impact device.

w [mm]	S [N]	U_s [J]	w [mm]	S [N]	U_s [J]
10	68.6	0.56	35	132.6	3.07
15	81.4	0.97	40	145.4	3.77
20	94.2	1.37	45	158.2	4.53
25	107.0	1.88	50	171.0	5.35
30	119.8	2.44	55 (max)	183.8	6.24

3. Results

The subsequent Sections 3.1 – 3.3 summarize the experimental results per experiment type. Relevant observations have been added.

3.1. Direct Four-Point Bending Tests

Tables H.4a – e present the results of the direct 4-point bending tests. They tabulate both the initial failure strength R_0 and the post-failure strength $R_{res,III}$ – if any. The results are primarily presented in terms of maximum bending moment (i.e. in kNm). The ratio M/t has been added to correct for the differences in section thickness. For stages in which the glass is still active, the failure stresses of the remaining part of the section have also been noted.

Note that, due to practical reasons of the execution of the experiment, specimen names in pictures may not correspond to those in the text. Principally, the names in the text and captions should be considered to be correct and consistent.

Observations with Table E.4a:

- In direct 4-point bending, most specimens (annealed, strengthened, and tempered) failed by simultaneous breakage of all layers at the same or almost the same location. Specimen 2.PVB.A_2 had a deviating failure mode: during loading a V-crack appeared in only one layer (thus, the specimen accumulated damage). Upon reloading, the specimen failed by two more dense V-cracks in both layers near each other. Thus, the failure behaviour was more similar to that of the specimens tested in 4-point bending after damage by impact and static load. Although not common, this type of failure behaviour has been witnessed before by the author in other experiments.
- The failure stress of the annealed specimens was as expected. The average failure stress of the strengthened and tempered specimens was well above the representative strengths given by glass engineering codes as well as previous research results presented by Veer et al.³ Especially with regard to the strengthened specimens it should be noted that they did not show a very dense cracking pattern, thus did not have too much prestress. Perhaps the edge work was of particularly fine quality, but a final explanation remains evasive.
- The annealed specimens had a very small amount of post-failure strength, just above or just below their self weight, depending on the specimen. The strengthened specimens, on the other hand, released so much energy at failure that the PVB ruptured and the specimens broke in two pieces, thus resulting in no post-failure strength whatsoever. Remarkably, although the tempered specimens held even more energy at failure, they did not break at failure. This should be attributed to the fact that the dense cracking pattern allows the energy release to be distributed over a large area of PVB, while with the strengthened specimens it is concentrated around a limited number of cracks. After failure, the tempered specimens slowly sag under their self weight until the maximum displacement of the experimental set-up is reached.

³ Veer, F.A., Louter, P.C., Bos, F.P., Romein, T., Ginkel, H. van, Riemsdag, A.C., *The Strength of Architectural Glass*, Proceedings of the Challenging Glass Conference, Delft, the Netherlands, May 2008.

Table E.4a Results of direct 4-point bending tests; double layer PVB laminated specimens.

Specimen	R_0			R_{III}	
	M_0 [kNm]	M_0/t [10 ³ kNm/mm]	σ_0 [MPa]	M_{III} [kNm]	M_{III}/t [10 ³ kNm/mm]
2.PVB.A					
1	2.43	121.5	50.6	0.015*	0.75
2	1.32****	66.1	27.6	0.010**	0.50
3	2.36	117.8	49.1	0.035	1.75
Ave	2.39	119.7	49.8	0.025	1.00
Rel. SD	2.22 %			56.6 %	
2.PVB.S					
1	6.07	303.3	126.4	0***	-
2	6.02	300.8	125.3	0***	-
3	5.84	292.0	121.7	0***	-
Ave	5.97	298.7	124.4	0	-
Rel. SD	1.98 %			0	
2.PVB.T					
1	7.99	399.5	166.5	0.010**	0.50
2	7.62	380.8	158.6	0.010**	0.50
3	7.94	397.0	165.4	0.010**	0.50
Ave	7.85	392.4	163.5	0.010	0.50
Rel. SD	2.59 %			0	

* The post-failure strength was approximately equal to the self weight of this specimen ($q_{sw} = 0.06$ kN/m; $M_{max,sw} = 0.015$ kNm).

** Although these specimens did not break, they slowly sagged under their self weight. Their post-failure strength was arbitrarily estimated at two-thirds of their self weight (i.e. 0.010 kNm).

*** These specimens broke into two pieces at failure.

**** This specimen had deviating failure behaviour and was not considered for the calculation of the average. See observations below.

Observations with Table E.4b:

- The average failure stress of the annealed and strengthened triple layer specimens is considerably lower – approximately 20 % – than the failure stress of the double layer specimens. This may be caused by the weakest link effect: the probability of a larger defect is higher in a triple layer specimen than in a double layer one. However, it is questionable whether this could explain such a big difference. Statistical effects (only small numbers of specimens were tested) may also play a role. The tempered triple layer specimens show only a minor drop in failure stress in comparison to the double layer ones.

- The failure behaviour and post-failure strength of strengthened and tempered triple layer specimens is comparable to the double layer ones. The annealed triple layer specimens however, yield considerably more post-failure strength, both absolutely ($M_{III, triple, ave} / M_{III, double, ave} = 3.2$) and relatively ($(M/t)_{III, triple, ave} / (M/t)_{III, double, ave} = 2.7$). Since the post-failure strength is more than doubled, the increase is higher than should be expected based on the increase in the amount of PVB alone. The extra amount of PVB increases the bending stiffness in the post-failure stage, which allows for a change in load transfer mechanism. This is further discussed in Section 4.3.2. Nevertheless, the post-failure strength is still very low compared to the failure strength ($R_{III, ave} / R_{0, ave} = 0.08 / 2.7 = 0.03$).

Table E.4b Results of direct 4-point bending tests; triple layer PVB laminated specimens.

Specimen	R_0			R_{III}	
3.PVB.A	M_0 [kNm]	M_0/t [10 ³ kNm/mm]	σ_0 [MPa]	M_{III} [kNm]	M_{III}/t [10 ³ kNm/mm]
1	2.67	89.1	37.1	0.12	4.0
2	2.80	93.2	38.8	0.05	1.6
3	2.70	89.9	37.5	0.09	3.1
4	2.65	88.2	36.8	0.07	2.3
Ave	2.70	90.1	37.5	0.08	2.7
Rel. SD	2.43 %			37.7 %	
3.PVB.S	M_0 [kNm]	M_0/t [10 ³ kNm/mm]	σ_0 [MPa]	M_{III} [kNm]	M_{III}/t [10 ³ kNm/mm]
1	9.00	299.9	125.0	0**	-
2	5.75	191.6	79.8	0**	-
Ave	7.37	245.8	102.4	0**	-
Rel. SD	31.17 %			0	
3.PVB.T	M_0 [kNm]	M_0/t [10 ³ kNm/mm]	σ_0 [MPa]	M_{III} [kNm]	M_{III}/t [10 ³ kNm/mm]
1	10.77	359.1	149.6	0.015*	0.5
2	11.22	374.1	155.9	0.015*	0.5
3	11.42	380.7	158.6	0.015*	0.5
Ave	11.14	371.3	154.7	0.015	0.5
Rel. SD	2.99 %			0	

*Although these specimens did not break, they slowly sagged under their self weight. Their post-failure strength was arbitrarily estimated at two-thirds of their self weight ($q_{sw} = 0.09$ kN/m; $M_{max, sw} = 0.022$ kNm, i.e. $M_{III} = 0.015$ kNm).

** These specimens broke into two pieces at failure.

Observations with Table E.4c:

- The glass in the SG laminated specimens came from another badge and manufacturer.
- The failure strength of the annealed specimens is rather low. This may depend on the glass edge quality and therefore on the manufacturer.
- Contrary to the PVB-laminated specimens, the heat strengthened SG laminated specimens did not break upon failure. This is not only due to the fact that SG is stronger, but also that it is twice as thick. The extremely small time frame in which the glass beam strain energy is released makes the higher SG Young's modulus irrelevant, as the time-dependency of polymer stiffness is irrelevant.
- The post-failure strength of the strengthened specimens is just below that of the annealed specimens. This may be caused by the somewhat more intense cracking pattern which allows less compression build-up in the broken glass, but it may also be due to statistical effects. As could be expected, the internal prestress in the glass does not play a role in the 2nd LTM.
- Final failure is eventually caused by the SG starting to rupture.⁴ This was not observed with the PVB specimens. The PVB failure strain is so high that final failure could not be obtained within the test set-up displacement limits.

Table E.4c Results of direct 4-point bending tests; double layer SG laminated specimens.

Specimen	R ₀			R _{III}	
	M ₀ [kNm]	M ₀ /t [10 ³ kNm/mm]	σ ₀ [MPa]	M _{III} [kNm]	M _{III} /t [10 ³ kNm/mm]
1	1.51	75.5	31.5	0.34	17.0
2	2.20	110.1	45.9	0.34	16.8
3	1.75	87.3	36.4	0.31	15.6
Ave	1.82	91.0	37.9	0.33	16.5
Rel. SD	19.4 %			4.45 %	
2.SG.S	M ₀ [kNm]	M ₀ /t [10 ³ kNm/mm]	σ ₀ [MPa]	M _{III} [kNm]	M _{III} /t [10 ³ kNm/mm]
	1	5.34	267.0	111.3	0.28

Observations with Table E.4d:

- The decrease in failure strength between annealed and strengthened 2- and 3-layer beams as observed with the PVB-laminated specimens, here only occurs for the strengthened specimens. Generally, it should be concluded too few specimens have been tested to make any definite conclusions on this issue.

⁴ In similar experiments, Belis et al. found that the SG started to rupture much earlier than should be expected based on tensile tests on SG samples: Belis, J., Depauw, J., Callewaert, D., Delincé, D., Impe, R. van, *Failure Mechanisms and Residual Capacity of Annealed Glass/SGP Laminated Beams at Room Temperature*, Engineering Failure Analysis, 2008 (article in press). The author suggests this may be due to notches (local damage, e.g. caused by sharp edges of broken glass). Some polymers, like e.g. PC, show have a high failure strain when undamaged. However, when a notch is present, the yielding concentrates around that notch, and the overall failure strain is significantly reduced. See AdDoc II, Section 4.2.8.

- Contrary to the PVB specimens, the post-failure strength of SG triple layer specimens is approximately twice as high as that of the double layer specimens – and thus proportional to the amount of SG in the section, which has also doubled. This indicates the 2nd LTM in the double and triple layer specimens work the same. See Section 4.3.2.

Table E.4d Results of direct 4-point bending tests; triple layer SG laminated specimens.

Specimen	R_0			R_{III}	
	M_0 [kNm]	M_0/t [10 ³ kNm/mm]	σ_0 [MPa]	M_{III} [kNm]	M_{III}/t [10 ³ kNm/mm]
1	2.72	90.7	37.8	0.72	23.9
2	2.80	93.2	38.8	0.64	21.3
3	3.25	108.2	45.1	0.63	20.9
Ave	2.92	97.4	40.6	0.66	22.0
Rel. SD	9.72 %			7.37 %	
3.SG.S	M_0 [kNm]	M_0/t [10 ³ kNm/mm]	σ_0 [MPa]	M_{III} [kNm]	M_{III}/t [10 ³ kNm/mm]
	1	5.87	195	5.7	0.63

Observations with Table E.4e:

- The SG-laminated reinforced specimens have a high failure strength, compared to all other annealed specimens. No specific cause could be identified for this difference.
- The post-failure strength and behaviour is completely different from that observed with the PVB- and SG-laminated specimens. The capacity of the 2nd LTM is consistently higher than of the 1st LTM. The behaviour of SG-laminated and GB368 bonded specimens is extensively discussed in Appendix I.

Table E.4e Results of direct 4-point bending tests; reinforced specimens.⁵

Specimen	$R_{0,pd}$			$R_{III,pd}$	
	M_0 [kNm]	M_0/t [10 ³ kNm/mm]	σ_0 [MPa]	M_{III} [kNm]	M_{III}/t [10 ³ kNm/mm]
1	2.87	130.5	50.0	3.54	161.0
2	2.74	124.6	47.9	3.22	146.2
3	2.34	106.5	40.9	3.57	162.1
4	2.19	99.6	38.3	3.67	166.7
5	2.47	112.1	43.1	3.49	158.7
6	2.49	113.3	43.5	3.54	161.0

⁵ Data taken from experimental research described in Appendix I.

Ave	2.52	114.4	43.9	3.50	159.3
Rel. SD	9.93 %			4.35 %	
3re.SG.A	M₀	M₀/t	σ₀	M_{III}	M_{III}/t
	[kNm]	[10³ kNm/mm]	[MPa]	[kNm]	[10³ kNm/mm]
1	2.87	130.3	50.0	4.24	192.8
2	2.69	122.4	47.0	4.39	199.6
3	3.22	146.2	56.1	4.47	203.1
4	3.27	148.5	57.0	4.52	205.3
5	2.95	134.2	51.5	4.38	199.2
Ave	2.95	134.2	51.5	4.38	199.2
Rel. SD	10.45 %			2.63 %	

3.2. Predamaged

In Table E.5a – e, the results of the 4-point bending tests on the specimens predamaged by impact are given. The sequence of impacts (in terms of impact energy) is listed, along with the failure load to level III (if any), and the post-failure strength (if any). In principal, the impact energies were chosen so as to obtain model level III damage in the specimens.

For a number of specimens, it was necessary to apply multiple impacts to find the right impact energy to create such damage. This is presented by the ‘impact sequence’ in the tables. ‘O_1’, ‘O_2’, and ‘Inn’ refer to the first outer layer, second outer layer, and the inner layer, respectively (obviously, only triple layer specimens have an inner layer).

Observations with Table E.5a, for the annealed specimens:

- In general, it proved difficult to obtain the desired extent of physical damage in laminated annealed glass specimens. Even with the impact device in maximally strained position, the right result was not always obtained after a single or sometimes multiple impacts, while with preliminary tests, on the other hand, it had proven to be quite easy to break single, annealed glass sheets of similar geometry. Thus, the presence of a laminate significantly reduces the elements damage sensitivity.
- Although not always obtained, the typical damage caused by an 6.24 J impact with the impact device consisted of a dent and a vertical crack as in Figure E.10 (specimen 2.PVB.A_2).
- Specimen 2.PVB.A_1 was not damaged completely to level III after the impacts (Figure E.11). Therefore, it was first tested to initial failure. It appeared the resistance of the damaged element was already diminished to only $\sigma_{0,pd,nom} = 5.40$ MPa (considering nominal section). Due to the low initial failure stress the post-failure strength was similar to the specimens which had been directly damaged to level III by the impact device.
- The post-failure resistance is significantly higher than for the directly tested specimens (Table E.4a). This is due to the small amount of cracks at (initial) failure ($M_{III,pd,ave} = 0.086$ kNm; $M_{III,dir,ave} = 0.025$ kNm). See Section 4.3.2.

Table E.5a Results of 4-point bending tests after predamage; double layer PVB laminated specimens.

Specimen	Impact Sequence [J]	R_{pd}			$R_{III,pd}$	
		M_{pd} [kNm]	M_{pd}/t [10 ³ kNm/mm]	σ_{pd} [MPa]	M_{III} [kNm]	M_{III}/t [10 ³ kNm/mm]
2.PVB.A						
1	O_1: 6.24 J O_2: 6.24 J	0.26	13.0	5.40	0.082	4.09
2	O_1: 6.24 J**	-			0.098	4.88
3	O_1: 6.24 J O_2: 6.24 J	-			0.080	3.98
Ave					0.086	4.32
Rel. SD					11.4 %	
2.PVB.S						
1	O_1: 2.44 J; 2.44 J; 2.44 J; 2.44 J; 2.44 J; 2.44 J; 2.44 J; 3.07 J O_2: 3.07 J; 3.07 J; 3.07 J; 3.77 J; 3.77 J***	1.32	66.0	27.5	0.032	1.61
2	O_1: 3.77 J O_2: 3.77 J	1.04	52.1	21.7	0.025	1.25
3	O_1: 3.77 J O_2: 3.77 J	2.08	103.8	43.2	0.010*	0.50
Ave		1.48	74.0	30.8	0.022	1.12
Rel. SD			69.3 %		50.6 %	
2.PVB.T						
1	O_1: 0.56 J; ; 0.56 J; 1.37 J; 1.37 J O_2: 1.37 J; 1.37 J; 1.37 J; 1.37 J; 1.37 J; 1.88 J***	-			0.010*	0.50
2	O_1: 1.88 J; 1.88 J; 1.88 J; O_2: 1.88 J; 1.88 J; 1.88 J; 2.44 J***	-			0.010*	0.50
3	O_2: 2.44 J O_1: 2.44 J	-			0.010*	0.50
Ave					0.010	0.50

Rel. SD		0
---------	--	---

* Although these specimens did not break, they slowly sagged under their self weight. Their post-failure strength was arbitrarily estimated at two-thirds of their self weight (i.e. 0.010 kNm).

** Hits both layers simultaneously and introduces a crack in both layers.

*** Searching for the appropriate impact.

Observations with Table E.5a, for the heat strengthened specimens:

- A lower impact energy was used, as it was expected heat strengthened glass would be more damage sensitive because of the internal stress that may be released upon failure (see also thermally tempered specimens). However, this assumption proved incorrect. The applied impacts only created dents in the glass (Figure E.12). There seems to be no significant difference in damage sensitivity between annealed and heat strengthened glass.
- As with the annealed specimen, a relatively small dent does introduce a very serious resistance reduction ($\sigma_{pd,nom,ave} = 30.8$ MPa, compared to $\sigma_{0,dir,ave} = 124.4$ MPa).
- The failure behaviour is fundamentally different from that exhibited by the directly tested specimens. Due to the much smaller energy release, the PVB does not tear, thus the specimen does not break. Instead, it goes into a weak post-failure stage. The post-failure resistance is significantly smaller than for the annealed specimens, caused by the more intense fracture pattern (Figure E.13), and actually compares to the directly tested annealed specimens.

Observations with Table E.5a, for the thermally tempered specimens:

- Compared to the annealed and heat strengthened specimens, the tempered specimens require much less impact energy to create level III damage (only 2.44 J per impact, instead of at least 6.24 J). The difference is caused by the release of internal strain energy which fractures the whole sheet once the impact device penetrates the compressive layer.
- The post-failure resistance is comparable to that witnessed in the direct tests. Since the density of the fracture pattern is governed mainly by the internal prestress strain energy rather than the introduced energy by loading, the experiment type has no influence on the post-failure resistance.

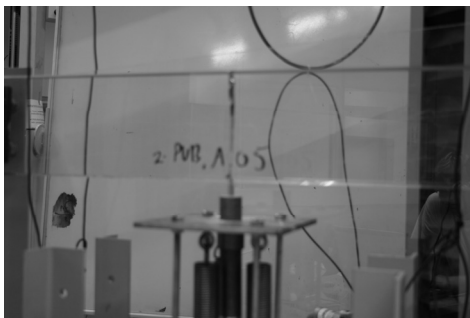


Fig. E.10 Typical physical damage in annealed glass specimens as caused by an 6.24 J impact from the impact device (specimen pd 2.PVB.A_2).

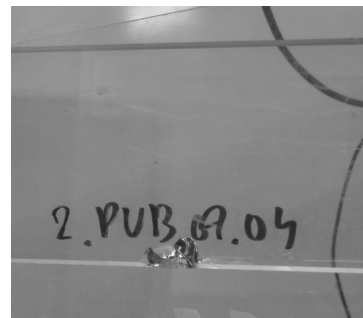


Fig. E.11 Level III damage could not be obtained in every annealed glass specimen, even with the impact device maximally strained (specimen pd 2.PVB.A_1).



Fig. E.12 Typical physical damage in heat strengthened as caused by an 3.77 J impact from the impact device (specimen pd 2.PVB.S_1).

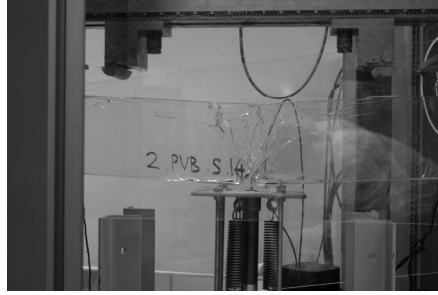


Fig. E.13 Post-failure behaviour of a double layer heat strengthened specimen (specimen pd 2.PVB.A_1).

Observations with Table E.5b:

- No thermally tempered triple layer specimens were tested with this experiment type as the result can reasonably be predicted from the directly tested triple layer specimens and the predamaged double layer specimens: they will sag under self-weight in the post-failure state.
- The post-failure strength both of annealed and heat strengthened triple layer specimens is approximately twice as high as that of the double layer specimens. Apparently, the amount of PVB in the section is governing for the 2nd LTM and the maximum post-failure resistance.
- As with the double layer specimens, the post-failure strength of the annealed specimens after predamage is significantly higher than in direct testing ($M_{III,pd,ave} = 0.16 \text{ kNm}$; $M_{III,dir,ave} = 0.082 \text{ kNm}$).
- The post-failure strength of the heat strengthened specimens is still significantly lower than that of the annealed specimens. Again, this is attributed to the crack pattern density.

Observations with Table E.5c:

- The laminate type has no noticeable influence on the elements damage sensitivity. It requires as much energy to create a certain amount of physical damage with PVB as with SG laminated specimens. The extremely small time frame in which the impact energy is transferred into the glass beam makes the higher SG Young's modulus irrelevant, as the time-dependency of polymer stiffness becomes irrelevant in this situation. Compare observations with Table E.4c.
- Contrary to the PVB laminated specimens, the SG laminated beams yield considerable post-failure resistance. The difference is greater than could be expected based on the difference in thickness and strength of the SG compared to the PVB. This indicates the load transfer mechanism is different. See Section 4.3.2.
- For both double and triple layer, the post-failure resistance is approximately 1.3 times as high as with the directly tested SG laminated specimens.

Table E.5b Results of 4-point bending tests after predamage; triple layer PVB laminated specimens.

Specimen	Impact Sequence [J]	R_{pd}			$R_{III,pd}$	
		M_{pd} [kNm]	M_{pd}/t [10 ³ kNm/mm]	σ_{pd} [MPa]	M_{III} [kNm]	M_{III}/t [10 ³ kNm/mm]
1	O_1: 6.24 J O_2: 6.24 J In: 6.24 J	-			0.14	4.78
2	O_1: 6.24 J O_2: 6.24 J In: 6.24 J; 6.24 J	0.33	11.2	4.6	0.18	5.98
Ave					0.16	5.38
Rel. SD					15.8 %	
3.PVB.S	Impact Seq. [J]	M_{pd} [kNm]	M_{pd}/t [10 ³ kNm/mm]	σ_{pd} [MPa]	M_{III} [kNm]	M_{III}/t [10 ³ kNm/mm]
1	O_1: 6.24 J O_2: 6.24 J In: 6.24 J; 6.24 J	2.08	69.3	28.9	0.043	1.44
2	O_1: 6.24 J O_2: 6.24 J In: 6.24 J; 6.24 J	1.96	65.2	27.2	0.039	1.30
Ave		2.02	67.3	28.0	0.041	0.91
Rel. SD			4.29 %		6.80 %	

Table E.5c Results of 4-point bending tests after predamage; SG laminated specimens.

Specimen	Impact Sequence [J]	R_{pd}			$R_{III,pd}$	
		M_{pd} [kNm]	M_{pd}/t [10 ³ kNm/mm]	σ_{pd} [MPa]	M_{III} [kNm]	M_{III}/t [10 ³ kNm/mm]
1	O_1: 6.24 J O_2: 6.24 J	-			0.51	25.4
2	O_1: 6.24 J O_2: 6.24 J	-			0.37	18.3
Ave		-			0.44	21.9
Rel. SD					23.1 %	
3.SG.A	Impact Seq. [J]	M_{pd} [kNm]	M_{pd}/t [10 ³ kNm/mm]	σ_{pd} [MPa]	M_{III} [kNm]	M_{III}/t [10 ³ kNm/mm]
1	O_1: 6.24 J O_2: 6.24 J	-			0.95	31.6

	In: 6.24 J			
2	O_1: 6.24 J; 6.24 J O_2: 6.24 J In: 6.24 J	-	0.74	24.7
Ave		-	0.84	28.2
Rel. SD				17.2 %

Observations with Table E.5d:

- The reinforced specimens could not be damaged in the same way the (triple layer) ordinary laminate beams were damaged. The reinforcement profile acts as a protective barrier to damage from the bottom edge. Repeated impacts on the reinforcement only resulted in some dents in the steel, but no visible consequences in the glass. Therefore, the specimens had to be turned upside down and impacted from above to obtain similar damage (Figures H.14a, b).
- The damage sensitivity of the outer layers may be somewhat larger than of the other specimens as they are thinner (6 mm instead of 10 mm). However, no significant differences have been observed.
- The influence of damage on both the initial R_{pd} and final resistance R_{III} is small in the GB368 bonded as well as the SG laminated specimens. Apparently, a local crack bridge is formed which causes cracks only to increase when the applied load comes close to the undamaged resistance. The relative differences are:

- o $R_{pd,ave,GB368} / R_{0,dir,ave,GB368} = 2.11/2.52 = 0.84,$
- o $R_{III,pd,ave,GB368} / R_{III,dir,ave,GB368} = 3.25/3.50 = 0.93,$
- o $R_{pd,ave,SG} / R_{0,dir,ave,SG} = 3.24/2.95 = 1.10,$
- o $R_{III,pd,ave,SG} / R_{III,dir,ave,SG} = 3.74/4.38 = 0.85.$

The differences are practically within the limits of the statistical variations. Thus, the damages hardly have any influence on the resistances.

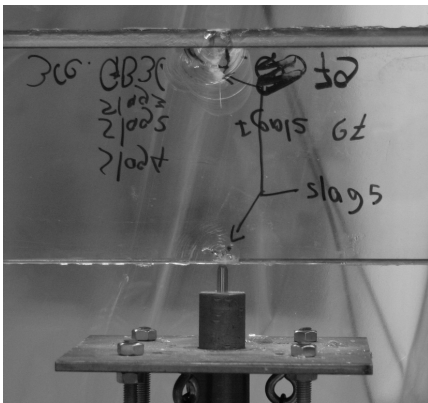


Fig. E.14a Typical physical damage in GB368 bonded, reinforced specimens (pd 3re.GB368.A_1).



Fig. E.13 Typical post-failure behaviour of a GB368 bonded, reinforced specimen (pd 3re.GB368.A_2).

Table E.5d Results of 4-point bending tests after predamage; reinforced specimens.

Specimen	Impact Sequence [J]	R_{pd}			$R_{III,pd}$	
		M_{pd} [kNm]	M_{pd}/t [10 ³ kNm/mm]	σ_{pd} [MPa]	M_{III} [kNm]	M_{III}/t [10 ³ kNm/mm]
3re. GB368.A	O_1: 6.24 J O_2: 6.24 J In: 6.24 J*; : 6.24 J**; : 6.24 J*	2.09	95.2	36.6	2.99	136.0
	O_1: 6.24 J O_2: 6.24 J In: 6.24 J**	2.50	113.5	43.6	3.59	163.3
	O_1: 6.24 J O_2: 6.24 J In: 6.24 J**, 6.24 J	1.74	79.1	30.4	3.17	144.0
	Ave	2.11	95.9	36.8	3.25	147.8
Rel. SD		18.0 %			9.49 %	
3re.SG.A	Impact Seq. [J]	M_{pd} [kNm]	M_{pd}/t [10 ³ kNm/mm]	σ_{pd} [MPa]	M_{III} [kNm]	M_{III}/t [10 ³ kNm/mm]
	O_1: 6.24 J O_2: 6.24 J In: 6.24 J**	3.39	154.2	59.2	3.87	175.8
	O_1: 6.24 J O_2: 6.24 J In: 6.24 J**	3.09	140.6	54.0	3.62	164.4
Ave	3.24	147.4	56.6	3.74	170.1	
Rel. SD		5.45 %			4.72 %	

* on reinforcement (bottom edge)

** specimen turned, on top edge.

Observations with Table E.5e:

- Even with repeated impact, the cracks in both specimens are limited to the directly affected layer (Figure E.15).
- Three impacts on the 2.PVB.A specimen cause a dent and some radial cracks; three impacts on the 3re.GB368.A specimen only causes a dent (Figures H.17 and I.18). The glass stiffness in the plane perpendicular to the impact direction seems to influence the amount of cracking that results from an impact (similar preliminary tests on a single layer glass sheet resulted in breakage).
- As could be expected, compared to the undamaged specimens, the 2.PVB.A shows a significant reduction in resistance ($R_{side-d,2,PVB.A} / R_{0,dir,ave,2,PVB.A} = 1.07/2.39 = 0.45$). Since only one layer was damaged, the results should best be compared with those of the static+impact tested specimens (Table E.6a).

Surprisingly (since the damage is on the neutral axis, rather than at the maximally stressed bottom edge), the resistance of the side impacted specimen is even lower than the resistance of those specimens ($R_{\text{side-d},2.\text{PVB.A}} / R_{0,\text{st+i,ave},2.\text{PVB.A}} = 1.07/1.65 = 0.65$). Other than possible statistical variations, no explanation for this was found.

- The high post-failure strength of the 2.PVB.A specimen is caused by the fact that the crack origins in both layers do not coincide (Figure E.18) (this may be coincidental). Thus, the PVB in the overlap is loaded in shear and can still transfer significant forces. This indicates that the post-failure strength of elements tested in a way that damages do not coincide, will be much higher than the results presented here. However, this falls outside the scope of this experiment and should be subject of further consideration and research.
- The resistance reduction with the 3re.GB368.A specimen is less severe than with the 2.PVB.A specimen, but still considerable ($R_{\text{side-d},3\text{re.GB368.A}} / R_{0,\text{dir,ave},3\text{re.GB368.A}} = 1.90/2.52 = 0.75$). Obviously, a smaller part of the section was influenced by the impact. Like the 2.PVB.A specimen, the R_0 resistance reduction is greater than that of the specimens damaged by static load and impact, while of those specimens *both* outer layers had been damaged ($R_{\text{side-d},3\text{re.GB368.A}} / R_{\text{II,st+i,ave},3\text{re.GB368.A}} = 1.90/2.23 = 0.85$). The result coincides with the lowest results from that series ($R_{\text{II,st+i,low},3\text{re.GB368.A}} = 1.88$). Thus, this, two, may be a statistical variation – especially since initial failure did not start from the dent caused by the impact (Figure E.19).
- The post-failure resistance of the reinforced specimen seemed to be hardly influenced by the side damage ($R_{\text{side-d},3\text{re.GB368.A}} / R_{0,\text{dir,ave},3\text{re.GB368.A}} = 3.49/3.50 = 1.00$).

Table E.5e Results of 4-point bending tests after predamage; side impacted specimens.

Specimen	Impact Sequence [J]	R_{pd}			$R_{\text{III,pd}}$	
		M_{pd} [kNm]	M_{pd}/t [10 ³ kNm/mm]	σ_{pd} [MPa]	M_{III} [kNm]	M_{III}/t [10 ³ kNm/mm]
2.PVB.A						
1	O_1, side: : 6.24 J; : 6.24 J; : 6.24 J	1.07	53.6	22.3	0.83	41.4
3re. GB368.A	Impact Seq. [J]	M_{pd} [kNm]	M_{pd}/t [10 ³ kNm/mm]	σ_{pd} [MPa]	M_{III} [kNm]	M_{III}/t [10 ³ kNm/mm]
1	O_1, side: : 6.24 J; : 6.24 J; : 6.24 J	1.90	86.5	33.2	3.49	158.7

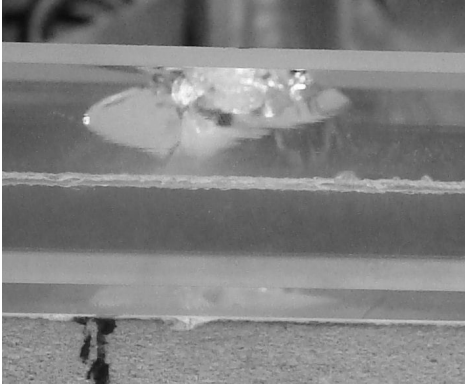


Fig. E.15 Side view of the 2.PVB.A specimen. Cracks stay limited to the directly affected layer with side impact. The same applies for the 3re.GB368.A specimen.

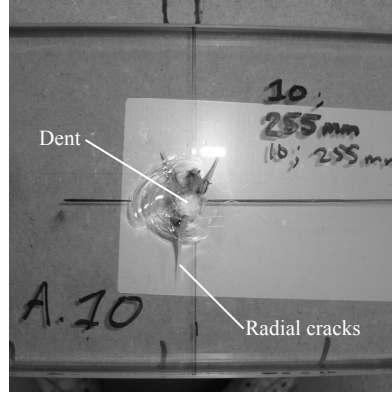


Fig. E.16 Frontal view of side impact in 2.PVB.A specimen. Besides a dent, some radial cracks appear.

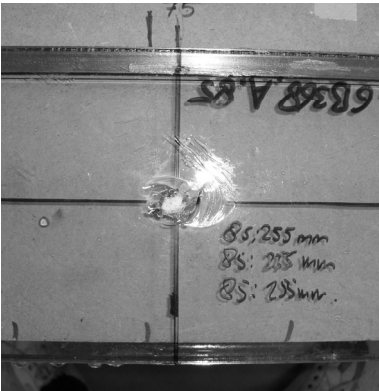


Fig. E.17 Frontal view of side impact in 3re.GB368.A specimen. Only a dent appears.

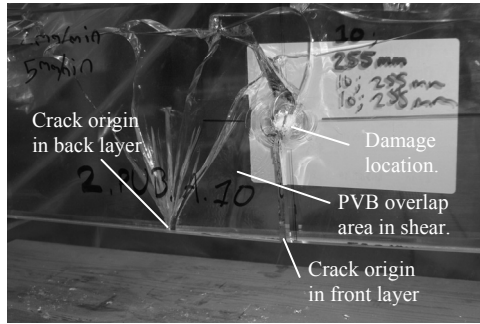


Fig. E.18 In the 2.PVB.A specimen, the crack origins in both layers (one as a consequence of the side impact, the other of 4-point bending) did not coincide. Therefore the beam could still carry significant post-failure loads through shear in the PVB overlap area.

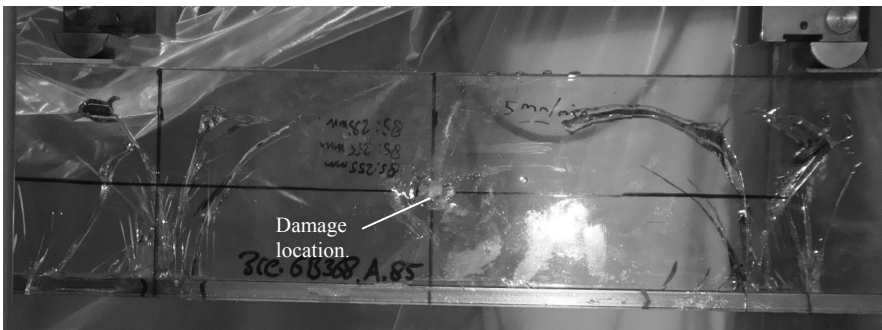


Fig. E.19 Initial failure in the side-impacted 3re.GB368.A specimen. Failure seems unrelated to the side damage.

3.3. Static + Impact

In Table E.6a – e the results of the 4-point bending tests on the specimens damaged by impact and static load, are given. The sequence of impacts (in terms of impact energy) is listed, along with the failure load to level III, and the post-failure strength. In principal, the impact energies were chosen so as to obtain model level I damage in the double layer specimens, and model level II damage in the triple layer specimens.

Table E.6a Results of 4-point bending tests after damage by simultaneous impact and static load; double layer PVB laminated specimens.

Specimen	Impact Sequence [J]	$R_{I, st+i}$			$R_{III, st+i}$	
		M_I [kNm]	M_I/t [10 ³ kNm/mm]	$\sigma_{I(one\ layer)}$ [MPa]	M_{III} [kNm]	M_{III}/t [10 ³ kNm/mm]
1	O_1: 3.77 J	1.46	72.9	60.7	0.02	1.10
2	O_1: 4.53 J	1.72	86.0	71.7	0.06	2.78
3	O_1: 4.53 J	1.79	89.3	74.4	0.05	2.34
Ave		1.65	82.7	68.9	0.041	2.07
Rel. SD			10.5 %		42.1 %	
2.PVB.S	Impact Seq. [J]	M_I [kNm]	M_I/t [10 ³ kNm/mm]	$\sigma_{I(one\ layer)}$ [MPa]	M_{III} [kNm]	M_{III}/t [10 ³ kNm/mm]
1	O_1: 3.77 J	3.24	162.0	135.0	0*	-
2	O_1: 4.53 J	3.39	169.5	141.3	0*	-
3	O_1: 4.53 J	2.82	140.8	117.3	0*	-
Ave		3.15	157.4	131.2	0	-
Rel. SD			9.47 %		0	
2.PVB.T	Impact Seq. [J]	M_I [kNm]	M_I/t [10 ³ kNm/mm]	$\sigma_{I(one\ layer)}$ [MPa]	M_{III} [kNm]	M_{III}/t [10 ³ kNm/mm]
1	O_1: 1.88 J	4.07	203.3	169.4	0.010**	0.50
2	O_1: 1.37 J	4.12	205.8	171.5	0.010**	0.50
3	O_1: 1.37 J	4.29	214.5	178.8	0.010**	0.50
Ave		4.16	207.9	173.2	0.010	0.50
Rel. SD			9.47 %		0	

* These specimens broke into two pieces at failure.

** Although these specimens did not break, they slowly sagged under their self weight. Their post-failure strength was arbitrarily estimated at two-thirds of their self weight (i.e. 0.010 kNm).

Observations with Table E.6a, general:

- The energy required to create a certain extent of damage is significantly less when a static load is applied during the impact. This observation is valid for all glass types. For annealed and heat strengthened glass, only 3.77 to 4.53 J was needed instead of 6.24 J applied in the previous tests, while for tempered glass instead of 2.44 J, only 1.37 J needed to be applied. Figures H.20a and b show the typical fracture pattern as a result of the impact during static load, for annealed and heat strengthened glass, respectively.
- After the impact, no or practically no subsequent crack growth occurred during the time the static load was applied (600 s for the double layer specimens, and 300 s for the triple layer specimens). Sometimes some extra cracks appeared during load removal (Figure E.21), due to possible incompatibility of closing cracks.

Observations with Table E.6a, for the annealed specimens:

- The failure strength of the undamaged layer is significantly higher than that of the undamaged beams tested in direct 4-point bending ($\sigma_{I, \text{st+I, ave, 2, PVB.A}} / \sigma_{0, \text{dir, ave, 2, PVB.A}} = 68.9/49.8 = 1.38$). This may be due to the fact that the broken layer still partially transfers compressive loads, thus shifting the centre of gravity of the beam section upwards and allowing the unbroken layer to transfer a higher tensile load. See section 4.3.1.
- The post-failure resistance is in between that observed in the direct tests and that found in the predamaged tests ($M_{III, \text{dir, ave, 2, PVB.A}} = 0.025$ kNm; $M_{III, \text{st+I, ave, 2, PVB.A}} = 0.041$ kNm; $M_{III, \text{dir, ave, 2, PVB.A}} = 0.086$ kNm). This supports the assumption that the strain energy content at failure influences the post-failure behaviour – in this case mainly through the fracture pattern density.

Observations with Table EI.6a, for the heat strengthened specimens:

- Contrary to the annealed specimens, the failure strength of the undamaged layer is only slightly higher than observed in the directly tested specimens ($\sigma_{I, \text{st+I, ave, 2, PVB.S}} = 131.2$ MPa; $\sigma_{0, \text{dir, ave, 2, PVB.S}} = 124.4$ MPa). Thus, for these specimens the broken layer apparently does not contribute to the section resistance (by transferring compressive forces). This difference in behaviour between annealed and heat strengthened glass is quite remarkable as in either case, a part of the damaged layer remains unbroken (Figures H.20a and b) – thus one would expect a contribution in compression of this layer also in the heat strengthened specimens. The more intense V-shaped fracture pattern in the heat strengthened specimens must be responsible for the fact that the damaged layer can not transfer any significant amount of compressive stresses in the top anymore (probably insufficient stiffness).
- At failure, the specimens break (PVB rupture), as they do when directly tested. Even with one layer damaged, they build up too much energy for the PVB to dissipate at failure.

Observations with Table E.6a, for the thermally tempered specimens:

- Again, σ_1 is not significantly higher than σ_0 . In this case, however, it can be attributed more convincingly to the fracture pattern density, which, in

combination with the low PVB stiffness, does not allow significant compression transfer in the broken layer.

- The post-failure behaviour is similar to that witnessed in the previous experiments: the beams slowly sag under self-weight. Since the density of the fracture pattern is governed mainly by the internal prestress strain energy rather than the introduced energy by loading, the experiment type has no influence on the post-failure resistance.
- After applying the impact and breakage of one layer, the beams are slightly bended by expansion of the broken layer (Figure E.22). This may influence the actual stress distribution somewhat, but since no instability phenomena have been noticed, this effect has been ignored in the calculations.

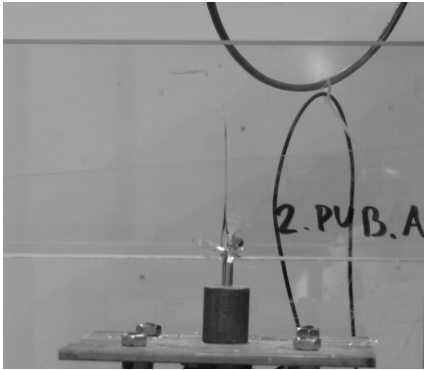


Fig. E.20a Typical fracture pattern in 2.PVB.A beam after impact in one layer while simultaneously applying a static load.

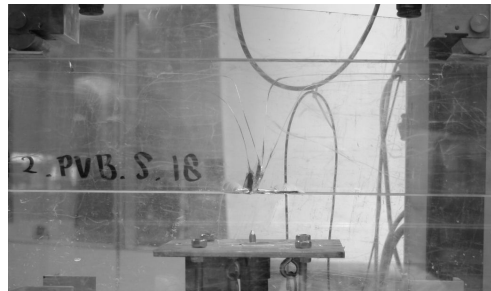


Fig. E.20b Typical fracture pattern in 2.PVB.S beam after impact in one layer while simultaneously applying a static load.

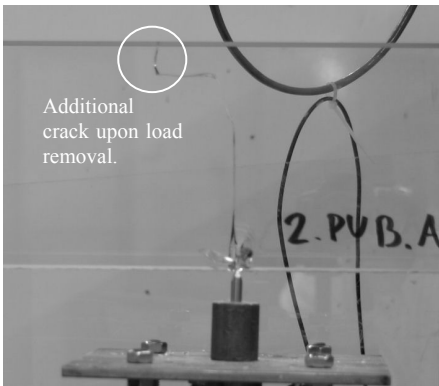


Fig. E.21 In some cases, cracks extended during load removal. This is probably caused by incompatibility of the cracks that are now pushed together again.

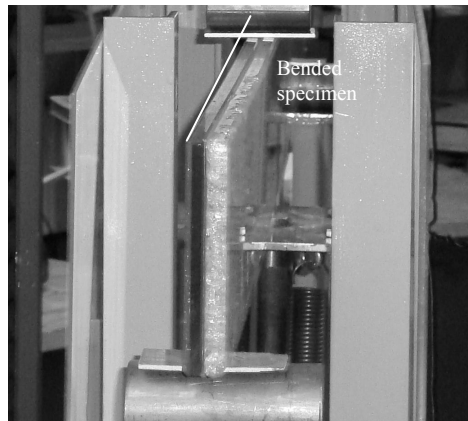


Fig. E.22 The thermally tempered specimens are slightly bended when one layer breaks due to extension of that layer.

Generally, it may be concluded that ignoring a broken layer in a laminate standing beam when calculating its resistance, is a valid, though for annealed glass beams slightly conservative, assumption.

Table E.6b Results of 4-point bending tests after damage by simultaneous impact and static load; triple layer PVB laminated specimens.

Specimen	Impact Seq. [J]	$R_{II, st+i}$			$R_{III, st+i}$		
		M_{II} [kNm]	M_{II}/t [10 ³ kNm/mm]	$\sigma_{II(one\ layer)}$ [MPa]	M_{III} [kNm]	M_{III}/t [10 ³ kNm/mm]	
3.PVB.A	O_1: 3.77 J O_2: 3.77 J	1.92	64.0	80.0	0.09	2.91	
	O_1: 3.77 J O_2: 3.77 J	1.86	61.0	77.5	0.07	2.32	
	O_1: 3.77 J O_2: 3.77 J	1.96	65.5	81.9	0.13	4.25	
	Ave	1.91	63.5	79.8	0.095	3.16	
Rel. SD		1.55 %			31.4 %		
3.PVB.S	Impact Seq. [J]	M_{II} [kNm]	M_{II}/t [10 ³ kNm/mm]	$\sigma_{II(one\ layer)}$ [MPa]	M_{III} [kNm]	M_{III}/t [10 ³ kNm/mm]	
		1***	O_1: 3.77 J O_2: 3.77 J	1.54	51.4	64.3	0.15
	2	O_1: 3.77 J O_2: 3.77 J	3.90	129.9	162.4	0*	-
3.PVB.T	Impact Seq. [J]	M_{II} [kNm]	M_{II}/t [10 ³ kNm/mm]	$\sigma_{II(one\ layer)}$ [MPa]	M_{III} [kNm]	M_{III}/t [10 ³ kNm/mm]	
		1	O_1: 1.37 J O_2: 1.37 J	4.95	164.9	206.1	0.015**
	2	O_1: 1.37 J O_2: 1.37 J	4.55	151.6	189.5	0.015**	0.50
	3	O_1: 1.37 J O_2: 1.37 J	4.52	150.7	188.4	0.015**	0.50
	Ave		4.67	155.7	194.7	0.015	0.50
Rel. SD		5.10 %			-		

* These specimens broke into two pieces at failure.

** Although these specimens did not break, they slowly sagged under their self weight. Their post-failure strength was arbitrarily estimated at two-thirds of their self weight (i.e. 0.015 kNm).

*** The results from this specimen were ignored due to the very low failure stress. See observations to this table.

Observations with Table E.6b, for the annealed specimens:

- Figure E.23 shows a typical cracking pattern for 3.PVB.A specimens after impact and simultaneous static load.
- Even more than with the double layer annealed specimens, the resistance of the remaining undamaged layer is higher than of the undamaged specimen ($\sigma_{II,st+i,ave,3.PVB.A} / \sigma_{0,dir,ave,3.PVB.A} = 79.8/37.5 = 2.13$). This should be attributed to the broken layers partially transferring compressive loads. See Section 4.3.1.
- Contrary to the double layer specimens, the post-failure strength is comparable to the directly tested specimens. It is significantly lower than of the predamaged specimens ($M_{III,dir,ave,3.PVB.A} = 0.082$ kNm; $M_{III,st+i,ave,3.PVB.A} = 0.095$ kNm; $M_{III,pd,ave,3.PVB.A} = 0.16$ kNm). Perhaps this can be attributed to the relatively high level II residual strength (which results in a high energy content at failure and thus low post-failure strength).
- The post-failure strength is over twice that of the double layer specimens. This can be attributed to the double amount of PVB in the section.

Observations with Table E.6b, for the heat strengthened specimens:

- The results of the two specimens tested significantly deviate from each other. There have been no errors in the execution of the experiment to account for this difference. The cracks in the first specimen after impact in both outer layers run much higher than in the second one. This probably influenced the subsequent M_{II} resistance. An explanation for this difference in fracture pattern, however, remains evasive (Figures H.24a and b).
- Especially the weak specimen deviates from what could be expected. The resistance is even below that of the annealed specimens. However, the fracture pattern in this specimen does not suggest it was not heat strengthened.
- The stronger specimen has a high resistance compared to previous results, but within the limits of what could reasonable be expected.
- As a consequence, the strong specimen behaves as the heat strengthened specimens in direct bending: it breaks upon failure. The weak one, on the other hand behaves as the annealed specimens and provides considerable post-failure strength.
- Due to the sub standard performance of the weak specimen, it has been ignored in further analysis and the construction of the ESDs in Chapter 7.

Observations with Table E.6b, for the thermally tempered specimens:

- σ_{II} is significantly higher than σ_0 ($\sigma_{II,st+i,ave,3.PVB.T} / \sigma_{0,dir,ave,3.PVB.T} = 194.7/154.7 = 1.26$). Perhaps the broken layers can transfer some compressive loads in triple layer specimens. However, since this was not possible with the double layer specimens, it is unclear why this would be much different with the triple layer specimens.
- The post-failure behaviour is similar to that witnessed in the previous experiments: the beams slowly sag under self-weight.

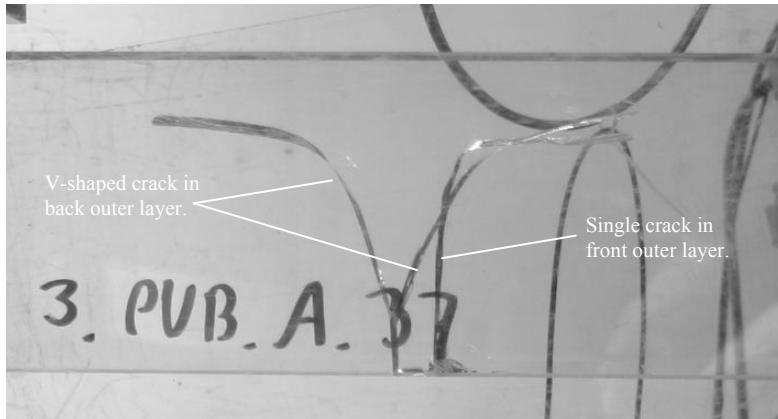


Fig. E.23 Typical fracture pattern in 3.PVB.A beam after impact in two outer layers while simultaneously applying a static load.

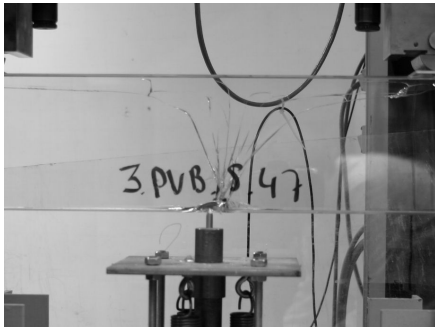


Fig. E.24a Fracture pattern in 3.PVB.S_1 (weak), after impact in two outer layers while simultaneously applying a static load.

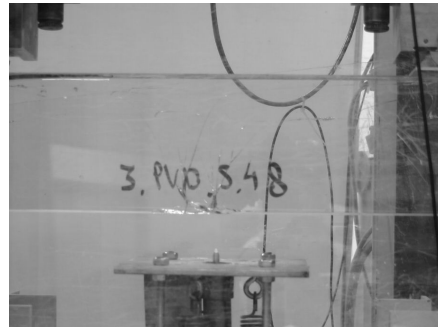


Fig. E.24b Fracture pattern in 3.PVB.S_2 (strong), after impact in two outer layers while simultaneously applying a static load.

Observations with Table E.6c, general:

- As with the impacts applied without static load, there seems to be no significant difference in damage sensitivity between PVB and SG-laminated glass beams (Figure E.25).

Observations with Table E.6c, for the annealed specimens:

- σ_1 is significantly lower than with the PVB-laminated specimens ($\sigma_{1, \text{st+i, ave, 2.SG.A}} = 56.7 \text{ MPa}$; $\sigma_{1, \text{st+i, ave, 2.PVB.A}} = 68.9 \text{ MPa}$). This is probably due to the fact that the glass for the SG-laminated specimens came from another manufacturer.
- The post-failure strength is approximately equal to that obtained from the direct bending tests and thus lower than from obtained from the predamaged specimens.

Observations with Table E.6c, for the heat strengthened specimen:

- There was only one double layer heat strengthened SG-laminated specimen. Its σ_1 was quite high. This is probably due to the fact that the glass for the SG-laminated specimens came from another manufacturer. The post-failure strength is approximately equal to both the direct tests and the annealed

specimens. Thus, the stiffness of the laminate makes the fracture pattern density less relevant for the post-failure resistance.

Table E.6c Results of 4-point bending tests after damage by simultaneous impact and static load; double layer SG laminated specimens.

Specimen	Impact Sequence [J]	$R_{I,St+i}$			$R_{III,St+i}$	
		M_I [kNm]	M_I/t [10 ³ kNm/mm]	$\sigma_{I(one\ layer)}$ [MPa]	M_{III} [kNm]	M_{III}/t [10 ³ kNm/mm]
1	O_1: 3.77 J	1.18	58.9	49.1	0.38	18.8
2	O_1: 3.77 J	1.55	77.5	64.6	0.31	15.3
3	O_1: 3.77 J	1.36	67.8	56.5	0.30	14.8
Ave		1.36	68.1	56.7	0.33	16.3
Rel. SD			13.7 %			33.0 %

2.SG.S	Impact Seq. [J]	M_I	M_I/t	$\sigma_{I(one\ layer)}$	M_{III}	M_{III}/t
		[kNm]	[10 ³ kNm/mm]	[MPa]	[kNm]	[10 ³ kNm/mm]
1	O_1: 1.37 J*	3.84	192.0	160.0	0.30	14.8

* The amount of thermal prestress is unclear before testing. The specimen turns out to be heat strengthened.



Fig. E.25 Typical fracture pattern in 3.SG.A beam after impact in two outer layers while simultaneously applying a static load. Disregard the ‘S’ in the name – this specimen turned out not to be heat strengthened.

Table E.6d Results of 4-point bending tests after damage by simultaneous impact and static load; triple layer SG laminated specimens.

Specimen	Impact Sequence [J]	$R_{II, st+i}$			$R_{III, st+i}$	
		M_{II} [kNm]	M_{II}/t [10 ³ kNm/mm]	$\sigma_{II(one\ layer)}$ [MPa]	M_{III} [kNm]	M_{III}/t [10 ³ kNm/mm]
1	O_1: 6.24 J* O_2: 3.77 J**	0.77	25.7	32.1	0.22	7.41
2	O_1: 3.77 J O_2: 3.77 J	1.76	58.7	73.3	0.70	23.5
3.SG.S	Impact Seq. [J]	M_{II} [kNm]	M_{II}/t [10 ³ kNm/mm]	$\sigma_{II(one\ layer)}$ [MPa]	M_{III} [kNm]	M_{III}/t [10 ³ kNm/mm]
1	O_1: 1.37 J; 1.37 J O_2: 3.77 J***	2.18	72.3	30.3	0.67	22.2

* Accidentally applied incorrect impact.

** Accidentally hits both the second outer layer and the inner layer. The impact causes cracks in both (thus in total, there is damage in all layers). This results in significantly lower resistance – comparable to the results of the previously discussed predamaged specimens with damage in all layers before 4-point bending. The result of this specimen is therefore ignored in further calculations and analysis.

*** The amount of thermal prestress is unclear before testing. The specimen turns out to be heat strengthened.

Observations with Table E.6d:

- As annealed specimens discussed earlier, the undamaged layer of the 3.SG.A specimen has a high failure strength. See section 4.3.1.
- The post-failure strength of both the annealed and heat strengthened specimen is approximately twice as high as that of the double layer specimens. This indicates the amount of SG in the section governs the post-failure strength and that the load transfer mechanism in the double and triple layer specimens is similar.
- The post-failure strength of both the annealed and heat strengthened specimen is approximately equal to that of the directly tested specimens. Apparently the stiff laminate makes the fracture pattern density less relevant for the residual strength
- As with the double layer specimens, the post-failure strength of the annealed specimens is somewhat lower than in the predamaged specimens. Thus, the fracture pattern density may be less relevant, but not completely irrelevant altogether.

Observations with Table E.6e:

- Figures H.26a and b present the typical fracture pattern after impact in the reinforced specimens. There are no important differences between the cracks originating in GB368 bonded specimens and SG laminated specimens.
- The physical damage caused by impact and static load does not seem to have a significant effect on R_{II} or R_{III} .

- σ_{II} in both the GB368 bonded and even more in the SG laminated reinforced specimens is high – even more so than in previously discussed annealed glass specimens. Especially for the SG-laminated specimens this resistance is difficult to explain. The 2nd LTM can not be responsible as it can not be activated before breakage of the inner glass layer. Alternatively, the reinforcement profile may act as a crack bridge on microscale along the glass sheet bottom edge that (partially) annuls the stress concentrations that would otherwise arise at the tips of the defects along the stressed edge (Figure E.27). However, this does not elucidate the significant difference between the GB368 bonded and SG laminated specimens ($\sigma_{II, st+i, ave, 3re, GB368.A} = 85.6$ MPa; $\sigma_{II, st+i, ave, 3re, SG.A} = 130.2$ MPa). No plausible explanation for this difference was found.

Table E.6e Results of 4-point bending tests after by simultaneous impact and static load; reinforced specimens.

Specimen	Impact Sequence [J]	$R_{II, st+i}$			$R_{III, st+i}$		
		M_{II} [kNm]	M_{II}/t [10 ³ kNm/mm]	$\sigma_{II(one\ layer)}$ [MPa]	M_{III} [kNm]	M_{III}/t [10 ³ kNm/mm]	
3re.GB368.A	1	O_1: 6.24 J O_2: 6.24 J	1.88	85.7	72.4	3.34	151.9
	2	O_1: 3.77 J O_2: 3.77 J	2.21	100.7	85.0	2.69	122.4
	3	O_1: 3.77 J O_2: 3.77 J	2.59	117.8	99.5	3.54	161.0
	Ave		2.23	101.4	85.6	3.19	145.1
	Rel. SD			15.9 %			13.9 %
3re.SG.A	1	O_1: 3.77 J O_2: 3.77 J	2.81	127.7	98.1	3.82	173.5
	2	O_1: 3.77 J O_2: 3.77 J	2.67	121.4	93.2	3.77	171.2
	Ave		2.74	124.6	95.6	3.79	172.4
	Rel. SD			3.61 %			0.93 %

* These specimens broke into two pieces at failure.

** Although these specimens did not break, they slowly sagged under their self weight. Their post-failure strength was arbitrarily estimated at two-thirds of their self weight (i.e. 0.015 kNm).

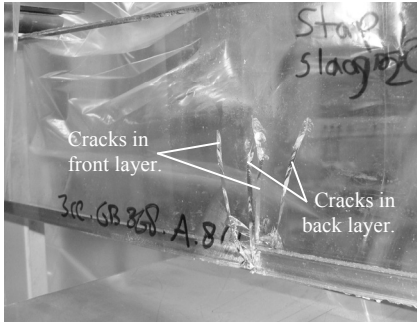


Fig. E.26a Typical fracture pattern in 3re.GB368.A specimen, after impact in two outer layers while simultaneously applying a static load.

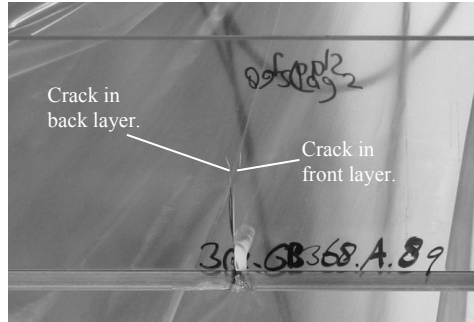


Fig. E.26b Typical fracture pattern in 3re.SG.A specimen, after impact in two outer layers while simultaneously applying a static load.

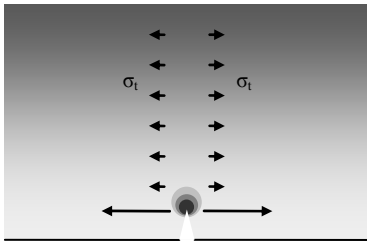


Fig. E.27a Stress concentrations around a defect tip in a glass sheet.

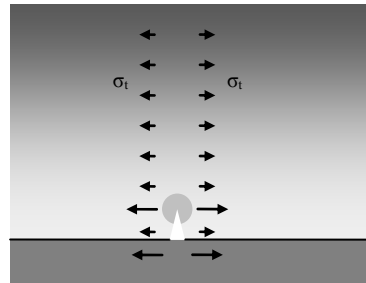


Fig. E.27b Suggested effect of reinforcement as micro scale crack bridge: de-intensification of the stress concentration.

4. Analysis

Many remarks concerning the resistances, crack growth, damage sensitivity, and failure behaviour of the tested glass beams have already been made. The experimental results per specimen type have been summarized in Section 4.1. The subsequent Sections treat the two principal issues of this experiment in general: damage sensitivity (4.2) and Level I, II, and III load transfer mechanisms (4.3).

4.1. Overview of Resistances per Specimen Type

Table E.7 summarizes the experimental results per specimen type. It lists the average values for R_0 , R_I , R_{II} , and R_{III} , per experiment type, taken from Tables H.4a – e, H.5a – d, and H.6a – e.

The post-failure strength (R_{III}) of the annealed and heat strengthened PVB-laminated specimens turns out to be highly dependent on the experiment type applied. Generally, the direct test yields the lowest post-failure strength, while the predamaged test (with level III damage applied by impacts before 4-point bending) gave the highest post-failure strength (Figures H.28a, b).

Table E.7 Summary of average resistances of all specimen types. The numbers between brackets indicate the number of specimen results on which the averages are based.

Specimen Type	$R_{0,dir}$ [kNm]	R_{pd}		$R_{I/II,st+i}$		R_{III} [kNm]	
		M_{pd} [kNm]	$M_{I/II,st+i}$ [kNm]	$M_{III,dir}$	$M_{III,pd}$	$M_{III,st+i}$	
2.PVB.A	2.39 (3)	-	1.65 (3)	0.025 (3)	0.086 (3)	0.041 (3)	
2.PVB.S	5.97 (3)	1.48 (3)	3.15 (3)	0 (3)	0.022 (3)	0 (3)	
2.PVB.T	7.85 (3)	-	4.16 (3)	0.010 (3)	0.010 (3)	0.010 (3)	
3.PVB.A	2.70 (4)	-	1.91 (3)	0.082 (4)	0.16 (2)	0.095 (3)	
3.PVB.S	7.37 (2)	2.02 (2)	3.90 (1)	0 (2)	0.041 (2)	0 (1)	
3.PVB.T	11.14 (3)	n/a	4.67 (3)	0.015 (3)	n/a	0.015 (3)	
2.SG.A	1.82 (3)	-	1.36 (3)	0.33 (3)	0.44 (2)	0.33 (3)	
2.SG.S	5.34 (1)	n/a	n/a	0.28 (1)	n/a	n/a	
2.SG.T	n/a	n/a	3.84 (1)	n/a	n/a	0.30 (1)	
3.SG.A	2.92 (3)	-	1.76 (1)	0.66 (3)	0.84 (2)	0.70 (1)	
3.SG.S	5.87 (1)	n/a	2.18 (1)	0.63 (1)	n/a	0.67 (1)	
3re.GB368.A	2.52 (6)	2.11 (3)	2.23 (3)	3.50 (6)	3.25 (3)	3.19 (3)	
3re.SG.A	2.95 (5)	3.24 (2)	3.39 (2)	4.38 (5)	3.74 (2)	3.79 (2)	

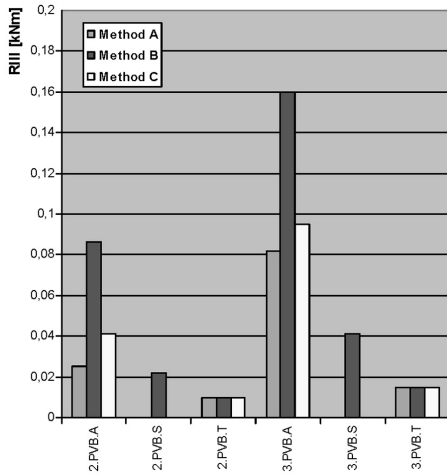


Fig. E.28a Average post-failure strengths for PVB-laminated glass beams, per test method (based on Table E.7). A = direct; B = predamaged; C = static+impact. Note the significant test method dependency.

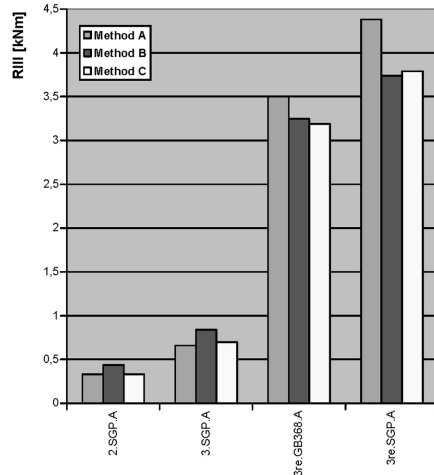


Fig. E.28b Average post-failure strengths for SG-laminated annealed glass beams and reinforced glass beams, per test method (based on Table E.7). A = direct; B = predamaged; C = static+impact.

This is attributed to the amount of elastic strain energy that is released at failure. In heat strengthened glass, high energy contents have caused PVB to rupture at failure resulting in no post-failure resistance. Furthermore, the energy content influences the amount of

crack surface area that is created and thus the fracture pattern density. This has been proven by the experiment described in Appendix G.

It should be mentioned that even in the best cases, the post-failure capacity of the PVB-laminated specimens is only several times their self weight and may thus be of little use in structural applications with external permanent loads. Additionally, the author notes that elastic strain energy, contrary to failure stress, is geometry dependent.⁶ Larger elements contain much more energy at failure than smaller ones, when failing at the same failure stress. Thus it may well be expected that PVB rupture could occur also in large annealed beams, or fracture patterns may be too dense to yield post-failure strength equal to or higher than self weight.

Contrary to the annealed and heat strengthened specimens, the post-failure behaviour of the thermally tempered PVB-laminated specimens is not influenced by the experiment type. The internal prestress energy is much higher⁷ and governs the fracture pattern, which is so dense that specimens sag under their self weight after failure, regardless of the test method applied.

The fracture pattern density of the SG-laminated specimens seems to play a much less significant role in the determination of the residual strength. The predamaged specimens have a higher failure strength than the other ones (1.3 times), but this difference is less than with the PVB-laminated specimens. The specimens tested directly and those tested after being damaged to level I/II, have equal residual strength. Furthermore, residual strength is proportional to the amount of SG in the section (thus for the triple layer specimens twice as high as for the double layer ones). This indicates the post-failure load transfer mechanism in the double and triple layer specimens works in the same way.

For most PVB-laminated specimens, this holds as well, but the directly tested double layer specimens have a post-failure strength significantly below half of the post-failure strength of the triple layer specimens.

The reinforced specimens seem to be hardly influenced by the test method, both in pre- and post-failure resistance. Remarkably, the average post-failure resistance of the predamaged and static+impact specimens is somewhat lower (contrary to other specimens) than of the directly tested specimens. This may be attributed to the fact that they came from different badges. The post-failure behaviour of the reinforced specimens is extensively discussed in Appendix I.

Generally, it is concluded that the post-failure resistance of PVB- and SG-laminated glass beams depends on:

- The laminate tensile strength,
- The laminate stiffness,
- The glass fracture pattern density.

⁶ Appendix F.

⁷ Appendix F.

The laminate tensile strength determines the tensile load that can be carried by the laminate. The laminate stiffness and fracture pattern density determine the amount of compressive stress that can be build up in the (broken) glass. When the laminate stiffness increases (e.g. SG instead of PVB), the fracture pattern density becomes less important or even irrelevant (as shown by the post-failure strength of the thermally tempered SG-specimen, which is on par with the other SG-laminated specimens).

4.2. Impact and Damage Sensitivity

The impact sensitivity (the amount of physical damage caused per unit of impact) seems to depend on the stiffness of the impacted body, probably both in the direction of the impact as well as perpendicular to it. Possibly, the resistance against deformation in the plane frontal to the cracks (i.e. the glass sheet face) is the most important parameter because for the crack to grow, the glass shards are moved in that plane⁸ (in principal perpendicular to the crack growth direction, Figure E.28). When this in-plane movement is resisted, so is crack growth.

The usually applied Young's modulus of the laminate appears to be of minor importance as the fracture takes place in a very short time frame in which the time-dependency of the Young's modulus becomes irrelevant. Thus PVB- and SG-laminated specimens yield approximately equal crack growth.

Surprisingly, the impact sensitivity of annealed and heat strengthened glass was comparable. It required as much impact energy to create a crack through an annealed glass sheet as it did through a strengthened one. Heat strengthened specimens did not suffer early failure from a release of internal stress. Thermally tempered ones, on the other hand, did: it required only about 35-40 % of the energy needed for the other glass types (without static load 39 %; with static load 36 %). Furthermore, it is expected that the required impact energy to completely fracture a tempered glass sheet is geometry independent, whereas to create a through-crack in a larger or thicker piece of annealed or strengthened glass would require (possibly proportionally) more energy.

The strength reduction (structural damage) caused by impact-originated dents (physical damage) is considerably disproportional to the decrease in moment of resistance W caused by them. Figure E.29 shows a damaged specimen. With W_{pd} down 31 %, M_{pd} dropped by 83 %. More dedicated experiments are required to determine the relation between impact, physical damage, and structural damage. This justified the assumption that a sheet in a laminate beam with a vertical crack running from the bottom to over half the section of the sheet will carry practically no tensile loads (contrary to e.g. steel).

⁸ This is the kinetic component U_k in Mott's expansion of the Griffith energy balance (Chapter 4, Section 1.1.1., Eq. 4.5).

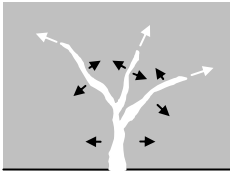


Fig. E.28 Crack growth direction and glass shard movement. The crack growth speed will be determined by the resistance the glass shards encounter to separate.

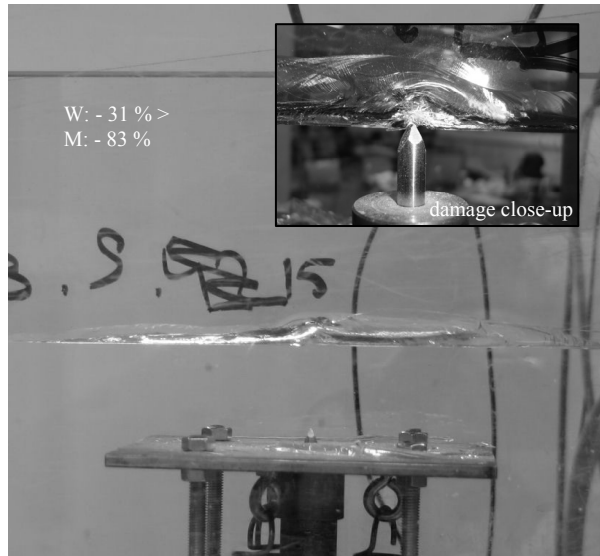


Fig. E.29 The effect of physical damage on the resistance of a glass beam: even a small reduction in moment of resistance (estimated loss of 20 mm of bottom of the section results in $W_{pd} = 33\,333\text{ mm}^3$, whereas $W_{mi} = 48\,000\text{ mm}^3$), causes a significant drop in strength (pd 2.PVB.S; $M_{pd} = 1.04\text{ kNm}$; $M_{0,dir,ave,2.PVB.S} = 5.97\text{ kNm}$).

The presence of static loads during impact will cause significantly more physical damage than an impact without a static load. Vice versa, it requires much less impact energy to create a certain amount of physical damage when a static load (as high as the calculable resistance M_d of the unaffected layer(s)) is applied during impact. The effect on annealed and heat strengthened glass, and thermally tempered glass was comparable. Impact energy reductions of 40 % and 44 %, respectively, were found.

This effect should be considered when testing structural glass elements for practice applications. When a governing, realistic impact has been identified, the elements should be tested for it in combination with a static load that may be expected at the time. This is not necessarily the momentary load, the impact type (e.g. falling person on a roof) may coincide with a specific variable load (e.g. maintenance). Alternatively, the applicable impact should be multiplied by a factor to account for the otherwise present static load. In the execution of experiments this may be easier, but it will probably predict the consequence of the impact less accurately. Additionally, it requires further research to determine a correct factor to multiply the impact with.

With regard to damage sensitivity, the reinforced specimens have the distinct advantage that their inner layer is protected from the bottom side by the reinforcement profile. This makes it extremely difficult to damage those layers from that side (impossible with the impact device used in this experiment). Assuming such beams will often also be protected from the top side by e.g. glazing, the inner layers of such beams will be very damage insensitive.

Finally, the tests showed that when the impact device head hits only one layer, the damage does not expand to other layers, but stay within the directly affected layer – independent of glass and laminate type. Shock waves inducing damage in other layers were not observed. Furthermore, no significant crack growth was found under static load after the initial impact.

4.3. Load Transfer Mechanisms

The LTMs of the reinforced specimens are extensively discussed in Appendices K and L.

4.3.1. Level I and II Mechanisms

Although principally the same, there is a minor change in the 1st LTM of some specimens after having reached level I or level II damage. It is not so much the mechanism itself that changes – it remains linear elastic bending – but the effective section. Instead of being a sum of the section of complete rectangular sheets, it becomes T-shaped, with the complete unbroken layer active, and the broken layer partially active, as in Figure E.30. The neutral axis shifts upwards which allows for a higher internal moment capacity, than that of just a single sheet. In the ESDs constructed in Section 2 of Chapter 7, this becomes apparent by a change of slope of the redundant curve. See further discussion there.

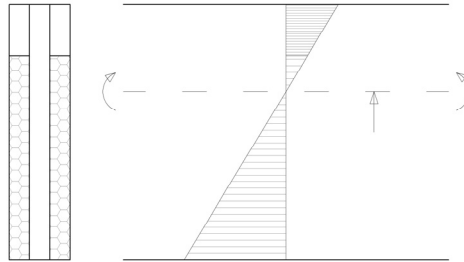


Fig. E.30 At level I or II, the active section in the 1st LTM (linear elastic bending of the glass) becomes T-shaped, rather than rectangular. The neutral axis shifts upwards, allowing the undamaged sheet to transfer a higher tensile load than it otherwise would.

4.3.2. Level III Mechanisms

In the laminated specimens, the laminate must carry the tensile loads after failure. In some cases the cracking pattern is too dense or the laminate is not stiff enough to allow compressive stresses in the (broken) glass, and the laminate thus remains the only active material. In others, the laminate works in composite action: the glass in compression and the laminate in tension.

Four LTMs are proposed (Figure E.31a – d): linear elastic bending, plastic bending, composite action with laminate in elastic bending, and composite action with laminate in plastic bending. The mechanisms linear elastic bending and plastic bending are self-evident. The capacity of the composite mechanisms is determined by the tensile capacity of the laminate which can now be activated over practically the entire beam height, but for a small top layer where the glass is in compression. The compressed

glass is assumed not to be governing (no compressive glass failure was observed). The theoretical capacity of each one was determined for PVB- and SG-laminated glass in double or triple layer configuration. Based on the experimental results, it was determined which one is applicable to each specimen and experiment type (Tables H.8 and H.9). In a considerable number of cases, the specimen resistance seems to be determined by an intermediate case as e.g. in Figure E.32.

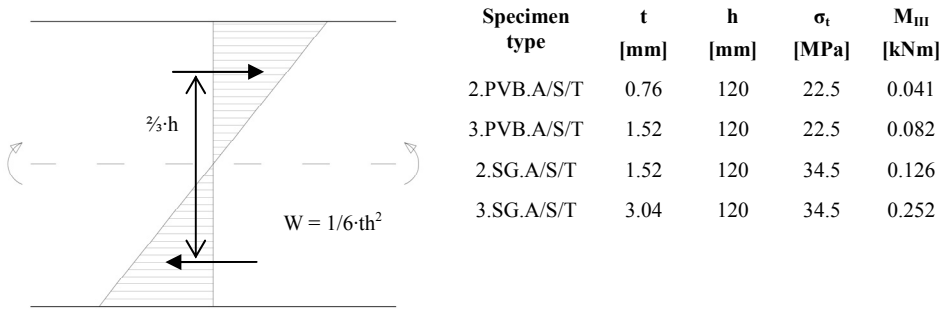


Fig. E.31a 2nd LTM 1: Linear Elastic Bending of the laminate, and theoretical moment capacities of the LTM in the different specimen types. The glass type is irrelevant for this calculation.

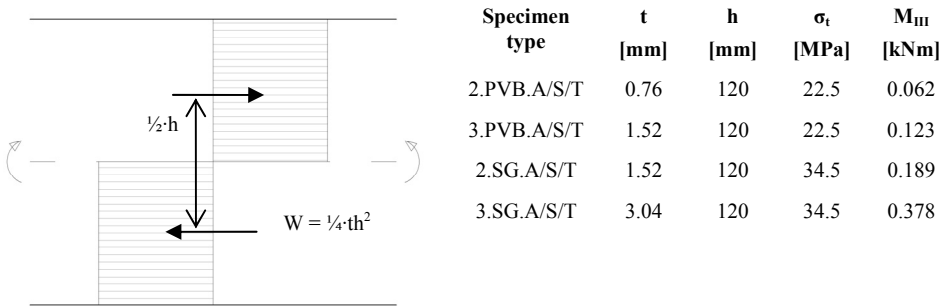


Fig. E.31b 2nd LTM 2: Linear Elastic Bending of the laminate, and theoretical moment capacities of the LTM in the different specimen types. The glass type is irrelevant for this calculation.

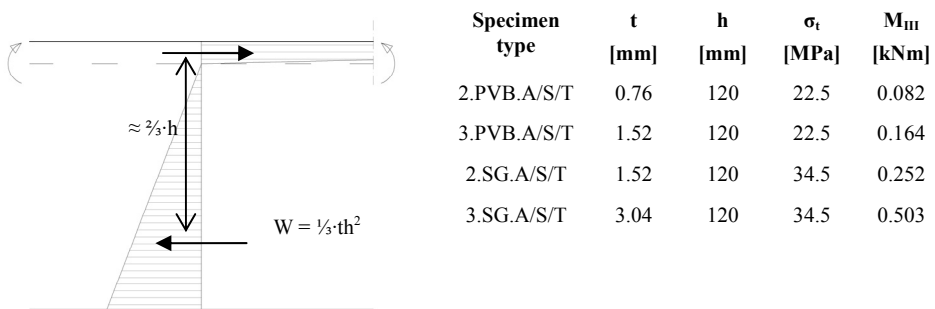
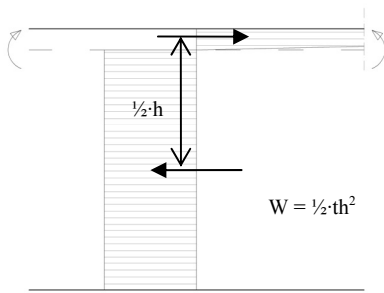


Fig. E.31c 2nd LTM 3: Linear Elastic Bending of the laminate, and theoretical moment capacities of the LTM in the different specimen types. The glass type is irrelevant for this calculation.



Specimen type	t [mm]	h [mm]	σ_t [MPa]	M_{III} [kNm]
2.PVB.A/S/T	0.76	120	22.5	0.123
3.PVB.A/S/T	1.52	120	22.5	0.246
2.SG.A/S/T	1.52	120	34.5	0.378
3.SG.A/S/T	3.04	120	34.5	0.755

Fig. E.31d 2nd LTM 4: Linear Elastic Bending of the laminate, and theoretical moment capacities of the LTM in the different specimen types. The glass type is irrelevant for this calculation.

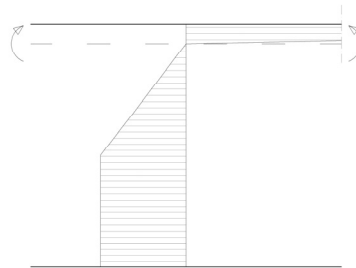


Fig. E.32 Intermediate state between 2nd LTM 3 and 4.

Table E.8 Post-failure Load Transfer Mechanism per specimen type, per test method – sorted by specimen type. A ‘0’ means there is no 2nd LTM is present; ‘0-1’ indicates the fracture pattern is too dense to allow LTM 1 to fully develop (to reach laminate tensile strength); ‘3-4’ points to an intermediate situation as in Figure E.32.

Specimen Type	2 nd LTM		
	Direct	Predamaged to Level III	Static+Impact to Level I/II
2.PVB.A	0 – 1	3	1
2.PVB.S	0	0 – 1	0
2.PVB.T	0 – 1	0 – 1	0 – 1
3.PVB.A	1	3	1
3.PVB.S	0	0 – 1	0
3.PVB.T	0 – 1	0 – 1	0 – 1
2.SG.A	3 – 4	4	3 – 4
2.SG.S	3 – 4	n/a	n/a
2.SG.T	n/a	n/a	3 – 4
3.SG.A	3 – 4	4	3 – 4
3.SG.S	3 – 4	n/a	3 – 4

As shown in Table E.8, the differences in post-failure resistance agree with different LTMs. The laminate stiffness and strain energy at failure determine which LTM can be activated. Thus, the post-failure resistance of an element can not be established without indicating the impact type with which failure is to be obtained.

Furthermore, Table E.8 shows that the 2nd LTM in SG-laminates differs from that in PVB-laminates. The difference in post-failure resistance not only stems from the greater strength and thickness of the laminate, but also from the fact that, because of its stiffness, it allows another LTM to be activated.

The number of glass layers has a minor influence on the 2nd LTM. There is a difference between 2.PVB.A and 3.PVB.A in the direct test method (LTM 0 – 1 and 1, respectively), and between 2.PVB.S and 3.PVB.S in the static+impact test method (LTM 0 and 1, respectively).

Table E.9 Load Transfer Mechanism per specimen type, per test method – sorted by LTM. A ‘0’ means there is no 2nd LTM is present; ‘0-1’ indicates the fracture pattern is too dense to allow LTM 1 to fully develop (to reach laminate tensile strength); ‘3-4’ points to an intermediate situation as in Figure E.32.

LTM	Specimen type and test method
0	2.PVB.S: direct, static + impact. 3.PVB.S: direct.
0 – 1	2.PVB.A: direct. 2.PVB.S: predamaged. 2.PVB.T: direct, predamaged, static+impact. 3.PVB.S: predamaged. 3.PVB.T: direct, predamaged, static+impact.
1	2.PVB.A: static+impact. 3.PVB.A: direct, static+impact. 3.PVB.S: static+impact.
3	2.PVB.A: predamaged. 3.PVB.A: predamaged.
3 – 4	2.SG.A: direct, static+impact. 2.SG.S: direct. 2.SG.T: static+impact. 3.SG.A: direct, static+impact. 3.SG.S: direct, static+impact.
4	2.SG.A: predamaged. 3.SG.A: predamaged.

5. Conclusions

With regard to impact and damage sensitivity:

- An impact applied on one layer in a laminate only results in fracture in that layer. This applies to impacts applied to the glass sheet edge as well as to its face. No shock wave or similar effect was found that induces fracture in the

other layers. Thus, it may be concluded that outer layers form a formidable protection for the inner one(s).

- The individual layers in a double or triple layer glass beam are almost equally impact sensitive. Overall, the triple layer beams are much less damage sensitive as the outer layers protect the inner layer well. Annealed and heat strengthened glass are approximately equally impact sensitive.
- Thermally tempered is about three times as impact sensitive as annealed and heat strengthened glass.
- A relatively minor amount of physical damage results in disproportional structural damage.
- The presence of a static load during impact greatly enhances the physical damage caused by that impact. Therefore, in testing for practice applications, the static loads that may be present during a governing impact should be considered and applied during testing. Alternatively, the applicable impact can be magnified.
- The reinforcement profiles in reinforced glass beams (as applied in this experiment) constitutes a significant protection for the inner layer. Impact on the reinforcement profile did not cause cracks in the inner glass sheet.

With regard to initial and post-failure behaviour:

- The combination of impact and a static load on a glass beam, with the static load equal to the calculable resistance of the layer(s) unaffected by the impact, does not induce premature failure of the beam. This is in agreement with the general assumption.
- When a layer in a laminate beam is fractured to an extent it can not carry tensile loads anymore, it may still transfer compressive loads depending on the fracture pattern density. This alters the active section from rectangular into T-shaped, thereby shifting the neutral axis upwards and allowing the undamaged glass sheet to carry more tensile loads. In effect, ignoring the damaged layer in strength calculations (as is often done) is a safe, slightly conservative approach.
- In laminated glass beams, the post-failure strength depends on the fracture pattern density, the laminate stiffness and the laminate tensile strength. The former two determine to which extent compressive forces can be build up in the (broken) glass and thereby the type of load transfer mechanism activated after initial failure. The latter determines the tensile capacity of that mechanism. The compressive strength of the glass was never governing.
- As the elastic strain energy released at failure determines the fracture pattern density, it also influences the 2nd LTM. Thus, different test methods which yield varying levels of energy at failure, result in different LTMs and thus differences in post-failure strength. Therefore, when a certain post-failure strength is required, the type of impact with which failure is to be obtained should always be specified.
- Generally, the directly tested specimens yielded the lowest post-failure strength, while those predamaged to level III gave the highest post-failure strength. The results of the specimens predamaged to level I and II (by impact and simultaneous static load) were mostly in between.
- Since strain energy content is geometry dependent, size effects are to be expected when determining post-failure behaviour of glass elements.

- In the heat strengthened, PVB-laminated specimens, failure often coincided with collapse as the energy release caused the PVB to rupture. Only with the predamaged (to level III) specimens this was not observed. The thermally tempered specimens did not show this behaviour as their fracture pattern is so dense that the energy release is distributed over a much larger area of the laminate. Neither did this occur with the SG specimens.
- The presence of damage has only minor influence on both the initial and post-failure resistance of reinforced glass beams.

The results of this study have been used in Chapter 7 to construct Element Safety Diagrams and discuss the safety of each design.

Appendix F: Calculating Elastic Strain Energy in Glass Beams

This appendix elucidates the mechanics concept of *elastic strain energy* by providing calculation examples for glass beams. It presents the general equation for the elastic strain energy in a body, and continues with three methods with which it can be calculated for beams in three-point bending. Subsequently, with the application of the second method, the elastic strain energy content of a beam loaded in four-point bending is also determined. As a comparison to the energy induced by static external load, this appendix closes with an approximate calculation of the energy stored in a glass sheet by heat treatment.

1. General Equation

The total elastic strain energy content in a body U_ε is obtained by integrating the strain energy density $\chi(x,y,z)$ over the body volume B , Eq. (I.1).¹ The elastic strain energy density may vary throughout the body, and is thus a function of place in the body. At a single point, $\chi_{x,y,z}$ results from integrating the stress over the elastic strain, Eq. (I.2).

$$U_\varepsilon = \int_B \chi(x, y, z) dx dy dz \quad (\text{I.1})$$

$$\chi_{x,y,z} = \int_{\varepsilon_{el,max}} \sigma_{x,y,z}(\varepsilon) d\varepsilon \quad (\text{I.2})$$

Note that, $\chi(x,y,z)$ and $\sigma_{x,y,z}(\varepsilon)$ are *functions* (of place in the body and strain at a place in the body, respectively), while $\chi_{x,y,z}$ is a *value* (of elastic strain energy density at the point with coordinates x,y,z). For linear elastic materials, Eq. (I.2) yields $\chi_{x,y,z} = \frac{1}{2}\sigma_{\max}\varepsilon_{\max} = \frac{1}{2}\varepsilon_{\max}^2 E$.

2. Beam in Three-Point Bending

There are several ways in which the elastic energy content in a glass beam, freely supported and loaded in three-point bending can be calculated. We consider a glass beam of dimensions and properties as provided in Table F.1 and Figure F.1, and assume a nominal bending tensile failure stress of $\sigma_f = 45$ MPa.

The beam is loaded in bending and shear. As we shall see later on, the energy absorbed by elastic shear is negligible compared to that absorbed by the bending. However, we shall calculate it anyway.

¹ See general literature on elasticity, e.g. Blaauwendraad, J., Theory of Elasticity; Energy Principles and Variational Methods, TU Delft, the Netherlands, 2004.

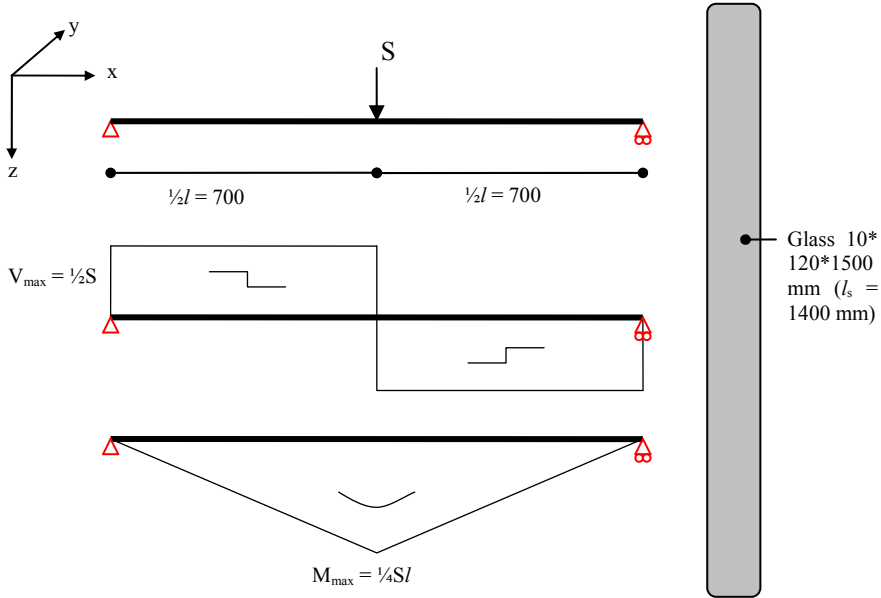


Fig. F.1 Section and distribution of load, moment and shear in freely supported example beam in three-point bending.

Table F.1 Dimensions and properties of example beam.

L	1500 mm	ν	0.22
l_s	1400 mm	I	$= \frac{1}{12}th^3 = 1.44 * 10^6 \text{ mm}^4$
h	120 mm	W	$= \frac{1}{6}th^2 = 24 * 10^3 \text{ mm}^3$
t	10 mm	σ_f	45 MPa
E	$70 \cdot 10^3$ MPa	M_{\max}	$= \sigma_f W = 45 * 24 * 10^3 = 1.08 * 10^6 \text{ Nmm}$
E_{shear}	$= E/(2(1+\nu)) = 28.7 \cdot 10^3$ MPa	S_{\max}	$= \frac{4M_{\max}}{l} = \frac{4 * 1.08 * 10^6}{1400} = 3085.7 \text{ N}$

2.1. Method 1: From Individual Stress and Strain Components

The most generally applicable – but also rather elaborate – method is to consider all stress-strain distributions through the beam. As will be shown in Section 4, this method can also be applied to calculate the strain energy induced by heat treatment.

If the elastic strain energy density is constant through the body, the total strain energy can be obtained simply through Eq. (I.1) from $U_e = \chi \cdot x_{\max} y_{\max} z_{\max}$. However, since the strain distribution is not constant, neither is the strain energy density. Therefore, the total strain energy has to be determined from integration of the strain energy density distribution function $\chi(x,y,z)$ over the body volume. To be able to do so, $\chi(x,y,z)$ can be

broken down in directional components (similar to stresses and strains), which for linear elastic materials, yields Eq. (I.3). This can be used to rewrite Eq. (I.1) as Eq. (I.4).

$$\chi_{ij}(x, y, z) = \frac{1}{2} \varepsilon_{ij}(x, y, z)^2 E \tag{I.3}$$

$$\begin{aligned} U_\varepsilon &= \frac{1}{2} \int_B (\sigma_{xx}(x, y, z) \varepsilon_{xx}(x, y, z)) dx dy dz + \frac{1}{2} \int_B (\sigma_{yy}(x, y, z) \varepsilon_{yy}(x, y, z)) dx dy dz \\ &+ \frac{1}{2} \int_B (\sigma_{zz}(x, y, z) \varepsilon_{zz}(x, y, z)) dx dy dz + \frac{1}{2} \int_B (\sigma_{xy}(x, y, z) \varepsilon_{xy}(x, y, z)) dx dy dz \\ &+ \frac{1}{2} \int_B (\sigma_{yx}(x, y, z) \varepsilon_{yx}(x, y, z)) dx dy dz + \frac{1}{2} \int_B (\sigma_{xz}(x, y, z) \varepsilon_{xz}(x, y, z)) dx dy dz \\ &+ \frac{1}{2} \int_B (\sigma_{zx}(x, y, z) \varepsilon_{zx}(x, y, z)) dx dy dz + \frac{1}{2} \int_B (\sigma_{yz}(x, y, z) \varepsilon_{yz}(x, y, z)) dx dy dz \\ &+ \frac{1}{2} \int_B (\sigma_{zy}(x, y, z) \varepsilon_{zy}(x, y, z)) dx dy dz \\ &= \frac{1}{2} E \int_B \varepsilon_{xx}(x, y, z)^2 dx dy dz + \frac{1}{2} E \int_B \varepsilon_{yy}(x, y, z)^2 dx dy dz + \frac{1}{2} E \int_B \varepsilon_{zz}(x, y, z)^2 dx dy dz \\ &+ \frac{1}{2} E \int_B \varepsilon_{xy}(x, y, z)^2 dx dy dz + \frac{1}{2} E \int_B \varepsilon_{yx}(x, y, z)^2 dx dy dz + \frac{1}{2} E \int_B \varepsilon_{xz}(x, y, z)^2 dx dy dz \\ &+ \frac{1}{2} E \int_B \varepsilon_{zx}(x, y, z)^2 dx dy dz + \frac{1}{2} E \int_B \varepsilon_{yz}(x, y, z)^2 dx dy dz + \frac{1}{2} E \int_B \varepsilon_{zy}(x, y, z)^2 dx dy dz \end{aligned} \tag{I.4}$$

Table F.2 Directional stress and strain components for beam in three-point bending.

Dir.	= 0 or ≠ 0	Dir.	= 0 or ≠ 0	Dir.	= 0 or ≠ 0
Xx	≠ 0	xy	= 0	zx	≠ 0
Yy	= 0	yx	= 0	yz	= 0
Zz	= 0	xz	≠ 0	zy	= 0

First, we investigate which components are equal to 0 and which are not, see Table F.2. It follows there are three components unequal to 0: xx, xz, and zx. By definition $xz = xz$. Thus, the contribution of two components has to be determined. Their stress distributions through the beam are presented in Figures I.2a and b and more unconventionally in Figures I.3a and b. The advantage of the latter Figures is that they show the distribution function shapes and indicate the total strain energy in the beam, i.e. the volumes enclosed by them. The following can be concluded with regard to the distribution functions:

- $\sigma_{xx}(x,y,z)$ is constant over y, thus: $\int \sigma_{xx}(x,y,z) dx dy dz = t \cdot \int \sigma_{xx}(x,z) dx dz$. Furthermore, $\sigma_{xx}(x,z)$ is linear over x and z.
- $\sigma_{xz}(x,y,z)$ is constant over x and y, thus: $\int \sigma_{xz}(x,y,z) dx dy dz = l \cdot t \cdot \int \sigma_{xz}(z) dz$. Furthermore, $\sigma_{xz}(z)$ is a second order function of z.

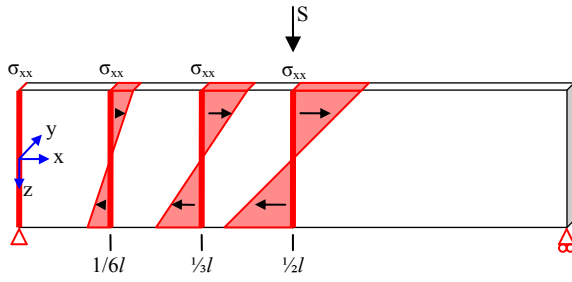


Fig. F.2a Normal stress σ_{xx} distribution through beam in three-point bending.

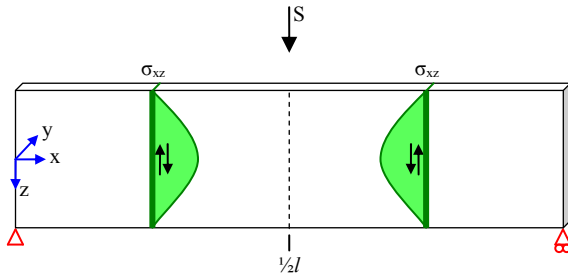


Fig. F.2b Shear stress σ_{xz} distribution through beam in three-point bending.

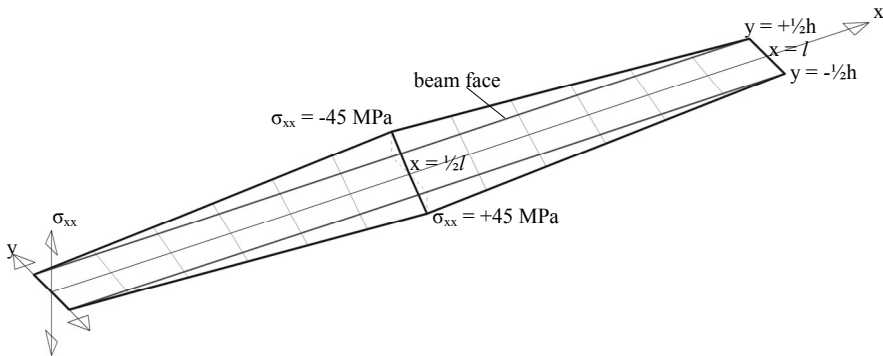


Fig. F.3a Normal stress σ_{xx} distribution through beam in three-point bending, 3D representation.

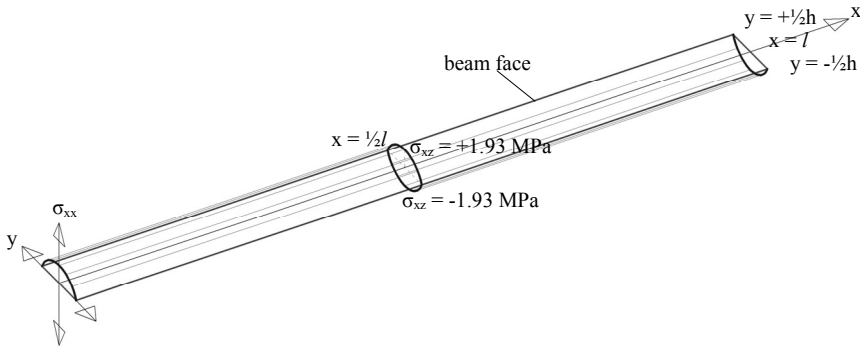


Fig. F.3b Shear stress σ_{xz} distribution through beam in three-point bending, 3D representation.

Thus, first the functions for $\sigma_{xx}(x,z)$ and $\sigma_{xz}(z)$ have to be determined.

- **For $\sigma_{xx}(x,z)$:** The function for the normal stress takes the general form: $\sigma_{xx} = axz + b$. It is easiest to consider the origin of the x,y,z axis system to lie at mid height of the beam, on one end (Figure F.3a). Then, $b = 0$ because $\sigma_{xx} = 0$ when x and z are 0. Consequently, a can be determined by considering that, at the midpoint of the beam, $\sigma_{xx} = \sigma_f = 45$ MPa:

$$45 = a \cdot 700 \cdot 60 \Leftrightarrow a = 45 / 700 \cdot 60 = 1.071429 \cdot 10^{-3} \Rightarrow$$

$$\sigma_{xx} = 1.071429 \cdot 10^{-3} xz$$

For the normal strain, the function can be found by dividing a through the Young's modulus. This yields:

$$\varepsilon_{xx} = \frac{\sigma_{xx}}{E} = \frac{1.071429 \cdot 10^{-3} xz}{70 \cdot 10^3} = 1.5306 \cdot 10^{-8} xz$$

- **For $\sigma_{xz}(z)$:** The shear stress is a second order function over the beam height. We again take the x,y,z -origin at midheight of the beam (Figure F.3b). Since the shear stresses are constant over the length, the position of $x = 0$ along the length of the beam is irrelevant. The function takes the form of: $\sigma_{xz} = az^2 + bz + c$. Here, c is equal to the maximum shear stress in the middle of the beam (because there, $z = 0$), which can be calculated through:

$$\sigma_{z_x, \max} = \frac{3V_{\max}}{2A} = \frac{3S_{\max}}{4th} = \frac{9257.1}{4800} = 1.9285625 \text{ MPa}, \text{ thus } c \approx 1.93.$$

Because $\sigma_{z_x}' = 2az + b$ has to be 0 for $z = 0$, b must also be equal to 0.

Now, a can be calculated by considering the shear stress has to be zero at the beam edges: $\sigma_{zx} = az^2 + 1.93 = 0$, for $z = \frac{1}{2}h = 60$. Thus:

$$a = -1.93 / 60^2 = -536 \cdot 10^{-6} \text{ N/mm}^4, \text{ so:}$$

$$\sigma_{zx} = -536 \cdot 10^{-6} z^2 + 1.93$$

Again, ε_{zx} can be obtained by dividing through the Young's modulus:

$$\varepsilon_{zx} = \frac{-536 \cdot 10^{-6} z^2 + 1.93}{70000} = -7.6543 \cdot 10^{-9} z^2 + 27.6 \cdot 10^{-6}$$

Now that both strain distribution functions are known, the elastic strain energy can be calculated through:

$$U_\varepsilon = \frac{1}{2} \cdot 4Et \int_{\frac{1}{2}l}^{\frac{1}{2}h} \varepsilon_{xx}^2 dx dz + \quad \mathbf{4A \text{ (Fig. F.4a)}}$$

$$\frac{1}{2} 2Et l \int_{\frac{1}{2}h} \varepsilon_{zx}^2 dz + \quad \mathbf{2B \text{ (Fig. F.4b)}}$$

$$\frac{1}{2} 2Et l \int_{\frac{1}{2}h} \varepsilon_{xz}^2 dz \quad \mathbf{2C; 2B = 2C}$$

$$\begin{aligned} 4A &= 2 \cdot 70000 \cdot 10 \int_{\frac{1}{2}l}^{\frac{1}{2}h} (2.342776 \cdot 10^{-16} x^2 z^2) dx dz = \\ &= 1.4 \cdot 10^6 \cdot \frac{1}{3} \frac{1}{3} 2.342776 \cdot 10^{-16} x^3 z^3 = \\ &= 1.4 \cdot 10^6 \cdot 2.603084 \cdot 10^{-17} \cdot 343000000 \cdot 216000 = \\ &= 1.4 \cdot 10^6 \cdot 0.00192857 = 2699 \text{ Nmm} = 2.7 \text{ J} \end{aligned}$$

$$\begin{aligned} 2B &= 70000 \cdot 10 \cdot 1400 \int_{\frac{1}{2}h} (5.859 \cdot 10^{-17} z^4 - 4.2251736 \cdot 10^{-13} z^2 + 76 \cdot 10^{-11}) dz = \\ &= 980 \cdot 10^6 \left(1.1718 \cdot 10^{-17} z^5 - 1.408 \cdot 10^{-13} z^3 + 76 \cdot 10^{-11} z \right) = \\ &= 980 \cdot 10^6 \left(0.911 \cdot 10^{-8} - 3.042 \cdot 10^{-8} + 4.571 \cdot 10^{-8} \right) = \\ &= 980 \cdot 10^6 \cdot 2.44 \cdot 10^{-8} = 24.4 \text{ Nmm} = 0.0244 \text{ J} \end{aligned}$$

Therefore, finally the total elastic strain energy in this beam becomes:

$$U_{\epsilon} = 2.699 + 0.024 + 0.024 = 2.748J$$

As we can see, the influence of the elastic shear strain energy is very small compared to the bending strain energy.

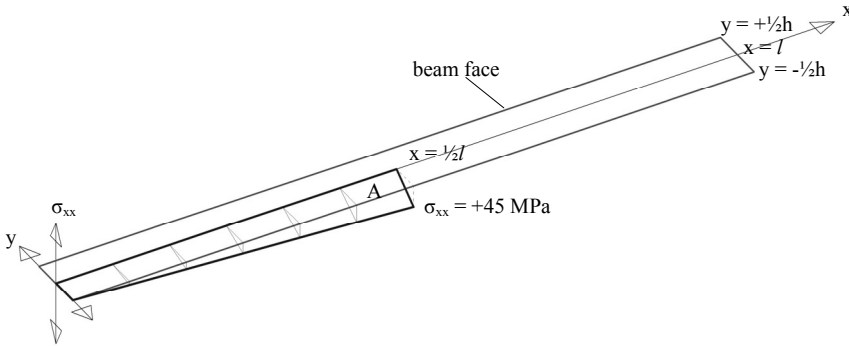


Fig. F.4a Volume representing A: $\frac{1}{4}$ of the elastic strain energy from normal stress σ_{xx} .

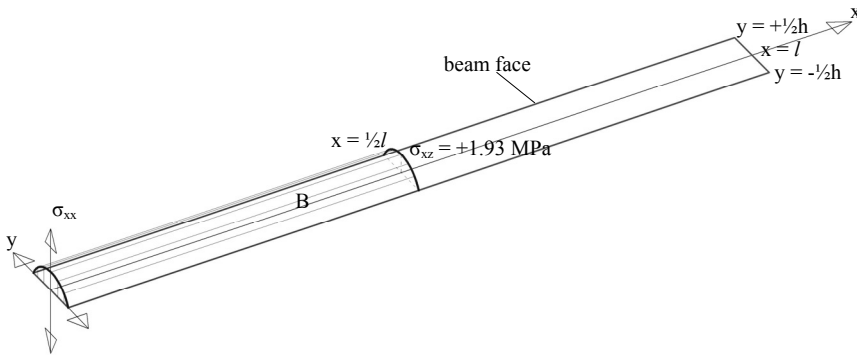


Fig. F.4b Volume representing B: $\frac{1}{2}$ of the elastic strain energy from shear stress σ_{xz} .

2.2. Method 2: From M, κ - and V, η^2 -curves

A second, more swift, method applies specifically to beams. It makes use of moment-curvature (M, κ) and shear force-shear angle rotation (V, η) diagrams. The elastic strain energy *per unit length* is the surface under the M, κ -diagram plus the surface under the V, η -diagram, Eq. (I.5). With Eqs. (I.6a), (I.6b), and (I.6c), this expression can be rewritten as Eq. (I.7), which has the advantage for this calculation that all variables except the strain energy are known or can be easily calculated.

$$\frac{U_{\epsilon}}{l} = \frac{1}{2} M \kappa + \frac{1}{2} V \eta \tag{I.5}$$

² Usually, for shear angle γ is used. However, in order to avoid confusion with abundantly used γ for safety factors in this publication, for shear angle η is used instead.

$$M = EI\kappa; V = E_{shear}A\eta \Leftrightarrow \eta = V / E_{shear}A; V = \frac{1}{2}S \quad (I.6a, b, c)$$

$$\frac{U_\varepsilon}{l} = \frac{1}{2}EI\kappa^2 + \frac{1}{8}\frac{S^2}{E_{shear}A} \quad (I.7)$$

However, since the moment M and thus the curvature κ are not constant throughout the beam length,³ the moment bending component in Eq. (I.7) has to be adjusted. The shear deformation component can remain unchanged since the shear stresses are constant over the beam length (except for a change from negative to positive). Consequently, Eq. (I.7) develops into Eq. (I.8) by integrating curvature over the beam length.

$$U_\varepsilon = \frac{1}{2}EI \int_l \kappa(l)^2 dl + \frac{1}{8}\frac{S^2}{E_{shear}A}l \quad (I.8)$$

Now $\kappa = \frac{M}{EI} = \frac{S}{4EI}l$, thus $\kappa^2 = \frac{S^2}{16E^2I^2}l^2$. The elastic strain is now:

$$U_\varepsilon = \frac{1}{2}EI \frac{1}{3}\frac{S^2}{16E^2I^2}l^3 + \frac{1}{8}\frac{S^2l}{E_{shear}A} = \frac{S^2l^3}{96EI} + \frac{1}{8}\frac{S^2l}{E_{shear}th}$$

For the given beam, this yields:

$$U_\varepsilon = \frac{3085.7^2 * 1400^3}{96 * 70000 * 1.44 * 10^6} + \frac{3085.7^2 * 1400}{8 * 28688.5 * 10 * 120} = \frac{2.612711808 * 10^{16}}{9.6768 * 10^{12}} + \frac{1.333 * 10^{10}}{275409600} = 2699.97 Nmm + 48.4 Nmm = 2.748J$$

The result is equal to the one previously obtained.

2.3. Method 3: From Load Displacement

Both outcomes can be checked by calculating the energy provided by the external load on the beam through Eq. (I.9). For linear elastic materials, this yields $U_\varepsilon = \frac{1}{2}F_{max}w_{max}$. The maximum load F_{max} has been determined above, and is equal to 3085.7 N. The maximum total displacement w_{max} consists of a bending component and a shear deformation component, Eq. (I.10).

$$U_\varepsilon = \int_{w_{max}} S(w)dw \quad (I.9)$$

³ M and κ are only constant in pure bending, e.g. the range between the loading points in four-point bending.

$$w_{\max} = \frac{Sl^3}{48EI} + \eta \frac{1}{2}l \tag{I.10}$$

$$\eta = \frac{V}{E_{\text{shear}}A} = \frac{\frac{1}{2}S}{E_{\text{shear}}th} = \frac{1542.85}{28688.5 \cdot 10 \cdot 120} = 44.816 \cdot 10^{-6}, \text{ thus:}$$

$$w_{\max} = \frac{3085.7 \cdot 2744 \cdot 10^6}{48 \cdot 70000 \cdot 1.44 \cdot 10^6} + 44.816 \cdot 10^{-6} \cdot 700 = 1.7500 + 0.0314 = 1.7814 \text{ mm}$$

This, again, yields $U_e = \frac{1}{2} \cdot 3085.7 \cdot 1.7814 = 2748 \text{ Nmm} = 2.748 \text{ J}$.

3. Beam in Four-Point Bending

The strain energy of the same beam loaded in four-point bending can also be calculated, e.g. by using the first method. Figure F.4 shows the load, moment, and shear distribution. The dimensions and all properties but one, are equal to the beam discussed in Section 2, and can thus be found in Table F.1. Only the maximum load is different, namely:

- $$S_1 = \frac{M_{\max}}{l_{\text{sec I}}} = \frac{1.08 \cdot 10^6}{500} = 2160 \text{ N};$$

$$S_{\text{tot}} = 2S_1 = 4320 \text{ N}$$

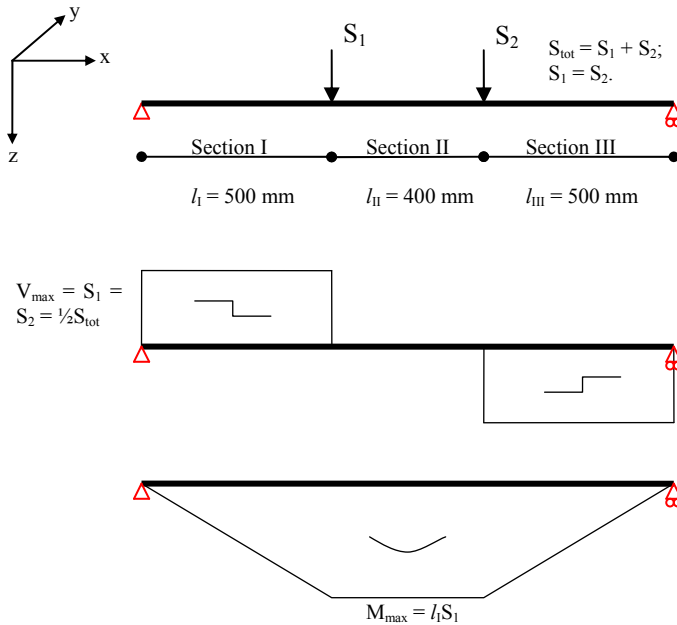


Fig. F.4 Distribution of load, moment and shear in freely supported example beam in four-point bending.

As shown in Figure F.4, the beam can be divided into three sections. The total strain energy in the beam is equal to the sum of the strain energy in each section:

$$U_{\varepsilon,tot} = U_{\varepsilon,I} + U_{\varepsilon,II} + U_{\varepsilon,III}, \text{ with } U_{\varepsilon,I} = U_{\varepsilon,III}.$$

Thus, we first calculate the energy content of Section I and Section II, separately.

3.1. Section I

The directional stresses and strains are similar to those in the beam in three-point bending. Thus, the observations of Table F.2 hold, as well as the previously drawn conclusions with regard to the stress distribution functions:

- $\sigma_{xx}(x,y,z)$ is constant over y , thus: $\int \sigma_{xx}(x,y,z) dx dy dz = t \cdot \int \sigma_{xx}(x,z) dx dz$. Furthermore, $\sigma_{xx}(x,z)$ is linear over x and z .
- $\sigma_{xz}(x,y,z)$ is constant over x and y , thus: $\int \sigma_{xz}(x,y,z) = l_1 \cdot t \cdot \int \sigma_{xz}(z) dz$. Furthermore, $\sigma_{xz}(z)$ is a second order function of z .

Again, the functions for $\sigma_{xx}(x,z)$ and $\sigma_{xz}(z)$ have to be determined. Since we follow the same steps as described in Section 2.1, only brief argumentation is provided.

- **For $\sigma_{xx}(x,z)$:** The function for the normal stress takes the general form: $\sigma_{xx} = axz + b$, with $b = 0$ (since $\sigma_{xx} = 0$ when x and z are 0). Consequently, a can be determined from $\sigma_{xx} = \sigma_f = 45 \text{ MPa}$:

$$45 = a \cdot 700 \cdot 60 \Leftrightarrow a = 45 / 700 \cdot 60 = 1.5 \cdot 10^{-3} \Rightarrow$$

$$\sigma_{xx} = 1.5 \cdot 10^{-3} xz$$

$$\varepsilon_{xx} = 2.143 \cdot 10^{-8} xz$$

- **For $\sigma_{zx}(z)$:** The function takes the form of: $\sigma_{zx} = az^2 + bz + c$.

$$\sigma_{zx,max} = \frac{3V}{2A} = \frac{3S_1}{2th} = \frac{6480}{2400} = 2.7 \text{ MPa}, \text{ thus } c = 2.7.$$

Because $\sigma_{zx}' = 2az + b$ has to be 0 for $z = 0$, b must be equal to 0.

Now, a can be calculated by considering the shear stress has to be zero at the beam edges: $\sigma_{zx} = cz^2 + 2.7 = 0$, for $z = \frac{1}{2}h = 60$. Thus:

$$a = -2.7 / 60^2 = -750 \cdot 10^{-6} \text{ N/mm}^4, \text{ so:}$$

$$\sigma_{zx} = -750 \cdot 10^{-6} z^2 + 2.7, \text{ and:}$$

$$\varepsilon_{zx} = -10.714 \cdot 10^{-9} z^2 + 38.6 \cdot 10^{-6}$$

With both strain distribution functions known, the elastic strain energy in section I can be calculated through:

$$U_{\varepsilon} = \frac{1}{2} \cdot 2Et \int_{l_I} \int_{\frac{1}{2}h} \varepsilon_{xx}^2 dx dz + \tag{2A}$$

$$\frac{1}{2} 2Etl_I \int_{\frac{1}{2}h} \varepsilon_{zx}^2 dz + \tag{2B}$$

$$\frac{1}{2} 2Etl \int_{\frac{1}{2}h} \varepsilon_{xz}^2 dz \tag{2C; 2B = 2C}$$

$$\begin{aligned} 2A &= 70000 \cdot 10 \int_{l_I} (4.592449 \cdot 10^{-16} x^2 z^2) dx dz = \\ &= 0.7 \cdot 10^6 \cdot \frac{1}{3} \frac{1}{3} 4.592449 \cdot 10^{-16} x^3 z^3 = \\ &= 0.7 \cdot 10^6 \cdot 5.069387778 \cdot 10^{-17} \cdot 125000000 \cdot 216000 = \\ &= 0.7 \cdot 10^6 \cdot 0.001368735 = 958.11429 Nmm = 0.958J \end{aligned}$$

$$\begin{aligned} 2B &= 70000 \cdot 10 \cdot 500 \int_{\frac{1}{2}h} (11.4789796 \cdot 10^{-17} z^4 - 8.271208 \cdot 10^{-13} z^2 + 148.996 \cdot 10^{-11}) dz = \\ &= 350 \cdot 10^6 (2.29579592 \cdot 10^{-17} z^5 - 2.757 \cdot 10^{-13} z^3 + 148.996 \cdot 10^{-11} z) = \\ &= 350 \cdot 10^6 (1.7852 \cdot 10^{-8} - 5.95512 \cdot 10^{-8} + 8.93976 \cdot 10^{-8}) = \\ &= 350 \cdot 10^6 \cdot 4.76984 \cdot 10^{-8} = 16.7 Nmm = 0.017J \end{aligned}$$

The total elastic strain energy in this section of the beam becomes:

$$U_{\varepsilon,sec I} = 0.958 + 0.017 + 0.017 = 0.992J$$

3.2. Section II

Table F.3 Directional stress and strain components for mid span section of beam in four-point bending.

Dir.	= 0 or ≠ 0	Dir.	= 0 or ≠ 0	Dir.	= 0 or ≠ 0
xx	≠ 0	xy	= 0	zx	≠ 0
yy	= 0	yx	= 0	yz	= 0
zz	= 0	xz	≠ 0	zy	= 0

Table F.3 lists which directional components of the stress and strain in the mid section (section II) are equal to 0 and which are not. Actually, only $\sigma_{xx} \neq 0$.

Additionally,

- $\sigma_{xx}(x,y,z)$ is constant over x and y , thus: $\sigma_{xx}(x,y,z) = l_{II} \cdot \sigma_{xx}(z)$. Furthermore, $\sigma_{xx}(z)$ is linear over z .

Thus, the function for $\sigma_{xx}(z)$ has to be determined.

- **For $\sigma_{xx}(z)$:** The function takes the general form: $\sigma_{xx} = az + b$, with $b = 0$. Then,

$$45 = a \cdot 60 \Leftrightarrow a = 45/60 = 0.75 \Rightarrow$$

$$\sigma_{xx} = 0.75z$$

$$\varepsilon_{xx} = 10.7143 \cdot 10^{-6} z$$

The elastic strain energy in section II can be calculated through:

$$U_{\varepsilon} = \frac{1}{2} \cdot 2Et l_{II} \int_{\frac{1}{2}h} \varepsilon_{xx}^2 dz \quad 2A$$

$$\begin{aligned} 2A &= 70000 \cdot 10 \cdot 400 \int_{\frac{1}{2}h} (114.7962245 \cdot 10^{-12} z^2) dz = \\ &= 280 \cdot 10^6 \cdot \frac{1}{3} 114.7962245 \cdot 10^{-12} z^3 = \\ &= 280 \cdot 10^6 \cdot 38.26540817 \cdot 10^{-12} \cdot 216000 = \\ &= 280 \cdot 10^6 \cdot 8.265328 \cdot 10^{-6} = 2314.29 Nmm = 2.314 J \end{aligned}$$

This result can easily be checked with the second method:

$$\frac{U_{\varepsilon}}{L} = \frac{1}{2} M \kappa + \frac{1}{2} V \eta.$$

Since $V = 0$ in section II and $\kappa = \frac{M}{EI}$, this transforms into: $U_{\varepsilon} = \frac{1}{2} \frac{M^2 l_{II}}{EI}$, in which all parameters except the strain energy are already known. This yields:

$$U_{\varepsilon} = \frac{1}{2} \frac{M^2 l_{sec II}}{EI} = \frac{(1.08 \cdot 10^6)^2 \cdot 400}{2 \cdot 70000 \cdot 1.44 \cdot 10^6} = \frac{1.1664 \cdot 10^{12} \cdot 400}{0.2016 \cdot 10^{12}} = 2314.29 Nmm = 2.314 J$$

(in agreement with the previous result).

3.3. Total

The total elastic strain energy in the beam is now:

$$U_{\epsilon,tot} = U_{\epsilon,I} + U_{\epsilon,II} + U_{\epsilon,III} = 0.992 + 2.314 + 0.992 = 4.3J$$

3.4. Load Displacement

If desired the vertical displacement at the point where the loads are applied can be determined from the previous result and Eq. (I.9):

$$U_{\epsilon} = \int S(w)dw = \frac{1}{2}S_{tot}w_1 \Leftrightarrow w_1 = \frac{U_{\epsilon}}{\frac{1}{2}F_{tot}} = \frac{4317.6}{2160} = 2.0mm$$

4. Strain Energy Induced by Heat Treatment

In heat treated glass, residual stresses are introduced by cooling rate differences. Effectively, forced deformations are introduced to the inner part of the glass sheet, which ‘wants’ to shrink more than the outer part, but is prevented from doing so. As a consequence, an amount of elastic strain energy is stored in the heat treated sheet. The amount of energy can be calculated by integrating the individual directional strain distribution functions over the body volume, similarly to method 1 applied to the externally loaded beam in Section 2.1.

In this example, the stored elastic strain energy caused by thermal prestress in a glass sheet is calculated. Its dimensions are equal to those of the sheet considered in the previous Section. It will be shown that, even with modest thermal stresses, the thermal elastic strain energy exceeds the strain energy caused by external loading by orders of magnitude.

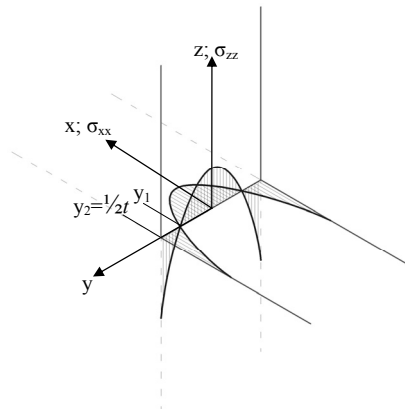


Fig. F.5 Through-the-thickness normal stress distribution in heat-treated glass.

The normal stress distribution through-the-thickness of a heat treated glass sheet, is usually idealized as a second order function (parabola; Figure F.5). When the sheet is in equilibrium, the integral from $y = 0$ to $y = \frac{1}{2}t$ must yield 0. Therefore, the maximum inner tensile stress at $y = 0$ has to be equal to half the maximum compressive surface stress at $y = \frac{1}{2}t$.⁴ Obviously, the normal stresses work in two perpendicular directions in planes parallel to the sheet outer surfaces, i.e. there is an σ_{xx} - and an σ_{zz} -component.

In a heat treated plate of finite size, shear stresses and normal stresses perpendicular to the surface would also arise. These may be of relevant size near the edges, but quickly diminish when moving towards the plate middle. In a plate of infinite size, they will disappear altogether. Their influence on the total strain energy is neglected in this calculation, not only because they are active in only a small portion of the plate, but also because there increasing influence at the edges is partially compensated by a decreasing influence of the normal stresses. Table F.4 lists all directional stress and strain components for a thermally prestressed glass sheet (of infinite length and width).

Edge-deviations of this idealized stress pattern have been neglected.

Table F.4 Directional stress and strain components for a thermally prestressed glass sheet.

Dir.	= 0 or ≠ 0	Dir.	= 0 or ≠ 0	Dir.	= 0 or ≠ 0
xx	≠ 0	xy	= 0	zx	= 0
yy	≠ 0	yx	= 0	yz	= 0
zz	= 0	xz	= 0	zy	= 0

Furthermore,

- $\sigma_{xx}(x,y,z) = \sigma_{zz}(x,y,z)$, and $\sigma_{xx}(x,y,z)$ is constant over x and z . Thus $\int \sigma_{xx}(x,y,z) dx dy dz = L \cdot H \cdot \int \sigma_{xx}(y) dy$.

When assuming a maximum compressive surface stress of -70 MPa, the normal strain functions can be determined.

- **For $\sigma_{xx}(z)$:** Due to equilibrium requirements, the maximum inner tensile stress is 35 MPa.

A stress of -70 MPa yields a strain of: $\epsilon = \frac{\sigma}{E} = \frac{-70}{70 \cdot 10^3} = -1.0 \cdot 10^{-3}$;

A stress of 35 MPa yields a strain of: $\epsilon = \frac{\sigma}{E} = \frac{35}{70 \cdot 10^3} = 0.5 \cdot 10^{-3}$.

The normal strain distribution over the thickness can be generally described as:

$\epsilon(z) = bz^2 + d$. Now, b and d can be determined by considering:

⁴ Both the parabolic shape of the normal stress distribution and the fact that the maximum inner tensile stress equals half the maximum compressive surface stress, were corroborated by preliminary investigations by the author using a SCALP-03 optical stress measurement device. Due to the fire at the Architecture Faculty, this study was abandoned and the results were not published. However, similar results can also be found with: Nielsen, J.H., Olesen, J.F., Stang, H., *Experimental Investigation of Residual Stresses in Toughened Glass*, Proceedings of the Challenging Glass Conference, Delft, the Netherlands, May 2008.

for $y = 0$, the strain is $\varepsilon = 0.5 \cdot 10^{-3}$, thus: $by^2 + d = 0.5 \cdot 10^{-3} \Leftrightarrow d = 0.5 \cdot 10^{-3}$,

while for $y = \frac{1}{2}t = 5$, the strain is $\varepsilon = -1.0 \cdot 10^{-3}$, thus:

$$by^2 + 0.5 \cdot 10^{-3} = -1.0 \cdot 10^{-3} \Leftrightarrow 5^2 b = -1.5 \cdot 10^{-3} \Leftrightarrow b = -0.00006.$$

Therefore:

$$\varepsilon_{xx} = -0.00006y^2 + 0.0005$$

Note that d is dimensionless, while $b = [1/\text{mm}^2]$.

With the strain function known, the zero strain point (y_l) can be calculated

$$\text{through: } 0 = 0.00006y^2 - 0.0005 \Leftrightarrow y = \sqrt{\frac{0.0005}{0.00006}} = 2.89\text{mm}$$

The stored thermal elastic strain energy can be calculated through:

$$U_\varepsilon = \frac{1}{2} 4ELh \int_0^{y_l} \varepsilon_{xx}^2 dy + \quad \text{A (caused by } \sigma_{xx}\text{)}$$

$$\frac{1}{2} 4ELh \int_0^{y_l} \varepsilon_{zz}^2 dy + \quad \text{B (caused by } \sigma_{zz}\text{);}$$

$$\quad \quad \quad \text{A = B}$$

$$A = 2 \cdot 70.000 \cdot 1500 \cdot 120 \int_0^{y_l} (0.00006y^2 - 0.0005)^2 dy =$$

$$2.52 \cdot 10^{10} \int_0^{y_l} (0.36 \cdot 10^{-8} y^4 - 0.6 \cdot 10^{-6} y^2 + 0.25 \cdot 10^{-6}) dy =$$

$$2.52 \cdot 10^{10} \left(\frac{1}{5} 0.36 \cdot 10^{-8} y_1^5 - \frac{1}{3} 0.6 \cdot 10^{-6} y_1^3 + 0.25 \cdot 10^{-6} y_1 \right) =$$

$$2.52 \cdot 10^{10} (0.145 \cdot 10^{-6} - 4.8275 \cdot 10^{-6} + 0.7225 \cdot 10^{-6}) =$$

$$2.52 \cdot 10^{10} \cdot |-3.96 \cdot 10^{-6}| = 99792\text{Nmm} = 99.8\text{J}$$

Therefore, finally the total elastic strain energy in the example glass sheet becomes:

$$U_\varepsilon = 99.8 + 99.8 = 199.6\text{J}$$

Considering the fact that the assumed prestress in this calculation was still moderate (70 MPa surface compression, whereas it can easily be more than 100 MPa), it is obvious the strain energy caused by thermal prestress is much larger than that caused by external loading (in this case about two orders of magnitude). The dense fracture pattern which results when this energy is released, is therefore not surprising.

In conjunction with the observations made in Appendix E concerning the failure behaviour of tempered and strengthened glass and the conclusions on the relation between strain energy release and crack growth drawn in Appendix G, it must be assumed that the thermal strain energy in heat strengthened glass is *not* released at breakage when it breaks in a annealed-like, though more dense, fracture pattern. The increased total crack length is probably due to the increased breaking strength and the larger external load induced strain energy associated with that. Otherwise, a much more dense fracture pattern – actually less dense but more similar to thermally tempered glass, rather than similar to annealed glass – would have to occur. Therefore, thermal strain energy and thermal prestress must still be present in broken heat strengthened glass. The calculations above support the hypothesis made in Appendix E, that there must be some critical prestress or energy threshold above which disintegration through thermal strain energy release will occur when cracking through the compressive layer occurs. This should be subject of further, experimental research.

Appendix G: Experimental Determination of the Relation between Elastic Strain Energy Release and Crack Growth in Standing, Single Sheet Glass Beams

It was experimentally investigated whether the total amount of crack growth in standing glass beams could be related to the elastic strain energy stored in the glass beam at the moment of failure – either directly or with some additional parameters. It was found that the total crack surface area that results in single sheet annealed glass beams could indeed be related to the elastic strain energy through the beam height, the thickness, a loading configuration factor, and a crack growth constant. From this relation the failure stress can be deducted with a relative standard deviation of only 8.7%. Attempted relations based on failure stress directly, provided significantly less accurate results. Relations based on strain energy density were less accurate than those based on total strain energy, but still gave relatively accurate results and require no knowledge of the load distribution at failure. The results have been published earlier¹, though less extensively.

1. Introduction

Structural glass elements with high residual strength, such as the stainless steel reinforced glass beams developed for the Zappi Glass & Transparency research², rely on broken glass to transfer compressive forces in the post-initial failure stage. The extent of crack growth upon failure is likely to affect the magnitude of the obtainable maximum residual strength, either through the extent of crushing or by the influence on stability issues.

When studying the failure behaviour of laminate glass plates, Kott and Vogel found³ the intensive cracking pattern in annealed glass after a direct loading-to-failure test eliminates any residual strength, while an annealed glass laminate with less intensive cracking (caused by incidental impact) could still carry significant loads. The importance of the crack growth intensity was also experienced by the author in the development of hybrid glass-acrylic façade struts⁴. Tested in bending, only limited crack growth occurred upon initial failure, resulting in considerable residual strength and stiffness. However, when subjected to a buckling test, much more intensive cracking occurred. Consequently, the broken glass could not provide any significant

¹ Bos, F.P., *Elastic Strain Energy and Crack Length in Glass Beams*, Proceedings of the 3rd International Symposium on the Application of Architectural Glass (ISAAG), Munich, Germany, October 2008.

² Chapters 2 and 8, *AdDoc I: Zappi, 1996 – February 2004*, additional document to this PhD, www.glass.bk.tudelft.nl, and the numerous publications to which is referred there.

³ Kott, A., Vogel, T., *Structural Behaviour of Broken Laminated Broken Safety Glass*, in: Crisinel, M., Eekhout, M., Haldimann, M., Visser, R. (Eds.), *EU Cost C13 Final Report, Glass & Interactive Building Envelopes*, Research in Architectural Engineering Series, Volume 1, IOS Press, Amsterdam, the Netherlands, 2007, pp. 123 – 132.

⁴ Chapter 2, Section 3.

residual stiffness (and thus neither significant residual strength, as buckling failure is stiffness governed).

It is well known similar sheets of glass may break at rather varying stress levels. It may then be observed the density of the cracking pattern which results from failure, increases with increasing stress levels. Therefore, it can be tempting to assert that the total crack surface area depends directly on the failure stress at the crack origin. However, the author suggests that the crack area is a function of the elastic strain energy stored in the glass element upon failure, rather than of the failure stress (although they are related properties). The importance of this suggestion is that, while the failure stress is beyond the influence of the structural glass designer (being a material property), the elastic strain energy at failure is not. Besides failure stress and Young's modulus, the strain energy at failure namely also depends on element geometry and loading configuration.

In this study, stress, strain energy density and total strain energy content⁵ have been compared as predictive indicators for the total crack area in standing single sheet annealed glass beams. It will be shown that, at least for such specimens, the total strain energy content predicts the total crack area best – and the failure stress predicts it worst. A simple equation was found that relates the total crack length through a crack area constant with the elastic strain energy at failure and some other geometrical parameters, with a fair amount of accuracy.

2. Investigated Relations

Several relations, listed in Table G.1, were proposed and compared. Their suitability was assessed through the relative standard deviation (RSD; the standard deviation as a percentage of the mean) of the constant C_n (with n the number of the relation) which results from them, taken over all specimens, as well as over sets of groups. Ideally, a constant relation would yield equal results for C_n for all specimens and an RSD equal to 0. However, due to several inaccuracies (e.g. geometry dimensions, loading configuration, crack length measurement, angle between crack and glass surface) as well as the generally observed scatter in glass failure results, a significant RSD may be expected even in the best obtainable relation.

In total, 15 relations were investigated, divided into three sets of five each. Each set takes similar shape and is based on the basic variables failure stress σ_f , failure strain energy density χ_f , and total elastic strain energy at failure $U_{e,f}$, respectively. Since strain energy density is dependent on failure stress squared and Young's modulus and only specimens with identical (nominal) Young's modulus were used, the second group of relations, (R6)-(R10), differs only from the first group, (R1)-(R5), in the fact that they are dependent on the failure stress *squared* instead of just the failure stress. Both these groups are independent of specimen geometry and load configuration, contrary to the last group. The total strain energy content is highly dependent both on specimen geometry and load configuration.

⁵ Both concepts have been introduced in Appendix F, along with example calculations.

Table G.1 Investigated hypothetical constant relations between crack length and other specimen parameters.

Stress-based relations	Strain Energy Density-based relations	Strain Energy-based relations
$\frac{l_{fr}}{\sigma_f} = C_{R1}$ (R1)	$\frac{l_{fr}}{\chi_f} = C_{R6}$ (R6)	$\frac{l_{fr}}{U_{\varepsilon,f}} = C_{R11}$ (R11)
$\frac{A_{fr}}{\sigma_f} = C_{R2}$ (R2)	$\frac{A_{fr}}{\chi_f} = C_{R7}$ (R7)	$\frac{A_{fr}}{U_{\varepsilon,f}} = C_{R12}$ (R12)
$\frac{l_{fr}}{\sigma_f h} = C_{R3}$ (R3)	$\frac{l_{fr}}{\chi_f h} = C_{R8}$ (R8)	$\frac{l_{fr}}{U_{\varepsilon,f} h} = C_{R13}$ (R13)
$\frac{A_{fr}}{\sigma_f h} = C_{R4}$ (R4)	$\frac{A_{fr}}{\chi_f h} = C_{R9}$ (R9)	$\frac{A_{fr}}{U_{\varepsilon,f} h} = C_{R14}$ (R14)
$\frac{A_{fr}}{\sigma_f h \alpha_{config}} = C_{R5}$ (R5)	$\frac{A_{fr}}{\chi_f h \alpha_{config}} = C_{R10}$ (R10)	$\frac{A_{fr}}{U_{\varepsilon,f} h \alpha_{config}} = C_{R15}$ (R15)
With:		
C_{Rn}	= hypothetical glass cracking constant of relation n [varies]	
l_{fr}	= Total crack length [mm]	
$U_{\varepsilon,f}$	= Elastic Strain Energy stored in glass beam at failure [Nmm] = $[10^{-3} \text{ J}]$	
$A_{fr} = 2l_{fr}t\alpha_t$	= Nominal total crack surface area [mm^2]	
t	= Nominal glass beam thickness [mm]	
h	= Nominal glass beam height [mm]	
$\alpha_t = 1.05$	= Thickness correction factor [-]	
$\alpha_{config} = \frac{M_{max}}{\int_0^l M(l)dl}$	= Load Configuration Factor (LCF) [mm^{-1}]	
$\chi_f = \frac{1}{2} \frac{\sigma_f^2}{E}$	= Failure Elastic Strain Energy Density [Nmm^{-2}]	
l	= Support span length [mm]	
M, M_{max}	= Nominal Moment, Nominal Maximum Moment [Nmm]	
σ_f	= Nominal failure stress [MPa]	
E	= Young's modulus of Elasticity [MPa]	

Relations (R1), (R6) and (R11) propose a simple linear proportion between crack length l_{fr} and the basic variables (σ_f , χ_f , and $U_{e,f}$). Alternatively, (R2), (R7) and (R12) propose a relation between the crack surface *area* A_{fr} and the basic variables. If crack growth is energy dependent, this would make more sense as it takes more energy to produce a crack through a thick surface than through a thin surface. The total crack surface area was estimated by multiplying two times the total crack length (a crack produces two surfaces) with the nominal thickness times a correction factor of 1.05. This factor accounts for cracks running not perpendicularly to the glass surface. This actually only occurred for a small portion of the cracks, well away from the crack origin. The value of 1.05 is a rough estimate based on visual inspection.

Relations (R3), (R8), (R13), and (R4), (R9), (R14), are similar to (R1), (R6), (R11), and (R2), (R7), (R12), respectively, but introduce the beam height in the denominator. This factor takes into account that crack growth is also geometry dependent. Provided it has enough driving energy, a crack will grow once started until it reaches the edge of a specimen. In a high beam a crack just needs to travel longer before it reaches the edge, thus a larger portion of energy may be dissipated by crack growth.

Finally, in relations (R5), (R10), and (R15), a correction factor for the load configuration is introduced. It was observed that a larger portion of the total strain energy was absorbed by crack growth if the load is more concentrated. The Load Configuration Factor (LCF) α_{config} is a unified factor for the moment distribution over the beam as illustrated in Figures J.1a through d. Since the moment distribution is similar to the maximum principal stress distribution as well as the strain energy density distribution, α_{config} can also be expressed in those parameters, Eq. (J.1).

$$\alpha_{config} = \frac{M_{max}}{\int_0^l M(l)dl} = \frac{\sigma_{max}}{\int_0^l \sigma(l)dl} = \frac{\chi_{max}}{\int_0^l \chi(l)dl} \quad (J.1)$$

For now, only symmetrical 3- and 4-point bending tests have been performed. Thus, the definition of α_{config} for distributed load or constant moment as presented in Figures J.2c and d is still theoretical. Perhaps contrary to expectation, α_{config} is *not* independent of specimen span. Rather, for mechanically determined, two-side supported beams:

$$\frac{1}{l_s} \leq \alpha_{config} \leq \frac{2}{l_s}.$$

Fig. G.1a: 4p-bending

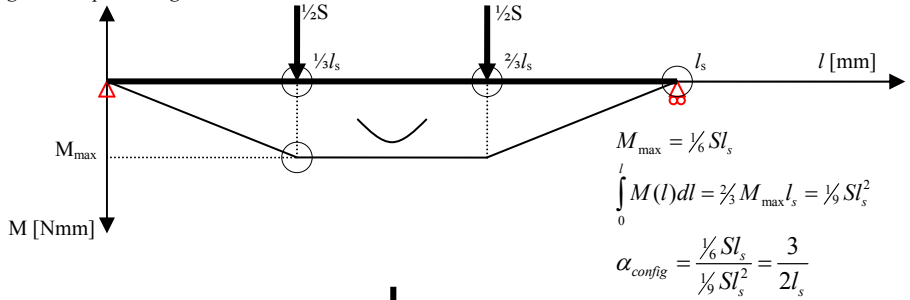


Fig. G.1b: 3p-bending

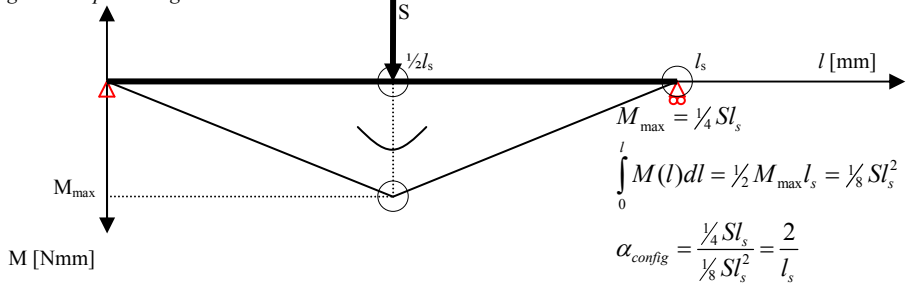


Fig. G.1c: Distributed load

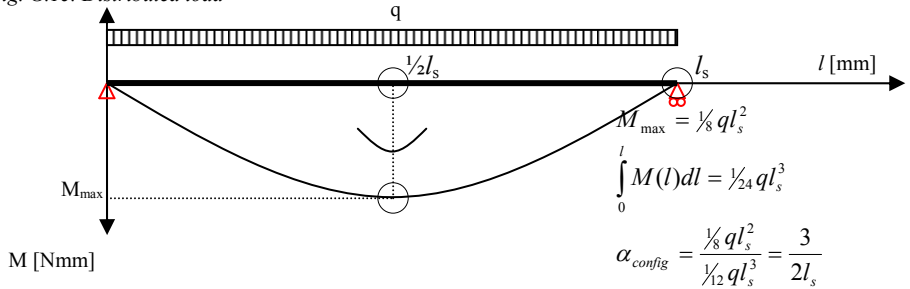


Fig. G.1d: Constant Moment

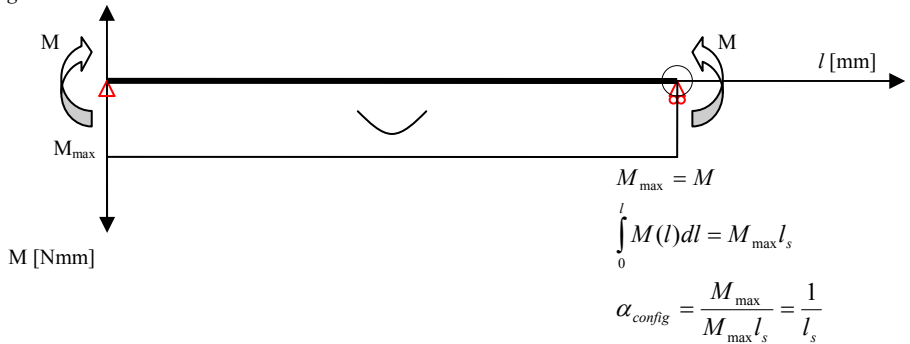


Fig. G.1a-d Determination of α_{config} for several load configurations.

3. Experimental Method

A large series of glass beams of various geometries has been subjected to 3- and 4p-bending tests in different load configurations, an overview of which is presented in Table G.2. All specimens had a solid section.

Table G.2 Overview of specimen geometry and loading configuration.

Group	Quantity	Geometry l x h x t [mm ³]	Loading Configuration (symmetrical)		
			3p/4p	Support span [mm]	Load span [mm]
G1	20	1000 x 100 x 10	4p	880	230
G2	2	1050 x 150 x 10	4p	880	230
G3	4	750 x 40 x 10	4p	700	230
G4	4	750 x 40 x 10	4p	530	160
G5	7	590 x 80 x 10	4p	530	160
G6	7	600 x 100 x 6	4p	530	160
G7	4	600 x 100 x 6	3p	470	0
G8	3	800 x 80 x 6	4p	700	230

All specimens were wrapped in plastic foil. The total crack length in each specimen was determined by photographing the specimens after failure, importing the pictures into AutoCad and drawing lines over all cracks (Figures J.2a and b). The elastic strain energy content of each specimen at failure was calculated based on the nominal dimensions of the specimens and the specimen failure stress with a specially prepared spreadsheet.

Subsequently, the hypothetical constant relations between specimen and failure parameters were investigated by determining their results and calculating the RSD of C_n for groups of specimens, sets of groups and all specimens.



Fig. G.2a Specimen G7-2 with highlighted cracks.

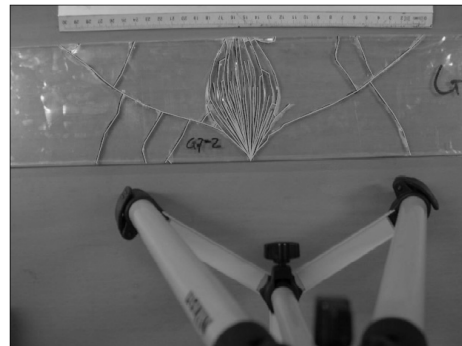


Fig. G.2b Crack pattern of the same specimen as drawn in AutoCad.

4. Results

For all specimens, the nominal maximum stress, nominal maximum elastic strain density, and nominal total strain energy at failure have been determined from the experimental failure loads. The total crack length was also measured (Table G.3). The results of several specimens had to be ignored for various reasons given in Table G.4. Subsequently, the hypothetical constants C_n of each specimen for each of the 15 proposed relations were determined (Table G.5). Then, the average, standard deviation and RSD values for C_n were calculated for each group of specimens, several sets of groups as well as for all specimens together (Table G.6). Finally, the energy dissipation as a percentage of the total stored strain energy at failure was determined, assuming a surface energy of $\gamma = 3 \text{ J/m}^2$ (Table G.7).

Table G.3 Experimental results and determined failure parameters.

Group	Specimen	S_f [N]	$\sigma_{\max,f}$ [N/mm ²]	$\chi_{\max,f}$ [N/mm ²]	$U_{el, str,f}$ [J]	l_{fr} [mm]
G1	G1-1	7843.4	76.5	0.0418	6.40	3032.3
	G1-2	4912.4	47.9	0.0164	2.51	1495.1
	G1-3	6875.9	67.0	0.0321	4.91	2266.3
	G1-4	5097.6	49.7	0.0176	2.70	1542.9
	G1-5	4941.5	48.2	0.0166	2.54	1498.0
	G1-6	8025.0	78.2	0.0437	6.68	3638.2
	G1-7	4272.9	41.7	0.0124	1.90	1143.3
	G1-8	5110.7	49.8	0.0177	2.71	1450.2
	G1-9	5698.8	55.6	0.0221	3.38	1660.4
	G1-10	5383.2	52.5	0.0197	3.01	1691.2
	G1-11	5248.8	51.2	0.0187	2.86	1393.2
	G1-12	5250.8	51.2	0.0187	2.86	1602.6
	G1-13	6484.3	63.2	0.0286	4.36	1926.6
	G1-14	5233.5	51.0	0.0186	2.84	1575.2
	G1-15	4963.2	48.4	0.0167	2.56	1452.4
	G1-16	5484.5	53.5	0.0204	3.13	1734.9
	G1-17	5070.0	49.4	0.0175	2.67	1802.8
	G1-18	4766.8	46.5	0.0154	2.36	1334.9
	G1-19	5045.8	49.2	0.0173	2.65	1472.1
	G1-20	5627.0	54.9	0.0215	3.29	1654.6
	G1-21	4353.1	42.4	0.0129	1.96	1010.3
	G1-22	4385.5	42.8	0.0131	2.00	1215.5
	G1-23	6698.9	65.3	0.0305	4.66	1977.8
	G1-24	4861.3	47.4	0.0160	2.46	1405.7

G2	G2-2	11354.0	49.2	0,0173	4,10	1885,4
	G2-6	13543.1	58.7	0,0246	5,84	3251,4
G3	G3-1	1651.2	72.8	0,0378	1,96	472,9
	G3-2	1169.7	51.5	0,0190	0,99	243,0
	G3-3	1603.4	70.6	0,0357	1,85	483,6
	G3-4	2240.4	98.7	0,0696	3,61	781,7
	G3-6	1936.1	85.3	0,0520	2,70	601,5
G4	G4-2	1911.7	66.3	0,0314	1,20	395,0
	G4-3	1754.6	60.9	0,0265	1,01	355,2
	G4-4	2210.0	76.7	0,0420	1,61	420,4
	G4-5	2625.6	91.1	0,0592	2,27	720,6
	G4-6	1915.4	66.4	0,0315	1,21	408,9
G5	G5-1	8431.3	73.1	0,0382	3,03	1587,1
	G5-2	10095.6	87.5	0,0547	4,34	1928,4
	G5-3	10322.5	89.5	0,0572	4,54	1760,5
	G5-4	10491.0	91.0	0,0591	4,69	2007,3
	G5-5	8862.9	76.9	0,0422	3,34	1607,5
	G5-6	10374.0	90.0	0,0578	4,58	2207,2
	G5-7	84987.0	73.7	0,0388	3,07	1603,0
G6	G6-1	6159.1	57.0	0,0232	1,41	1598,9
	G6-2	5722.8	52.9	0,0200	1,22	1620,4
	G6-3	8540.1	79.0	0,0446	2,72	3060,8
	G6-4	5790.2	53.6	0,0205	1,25	1863,6
	G6-5	4780.7	44.2	0,0140	0,85	1273,4
	G6-6	5674.5	52.5	0,0197	1,20	1669,7
	G6-7	4981.2	46.1	0,0152	0,93	1331,7
G7	G7-1	5901.2	69.3	0,0343	1,19	2256,1
	G7-2	6082.9	71.5	0,0365	1,27	2627,1
	G7-4	5850.4	68.7	0,0338	1,17	1784,0
	G7-5	5898.4	69.3	0,0343	1,19	2217,0
G8	G8-1	4290.4	78.8	0,0443	2,82	1989,3
	G8-2	3254.4	59.7	0,0255	1,62	1248,0
	G8-3	2689.6	49.4	0,0174	1,11	825,3

Table G.4 Specimens of which results were ignored.

Specimen	Reason for ignoring result
G2-1, G2-3, G2-4, G2-5	Foil tearing after failure, consequent falling onto the ground resulting in many extra cracks.
G3-5	Double origin failure, see Fig. G.3.
G4-1	Wrong load span applied.
G7-3, G7-6	Non-edge failure, see Fig. G.4a and b.

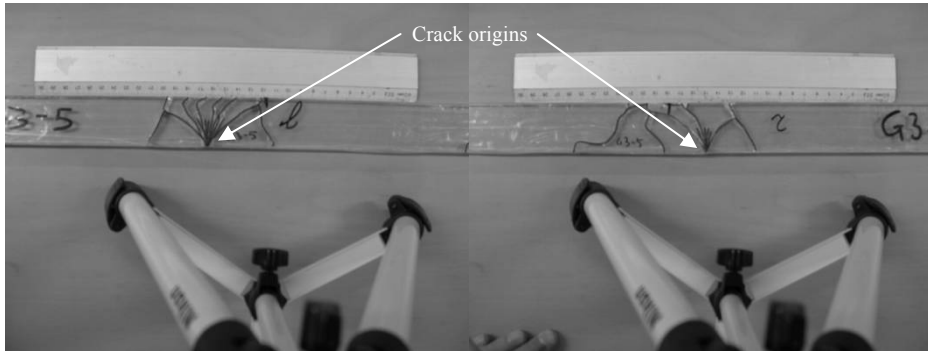


Fig. G.3 Double origin failure in specimen G3-5.

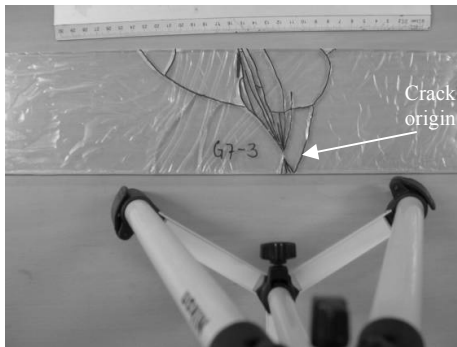


Fig. G.4a Non-edge failure in specimen G7-3.

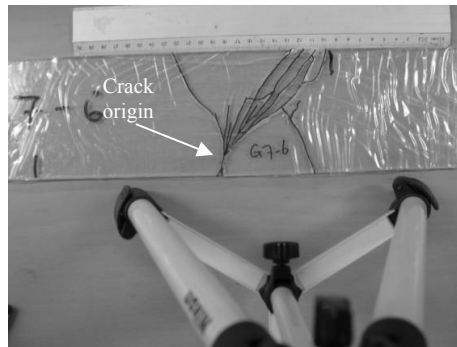


Fig. G.4b Non-edge failure in specimen G7-6.

Table G.5 Values of C of each specimen for proposed relations (1)-(15).

Spec	R1	R2	R3	R4	R5 10^3	R6 10^3	R7 10^3	R8 10^3	R9 10^3	R10 10^6	R11	R12	R13	R14	R15 10^3
G1-1	39,7	397	0,397	3,97	2,20	72,6	726	0,726	7,26	4,03	474	4741	4,74	47,41	26,3
G1-2	31,2	312	0,312	3,12	1,73	91,2	912	0,912	9,12	5,06	596	5963	5,96	59,63	33,1
G1-3	33,8	338	0,338	3,38	1,88	70,6	706	0,706	7,06	3,92	462	4620	4,62	46,20	25,6
G1-4	31,0	310	0,310	3,10	1,72	87,4	874	0,874	8,74	4,85	572	5716	5,72	57,16	31,7
G1-5	31,1	311	0,311	3,11	1,73	90,3	903	0,903	9,03	5,01	590	5901	5,90	59,01	32,7
G1-6	46,5	465	0,465	4,65	2,58	83,2	832	0,832	8,32	4,62	544	5444	5,44	54,44	30,2
G1-7	27,4	274	0,274	2,74	1,52	92,2	922	0,922	9,22	5,12	602	6017	6,02	60,17	33,4

G1-8	29,1	291	0,291	2,91	1,62	81,8	818	0,818	8,18	4,54	535	5351	5,35	53,51	29,7
G1-9	29,9	299	0,299	2,99	1,66	75,3	753	0,753	7,53	4,18	491	4915	4,91	49,15	27,3
G1-10	32,2	322	0,322	3,22	1,79	85,9	859	0,859	8,59	4,77	561	5615	5,61	56,15	31,2
G1-11	27,2	272	0,272	2,72	1,51	74,5	745	0,745	7,45	4,13	486	4863	4,86	48,63	27,0
G1-12	31,3	313	0,313	3,13	1,74	85,6	856	0,856	8,56	4,75	559	5594	5,59	55,94	31,0
G1-13	30,5	305	0,305	3,05	1,69	67,5	675	0,675	6,75	3,75	441	4414	4,41	44,14	24,5
G1-14	30,9	309	0,309	3,09	1,71	84,7	847	0,847	8,47	4,70	554	5542	5,54	55,42	30,8
G1-15	30,0	300	0,300	3,00	1,67	86,8	868	0,868	8,68	4,82	567	5674	5,67	56,74	31,5
G1-16	32,4	324	0,324	3,24	1,80	84,9	849	0,849	8,49	4,71	555	5547	5,55	55,47	30,8
G1-17	36,5	365	0,365	3,65	2,02	103,3	1033	1,033	10,3	5,73	676	6760	6,76	67,60	37,5
G1-18	28,7	287	0,287	2,87	1,59	86,5	865	0,865	8,65	4,80	565	5649	5,65	56,49	31,4
G1-19	29,9	299	0,299	2,99	1,66	85,2	852	0,852	8,52	4,73	557	5565	5,57	55,65	30,9
G1-20	30,2	302	0,302	3,02	1,67	77,0	770	0,770	7,70	4,27	502	5024	5,02	50,24	27,9
G1-21	23,8	238	0,238	2,38	1,32	78,5	785	0,785	7,85	4,36	514	5143	5,14	51,43	28,5
G1-22	28,4	284	0,284	2,84	1,58	93,1	931	0,931	9,31	5,17	607	6072	6,07	60,72	33,7
G1-23	30,3	303	0,303	3,03	1,68	64,9	649	0,649	6,49	3,60	424	4244	4,24	42,44	23,6
G1-24	29,7	297	0,297	2,97	1,65	87,6	876	0,876	8,76	4,86	573	5725	5,73	57,25	31,8
G2-2	38,3	383	0,26	2,55	1418	109,0	1090	0,727	7,27	4,03	460	4597	3,06	30,65	17,0
G2-6	55,4	554	0,37	3,69	2050	132,2	1322	0,881	8,81	4,89	557	5572	3,71	37,15	20,6
G3-1	6,5	65	0,16	1,62	756	12,5	125	0,313	3,13	1,45	241	2409	6,02	60,21	28,0
G3-2	4,7	47	0,12	1,18	548	12,8	128	0,320	3,20	1,49	247	2467	6,17	61,67	28,7
G3-3	6,8	68	0,17	1,71	796	13,6	136	0,339	3,39	1,58	261	2613	6,53	65,32	30,4
G3-4	7,9	79	0,20	1,98	921	11,2	112	0,281	2,81	1,31	216	2163	5,41	54,07	25,1
G3-6	7,1	71	0,18	1,76	820	11,6	116	0,289	2,89	1,35	223	2229	5,57	55,71	25,9
G4-2	6,0	60	0,15	1,49	514	12,6	126	0,314	3,14	1,08	329	3289	8,22	82,23	28,4
G4-3	5,8	58	0,15	1,46	503	13,4	134	0,336	3,36	1,16	351	3511	8,78	87,78	30,3
G4-4	5,5	55	0,14	1,37	473	10,0	100	0,250	2,50	0,86	262	2619	6,55	65,47	22,6
G4-5	7,9	79	0,20	1,98	682	12,2	122	0,304	3,04	1,05	318	3180	7,95	79,51	27,4
G4-6	6,2	62	0,15	1,54	531	13,0	130	0,324	3,24	1,12	339	3391	8,48	84,77	29,2
G5-1	21,7	217	0,27	2,71	936	41,6	416	0,520	5,20	1,79	525	5246	6,56	65,57	22,6
G5-2	22,0	220	0,28	2,75	950	35,2	352	0,440	4,40	1,52	444	4445	5,56	55,56	19,2
G5-3	19,7	197	0,25	2,46	848	30,8	308	0,384	3,84	1,33	388	3881	4,85	48,51	16,7
G5-4	22,1	221	0,28	2,76	951	34,0	340	0,424	4,24	1,46	428	4284	5,36	53,55	18,5
G5-5	20,9	209	0,26	2,61	902	38,1	381	0,476	4,76	1,64	481	4807	6,01	60,09	20,7
G5-6	24,5	245	0,31	3,07	1058	38,2	382	0,477	4,77	1,65	482	4818	6,02	60,23	20,8
G5-7	21,8	218	0,27	2,72	938	41,3	413	0,517	5,17	1,78	522	5217	6,52	65,21	22,5
G6-1	28,1	168	0,28	1,68	581	69,0	414	0,690	4,14	1,43	1131	6785	11,3	67,85	23,4
G6-2	30,6	184	0,31	1,84	634	81,0	486	0,810	4,86	1,68	1327	7963	13,3	79,63	27,5
G6-3	38,7	232	0,39	2,32	802	68,7	412	0,687	4,12	1,42	1126	6754	11,3	67,54	23,3
G6-4	34,8	209	0,35	2,09	720	91,0	546	0,910	5,46	1,88	1491	8947	14,9	89,47	30,9
G6-5	28,8	173	0,29	1,73	596	91,2	547	0,912	5,47	1,89	1495	8969	15,0	89,69	30,9

G7	Ave	31,8	191	0,32	1,91	0,45	63,7 9	383	0,64	3,83	0,90	1837	1101 8	18,3	110	25,9
	SD	4,45	26,7	0,04	0,27	0,06	7,98	47,9	0,08	0,48	0,11	230	1379	2,30	13,8	3,24
	RSD [%]	14,0	14,0	14,0	14,0	14,0	12,5	12,5	12,5	12,5	12,5	12,5	12,5	12,5	12,5	12,5
G8	Ave	21,0	126	0,26	1,57	0,73	47,1	282	0,59	3,53	1,64	740	4440	9,25	55,5 0	25,8 1
	SD	4,27	25,6 3	0,05	0,32	0,15	2,05	12,3	0,03	0,15	0,07	32,2	193	0,40	2,41	1,12
	RSD [%]	20,4	20,4	20,4	20,4	20,4	4,4	4,4	4,4	4,4	4,4	4,3	4,3	4,3	4,3	4,3
G1, G2 *	Ave	32,5	325	0,31	3,13	1,74	85,8	858	0,83	8,28	4,59	539	5395	5,26	52,6	29,2
	SD	6,47	65	0,05	0,46	0,25	13,7	137	0,09	0,89	0,49	58,3	583	0,79	7,91	4,39
	RSD [%]	19,9	19,9	14,6	14,6	14,6	16,0	16,0	10,7	10,7	10,7	10,8	10,8	15,0	15,0	15,0
G3, G8 *	Ave	12,0	88,4	0,20	1,62	0,75	25,4	183	0,41	3,25	1,51	426	3150	7,18	57,9	26,9
	SD	7,82	34,9	0,06	0,28	0,13	18,0	82,9	0,15	0,30	0,14	261	1082	1,76	4,19	1,95
	RSD [%]	65,2	39,5	30,7	17,5	17,5	71,1	45,3	35,5	9,33	9,33	61,3	34,4	24,5	7,23	7,23
G4, G5, G6 *	Ave	21,4	167	0,26	2,12	0,73	47,0	350	0,55	4,32	1,49	751	5531	9,20	72,2	24,9
	SD	10,5	67,2	0,07	0,54	0,19	29,7	155	0,23	0,91	0,31	478	2166	3,59	13,3	4,60
	RSD [%]	49,3	40,3	27,4	25,4	25,4	63,3	44,3	41,2	21,1	21,1	63,7	39,2	39,0	18,5	18,5
G3, G4 **	Ave	6,44	64,4	0,16	1,61	0,65	12,3	123	0,31	3,07	1,24	279	2787	6,97	69,6 8	27,6
	SD	1,03	10,3	0,03	0,26	0,16	1,09	10,9	0,03	0,27	0,23	50,6	506	1,26	12,6 4	2,44
	RSD [%]	15,9	15,9	15,9	15,9	24,5	8,84	8,84	8,84	8,84	18,2	18,2	18,2	18,2	18,2	8,84
G6, G7 **	Ave	31,7	190	0,32	1,90	0,58	75,3	452	0,75	4,52	1,41	1522	9134	15,2 2	91,3	25,1
	SD	3,86	23,2	0,04	0,23	0,13	12,6	75	0,13	0,75	0,43	305	1827	3,05	18,3	5,64
	RSD [%]	12,2	12,2	12,2	12,2	21,8	16,7	16,7	16,7	16,7	30,9	20,0	20,0	20,0	20,0	22,5
G1 - G5 ** *	Ave	24,7	247	0,27	2,71	1,36	60,8	608	0,65	6,47	3,33	467	4671	5,75	57,5	27,4
	SD	12,0	120	0,07	0,74	0,53	34,0	340	0,24	2,42	1,64	121	1209	1,13	11,3	4,92
	RSD [%]	48,6	48,6	27,1	27,1	39,1	56,0	56,0	37,4	37,4	49,2	25,9	25,9	19,6	19,6	18,0
G6, G7, G8 ** *	Ave	27,6	165	0,29	1,71	0,56	69,3	416	0,72	4,31	1,34	1312	7873	13,5	80,8	25,3
	SD	7,48	44,9	0,07	0,42	0,19	16,3	98,0	0,13	0,79	0,49	414	2486	3,67	22,0	5,07
	RSD [%]	27,1	27,1	24,2	24,2	33,9	23,6	23,6	18,3	18,3	36,9	31,6	31,6	27,3	27,3	20,1
G1, G6, G7 ** **	Ave	31,4	275	0,31	2,75	1,37	80,5	711	0,81	7,11	3,43	850	6588	8,50	65,9	29,1
	SD	4,22	69,6	0,04	0,70	0,59	10,6	197	0,11	1,97	1,69	493	2067	4,93	20,7	3,48
	RSD [%]	13,4	25,4	13,4	25,4	42,6	13,2	27,7	13,2	27,7	49,3	58,0	31,4	58,0	31,4	12,0
G5,	Ave	21,6	190	0,27	2,38	0,88	40,0	344	0,50	4,30	1,61	549	4602	6,86	57,5	21,8

*Experimental Determination of the Relation between Elastic Strain Energy Release and Crack Growth
in Standing, Single Sheet Glass Beams* **501**

G8	SD	2,38	47,8	0,03	0,60	0,13	5,91	53,6	0,07	0,67	0,14	139	432	1,73	5,40	3,29
**	RSD [%]	11,0	25,1	11,0	25,1	15,2	14,8	15,6	14,8	15,6	8,99	25,3	9,39	25,3	9,39	15,1

		(1)	(2)	(3)	(4)	(5)	(6)	(7)	(8)	(9)	(10)	(11)	(12)	(13)	(14)	(15)
						10 ³	10 ³	10 ³	10 ³	10 ³	10 ⁶					10 ³
AL L	Ave	27,0	240	0,29	2,55	1,20	65,6	585	0,68	6,09	2,94	709	5688	7,85	64,0	27,1
	SD	10,2	105	0,06	0,73	0,57	29,1	301	0,21	2,30	1,66	449	2146	4,19	18,9	4,60
	RSD [%]	37,8	43,9	22,1	28,8	47,4	44,4	51,4	30,9	37,8	56,4	63,4	37,7	53,4	29,4	16,9

* Specimen groups with equal load configuration.

** Specimen groups with equal specimen geometry.

*** Specimen groups with equal specimen thickness.

**** Specimen groups with equal specimen height.

Table G.7 Energy dissipation by crack growth

Spec.	$U_\gamma = A_{fr}\gamma^*$	$U_\gamma/U_\epsilon \cdot 100\%$	Spec.	$U_\gamma = A_{fr}\gamma^*$	$U_\gamma/U_\epsilon \cdot 100\%$	Spec.	$U_\gamma = A_{fr}\gamma^*$	$U_\gamma/U_\epsilon \cdot 100\%$
G1-1	0,182	2,84%	G1-20	0,099	3,01%	G5-3	0,106	2,33%
G1-2	0,090	3,58%	G1-21	0,061	3,09%	G5-4	0,120	2,57%
G1-3	0,136	2,77%	G1-22	0,073	3,64%	G5-5	0,096	2,88%
G1-4	0,093	3,43%	G1-23	0,119	2,55%	G5-6	0,132	2,89%
G1-5	0,090	3,54%	G1-24	0,084	3,44%	G5-7	0,096	3,13%
G1-6	0,218	3,27%	G2-2	0,113	2,76%	G6-1	0,058	4,07%
G1-7	0,069	3,61%	G2-6	0,195	3,34%	G6-2	0,058	4,78%
G1-8	0,087	3,21%	G3-1	0,028	1,45%	G6-3	0,110	4,05%
G1-9	0,100	2,95%	G3-2	0,015	1,48%	G6-4	0,067	5,37%
G1-10	0,101	3,37%	G3-3	0,029	1,57%	G6-5	0,046	5,38%
G1-11	0,084	2,92%	G3-4	0,047	1,30%	G6-6	0,060	5,01%
G1-12	0,096	3,36%	G3-6	0,036	1,34%	G6-7	0,048	5,18%
G1-13	0,116	2,65%	G4-2	0,024	1,97%	G7-1	0,081	6,81%
G1-14	0,095	3,33%	G4-3	0,021	2,11%	G7-2	0,095	7,46%
G1-15	0,087	3,40%	G4-4	0,025	1,57%	G7-4	0,064	5,48%
G1-16	0,104	3,33%	G4-5	0,043	1,91%	G7-5	0,080	6,70%
G1-17	0,108	4,06%	G4-6	0,025	2,03%	G8-1	0,072	2,54%
G1-18	0,080	3,39%	G5-1	0,095	3,15%	G8-2	0,045	2,77%
G1-19	0,088	3,34%	G5-2	0,116	2,67%	G8-3	0,030	2,68%

* Assuming $\gamma = 3 \text{ J/m}^2$

**Average 3.42 %
RSD 37.0 %**

5. Discussion

5.1. Hypothetical Relations

Three sets of equations have been introduced, based on σ_f , χ_f , and $U_{\epsilon,f}$, respectively, by which the relations between failure parameters and the experimentally determined crack length parameter l_{fr} have been investigated with the purpose of finding a constant relation. The first equation in each set, i.e. (R1), (R6), and (R11), divides l_{fr} by the failure parameter to find a direct relation through a simple constant. In the other equations, geometry and load configuration parameters (t , h , α_{config}) have been added to investigate if they might help to relate the results in different specimen groups with each other.

The quality of a proposed relation was evaluated by the RSD found over all tested specimens as well as the RSD's over specimen groups and sets of groups. A low RSD points to a relatively consistent relation.

5.2. Results for Individual Groups

Table G.8 sums up the RSD's for the relation sets and concludes which set performs best per specimen group. When comparing the results for the individual specimen groups, it is immediately apparent that the χ - and U_{ϵ} -based relations (sets 2 and 3) provide much more consistent results than the σ -based ones (set 1). Generally, they yield a RSD of approximately 10 %, with G2 and G8 being the upper and lower limits at 13.6% and 4.4% respectively. Only for group 5 the σ -based relations yield significantly better results with a RSD of 6.7% where the other sets score 10.7%. For groups 6 and 7 the results are comparable for all sets. The RSD's for the σ -based relations vary from 6.7% for group 5 up to 25.8% for group 2.

5.3. Influence of added geometry and loading configuration parameters

Table G.8 Overview of RSD's per relation set for individual specimen groups.

Specimen Group	Relative Standard Deviation [%]			Best performing
	Set 1 (R1)-(R5)	Set 2 (R6)-(R10)	Set 3 (R11)-(R15)	
G1	14.2	10.8	10.8	Sets 2 and 3
G2	25.8	7.7	7.7	Sets 2 and 3 (Rel. SD \pm 3 times lower)
G3	17.9	10.8	10.8	Sets 2 and 3
G4	15.2	10.8	10.8	Sets 2 and 3
G5	6.73	10.7	10.7	Set 1
G6	12.2	11.7	11.7	Approximately equal
G7	14.0	12.5	12.5	Approximately equal
G8	20.4	4.4	4.3	Sets 2 and 3 (Rel. SD \pm 5 times lower)

The proportion between l_{fr} and χ_f or $U_{\epsilon,f}$ has shown to be fairly constant for different specimens with equal geometry and loading configuration. However, it was found that

these proportions yield a wide range of results when comparing the different groups of specimens. This also goes for the l_{fr}/σ_f -proportion. Thus geometry and loading configuration parameters have introduced to try to find a constant value for the crack factor C_n for different specimen groups.

5.4. Specimen Thickness t

The specimen thickness parameter t was introduced to estimate the total crack surface area, rather than the crack length. It was expected that σ_f , χ_f and $U_{e,f}$ are actually not related to l_{fr} but to A_{fr} .

Table G.9a Influence of adding parameter t on the consistency of σ_f -based relations.

Specimen Groups	Relative Standard Deviation [%]				Best performing
	(R1)	(R2)	(R3)	(R4)	
G3, G8	65,2	39,5	30,7	17,5	Relation (R4), with t .
G4, G5, G6	49,3	40,3	27,4	25,4	Relation (R4), with t .
G1, G6, G7	13,4	25,4	13,4	25,4	Relations (R1) and (R3), without t .
G5, G8	11,0	25,1	11,0	25,1	Relations (R1) and (R3), without t .
All	37,8	43,9	22,1	28,8	Relation (R3), without t .

Table G.9b Influence of adding parameter t on the consistency of χ_f -based relations.

Specimen Groups	Relative Standard Deviation [%]				Best performing
	(R6)	(R7)	(R8)	(R9)	
G3, G8	71,1	45,3	35,5	9,33	Relation (R4), with t .
G4, G5, G6	63,3	44,3	41,2	21,1	Relation (R4), with t .
G1, G6, G7	13,2	27,7	13,2	27,7	Relations (R1) and (R3), without t .
G5, G8	14,8	15,6	14,8	15,6	Relations (R1) and (R3), without t .
All	44,4	51,4	30,9	37,8	Relation (R3), without t .

Table G.9c Influence of adding parameter t on the consistency of $U_{e,f}$ -based relations.

Specimen Groups	Relative Standard Deviation [%]				Best performing
	(R11)	(R12)	(R13)	(R14)	
G3, G8	61,3	34,4	24,5	7,23	Relations with t better. (R12) better than (R11) and (R14) better than (R13).
G4, G5, G6	63,7	39,2	39,0	18,5	Relations with t better.
G1, G6, G7	58,0	31,4	58,0	31,4	Relations with t better.
G5, G8	25,3	9,39	25,3	9,39	Relations with t better.
All	63,4	37,7	53,4	29,4	Relations with t better.

However, when considering the RSD's for all specimens as well as for those of the various sets of groups, it turns out the σ - and χ -based relations provide a diffuse picture

when using A_{fr} in the equations instead of l_{fr} . Tables J.9a and b provide an overview of the influence of t in the σ - and χ -based relations. In some sets of groups, the consistency increases (i.e. the RSD's decrease), while for others the consistency decreases.

Contrary to the σ - and χ -based relations, the U_e -based relations all show significant improvements in consistency when the thickness parameter is applied, see Table G.9c. The fact that the thickness parameter has a positive influence on the U_e -based relations but not on the σ - and χ -based relations can be explained by the nature of the stress and strain energy density on the one hand and the total strain energy on the other. The former are geometry independent quantities working on a point without a finite size. The latter, though, is a global quantity the magnitude of which is directly dependent on specimen geometry (since it is strain energy density integrated over the specimen volume). From a physical point of view it is also immediately understandable why $U_{e,f}$ is related to A_{fr} rather than to l_{fr} ; the creation of crack surface is what dissipates energy. The created crack length is only a consequence of the formation of a certain crack surface area. Since there is no direct physical relation between stress or strain energy density and crack surface area, the positive influence of t on some of the σ - and χ -based relations should be considered accidental.

5.5. Specimen Height h

Cracks in a (standing) glass beam start from the tensile stressed area at the bottom. Then they usually fork and run upwards until they meet the end of the beam. The beam height h was therefore introduced as the second geometry parameter to obtain more consistency in the relations. A beam twice as high as another one simply provides the opportunity for cracks to grow twice as long.

Tables J.10a, b, and c give an overview of the influence of the parameter h . Contrary to beam thickness t , adding the beam height h to the equations improves the consistency in the σ - and χ -based relations without exception. Remarkably, the RSD *increases* when evaluating the set of G1 and G2 for U_e -based relations. The reason for this is unclear. For all other sets of groups, the RSD *decreases*, like it does for the σ - and χ -based relations. Since the RSD also decreases significantly over all specimens, adding h should be considered to generally improve the consistency even for the U_e -based relations.

Table G.10a Influence of adding parameter h on the consistency of σ -based relations.

Specimen Groups	Relative Standard Deviation [%]				Best performing
	(R1)	(R2)	(R3)	(R4)	
G1, G2	19,9	19,9	14,6	14,6	Relations with h better. (R3) better than (R1) and (R4) better than (R2).
G3, G8	65,2	39,5	30,7	17,5	Relations with h better.
G4, G5, G6	49,3	40,3	27,4	25,4	Relations with h better.
G1-G5	48,6	48,6	27,1	27,1	Relations with h better.
G6, G7, G8	27,1	27,1	24,2	24,2	Relations with h better.
All	37,8	43,9	22,1	28,8	Relations with h better.

Table G.10b Influence of adding parameter h on the consistency of χ -based relations.

Specimen Groups	Relative Standard Deviation [%]				Best performing
	(R6)	(R7)	(R8)	(R9)	
G1, G2	16,0	16,0	10,7	10,7	Relations with h better. (7) better than (6) and (9) better than (8).
G3, G8	71,1	45,3	35,5	9,33	Relations with h better.
G4, G5, G6	63,3	44,3	41,2	21,1	Relations with h better.
G1-G5	56,0	56,0	37,4	37,4	Relations with h better.
G6, G7, G8	23,6	23,6	18,3	18,3	Relations with h better.
All	44,4	51,4	30,9	37,8	Relations with h better.

Table G.10c Influence of adding parameter h on the consistency of $U_{e,r}$ -based relations.

Specimen Groups	Relative Standard Deviation [%]				Best performing
	(R11)	(R12)	(R13)	(R14)	
G1, G2	10,8	10,8	15,0	15,0	Relations with h worse. (R13) worse than (R11) and (R14) worse than (R12)
G3, G8	61,3	34,4	24,5	7,23	Relations with h better. (R13) better than (R11) and (R14) better than (12).
G4, G5, G6	63,7	39,2	39,0	18,5	Relations with h better.
G1-G5	25,9	25,9	19,6	19,6	Relations with h better.
G6, G7, G8	31,6	31,6	27,3	27,3	Relations with h better.
All	63,4	37,7	53,4	29,4	Relations with h better.

5.6. Specimen Loading Configuration Factor α_{config}

Table G.11a Influence of adding parameter α_{config} on the consistency of σ_r -based relations.

Specimen Groups	Relative Standard Deviation [%]		Best performing
	(R4)	(R5)	
G3, G4	15.9	24.5	Relation (R4), without α_{config} .
G6, G7	12.2	21.8	Relation (R4), without α_{config} .
G1-G5	27.1	39.1	Relation (R4), without α_{config} .
G6, G7, G8	24.2	33.9	Relation (R4), without α_{config} .
G1, G6, G7	25.4	42.6	Relation (R4), without α_{config} .
G5, G8	25.1	15.2	Relation (R5), with α_{config} .
All	28.8	47.4	Relation (R4), without α_{config} .

The background to the LCF α_{config} has been previously introduced. Tables J.11a, b, and c compare the equations with and without this factor. For the σ - and χ -based relations, adding α_{config} means a significant loss of consistency. Only for the combination of G5

and G8 is the RSD lower. For all other combinations, including all specimens combined, the RSD is approximately 10-20 percent points higher for equations with α_{config} . The U_{ε} -based relations show exactly the opposite effect. The RSD decreases approximately 10-20 percent points for all sets of groups, except for the set of G1-G5 which yields an approximately equal RSD and set G5 and G8 which results in an increased RSD. It is unclear why the behaviour of set G5 and G8 deviates from all other sets of relations.

Table G.11b Influence of adding parameter α_{config} on the consistency of χ_t -based relations.

Specimen Groups	Relative Standard Deviation [%]		Best performing
	(R9)	(R10)	
G3, G4	8.84	18.2	Relation (R9), without α_{config} .
G6, G7	16.7	30.9	Relation (R9), without α_{config} .
G1-G5	37.4	49.2	Relation (R9), without α_{config} .
G6, G7, G8	18.3	27.1	Relation (R9), without α_{config} .
G1, G6, G7	27.7	43.9	Relation (R9), without α_{config} .
G5, G8	15.6	8.99	Relation (R9), with α_{config} .
All	37.8	56.4	Relation (R9), without α_{config} .

Table G.11c Influence of adding parameter α_{config} on the consistency of $U_{\varepsilon,t}$ -based relations.

Specimen Groups	Relative Standard Deviation [%]		Best performing
	(R14)	(R15)	
G3, G4	18.1	8.84	Relation (15), with α_{config} .
G6, G7	20.0	11.9	Relation (15), with α_{config} .
G1-G5	19.6	18.0	Relation (15), with α_{config} .
G6, G7, G8	27.3	20.1	Relation (15), with α_{config} .
G1, G6, G7	31.4	11.9	Relation (15), with α_{config} .
G5, G8	9.4	15.1	Relation (4), without α_{config} .
All	29.5	16.9	Relation (15), with α_{config} .

The fact that the parameter α_{config} influences the U_{ε} -based relations positively, but not the σ - and χ -based relations, probably has a similar explanation as for the parameter t , although the RSD's more consistently decrease by use of α_{config} than by applying t . Again it is suggested that this is due to the geometry independency of σ and χ as opposed to the geometry dependent character of U_{ε} .

5.7. Results for All Specimens

Except for equation (R15), the RSD's for the χ - and U_{ε} -based relations are remarkably higher than those for the σ -based relations, even though the χ - and U_{ε} -based relations performed considerably better for most individual specimen groups.

The RSD values for C_n for all specimens (see also Table G.6) have been reproduced in Figure G.5. Additionally, for the χ - and U_{ε} -based relations, the prediction accuracy for

the σ_f has been shown. Because of the squared relation between stress and strain energy, the RSD for predicting σ_f from the χ - and $U_{e,f}$ -based relations is only approximately half that of the RSD for predicting $\chi_{f,r}$ or $U_{e,f}$. Now, it is apparent that the χ - and $U_{e,f}$ -based relations predict the failure stress *better* than the σ -based relations.

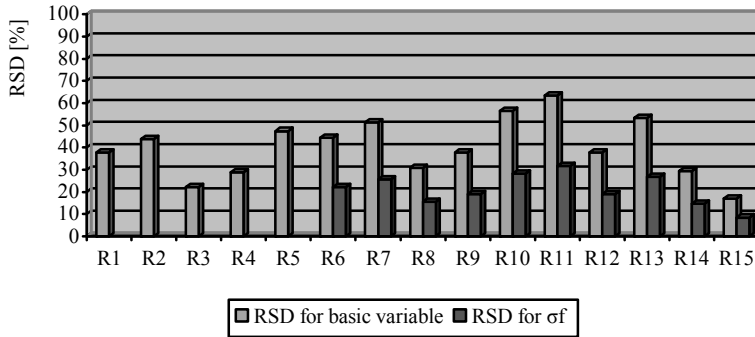


Fig. G.5 RSD's for predicting the basic variable (σ_f , $\chi_{f,r}$ or $U_{e,f}$) and for predicting the failure stress σ_f , over all specimens.

Especially relation (R15) provides a fairly accurate prediction of failure stress from determining the crack length, specimen geometry and loading configuration, with a RSD of only 8.7%. The value for the constant C_{R15} , which the author proposes to call the (*elastic strain energy*) *cracking constant*, is $C_{R15} = C_{U_{e,f}} = 27.1 \cdot 10^3 \text{ mm/N} = 27.1 \text{ m}^2/\text{J}$ (Table G.6)⁶. Thus, relation (R15) can be rewritten as Eq. (J.2).

$$U_{\varepsilon,f} = \frac{A_{fr}}{C_{U_{\varepsilon,f}} h \alpha_{config}} = \frac{A_{fr}}{27.1 \frac{\text{m}^2}{\text{J}} \cdot h \alpha_{config}} \quad (\text{J.2})$$

Using (R15) to determine the failure stress σ_f it can be difficult because it requires not only the specimen geometry but also the loading configuration to be known, both to calculate α_{config} and to relate σ_f to $U_{e,f}$. If you want to determine the failure stress of a glass beam from its fracture pattern in an forensic situation, it may be especially problematic to determine the loading configuration. In such cases, relation (R8) provides an easy alternative. The results are less accurate, but with a RSD of 15.5% still quite acceptable as an approximation. To solve this equation, only the proportion between the crack length l_{fr} and the beam height h needs to be known.

5.8. Ignored specimens G3-5, G7-3, G7-6

Three of the ignored specimens were disregarded because they had an abnormally deviating crack length l_{fr} (other specimens were ignored because of errors in experiment execution). Specimen G3-5 had failed simultaneously from two crack origins (see Fig.

⁶ The unit of the cracking constant $U_{e,f}$ [m^2/J] is not to be read as a crack surface area created per amount of strain energy stored in the beam at failure, as the unit may suggest. For now, no physical meaning is suggested. Further (theoretical) research is required. The similarity of unit of $U_{e,f}$ with that of the surface energy γ [J/m^2] may be coincidental because the units of beam height h and loading configuration α_{config} cancel each other out.

G.3). Although this is quite rare, it is not unique. The author has witnessed this several times over the last years in various studies. It resulted in a total crack length of $l_{fr} = 883$ mm at a failure stress σ_f of 61.3 MPa. This yielded a elastic strain energy cracking constant of $C_{U_{\epsilon,f}} = 73.7 \text{ m}^2/\text{J}$, over twice the average over the other specimens in group 3, which was $C_{U_{\epsilon,f}} = 27.6 \text{ m}^2/\text{J}$ (RSD = 7.66%).

Failure of specimens G7-3 and G7-6, surprisingly, did not originate from the beam edge, but from the surface a little way above the edge (see Figure G.4a and b). This resulted in significantly lower elastic strain energy cracking constants of $C_{U_{\epsilon,f}} = 14.5 \text{ m}^2/\text{J}$ and $C_{U_{\epsilon,f}} = 14.1 \text{ m}^2/\text{J}$, while the average over the other specimens in group 7 was $C_{U_{\epsilon,f}} = 25.9 \text{ m}^2/\text{J}$ (RSD = 15.2%).

Thus it is suggested to extent Eq. (J.2) to Eq (J.3) with a crack origin number factor $\alpha_{o\#}$ and crack origin location factor α_{ol} .

$$U_{\epsilon,f} = \frac{A_{fr}}{27.1 \frac{\text{m}^2}{\text{J}} \cdot h \cdot \alpha_{o\#} \cdot \alpha_{ol} \cdot \alpha_{config}} \quad (\text{J.3})$$

The proposed values are:

- $\alpha_{o\#} = n$, where n is the number of crack origins.
- $\alpha_{ol} = 1$ for a crack from the edge and $\alpha_{ol} = 0.5$ for a crack from the surface.

However, too little data exist to statistically validate these suggestions.

5.9. Energy Dissipation by Crack Growth

It is noteworthy that in all specimens, only a small portion of 3.4 % on average of the stored strain energy is dissipated by crack surface formation (Table G.7). A small amount of energy is released by means of sound, but most is transformed into kinetic energy. This explains the fact that glass shards tend to fly away from the broken specimen, rather than to just fall on the floor. For the development of glass elements with residual strength (and thus second load transfer mechanisms) it is important to realize that this energy has to be dissipated by the other materials (e.g. adhesive layers and/or reinforcement) in a composite glass element at the moment of failure. This may lead to premature tearing or adhesive failure, especially when brittle materials are used.

6. Conclusions

The amount of crack growth through a glass beam loaded in 3- or 4-point bending is linearly related to the total strain energy at failure through a constant and several geometry and loading configuration parameters.

The extent of crack growth can be predicted from the total strain energy at failure or vice versa, with a considerable degree of accuracy. The experiments have shown a relatively simple relation exists between crack length l_{fr} , beam thickness t , beam height h , loading configuration factor α_{config} and total strain energy at failure $U_{\epsilon,f}$, presented by Eq. (K.7), through the elastic strain energy cracking constant $C_{U_{\epsilon,f}}$, experimentally determined to be $C_{U_{\epsilon,f}} = 27.1 \text{ m}^2/\text{J}$. Eq. (7) predicts the $U_{\epsilon,f}$ for a certain crack length

with a coefficient of variation of 16.9% and the failure stress σ_f with a coefficient of variation of only 8.5%.

Deviating failure patterns in three specimens seem to suggest that the amount of crack growth per amount strain energy is approximately proportional to amount of failure origins (i.e. a simultaneous failure from two origins, which occasionally occurs, will yield twice the crack length as an ordinary failure from one origin). Furthermore, failure started from the surface of a glass beam rather than from the edge, seems to decrease the total crack length by half.

Attempts at finding a similar linear relation between crack length and failure stress have not produced satisfying results. Relation (R3) predicts the failure stress from the crack length with a coefficient of variation of 22.1%, considerably more than χ - and U_e -based relations. Thus, it is concluded that crack length is not directly dependent on failure stress, but only indirectly through its influence of the total strain energy and strain energy density.

Since the extent of cracking in beams depends on the stored elastic strain energy, it may be sensible to design structural glass members in a way that they will store as little elastic strain energy as possible at a certain failure stress (i.e. optimize stiffness).

Appendix H: Comparison between Failure Behaviour of Reinforced Glass Beams with Varying Elastic Strain Energy Content

The failure behaviour of two reinforced glass beam designs has been compared in a four-point bending test. One design featured a slim section with a high moment of inertia and thus relatively low elastic strain energy absorption. The section of the other design, on the contrary, was stocky with a low moment of inertia and therefore high elastic strain energy absorption. The moment of resistance of both designs was approximately equal, so that the initial failure load was also practically the same. The energy release of the stocky beams at initial failure was significantly higher than for the slim beams. Also, the post-initial failure strength was significantly lower. However, this could be attributed mainly to the difference in internal moment arm for the tension carrying part of the section (i.e. the steel reinforcement) in the post initial failure stage. Contrary to the stocky beams, failure of the slim beams was, without exception, governed by adhesive failure. This is due to the higher shear stress. The amount of energy release did seem to have an effect on crack growth and consequently on failure behaviour, but the other mechanics parameters have an overriding effect.

1. Introduction

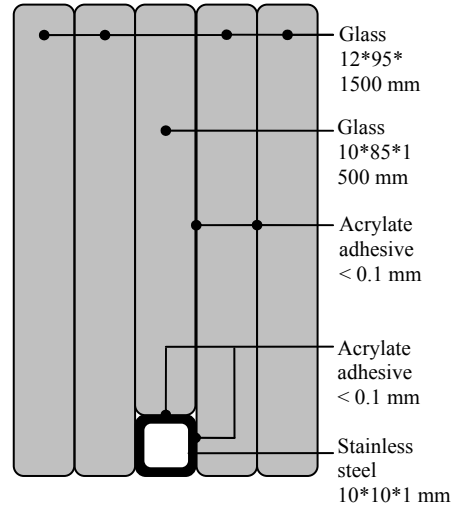
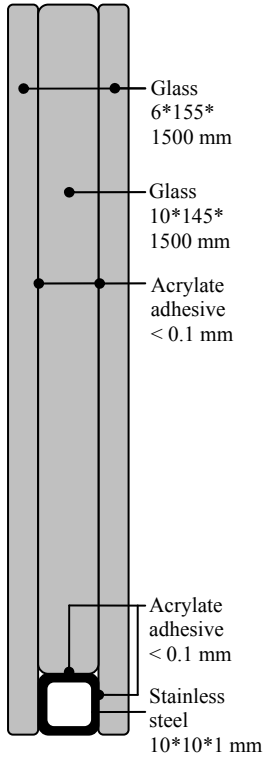
The experiments presented in Appendix G have convincingly shown that the extent of crack growth in standing, single sheet annealed glass beams depends on the amount of elastic strain energy at failure and some geometry parameters. It was assumed the extent of crack growth would, in turn, influence the failure behaviour of structural glass elements in the post-initial failure stage. Therefore, the failure behaviour of two reinforced glass beam designs with varying energy content has been compared by subjecting them to a four-point bending test.

It was investigated whether beams with low energy content at initial failure would show more favourable post-initial failure behaviour (most notably a higher maximum post-initial failure strength) than beams with high energy absorption.

2. Experimental Method

Two reinforced glass beams were designed. They were both 1.5 m long, but had different section dimensions (width and height), so that their moments of resistance were approximately equal ($88.1 \cdot 10^3 \text{ mm}^3$ and $87.2 \cdot 10^3 \text{ mm}^3$) while their moments of inertia varied by a factor 1.6 ($6.83 \cdot 10^6 \text{ mm}^4$ and $4.14 \cdot 10^6 \text{ mm}^4$). Thus, when they are loaded with an equal load, the displacement as well as the elastic strain energy content of both beams would also vary by a factor 1.6 (see Chapter 9, Section 2 or Appendix F). The slim beams are referred to as type I, the stocky beams as type II. Their geometrical and mechanics properties are presented in Figures K.1 and K.2.¹

¹ For easy computation, the pre-failure calculations are based on massive rectangular glass sections rather than composite sections. As the steel section area is only a little over one third of the equivalent 10 x 10 mm glass



Type I Properties		Type II Properties	
L	1500 mm	L	1500 mm
h	155 mm	h	95 mm
t	22 mm	t	58 mm
W_y	$88.1 \cdot 10^3 \text{ mm}^3$	W_y	$87.2 \cdot 10^3 \text{ mm}^3$
I_y	$6.83 \cdot 10^6 \text{ mm}^4$	I_y	$4.14 \cdot 10^6 \text{ mm}^4$
$S_{45\text{MPa}}$	15.9 kN	$S_{45\text{MPa}}$	15.7 kN
$W_{45\text{MPa}}$	2.22 mm	$W_{45\text{MPa}}$	3.61 mm
$U_{e,45\text{MPa}}$	12.4 J	$U_{e,45\text{MPa}}$	19.7 J

Fig. H.1 Section design of the slim glass beam, Type I.

Fig. H.2 Section design of the stocky glass beam, Type II.

section and the Young's modulus, on the other hand, is three times as high, this has practically no influence on the beams neutral axis or stress distribution. Actually, the distance of the neutral axis from the top of the section would be $z = 79.3 \text{ mm}$ for type I compared to $\frac{1}{2} h = 77.5 \text{ mm}$, and $z = 48.2$ for type II, with $\frac{1}{2} h = 47.5 \text{ mm}$ (with $E_{\text{steel}} \approx 3 \cdot E_{\text{glass}}$).

Also, the load to obtain a maximum tensile stress level of 45 MPa is given, as well as the (theoretical) elastic strain energy content and displacement *under one of the load points*², at that load. The displacement was determined by Eq. (K.1). For the equations to determine the elastic strain energy content, refer to Appendix F or Section 2 of Chapter 9.

$$w = \frac{\frac{1}{2} Sa^2 b + \frac{1}{3} Sa^3}{(EI)_{\text{glassbeam}}} \quad (\text{K.1})$$

For *a* and *b*, see Figure H.3.

Of type I, 6 specimens were prepared while 5 type II specimens have been manufactured. All specimens have been subjected to displacement controlled four-point bending (Figure H.3). The support span was 1400 mm; the load span 400 mm, symmetrically applied.

The bending tests were executed in two stages. In the first stage, a specimen was loaded at 2.0 mm/min. until the first significant cracking and drop in applied load (> ~10 %) occurred. The load was then released. The crack pattern was photographed. Then, the load was reapplied at 5.0 mm/min. until final failure took place or the maximum displacement of the experimental set-up was reached.

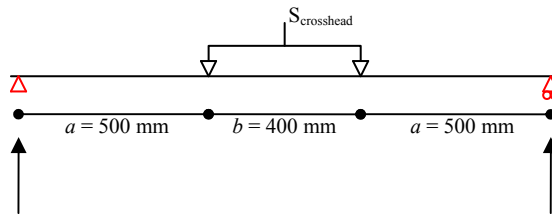


Fig. H.3 Lay-out of four-point bending test.

The experiments were executed in a laterally supported set-up to exclude lateral torsional buckling. In reality, it may well be that stability phenomena will play an important role in cracked glass in the post-initial failure stage. However, the presence of multiple possible failure mechanisms would cloud observations too much.

3. Results

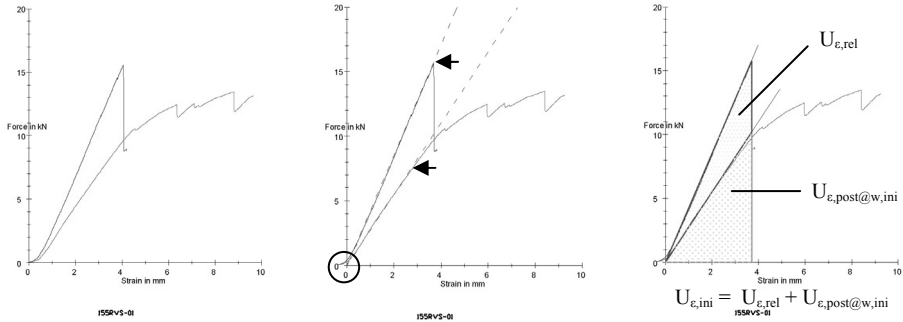
Table H.1 lists the maximum initial and post-initial failure loads, the initial glass tensile failure stress, the uncorrected maximum initial and post-initial displacements, the relative residual strength, and the final failure cause.

² This is *not* the maximum displacement at mid span. The testing machine tracks the displacement of the loading points. Thus, the experimental results can be compared with these theoretical values.

Table H.1 Direct experimental results.

Spec.	S_{ini} [kN]	σ_{ini} [MPa]	w_{ini} [mm]	$S_{post,max}$ [kN]	$w_{post,max}$ [mm]	Rel. Res. Strength	Final Failure Cause
I-01	15.6	44.2	4.05	13.5	8.8	86 %	Steel-glass adhesive
I-02	16.6	47.2	5.59	17.8	15.4	107 %	Steel-glass adhesive
I-03	14.0	39.7	5.21	17.1	50.9	122 %	Steel-glass adhesive
I-04	15.0	42.5	4.15	16.7	11.4	112 %	Steel-glass adhesive
I-05	12.1	34.5	4.27	17.6	20.2	145 %	Steel-glass adhesive
I-06	17.8	50.5	5.19	17.9	45.7	101 %	Steel-glass adhesive.
Average	15.2	43.1	6.2	16.8	25.4	1.12	
St. Dev.	1.99	5.66	0.58	1.68	18.22	0.20	
Rel. St. Dev.	13.1 %	13.1 %	9.4 %	10.0 %	71.7 %	17.9 %	
II-01	14.0	40.1	5.84	12.3	39.2	88 %	Reached max. displacement.
II-02	13.2	37.8	6.68	11.0	44.9	83 %	Reached max. displacement.
II-03	15.5	44.5	5.86	12.1	35.6	78 %	Steel-glass adhesive.
II-04	15.1	43.2	5.57	9.9	44.8	66 %	Reached max. displacement.
II-05	16.4	46.9	6.89	10.6	43.8	65 %	Reached max. displacement.
Average	14.8	42.5	4.7	11.2	41.6	0.76	
St. Dev.	1.26	5.66	0.66	1.01	4.14	0.10	
Rel. St. Dev.	8.5 %	8.5 %	14.0 %	9.1 %	9.9 %	13.7 %	

The elastic strain energy was determined from the crosshead displacement and crosshead loads. However, most specimens had a (small) initial trajectory of set-up settlement before the graph entered a linear elastic stage until initial failure. To accurately assess the energy levels, the graphs therefore had to be shifted horizontally so that the linear elastic trajectory would extend through the origin. This was done using Autocad (Figure H.4a – c). It resulted in a corrected displacement at initial failure, given in Table H.2, along with the values for the elastic strain energy at initial failure, the elastic strain energy during reloading at the displacement of initial failure, and the released elastic strain energy, both absolute and relative to the elastic strain energy at initial failure.



K.4a, b, and c (left to right) Load-displacement graph of specimen I-01 in Autocad. Figure a) original graphs; Figure b) Shifting of graphs to match linear elastic curves from origin; Figure c) determination of elastic strain energy release at failure and content before and after failure at the initial failure displacement. Note that the Figures only show part of the post-initial behaviour graph. The full graphs are presented in Figures K.8a – f and K.9a – e.

Table H.2 Elastic strain energy related results.

Spec.	$w_{ini,cor}$ [mm]	$U_{e,ini}$ [J]	$U_{e,post@w,ini}$ [J]	$U_{e,rel}$ [J]	Rel. $U_{e,rel}$ [%]
I-01	3.7	29.3	18.9	10.4	35.4
I-02	3.9	32.1	21.1	11.0	34.3
I-03	3.4	24.6	18.6	6.1	25.6
I-04	3.5	26.3	17.2	9.0	34.3
I-05	2.9	17.6	13.4	4.3	24.2
I-06	4.0	35.7	24.5	11.9	33.4
Average	3.6	27.6	18.9	8.8	31.0
St. Dev.	0.40	6.30	3.72	3.01	5.20
Rel. St. Dev.	11.3 %	22.8 %	19.7 %	34.3 %	16.8 %
II-01	4.2	29.7	15.6	14.1	47.6
II-02	3.9	25.8	14.7	11.2	43.3
II-03	3.9	25.9	15.4	10.5	40.5
II-04	4.3	32.7	16.4	16.3	49.9
II-05	4.7	38.6	15.8	22.8	59.1
Average	4.2	30.6	15.6	15.0	48.1
St. Dev.	0.34	5.31	0.62	4.94	7.15
Rel. St. Dev.	8.0 %	17.4 %	4.0 %	33.0 %	14.9 %



Fig. H.5 Photograph of initial crack pattern of specimen I-01 in Autocad. Determination of crack related results crack height and total crack width.

Table H.3 Crack growth related results.

Spec.	Crack origin	h_c [mm]	Rel. h_c [%]	w_c [mm]	Rel. w_c [%]
I-01	Inside load span	138.1	89.1	301.6	194.6
I-02	Under load point	138.8	89.5	270.1	174.3
I-03	Under load point	135.9	87.7	211.6	136.5
I-04	Under load point	142.5	91.9	219.7	141.7
I-05	Inside load span	128.5	82.9	183.2	118.2
I-06	Outside load span	141.5	91.3	377.9	243.8
Average		137.6	88.7	260.7	1.68
St. Dev.		5.03	3.25	71.54	0.46
Rel. St. Dev.		3.7 %	3.7 %	27.5 %	27.5 %
II-01	Outside load span	89.1	93.8	285.9	301.0
II-02	Inside load span	88.0	92.6	146.8	154.5
II-03	Outside load span	87.6	92.2	144.4	152.0
II-04	Inside load span	90.1	94.8	231.7	243.9
II-05	Inside load span	95.0	100.0	281.8	296.6
Average		90.0	94.7	218.1	2.29
St. Dev.		2.98	3.14	69.56	0.73
Rel. St. Dev.		3.31 %	3.31 %	31.9 %	31.9 %

Some crack growth parameters were also determined by importing photographs of the crack patterns into Autocad and measuring distances (Figure H.5). Table H.3 provides the initial crack origin, initial crack height h_c and total width w_c (absolute and relative to beam height h_b).

In both specimen types, cracks concentrated around one origin at initial failure. During reloading, in some specimens a second major crack area occurred. These crack concentrations resulted in plastic hinges which governed the overall deformation behaviour of the beams. Figures K.6a – d and K.7a – d provide some insight into typical crack development in type I and type II beams, respectively.

The shifted load-displacement graphs of type I and type II specimens, as well as the initial failure crack patterns are shown in Figures K.8a – f and Figures K.9a – e.

Several important points can be deduced from the results presented in Tables K.1, K.2, and K.3:

- The average initial failure load of type I and II specimens is approximately equal ($S_{ini,max,ave,I} = 15.2$ kN; $S_{ini,max,ave,II} = 14.8$ kN), as was expected based on their moment of resistance.
- The average post-initial failure load of type I and II specimens varies significantly, by a factor of 1.5 ($S_{post,max,ave,I} = 16.8$ kN; $S_{post,max,ave,II} = 11.2$ kN).
- The average measured displacement for both types at initial failure is much larger than the theoretical displacement by bending of the glass beams, as determined by Eq. (K.1) and given in Figure H.1 and K.2.
- While all type I specimens finally failed by failure of the glass-steel reinforcement adhesive bond, only 1 type II specimen finally failed that way. The other type II specimens could not be tested to final failure as the maximum displacement of the test set-up was reached.

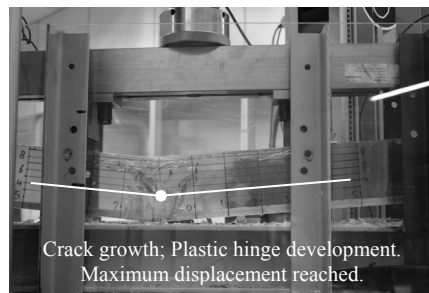
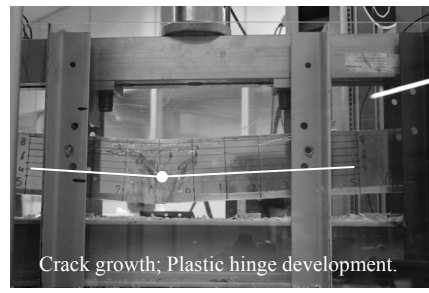
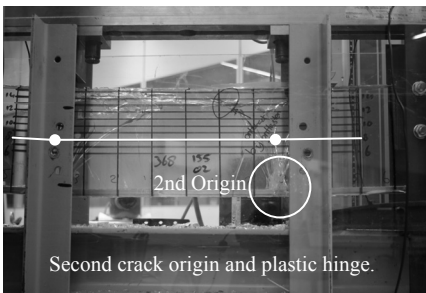
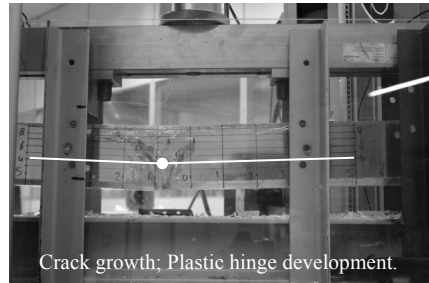
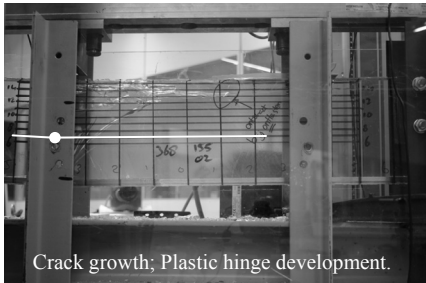
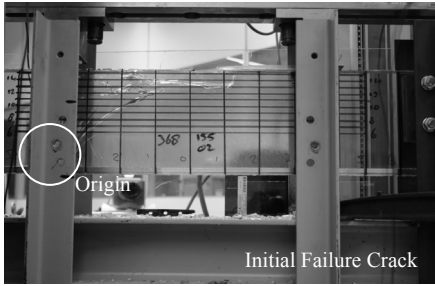


Figure H.6a – d (top to bottom) Crack development in specimen I-02.

Figure H.7a – d (top to bottom) Crack development in specimen II-02.

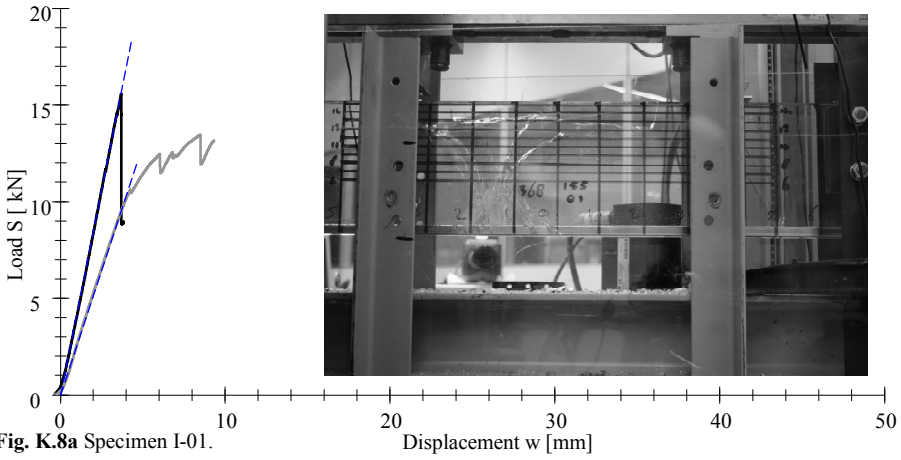


Fig. K.8a Specimen I-01.

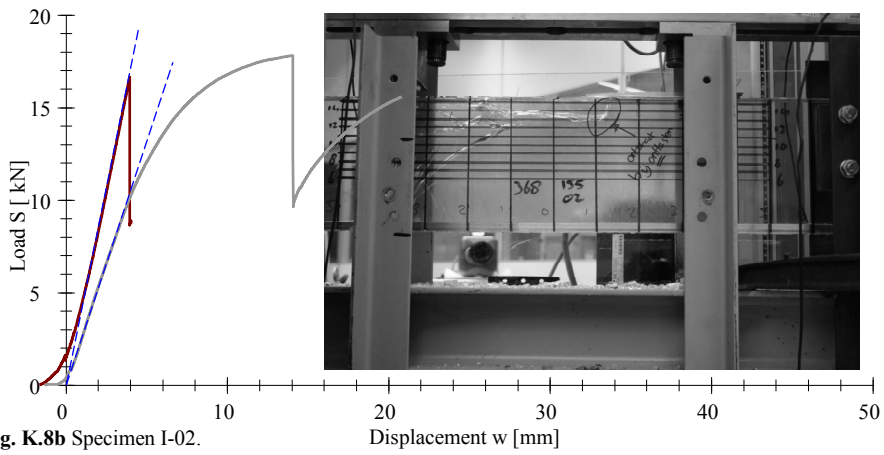


Fig. K.8b Specimen I-02.

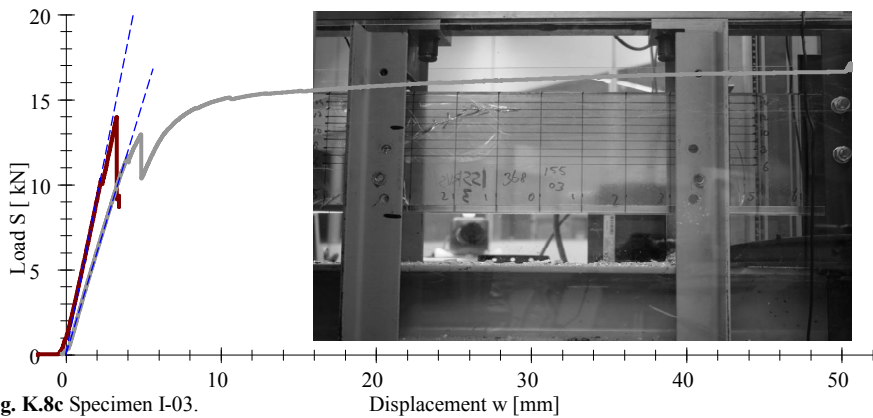
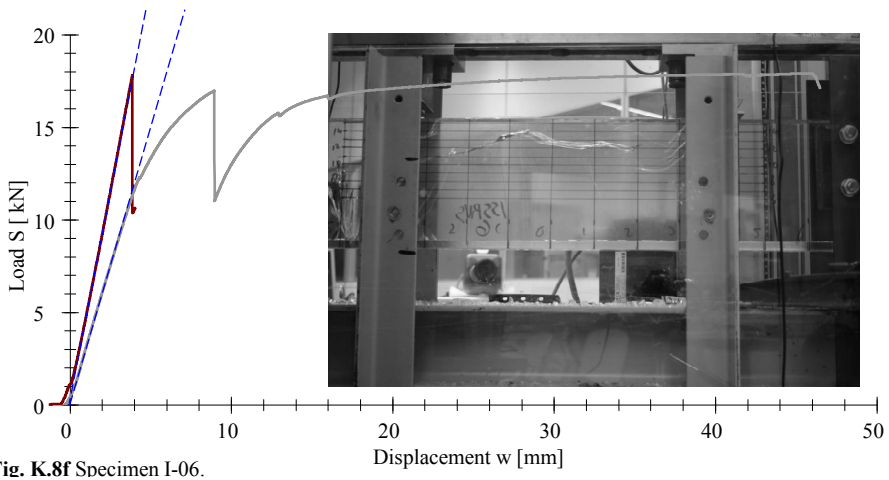
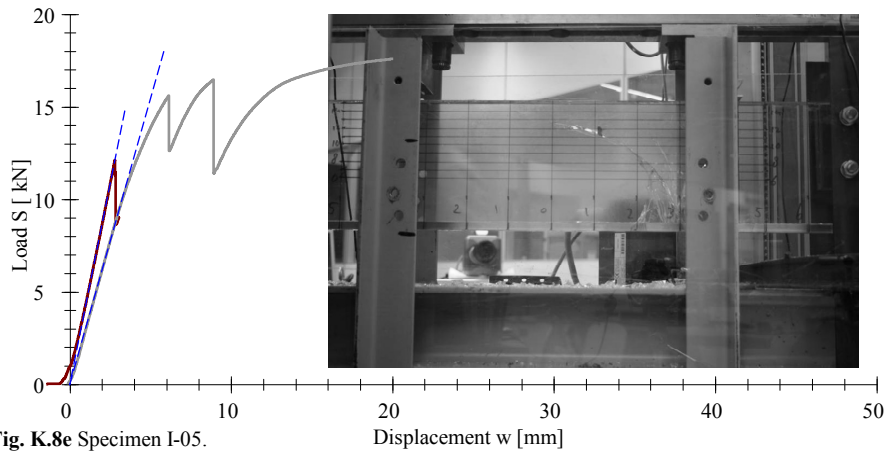
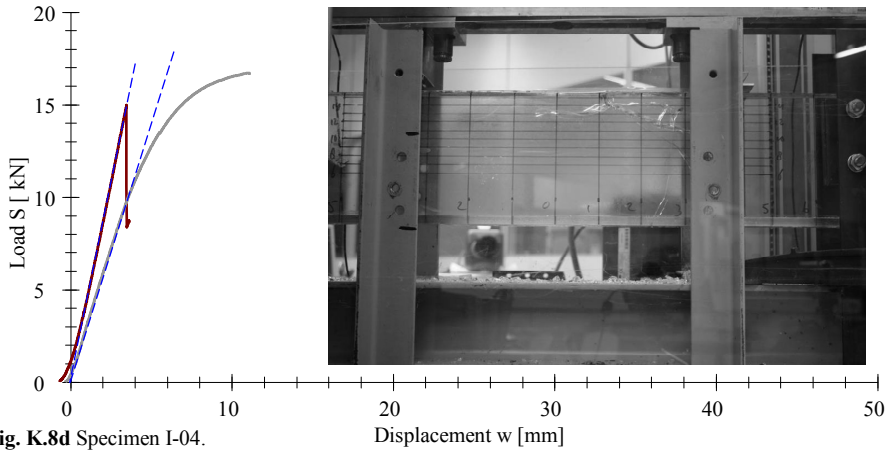


Fig. K.8c Specimen I-03.



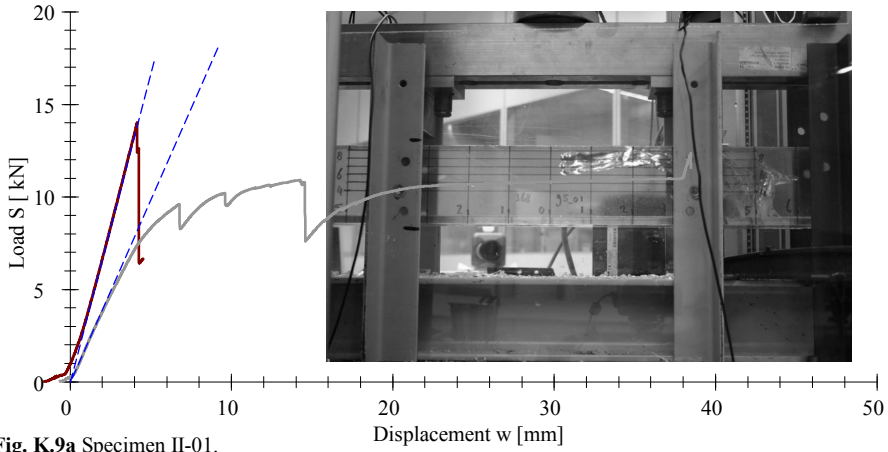


Fig. K.9a Specimen II-01.

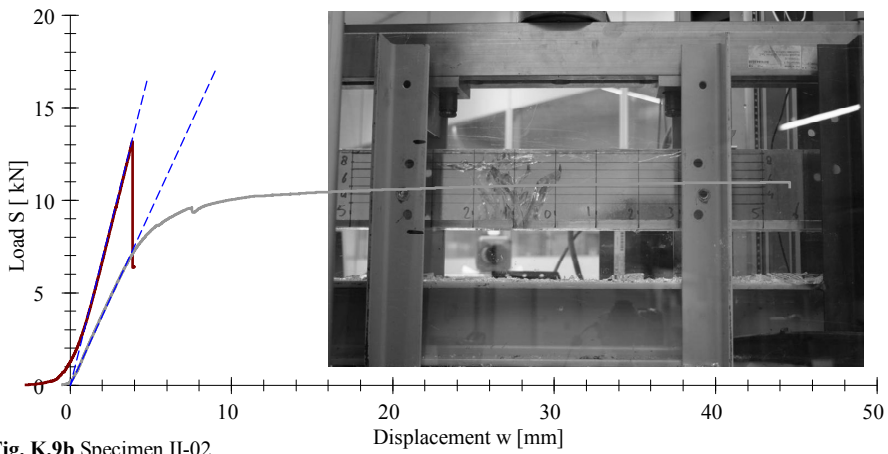


Fig. K.9b Specimen II-02.

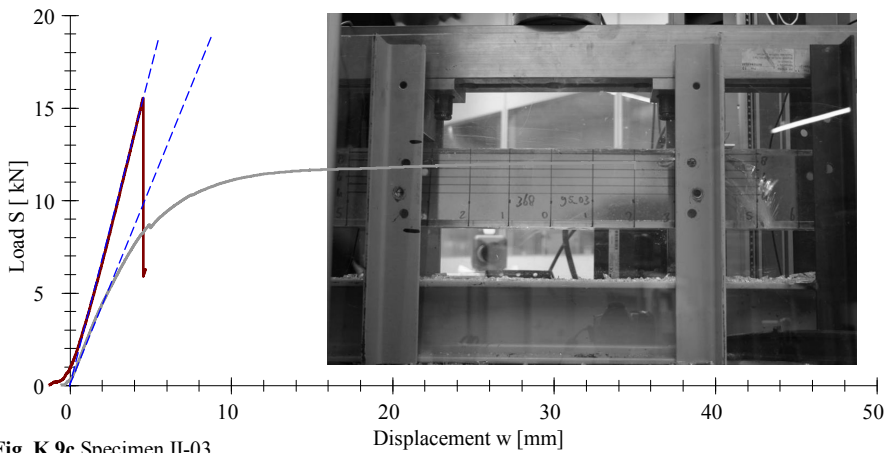


Fig. K.9c Specimen II-03.

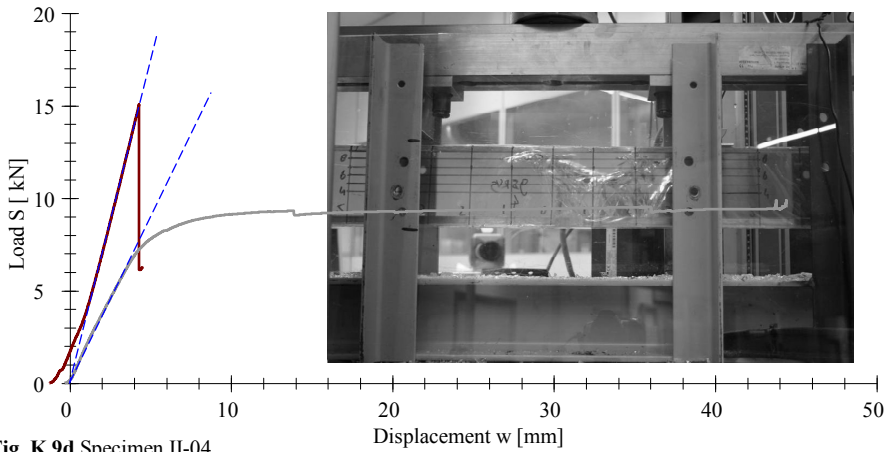


Fig. K.9d Specimen II-04.

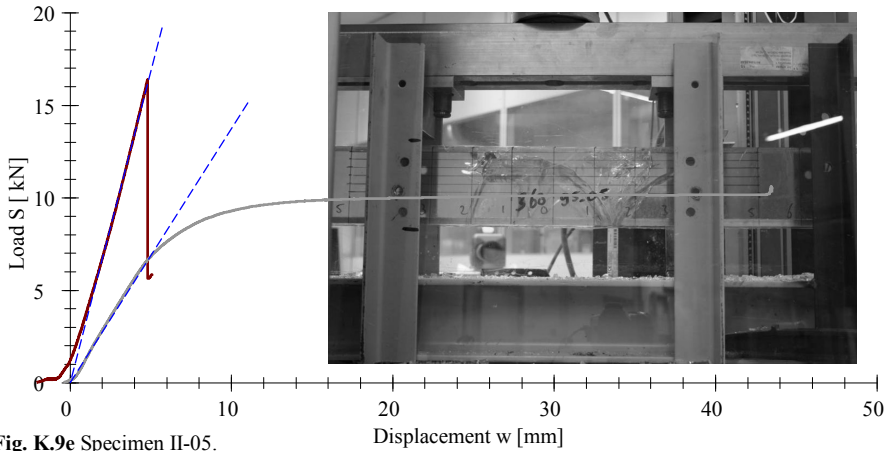


Fig. K.9e Specimen II-05.

4. Discussion

As expected, both beam types showed similar initial failure strengths, averaging at 15.2 and 14.8 kN for type I and II, respectively (Table H.1). Since the moment of resistance of both beams is equal, so are the occurring maximum tensile stresses in the outer grain before initial failure (Eq. (K.2)). With relative standard deviations of 13.1 % and 8.50 %, the initial failure results are also fairly consistent for glass beam specimens.

$$\sigma = \frac{M}{W} = \frac{1}{2} \frac{Sa}{W} \tag{K.2}$$

In the post-initial failure stage, however, an important difference in residual strength was encountered. For type I, this averaged on 16.8 kN or 112 %, while for type II it was only 11.2 kN or 75.9 %. This would seem to justify a swift conclusion that low energy

content beams indeed perform much better in the post-initial failure stage than high energy content beams. However, this line of thought would be erroneous.

Consider, therefore, the load transfer mechanisms in the beam before and after initial failure, as presented in Figures K.10a and b. In the post-initial failure stage, the external moment ($\max = Sa$) is counteracted by a couple of internal forces multiplied by the internal moment arm z : compression in the top part of the glass section and tension in the steel reinforcement. The exact magnitude of the internal moment arm is hard to estimate as it is not directly obvious what the height of the active glass compression zone is, but it seems reasonable to assume the internal moment arm z is approximately proportional to the beam height h ($z_I / z_{II} \approx h_I / h_{II}$). Thus, the moment capacity of the section depends on the steel tensile strength, the glass compressive strength and the internal moment arm.

Tensile experiments³ on the reinforcement profile have shown the applied steel type does not show a 'traditional' yield stage with increasing displacement at constant load and a consequent hardening stage, but rather a weakening trajectory at which an increasing load induces much larger displacements than in the linear elastic stage (Figure H.11).

The theoretical moment capacity of the beam sections in the post-initial failure state can be calculated from the height of the active glass compression zone, estimated to be equal to the top of the glass beam section without cracks after initial failure. In reality, the compressive zone may decrease in height during the post-initial failure stage through increased cracking. However, as reliable data for this are lacking, this is further ignored. Using the geometrical values as presented in Figures K.10a and b, the internal moment capacity of beam type I (average) is 4.1 kNm, which corresponds to a crosshead load of 16.3 kN. For a type II beam, internal moment capacity is 2.5 kNm, corresponding to 10.1 kN crosshead load. These values are governed by yielding of the reinforcement and correspond relatively well to the obtained experimental values of $S_{\text{post,max,I,ave}} = 16.8$ kN and $S_{\text{post,max,II,ave}} = 11.2$ kN. The maximum compressive stress in the glass at the top of the beams can also be calculated. This yields 248 MPa and 211 MPa for type I and II, respectively. Although the moment capacity of both beams is significantly different, the maximum glass compressive stresses are quite close.

Since $S_{\text{post,max,ave,I}} / S_{\text{post,max,ave,II}} = 16.8 \text{ kN} / 11.2 \text{ kN} = 1.5$ and $h_I / h_{II} = 155 \text{ mm} / 95 \text{ mm} = 1.63$, it can now easily be seen that the difference in maximum post-initial failure strength between the type I and type II beams is likely to be caused primarily by the difference in beam height, rather than by the difference in elastic strain energy release. The beam height h and elastic strain energy U_e are not independent properties, but in this argument, the relation between internal moment capacity directly depends on beam height, while the relation with elastic strain energy is only indirect.

Nevertheless, there are some important additional comments to be made.

³ Conducted by P.C. Louter, to be published in his forthcoming dissertation. Expected late 2009 – early 2010.

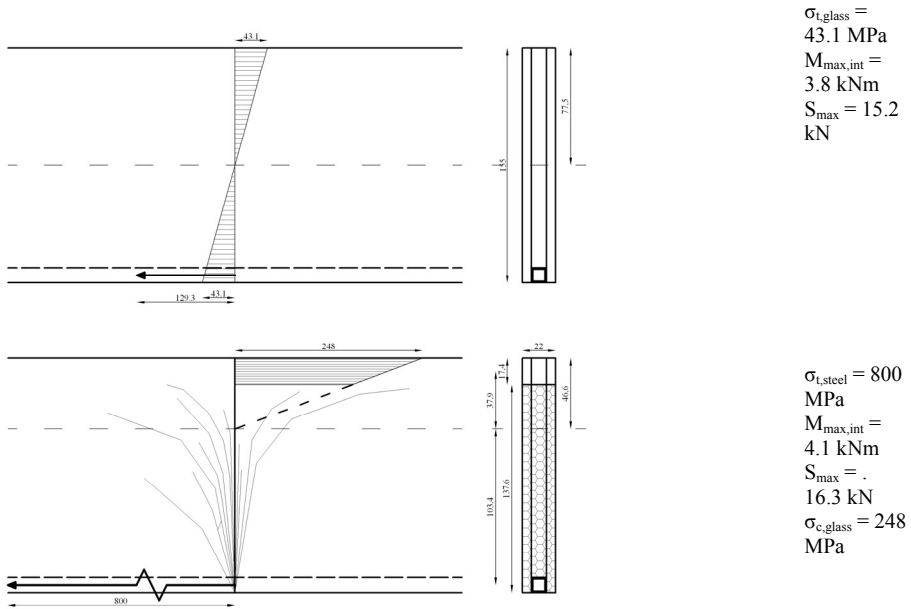


Fig. H.10a Load transfer mechanism of type I specimens in pre- and post-initial failure stage (top and bottom, respectively).

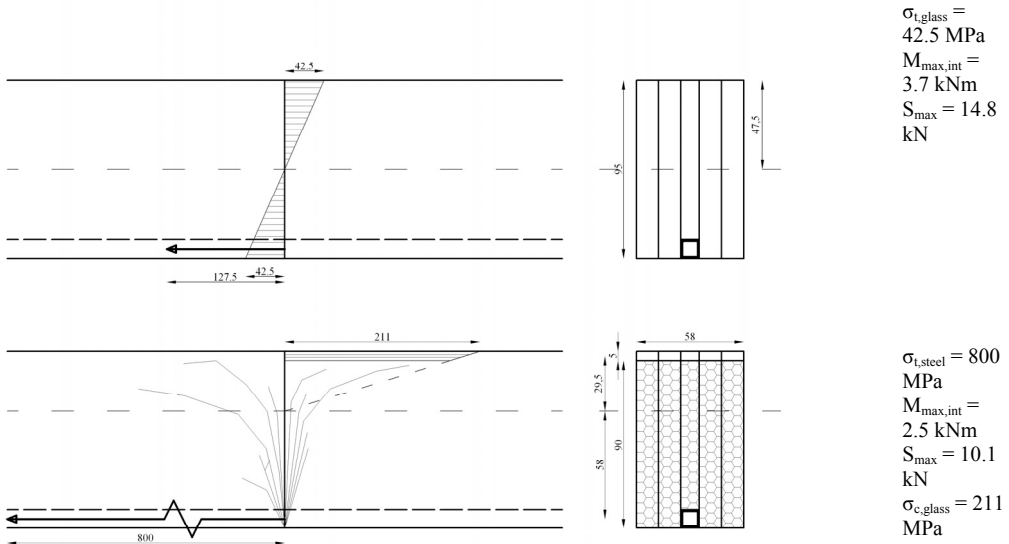


Fig. H.10b Load transfer mechanism of type II specimens in pre- and post-initial failure stage (top and bottom, respectively).

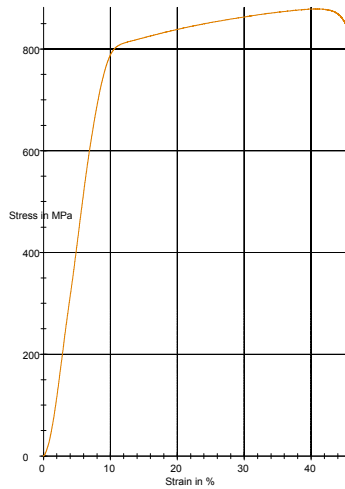


Fig. H.11 Stress-strain curve of tensile test on reinforcement profile.

4.1. Theoretical and Experimental Energy Release

The calculated theoretical displacement under the load points deviates significantly from the experimentally obtained values, see Table H.4. This is caused by the experimental set-up. To be able to test the specimens in the available standard Zwick testing rigs, an auxiliary steel frame was made to support the glass beams, see Figure H.12a and b. The steel frame main longitudinal element was a HEA 100 profile. With a moment of inertia $I_{y,HEA100} = 3.49 \cdot 10^6 \text{ mm}^4$ ($I_{y,I} = 6.83 \cdot 10^6 \text{ mm}^4$; $I_{y,II} = 4.14 \cdot 10^6 \text{ mm}^4$) and the spans as given in Figure H.12, the contribution of the frame to the overall displacement can not be ignored. Actually, it means approximately 36 % of the total displacement with type I beams and 25 % with type II beams is caused by deformation of the steel frame. When the corrected deformations are split according to these proportions, in a part caused by bending of the glass beam and a part caused by bending of the steel beam, it turns out the displacement caused solely by the glass beams is much closer to the theoretical displacement values (Table H.5).

Table H.4 Calculated theoretical and experimental displacements under load points.

Beam	Theoretical $w_{45MPa,glass}$ [mm]	Corrected experimental results $w_{cor,ini,max}$			
		Range [mm]	Average [mm]	St. dev. [mm]	Rel. St. Dev. [%]
Type I	2.22	2.86 – 3.98	3.56	0.40	11.31
Type II	3.61	3.90 – 4.72	4.21	0.34	8.04

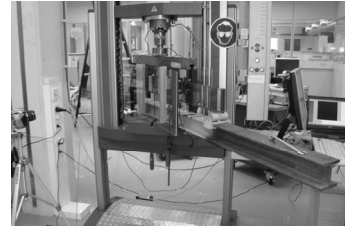
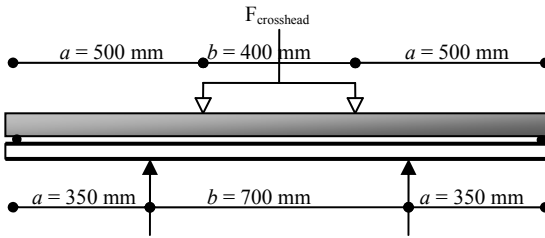


Fig. H.10 Glass beam specimens supported by HEA 100 frame.

Table H.5 Displacements split in part caused by glass beam bending and part caused by steel frame bending.

Specimen	$w_{cor,tot}$	=	w_{glass}	+	w_{frame}
I-01	3.71	=	2.38	+	1.33
I-02	3.88	=	2.49	+	1.39
I-03	3.41	=	2.19	+	1.22
I-04	3.50	=	2.24	+	1.26
I-05	2.86	=	1.83	+	1.03
I-06	3.98	=	2.55	+	1.43
Average			2.28		
St. Dev.			0.24		
Rel. St. Dev.			10.38 %		
II-01	4.19	=	3.13	+	1.06
II-02	3.91	=	2.92	+	0.99
II-03	3.90	=	2.91	+	0.99
II-04	4.34	=	3.24	+	1.10
II-05	4.72	=	3.53	+	1.19
Average			3.15		
St. Dev.			0.25		
Rel. St. Dev.			8.08 %		

The steel contribution to the total deformation has considerable consequences for the release of elastic strain energy, as $U_e = \frac{1}{2} Sw$. At an average failure stress for type I of 43.1 MPa and type II of 42.5 MPa, the theoretical strain energy content at failure would be 11.4 J and 17.6 J, respectively. However, as the crosshead displacement increases by $36/64 = 56\%$ and $25/75 = 33\%$, the theoretical strain energy content at failure increases to 17.8 J and 23.5 J. Note that, because the relative stiffness compared to the steel frame of the type I beam is higher than that of the type II beam, the difference in strain energy content at failure between type I and type II beams, gets *smaller* (was 6.2 J but decreases to 5.7 J).

These values, however, are still well below the strain energy quantities determined from the shifted load-displacement graphs (Table H.2). With averages of $U_{e,ini,cor,I} = 27.6$ J and $U_{e,ini,cor,II} = 30.6$ J, they differed only a factor 1.1. The difference between theoretical and experimental energy values must be caused by extra deformations in the experimental set-up, as the initial failure loads were as expected. However, it is not clear what causes these extra deformations.

Remarkably though, although the strain energy values at initial failure are close, the amount of energy released upon initial failure is not. For type II, this is on average 15.0 J or 48.1 %, while for type I it is only 8.8 J (31.0 %). This relative difference – a factor 1.55 – should probably be attributed to the beams stiffness in broken state, which is governed by the internal moment arm z (and $z_I / z_{II} \approx h_I / h_{II}$; $h_I / h_{II} = 1.63$).

4.2. Crack Growth

The elastic strain energy released at initial failure is absorbed by damage to the specimen (it can not be dissipated by kinetic energy as the specimens do not move upon initial failure and the contribution of heat and sound is ignored, see also Chapter 9 Section 5). Three damage mechanisms can be distinguished:

- Yielding of the steel profile,
- Adhesive or cohesive failure of the adhesive layers,
 - o Glass-steel,
 - o Glass-glass,
- Crack growth through the glass.

The extent of yielding or adhesive failure could not be established in this experiment. Neither could the exact amount of crack growth be determined.⁴ However, two overall crack parameters, the total (relative) crack width and (relative) crack height, could be determined from photographs imported into Autocad (Figure H.5). Their values are summarized in Table H.6

Table H.6 Summarized crack growth parameters.

Crack growth parameters, average values				
Specimen	h_c [mm]	Rel. h_c	$w_{tot,c}$ [mm]	Rel. $w_{tot,c}$
Type I	137.6	88.7 %	260.7	168 %
Type II	90.0	94.7 %	218.1	229 %

Assuming these parameters roughly relate linearly to the total crack length (the photographs of the specimens showed no obvious difference in cracking pattern density), Table H.6 shows there is less crack length⁵ in type II specimens in absolute terms, but more in relative⁶ terms. Although not observed in this experiment, a greater crack height

⁴ the method used in Appendix G could not be applied as the multiple layer character of the beams made it practically impossible to determine which crack occurred in which layer

⁵ This does not necessarily mean there is less crack surface area created. Since $t_{II}/t_I = 2.64$, it requires more than a crack length in type I of more than two and a half times that in type II to obtain equal crack surface area.

⁶ To the beam height.

and/or total crack width in relative terms could indicate earlier stability problems or less (effective) strength of the compressive zone.

4.3. Final Failure

An important difference between both beam types was found in the mode of final failure. While all type I specimens lost their load carrying capacity through failure of the glass-steel adhesive bond, final failure could not be established for all but one of the type II specimens. The maximum test set-up displacement was reached before final failure.

Again, the difference in internal moment arm z explains this difference. The adhesive layer between the glass and the steel reinforcement is loaded in shear stress τ , given by eq. (K.3). As $A_{s,I} = A_{s,II}$, the ratio of shear stress in type I and type II is given by $z_{s,I} / z_{s,II} \approx 1.78$.

$$\tau = \frac{VS}{bI} = \frac{VA_s z_s}{bI} \quad (\text{K.3})$$

For two reasons, adhesive failure occurs only after a certain post-initial failure trajectory (for pure yielding of the steel one would not expect a further increase in load on the steel and the adhesive and thus either the adhesive would have failed before the yielding starts or not to fail at all). First, as shown in Figure H.9, there is an increase in load in the steel during yielding, and thus also a load increase on the adhesive. Probably more importantly, initial failure starts local adhesive debonding from around the initial crack outwards (probably due to peak stresses), thus gradually decreasing the total bond surface area which increases stresses and eventually causes adhesive failure.

Since adhesive failure was governing for the type I beams and no governing failure mechanism could be established for type II beams, the effect of crack growth in both beams types on the post-initial failure behaviour could neither be determined.

5. Conclusions

The experiment did not yield a conclusive proof for the hypothesis that low strain energy content reinforced glass beams have more favourable post-initial failure behaviour than high strain energy content beams because of the amount of strain energy. Rather, it has shown that, for the chosen designs and materials, post-initial failure strength is governed by internal moment arm and yielding of the reinforcement. Final failure occurs for the low energy content beams through adhesive failure. For the high energy content beams, final failure could not be established within the displacement limits of the experimental set-up because the shear stresses on the adhesive are considerably lower.

Furthermore, the deformations in the test frame caused the differences in elastic strain energy at initial failure to be almost equal, differing only a factor 1.1 instead of 1.6, as would be expected from the difference in moment of inertia of both beam designs. Therefore, the type I beams could hardly profit from their energy characteristics over the type II beams.

Nevertheless, some important indications were found that low energy content beams could perform better in the post-initial failure stage than high energy beams. Most importantly, the amount of elastic strain energy released upon initial failure, both in relative and in absolute terms, was considerably lower (even though the strain energy content was almost the same). Thus, the specimens must have suffered less damage at initial failure. This difference in energy release is probably caused by the section stiffness $(EI)_{\text{eff,I}}$.

The relative crack height and total crack width was smaller. This leaves a larger effective glass compression zone and is less likely to cause stability problems in the post-initial failure stage. The difference in crack height could be expected to be much larger in a set-up which features ignorable deformations in the test frame (a much stiffer test frame would be required).

In these designs, the advantages in crack growth could not be profited from as post-initial failure was governed by yielding of the reinforcement and adhesive failure. A stronger adhesive and reinforcement, however, could be applied to maximize the post-failure strength.

The maximum compressive stress in type II beams was close to that in beam type I in this experiment, despite its much lower post-initial strength. Decreasing the test frame contribution to the glass beam energy absorption at initial failure by increasing the frame stiffness, might result in a larger active glass compression zone from which the slim beams are likely to benefit most. This could even result in maximum compressive stresses in the slim beams to be lower than in the stocky ones. This would allow more reinforcement to be applied without glass compressive failure becoming the governing post-initial failure mechanism.

Based on observed crack growth behaviour and measured strain energy release, there seems to be more room for such maximization of post-initial failure strength in low energy content beams than in large energy content ones.

Appendix I: Comparison between Failure Behaviour of SG and GB368 Laminated Reinforced Glass Beams

The failure behaviour of two reinforced glass beam designs has been compared in a four-point bending test. One design featured a UV-curing adhesive (Delo GB368) to bond glass to glass and glass to steel reinforcement, while in the other an ionomer laminate (DuPont SG) was applied. A significantly different behaviour was observed. In the former, extensive cracking occurred in one or two locations along the beam length, resulting in plastic hinges in which the moment capacity depended largely on the internal moment arm and the steel yield strength. On the other hand, smaller, evenly distributed cracks appeared in the latter. In the specimens bonded with UV-curing adhesive, the cracks ran through the complete glass thickness, while the in the SG laminated beams, the cracks were limited to the glass layer from which they originated. As a result the latter beam type had a different post-initial failure load transfer mechanism, in which the glass kept transferring an amount of tensile actions through shear loaded glass-SG-glass bonds. Thus, the post-initial failure strength was considerably higher. Analysis of strain energy release upon initial failure confirmed the energy release in the SG laminated specimens was much lower. SG thus functions as a shock absorber which positively influences the post-initial failure behaviour.

1. Introduction

The failure behaviour of two reinforced glass beam designs has been compared in a four-point bending test. One design featured a UV-curing adhesive (Delo GB368) to bond glass to glass and glass to steel reinforcement, while in the other an ionomer laminate (DuPont SG) was applied.¹

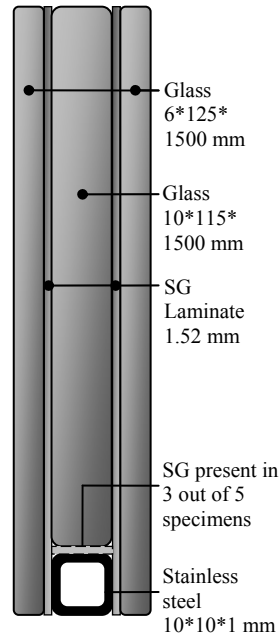
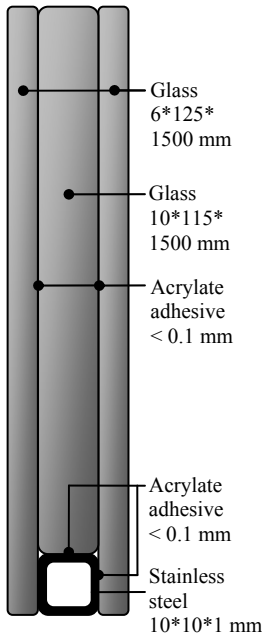
The experiments presented in Appendix H showed that failure of stainless steel reinforced glass beams with high residual strength was governed by adhesive failure of the glass-steel bond. Thus, it was investigated whether the post-initial failure behaviour could be improved by applying SG rather than GB368 to bond the steel to the glass. Although both can theoretically provide high strength glass to metal bonds, it was expected the energy absorption of SG upon initial failure would be higher (because of its volume) resulting in less glass cracking and less damage to the adhesive layer and thus better post-initial failure behaviour.

2. Experimental Method

Two reinforced glass beams were designed. They were both 1.5 m long. The glass and steel dimensions in both sections were equal, but in one type the glass layers and

¹ This experiment was carried out together with P.C. Louter. The results have been published as Louter, P.C., Bos, F.P., Veer, F.A., *Performance of SGP and adhesively bonded metal reinforced glass beams*, Proceedings of the International Symposium on the Architectural Application of Glass, Munich, Germany, 2008. This appendix, however, features an analysis, especially of strain energy and crack growth behaviour, independent from and additional to that publication.

reinforcement were bonded with Delo GB368, a UV-curing adhesive, while in the other DuPont's SentryGlas (SG) was applied (Figures L.1 and L.2). The SG was placed between the glass layers and the left and right sides of the reinforcement. In 3 out of 5 specimens of type IV, a small strip of SG was also placed on top of the reinforcement. No difference in behaviour has been noted between the specimens with and those without this top strip. This is thus ignored henceforth.



Properties	
L	1500 mm
h	125 mm
t	22 mm
W_y	$57.3 \cdot 10^3 \text{ mm}^3$
I_y	$3.58 \cdot 10^6 \text{ mm}^4$
$S_{45\text{MPa}}$	10.3 kN
$w_{45\text{MPa}}$	2.74 mm
$U_{e,45\text{MPa}}$	9.9 J

Fig. I.1 Section design of the glass beam bonded with GB368 (Type III)

Fig. I.2 Section design of the glass beam bonded with SG (Type IV).

Also, the load to obtain a maximum tensile stress level of 45 MPa is given, as well as the (theoretical) elastic strain energy content and displacement *under one of the load*

points², at that load. The displacement was determined by Eq. (L.1). For the equations to determine the elastic strain energy content, refer to Appendix F or Section 2 of Chapter 8.

$$w = \frac{\frac{1}{2} Sa^2 b + \frac{1}{3} Sa^3}{(EI)_{\text{glassbeam}}} \tag{L.1}$$

For *a* and *b*, see Figure I.3.

Of the GB368 beams, 6 specimens were prepared while 5 SG laminated specimens have been manufactured. They have all been subjected to displacement controlled four-point bending (Figure I.3). The support span was 1400 mm; the load span 400 mm, symmetrically applied.

The bending tests were executed in two stages. In the first stage, a specimen was loaded at 2.0 mm/min. until the first significant cracking and drop in applied load (> ~10 %) occurred. The load was then released. The crack pattern was photographed. Then, the load was reapplied at 5.0 mm/min. until final failure took place or the maximum displacement of the experimental set-up was reached.

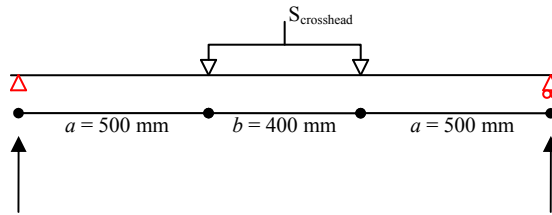


Fig. I.3 Lay-out of four-point bending test.

The experiments were executed in a laterally supported set-up to exclude lateral torsional buckling. In reality, it may well be that stability phenomena will play an important role in cracked glass in the post-initial failure stage. However, the presence of multiple possible failure mechanisms would cloud observations too much.

3. Results

Table I.1 lists the maximum initial and post-initial failure loads, the initial glass tensile failure stress, the uncorrected maximum initial and post-initial displacements, the relative residual strength, and the final failure cause.

² This is *not* the maximum displacement at mid span. The testing machine tracks the displacement of the loading points. Thus, the experimental results can be compared with these theoretical values.

Table I.1 Direct experimental results.

Spec.	S_{ini} [kN]	σ_{ini} [MPa]	w_{ini} [mm]	$S_{post,max}$ [kN]	$w_{post,max}$ [mm]	Rel. Res. Strength	Final Failure Cause
GB368-01	11.4	49.7	4.9	14.1	25.7	124 %	Steel-glass adhesive
GB368-02	10.9	47.6	5.4	12.8	17.6	117 %	Steel-glass adhesive
GB368-03	9.3	40.5	4.8	14.2	35.8	153 %	Steel-glass adhesive
GB368-04	8.7	37.8	4.1	14.6	16.8	169 %	Steel-glass adhesive
GB368-05	9.8	42.9	4.3	13.9	52.8	142 %	Reached max. displacement.
GB368-06	9.9	43.1	4.4	14.1	49.7	143 %	Reached max. displacement.
Average	10.0	43.6	4.7	14.0	33.1	1.41	
St. Dev.	1.0	4.41	0.48	0.61	15.7	0.19	
Rel. St. Dev.	10.1 %	10.1 %	10.2 %	4.4 %	47.5 %	13.3 %	
SG-01	11.4	49.6	5.2	16.9	50.0	149 %	Reached max. displacement.
SG -02	10.7	46.5	4.9	17.5	55.0	165 %	Reached max. displacement.
SG -03	10.8	47.1	4.8	17.1	54.3	158 %	Reached max. displacement.
SG -04	12.8	56.0	4.9	17.8	53.2	139 %	Reached max. displacement.
SG -05	13.0	56.7	4.7	18.0	50.2	139 %	Reached max. displacement.
Average	11.7	51.2	4.9	17.5	52.5	1.50	Reached max. displacement.
St. Dev.	1.1	4.88	0.21	0.48	2.31	0.12	
Rel. St. Dev.	9.54 %	7.54 %	4.3 %	2.77 %	4.39 %	7.72 %	

The elastic strain energy was determined from the crosshead displacement and crosshead loads. However, most specimens had a (small) initial trajectory of set-up settlement before the graph entered a linear elastic stage until initial failure. To accurately assess the energy levels, the graphs therefore had to be shifted horizontally so that the linear elastic trajectory would extend through the origin. This was done using Autocad (Figure I.4a – c). It resulted in a corrected displacement at initial failure, given in Table I.2, along with the values for the elastic strain energy at initial failure, the elastic strain energy during reloading at the displacement of initial failure, and the released elastic strain energy, both absolute and relative to the elastic strain energy at initial failure.

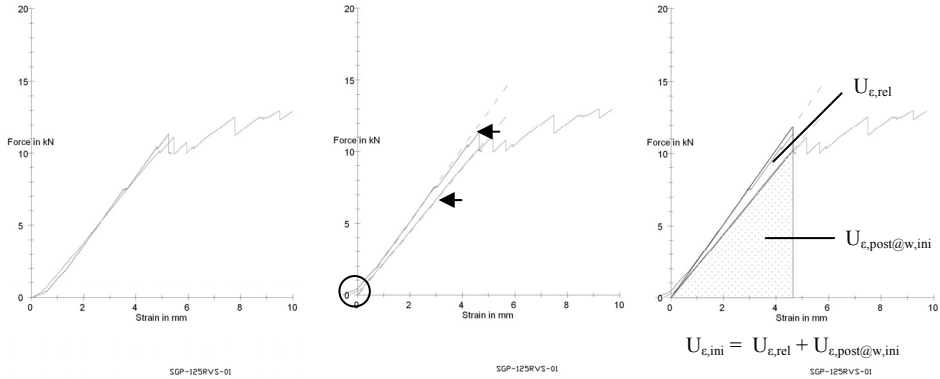


Fig. I.4a, b, and c (left to right) Load-displacement graph of specimen SG-01 in Autocad. Figure a) original graphs; Figure b) Shifting of graphs to match linear elastic curves from origin; Figure c) determination of elastic strain energy release at failure and content before and after failure at the initial failure displacement. Note that the Figures only show part of the post-initial behaviour graph. The full graphs are presented in Figures L.6a – f and L.7a – e.

Table I.2 Elastic strain energy related results.

Spec.	$w_{ini,cor}$ [mm]	$U_{e,ini}$ [J]	$U_{e,post@w,ini}$ [J]	$U_{e,rel}$ [J]	Rel. $U_{e,rel}$
GB368-01	4.0	23.4	15.4	8.0	34.0 %
GB368-02	3.5	19.4	12.5	6.9	35.6 %
GB368-03	3.4	17.5	12.7	4.8	27.6 %
GB368-04	2.8	12.6	9.7	2.9	22.9 %
GB368-05	3.1	15.2	11.0	4.1	27.3 %
GB368-06	3.1	15.4	12.0	3.4	23.0 %
Average	3.3	17.2	12.2	5.0	28.4
St. Dev.	0.39	3.78	1.91	1.99	5.41
Rel. St. Dev.	11.81 %	21.95 %	15.63 %	39.43 %	19.04 %
SG -01	4.6	27.6	23.7	3.9	14.1
SG -02	3.5	19.5	16.2	3.3	17.0
SG -03	4.1	22.7	19.9	2.8	12.4
SG -04	4.1	26.9	22.2	4.6	17.2
SG -05	4.4	30.4	26.3	4.1	13.6
Average	4.1	25.4	21.7	3.8	14.9
St. Dev.	0.42	4.32	3.85	0.71	2.14
Rel. St. Dev.	10.05 %	16.98 %	17.77 %	18.80 %	14.38 %

Some crack growth parameters were also determined by importing photographs of the crack patterns into Autocad and measuring distances (Figure I.5). Table I.3 provides the initial crack height h_c and total width w_c (absolute and relative to beam height h_b).



Fig. I.5 Photograph of initial crack pattern of specimen GB368-03 in Autocad. Determination of crack related results crack height and total crack width (upon initial failure).

Table I.3 Crack growth related results.

Spec.	h_c [mm]	Rel. h_c	w_c [mm]	Rel. w_c [%]
GB368-01	111.5	89.2 %	228.3	183 %
GB368-02	113.0	90.4 %	206.8	165 %
GB368-03	100.5	80.4 %	159.1	127 %
GB368-04	98.1	78.5 %	141.9	114 %
GB368-05	110.6	88.5 %	124.9	100 %
GB368-06	109.6	87.7 %	169.7	136 %
Average	107.2	85.8	171.8	137
St. Dev.	6.27	5.02	39.18	0.31
Rel. St. Dev.	5.86 %	5.86 %	22.81 %	22.81 %
SG-01	94.8	75.8 %	172.8	138 %
SG -02	95.4	76.3 %	163.5	131 %
SG -03	97.9	78.3 %	99.2	79.4 %
SG -04	98.5	78.8 %	135.5	108 %
SG -05	92.9	74.3 %	93.6	74.9 %
Average	95.9	76.7	132.9	106
St. Dev.	2.30	1.84	36.10	0.29
Rel. St. Dev.	2.40 %	2.40 %	27.17 %	27.17 %

Typical crack development of GB368 bonded and SG laminated beams is presented in Figures L.6a – d and L.7 a – d, respectively. Like the beams discussed in Appendix H, the GB368 bonded ones develops a plastic hinge (or sometimes two) at a location of concentrated crack growth. The SG laminated beams, however, shows a much more evenly distributed cracking pattern were each crack stays limited to the glass sheet of its origin. Consequently, those specimens also show a smoother bending curve.

As experienced in the experiments described in Appendix H, a considerable amount of measured displacement can be attributed to bending of the test frame (see Appendix H, Section 4.1). Table I.4 splits the total displacement in a part caused by glass beam bending and a part caused by steel frame bending.

The crack patterns after initial failure as well as the shifted load-displacement graphs are shown in Figures L.8a – f (GB368 bonded) and Figures L.9a – e (SG laminated).

Several important points can be deduced from the results presented in Tables L.1, L.2, and L.3:

- The average initial failure load of GB368 bonded and SG laminated specimens differs considerably ($S_{ini,max,ave,III} = 10.0$ kN; $S_{ini,max,ave,IV} = 11.7$ kN). With a short term Young's modulus of only 0.3 GPa, the presence of SG in SG laminated specimens does not explain this difference.
- The average post-initial failure load of GB368 bonded and SG laminated specimens varies significantly, especially in absolute terms ($S_{post,max,ave,GB368} = 14.0$ kN; $S_{post,max,ave,SG} = 17.5$ kN). When presented as percentage of the initial failure strength, the difference is smaller because of the higher average initial failure load with the SG laminated specimens.
- The average displacement at initial failure w_{ini} was 4.1 mm for SG laminated beams, but only 3.3 mm for GB368 bonded ones.
- Because of the higher displacement and initial failure load of the SG laminated specimens, their strain energy content U_e at failure was also much higher ($U_{e,ave,GB368} = 17.2$ J; $U_{e,ave,SG} = 25.4$ J). Nevertheless, the strain energy release $U_{e,rel}$ upon initial failure was significantly lower, both in absolute and relative terms ($U_{e,rel,ave,GB368} = 5.0$ J (28.4 %); $U_{e,rel,ave,SG} = 3.8$ J (14.9 %)).
- The GB368 bonded and SG laminated beams showed considerably different fracture patterns. The average crack height and total crack width in SG laminated beams were smaller. More importantly though, while the cracks in GB368 bonded beams concentrated around one or two origins, in SG laminated ones they were distributed very evenly along the beam length.
- Final failure could not be established for any of the SG laminated specimens. Four out of six GB368 bonded specimens, on the other hand, collapsed by adhesive failure of the glass-reinforcement bond.

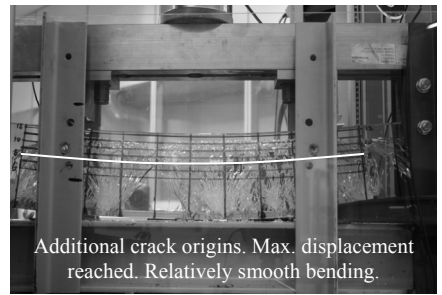
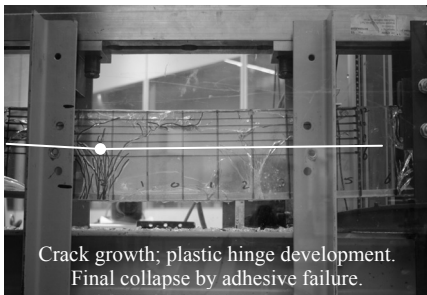
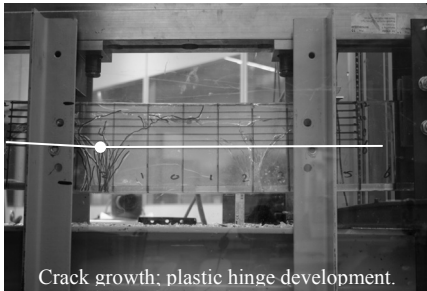
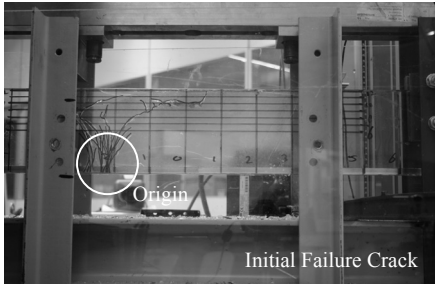


Figure I. 6a – d (top to bottom) Crack development in specimen GB368-02.

Figure I. 7a – d (top to bottom) Crack development in specimen SG-02.

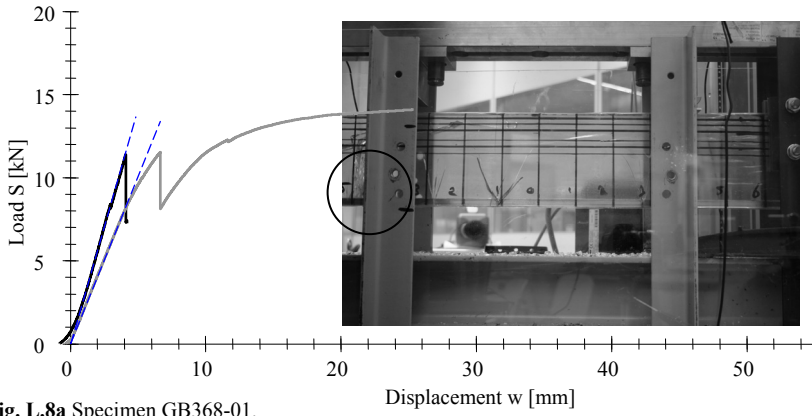


Fig. L.8a Specimen GB368-01.

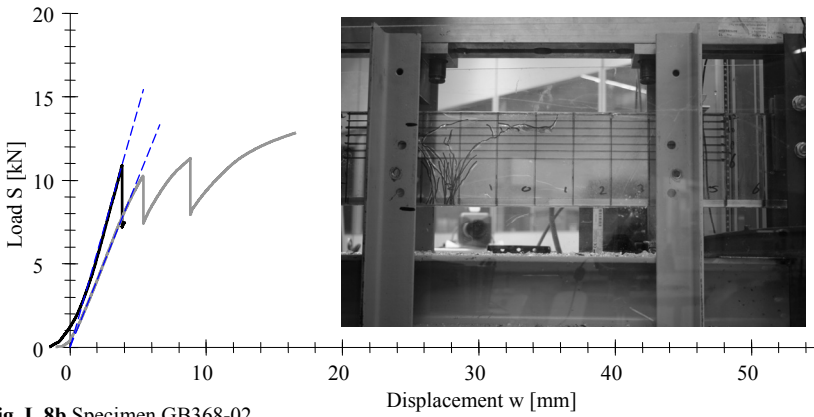


Fig. L.8b Specimen GB368-02.

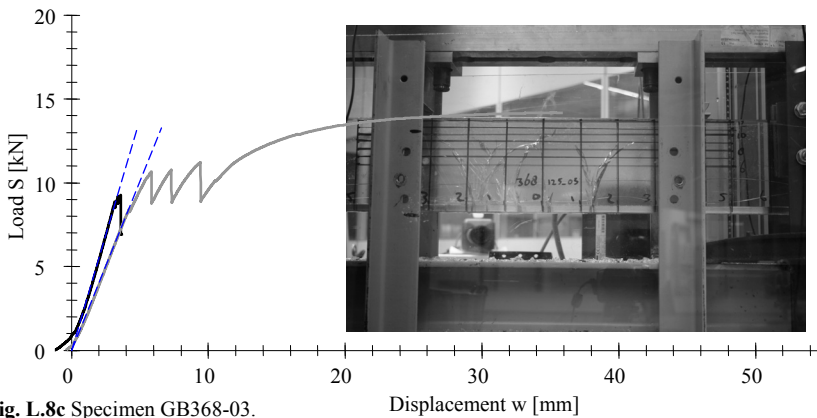


Fig. L.8c Specimen GB368-03.

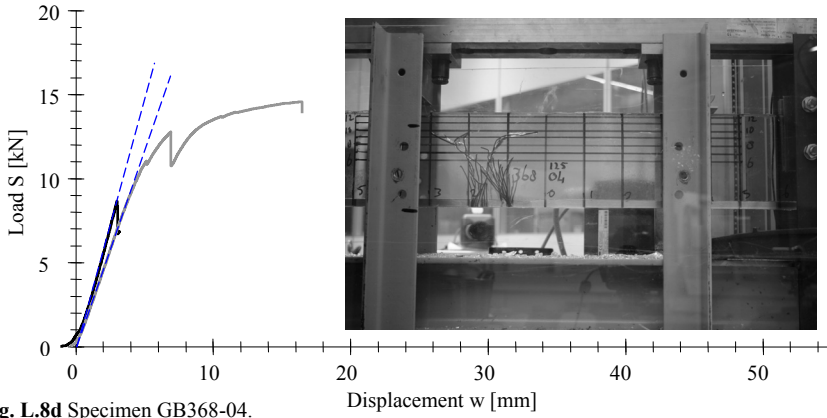


Fig. L.8d Specimen GB368-04.

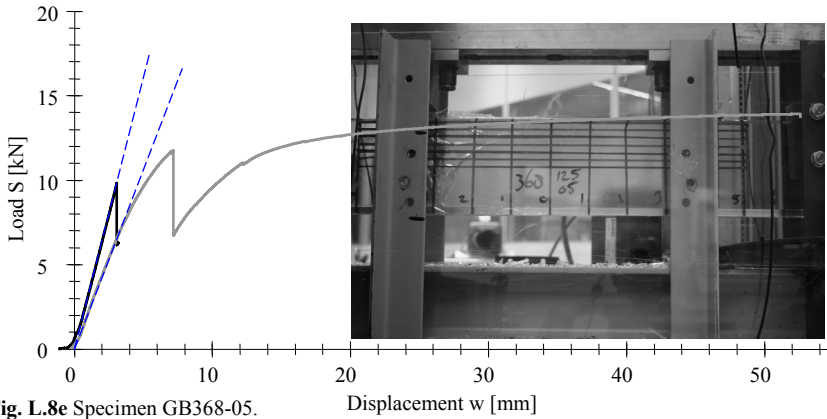


Fig. L.8e Specimen GB368-05.

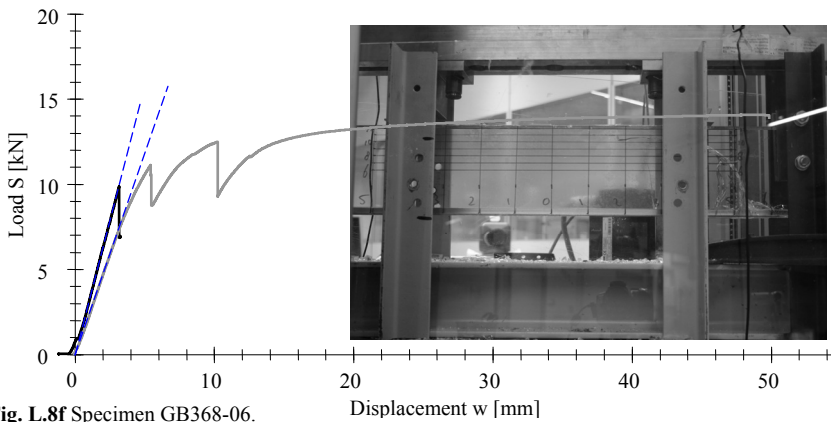


Fig. L.8f Specimen GB368-06.

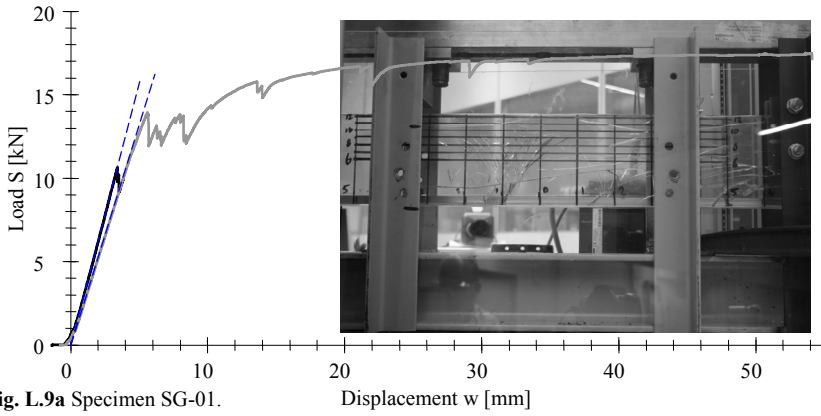


Fig. L.9a Specimen SG-01.

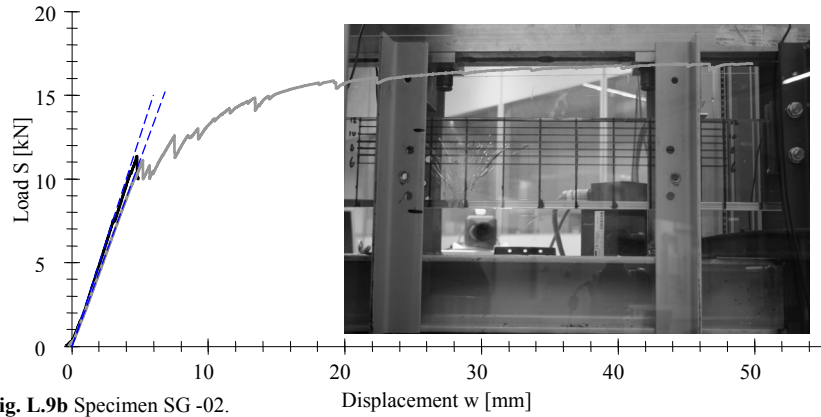


Fig. L.9b Specimen SG-02.

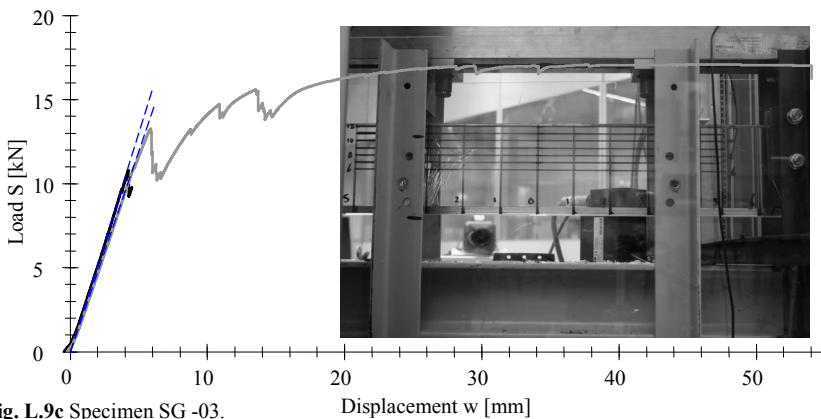


Fig. L.9c Specimen SG-03.

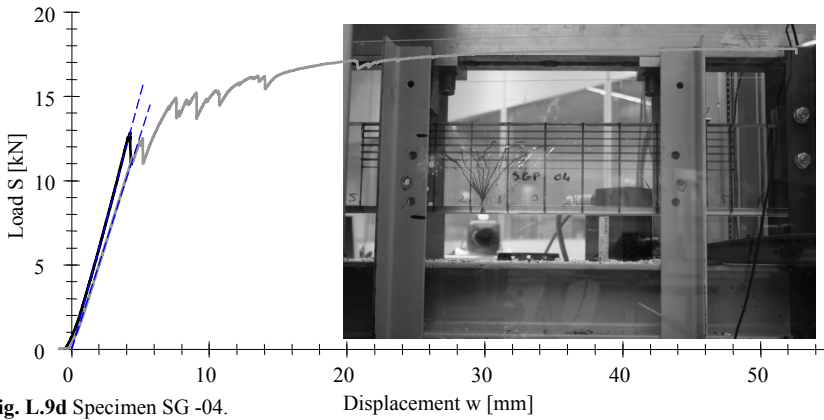


Fig. L.9d Specimen SG -04.

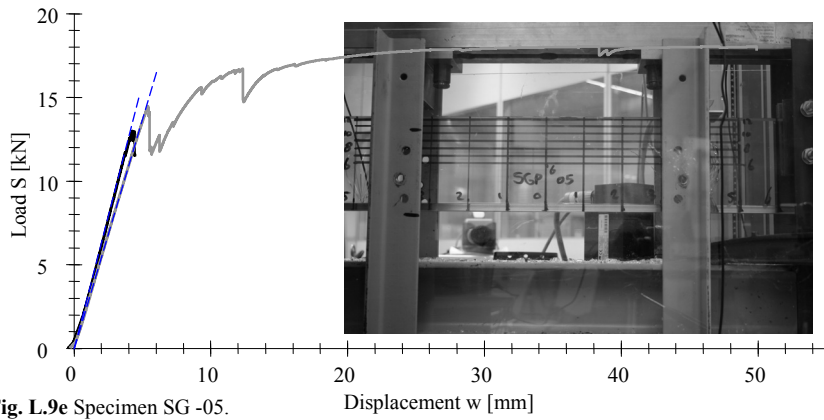


Fig. L.9e Specimen SG -05.

Table I.4 Displacements split in part caused by glass beam bending and part caused by steel frame bending.

Specimen	$w_{cor,tot}$	=	w_{glass}	+	w_{frame}
GB368-01	4.0	=	3.1	+	0.9
GB368-02	3.5	=	2.7	+	0.8
GB368-03	3.4	=	2.7	+	0.8
GB368-04	2.8	=	2.2	+	0.6
GB368-05	3.1	=	2.4	+	0.7
GB368-06	3.1	=	2.4	+	0.7
Average			2.6		
St. Dev.			0.28		
Rel. St. Dev.			10.8 %		

Table I.4 (continued)

Specimen	$w_{cor,tot}$	=	w_{glass}	+	w_{frame}
SG -01	4.6	=	3.6	+	1.1
SG -02	3.5	=	2.7	+	0.8
SG -03	4.1	=	3.2	+	0.9
SG -04	4.1	=	3.2	+	0.9
SG -05	4.4	=	3.4	+	1.0
Average			3.2		
St. Dev.			0.32		
Rel. St. Dev.			10.1 %		

4. Discussion

Although similar at first sight, there are important differences in the failure behaviour of the investigated beam types.

4.1. Failure Behaviour of GB368 Bonded Reinforced Glass Beams

Failure in the GB368 bonded specimens initiated by extensive cracking from a single origin. The crack goes through the thickness of the complete glass section and extents on average over 85.8 % of the beam height (107.2 mm). At the location of the initial cracks, a plastic hinge develops. In some cases a second origin of extensive cracking occurs and a second hinge develops at that location. No more than two such hinges in any one specimen have been observed. After the creation of these hinges, the load transfer mechanism has definitively shifted from solid section in linear elastic bending to composite action with the (uncracked) top part of the glass in compression and the steel reinforcement in tension.

As discussed in Section 4 of Appendix H, the moment capacity of the plastic hinge is determined by the internal moment arm z , the steel yield strength, the glass compressive strength and the adhesive shear strength of the glass-reinforcement bond. The stress distribution before initial failure and at the maximum post-initial failure strength are presented in Figure I.10 (z has been determined as in Appendix H, by considering the uncracked glass section upon initial failure to present the compression zone).

Four out of six GB368 bonded specimens finally collapsed by failure of the glass-steel adhesive bond. The shear stress on the adhesive layer depends on the internal moment arm z through Eq. (L.2)

$$\tau = \frac{VS}{bI} = \frac{VA_s z_s}{bI} \tag{L.2}$$

For two reasons, adhesive failure occurs only after a certain post-initial failure trajectory (for pure yielding of the steel one would not expect a further increase in load on the steel and the adhesive and thus either the adhesive would have failed before the yielding starts or not to fail at all). First, there is an increase in load in the steel during yielding

(see Figure K.11 in Appendix H), and thus also a load increase on the adhesive. Probably more importantly, initial failure starts local adhesive debonding from around the initial crack outwards (probably due to peak stresses), thus gradually decreasing the total bond surface area which increases stresses and eventually causes adhesive failure.

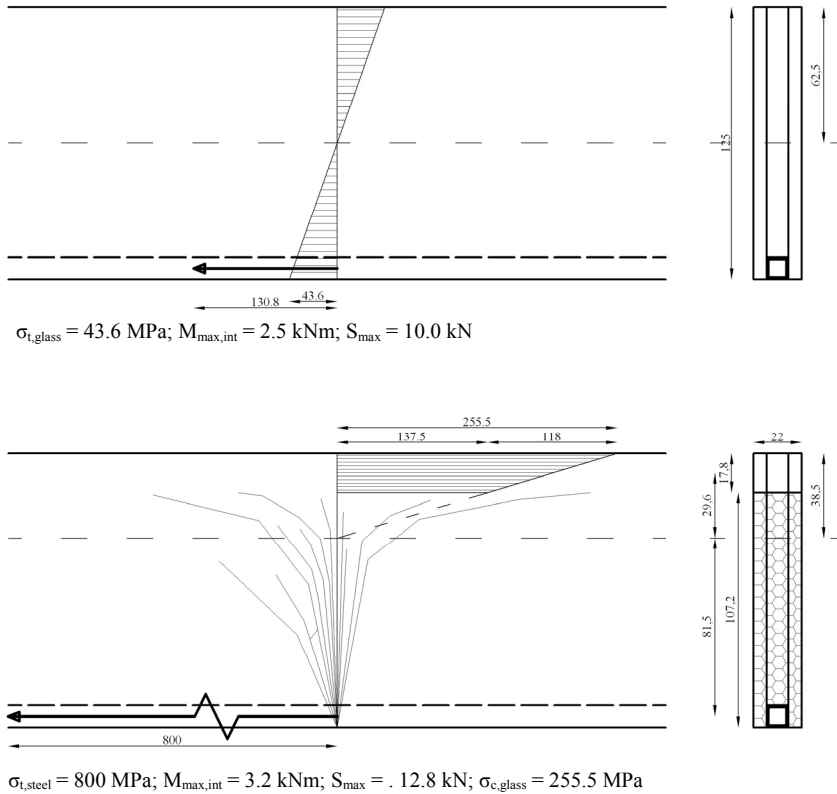


Fig. I.10 Load transfer mechanism of GB368 bonded specimens in pre- and post-initial failure stage (top and bottom, respectively).

4.2. Failure Behaviour of SG Bonded Reinforced Glass Beams

The average initial failure strength of the SG laminated specimens is remarkably higher than of the GB368 bonded ones ($S_{\text{ini, GB368}} = 10.0 \text{ kN}$; $S_{\text{ini, SG}} = 11.7 \text{ kN}$; $\sigma_{\text{ini, GB368}} = 43.6 \text{ MPa}$; $\sigma_{\text{ini, SG}} = 51.2 \text{ MPa}$). Since the Young's modulus of SG is only 0.3 GPa at room temperature compared to $E_{\text{glass}} = 70 \text{ GPa}$, the additional load carrying capacity of the SG can not explain this difference (at 45 MPa tensile stress in the glass, the SG could carry only 0.006 kN of the applied load).

Since the geometry of the GB368 bonded and SG laminated specimens is otherwise identical and thus in absence of an explanation from a mechanics point of view, the difference probably has to be attributed to the fact that the glass for each type came from different glass processors (thus the edge quality may have been different).

The variation in initial failure load explains the established gap between the corrected average initial displacement values of $w_{ini,cor,III} = 3.3$ mm and $w_{ini,cor,IV} = 4.1$ mm ($S_{ini,GB368}/S_{ini,SG} = 0.85$, while $w_{ini,cor,GB368}/w_{ini,cor,SG} = 0.80$).

A more fundamental difference in failure behaviour of both types occurs in the post-initial failure stage. SG laminated beams yielded an average maximum post-failure strength of $S_{post,max,ISG} = 17.5$ kN ($S_{post,max,GB368} = 14.1$ kN). However, if the post-failure strength is considered to be governed by one or more plastic hinges as in Figure I.10 with a glass compression zone, a steel tensile zone and an inactive cracked zone in between, $S_{post,max,SG}$ is *well above the theoretical maximum*.

Although the internal moment arm can not be established very accurately, it can not be more than the distance from the beam top to the middle of the steel profile. Thus the maximum theoretical moment capacity of the plastic joint would be given by Eq. (L.3a) and the required external load in the applied test set-up by Eq. (L.3b).

$$M_{max} = \sigma_{y,steel} A_{profile} (h_{IV} - \frac{1}{2} h_{profile}) \quad (L.3a)$$

$$S_{ext} = 2 \cdot M_{max} / a \quad (L.3b)$$

When applying the maximum strength $\sigma_{steel} = 830$ MPa, found for the reinforcement profiles (Section 4 and Figure K.9, Appendix H), this still only yields $M_{int,max} = 3.59$ kNm and $S_{post,max} = 14.3$ kN. Therefore, there has to be another load transfer mechanism in the post-initial failure stage. More specifically, there has to be an additional tension carrying component. The most obvious candidate is, off course, the SG laminate. However, simply adding the SG layers to the section assumed earlier (glass compression part, steel tension part, and inactive, broken glass part in between) does not explain the difference as its strain is governed by the steel strain (it can not be larger) and the developed forces are therefore determined by the stiffness ratio of both materials and the internal moment arm ($\approx \frac{1}{3} z^2 (tE)_{SG} / z(AE)_{steel} = 14592 / 907200 = 0.016$).

Consider the crack growth behaviour in both beam types. Both the average initial crack height ($h_{c,GB368} = 107.2$ mm; $h_{c,SG} = 95.9$ mm) and initial total crack ($w_{c,GB368} = 171.8$ mm; $w_{c,SG} = 132.9$ mm) width are significantly smaller for SG laminated beams.

Even more importantly though, is the difference in crack distribution. Whereas the initial cracks in the GB368 bonded beams run through the beam thickness completely as it was a solid piece of glass, in the SG laminated beams they stay limited to the glass layer in which the crack originated. In the post-initial failure stage, new cracks origins occurred more or less evenly distributed over the beam length and the beam layers. As a result, even far in the post-initial failure stage, there are no locations along the beam length where the cracks run through the glass thickness completely; there is always at least one glass layer active in each section.

This does not mean, however, the section can be considered to carry actions as suggested in Figure I.11. This would require linear elastic behaviour (as the unbroken

glass can only act linear elastically), which is clearly contradicted by the shape of the post-initial failure curves in Figure I.9. Rather, the SG and broken glass form a tensile load transfer mechanism through multiple shear bonds as clarified in Figure I.12. The stiffness of these bonds is much higher than of SG only (but not necessarily linear elastic as glass), thus this system can carry significant loads at relatively limited, and reinforcement governed, strains. The gradual increase of cracks observed in the post-initial failure stage explains the steady decrease in overall stiffness.³

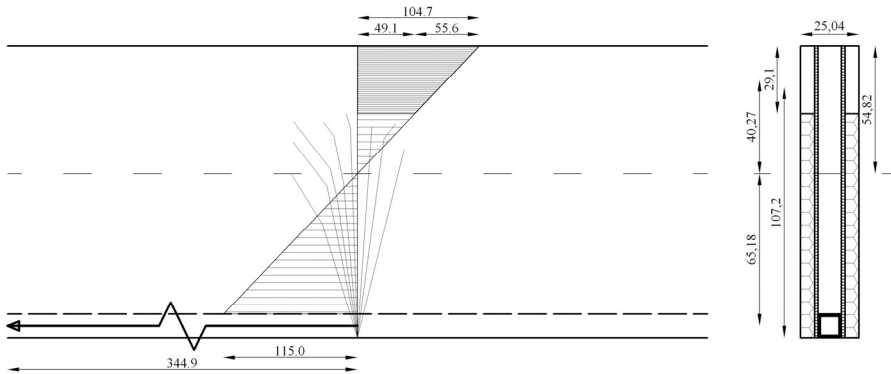


Fig. I.11 Suggested but incorrect post-initial failure load transfer mechanism in SG laminated beams.

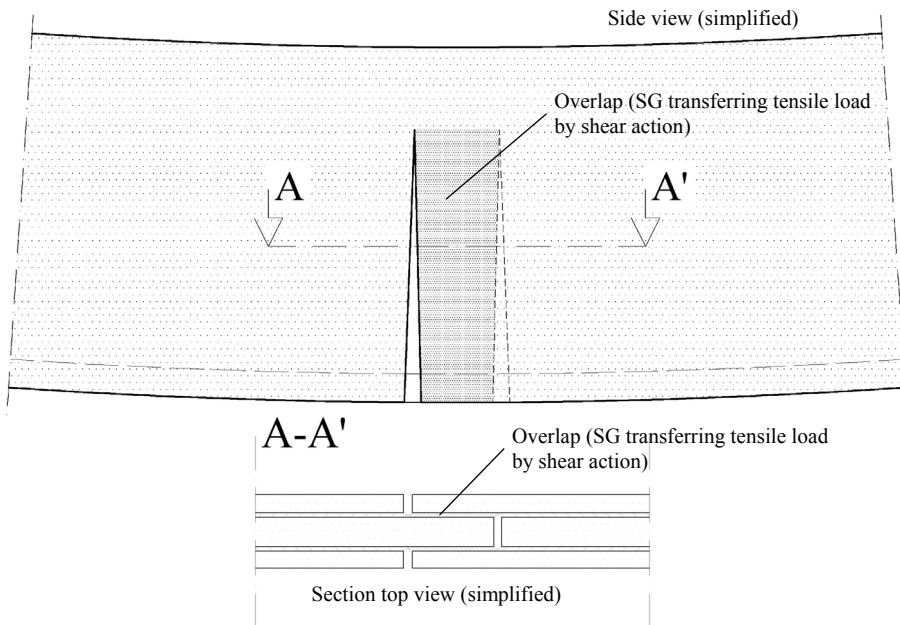


Fig. I.12 Simplified representation of the extra tensile capacity provided by shear loaded SG.

³ Quantification of the stiffness of these bonds and the forces through the glass and SG would require extensive FE-analysis. This falls outside the scope of this study.

4.3. Causes for the Differences in Failure Behaviour

The essence of the observed difference in failure behaviour is the absence (GB368) or presence (SG) of overlapping glass transferring shear loads through the laminate. The SG layers between the glass sheets specimens act as crack stoppers. Compared to the GB368 bonds, the SG laminates are relatively weak through their lower Young's modulus ($E_{SG} = 0.3 \text{ GPa}$ vs $E_{GB368} = 0.9 \text{ GPa}^4$), but more importantly through their thickness ($t_{SG} = 1.52 \text{ mm}$ vs $t_{GB368} < 0.1 \text{ mm}$). Thus, the peak stress around an advancing crack is dissipated once reaching the SG interlayer. The resulting peak stress on the glass layer on the other side is much lower and therefore the crack is stopped – at least to proceed into another layer. A similar effect would be expected if even weaker laminates, such as PVB, would be applied. On the other hand, a very stiff bond (such as obtained with GB368) does not decrease the stress peak at the crack tip, and therefore the crack will continue in the subsequent glass layer.

4.4. Crack Growth Behaviour and Elastic Strain Energy Release

A secondary difference in failure behaviour is the extent of crack growth upon initial failure. The average relative crack height and total crack width are both significantly smaller in the SG laminated specimens (rel. $h_{c,GB368} = 85.8 \%$ vs rel. $h_{c,SG} = 76.7 \%$; rel. $w_{c,GB368} = 137 \%$ vs rel. $w_{c,SG} = 106 \%$). The photographs also clearly show a less extensive cracking pattern (Figures L.6 and 7).

These observations are backed by the determined values of elastic strain energy release. In the SG laminated specimens, the elastic strain energy at initial failure is higher than in the GB368 bonded specimens because the average initial failure strength is higher.⁵ However, the elastic strain energy release is *lower*, not only in relative terms but even in absolute values: $U_{e,SG} = 3.8 \text{ J}$ vs $U_{e,GB} = 5.0 \text{ J}$; rel. $U_{e,SG} = 28.4 \%$ vs rel. $U_{e,GB368} = 14.9 \%$. Thus, less crack growth would be expected in SG laminated specimens.

Off course, the fact that the initial cracks stay limited to one sheet would directly lead to the conclusion that less energy is released. But the available glass for crack growth is also significantly less thus that does not automatically mean less crack growth.

Rather, the reason for the limited amount of crack growth upon initial failure (even in one sheet) is the fact that the elastic strain energy released by the breaking glass sheet is absorbed by elastic strain energy build-up in the SG⁶. The capacity of the absorbance is determined by the Young's modulus, thickness and adhesive strength to the glass.⁷ The GB368 bonds therefore possess much less elastic energy absorbance capacity.

Alternatively, the limited strain energy release can be attributed to the post-initial failure stiffness (as the strain energy release is determined by subtracting the pre- and post-

⁴ DELO, *Glassbond selection chart*, www.delo.de.

⁵ Therefore the displacement is also higher. Note that the elastic strain energy content depends linearly on the *product* of applied load and displacement.

⁶ By *elastic* deformation. The SG does not deform plastically at initial failure can be deduced from the high post-initial failure stiffness (post-initial load-displacement curves in Figures L.7a – e) and the low elastic strain energy release. Instead of the elastic strain energy being released by damage or plastic deformation, it is partially transferred from the glass to the SG around the developing crack tip.

⁷ Therefore, a PVB laminate would be expected to be less effective as it can absorb much less elastic strain energy at equal deformation than SG.

initial failure curves, see Figure I.4). However, the post-initial failure stiffness is determined by the same parameters as the elastic strain energy absorbance capacity, thus this actually amounts to the same. The former explanation is more fundamental as it relates to the relevant processes during fracture, while the latter deduces from the post-initial failure state and is thus retrospective.

5. Conclusions

The SG laminated reinforced glass beams have shown consistently higher levels of residual strength and displacement than those bonded with GB368. This can be attributed to a fundamentally different load transfer mechanism in the post-initial failure stage, made possible by a) the crack stopping properties of the interlayer, and b) the elastic strain energy absorbance capacity of the interlayer.

The post-initial failure strength of the GB368 bonded specimens was governed by the moment capacity of one or two plastic hinges which occurred along the beam length, like those in both beam types reported in Appendix H. These plastic hinges consist of a compressive glass zone in the top and a tensile steel zone at the bottom. The capacity of these hinges can be determined by quite simple two dimensional analytical calculations.

On the other hand, for their maximum post-initial failure strength, the SG bonded specimens had the advantage of an additional tensile capacity provided by overlapping glass segments transferring tensile actions through shear loaded glass-SG-glass bonds. For this mechanism to work, the non-coincidence of glass cracks in the various layers, is crucial. This is ensured by the crack stopping properties of the SG laminate and the natural variation of bending tensile strength along the edges of glass sheets.

Curriculum Vitae



Freek Paul Bos

Freek Bos was born March 1st 1977 in Amsterdam. He grew up in Leiden, where he attended the municipal grammar school (*Stedelijk Gymnasium*). He graduated in 1995 and began his academic education at the Architecture Faculty of the Delft University of Technology.

During his study, Freek was chairman of BouT, the students association for Building Technology, after having spent half a year at the *Politecnico* in Milan, Italy. Besides his study, he worked as a draughtsman at a small architecture firm, and later as student-assistant at the Chair of Mechanics in Buildings. In 2002, he obtained his Masters degree in two specializations (Architecture and Building Technology) on an exploration of the possibilities of structural optimization methods for the design of free-form architecture.

After his study, Freek briefly worked as a structural engineer at ABT, before starting this doctorate research. In 2004, he coordinated the All Transparent Pavilion project and organized the symposium *There / Not there*. He is a member of the IABSE Working Group Structural Glass and the Scientific Committee to the ICSA2010 conference, and a lecturer at the post-academic *Glass in Construction* course at the TU Delft (2005, 2007, 2009 editions). The *Challenging Glass* conferences (2008, 2010) are organized by Freek and his close colleague Christian Louter.

Besides his work at the university, Freek has been an editor to *Bouwen met Staal* and frequently edited articles for other professional magazines in the building industry on a freelance basis since 2003.

Freek's hobbies include travelling, mountain hiking, and skiing. He is married to Lonneke. They have two children: Caspar and Emilia.

